

INVESTIGATION OF NORMALIZED BEHAVIOR OF RESEDIMENTED
BOSTON BLUE CLAY USING
GEONOR DIRECT SIMPLE SHEAR APPARATUS

by

Imtiaz Ahmed

B. Sc. (Civil Engineering)
Military College of Engineering
Risalpur, Pakistan
(1982)

Submitted to the Department of
Civil Engineering in partial fulfillment
of requirements for the degree of

Master of Science in Civil Engineering

at the

MASSACHUSETTS INSTITUTE OF TECHNOLOGY

May 1990

© Massachusetts Institute of Technology 1990

Signature of Author:.....
Dept. of Civil Engineering, May 18, 1990

Certified by:.....
Dr. John T. Germaine, Thesis Co-Supervisor

Certified by:.....
Prof. Charles C. Ladd, Thesis Co-Supervisor

Accepted by:.....
Prof. Ole S. Madsen
Chairman, Departmental Committee on Graduate Students

MASSACHUSETTS INSTITUTE
OF TECHNOLOGY

JUN 15 1990

LIBRARIES

بِسْمِ اللَّهِ الرَّحْمَنِ الرَّحِيمِ

In the name of Allah, THE BENEFICENT, THE MERCIFUL.

"...and of His signs is that He created you of dust"

Al Quran

INVESTIGATION OF NORMALIZED BEHAVIOR OF RESEDIMENTED BOSTON BLUE CLAY USING GEONOR DIRECT SIMPLE SHEAR APPARATUS

by

Imtiaz Ahmed

Submitted to the Department of Civil Engineering on
May 18, 1990, in partial fulfillment of the requirements
for the Degree of Master of Science in Civil Engineering.

ABSTRACT

This thesis investigates the normalized undrained stress-strain-strength behavior of resedimented Boston Blue Clay in the Geonor Direct Simple Shear (DSS) apparatus. The experimental study included a number of K_0 consolidated-undrained shear tests on specimens of normally consolidated resedimented Boston Blue Clay III (BBC) at different consolidation stress levels (σ'_{vc}) and also on specimens rebounded to varying overconsolidation ratios (OCR's). Additionally, constant rate of strain consolidation (CRSC) tests were conducted to obtain well defined compression curves for comparison with the consolidation data from the CK_0 UDSS tests.

The evaluation of data from the consolidation phase of the CK_0 UDSS tests show that the Geonor DSS gives consistent and good estimates of the 1-D consolidation response of BBC, except for tests influenced by deformation of "bent" metal porous stones. The DSS compression curves are in reasonable agreement with those obtained from the end of primary incremental oedometer and CRSC tests conducted at strain rates which result in normalized pore pressure (u_b/σ_v) values between 2 to 5%. The virgin compression ratio for BBC is found to decrease with increasing stress levels. The new BBC III gives a lower rate of secondary compression than BBC II and the ratio $C_{\alpha\epsilon}/CR$ falls somewhat below the range found for most inorganic soft clays.

The results from the CK_0 UDSS tests on normally consolidated BBC at σ'_{vc} ranging from 1.44 to 12 ksc are generally consistent and demonstrate good normalized behavior with respect to the undrained shear strength ratio (c_u/σ'_{vc}). However, the following trends were found with increasing σ'_{vc} : increase in strain at failure; decrease in $\Delta u/\sigma'_{vc}$ versus shear strain; and a significant decrease in Young's modulus expressed as E_u/c_u or E_u/σ'_{vc} versus shear stress level or shear strain. The values of τ_h/σ'_{vc} at maximum obliquity appear reasonable in the light of ϕ' obtained from CK_0U triaxial tests, but show large scatter. All the specimens exhibit significant strain softening at large shear strains, which is suspected to be partially due to "unloading" caused by nonuniform stresses within the DSS device.

The undrained shearing of overconsolidated specimens produces negative pore pressures which increase with increasing OCR and reach a minimum value near the peak strength. They then become less negative, and even become positive for OCR's < 3.25. This pore pressure behavior is the principal reason for the large increase in c_u/σ'_{vc} with increase in OCR, which is also accompanied by an increasing strain at failure. The effective stress path from normally consolidated sample forms an envelope for the paths of the overconsolidated samples. All the paths from the overconsolidated samples rise up to the normally consolidated stress path, reaching the envelope at the peak shear resistance, and then follow the OCR = 1 curve while strain softening and eventually reaching maximum obliquity. The normalized modulus E_u/c_u versus τ_h/c_u decreases with increasing OCR, whereas E_u/σ'_{vc} versus shear strain shows the opposite trend. The effect of changes in the maximum past pressure (σ'_{vm}) on the behavior of specimen with the same OCR showed the same effect as for normally

consolidated specimens, e.g., lower normalized stiffness with increasing value of σ'_{vm} . The overconsolidated specimens also exhibited significant strain softening, but generally less pronounced than at $OCR = 1$, which was again partially due to the device "unloading".

Thesis Co—Supervisor: Dr. John T. Germaine
Title: Lecturer in Civil Engineering

Thesis Co—Supervisor: Dr. Charles C. Ladd
Title: Professor of Civil Engineering

*to
Musarrat
Aisha
Saad
and
Hammad*

ACKNOWLEDGEMENTS

I am indebted to the Government of Pakistan for the generous financial support for my studies at MIT.

I wish to express my sincere thanks and profound sense of gratitude to Lieutenant General Syed Shujaat Hussain, H.I.(M), S.Bt., Engineer-in-Chief of the Pakistan Army, for his deep interest in my studies. It was through his personal efforts that I got the unique opportunity to study at MIT.

My sincere gratitude and heartfelt thanks to Professor Charles C. Ladd, my academic advisor and co-thesis supervisor, for his genuine concern, advice and enthusiastic encouragement through all the stages of my studies at MIT. During the thesis writing phase, he provided invaluable guidance and constructive criticism. I am personally indebted to him.

I am immensely grateful to Dr. John T. Germaine, my thesis co-supervisor, for providing me constant guidance and motivation during the course of this research. He also suggested me the topic upon which this thesis is based. It has been a great learning experience to complete the experimental phase of this research under his close supervision.

My thanks to all the friends and officemates I have had over the past years, who made my life at MIT a little less trying and a little more enjoyable. I especially extend my thanks to Tian Ho Seah for his eagerness to help, and also for providing soil samples for this research.

I am grateful to my family, especially my parents, for their encouragement, prayers and continuous guidance through all the stages of my life.

Finally, I greatly appreciate the patience and sacrifice of my wife and children throughout the course of my studies at MIT. To them this work is dedicated.

All Thanks and Praise be to God

TABLE OF CONTENTS

Abstract	3
Acknowledgements	6
Table of Contents	7
List of Tables	10
List of Figures	12
List of Symbols	20
1. INTRODUCTION	24
2. BACKGROUND	26
2.1 Normalized Soil Parameter Concept	26
2.2 Review of Existing Simple Shear Devices (reproduced from DeGroot, 1989; edited by Ladd, 1990)	29
2.3 State of Stresses in Direct Simple Shear Testing (abstracted from DeGroot, 1989)	30
2.3.1 Uniformity of Stress and Strain	30
2.3.2 State of Stress at Failure	33
2.4 Summary and Conclusions	37
3. DESCRIPTION OF EQUIPMENT AND EXPERIMENTAL PROCEDURES	56
3.1 Introduction	56
3.2 Description of Testing Apparatus	57
3.3 Experimental Procedures	61
4. TESTING MATERIAL AND LABORATORY TESTING PROGRAM	68
4.1 Preparation and Engineering Properties of Testing Material	68
4.1.1 Preparation of Resedimented Boston Blue Clay III.	68
4.1.2 Summary of Soil Properties	72
4.2 Laboratory Testing Program	74

5. CONSOLIDATION BEHAVIOR	90
5.1 Introduction	90
5.2 Presentation of Consolidation Results	91
5.3 Discussion on the Consolidation Behavior of BBC III	93
5.3.1 Preconsolidation Pressure	93
5.3.2 Compression Curves	93
5.3.3 Analysis of Discrepancy in DSS Compression Curves	95
5.3.4 Compression Ratio and Swelling Ratio	98
5.3.5 Rate of Secondary Compression	99
5.4 Summary and Conclusions	100
6. UNDRAINED SHEAR BEHAVIOR OF NORMALLY CONSOLIDATED BOSTON BLUE CLAY	119
6.1 Introduction	119
6.2 Results of CK_0 UDSS Tests on Normally Consolidated BBC	120
6.2.1 Presentation of Results	120
6.2.2 Discussion of the Normally Consolidated CK_0 UDSS Results	121
6.3 Comparison of CK_0 UDSS Tests with Published Data	124
6.4 Effect of Consolidation Stress Level on Normalized Behavior for DSS Tests on Normally Consolidated BBC	127
6.5 Summary and Conclusions	132
7. UNDRAINED SHEAR BEHAVIOR OF OVERCONSOLIDATED BBC	167
7.1 Introduction	167
7.2 Presentation and Discussion of Results from CK_0 UDSS Tests on Overconsolidated Boston Blue	168
7.3 Comparison with the Previous Research	174
7.4 Summary and Conclusions	176
8. SUMMARY, CONCLUSIONS AND RECOMMENDATIONS	211
8.1 Background	211
8.2 Consolidation Behavior	213
8.3 Normally Consolidated Undrained Shear Behavior	214
8.4 Overconsolidated Undrained Shear Behavior	216
8.5 Recommendations	218
9. REFERENCES	220
Appendix A. K_0-CONSOLIDATION RESULTS FROM GEONOR DSS	227
Appendix B. UNDRAINED SHEAR RESULTS FROM GEONOR DSS	224

Appendix C. CONSOLIDATION AT CONSTANT RATE OF STRAIN	304
C.1 Introduction	305
C.2 CRSC Testing Procedures	306
C.3 Presentation and Discussion of Test Results	307
C.3.1 Preconsolidation Pressure	308
C.3.2 Compression Curves	313
C.3.3 Coefficient of Permeability	314
C.4 Conclusions	317

LIST OF TABLES

Table 2.1: State of Stress in Geonor CK_0UDSS Tests on Normally Consolidated BBC Using Different Assumptions (after Ladd and Edgers, 1972; from DeGroot, 1990)	40
Table 4.1: Index Properties of Resedimented BBC III (from Seah, 1990)	77
Table 4.2: Results of Batch Consolidometer Tests for Resedimented BBC III (from Seah, 1990)	78
Table 4.3: Results of Oedometer Tests on Samples from Batches of BBC III (from Seah, 1990)	79
Tables 4.4: Unconsolidated–Undrained Triaxial Compression Tests on Resedimented BBC III (from Seah, 1990)	81
Table 4.5: Index Properties of the Different Batches of Resedimented BBC (after Fayad, 1986; from Seah, 1990)	82
Table 4.6: Comparison of Experimental Data Between the Resedimented Boston Blue Clay and Natural Boston Blue Clay (from Seah, 1990)	83
Table 4.7: Loading Programs of Constant Rate of Strain Testing	84
Table 4.8: Overview of CK_0UDSS Testing Program on Normally Consolidated Samples of BBC III.	85
Table 4.9: Summary of CK_0UDSS Tests Performed on Overconsolidated Samples of BBC III	86
Table 5.1: Consolidation Results of Geonor DSS Tests on Batch 204 of BBC III	102
Table 5.2: Consolidation Results of DSS Tests on Batch 205 of BBC III	103
Table 5.3: Consolidation Results of Geonor DSS Tests on Batch 207 of BBC III	104
Table 5.4: Results of Consolidation Tests on Samples from Batches of BBC III	105
Table 6.1: Summary of Geonor CK_0UDSS Tests on Normally Consolidated BBC III	136
Table 6.2: Results of Geonor CK_0UDSS Tests on Different Series of Normally Consolidated BBC	137
Table 6.3: Summary of Results from Geonor CK_0UDSS Tests on Normally Consolidated BBC	139
Table 6.4: Results from Geonor CK_0UDSS Tests at Various Stress Levels on Normally Consolidated BBC	140

Table 6.5: Comparison of Results with CK_0 UDSS Tests at Same σ'_{vc} on Normally Consolidated BBC	141
Table 7.1: Results from Geonor CK_0 UDSS Tests on Overconsolidated BBC III	180
Table 7.2: Results of CK_0 UDSS Tests on Overconsolidated BBC (from Ladd and Edgers, 1972)	181
Table 7.3: Comparison of Results from Geonor CK_0 UDSS Tests on Overconsolidated BBC III	182
Table 7.4: Comparison of m Values for CK_0 UDSS Tests on Overconsolidated BBC	183
Table A.1: Summary of Consolidation Results from CK_0 UDSS Tests on BBC III	228
Table C.1: Results of CRSC Tests on Boston Blue Clay III	319
Table C.2: Results of CRSC Tests on BBC III (after Walbaum, 1988)	320
Table C.3: Summary of Consolidation Results from CRS and Oedometer Tests on BBC III	321
Table C.4: Linear Regression Results for $e-k$ Relationship for Tests on BBC III	322

LIST OF FIGURES

- Figure 2.1:** Cross-Section of the SGI Simple Shear Apparatus (after Kjellman, 1951; from DeGroot, 1989) 41
- Figure 2.2:** Schematics of: (a) Cambridge University Direct Simple Shear Device; (b) NGI Direct Simple Shear Device (after Franke, et al. 1979; from DeGroot, 1989) 41
- Figure 2.3:** Cambridge University Mk7 Simple Shear Apparatus: (a) Cross-Section; (b) Arrangement of Load Transducers; (c) Typical Set of Forces Measured; (d) Stresses Deduced for Sample Core (after Budhu, 1985; from DeGroot, 1989) 42
- Figure 2.4:** Cambridge University Cylindrical Simple Shear Apparatus (CSSA); (a) Cross-Section; (b) Typical Set of Forces Measured (after Budhu, 1989; from DeGroot, 1989) 42
- Figure 2.5** Comparison of Ideal Set of Stresses Imposed to a Simple Shear Specimen Versus Stresses Which can Realistically be Imposed (from DeGroot, 1989) 43
- Figure 2.6:** Elastic Stresses in Cambridge Simple Shear Apparatus Computed by Roscoe (1953; from Ladd and Edgers, 1972) 44
- Figure 2.7:** Elastic Stresses in Geonor DSS Apparatus Computed by Luck et al. (1972; from DeGroot, 1989) 45
- Figure 2.8:** Stress Distribution on the Principal Third for a Constant Volume Test on Kaolin in the Cambridge CSSA: (a) Principal Third Load Cells; (b) Normal Stress; (c) Shear Stress ($\alpha =$ shear distortion γ_{yx} ; after Airey and Wood; from DeGroot, 1989) 46
- Figure 2.9:** Definition of Stresses and Angles for Initial and Failure States in the Direct Simple Shear Test (after Ladd and Edgers, 1972; from DeGroot, 1989) 47
- Figure 2.10:** Direct Simple Shear Failure Criterion I: Applied Stress System in Pure Shear (after Ladd and Edgers, 1972; from DeGroot, 1989) 48
- Figure 2.11:** Direct Simple Shear Failure Criterion II: Horizontal Plane is Failure Plane (from DeGroot, 1989) 49
- Figure 2.12:** Stress Ratio on Horizontal Plane in Central Third, Average Void Ratio Change for Whole Sample and Inclination to Horizontal of Major Principal Planes of Stress (ψ), Stress Increment (\mathcal{N}), Strain Increment (ζ), as well as Planes of Maximum Shear Stress (β) and Maximum Obliquity (ω) for Drained Tests in the Cambridge DSS on: (a) Medium Loose Sand ($e_o = 0.68$); (b) Dense Sand ($e_o = 0.53$); after Roscoe, et al. 1985; from DeGroot, 1989) 50

Figure 2.13: Rupture Observer in Radiograph of Simple Shear Test on Kaolin (sketches of radiographs of threads of lead paste; after Airey, et al. 1985; from DeGroot, 1989)	50
Figure 2.14: Direct Simple Shear Failure Criterion III: Horizontal Plane is Plane of Maximum Shear Stress (from DeGroot, 1989)	51
Figure 2.15: Direct Simple Shear Failure Criterion IV: Assume Mohr–Coulomb Failure Envelope (from DeGroot, 1989)	52
Figure 2.16: Direct Simple Shear Failure Criterion V: Failure Occurs on Vertical Planes (from DeGroot, 1989)	53
Figure 2.17: Direct Simple Shear Criterion VI: Linear Relationship Between τ_h/σ'_v and $\kappa \tan \delta$ (from DeGroot, 1989)	54
Figure 2.18: Direct Simple Shear Failure Criterion VII: Coincidence of Principal Axis of Strain Increment and Stress (from DeGroot, 1989)	55
Figure 3.1: Geonor Model 4 Direct Simple Shear Device (Geonor DSS Manual)	63
Figure 3.2: Sample Assembly of Geonor Model 4 Direct Simple Shear Apparatus (Geonor DSS Manual)	64
Figure 3.3: Schematic Diagram of the Modified Geonor Model 4 DSS Apparatus	65
Figure 3.4: Location of Constant Height DCDT in the Geonor DSS Apparatus (from DeGroot, 1989)	66
Figure 3.5: Schematic of Geonor Constant Height Servo Control System (from DeGroot, 1989)	67
Figure 4.1: Location of the Site from where Boston Blue Clay III was collected (from Seah, 1990).	87
Figure 4.2: Schematic of General Layout (from Seah, 1990).	88
Figure 4.3: Compression Curves (ϵ_v versus $\log \sigma'_{vc}$) from Oedometer Tests on Batch 204, 205 and 207 of BBC III (after Seah, 1990).	89
Figure 5.1: Definition of Swelling Ratio (SR).	106
Figure 5.2: Compression Curves (ϵ_v versus $\log \sigma'_{vc}$) from DSS Tests on Batch 204.	107
Figure 5.3: Compression Curves (ϵ_v versus $\log \sigma'_{vc}$) from DSS Tests on Batch 205.	108
Figure 5.4: Compression Curves (ϵ_v versus $\log \sigma'_{vc}$) from DSS Tests on Batch 207.	109

Figure 5.5: Compression Curves (ϵ_v versus $\log \sigma'_{vc}$) from DSS Tests on BBC III.	110
Figure 5.6: Compression Curves (ϵ_v versus $\log \sigma'_{vc}$) from DSS Tests on Batches 204 and 207 (from Werner, 1990).	111
Figure 5.7: Compression Curves (ϵ_v versus $\log \sigma'_{vc}$) from Oedometer Tests on Batches 204, 205, and 207 (from Seah, 1990).	112
Figure 5.8: Comparison of Compression Curves (ϵ_v versus $\log \sigma'_{vc}$) from Tests on Batch 204 (Results from DSS and Oedometer Tests).	113
Figure 5.9: Comparison of Compression Curves (ϵ_v versus $\log \sigma'_{vc}$) from Tests on Batch 205 (Results from DSS and Oedometer Tests).	114
Figure 5.10: Comparison of Compression Curves (ϵ_v versus $\log \sigma'_{vc}$) from Tests on Batch 207 (Results from DSS and Oedometer Tests).	115
Figure 5.11: Comparison of Compression Curves (ϵ_v versus $\log \sigma'_{vc}$) from tests on Batches 204, 205, and 207 of BBC III.	116
Figure 5.12: Comparison of Compression Curves (ϵ_v versus $\log \sigma'_{vc}$) from All the DSS, Oedometer, and CRSC tests on Batches 204, 205, and 207 of BBC III.	117
Figure 5.13: Typical Compression Curve for BBC III in the DSS Test.	118
Figure 6.1: Normalized Stress Paths from CK_0 UDSS Tests on Normally Consolidated Boston Blue Clay.	142
Figure 6.2: Normalized Shear Stress Versus Shear Strain from CK_0 UDSS Tests on Normally Consolidated Boston Blue Clay.	143
Figure 6.3: Applied Shear Stress Ratio Versus Shear Strain from CK_0 UDSS Tests on Normally Consolidated Boston Blue Clay.	144
Figure 6.4: Normalized Pore Pressure Versus Shear Strain from CK_0 UDSS Tests on Normally Consolidated Boston Blue Clay.	145
Figure 6.5: Vertical Strain Versus Shear Strain from CK_0 UDSS Tests on Normally Consolidated Boston Blue Clay.	146
Figure 6.6: Normalized Undrained Young's Modulus Versus Applied Shear Stress Ratio from CK_0 UDSS Tests on Normally Consolidated Boston Blue Clay.	147
Figure 6.7: Normalized Stress Paths from CK_0 UDSS Tests on Normally Consolidated Boston Blue Clay (From DeGroot, 1989).	148
Figure 6.8: Normalized Shear Stress Versus Shear Strain from CK_0 UDSS Tests on Normally Consolidated BBC (From DeGroot, 1989).	149
Figure 6.9: Applied Shear Stress Ratio Versus Shear Strain from CK_0 UDSS Tests on Normally Consolidated BBC (From DeGroot, 1989).	150

Figure 6.10: Normalized Pore Pressure Versus Shear Strain from CK_0 UDSS Tests on Normally Consolidated BBC (From DeGroot, 1989).	151
Figure 6.11: Normalized Undrained Young's Modulus Versus Applied Shear Stress Ratio from CK_0 UDSS Tests on Normally Consolidated BBC (From DeGroot, 1989).	152
Figure 6.12: Stress Paths for CK_0 UDSS Tests on Normally Consolidated BBC.	153
Figure 6.13: Normalized Shear Stress Versus Shear Strain for CK_0 UDSS Tests on Normally Consolidated BBC.	154
Figure 6.14: Applied Shear Stress Ratio Versus Shear Strain for CK_0 UDSS Tests on Normally Consolidated BBC.	155
Figure 6.15: Pore Pressure Versus Shear Strain for CK_0 UDSS Tests on Normally Consolidated BBC.	156
Figure 6.16: Young's Modulus Versus Applied Shear Stress Ratio for CK_0 UDSS Tests on Normally Consolidated BBC.	157
Figure 6.17: Young's Modulus (E_u/σ'_{vc}) versus Shear Strain (γ) for CK_0 UDSS Tests on Normally Consolidated BBC (Tests by Author and DeGroot, 1989).	158
Figure 6.18: Maximum Normalized Shear Stress Versus Vertical Consolidation Stress for CK_0 UDSS Tests on Normally Consolidated BBC (Data from Tables 6.1 and 6.2).	159
Figure 6.19: Shear Strain at Peak Shear Strength Versus Vertical Consolidation Stress for CK_0 UDSS Tests on Normally Consolidated BBC (Data from Tables 6.1 and 6.2).	160
Figure 6.20: Normalized Vertical Effective Stress at Peak Strength Versus Consolidation Stress for CK_0 UDSS Tests on Normally Consolidated BBC (Data from Tables 6.1 and 6.2).	161
Figure 6.21: Normalized Pore Pressure at Peak Strength Versus Shear Strain at Failure for CK_0 UDSS Tests on Normally Consolidated BBC (Data from Tables 6.1 and 6.2).	162
Figure 6.22: Angle ψ at Peak Shear Stress Versus Consolidation Stress for CK_0 UDSS Tests on Normally Consolidated BBC (Data from Tables 6.1 and 6.2).	163
Figure 6.23: Angle ψ at Peak Shear Stress Versus Shear Strain at Failure for CK_0 UDSS Tests on Normally Consolidated BBC (Data from Tables 6.1 and 6.2)	164
Figure 6.24: Normalized Undrained Young's Modulus Versus Vertical Consolidation Stress for CK_0 UDSS Tests on Normally Consolidated BBC (Data from Tables 6.1 and 6.2).	165

Figure 6.25: Young's Modulus (E_u/σ'_{vc}) Versus Vertical Consolidation Stress for CK_oUDSS Tests on Normally Consolidated BBC (Data from Tables 6.1 and 6.2).	166
Figure 7.1: Normalized Stress Paths from CK_oUDSS Tests on Overconsolidated Boston Blue Clay.	184
Figure 7.2: Normalized Shear Stress Versus Shear Strain from CK_oUDSS Tests on Overconsolidated Boston Blue Clay.	185
Figure 7.3: Applied Shear Stress Ratio Versus Shear Strain from CK_oUDSS Tests on Overconsolidated Boston Blue Clay.	186
Figure 7.4: Normalized Pore Pressure Versus Shear Strain from CK_oUDSS Tests on Overconsolidated Boston Blue Clay.	187
Figure 7.5: Vertical Strain Versus Shear Strain from CK_oUDSS Tests on Overconsolidated Boston Blue Clay.	188
Figure 7.6: Normalized Undrained Young's Modulus Versus Applied Shear Stress Ratio from CK_oUDSS Tests on Overconsolidated Boston Blue Clay.	189
Figure 7.7: Normalized Undrained Young's Modulus (E_u/σ'_{vc}) Versus Shear Strain from CK_oUDSS Tests on Overconsolidated Boston Blue Clay.	190
Figure 7.8: Normalized Young's Modulus Versus OCR from CK_oUDSS Tests on Overconsolidated Boston Blue Clay.	191
Figure 7.9: Undrained Shear Strength Ratio Versus OCR from CK_oUDSS Test on Overconsolidated Boston Blue Clay.	192
Figure 7.10: Comparison of Stress Paths from CK_oUDSS Tests on BBC at the Same OCR with Different σ'_{vm}.	193
Figure 7.11: Normalized Shear Stress Versus Shear Strain from CK_oUDSS Tests at the Same OCR with Different σ'_{vm}.	194
Figure 7.12: Normalized Pore Pressure Versus Shear Strain from CK_oUDSS Tests at the Same OCR with σ'_{vm}.	195
Figure 7.13: Normalized Undrained Young's Modulus Versus Applied Shear Stress Ratio from CK_oUDSS Tests on BBC at the Same OCR with Different σ'_{vm}.	196
Figure 7.14: Normalized Stress Paths from CK_oUDSS Tests on Overconsolidated Boston Blue Clay (from Ladd and Edgers, 1972).	197
Figure 7.15: Normalized Shear Stress Versus Shear Strain from CK_oUDSS Tests on Overconsolidated Boston Blue Clay (from Ladd and Edgers, 1972).	198

Figure 7.16: Applied Shear Stress Ratio Versus Shear Strain from CK₀UDSS Tests on Overconsolidated Boston Blue Clay (from Ladd and Edgers, 1972).	199
Figure 7.17: Normalized Pore Pressure Versus Shear Strain from CK₀UDSS Tests on Overconsolidated Boston Blue Clay (from Ladd and Edgers, 1972).	200
Figure 7.18: Normalized Undrained Young's Modulus Versus Applied Shear Stress Ratio from CK₀UDSS Tests on Overconsolidated Boston Blue Clay (from Ladd and Edgers, 1972).	201
Figure 7.19: Normalized Undrained Young's Modulus (E_u/σ'_{vc}) Versus Shear Strain from CK₀UDSS Tests on Overconsolidated Boston Blue Clay (from Ladd and Edgers, 1972).	202
Figure 7.20: Normalized Stress Paths from CK₀UDSS Tests on Overconsolidated Boston Blue Clay (Curves from Figures 7.1 and 7.14).	203
Figure 7.21: Normalized Shear Stress Versus Shear Strain from CK₀UDSS Tests on Overconsolidated Boston Blue Clay (Curves from Figures 7.2 and 7.15).	204
Figure 7.22: Applied Shear Stress Ratio Versus Shear Strain from CK₀UDSS Tests on Overconsolidated Boston Blue Clay (Curves from Figures 7.3 and 7.16).	205
Figure 7.23: Normalized Pore Pressure Versus Shear Strain from CK₀UDSS Tests on Overconsolidated Boston Blue Clay (Curves from Figures 7.4 and 7.17).	206
Figure 7.24: Normalized Undrained Young's Modulus Versus Applied Shear Stress Ratio from CK₀UDSS Tests on Overconsolidated Boston Blue Clay (Curves from Figures 7.6 and 7.18).	207
Figure 7.25: Normalized Undrained Young's Modulus (E_u/σ'_{vc}) Versus Shear Strain from CK₀UDSS Tests on Overconsolidated Boston Blue Clay (Curves from Figures 7.7 and 7.19).	208
Figure 7.26: Normalized Young's Modulus Versus OCR from CK₀UDSS Tests on Overconsolidated Boston Blue Clay (Tests by Author and from Ladd and Edgers, 1972).	209
Figure 7.27: Normalized Undrained Shear Strength Ration Versus OCR from CK₀UDSS Tests on Boston Blue Clay (Results from Tables 7.1 and 7.2)	210
Figure A.1: Compression Curve (ϵ_v versus $\log \sigma'_{vc}$) from DSS Test 14.	232
Figure A.2: Compression Curve (ϵ_v versus $\log \sigma'_{vc}$) from DSS Test 18.	233
Figure A.3: Compression Curve (ϵ_v versus $\log \sigma'_{vc}$) from DSS Test 22.	234
Figure A.4: Compression Curve (ϵ_v versus $\log \sigma'_{vc}$) from DSS Test 25.	235
Figure A.5: Compression Curve (ϵ_v versus $\log \sigma'_{vc}$) from DSS Test 31.	236

Figure A.6: Compression Curve (ϵ_v versus $\log \sigma'_{vc}$) from DSS Test 37.	237
Figure A.7: Compression Curve (ϵ_v versus $\log \sigma'_{vc}$) from DSS Test 40.	238
Figure A.8: Compression Curve (ϵ_v versus $\log \sigma'_{vc}$) from DSS Test 44.	239
Figure A.9: Compression Curve (ϵ_v versus $\log \sigma'_{vc}$) from DSS Test 48.	240
Figure A.10: Compression Curve (ϵ_v versus $\log \sigma'_{vc}$) from DSS Test 50.	241
Figure A.11: Compression Curve (ϵ_v versus $\log \sigma'_{vc}$) from DSS Test 51.	242
Figure A.12: Typical Settlement–Time Curve of a Consolidation Increment in the DSS.	243
Figure C.1: Schematic of MIT General Purpose Consolidometer (from Wissa and Heiberg, 1969).	323
Figure C.2: Compression Curve (ϵ_v Vs. $\log \sigma'_{vc}$) from CRSC TEST No. 1.	324
Figure C.3: Compression Curve (ϵ_v Vs. $\log \sigma'_{vc}$) from CRSC TEST No. 2.	325
Figure C.4: Compression Curve (ϵ_v Vs. $\log \sigma'_{vc}$) from CRSC TEST No. 3.	326
Figure C.5: Compression Curve (ϵ_v Vs. $\log \sigma'_{vc}$) from CRSC TEST No. 8.	327
Figure C.6: Comparison of Compression Curves (ϵ_v Vs. $\log \sigma'_{vc}$) from All CRS Tests.	329
Figure C.7: Comparison of Compression Curves (ϵ_v Vs. $\log \sigma'_{vc}$) from CRS and Oedometer Tests.	330
Figure C.8: Plot of Constrained Modulus (D) Vs. Vertical Effective Stress (σ'_{vc}) for CRSC Test No. 1.	331
Figure C.9: Plot of Constrained Modulus (D) Vs. Vertical Effective Stress (σ'_{vc}) for CRSC Test No. 2.	332
Figure C.10: Plot of Constrained Modulus (D) Vs. Vertical Effective Stress (σ'_{vc}) for CRSC Test No. 3.	333
Figure C.11: Plot of Constrained Modulus (D) Vs. Vertical Effective Stress (σ'_{vc}) for CRSC Test No. 8.	334
Figure C.12: Compression Curve (e Vs. $\log \sigma'_{vc}$) from CRSC TEST No. 1.	335
Figure C.13: Compression Curve (e Vs. $\log \sigma'_{vc}$) from CRSC TEST No. 2.	336
Figure C.14: Compression Curve (e Vs. $\log \sigma'_{vc}$) from CRSC TEST No. 3.	337
Figure C.15: Compression Curve (e Vs. $\log \sigma'_{vc}$) from CRSC TEST No. 8.	338
Figure C.16: Comparison of Compression Curves (e Vs. $\log \sigma'_{vc}$) from All the CRS Tests.	339

Figure C.17: Graph of Void Ratio (e) Vs. Logarithm of Coefficient of Permeability (k) for CRSC Test No. 1.	340
Figure C.18: Graph of Void Ratio (e) Vs. Logarithm of Coefficient of Permeability (k) for CRSC Test No. 2.	341
Figure C.19: Graph of Void Ratio (e) Vs. Logarithm of Coefficient of Permeability (k) for CRSC Test No. 3.	342
Figure C.20: Graph of Void Ratio (e) Vs. Logarithm of Coefficient of Permeability (k) for CRSC Test No. 8.	343
Figure C.21: Graph of Void Ratio (e) Vs. Logarithm of Coefficient of Permeability (k) for All the CRS Tests.	344
Figure C.22: Graph of Logarithm of Void Ratio (e) Vs. Logarithm of Coefficient of Permeability (k) for CRSC Test No. 1.	345
Figure C.23: Graph of Logarithm of Void Ratio (e) Vs. Logarithm of Coefficient of Permeability (k) for CRSC Test No. 2.	346
Figure C.24: Graph of Logarithm of Void Ratio (e) Vs. Logarithm of Coefficient of Permeability (k) for CRSC Test No. 3.	347
Figure C.25: Graph of Logarithm of Void Ratio (e) Vs. Logarithm of Coefficient of Permeability (k) for CRSC Test No. 8.	348
Figure C.26: Graph of Logarithm of Void Ratio (e) Vs. Logarithm of Coefficient Permeability (k) for All the CRS Tests.	349
Figure C.27: Plot of Normalized Excess Pore Pressure (u_b/σ'_v) versus Vertical Effective Stress (σ'_v) for CRSC Test No. 1.	350
Figure C.28: Plot of Normalized Excess Pore Pressure (u_b/σ'_v) versus Vertical Effective Stress (σ'_v) for CRSC Test No. 2.	351
Figure C.29: Plot of Normalized Excess Pore Pressure (u_b/σ'_v) versus Vertical Effective Stress (σ'_v) for CRSC Test No. 3.	352
Figure C.30: Plot of Normalized Excess Pore Pressure (u_b/σ'_v) versus Vertical Effective Stress (σ'_v) for CRSC Test No. 8.	353
Figure C.31: Graph of Permeability Change Index, C_k , Versus Void Ratio, e_0 , for All Clays Tested (after Tavenas et al., 1983).	354
Figure C.32: Graph of Permeability Change Index, C_k , Versus Void Ratio, e_0 , for BBC III.	355

LIST OF SYMBOLS

Note:

1. Prefix Δ indicates a change.
2. Suffix f indicates a final or failure condition.
3. A superscript prime on a stress indicates an effective stress.
4. A superscript prime on a property indicates value in terms of effective stress.

GENERAL

BBC	Boston Blue Clay
COV	Coefficient of variation = SD/Mean
DCDT	Direct current displacement transducer
n,r	Linear regression parameters; n = number of observations; r = correlation coefficient
SD	Standard deviation

INDEX AND CLASSIFICATION PROPERTIES

e	Void ratio
e ₀	Initial void ratio
G	Specific Gravity
I _l	Liquidity index
I _p	Plasticity index
LL	Liquidity limit
PL	Plastic Limit
S	Degree of saturation
w	Water content
w _l	Liquid limit
w _p	Plastic limit

STRESSES, STRAINS, MODULI AND STRENGTH PARAMETERS

c_u	Undrained shear strength from DSS ($= \tau_{hmax}$)
E	Young's modulus
E_u	Undrained secant E
$E_u(50)$	E_u fifty percent to failure
G	Shear modulus
K_o	Coefficient of earth pressure at rest
m, n	OCR exponents
OCR	Overconsolidation ratio $= \sigma'_p / \sigma'_{vc}, \sigma'_p / \sigma'_{vm}$
p'	$0.5(\sigma'_v + \sigma'_h)$
q	$0.5(\sigma_v - \sigma_h)$ or $(\sigma_1 - \sigma_2)$
q_f	q at failure
S	Normally consolidated undrained strength ratio
NSP	Normalized Soil Parameter
SHANSEP	Stress History And Normalized Soil Engineering Properties
t_c	Consolidation time under last increment
t_f	Time to failure
t_s	Storage time
u	Pore water pressure
u_b	Pore water pressure at the base of specimen
ϵ_{vol}	Volumetric strain
$\epsilon_1, \epsilon_2, \epsilon_3$	Principal strains
δ	Angle between σ_{1f} and vertical direction
γ	Shear strain
σ, σ'	Normal total stress, normal effective stress
$\sigma_1, \sigma_2, \sigma_3$	Principal stresses

$\sigma_{ff}, \sigma'_{ff}$	Normal stress on failure plane at failure
σ_v	Vertical normal stress
σ_h	Horizontal normal stress
σ_r	Radial normal stress
τ	Shear stress
τ_{ff}	τ on failure plane at failure
ϕ, ϕ'	Slope of Mohr–Coulomb failure envelope
θ_f	Orientation of the failure plane relative to the horizontal
θ_p	Orientation of the major principal stress relative to the horizontal
ψ	Arctan (τ_h/σ'_v) for direct simple shear tests.
ν	Poisson's ratio

CONSOLIDATION PARAMETERS

a_v	Coefficient of Compressibility = $\Delta e/\Delta \sigma_v$
c_v	Coefficient of consolidation for vertical flow
C_c	Virgin compression index
C_k	Permeability change index = $\Delta e/\Delta \log k$
C_r	Recompression index
C_s	Swelling index
C_α	Rate of secondary compression = $\Delta \epsilon_v/\Delta \log t$
CR	Virgin compression ratio = $\Delta \epsilon_v/\Delta \log \sigma'_{vc}$
k	Permeability
m_v	Coefficient of volume change = $\Delta \epsilon_v/\Delta \sigma_v$
RR	Recompression Ratio
SR	Swelling Ratio
t	Time

t_p, t_{100}	t required for primary consolidation
ϵ_v	Vertical Strain
σ'_{vc}	Vertical consolidation stress
σ'_{vo}	Initial vertical effective stress
σ'_p	Preconsolidation pressure
σ'_{vm}	Maximum Past Pressure

CONSOLIDATION AND STRENGTH TESTS

CAU	Anisotropically consolidated–undrained shear test
CAUDSS	CAU direct simple shear test
CIUC	Isotropically consolidated–undrained triaxial compression test
CK ₀ U	K ₀ consolidated–undrained shear test
CK ₀ UC	CK ₀ U triaxial compression test
CK ₀ UDSS	CK ₀ U direct simple shear test
CRSC	Constant rate of strain consolidation test
DSS	Direct simple shear
PCE	Plane strain compression test
PSE	Plane strain extension test
TC	Triaxial compression
TE	Triaxial extension
UU	Unconsolidated–undrained shear test
UUC	UU triaxial compression test

CHAPTER 1

INTRODUCTION

The objective of this research is to investigate the normalized undrained strength and stress–strain behavior of resedimented Boston Blue Clay (BBC) using Geonor Direct Simple Shear (DSS) apparatus. This is achieved by conducting a number of K_o –consolidated–undrained Direct Simple Shear (CK_oUDSS) tests on specimens of normally consolidated BBC at different consolidation stress levels and also on specimens rebounded to varying overconsolidation ratios (OCR's). The results are then expressed in terms of Normalized Soil Parameters (NSP) to evaluate the normalized behavior of normally consolidated and overconsolidated Boston Blue Clay. Additionally, a number of constant rate of strain consolidation (CRSC) tests were performed to obtain well defined compression curves for comparison with the data from the consolidation phase of CK_oUDSS tests.

Chapter 2 describes the NSP concept along with an outline of the SHANSEP (an acronym for Stress History And Normalized Soil Engineering Properties) design method and laboratory testing technique (Ladd and Foott, 1974). It also contains a review of simple shear devices and the state of stress in DSS testing, with emphasis on the Geonor type DSS apparatus.

The tests for this research were conducted in MIT's Geonor Model 4 Direct Simple Shear apparatus using the SHANSEP reconsolidation technique. Chapter 3 contains a description of the testing equipment and summarizes the experimental procedures.

Chapter 4 gives a summary of batching procedures and properties of resedimented BBC. The chapter also contains an outline of the laboratory testing program.

The data from the consolidation phase of the CK_oUDSS tests are presented and

analyzed in Chapter 5. The chapter compares the Geonor DSS consolidation results with data from incremental oedometer and constant rate of strain consolidation tests on resedimented BBC III and draws relevant conclusions based on comparison and analyses.

Chapter 6 presents and analyzes the results of CK_o UDSS tests on normally consolidated specimens of BBC. The chapter summarizes the available data from SHANSEP type undrained shear tests performed in the Geonor DSS on normally consolidated specimens of BBC and subsequently compares data from the writer's tests with the prior data. The chapter then discusses the undrained shear behavior of normally consolidated resedimented BBC in the Geonor DSS and summarizes the salient conclusions.

Chapter 7 presents and discusses the results of CK_o UDSS tests on overconsolidated specimens of BBC. The chapter compares the data from the author's tests with those from previous research and finally summarizes the relevant conclusions pertaining to undrained shear behavior of overconsolidated resedimented BBC in the Geonor DSS.

Chapter 8 summarizes the main conclusions of the experimental study and provides recommendations for further research. Chapter 9 gives a list of references. Three Appendices are attached. Appendix A contains the tabulated stress-strain data and compression curves from the individual tests for the consolidation phase of the DSS testing. Appendix B presents the tabulated undrained shear experimental data from the individual CK_o UDSS tests on resedimented BBC. Appendix C describes consolidation at constant rate of strain. The Appendix contains an outline of the CRSC testing procedures, presents and analyzes the CRSC test results and finally provides a summary of important conclusions from the experimental study. The tabulated data from each CRSC test are also contained in Appendix C.

CHAPTER 2

BACKGROUND

2.1 Normalized Soil Parameter Concept

The Normalized Soil Parameter (NSP) concept is based on the empirical observation that the results of laboratory test on clay samples having the same overconsolidation ratio (OCR), but different consolidation stresses (σ'_{vc}) and therefore different maximum past (or preconsolidation) pressures (σ'_{vm} or σ'_p), exhibit similar properties (i.e., strength, stress-strain, pore pressure parameters, moduli, etc) when normalized with respect to the consolidation stress (Ladd and Foott, 1974). The concept has significant practical value for it provides a very convenient format for presenting and evaluating clay behavioral characteristics. This concept will be described in some detail in the succeeding paragraphs since the intent of this research is to evaluate the normalized behavior of resedimented Boston Blue Clay (BBC)—a test soil (see Chapter 4) being widely used at MIT for understanding the behavior of typical cohesive soils.

The normalized method of plotting the data has been extensively used at MIT during the past two decades and it has been found that many cohesive soils exhibit normalized behavior. Ladd and Foott (1974) compared undrained strength data for five cohesive soils tested in the Geonor DSS and found that the soils exhibit very similar trends with increasing OCR, even though the index properties of the five soils covered a wide range of values. Cohesive soils are also found to exhibit normalized behavior in the other types of shear tests (e.g., Ladd and Foott, 1980).

The NSP concept has significance beyond being a convenient way of presenting test results, since it provides a very useful framework for comparing and relating the behavioral characteristics of different cohesive soils. The concept has led to the development of a very valuable design method, called SHANSEP (an acronym for

Stress History And Normalized Soil Engineering Properties), to evaluate the in-situ strength and stress-strain properties for stability analyses (Ladd and Foott, 1974). The method, though based on empirical observations of normalized behavior, has become adopted by many in engineering practice over the past decade or so because of its successful practical application on a variety of different soils. This design method encompasses the following major steps for a thorough and reliable evaluation of design parameters (from Jamiolkowski et al. 1985):

- Establish the stress history, i.e., the profile of σ'_{v0} and σ'_p , which determines the range of OCR values for which data are required.
- Perform a series of CK_0U shear tests, with representative modes of failure, on specimens consolidated beyond the in situ preconsolidation pressures (to σ'_{vc} greater than 1.5 to 2 times the σ'_p) to measure the behavior of normally consolidated clay and also on specimens rebounded to varying OCR to measure overconsolidated behavior.
- Express the results in terms of NSP and establish NSP versus OCR relationships, i.e., c_u/σ'_{vc} versus OCR (the resulting relationship can be expressed as, $c_u/\sigma'_{vc} = S (\text{OCR})^m$; where, $S = c_u/\sigma'_{vc}$ for normally consolidated soil)
- Use these NSP relationships and the stress history information to compute profile of c_u , etc.

Ladd and Foott (1974) suggested a laboratory testing technique to yield NSP values which requires that the sample be K_0 -consolidated back onto the virgin compression line before testing (step 2 above), primarily to reduce the adverse effects of the sample disturbance. They also recommended to standardize the effects of the secondary compression, the last consolidation increment should be left on the sample

for about one log cycle of secondary compression prior to undrained shear. They suggested that a shear strain rate of 5 % per hour is appropriate for CK_0 UDSS tests.

Critics of SHANSEP (Mesri, 1975; Tavenas and Leroueil, 1977, 1980) argue that consolidating the sample well beyond the in situ stresses will destroy some important aspects of soil structure that have been developed during and after clay deposition. Ladd and Foott (1974, 1980) agree that this argument is valid with "highly structured" and naturally cemented deposits and hence the SHANSEP reconsolidation method is not recommended with such soils. However, they state that with more ordinary clays (e.g., I_1 typically less than unity), the real question from a practical point of view is the degree to which the SHANSEP reconsolidation procedure will provide reasonable estimates of in-situ properties, specially when compared with other available techniques commonly used in practice. Ladd (1988, 1990) recommends that the method should be applied to tube samples of soils with moderate to low OCR's having low I_1 (≤ 1) and especially for all truly normally consolidated soils.

In view of the preceding discussion, it is evident that the normalized parameter concept provides a powerful tool for evaluating and synthesizing experimental data. The SHANSEP method also has established its credibility because of its successful use for designs involving a variety of different soils and has been further refined over the past years. However, the method is expensive and is applicable only to those soils which exhibit reasonable normalized behavior (i.e., yield reasonably constant c_u/σ'_{vc} at different consolidation stress levels for normally consolidated soils and result in a consistent curve for CK_0 UDSS test data of c_u/σ'_{vc} versus logarithm of OCR plot in case of overconsolidated samples independent of preconsolidation pressure). It is found (Ladd et al. 1977) that normalized behavior applies only to those cohesive soils which maintain their same basic structure during loading beyond the in situ stresses and into the virgin compression range. These soils generally have a reasonably constant virgin compression index. Soils such as quick clays and naturally cemented soils do not

exhibit normalized behavior since their structure is drastically altered when loaded beyond their "apparent" preconsolidation pressure (e.g., Koutsoftas and Ladd, 1984).

2.2 Review of Existing Simple Shear Devices (reproduced from DeGroot, 1989; edited by Ladd, 1990)

The first direct simple shear apparatus capable of uniformly deforming a soil specimen was built in 1936 at the Royal Swedish Geotechnical Institute (SGI; Kjellman, 1951). The SGI apparatus used a circular soil specimen (6 cm diameter by 2 cm height) which is placed between a lower and upper grooved plate (Figure 2.1). The specimen is confined laterally by a rubber membrane and a series of stacked aluminum rings. The ring spacing is small enough to allow vertical compression of the sample while minimizing lateral expansion of the membrane. Dead weights are used to apply both the vertical stress and horizontal shear stress to the sample. The sample is sheared under stress controlled conditions.

In the early 1960's, the Norwegian Geotechnical Institute (NGI) developed a direct simple shear device based on the SGI apparatus (Bjerrum and Landva, 1966). The new device was designed to K_0 -consolidate undisturbed sensitive clay specimens and to allow the specimens to strain in simple shear. These conditions are satisfied by confining a circular specimen (8 cm diameter by 1 cm height) within a wire reinforced rubber membrane which allows the sample to deform vertically and horizontally with minimal changes in diameter (Figure 2.2b). A special trimming apparatus was also developed so that soft sensitive clay could be prepared with minimum disturbance. Constant volume tests are run by varying the normal stress acting on a sample via a screw-controlled loading system. This device is sold commercially by Geonor as the Direct Simple Shear (DSS) apparatus (From here on the NGI type DSS will be referred to as the Geonor direct simple shear device or the Geonor DSS). MIT currently uses the Geonor Model 4 DSS which is described in more detail in Chapter 3.

In 1953, Cambridge University developed a simple shear apparatus which can impose simple shear strain to a rectangular (6 cm square by 2 cm high) sand specimen while also permitting the measurement of volume changes during shear (Roscoe, 1953). The apparatus deforms an initially cuboidal sample into a parallelepiped shape by allowing two initially vertical sides of the box containing the sample to rotate as the top or bottom faces displace horizontally (Figure 2.2a). Since 1953, seven versions of the Cambridge simple shear device have been developed (MK1 to MK7). The newer models have been elaborately instrumented to measure normal and shear forces along the faces of the sample and are also capable of testing cohesive soils (Figure 2.3). Cambridge has also developed a fully instrumented circular simple shear apparatus (Figure 2.4).

Since the late 1960's, many other types of direct simple shear devices have been developed. Several were primarily built to conduct cyclic tests on soil samples, including those described by Peacock and Seed (1968), Finn et al. (1971) and Hara and Kiyota (1977), Ansell and Brown (1978), Sidney et al. (1978) and Idriss et al. (1980). Several other devices are equipped with pressure chambers as described by Franke et al. (1979), Silver, et al. (1980) and Tatsuoka and Silver (1981).

2.3 State of Stresses in Direct Simple Shear Testing (abstracted from DeGroot, 1989)

2.3.1 Uniformity of Stress and Strain

The direct simple shear apparatus was developed to provide a soil testing device which can evaluate the stress strain behavior of soils under simple shear strain conditions. It enables soil specimens to be tested wherein the major principal stress axis rotates during shear while the sample is kept under a condition of plane strain. Since its inception the direct simple shear apparatus has been known to be unable to impose uniform normal and shear stresses to a test specimen. This problem mainly

arises from the fact that existing simple shear devices can not impose complementary shear forces to the vertical sides of specimen (Figure 2.5).

Many studies have been conducted to predict the state of stress within a soil sample tested in a simple shear device. The succeeding paragraphs present a summary of important theoretical and experimental studies for drawing relevant conclusions subsequently.

Roscoe (1953) conducted a mathematical analysis of the rectangular Cambridge apparatus for an elastic material. The results show (Figure 2.6) that the application of a shear force to the top and bottom faces is counterbalanced by a couple due to normal stresses acting on the sample sides. The development of the counteracting couple on the faces causes tension zones to develop at the upper leading edge and the lower trailing edge. However, these tension zones can be overcome if a normal force, equivalent or greater than the shear force, is applied to the sample. The results also show that the shear stress on the sample faces is approximately uniform across only the middle third of each face.

Duncan and Dunlop (1969) also analyzed the Cambridge apparatus and reported that, for horizontal equilibrium, the shear stress increases from the top and bottom towards the middle, reaching a maximum value at the middle height. For Roscoe's analysis the difference between the average values of shear stress at the top and at the middle height is equal to 7 %, whereas for the nonlinear finite element analysis the difference ranges from 4% to 8%.

Lucks et al. (1972) used a three dimensional finite element method with linear elastic isotropic material properties and with the assumption of infinitesimal strains to study the stress conditions in the circular Geonor DSS. Their results (Figure 2.7) indicate that local stress concentrations occur at the edges of an elastic material in the device. However, overall 70% of the sample has a uniform stress condition and the horizontal shear stress acting at the middle height of the sample is uniform over the

central 80% of the sample. Finally they concluded that it is reasonable to assume that the test is measuring the horizontal shear stress and that progressive yielding is of minimum importance unless the soil is significantly strain softening.

Shen et al. (1978) conducted a parametric study of the Geonor DSS using a three dimensional elastic finite element analysis of a nonaxisymmetrically loaded axisymmetric solid. The cases investigated used different combinations of material properties, membrane stiffness, specimen geometry and boundary displacements. The study concluded that the uniformity of the shear stress—strain distribution in the sample improves as the:

- specimen height—diameter ratio decreases;
- percent of wire reinforcement increases;
- elastic modulus of the soil decreases;
- Poisson's ratio of the soil decreases;
- applied horizontal displacement increases.

Vucetic and Lacasse (1982) performed a laboratory investigation of the influence of the height to diameter ratio and of the membrane stiffness on the undrained behavior of clay in the Geonor DSS. The study included 21 strain—controlled constant volume tests on undisturbed specimens of the medium—stiff Haga CL clay. The results indicated no significance influence of the height to diameter ratio or wire reinforcement on the measured soil strength. Based on these results they concluded that the theoretical elastic analysis of the direct simple shear device presents a pessimistic view of the expected influence of stress nonuniformities, primarily because such analyses cannot take into account the influence of soil yielding during shear which will reduce the predicted stress concentrations.

Airey and Wood (1987) conducted constant volume tests on Kaolin in the

Cambridge simple shear device and, based on comparison with the results from tests on sand (Airey et al. 1985), state that uniformity of boundary stresses and internal deformations is much better for clays (Figure 2.8) than for sands in the simple shear device.

The conclusions from various studies on the uniformity of stress in the simple shear apparatus, summarized above, indicate that the theoretical (or numerical) analyses assuming elastic behavior of the specimen tend to exaggerate the situation because the stress concentrations at the specimen edges represent an extreme case for the non-yielding elastic material. This would not be expected for a plastic material such as clay that yields, as reported by Airey and Wood (1987) for tests on Kaolin and Vucetic and Lacasse's (1982). Furthermore, Airey and Wood justifiably state that the uniformity of stress and strain is better in the DSS than in a standard triaxial apparatus at large strains with rough ends wherein considerable bulging of the sample may occur as the test approaches failure. Yet triaxial test results do not receive the same degree of suspicion as simple shear test results.

2.3.2 State of Stress at Failure

The state of stress at failure in simple shear testing remains a controversial issue since in most of the direct simple shear devices there is not enough information to construct the Mohr's circle of stress during shear. For example, in the Geonor DSS only the vertical stress (σ'_v) and shear stress (τ_h) on a horizontal plane are known (this fixes only one point on Mohr's circle of stress). It is only in the more sophisticated devices like those developed at Cambridge University that the complete state of stress is known. However, the Cambridge devices are clearly suited only for research purposes while the simpler Geonor type device is much more commonly used in practice. It is therefore important to be able to evaluate the state of stress in this type of device. The purpose of this subsection is to summarize the conclusions from

various approaches in order to find the most suitable method for interpretation of stresses at failure in the Geonor DSS.

Seven approaches have been proposed to determine Mohr's circle of stress at failure in the Geonor type direct simple shear device. Each procedure makes an assumption with respect to determining the orientation of the major principal stress at failure, thereby allowing σ_1' and σ_3' to be calculated. Figure 2.9 shows Mohr's circle of stress for the initial and failure conditions in a DSS test. The initial stresses conform to K_0 conditions and the Mohr–Coulomb failure criterion is assumed to be valid (i.e., the stresses on the failure plane at failure, τ_{ff} and σ'_{ff} correspond to the point of tangency between the Mohr's circle at failure and the failure envelope. Table 2.1 presents results of the computed state of stress for a representative CK_0 UDSS test on a normally consolidated BBC specimen using the different failure criteria.

Failure Criterion I (Figure 2.10), proposed by Roscoe (1953) and Duncan and Dunlop (1969), is based on the assumption that the applied stress system is one of pure shear. Table 2.1 indicates that it results in the highest q_f/σ'_{vc} , the least amount of rotation of the principal axes and gives an unrealistically high friction angle ϕ' .

Failure Criterion II (Figure 2.11) assumes that the horizontal plane is the failure plane. The analysis of measured data, by Roscoe et al. (1967), from drained tests in the Cambridge Mk6 simple shear apparatus (Figure 2.12) and the observed rupture surface in the Cambridge circular simple shear device from tests on Kaolin (Figure 2.13) by Airey et al (1985) indicate that using this assumption is incorrect. Table 2.1 shows that it yields the largest ratio of $(\sigma'_h/\sigma'_v)_f$, largest rotation of the principal axes and an unreasonably small friction angle ϕ' .

Failure Criterion III assumes that the horizontal plane is a plane of maximum shear stress (Figure 2.14). Roscoe et al. (1967) showed this assumption to be valid for their drained tests on medium–loose sand, but not for the tests on dense sand (Figure 2.12). As discussed in the previous subsection, the shear stress in the direct simple

shear devices varies within the sample, i.e., it increases from the top and bottom towards the middle. Hence, in this case the measured τ_h at the sample top may not be equal to the maximum horizontal shear stress within the sample, implying that predictions for q_f/σ'_{vc} and ϕ' are conservative.

Failure Criterion IV assumes a location for the Mohr–Coulomb failure envelope (Figure 2.15). In this case the Mohr circle at failure must pass through the measured normal and shear stresses on the horizontal plane (σ'_v and τ_h) and be tangent to the Mohr–Coulomb envelope. The smaller of the two Mohr's circles is the more reasonable state of stress (Ladd and Edgers, 1972). In this case, to assume an appropriate value of ϕ' will be difficult unless sufficient laboratory data on the soil being tested is available for a reliable estimate of ϕ' . In addition, if one selects ϕ' from triaxial compression data, one has to decide between ϕ' at q_f or at maximum obliquity or some intermediate value.

Failure Criterion V, proposed by de Josselin de Jong, assumes that failure occurs on vertical planes (Figure 2.16). Subsequent researchers (e.g., Randolph and Wroth 1981; Wroth 1984; Wroth 1987; Airey et al. 1985), based on analyses of theoretical and experimental results, reported that the assumption appears to give very good results for normally consolidated cohesive soils with low undrained shear strengths, which also corresponds to low values of $\psi [= \arctan(\tau_h/\sigma'_v)]$. However, this criterion reaches a theoretical limit at $(\tau_h/\sigma'_{vc})_{\max} \simeq 0.22$, which proves unrealistic based on almost half of MIT's experimental DSS results reported by DeGroot (1989).

Failure Criterion VI, proposed by Oda and Konishi (1974), assumes a linear relationship between τ_h/σ'_v and $\kappa \tan \delta$, expressed as:

$$\tau_h/\sigma'_v = \kappa \tan \delta \quad (2.1)$$

The material constant κ is expressed by the following equation (Ochiai, 1975, 1976a,

1976b),

$$\kappa = 1 - K_o = \sin \phi_{cv} = \frac{2 \sin \phi_u}{(1 + \sin \phi_u)} \quad (2.2)$$

where:

K_o = earth pressure coefficient at rest;

ϕ_{cv} = internal friction angle at the critical void ratio;

ϕ_u = interparticle friction angle.

Equation 2.1 inherently assumes that $\sigma'_3 = K_o \sigma'_v$ throughout the test. Based on Equations 2.1 and 2.2 certain relationships for the major and minor principal stresses can be derived from consideration of Mohr's circle of stress (Figure 2.17).

The analyses (see DeGroot, 1989) reveal that the Criterion VI gives reasonable results that do not differ much from assuming the horizontal plane is the plane of maximum shear stress. However, sufficient experimental data on natural clays showing that the relationship holds at $(\tau_h)_{max}$ are not available. Furthermore, it requires a value of K_o which is not easy to obtain.

Failure Criterion VII, based on the assumption that the principal axes of strain increment and stress increment coincide (Figure 2.18), appears rational based on theoretical analyses (Hill, 1950). Roscoe et al. (1967) found the Criterion holds for drained DSS tests on sand. However, there is no experimental evidence indicating that this assumption is valid for natural clays. In the case of undrained tests, using this criterion gives the same results as assuming the horizontal plane is the plane of maximum shear stress (i.e., Criterion III).

Ladd and Edgers (1972) in their review of the state of stress at failure in CK_oUDSS tests conclude that the undrained shear strength based on $(\tau_h)_{max}$ lies between q_f and $\tau_{ff} = q_f \cos \phi'$. They further state that the test cannot be used to evaluate Mohr-Coulomb failure envelopes, except at very large shear strains. Wroth

(1987) also conclude that $(\tau_h)_{\max}$ is less than q_f and further states that simple shear tests produce a complex pattern of behavior where the maximum values of shear stress acting on different planes in the specimen vary widely and occur at different stages of the test.

2.4 Summary and Conclusions

Keeping in view the intent of this research, i.e., investigation of normalized behavior of resedimented BBC using the Geonor DSS, it was considered appropriate to include an overview of following aspects:

- Normalized Soil Parameter (NSP) concept.
- Review of existing simple shear devices.
- State of stresses in DSS testing

The NSP is based on the empirical observation that the results of laboratory tests on clay samples having the same OCR, but different consolidation stresses and therefore different maximum past pressures, exhibit very similar strength and stress–strain characteristics when normalized with respect to the consolidation stress. This concept lead to the development of a new design method, called SHANSEP, to evaluate the in situ strength and stress–strain properties of cohesive soils for stability analyses. The design method has been applied successfully in the engineering practice to a variety of cohesive soils. However the method is strictly applicable only to mechanically overconsolidated and truly normally consolidated soils exhibiting normalized behavior (Ladd, 1988).

The direct simple shear apparatus was developed to provide a soil testing device which can evaluate the stress–strain behavior of soil under simple shear. It enables soil specimens to be tested wherein the major principal stress axis rotates during shear

while the sample is kept under a condition of plane strain. Most DSS devices cannot, however, impose complementary shear stresses to the sides of the specimen. Hence a condition of nonuniform stress and strain occurs within the specimen. This deficiency has subjected the device to considerable criticism. However, many theoretical and experimental studies conducted in DSS reveal that for plastic soils the degree of uniformity of stress and strain in the device is acceptable up to the peak shear resistance.

The state of stress at failure in the Geonor type device is not known since, based on the measured vertical effective stress (σ'_v) and the shear stress (τ_h), the Mohr's circle of stress can not be determined. Hence, at the peak horizontal shear resistance the undrained maximum shear stress, $q_f = 0.5(\sigma_1 - \sigma_3)$, of the soil cannot be computed. Seven criteria have been proposed to obtain the Mohr's circle of stress at failure in the Geonor type DSS. Each criterion makes an assumption which determines the orientation of major principal stress at failure, thereby allowing σ'_1 and σ'_3 to be calculated. Many theoretical and experimental studies have been conducted in order to determine the feasibility of various criteria, but the issue is not yet fully resolved. DeGroot (1989), in his review of the current state of the art of simple shear testing, analyzed the state of stress at failure (abstract presented in Section 2.3) based on the available evidence and made the following statements with respect to the state of stress at $(\tau_h)_{\max}$ for CK_0 UDSS tests on normally consolidated cohesive soils:

- The undrained shear strength based on $(\tau_h)_{\max}$ probably lies between q_f and $\tau_{ff} = q_f \cos \phi'$ (Ladd and Edgers, 1972).
- Assuming that the applied stress system is one of pure shear (Criterion I) or that the failure plane is horizontal (Criterion II) is unreasonable.
- The experimental studies on a variety of soils show that the vertical effective stress ratio σ'_v / σ'_{vc} at $(\tau_h)_{\max}$ lies within a narrow band. As a

result, a strong correlation exists between $\psi [= \arctan (\tau_h / \sigma'_{vc})]$ and $(\tau_h / \sigma'_{vc})_{\max}$.

- Assuming the failure plane is vertical (Criterion V) compares well with experimental results when the values of the undrained strength ratio $(\tau_h / \sigma'_{vc})_{\max}$ are equal to or less than 0.22.

Table 2.1: State of Stress in Geonor K_0 UDSS Test on Normally Consolidated BBC Using Different Assumptions (after Ladd and Edgers, 1972; from DeGroot, 1989)

Failure Criterion	Assumption	At Failure (Maximum τ_h)							
		q_f/σ'_{vc}	τ_{ff}/σ'_{vc}	p'_f/σ'_{vc}	$(\sigma'_1/\sigma'_3)_f$	$(\sigma'_h/\sigma'_v)_f$	ϕ'_f	θ_p	θ_f
I	Applied Stresses Are Pure Shear	0.320	Indeter.	0.320	∞	0.5	90.0	19.3	Indeter.
II	Horizontal Failure Plane	0.212	0.200	0.640	1.99	1.246	19.3	54.7	0
III	$\tau_h = q_f$	0.200	0.187	0.570	2.08	1	20.6	45.0	10.3
IV	$\phi'_f = 30^\circ$	0.230	0.199	0.459	3.00	0.611	30.0	30.4	29.6
V	Vertical Failure Plane	0.236	0.200	0.445	3.26	0.561	32.0	29.0	90.0
VI	$\tau_h/\sigma'_v = \kappa \tan \psi$	0.213	0.193	0.498	2.49	0.747	25.3	35.1	22.6
VII	Plasticity Theory	0.200	0.187	0.570	2.08	1	20.6	45.0	10.3

Notes:

- a) Measured Data: at $(\tau_h)_{max}$, $\tau_h/\sigma'_{vc}=0.200$ and $\sigma'_v/\sigma'_{vc}=0.570$; assume $K_0=0.5$.
b) See Figure 2.9 for definition of stresses and angles.

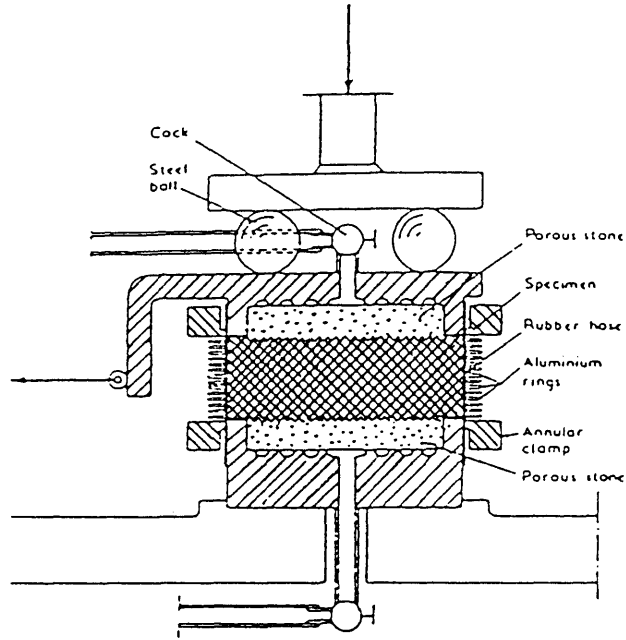


Figure 2.1: Cross-Section of the SGI Simple Shear Apparatus (after Kjellman, 1951; from DeGroot, 1989).

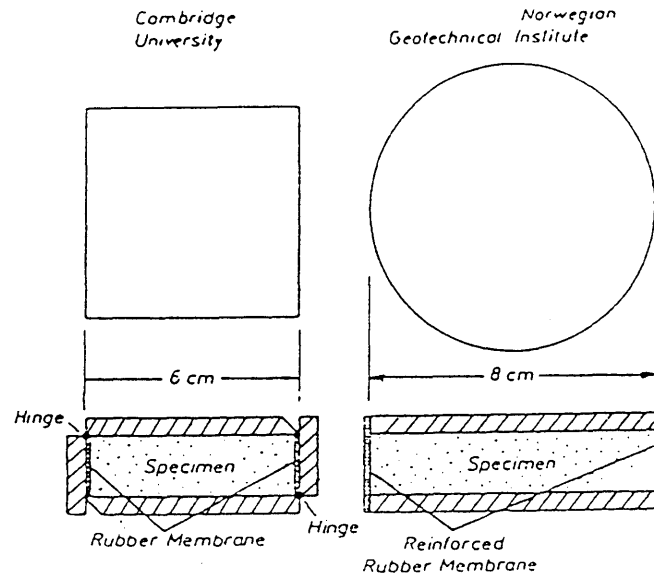


Figure 2.2: Schematics of: (a) Cambridge University Direct Simple Shear Device; (b) NGI Direct Simple Shear Device (after Franke, et al., 1979; from DeGroot, 1989).

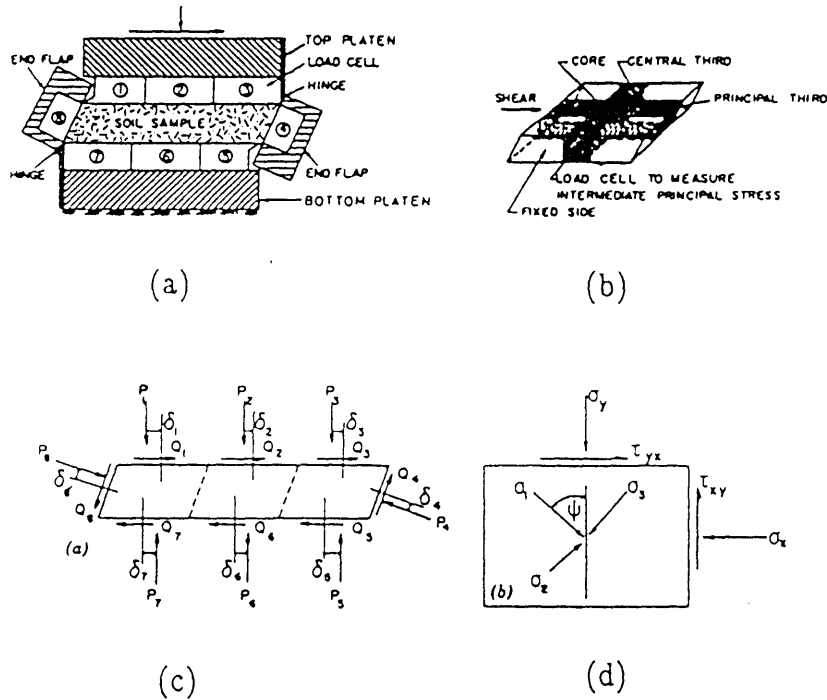


Figure 2.3: Cambridge University Mk7 Simple Shear Apparatus: (a) Cross-Section; (b) Arrangement of Load Transducers; (c) Typical Set of Forces Measured; (d) Stresses Deduced for Sample Core (after Budhu, 1985; from DeGroot, 1989).

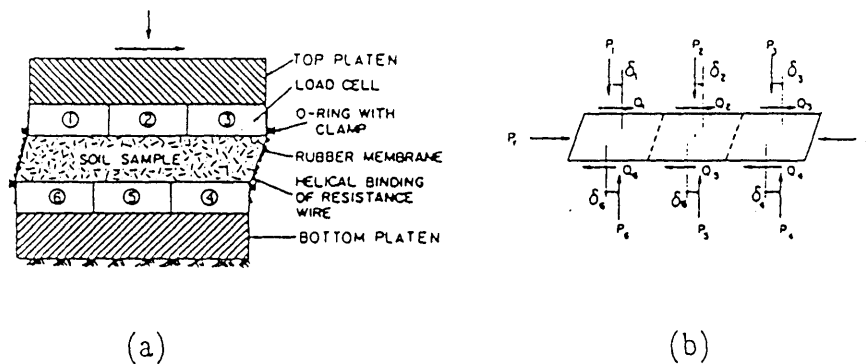


Figure 2.4: Cambridge University Cylindrical Simple Shear Apparatus (CSSA): (a) Cross-Section; (b) Typical Set of Forces Measured (after Budhu, 1985; from DeGroot, 1989).

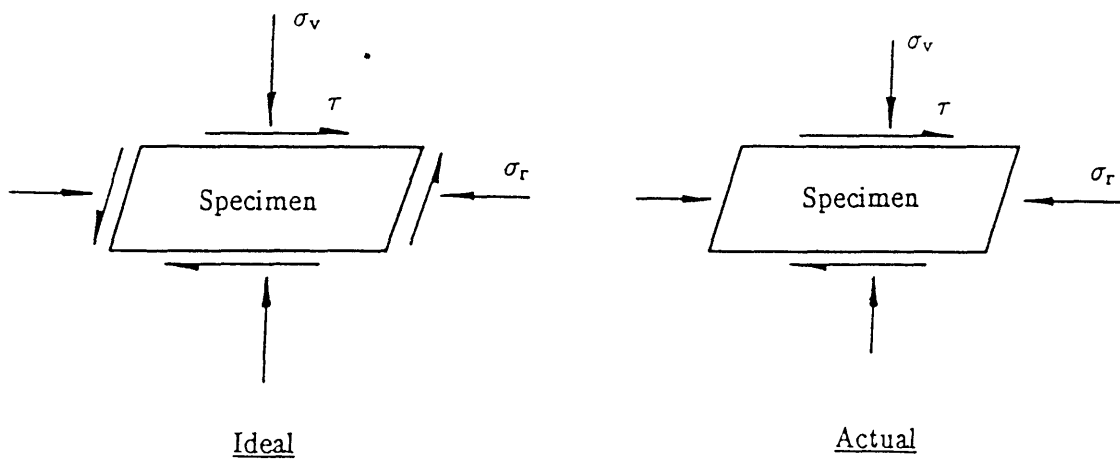


Figure 2.5: Comparison of Ideal Set of Stresses Imposed to a Simple Shear Specimen Versus Stresses Which can Realistically be Imposed (from DeGroot, 1989).

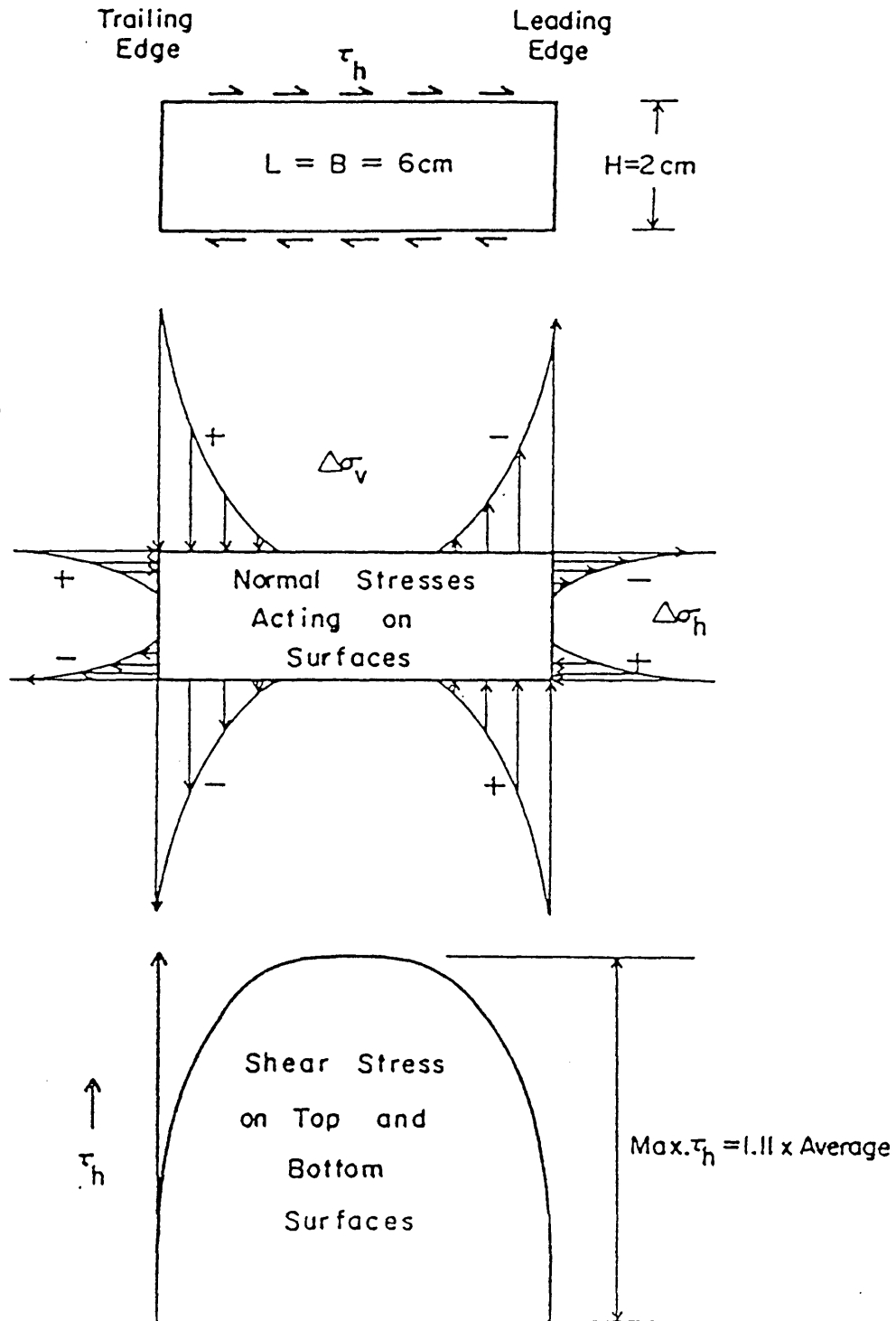


Figure 2.6: Elastic Stresses in Cambridge Simple Shear Apparatus Computed by Roscoe (1953; from Ladd and Edgers, 1972).

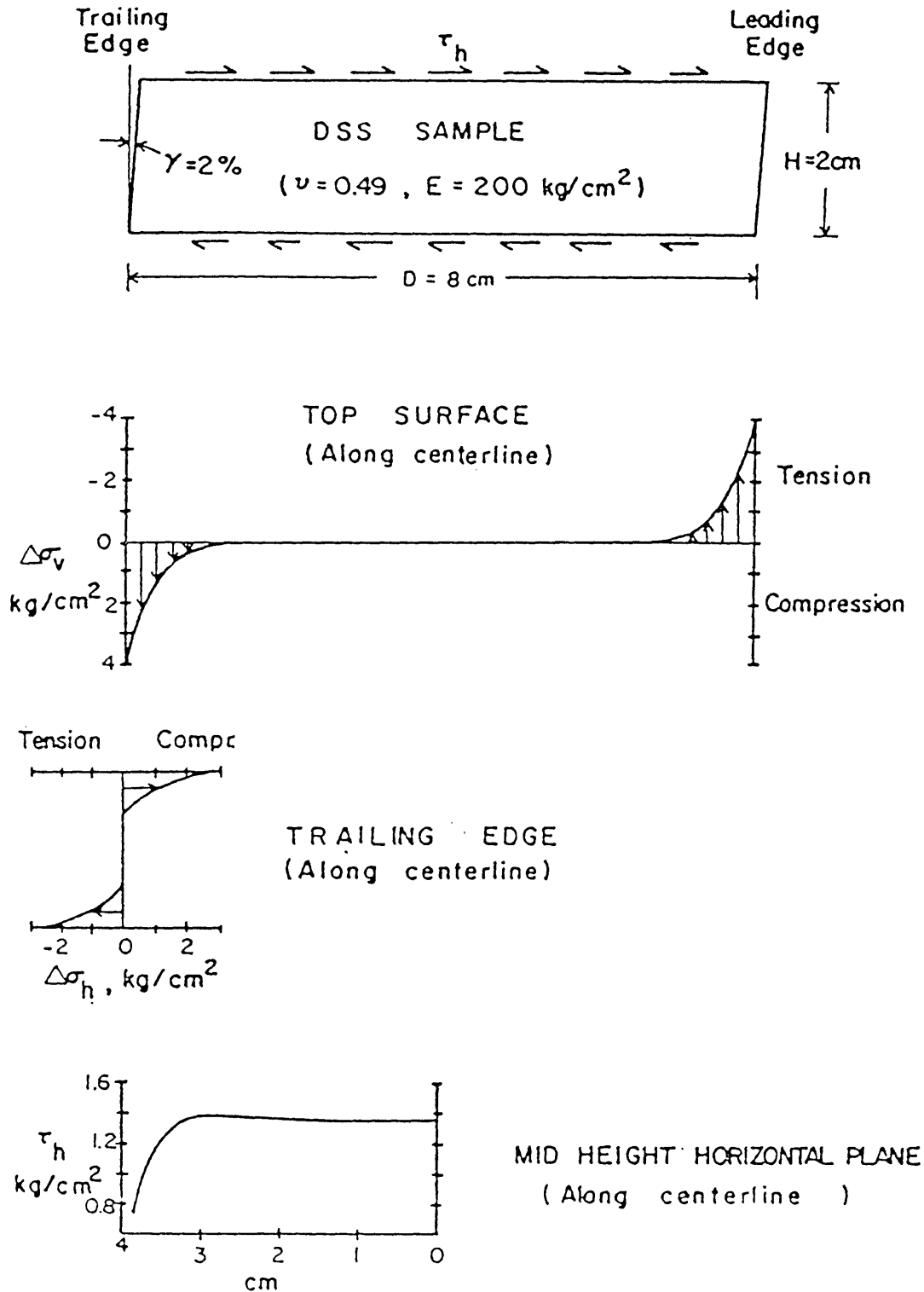


Figure 2.7: Elastic Stresses in Geonor DDS Apparatus Computed by Lucks et al. (1972; from Ladd and Edgers, 1972)

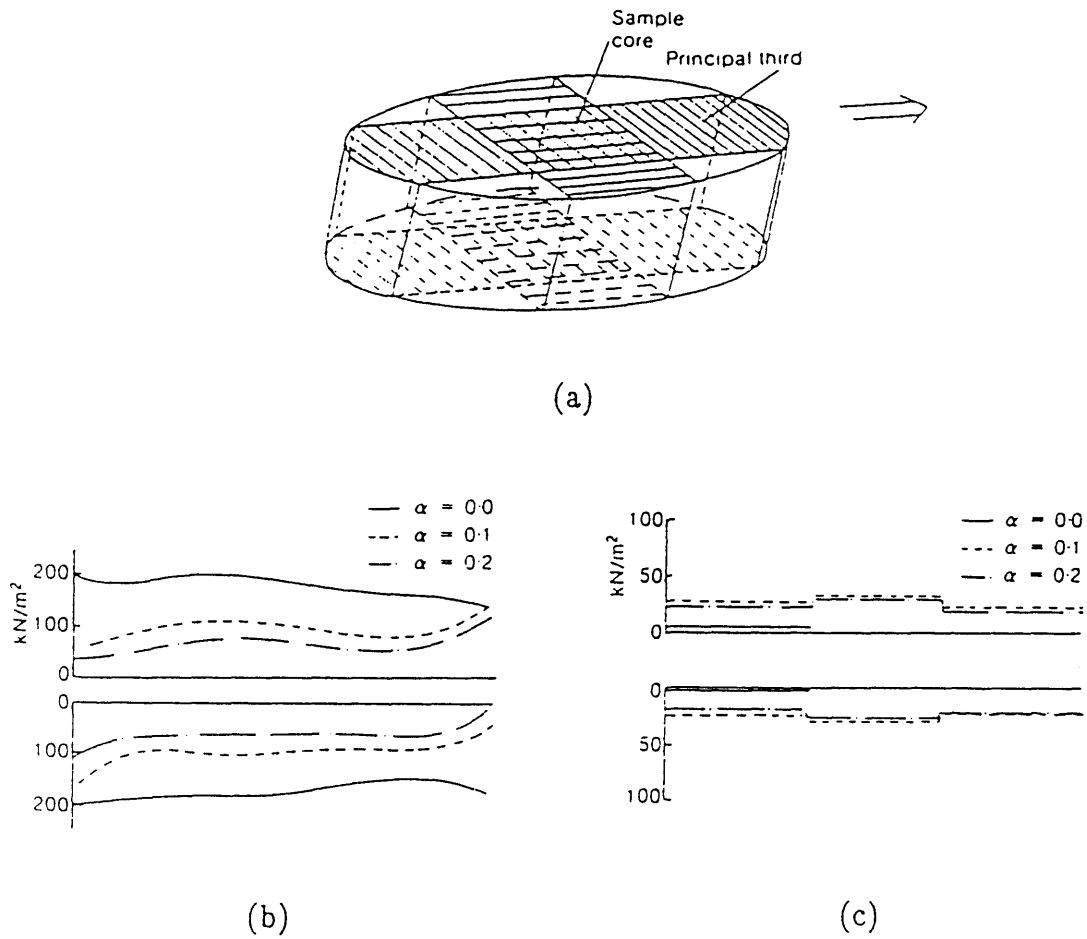
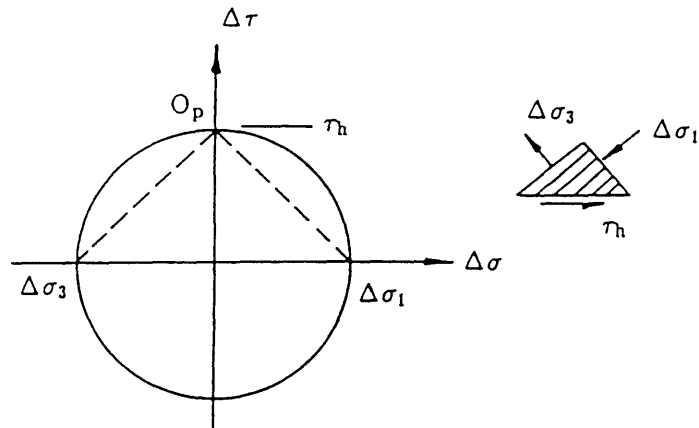
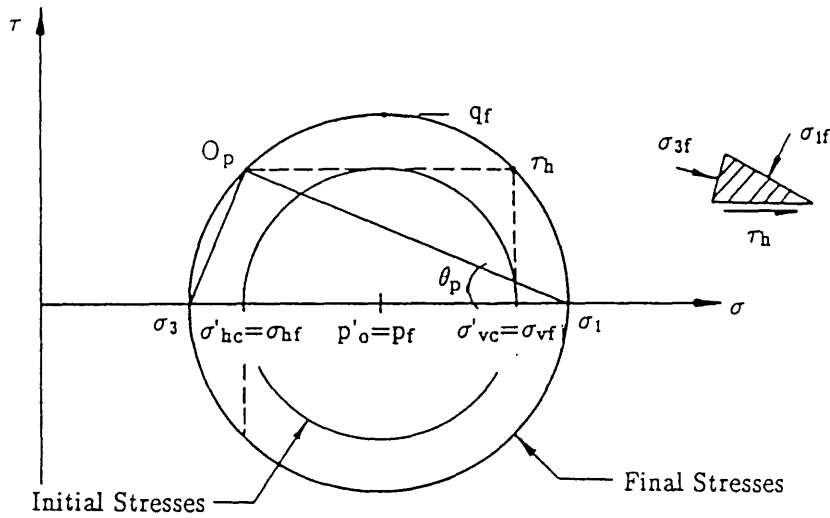


Figure 2.8: Stress Distributions on the Principal Third for a Constant Volume Test on Kaolin in the Cambridge CSSA: (a) Principal Third Load Cells; (b) Normal Stress; (c) Shear Stress ($\alpha =$ shear distortion γ_{yx} ; after Airey and Wood, 1987; from DeGroot, 1989).



Applied Stresses for Pure Shear



$$q_f / \sigma'_{vc} = \sqrt{\frac{(1 - K_o)^2}{4} + (\tau_h / \sigma'_{vc})^2}$$

$$\tau_{ff} = q_f \cos \phi'$$

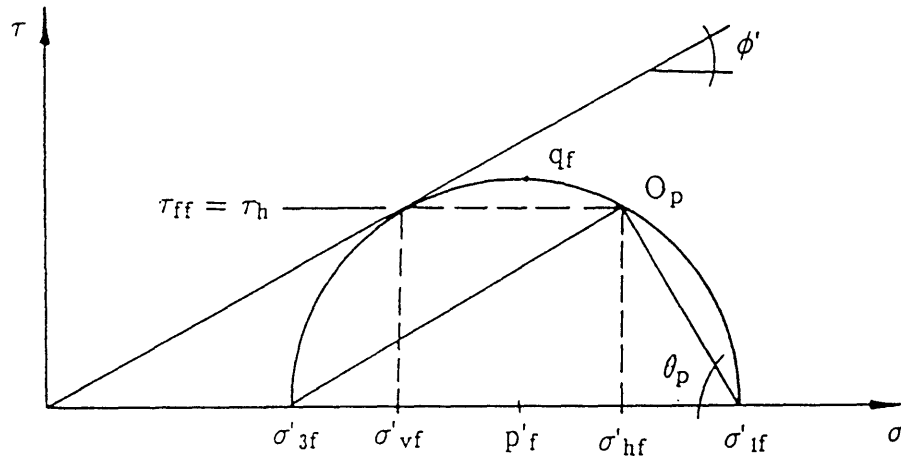
$$p'_f / \sigma'_{vc} = (p'_o - \Delta U) / \sigma'_{vc}$$

$$\sin \phi' = q_f / p'_f$$

$$\theta_f = 45^\circ = \phi' / 2 - \theta_p$$

$$\tan \theta_p = \frac{\tau_h / \sigma'_{vc}}{0.5(1 - K_o) + q_f / \sigma'_{vc}}$$

Figure 2.10: Direct Simple Shear Failure Criterion I:
Applied Stress System is Pure Shear (after Ladd and Edgers, 1972;
from DeGroot, 1989).



$$q_f / \sigma'_{vc} = \frac{\tau_h / \sigma'_{vc}}{\cos \phi'} \quad \tau_{ff} = \tau_h$$

$$p'_f / \sigma'_{vc} = \sigma'_{vf} / \sigma'_{vc} + (\tau_h / \sigma'_{vc}) \tan \phi'$$

$$\sigma'_{hf} / \sigma'_{vf} > 1 \quad \tan \phi' = \tau_h / \sigma'_{vf}$$

$$\theta_p = 45^\circ + \phi' / 2 \quad \theta_f = 0^\circ$$

Figure 2.11: Direct Simple Shear Failure Criterion II: Horizontal Plane is Failure Plane (from DeGroot, 1989).

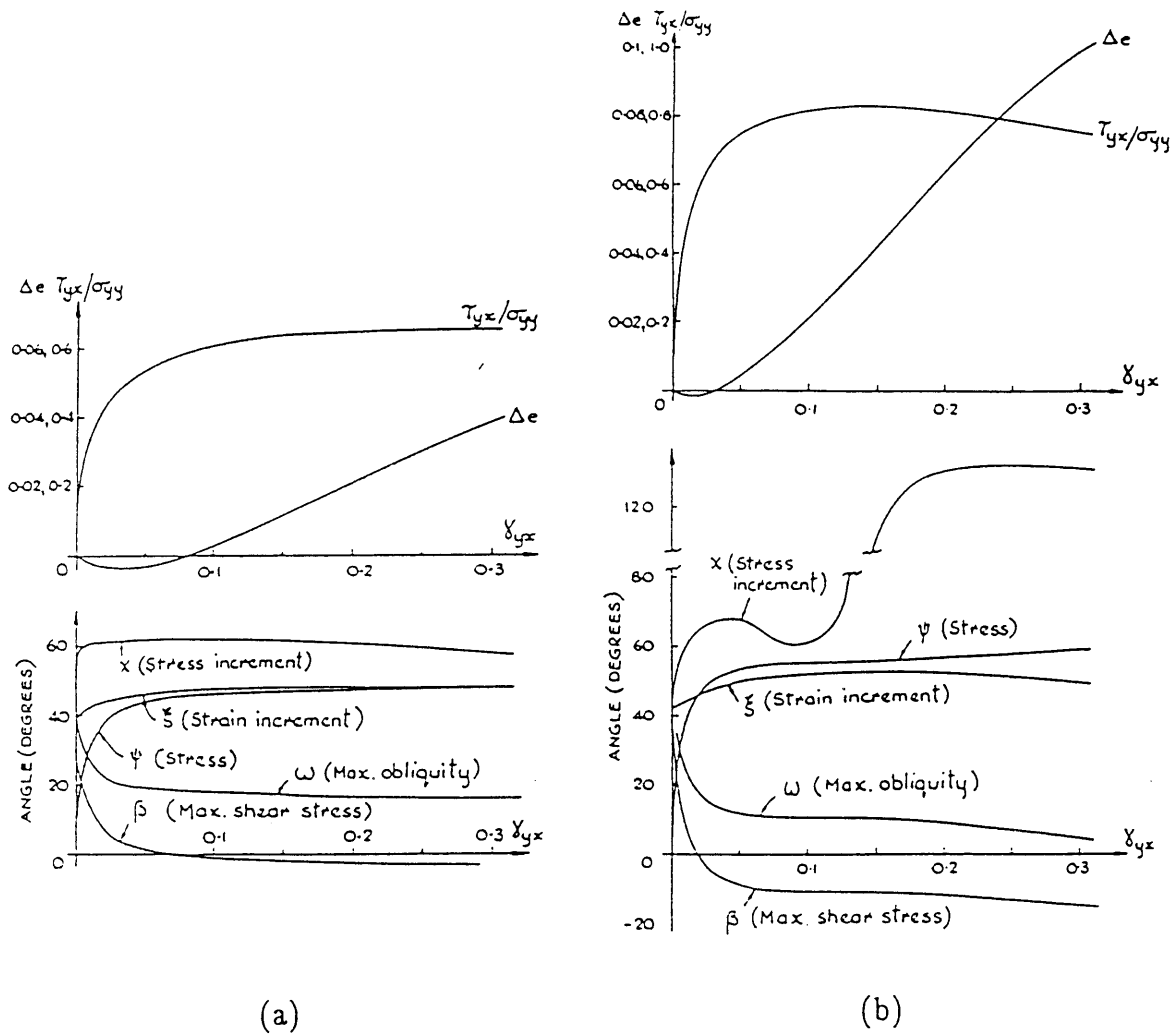
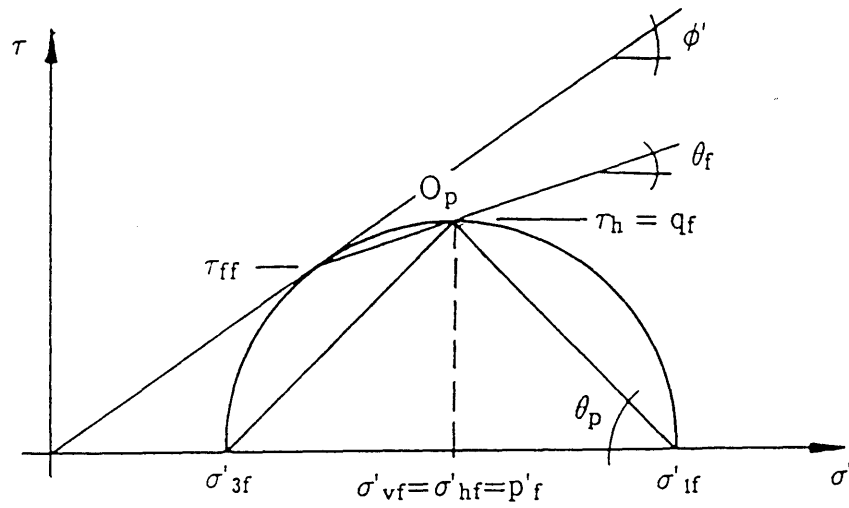


Figure 2.12: Stress Ratio on Horizontal Plane in Central Third, Average Voids Ratio Change for Whole Sample and Inclination to Horizontal of Major Principal Planes of Stress (ψ), Stress Increment (χ), Strain Increment (ξ), as Well as Planes of Maximum Shear Stress (β) and Maximum Obliquity (ω) for drained tests in the Cambridge DSS on: (a) Medium Loose Sand ($e_0=0.68$); (b) Dense Sand ($e_0=0.53$; after Roscoe, et al., 1967; from DeGroot, 1989).

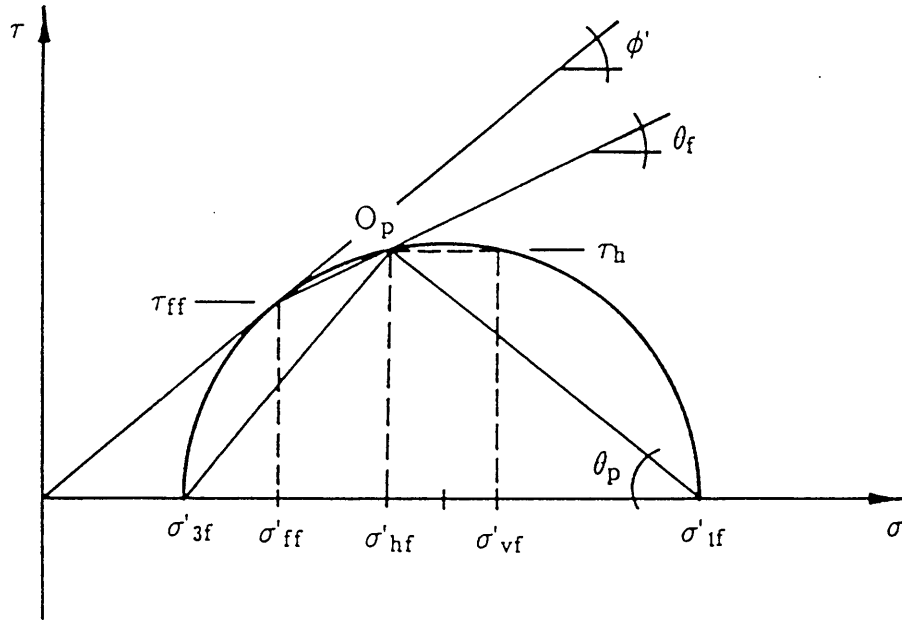


Figure 2.13: Ruptures Observed in Radiograph of Simple Shear Test on Kaolin (sketches of radiographs of threads of lead paste; after Airey, et al., 1985; from DeGroot, 1989).



$$\begin{aligned}
 q_f / \sigma'_{vc} &= \tau_h / \sigma'_{vc} & \tau_{ff} &= q_f \cos \phi' \\
 p'_f / \sigma'_{vc} &= \sigma'_{vf} / \sigma'_{vc} \\
 \sigma'_{hf} / \sigma'_{vf} &= 1 & \sin \phi' &= \tau_h / \sigma'_{vf} \\
 \theta_p &= 45^\circ & \theta_f &= \phi' / 2
 \end{aligned}$$

Figure 2.14: Direct Simple Shear Failure Criterion III: Horizontal Plane is Plane of Maximum Shear Stress (from DeGroot, 1989).



$$q_f/\sigma'_{vc} = (\tau_{ff}/\sigma'_{vc})/\cos\phi'$$

$$p'_f/\sigma'_{vc} = \sigma'_{ff}/\sigma'_{vc} + (q_f/\sigma'_{vc})\sin\phi'$$

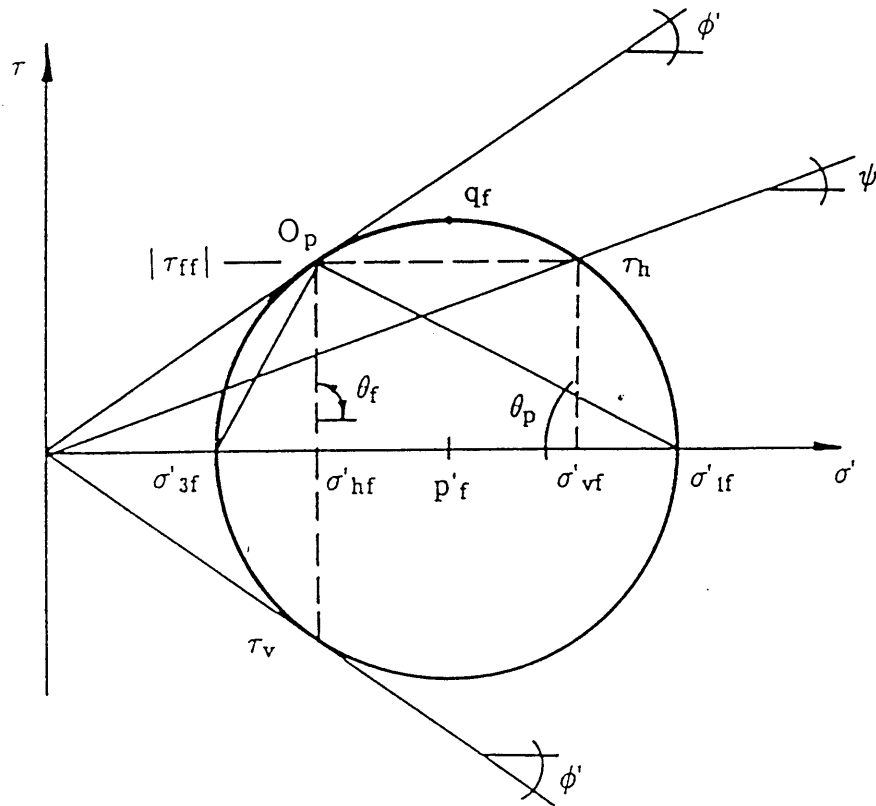
$$\sigma'_{3f} = p'_f - q_f$$

$$\phi' = \text{assumed}$$

$$\theta_f = 45^\circ + \phi'/2 - \theta_p$$

$$\tan\theta_p = \tau_h/(\sigma'_{vf} - \sigma'_{3f})$$

Figure 2.15: Direct Simple Shear Failure Criterion IV:
Assume Mohr–Coulomb Failure Envelope (from DeGroot, 1989).



$$q_f / \sigma'_{vc} = \frac{\tau_h / \sigma'_{vc}}{\cos \phi'}$$

$$\tau_h / \sigma'_{vf} = \frac{\sin \phi' \cos \phi'}{1 + \sin^2 \phi'}$$

$$\tau_{ff} = q_f \cos \phi'$$

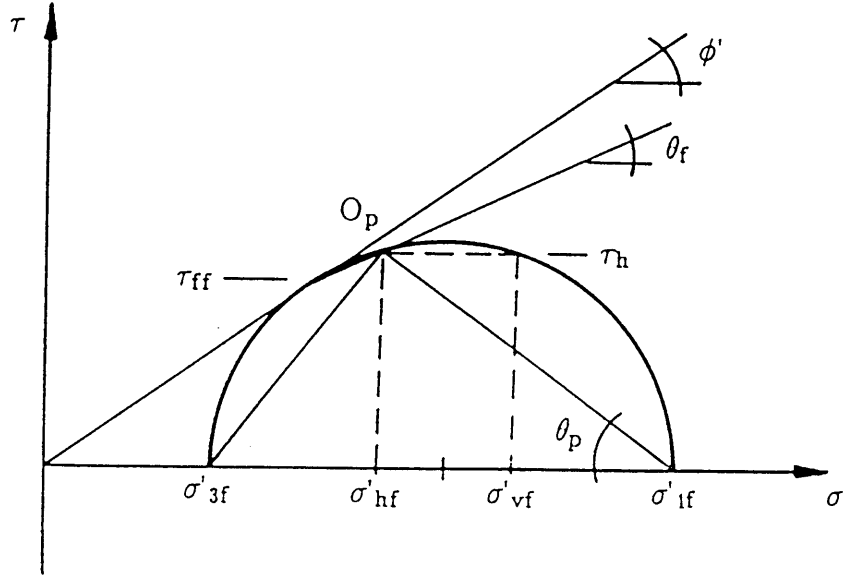
$$p'_f / \sigma'_{vc} = \sigma'_v / \sigma'_{vc} - (\tau_h / \sigma'_{vc}) \tan \phi'$$

$$\theta_p = 45^\circ - \phi' / 2$$

$$\psi = \arctan(\tau_h / \sigma'_{vf})$$

$$\theta_f = 90^\circ$$

Figure 2.16: Direct Simple Shear Failure Criterion V:
Failure Occurs on Vertical Planes (from DeGroot, 1989).



$$\tau_h/\sigma'_{vc} = \kappa \tan \delta \quad \theta_p = \delta \quad \kappa = 1 - K_o$$

$$\beta = 1 - \Delta U/\sigma'_{vc} \quad \tau_{ff} = q_f \cos \phi'$$

$$\sigma'_{3f}/\sigma'_{vc} = K_o \beta \quad \theta_f = 45^\circ + \phi'/2 - \theta_p$$

$$q_f/\sigma'_{vc} = \frac{\beta^2(1 - K_o)^2 + (\tau_h/\sigma'_{vc})^2}{2\beta(1 - K_o)}$$

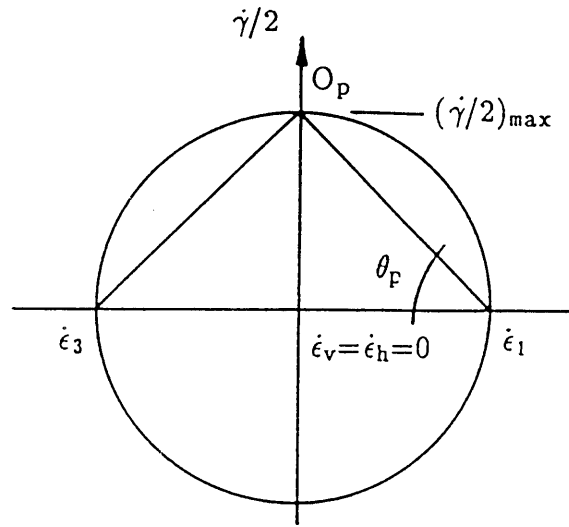
$$\sigma'_{1f}/\sigma'_{vc} = \frac{\beta^2(1 - K_o) + (\tau_h/\sigma'_{vc})^2}{\beta(1 - K_o)}$$

$$\sin \phi' = \frac{\beta^2(1 - K_o)^2 + (\tau_h/\sigma'_{vc})^2}{\beta^2(1 - K_o)^2 + (\tau_h/\sigma'_{vc})^2}$$

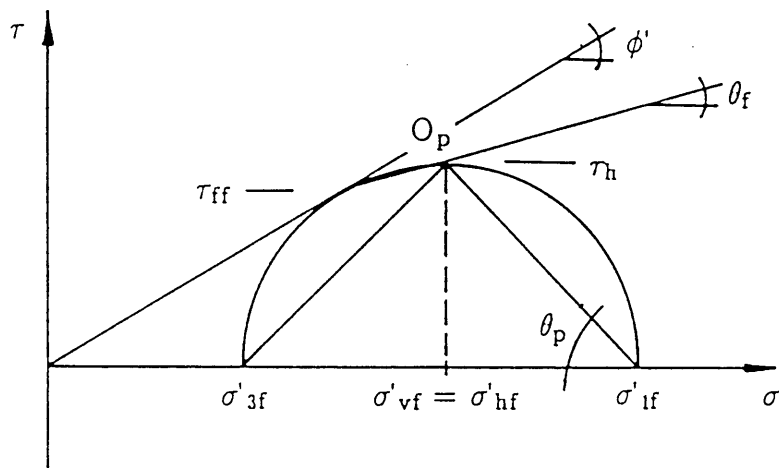
$$p'_{ff}/\sigma'_{vc} = 0.5(\sigma'_{1f}/\sigma'_{vc} + \sigma'_{3f}/\sigma'_{vc})$$

$$\tan \theta_p = \frac{\tau_h}{(\sigma'_{vf} - \sigma'_{3f})}$$

Figure 2.17: Direct Simple Shear Failure Criterion VI:
Linear Relationship Between τ_h/σ'_{vc} and $\kappa \tan \delta$ (from DeGroot, 1989).



Mohr's Circle of Strain Increment
(undrained test)



$$q_f / \sigma'_{vc} = \tau_h / \sigma'_{vc} \quad \tau_{ff} = q_f \cos \phi'$$

$$p'_f / \sigma'_{vc} = \sigma'_{vf} / \sigma'_{vc}$$

$$\sigma'_{hf} / \sigma'_{vf} = 1$$

$$\sin \phi' = \tau_h / \sigma'_{vf} \quad \theta_p = 45^\circ$$

$$\theta_f = \phi' / 2$$

Figure 2.18: Direct Simple Shear Failure Criterion VII:
Coincidence of Principal Axes of Strain Increment and Stress
(from DeGroot, 1989).

CHAPTER 3

DESCRIPTION OF EQUIPMENT AND EXPERIMENTAL PROCEDURES

3.1 Introduction

The tests conducted for this research were performed in MIT's Geonor Model 4 DSS apparatus that has been extensively used for direct simple shear research and testing at MIT since 1965. It was originally developed by the Norwegian Geotechnical Institute and manufactured by Geonor. The device is very similar to the one used for tests described by Bjerrum and Landva (1966). Several modifications have been made to this particular apparatus, acquired by MIT in 1984, in order to use 35 cm² samples, refine data measurement procedures, and to enable fully automated testing so that readings during consolidation/shear can be taken by MIT's central data acquisition system.

The Geonor DSS apparatus was designed for testing undisturbed cohesive samples of soils in order to evaluate the stress-strain behavior under simple shear strain conditions. It enables soil specimens to be tested where in the major principal stress axis rotates during shear while the specimen is kept under a condition of plane strain. Plane strain conditions are often encountered in practical situations and the horizontal portion of a failure surface can be simulated in the laboratory by means of DSS mode of shearing. The test provides one dimensional consolidation parameters as well as undrained strength and modulus values (after K_0 or anisotropic consolidation (CAU) i.e., by also applying a horizontal shear stress during consolidation) suitable for embankment design and evaluation of anisotropy via the "ADP" Recompression (Bjerrum, 1973) and the SHANSEP techniques (Ladd and Foot, 1974). Despite inherent drawbacks of the apparatus (e.g. its inability to impose uniform states of stress and strain in order to treat the specimen as a single element, as discussed in the previous chapter), it is considered a valuable device for engineering practice since it

provides consistent and reasonable estimates of one dimensional consolidation behavior and average undrained shear strength parameters for stability analyses with simple testing procedures at low operating cost (Ladd and Edgers, 1972; Ladd, 1981; Germaine, 1985; Ladd, 1988; DeGroot, 1989).

Subsequent sections of this chapter contain a brief description of the testing apparatus and experimental procedures, portions of which have been excerpted from DeGroot (1989). The reader is referred to Ladd and Edgers (1972), and DeGroot (1989) for comprehensive study of soil behavior in undrained direct simple shear.

3.2 Description of Testing Apparatus

Figure 3.1 schematically shows the original Geonor Model 4 DSS device. The apparatus consists of the sample assembly and vertical and horizontal load units. The sample assembly (Figure 3.2) comprises a top cap and bottom pedestal; both containing porous stones for providing drainage at the top and bottom of the sample. The stones also provide the frictional interface for transferring the horizontal shear force during testing to the sample. The trimmed sample is confined within a wire reinforced rubber membrane between the top cap and bottom pedestal. The sample is surrounded by a plexiglas water bath for keeping it immersed. The device was originally designed for testing samples with an area of 50 cm^2 . This, however, is incompatible with the diameter of sampling tubes typically used in North America (3 in. diameter or 45 cm^2); hence a 35 cm^2 sample with an approximate height of 2.3 cm is used at MIT.

The sample is incrementally consolidated to the desired stress state. Increments of vertical stress are applied to the sample using dead weights loaded on to a lever arm acting on the sample. The lever arm ratio is approximately 1:10. The vertical load was originally measured with a displacement transducer (DCDT) mounted inside a proving ring, however, this has been replaced during this research with a load cell (Figure 3.3)

to eliminate the possibility of any error in measurement of vertical load due to compliance in the proving ring and to stiffen the system in order to improve height control. The installation of the 1000 pounds capacity load cell stiffened the vertical load measuring system which has further reduced the response time of the height controller. Vertical displacements are measured with a dial guage/DCDT assembly which is connected to the top loading platen adjacent to the sample. The DCDT is connected to the dial guage so that vertical displacement readings can be made with data acquisition system. The consolidation is performed under one dimensional loading conditions (K_0 -consolidation) since the wire reinforced rubber membrane prevents lateral deformations. However, the apparatus can also be used to perform anisotropically consolidated (CAU) tests by also applying a horizontal shear stress during consolidation.

After consolidation, the sample is sheared by application of a horizontal force to the top cap (i.e., the top of the sample moves relative to the bottom in a simple shear strain mode). The top is driven at a constant rate of displacement and require force measurement. However, stress control testing is also possible. The horizontal force was originally measured with a proving ring and a dial guage. A DCDT was added for recording reading by a data acquisition system. The compliance of the proving ring resulted in variation of strain rate, specially at the beginning of a test. The proving ring has therefore been replaced with a 500 pounds capacity load cell (Figure 3.3), which has substantially improved the accuracy of stress-strain data measured during initial stages of the test. The horizontal displacement of the sample top relative to its fixed bottom is measured using a DCDT.

Shearing can be performed under drained or undrained conditions. Drained tests are performed by deforming the sample under constant vertical stress at a strain rate which is sufficiently slow to allow dissipation of excess pore pressure. However, it is rarely practiced. Undrained shear is conducted by maintaining the volume of sample

constant during shear. Due to the high radial stiffness of the wire reinforced rubber membrane, changes in the area of the specimen are negligible compared to the changes in height. Therefore, only the height needs to be kept constant to run a constant volume test. Sample height is kept constant by varying the vertical stress. Changes in vertical stress, required to keep the height constant are assumed to be equal to the pore pressure that would develop if the specimens were sealed and pore pressure measurements made.

The sample height is maintained constant during undrained shear using a closed loop servo control system consisting of a DCDT, a controller box, and an Electrocraft analog motor. The DCDT (Collins \pm 0.125 in.) is positioned adjacent to the sample on the opposite side of where the horizontal shear force is applied (Figure 3.4). It monitors the height changes in the top loading platen which is directly connected to the top cap of the sample assembly. The control box compares the DCDT reading to a reference voltage and sends the amplified voltage difference to the Electrocraft motor driver. The motor driver turns the motor at a rate which is proportional to the voltage difference. The motor in turn drives a worm-screw mechanism that is connected to the lever arm which applies the vertical load to the sample. Consequently, the vertical load acting on the sample can be automatically changed in response to changes in the sample height. Although the system is fairly efficient, a small change in height is required to activate the system. It is a closed loop analog feedback system, which is shown schematically in Figure 3.5. The control box was built by Dr. John T. Germaine, Principal Research Associate and MIT's Geotechnical Laboratory Director.

The system does not correct for the apparatus compressibility during shear. This can be done manually by gradually adjusting the reference voltage of the constant height DCDT according to the vertical stress acting on the sample and the load deflection curve (i.e., apparatus compressibility) of the device. However, this is not typically done as a standard procedure. The variation in the sample height during

shear is recorded by the vertical displacement DCDT. Chapters 6 and 7 discuss the measured vertical deformation during shear for all the CK UDSS tests performed for this research. The measured sample deformation indicate an average sample deflection, at peak shear resistance, of +0.095% (compression) and -0.10% (expansion) of the pre-shear sample height for normally consolidated and overconsolidated samples of BBC, respectively (Figures 6.5 and 7.5). The measured vertical deflection during shear is considered very small for clays and therefore ignored. However, this amount of deflection would lead to a significant error in undrained tests on sand specimens.

Transducer readings during consolidation and shear are recorded by MIT's central data acquisition system. The latest version of this system was installed in August 1988. It consists of an NEC APCIV Power Mate 1 personal computer (IBM PC/AT compatible) and Hewlett Packard # 3497A data acquisition control unit. All readings are triggered and taken by the central data acquisition's main software program and are subsequently transferred to 5 1/4 in. floppy disks for reduction and plotting. The data reduction program used for this research was written by Dr. Germaine.

Corrections are made to the measured data for apparatus compressibility during consolidation and for piston friction and membrane resistance during undrained shear. All consolidation displacements are corrected using the load deflection relationship for the apparatus as the data are being reduced for each consolidation increment. The measured horizontal resistance of a sample during undrained shear is corrected for piston friction and membrane resistance using the following equation:-

$$\text{Shear Resistance Correction (ksc)} = 0.004 + 0.00075 (\gamma \text{ in percent}) \quad (3.1)$$

In the above equation, the first part represents the frictional component and the second part represents the membrane resistance.

3.3 Experimental Procedures

The clay samples for this research came from batches of resedimented BBC. Chapter 4 summarizes the batching procedures and engineering properties of the test soil. This section describes the procedures used for undrained shear testing of cohesive soils in the Geonor DSS apparatus. The experimental procedures can be divided into three stages; preparation and setting— up of sample in the device, K_0 —consolidation of sample, and shearing of sample under constant volume conditions.

Each specimen of BBC is unwrapped from its aluminum foil cover and protective wax coating and trimmed in MIT's humid room (About 15 to 20 gm of soil are taken from corners of the specimen for 3 to 4 water content measurements by drying overnight in a forced draught oven maintained at 105 C°). The sample is then carefully placed on the bottom pedestal and into the Geonor trimming frame which holds and aligns the cutting ring and sample membrane. The edges of the sample are trimmed using the Geonor cutting shoe and a surgical knife. The sample is trimmed into a circular shape of 35 cm² area. The cutting shoe allows the top and bottom of the sample to be smoothly trimmed with a wire saw to an approximate height of 2.3 cm. The sample is then transferred to the testing laboratory where a vacuum pump is used to place the wire reinforced rubber membrane around it. The top cap is placed on the sample before the vacuum is released. At this stage the sample height is measured with a micrometer and vertical and horizontal load cell zero readings are taken. The sample is then assembled in the device and immediately a seating load is applied to the sample. The DCDT zero readings are then recorded.

Vertical consolidation increments are applied to the sample through application of dead weights on the vertical loading system lever arm. The sample is consolidated to 0.125 ksc before adding water to the bath. Consolidation continues using a load increment ratio between 0.75 and 1.0 to obtain the desired stress history and final stress state. The time—deformation data are recorded by the data acquisition system

for each consolidation increment and can be simultaneously plotted for consolidation analysis. The consolidation increments are left on the sample usually between the end of primary and 24 hours. The maximum consolidation stress (and also the final consolidation stress for the overconsolidated samples) is applied for approximately 24 hours to allow at least one cycle of secondary compression prior to undrained shear.

On completion of K_0 -consolidation, the sample is sheared under constant volume conditions. The constant height DCDT is placed in its position adjacent to the sample and the control box is turned on and allowed to warm up for about 30 minutes. The vertical loading lever arm is pinned in place and dead loads are removed. The Electrocraft motor is connected to the worm-gear which controls the force acting through the lever arm thereby allowing the vertical stress to be changed in response to changes in the sample height. At this stage the motor is turned on and a horizontal shear stress is applied at a constant strain rate of approximately 5% per hour. All the transducer readings are taken by the data acquisition system at a specified interval.

At the end of undrained shear, the pin holding the vertical loading lever arm is removed and a seating load is applied to the sample. The sample is then brought back to its pre-shear configuration and allowed to sit overnight. The following day the sample is removed from the device and a final water content is taken (however, the final water content is not equal to the water content during undrained shearing due to post shear vertical straining).

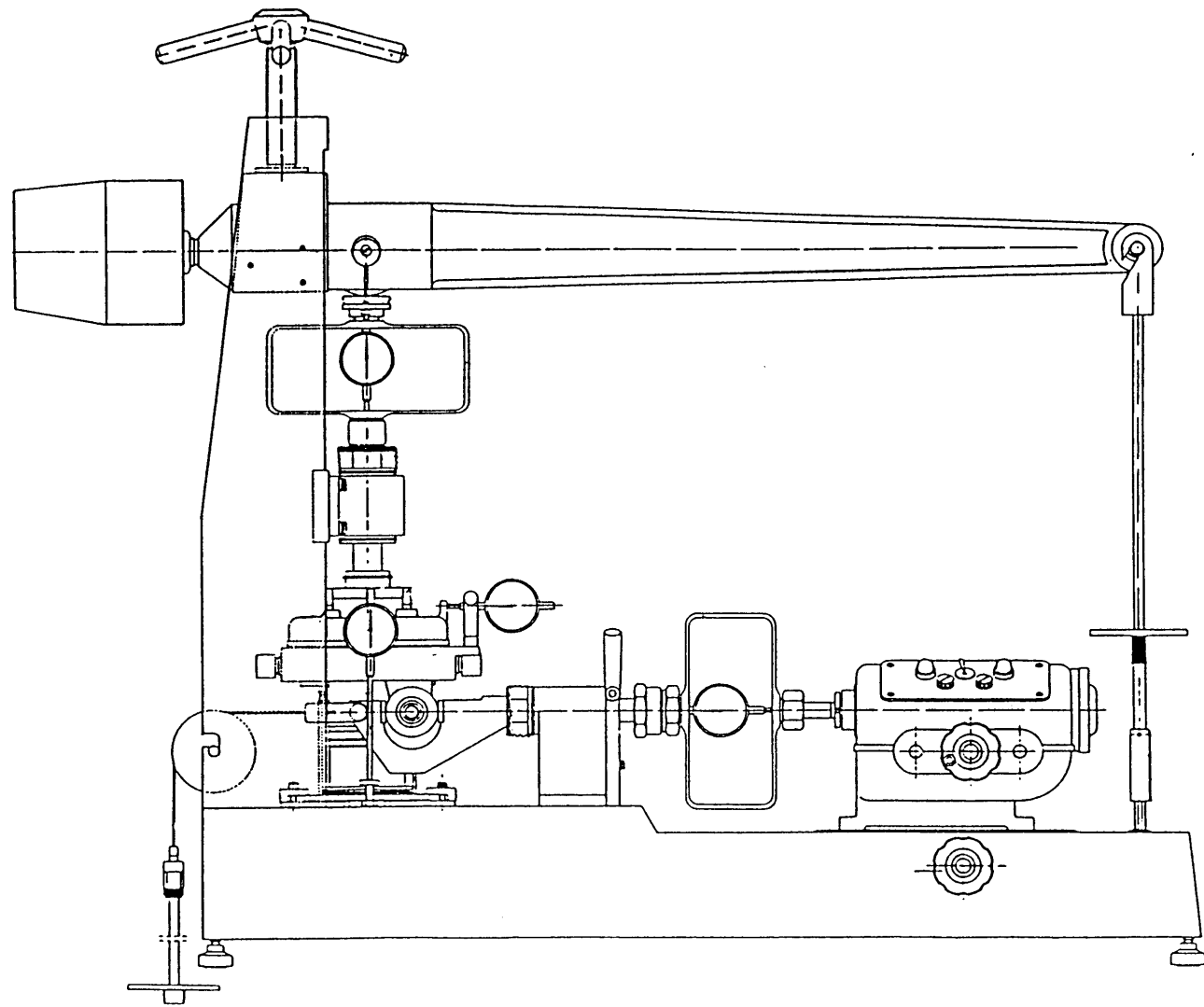


Figure 3.1: Geonor Model 4 Direct Simple Shear Device (Geonor DSS Manual)

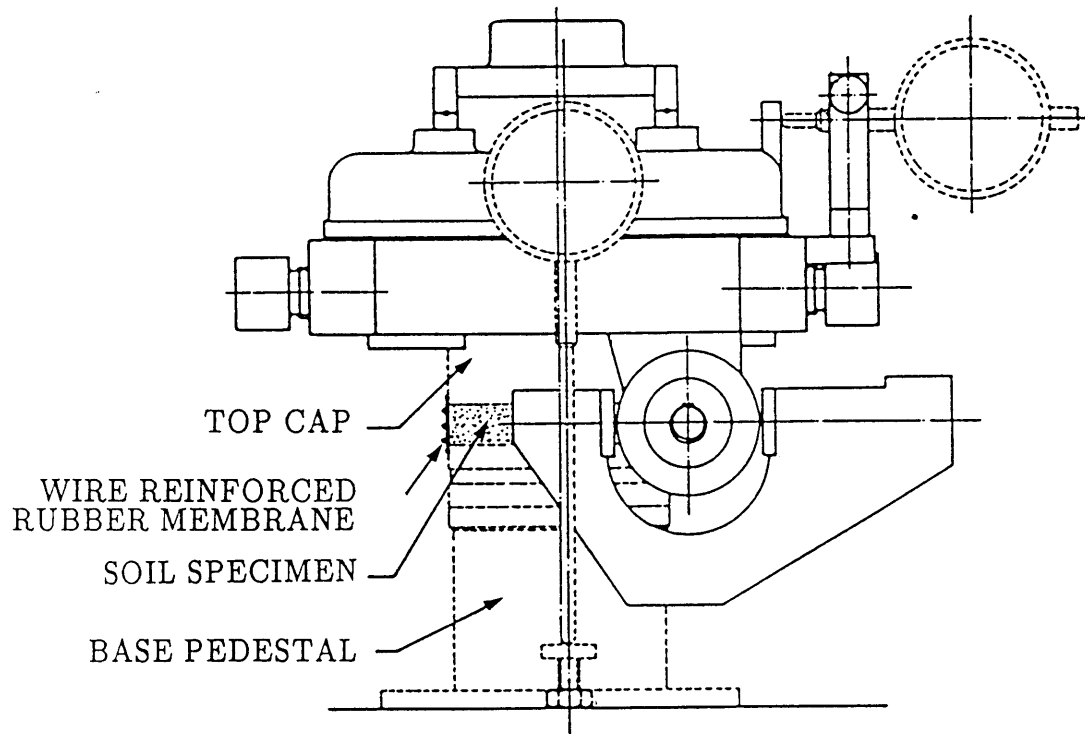


Figure 3.2 Sample Assembly of Geonor Model 4 Direct Simple Shear Apparatus
(Geonor DSS Manual)

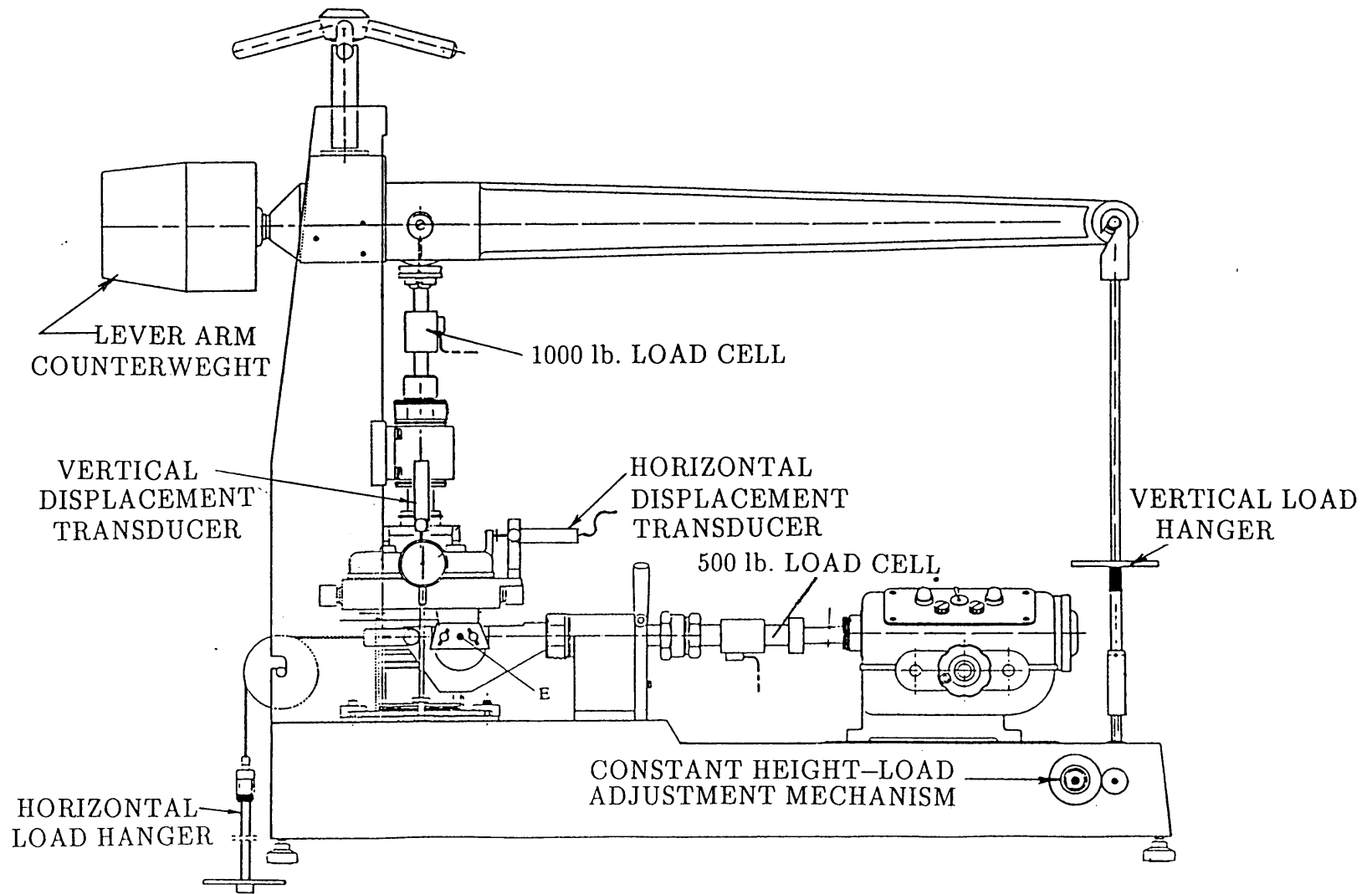
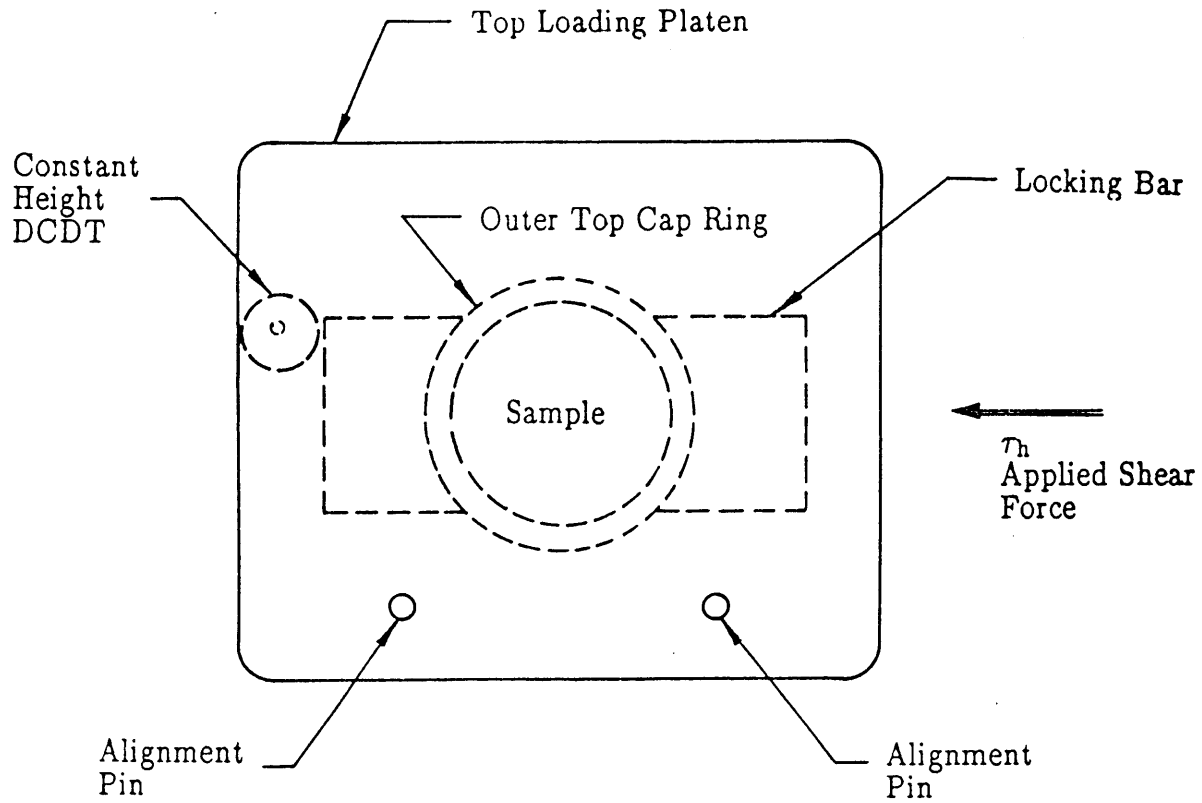


Figure 3.3 Schematic Diagram of the Modified Geonor Model 4 DSS Apparatus



Plan View

Scale Approx. $1/2'' = 1''$

Figure 3.4 Location of Constant Height DCDT in the Geonor DSS Apparatus
(From DeGroot, 1989)

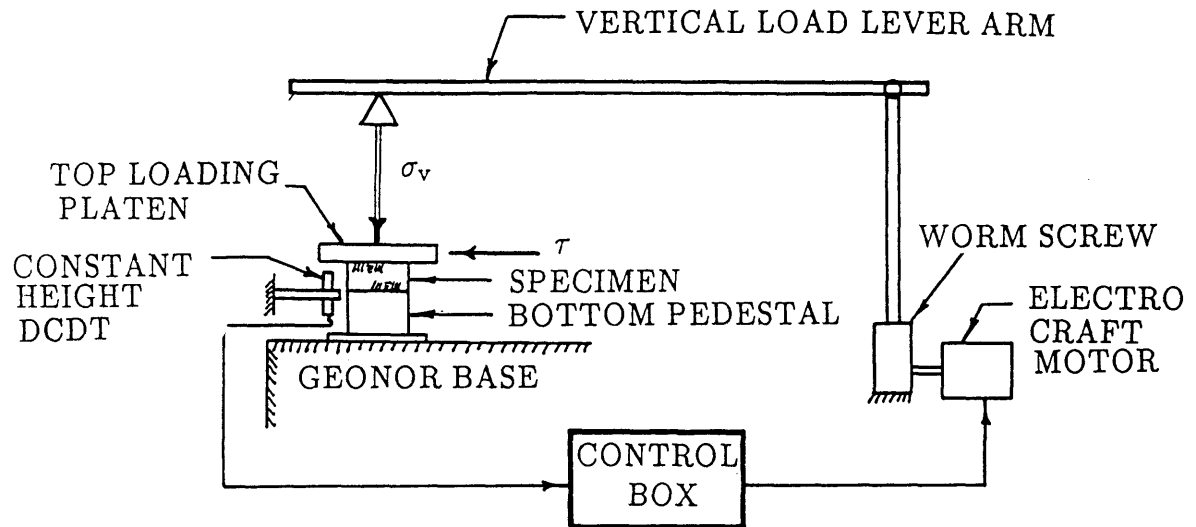


Figure 3.5 Schematic of Geonor Constant Height Servo Control System

(From DeGroot, 1989)

CHAPTER 4

TESTING MATERIAL AND LABORATORY TESTING PROGRAM

4.1 Preparation and Engineering Properties of Testing Material

Experimental parametric and material behavior studies require that soil samples be uniform (e.g., have identical basic index properties such as grain size and Atterberg limits) and have a well defined stress history. Natural soil samples, besides being difficult to procure, rarely meet these requirements. Careful consideration of various factors, namely: supply of samples, quality of samples (Germaine, 1982; Seah, 1990), and availability of prior data on the material (e.g. Ladd and Edgers, 1972) lead to the conclusion that the research objectives could best be accomplished by using reconstituted samples of Boston Blue Clay.

Boston Blue Clay is an illitic glacio-marine clay of low to medium sensitivity deposited in the Boston Basin approximately 12,000 to 14,000 years ago (Kenny, 1964). Development in Boston and its environs provided opportunities of extensive research on natural BBC at MIT, which stimulated interest in understanding its basic behavior. Spatial variability in the properties of natural material made it difficult to generalize the behavior of soil. The need therefore arose to reconstitute BBC samples under controlled conditions in the laboratory. Wissa (1961) pioneered the technique of resedimentation of BBC which has been modified and significantly improved by subsequent researchers. Germaine (1982) developed the resedimentation technique to produce fully saturated and uniform samples of BBC. The procedure has been further refined and simplified by Seah (1990), as described in the following section.

4.1.1 Preparation of Resedimented Boston Blue Clay III

The BBC III used for this research (called 200 series source material) was obtained from a depth of approximately 75 feet by augering during the construction of

a parking garage on Spring Street behind Kendall Square, Cambridge, Massachusetts (Figure 4.1). The original soil was described as a "medium stiff, grey-green silty clay with occasional partings" (Walbaum. 1988). The index properties of the natural soil were obtained to ensure that the material properties were representative of typical BBC. The soil was then subjected to a process of resedimentation prior to laboratory testing.

The underlying concept of the resedimentation is to mix dry clay with a known volume of water in the laboratory and then one dimensionally consolidate the slurry to a known vertical stress, thus approximately simulating the actual resedimentation process in the ground that took place during the glaciation period. The resedimentation technique broadly comprises processing of natural soil to obtain clean, uniform fine de-aired powder, mixing of soil with other ingredients in right proportion under vacuum to form a uniform dilute slurry and consolidating the slurry in a cylindrical container. The soil cake is then removed from the consolidometer, trimmed into small specimens of required sizes, sealed and stored in a humid room.

The resedimentation process begins by wet sieving the natural soil through a US Standard # 40 sieve to remove any coarse sand, large shells or organic materials in the clay. The soil is then oven dried at 105 C° and subsequently crushed to a fine powder by a ball-grinding process ensuring that at least 95% of the crushed soil should pass through US Standard # 100 sieve to reduce clumps to a reasonably fine state and eliminate all but fine sand size. This ensures consistency in the material size, which is essential to achieve uniformity within the batch, and also facilitates pouring of soil into the mixing chamber. A typical batch of BBC requires 15 kg of oven dried powder clay. The other ingredients are 15 kg of distilled de-aired water to make a slurry at 100% water content, 2 ml of phenol to prevent bacterial growth and some quantity of salt (exact quantity to be determined by measuring the salt concentration of crushed material) to ensure a pore fluid salt (Na Cl) concentration of 16 g/l which is considered

optimum to produce a flocculated clay structure (i.e., to prevent segregation of the soil particles during sedimentation) and yet minimize the potential for severe corrosion of the testing equipment.

The layout of the batching equipment is given in Figure 4.2. A dilute slurry is formed by thoroughly mixing the batch ingredients under vacuum in a plexiglas mixing cylinder. It is then rained through a 1.25 cm diameter nylon tube into a 30 cm diameter sedimentation chamber which consists of a plastic free fall cylinder and a stainless steel consolidometer. The slurry is incrementally consolidated in the consolidometer starting from a vertical stress of 0.063 ksc using a load increment ratio of one. Each increment is maintained on the sample until the end of primary consolidation. The last loading increment to one ksc is kept on the sample for one cycle of secondary compression. The sample is then incrementally unloaded to 0.25 ksc (i.e., OCR = 4). The vertical stress of 0.25 ksc is maintained for about four days to ensure complete dissipation of pore pressure before extrusion of the soil cake from the consolidometer.

O'Neill (1985) and Seah (1990) found that the value of K_o (swelling) is 0.9 for BBC at an overconsolidation ratio of four based on lateral stress oedometer and triaxial tests results. This implies that the sample in the consolidometer is almost in a hydrostatic state of stress, which would minimize the disturbance due to release of shear stresses during extrusion. Seah (1990) also evaluated the effects of lubrication on the inner walls of consolidometer prior to pouring the slurry. It was found that application of a thick grease layer (greater than 1 mm thick) on the inner walls of the consolidometer facilitates extrusion of the soil cake, besides improving the uniformity of the samples and minimizing disturbance.

After the sample is extruded, it is trimmed into different sizes according to the requirements using a wire saw and a special trimming device. Each specimen is then protected and sealed to prevent any damage or loss of water by coating it with a 50–50

mixture of paraffin and petroleum jelly, wrapped in a plastic wrap, another wrap of wax coated aluminum foil and a final thick layer of wax. During the entire process of trimming and wrapping, the specimens are handled very carefully using glass plates to minimize disturbance. The sealed specimens are then stored in a humid room which is maintained at 95% to 100% relative humidity.

Germaine (1982) evaluated the quality of resedimented BBC samples prepared by the procedure described above. Uniformity of individual batches was confirmed by measurement of the variation in water content with depth, x-ray diffraction pattern on different samples and the absence of stratification on air dried vertical slices. Seah (1990) also verified uniformity within a batch by conducting hydrometer analyses at varying depth which indicated no sign of particle segregation in the resedimented clay. Seah (1990) reported extensive reference tests to quantify the batch to batch variability of the resedimented BBC. Comparison of index properties (water content and Atterberg limits), preconsolidation pressures and general consolidation characteristics indicated little variation among the various batches. Unconsolidated-undrained triaxial compression tests were performed on different batches to check the degree of saturation. Measurements of Skempton's pore pressure parameter B indicated full saturation, which was further verified by measurements of phase quantities (i.e., measurement of water and soil weights and total volume of specimens). The results of the measured initial effective stress of the sample and consolidation strain data revealed some disturbance, which might have been caused during initial extrusion/trimming or during setting up of test samples despite the careful preparation procedure.

O'Neill (1985) confirmed by extensive laboratory testing that resedimented BBC II exhibited changes in strength and compressibility as the time of storage between batch preparation and testing is varied. This phenomenon was attributed to the thixotropic nature of the material. She found that the susceptibility of the material

to thixotropy (defined by Mitchell, 1976; as " an isothermal, reversible, time dependent process occurring under conditions of constant composition and volume whereby a material stiffens while at rest and softens or liquefies upon remolding ") can be detected based on measured increases in preconsolidation pressure with storage time. Seah (1990) conducted oedometer tests on samples of resedimented BBC III with varying storage time to examine the possibility of any thixotropic hardening. Based on tests results, which indicated no change in preconsolidation pressure with time, it was concluded that BBC III is a non-thixotropic material.

It takes approximately 3 to 4 weeks to prepare a batch of BBC, which typically yields two specimens for Directional Shear Cell, 12 to 16 DSS/oedometer specimens and four triaxial specimens. Resedimentation of BBC, though expensive in terms of labor and time, enjoys several advantages over field samples. One can produce a large quantity of high quality, uniform, saturated samples, with a known stress history. The resedimented samples of BBC III exhibit behavior which is non-thixotropic as opposed to BBC II. Thus the resedimentation procedure is considered extremely useful for research purposes.

4.1.2 Summary of Soil Properties

The new 200 series BBC is being extensively used for research at MIT. The author and his contemporary researchers at MIT have used specimens from Batch 200 to 207 for various testing programs. Table 4.1 summarizes the results of specific gravity, water content, Atterberg limits, clay fraction and salt concentration tests performed on the soil samples from Batch 200 to 207. These tests provide an important check on the uniformity of the batches. The results indicate very little variation among the different batches of resedimented BBC III.

Tables 4.2 and 4.3 contain a summary of the results of batch consolidometer and oedometer tests performed on various batches of BBC III. Besides the information

about test specimens (i.e., initial height, initial water content, initial void ratio etc.), the tables summarize the computed preconsolidation pressures (σ'_p), compressibilities for various stress ranges and permeability change index, C_k (computed based on the relationship, $C_k = \frac{\Delta e}{\Delta \log(k)}$; where, Δe = change in void ratio and k = coefficient of permeability). The consolidation results indicate little variation among the various batches in terms of compressibilities (C_c , C_r and C_s), with preconsolidation pressures fairly close to the applied values from the large consolidometer tests. The compression index, C_c , decreases with increasing vertical effective stress (σ'_v) from a C_c value of about 0.56 at $\sigma'_v = 0.2$ ksc to a C_c value of about 0.45 at $\sigma'_v = 0.8$ ksc (Table 4.2). A similar trend is observed from oedometer tests on specimens of BBC (Table 4.3). The samples of resedimented BBC used for this research came from Batch 204, 205 and 207. Figure 4.3 is a plot of the compression curves for four oedometer tests performed on batches of resedimented BBC III used for this research. The curves show good agreement in the consolidation results from various batches. The detailed consolidation behavior of BBC III is discussed in the subsequent chapter.

Table 4.4 summarizes the results of eight unconsolidated–undrained triaxial compression tests with pore pressure measurements performed on the samples from resedimented BBC III. The tests were mainly performed to check the degree of saturation. The results of all the tests indicate a "low" initial effective stress of the samples which implies some sample disturbance (ideally, the measured effective stress of the undisturbed soil specimens should be equal to the average effective stress of the soil in the consolidometer during the last load increment, i.e., 0.25 ksc for $K_o = 1$). The measured values of Skempton's pore pressure parameter B (B is equal to one for all the tests) indicate that the samples were fully saturated.

There are three different series of resedimented BBC used for research at MIT during the past three decades. Comparison of index properties of these series (Table 4.5) reveals a fairly consistent value of specific gravity, G_s , (ranging from 2.75 to 2.78)

while a greater scatter is observed in Atterberg limits, especially among old batches. The variation in Atterberg limits is related mainly to change in the liquid limit (35–45%), whereas the plastic limit generally remains constant (20–23%).

Extensive research has been conducted at MIT on resedimented BBC II and BBC III series during recent years. Table 4.6 summarizes the properties of BBC II, BBC III, and natural BBC (Ladd and Luscher, 1965) in terms of index properties, consolidation characteristics and some normally consolidated undrained strength parameters. The comparison reveals small differences between the two series of resedimented BBC for index properties, consolidation characteristics (except for coefficient of consolidation, which is significantly higher for BBC II and the effect of thixotropy on the consolidation behavior of BBC II) and normally consolidated undrained strength parameters. The most important difference between the series, as discussed earlier, is that BBC II exhibits thixotropic behavior while BBC III is non-thixotropic. The comparison with natural BBC show good agreement in various parameters, with the exception of coefficient of consolidation, which makes the resedimented clay very useful for studying realistic behavioral trends. It is, therefore, "strongly advised to recycle the BBC III, since this batch of clay has properties representative of the natural material. Furthermore, this clay is non-thixotropic and has a small rate of secondary compression which is ideal for research purposes" (Seah, 1990).

4.2 Laboratory Testing Program

The laboratory testing program was formulated to accomplish the research objectives set forth in Chapter One. The experimental program on samples of resedimented BBC consisted of four constant rate of strain consolidation (CRSC) tests, five K_0 -consolidated-undrained direct simple shear (CK_0UDSS) tests on normally consolidated soil, and six CK_0UDSS tests on overconsolidated soil. The results of these

tests are presented and discussed in chapters 5, 6 and 7.

The CRSC tests were performed using the general purpose consolidometer developed at MIT by Wissa et al. (1971) with a view to obtain well defined compression curves for comparison of general consolidation characteristics of resedimented BBC with CK_0UDSS consolidation results. All the samples were loaded at a constant rate of strain to a maximum vertical consolidation stress of about 20 ksc (i.e., the maximum vertical consolidation stress which can be achieved with a sample of area 31.6 cm^2 using MIT's general purpose consolidometer) and then unloaded to about 0.40 ksc. CRSC Tests No. 1 and 2 were also rebounded from a vertical stress of about 4 ksc to 0.40 ksc before reloading to the maximum vertical consolidation stress. At the end of each loading/unloading all the samples were equilibrated for 24 hours at constant vertical stress before they were rebounded/reloaded. The loading program of each test is given in Table 4.7.

CK_0UDSS tests were performed on normally consolidated samples of resedimented BBC using MIT's Geonor Model 4 DSS apparatus. The main objective of these tests was to investigate the normalized undrained shear behavior of normally consolidated samples under variable consolidation stresses. The minimum vertical consolidation stress was chosen as 1.5 ksc (i.e., $1.5 \times$ preconsolidation pressure of clay, $\sigma'_p = 1 \text{ ksc}$. This is the minimum vertical consolidation stress recommended by Ladd and Foott, (1974) to obtain normally consolidated behavior as being 1.5 to 2 times the preconsolidation pressure of the soil to reduce the adverse effects of the sample disturbance). The maximum stress was about 12 ksc based on the capacity of the wire reinforced rubber membrane which prevents lateral straining of the sample. All the samples were subjected to undrained shear by keeping the volume of the samples constant. The undrained shear was applied at a constant rate of strain of approximately 5 % per hour (as recommended by Ladd and Edgers, 1972 and Ladd and Foott, 1974). Table 4.8 gives an overview of CK_0UDSS testing program on normally

consolidated samples of resedimented BBC III.

In the subsequent phase of the DSS testing program, samples were consolidated well beyond the batch maximum past pressure to investigate the undrained shear behavior of resedimented BBC at different OCR's along the swelling curve. Five CK_0 UDSS tests were performed with a maximum past pressure of about 12 ksc at OCR's ranging from 1 to 32 (maximum OCR of 32 was selected keeping in view the minimum vertical stress required to prevent sliding between the top cap and the sample). One CK_0 UDSS test was performed at an OCR of 8 with a maximum past pressure of 3 ksc to determine the influence of maximum past pressure on the undrained shear behavior of overconsolidated samples of resedimented BBC. All the samples were subjected to undrained shear in the manner as described above. A summary of the tests conducted on overconsolidated samples of resedimented BBC is contained in Table 4.9.

Table 4.1: Index Properties of resedimented BBC III (from Seah, 1990)

Batch Number	σ'_{vm} * (ksc)	σ'_p † (ksc)	w (%)	LL (%)	PL (%)	PI † (%)	LI †	Clay Fr. <2 μ , (%)	Salt Conc. g/l	Remarks
(Ground)	-	-	-	44.90 ±0.14	22.45 ±0.07	22.45	-	52.1 ±4.1	1.98(g/kg) ±0.10	G _s = 2.785 (97% passed S. No.100)
200	1.00	1.04(3) ±0.04	41.10 ±0.80	45.90	21.95 ±0.35	23.95	0.80		22.13 ±2.02	
201	1.00	0.98(1)	39.42 ±1.90	44.82	21.19 ±0.35	23.63	0.77	57.6 ±1.1	14.53 ±1.43	
202	1.03	0.99(2) ±0.02	40.67 ±0.40	45.46	22.27 ±0.62	23.19	0.79		15.05 ±0.95	
203	1.00	1.00(1)	40.70 ±0.50	44.50	21.18 ±0.58	23.32	0.84		15.90 ±3.20	
204	1.01	0.97(2) ±0.02	40.19 ±0.40	45.60	21.47 ±0.58	24.13	0.78		13.63 ±3.02	
205	1.00	1.00(2) ±0.00	40.66 ±0.27	45.01	21.62 ±0.63	23.39	0.81		15.69 ±3.65	
206	0.98	0.98(2) ±0.00	41.24 ±0.30	45.17	22.10 ±0.64	23.07	0.83		17.38 ±2.52	
207	1.00	1.00(1)	40.75 ±0.10	45.12	22.15 ±0.57	22.97	0.81		16.25 ±1.73	
Mean, S.D.	-	-	40.59 ±0.57	45.20 ±0.44	21.74 ±0.44	23.46 ±0.42	0.82 ±0.02		16.34 ±2.60	

Notes: * Maximum applied vertical stress in the batch consolidometer.
 † Preconsolidation pressure obtained from Casagrande Construction method.
 ‡ Calculated from the mean.
 No Standard Deviation means one measurement only.

Table 4.2: Results of Batch Consolidometer Tests for Resedimented BBC III
(from Seah, 1990).

Batch No.	H_c^* (cm)	w_c^\dagger (%)	e_c^\ddagger	σ'_{vm}^* (ksc)	C_c (stress range, ksc)			C_s (stress range, ksc)		C_k from e- lgk	Remarks
					0.125-0.25	0.25-0.50	0.50-1.00	1.00-0.50	0.50-0.25		
200	10.272	41.10	1.145	1.00	0.482	0.509	0.409	-	0.010	0.686	
201	13.490	39.42	1.100	1.00	0.641	0.419	0.522	0.010	0.020	0.748	low w_c
202	13.822	40.67	1.132	1.03	0.568	0.453	0.453	0.011	0.006	0.813	
203	13.757	40.70	1.133	1.00	0.568	0.608	0.518	-	-	0.928	
204	13.238	40.19	1.119	1.01	0.512	0.487	0.463	-	-	0.676	
205	13.682	40.66	1.132	1.00	0.661	0.508	0.402	-	-	0.772	
206	11.646	41.24	1.148	0.98	0.548	0.439	0.416	0.023	0.025	0.728	
207	14.624	40.75	1.135	1.00	0.477	0.412	0.409	0.023	0.023	0.659	
Mean S.D.	-	40.59 ±0.57	-	-	0.557 ±0.068	0.479 ±0.064	0.449 ±0.049	0.017 ±0.007	0.017 ±0.008	0.751 ±0.088	

Notes:

- * Final measured sample height.
- † Final water content from Table 4.1.
- ‡ Final void ratio computed based on $G_w = S_e$, assuming $S = 1$.
- * Maximum applied vertical stress.

Table 4.3: Results of Oedometer Tests on Samples from Batches of BBC III
(from Seah, 1990)

Sheet 1/2

Test No.	Batch Label	Age t_s (days)	e_i	w_i^5 (%)	σ'_p (ksc)	CR (stress range, ksc)			RR 8-2-8	SR 16-2	$\frac{RR}{SR}$	$\frac{CR^\dagger}{RR}$ OCR=4	C_k from e-1gk
						1-2	2-4	4-8					
1	200-1 ¹	23	1.127	40.47	1.05	0.187	0.162	0.141	0.012	0.015	0.76	11.8	0.44
2	200-2	24	1.179	42.33	1.08	0.152	0.173	0.139	0.010	0.018	0.54	13.9	0.49
3	200-3	79	1.160	41.66	1.00	0.187*	0.154	0.138	0.015	0.015	1.06	9.2	0.43
4	201	1	1.168	41.94	0.98	0.147*	0.165	0.138	0.012	0.016	0.77	11.5	0.57
5	202	9	1.164	41.80	0.98	0.159*	0.165	0.154	0.012	0.018	0.67	12.8	0.50
6	202-D ²		1.133	40.70	1.00		0.189†						0.30
7	203-D		1.139	40.90	1.00		0.183†						0.33
8	204-T ³	61	1.135	40.76	0.98	0.176*	0.156	0.152	0.025	0.010	2.45	6.1	0.45
9	204-B ⁴	61	1.127	40.47	0.95	0.182*	0.155	0.165	0.008	0.015	0.55	20.6	0.55
10	205-T	248	1.115	40.03	1.00	0.156*	0.159	0.142	0.012	0.013	0.93	11.8	0.49
11	205LS0	257	1.115	40.04	1.00	0.172*	0.164	0.135	0.011	0.020	0.55	12.5	0.49

Table 4.3 (Cont.)

Sheet 2/2

Test No.	Batch Label	Age t_s (days)	e_i	w_i (%)	σ'_p (ksc)	CR (stress range, ksc)			RR	SR	$\frac{RR}{SR}$	$\frac{CR^\dagger}{RR}$ OCR=4	C_k from e-1gk
						1-2	2-4	4-8					
12	206-T	1	1.147	41.18	0.98	0.134	0.150	0.145	0.013	0.015	0.88	11.2	0.47
13	206-B	1	1.145	41.11	0.98	0.139	0.156	0.155	0.014	0.016	0.88	11.1	0.57
14	207-T	40	1.114	40.00	1.00	0.132*	0.159	0.152	0.016	0.017	0.96	9.5	0.50
Mean S.D	-	-	-	-	-	0.160 ±0.020	0.164 ±0.011	0.146 ±0.009	0.013 ±0.004	0.016 ±0.002	0.92 ±0.51	11.8 ±3.4	0.47 ±0.08

- Note:
- ¹ Test Number on the Batch.
 - ² Results obtained from DSS consolidation.
 - ³ Specimen taken at the top of the Consolidometer.
 - ⁴ Specimen taken at the bottom of the Consolidometer.
 - ⁵ Based on average of 3 to 4 measured water content.
- CR taken from 1.2-2 ksc load increment.
[†] CR taken from 4-8 ksc load increment.
[‡] CR taken from 1.5-3 ksc load increment.

**Table 4.4: Unconsolidated-Undrained Triaxial Compression Tests on Resedimented BBC III
(from Seah, 1990)**

Test Number	Batch Number	Initial W_c (%)	σ'_s * (ksc)	B value	S_u (ksc)	ϵ_a (%) at Failure	Type of Failure	Remarks
1	203	41.0	0.125	1.00	0.175	2.1	Bulge	
2	204	40.5	0.068	1.00	0.083	1.2	Wedge†	low u_c
3	204	41.0	0.110	1.00	0.171	2.4	Bulge	
4	205	41.0	0.037	1.00	0.121	1.2	Wedge†	low u_c
7	206	41.0	0.113	1.00	0.202	4.0	Bulge	
8	207	40.8	0.060	1.00	0.112	1.5	Wedge†	low u_c
9	205	40.5	0.138	1.00	-	-	-	Half Height Sample
10	207	40.5	0.121	1.00	-	-	-	Half Height Sample

Notes:

* Initial effective stress.

† Distinct rupture surface.

**Table 4.5: Index Properties of the Different Batches of Resedimented BBC
(after Fayad, 1986; from Seah, 1990)**

Year	Researchers	Series	Source Batch	G _s	LL (%)	PL (%)	PI (%)	Clay Fr. <2μ (%)	Salt (g/l)	Remarks	
1961	Bailey	Ia	MIT 1139	2.77	30.0 34.7	17.5 17.7	12.5 17.0	40	2-3 35	Low PI	
1963	Jackson				36.2	19.5	16.7		16.7	Low PI	
1964	Varallyay		S4 S5 S6			32.6 33.3 32.8	19.5 20.4 20.3	13.1 12.9 12.5	35	16.8 16.0	Low PI
1965	Ladd R.S.	Ib		2.77	45	22	23		16		
1965	Preston		S1	2.77	45.6	23.4	22.2	35	24		
1966	Braathen		S2	2.77	45.4	23.1	22.3		22		
1967	Dickey				34.5	23.9	19.6				
1970	Kinner			100	2.78	43.5	19.6	23.9	50	8	
				150		43.5	19.6	23.9			
			200	38.1		17.8	20.3	52	10		
			300	39.7		21.6	18.1				
			400	39.4		21.3	18.1	52	10		
			800	41.5		19.5	22.0	48	16		
			900	41.2		18.7	22.5	54	16		
	1000	41.1	19.5	22.6	58	16					
	1100	42.0	20.6	21.4		16					

Table 4.6: Comparison of Experimental Data Between the Resedimented Boston Blue Clay and Natural Boston Blue Clay (from Seah, 1990)

Experimental Parameters		Resedimented BBC III	Resedimented BBC II*	Natural BBC (MIT Campus)†
Index Properties	G_s	2.78	2.78	≈ 2.75
	LL(%)	45.2±0.4 (8)	41.3± ? (5)	44.4±5.4 (18)
	PL(%)	21.7±0.4 (8)	22.1± ? (5)	22.6±2.8 (18)
Consolid. Properties	C_c	0.34±0.02(12) ¹	0.33±0.02 (7)	0.37±0.08(30)
	C_r	0.03±0.01(12) ²	0.03±0.001(2)	0.06±0.02(13)
	C_s	0.03±0.01(12) ³	-	0.06±0.01(30)
	$C_v(4-8)$ (cm ² /s)	0.0024 ±0.0005(12)	0.004 ± ? (7)	0.0095 ±0.0030 (4)
Triaxial (CK ₀ UC) OCR = 1	S_u/σ'_{vc}	0.318±0.008(3)	0.317±0.004(2)	0.32±0.01 (2)
	ϵ_a (%)	0.147±0.029	0.183±0.023	0.28±0.11
	A_f	0.44±0.09	0.53±0.04	0.55±0.04
Triaxial (CK ₀ UE) OCR = 1	S_u/σ'_{vc}	0.135 (1)	0.156 (1)	0.143 (1)
	ϵ_a (%)	14.3	13.5	11.6
	A_f	1.16	1.14	1.16

Notes:

* Data from O'Neill (1985)

† Data from Ladd & Luscher (1965)

¹ Values taken from a stress of 4-8 ksc

² Values taken from a stress of 2-8 ksc

³ Values Taken from a stress of 16-2 ksc

Parathesis = number of tests.

Table 4.7: Loading Programs of Constant Rate of Strain Testing

Test Number	Batch Number	t_s^1 (Days)	w_c^2 (%)	Rate of Strain (Per Second)	Loading Program
CRS-1	204B ⁴	403	39.58	2.26×10^{-6}	Loaded at constant rate of strain to 4 ksc then rebounded to 0.40 ksc before reloading to 20 ksc. Finally unloaded to 0.40 ksc. Equilibrated for 24 hrs at 4 ksc, 0.40 ksc and 20 ksc vertical consolidation stresses ³
CRS-2	204B	416	39.55	2.27×10^{-6}	Same as CRS Test No.1.
CRS-3	207MT ⁵	61	41.02	2.29×10^{-6}	Loaded at constant rate of strain to 20 ksc, equilibrated for 24 hrs at constant vertical stress and then to 0.4 ksc.
CRS-4	205B	377	39.59	2.02×10^{-5}	Same as CRS Test No. 3.

- Notes:
1. Elapsed time of storage = $t_s - t_r - 5$ (O'Neill, 1985),
 t_r = Date on which sample reconsolidated to $\sigma' = 0.25$ ksc in the laboratory.
 t_c = Date on which the final batch consolidation stress of $\sigma' = 0.25$ ksc was applied
 2. Initial water content.
 3. Some fluctuation in vertical stress occurred due to defective Bellofram and variation in temperature during 24 hours.
 4. Specimen taken at the bottom of the consolidometer.
 5. Specimen taken at the middle top of the consolidometer.

Table 4.8: Overview of CK_0 UDSS Testing Program on Normally Consolidated Samples of BBC III.

Test Number	Batch Number	t_s^1 (Days)	w_c^2 (%)	σ'_{vc}^3 (ksc)	Remarks
DSS 14	207T ⁴	53	40.55	11.992	.d γ /dt = 5% per hour for all tests.
DSS 18	207MB ⁵	75	40.66	9.030	
DSS 22	207MB	85	40.64	5.992	
DSS 25	207B	92	40.78	2.955	
DSS 31	205M	302	40.48	1.441	

- Notes:**
1. As explained under Table 4.7.
 2. Initial water content.
 3. Vertical consolidation stress.
 4. Specimen taken at the top of the consolidometer.
 5. Specimen taken at the middle bottom of the consolidometer.

Table 4.9: Summary of CK_0 UDSS Tests Performed on Overconsolidated Samples of BBC III.

Test Number	Batch Number	t_s^1 (Days)	w_c^2 (%)	Stress History			Remarks
				σ'_{vm}^3 (ksc)	σ'_{vc}^4 (ksc)	OCR ⁵	
DSS 37	205B ⁶	364	39.70	11.407	3.512	3.248	.dy/dt = 5% per hour for all tests.
DSS 40	204T ⁷	540	40.12	11.394	5.798	1.965	
DSS 44	204M	554	39.75	11.420	1.447	7.892	
DSS 48	204T	562	40.21	11.342	0.772	14.692	
DSS 50	204B	570	40.00	2.956	0.379	7.823	
DSS 51	204B	574	39.80	11.897	0.373	31.895	

- Notes:**
1. As explained under Table 4.7.
 2. Initial water content.
 3. Maximum applied vertical effective stress.
 4. Vertical consolidation stress.
 5. $OCR = \sigma'_{vm} / \sigma'_{vc}$
 6. Specimen taken at the bottom of the consolidometer.
 7. Specimen taken at the top of the consolidometer.

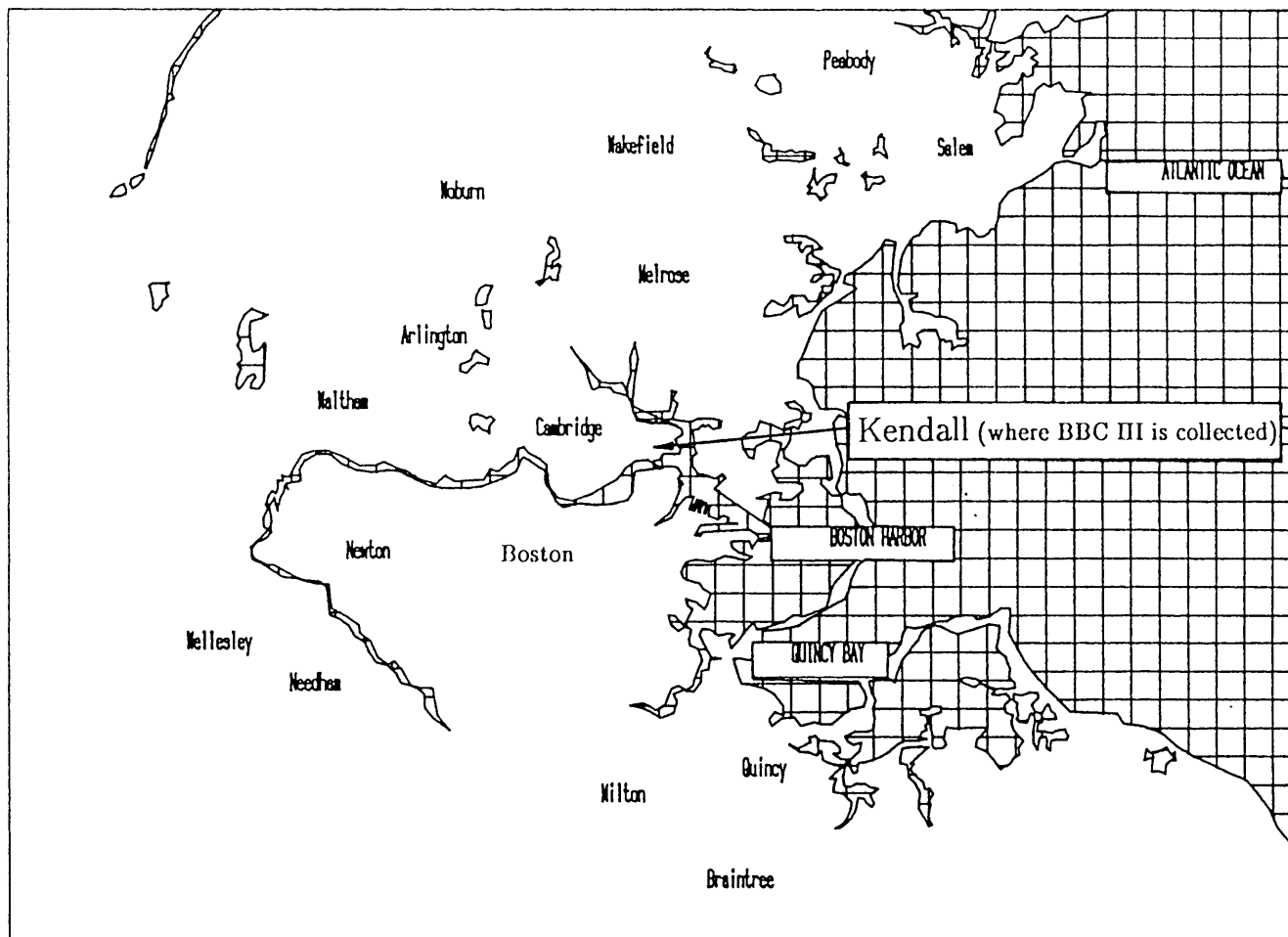


Figure 4.1: Location of the Site from where Boston Blue Clay III was collected
(from Seah, 1990).

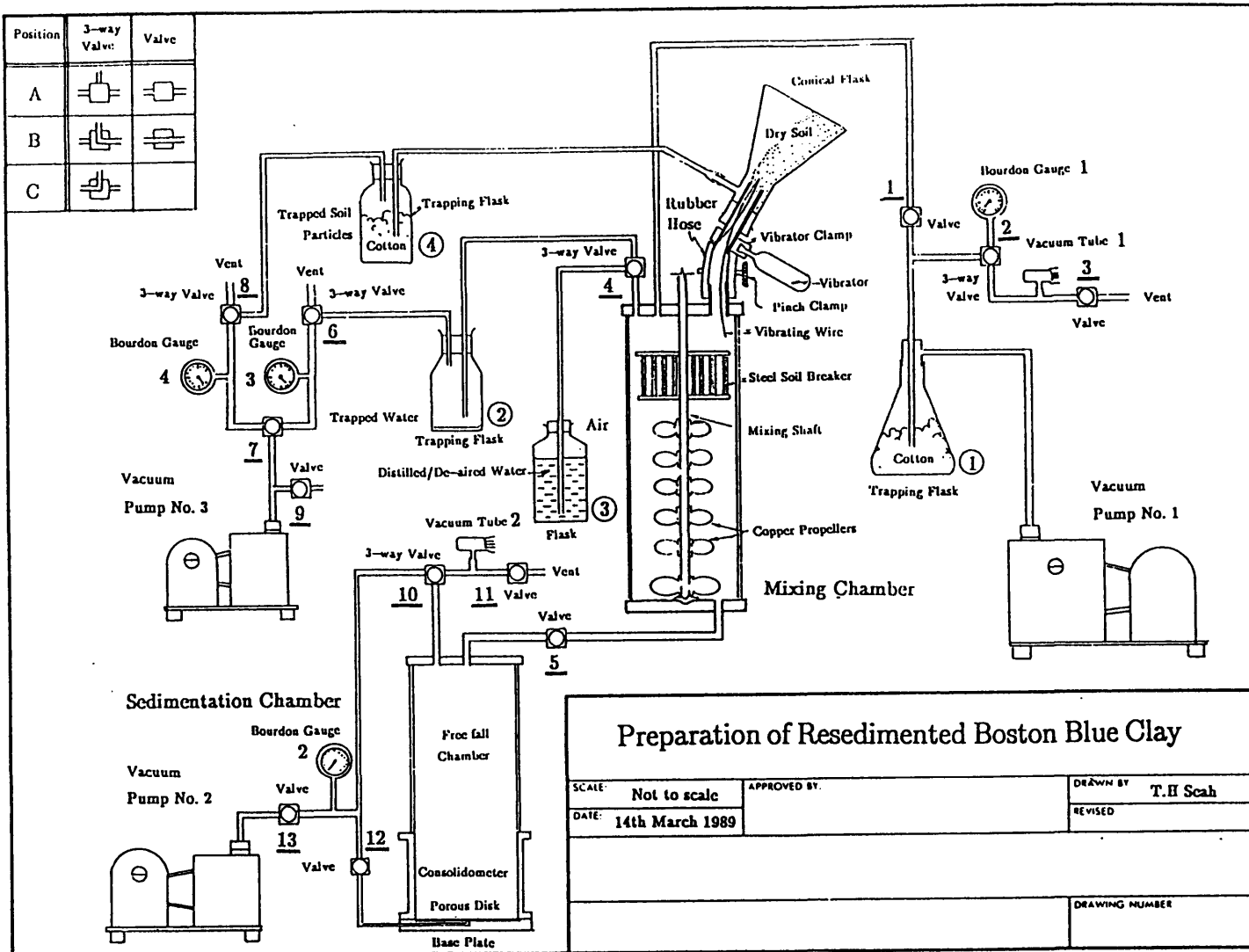


Figure 4.2: Schematic of General Layout (from Seah, 1990).

OEDOMETER TESTS ON BBC III (Batches 204,205&207)

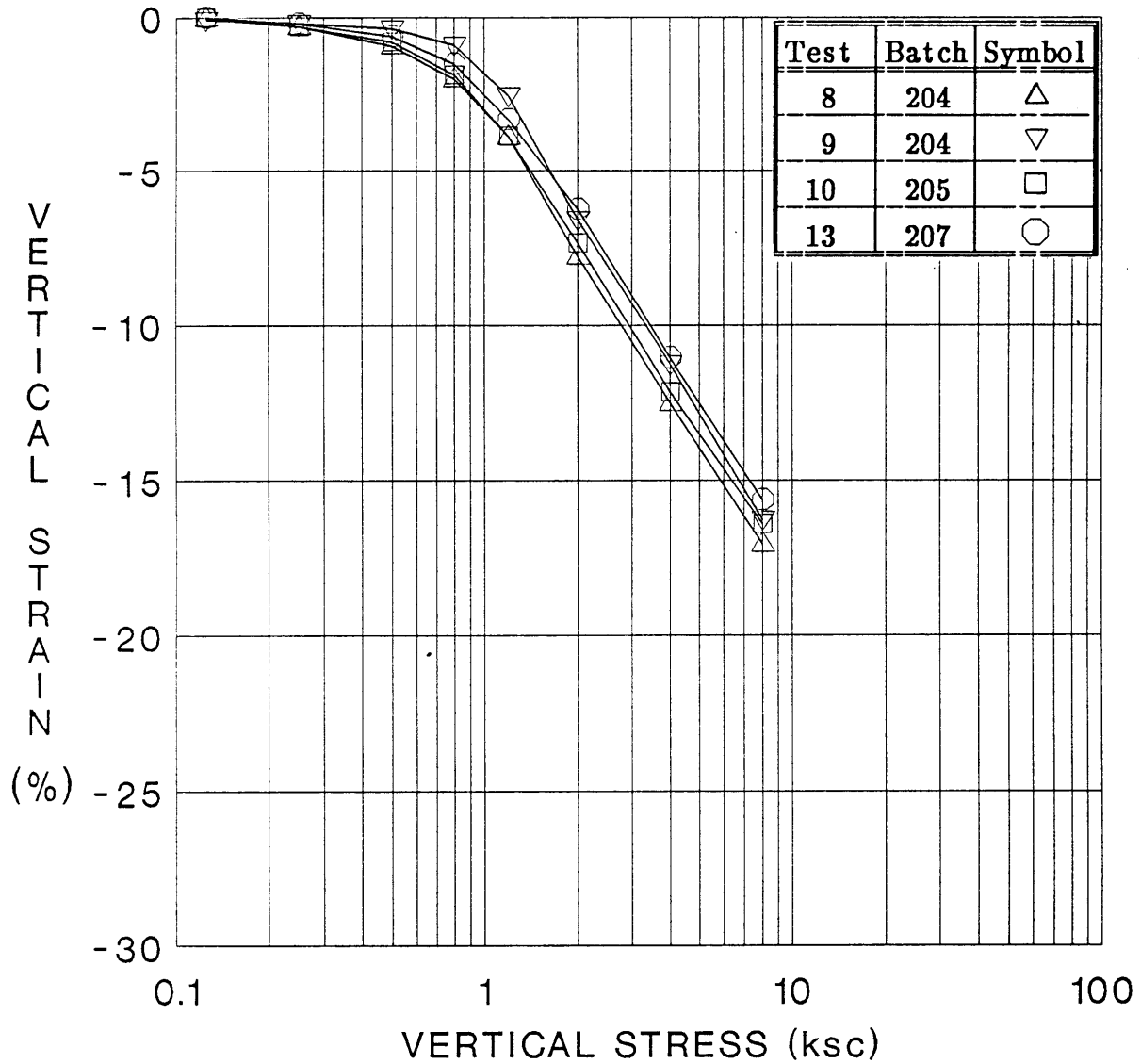


Figure 4.3: Compression Curves (ϵ_v versus $\log \sigma'_{vc}$) from Oedometer Tests on Batch 204, 205 and 207 of BBC III (after Seah, 1990).

CHAPTER 5

CONSOLIDATION BEHAVIOR

5.1 Introduction

MIT's Geonor Direct Simple Shear apparatus was used to perform K_0 -consolidated-undrained shear tests with the intended purpose of investigating the normalized stress-strain-strength behavior of resedimented Boston Blue Clay. The testing equipment and procedures are described in Chapter 3. As part of the SHANSEP (Stress History And Normalized Soil Engineering Properties) testing program, the first phase of the tests consisted of consolidating samples into the normally consolidated range. The maximum consolidation stress (and also the final consolidation stress for the overconsolidated samples) was applied for approximately 24 hours to allow at least one cycle of secondary compression prior to undrained shear. The specimens were unloaded to the desired OCR in the case of tests on overconsolidated samples.

The Geonor DSS has been shown to give the same K_0 -consolidation response as measured in a conventional oedometer test (Ladd and Edgers, 1972; Ladd, 1981; Germaine, 1985). The consolidation data from CK_0 UDSS tests are, therefore, presented and analyzed in this chapter to verify this for the resedimented BBC III. Four constant rate of strain consolidation (CRSC) tests were also performed on samples from the same batches of resedimented BBC in order to obtain well defined compression curves for comparison with CK_0 UDSS consolidation results. Appendix C discusses the consolidation behavior of resedimented BBC in CRSC testing.

The consolidation data obtained from the CRSC tests conducted at standard strain rates compared well with the EOP incremental oedometer compression data on BBC III. The salient conclusions drawn based on the experimental study on consolidation at constant rate of strain for 200 series of Boston Blue Clay are

summarized below:—

- The strain rate best suited for resedimented BBC to be used in CRSC tests in order to obtain the same preconsolidation pressure as obtained from EOP incremental tests is that which results in u_b/σ_v values between 2% to 5%.
- CRS consolidation performed at significantly faster strain rates that result in u_b/σ_v values greater than 5% can result in values of σ'_p which are higher than obtained from oedometer EOP curves.
- Janbu's (1969) method for determining preconsolidation pressure yields much higher values compared to Casagrande's (1936) construction method. Jonas's (1970) technique gives a range of σ'_p values
- The values of virgin compression ratio obtained from "standard" CRSC tests on resedimented BBC III decrease significantly with increase in the consolidation stress and compare well with values obtained from EOP oedometer curves at high stresses. CRSC test conducted at a strain rate approximately 9 times faster than standard test gave a significantly higher virgin compression ratio.
- Standard CRSC tests yield higher coefficient of permeability than those obtained from incremental consolidation tests.

5.2 Presentation of Consolidation Results

The clay samples for this research came from Batches 204, 205, and 207 of resedimented BBC III. Chapter 4 summarizes the batching procedures and the properties of the test soil. Appendix A contains the summary of stress–deformation data for each increment, compression curves for the individual tests and the tabulated data from consolidation phase of the CK_0 UDSS tests. This section will present the

results for the consolidation phase of DSS testing.

The experimental phase of this research was spread over a period of approximately seven months. The specimens from Batches 207, 205, and 204 were tested in that order (see laboratory testing program given in Chapter 4). Although the batching technique produces essentially uniform specimens and very little variability is observed among the various batches (as discussed in Chapter 4), significant variation is observed in the consolidation data obtained from DSS tests on specimens from different batches. It is, therefore, considered more appropriate to present the consolidation results batchwise to evaluate the fundamental cause of variation in the test results.

Tables 5.1, 5.2, and 5.3 contain the consolidation results from DSS tests on Batch 204, 205, and 207, respectively. The consolidation results from all the DSS tests are summarized in Table 5.4. The tables present the following important results:

- The preconsolidation pressure, σ'_p , determined by Casagrande's (1936) construction method. The strain (rather than void ratio) versus $\log \sigma'_{vc}$ plots have been used to determine the values of σ'_p since Ladd and Foott (1974) suggested that ϵ_v versus $\log \sigma'_{vc}$ plots yield more reliable values of preconsolidation pressure.
- The virgin compression ratio (CR), defined as the slope of the strain versus $\log \sigma'_{vc}$ in the normally consolidated region. The values of CR for various stress ranges are given since its value changes with stress level (Seah, 1990).
- Swelling ratio (SR), defined as shown in Figure 5.1, is given for various stress ranges along the swelling curve.
- The rate of secondary compression ($C\alpha\epsilon$), defined as the change in vertical strain per log cycle of time after the end of primary consolidation.

- The ratio of $C\alpha\epsilon/CR$ for comparison of results with the prior data on BBC and the range of values reported for the inorganic clays.

The data are also presented in the form of vertical strain versus $\log \sigma'_{vc}$ plots for comparison. Figures 5.2, 5.3, and 5.4 are the compression curves from the DSS tests on Batches 204, 205, and 207, respectively. Figure 5.5 compares the compression data on vertical strain versus $\log \sigma'_{vc}$ plot for all the DSS tests performed for this research.

5.3 Discussion on the Consolidation Behavior of BBC III

5.3.1 Preconsolidation pressure

The values of preconsolidation pressure, σ'_p , given in Tables 5.1, 5.2, and 5.3 for the DSS tests on Batches 204, 205, and 207, are fairly close to the values actually applied to the large consolidometer (Table 4.2). Table 5.4 compares the average ± 1 SD values of σ'_p determined for DSS tests with the results of the incremental and standard CRSC tests on samples from the same batches of BBC. The values of σ'_p determined from DSS tests are in good agreement with those obtained from the incremental and CRSC tests.

5.3.2 Compression Curves

Figures 5.2 through 5.4 compare the consolidation data using ϵ_v versus logarithm of σ'_{vc} plots for DSS tests on Batches 204, 205 and 207, respectively. The compression curves indicate a remarkable consistency within the tests performed on each batch. The comparison of the consolidation ϵ_v versus $\log \sigma'_{vc}$ plots from all the DSS tests (Figure 5.5) indicate a significant variation among compression curves from tests on Batches 204 and 205 versus 207. In particular, Batches 204 and 205 show considerably more consolidation strains than tests on Batch 207 (e.g., a difference of

approximately 2.5 % at $\sigma'_{vc} \simeq 12$ ksc).

Figures 5.6 and 5.7 are the plots of vertical strain versus logarithm of vertical stress for three Geonor DSS (from Werner, 1990) and four oedometer tests (from Seah, 1990) respectively, performed on the specimens from the same batches of clay. Figures 5.8 through 5.10 compare the batchwise compression curves from DSS tests performed for this research and those obtained from the available data for DSS and oedometer tests (Werner, 1990 and Seah, 1990). The comparison show that:

- the compression curves for the writer's DSS tests on Batch 204 compare well with those performed by Werner, but show more consolidation strains than oedometer tests on the same batch of clay at corresponding stress levels (Figure 5.8);
- in Figure 5.9, the writer's DSS tests on Batch 205 give considerably higher consolidation strains than the oedometer test on the same batch of clay;
- the compression curves in Figure 5.10 from the writer's four DSS tests on Batch 207 compare vary well with the oedometer test, whereas Werner's DSS test on the same batch of clay gives significantly larger consolidation strains than the oedometer test;
- the DSS tests performed for this research on Batch 207 compare very well with the range of compression curves from four oedometer tests on Batches 204, 205 and 207 (Figure 5.11; the small difference observed in the compression curves from the DSS tests and the range of oedometer tests, especially during the initially stages of the tests, is due to the greater seating error in the DSS because of the fixed top cap compared to the oedometer tests in which case the ball seating reduces the error and the error in determining the end of primary by Casagrande's method ,

since the load increments in the DSS tests were generally left for approximately 2 to 6 hours, with the exception of the last increments), whereas DSS tests on Batches 204 and 205 give significantly larger consolidation strains than the DSS tests on Batch 207 and the oedometer tests.

Figure 5.12 shows a remarkable agreement in the compression curves from the DSS tests on Batch 207 and the three CRSC tests on Batches 204 and 207, performed at strain rates which resulted in the values of u_b/σ_v between 2% to 5% in the normally consolidated region. However, the compression curves from the DSS tests on Batch 204 and 205 indicate considerably larger consolidation strains than the CRSC tests at corresponding stress levels.

5.3.3 Analysis of Discrepancies in DSS Compression Curves

Unfortunately, the large variation in the consolidation results from the DSS tests on different batches was not detected until the end of the testing program. A detailed investigation was then carried out to identify and evaluate the causes leading to the variation in the consolidation results from the different DSS tests. The possible reasons for this unexpected behavior are identified and evaluated in the succeeding paragraphs.

The consolidation results from DSS tests on Batches 204 and 205 showed considerably larger strains than measured in the DSS tests on Batch 207. The variation among batches was suspected as a cause of this behavior. However, based on the following evidence, batch variability is not considered to be the main cause leading to this behavior:

- The technique of reconstituting the samples of BBC under the controlled

laboratory conditions was initiated at MIT by Wissa (1961). It has been consistently evaluated and improved over the past three decades. The specimens for this research came from the batches of BBC III which were produced using the technique developed by Germaine (1982) and further refined by Seah (1990). Extensive laboratory testing by Germaine and Seah indicated very little variability among batches produced using the latest resedimentation technique (see Chapter 4 for detail discussion).

- The consolidation results from DSS tests on Batch 207 compared well with the oedometer tests on all the batches of the new 200 series BBC and also with the CRSC tests on Batches 204 and 207 (Figure 5.12).
- The DSS tests performed by Werner on specimens from Batch 204 and 207 show considerably more strains than measured in the writer's DSS tests on specimens from Batch 207.

Sample disturbance is known to result in an increase in consolidation strain at a given stress level (e.g., Ladd 1973), but it is also not considered to be the significant factor in this case because of the following reasons:

- Very careful specimen preparation procedures are followed at MIT to minimize disturbance (see Chapter 3), which is evident from the remarkable consistency observed in the compression curves for the author's DSS tests on the specimens from various batches (Figure 5.5.) and from the CRSC tests (Figure 5.12).
- It is known that sample disturbance may give a lower estimated value of σ'_p from Casagrande's (1936) construction method and a decrease in the compressibility in the virgin compression region (e.g., Jamiolkowski et al. 1985), but these trends were not observed from the

experimental results under discussion (Figure 5.5 and Table 5.4).

The possibility of excessive consolidation strains due to the lateral deformation of the wire reinforced rubber membrane was also considered and evaluated. The specimens in the Geonor DSS are confined in 0.56 mm thick rubber membranes, reinforced with 0.15 mm diameter constantan wire at a spacing of 0.5 mm having Young's modulus of 1.55×10^8 kn/m². DeGroot (1989) measured the lateral deformation of the membrane using two displacement transducers to measure the external diameter of the membrane during consolidation. At $\sigma'_{vc} = 3$ ksc, the radial strain of the membrane was found to be 0.07%. This radial strain corresponds to an increase in ϵ_v of 0.15% , which is considered insignificant. Vucetic (1984) measured the radial strain of the Geonor DSS constantan membrane using a π tape and found that, for a very soft silty clay, the radial strain averaged 0.16% for $\sigma'_{vc} = 1.02$ ksc. Figures 5.11 and 5.12 show reasonable agreement in the consolidation results for Batch 207 from DSS tests and from oedometer and CRSC tests, even at higher consolidation stresses (i.e., $\sigma'_{vc} \approx 8$ to 12 ksc). Hence, it is concluded that the membrane effects are very small and negligible compared to the discrepancy in the vertical strains for the DSS tests on Batches 204 and 205.

Having determined that the above mentioned factors were not the source of variation in the consolidation results, the focus shifted to the apparatus compressibility. Tests on a steel specimen indicated that the porous stones used in the Geonor DSS, which are made of cindered bronze, were bent and this bending influenced the vertical strains to an indeterminate degree. The evaluation of consolidation data, in the light of this discovery, revealed that DSS Test 31 and those run subsequently (including DSS 36,38, and 39 performed by Werner, 1990) showed considerably larger strains than those measured in the DSS tests performed earlier (the tests on Batch 207 all involved DSS tests of lower numbers, i.e., ranging from 14 to 25; Figure 5.4). Hence,

it is concluded that the bent porous stones probably influenced the measured vertical strains for the DSS tests on Batch 204 and 205 (i.e., DSS test numbers ranging from 31 to 51).

Based on the above discussion and the consolidation results from DSS tests on Batch 207, it is appropriately concluded that the K_0 -consolidation behavior of BBC III in the Geonor DSS can be determined with an acceptable accuracy. A typical compression curve for the BBC in the DSS tests based on the average results from the four DSS tests, not affected by the bent porous stones, is shown in Figure 5.13. The influence of bent porous stones on the vertical consolidation strains measured for the DSS tests on Batches 204 and 205 can not be determined accurately. To eliminate the possibility of error in consolidation strains, the cinkered bronze porous stones should either be flattened before each test or preferably replaced with ceramic porous stones, which break instead of bending if dropped accidentally or use some quality control standard prior to each test in order to confirm the flatness of stones.

5.3.4 Compression Ratio and Swelling Ratio

Tables 5.1 to 5.3 show that the DSS tests on each batch of clay yield very consistent results in terms of compressibilities (CR and SR), (Note: But the values of CR vary between batches due to the problem with bent stones discussed in Section 5.3.3). The virgin compression ratios decrease with increase in the consolidation stress. Table 5.4 compares the DSS consolidation results with other results from DSS and oedometer consolidation tests by Werner (1990) and Seah (1990) on the same clay. The virgin compression ratio from DSS tests on Batch 207 compare well with those from the oedometer tests, except at the stress levels from 1.2 to 2 ksc for which oedometer tests give lower values of CR. The CR values from DSS tests on Batches 204 and 205 are significantly larger than those obtained from oedometer tests at the corresponding stress levels and are in agreement with results from the DSS tests performed by

Werner on Batch 204 and 207, (Note: the latter agreement suggests that the bent stones all had similar compressibilities).

Table 5.4 shows a good agreement in the values of compression ratio from the DSS tests on Batch 207 and the three CRSC tests on Batches 204 and 207.. However, the the DSS tests on Batches 204 and 205 give significantly larger values of compression ratio than the CRSC tests at the corresponding stress levels. These DSS tests also tended to give somewhat larger values of the swelling ratio. This difference is believed to be due the error caused by bent stones.

5.3.5 Rate of Secondary Compression

The computed values of the rate of secondary compression, $C\alpha\epsilon$, for the DSS tests range from 0.30% to 0.56%, with a ratio of $C\alpha\epsilon/CR$ varying from 0.016 to 0.035 (the lower values are obtained from DSS tests on Batch 207). The $C\alpha\epsilon$ value for the each test has been computed for the maximum increment of stress, which was left on the sample for approximately one 24 hours. Seah (1990) obtained $C\alpha\epsilon$ values ranging from 0.26% to 0.60%, with a mean ratio of $C\alpha\epsilon/CR$ equal to 0.02 ($C\alpha\epsilon/CR = 0.017$ to 0.045) from 13 oedometer tests on BBC III (Table 4.4). Mesri and Choi (1985) reported that for the majority of inorganic soft clays this ratio ranges from 0.03 to 0.05. The ratio of $C\alpha\epsilon/CR$ from the DSS tests compares well with the average values obtained from oedometer tests on the same clay, but is lower than the values reported by Mesri and Choi. The $C\alpha\epsilon$ values for the DSS tests have been computed from the last increment of stress, which was left on the sample for approximately 24 hours (a typical settlement–time curve of a consolidation increment in the DSS is shown in Figure A.12) .

O'Neill (1985) found for BBC II that $C\alpha\epsilon/CR$ averaged 0.035. The comparison between the two series indicate that BBC III is a non–thixotropic material and has a higher average value of virgin compression index than BBC II, which is closer to the

average values for natural BBC (Table 4.6). Hence, it may be concluded that BBC III exhibits a lower rate of secondary compression than found for many inorganic soft clays.

5.4 Summary and Conclusions

The experimental results from the consolidation phase for the Geonor DSS testing have been presented and evaluated in this chapter. The analysis of the tests data reveal that the porous stones used in the Geonor DSS were bent during DSS testing on samples from Batches 204 and 205, which resulted in larger vertical consolidation strains than those measured in the DSS tests performed on samples from Batch 207 and from the oedometer tests on the same batches of clay. However, the consolidation data from Batch 207 compare very well with the data obtained from the oedometer and the CRSC tests on BBC III. Hence, the conclusions are mainly based on the consolidation results of the DSS tests on Batch 207 and are valid subject to the condition that the possibility of error in the consolidation data due to the bending of porous stones, used in the Geonor DSS, is eliminated.

The following conclusions are drawn for the one dimensional K_0 -consolidation behavior of BBC III in the Geonor DSS apparatus:

- The test gives consistent and good estimates of the compression response. The K_0 -consolidation parameters obtained from the DSS tests on BBC are in reasonable agreement with those obtained from EOP incremental oedometer curves.
- The consolidation results from the Geonor DSS show very good agreement with CRS consolidation at strain rates that result in the values of u_b/σ_v between 2% to 5% in the normally consolidated range.
- The virgin compression ratio (CR) for resedimented BBC III decreases

with increase in the stress level.

- The new 200 series BBC exhibits a lower rate of secondary compression than BBC II and the ratio of $C_{\alpha\epsilon}/CR$ for BBC III falls somewhat below the range found for most inorganic soft clays.

It is recommended that the porous stones used in the Geonor DSS, which are made of cindered bronze, should either be flattened before each test, or preferably replaced with ceramic porous stones which will break instead of bending if accidentally dropped. This will reduce the possibility of a serious error in the measured consolidation strains, thus improving the reliability of data obtained from the Geonor DSS

Table 5.1: Consolidation Results of Geonor DSS Tests on Batch 204 of BBC III

Test No.	w_c (%)	σ'_{vc}	CR (Stress Range in ksc)				SR (Stress Range in ksc)					$C_{a\epsilon}$ (%)	$C_{a\epsilon}$ --- CR
	σ'_p (ksc)	OCR	1.2-2	2-4	4-7	7-12	12-6	12-3	12-1.5	12-0.75	12-.375		
DSS40	40.12	5.798	0.212	0.189	0.168	0.160	0.013	-	-	-	-	0.556	0.035
	0.92	1.965											
DSS44	39.75	1.447	0.200	0.187	0.172	0.171	0.014	0.018	0.022	-	-	0.540	0.032
	0.98	7.892											
DSS48	40.21	0.772	0.195	0.183	-	0.179	0.013	0.018	0.023	0.026	-	0.512	0.029
	0.98	14.692											
DSS 50	40.00	0.379	0.203	-	-	-	0.011	0.015	0.019	-	-	0.393	0.019
	1.03	7.800											
DSS51	39.80	0.373	0.200	0.186	0.179	0.179	0.004	0.015	0.020	0.023	0.026	0.392	0.022
	1.05	31.904											
Mean ±1 SD	39.98	-	0.202	0.186	0.173	0.172	0.011	0.017	0.021	0.025	0.026	0.479	0.027
	0.20	-											
	0.99	-											
	0.05	-											
			0.006	0.002	0.006	0.009	0.004	0.002	0.002	-	-	0.080	0.007

Notes: 1. Ratio of $C_{a\epsilon}$ /CR computed for last increment.
2. CR data affected by stone bending.

Table 5.2: Consolidation Results of DSS Tests on Batch 205 of BBC III

Test No.	w _c (%)	σ'_{vc} OCR	CR (Stress Range in ksc)				SR†		C _{aε} (%)	C _{aε} --- CR
			1.2-2	2-4	4-7	7-12	12-6	12-3		
DSS31	40.48	1.441	-	-	-	-	-	-	0.448	-
	1.08	1.00								
DSS37	39.70	3.512	0.187	0.185	0.167	0.170	0.012	0.015	0.410	0.023
	0.98	3.248								
Mean	40.09	-	0.187	0.185	0.167	0.170	0.012	0.015	0.429	0.023

Notes: 1. Ratio of C_{aε}/CR is computed for last increment.
 2. CR data is affected by stone bending.
 † Stress range in ksc.

Table 5.3: Consolidation Results of Geonor DSS Tests on Batch 207 of BBC III

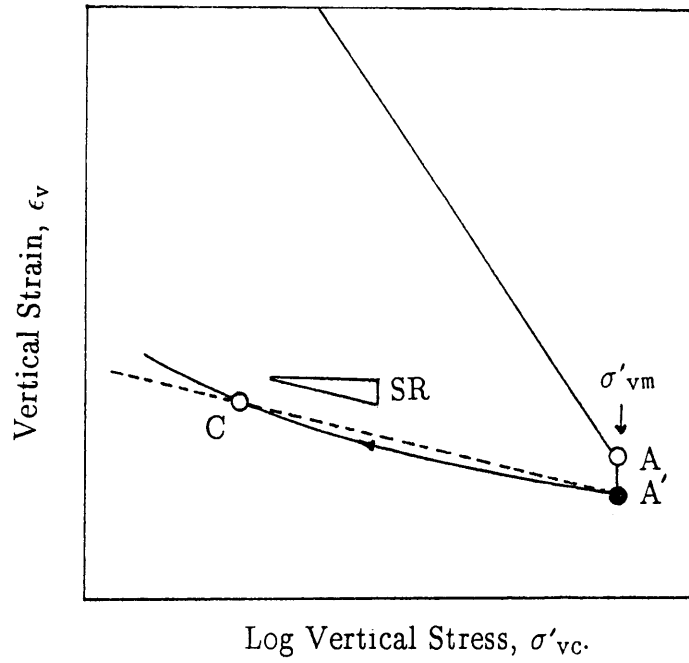
Test No.	w_c (%)	σ'_{vc} (ksc)	CR (Stress Range in ksc)				$C_{a\epsilon}$ (%)	$C_{a\epsilon}$ --- CR	Remarks
	σ'_p (ksc)	OCR	1.2-2	2-4	4-7	7-12			
DSS14	40.55 1.00	11.992 1.00	0.2140	0.1607	0.1504	0.1676	0.299	0.018	Excellent ϵ_v data. The data from this batch are not affected by stone bending.
DSS18	40.66 1.00	9.030 1.00	0.2083	0.1559	0.1540	-	0.302	0.020	
DSS22	40.64 1.00	5.992 1.00	0.2108	0.1604	-	-	0.336	0.021	
DSS25	40.78 1.05	2.955 1.00	0.2117	-	-	-	0.340	0.016	
Mean ± 1 SD	40.66 0.09 1.010 0.025	- -	0.2112 0.0020	0.1590 0.0030	0.1522 -	0.1676 -	0.319 0.022	0.019 0.002	

Table 5.4: Results of Consolidation Tests on samples from Batches of BBC III

Refer - ence Batch	No. & Type of Tests w_c (%)	σ'_p (ksc)	CR (Stress Range in ksc)				SR (Stress Range in ksc)					Ca ϵ (%)	Ca ϵ --- CR
			1.2-2	2-4	4-7	7-12	12-6	12-3	12-1.5	12-0.75	12-.375		
Author† 204	5, DSS 39.98 0.20	0.99 0.05	0.202 0.006	0.186 0.002	0.173 0.006	0.172 0.009	0.011 0.004	0.017 0.002	0.021 0.002	0.025	0.026	0.479 0.080	0.027 0.007
Author† 205	2, DSS 40.09 -	1.03	0.187	0.185	0.170	0.177	0.012	0.015	-	-	-	0.429 -	0.023
Author 207	4, DSS 40.66 0.09	1.01 0.03	0.211 0.002	0.159 0.003	0.152 -	0.168 -	-	-	-	-	-	0.319 0.022	0.019 0.002
Werner† (1990) 204, 207	3, DSS ¹ 40.43 0.45	1.03 0.03	0.195 0.020	0.183 0.003	0.162 0.013	- -	-	-	-	-	-	0.241 0.010	0.014 0.002
Seah (1990) 2	4, Oed ³ 40.32 0.37	0.98 0.02	0.162 0.023	0.157 0.002	0.153 ⁴ 0.009	- -	-	-	0.014 ⁵ 0.003	-	-	0.26 to 0.60	0.017 to 0.039
Author (ApxC) 204, 207	3, CRS ⁶ 40.05 0.84	1.05 0.05	0.184 0.008	0.169 0.003	0.148 -	0.134 0.002	0.010 0.001	0.013 0.001	0.016 0.002	0.020 0.001	0.023 0.001	- -	- -

Notes: 1 Results from DSS 36, 38 and 39 (Figure.5.6). 2 Batch 204, 205 and 207.
 3 Results from Test 8,9,10 and 13 (Figure 5.7). 4 CR for stress Range 4 to 8 ksc.
 5 SR for Stress Range 16-2 ksc (i.e., OCR=8). 6 Average $\epsilon = 2.27 \times 10^{-6}$ per second.
 † Data affected by stone bending.

DEFINITION OF SWELLING RATIO (SR)



$$SR = \frac{(\epsilon_{at A'} - \epsilon_{at C})}{\log \left(\frac{\sigma'_{vm}}{\sigma'_{at C}} \right)}$$

Figure 5.1: Definition of Swelling Ratio (SR).

DSS TESTS ON BATCH 204

(DSS 40,44,48,50&51)

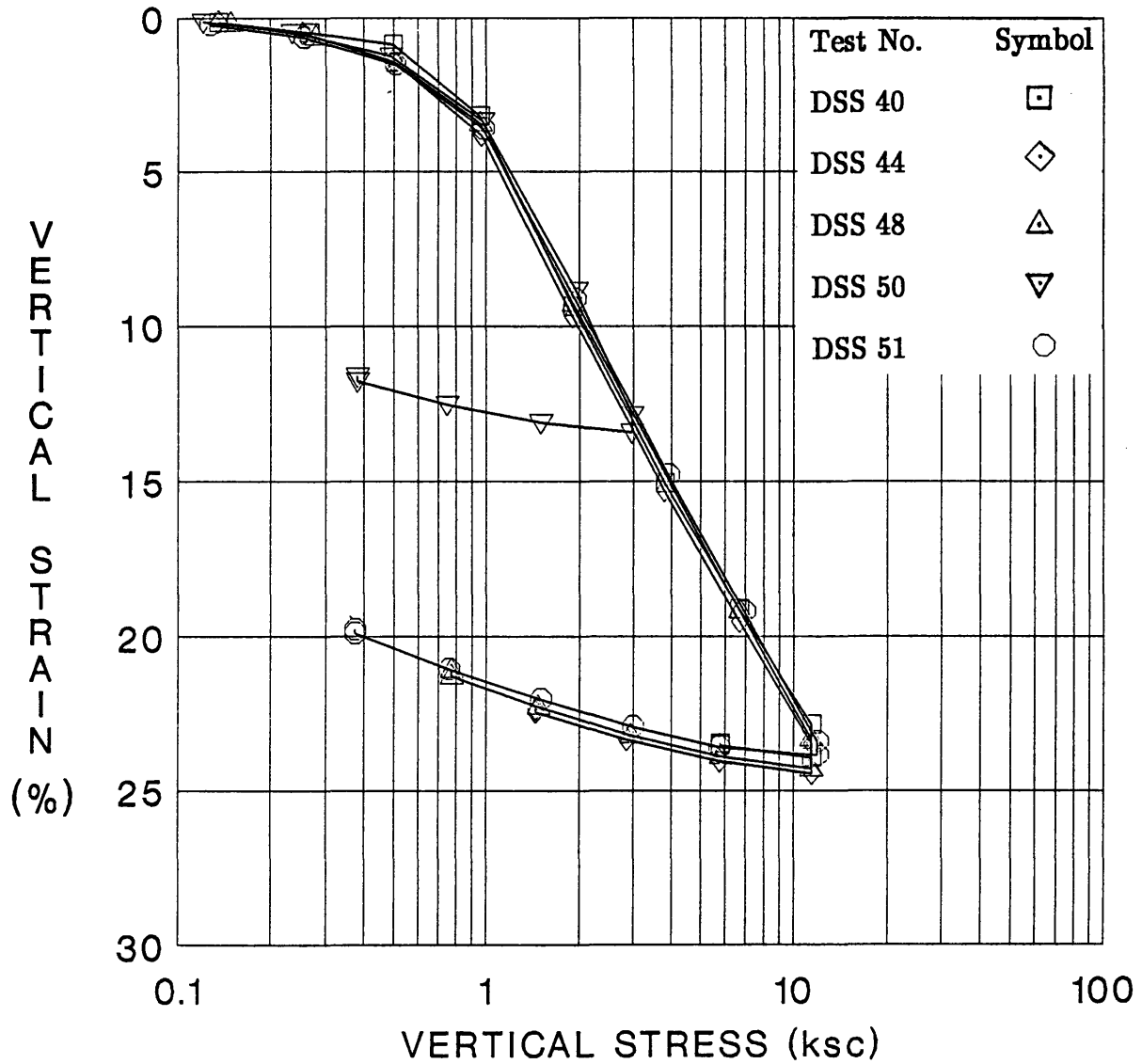


Figure 5.2 Compression Curves (ϵ_v versus $\log \sigma'_{vc}$) from DSS Tests on Batch 204.

DSS TESTS ON BATCH 205 (DSS 31&37)

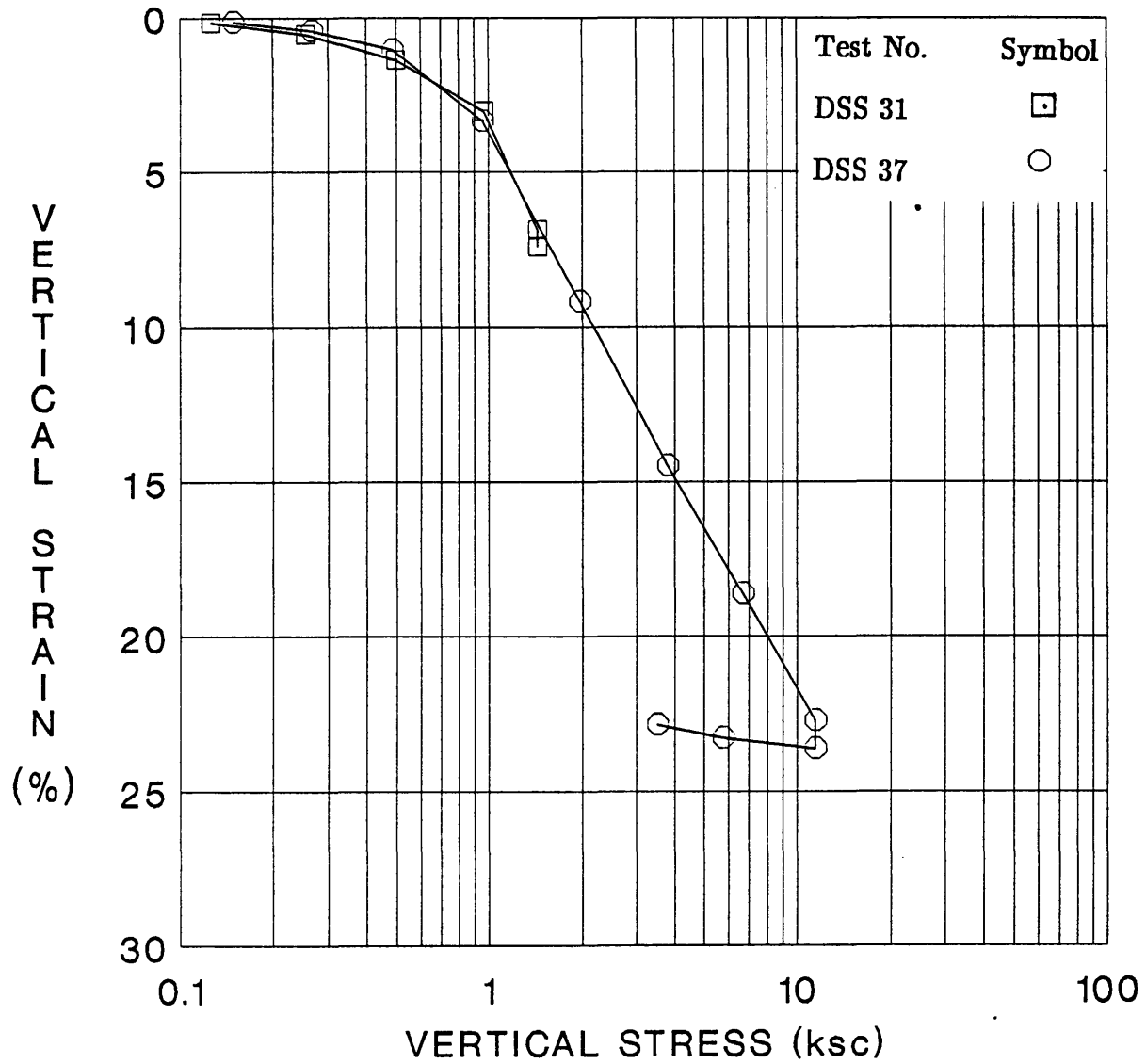


Figure 5.3 Compression Curves (ϵ_v versus $\log \sigma'_{vc}$) from DSS Tests on Batch 205.

DSS TESTS ON BATCH 207

(DSS 14,18,22,& 25)

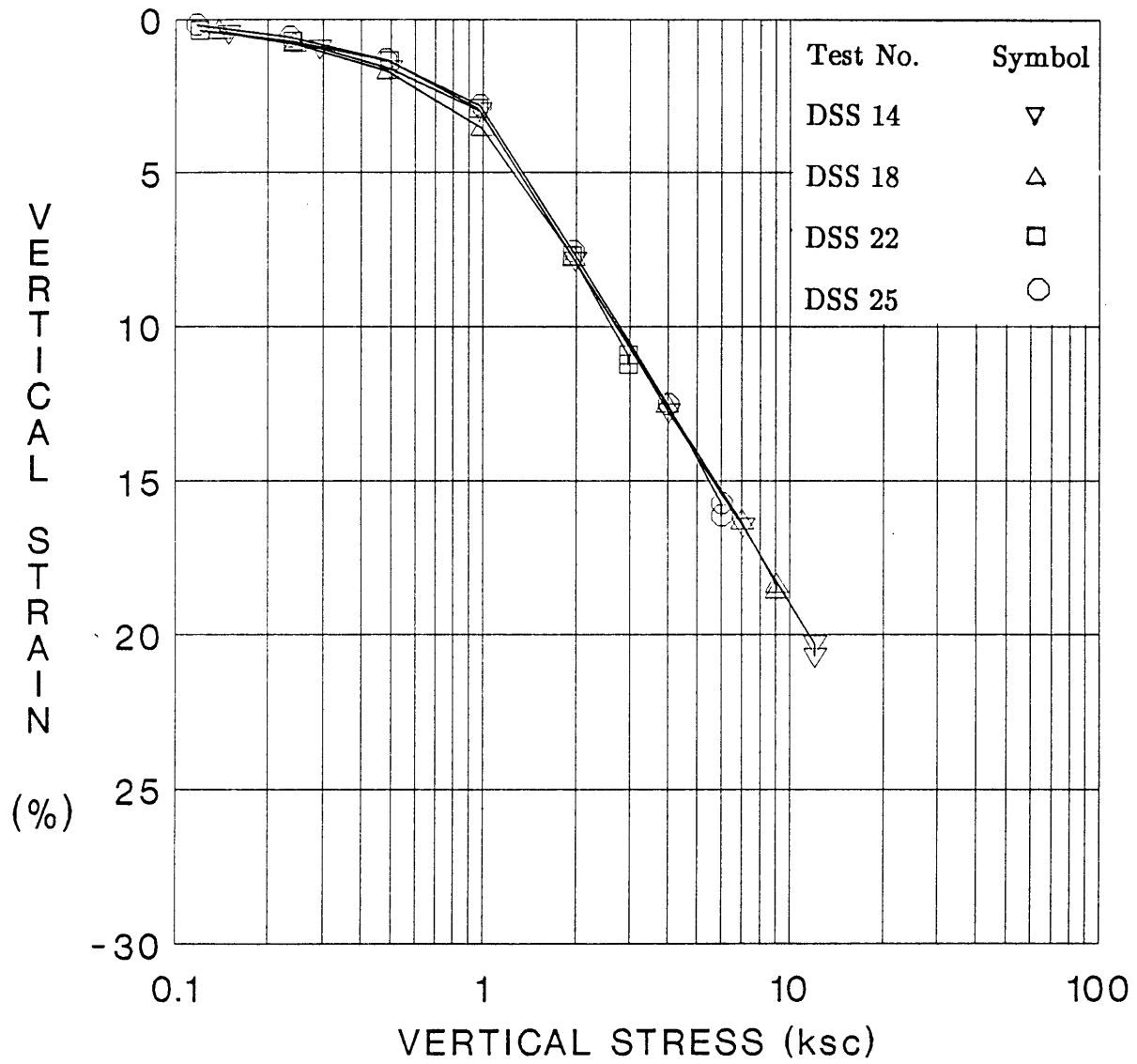


Figure 5.4 Compression Curves (ϵ_v versus $\log \sigma'_{vc}$) from DSS Tests on Batch 207.

DSS TESTS ON BBC III

(Batches 204, 205 & 207)

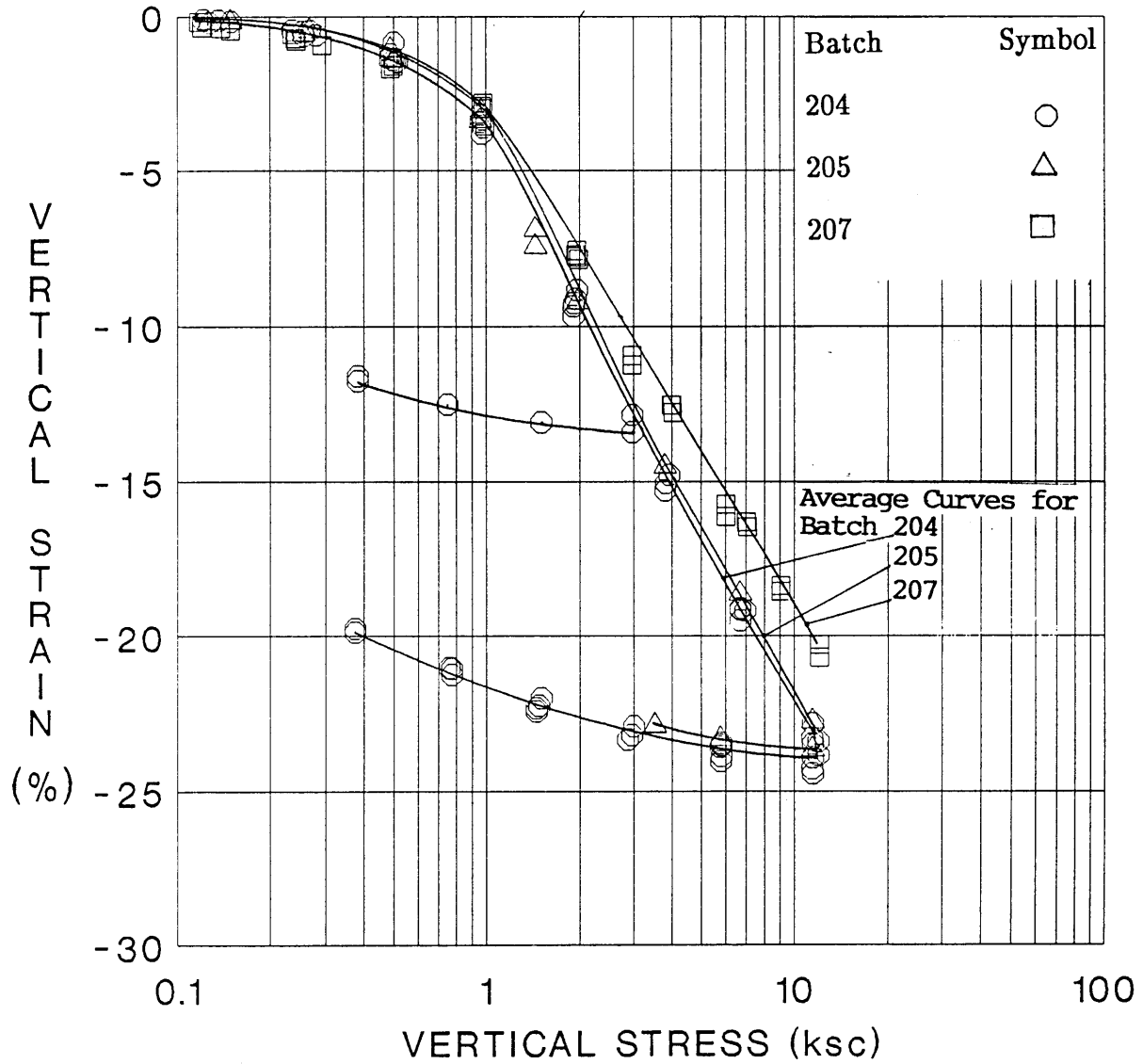


Figure 5.5 Compression Curves (ϵ_v versus $\log \sigma'_{vc}$) from DSS Tests on BBC III.

DSS TESTS ON BATCHES 204 AND 207 (DSS 36,38&39)

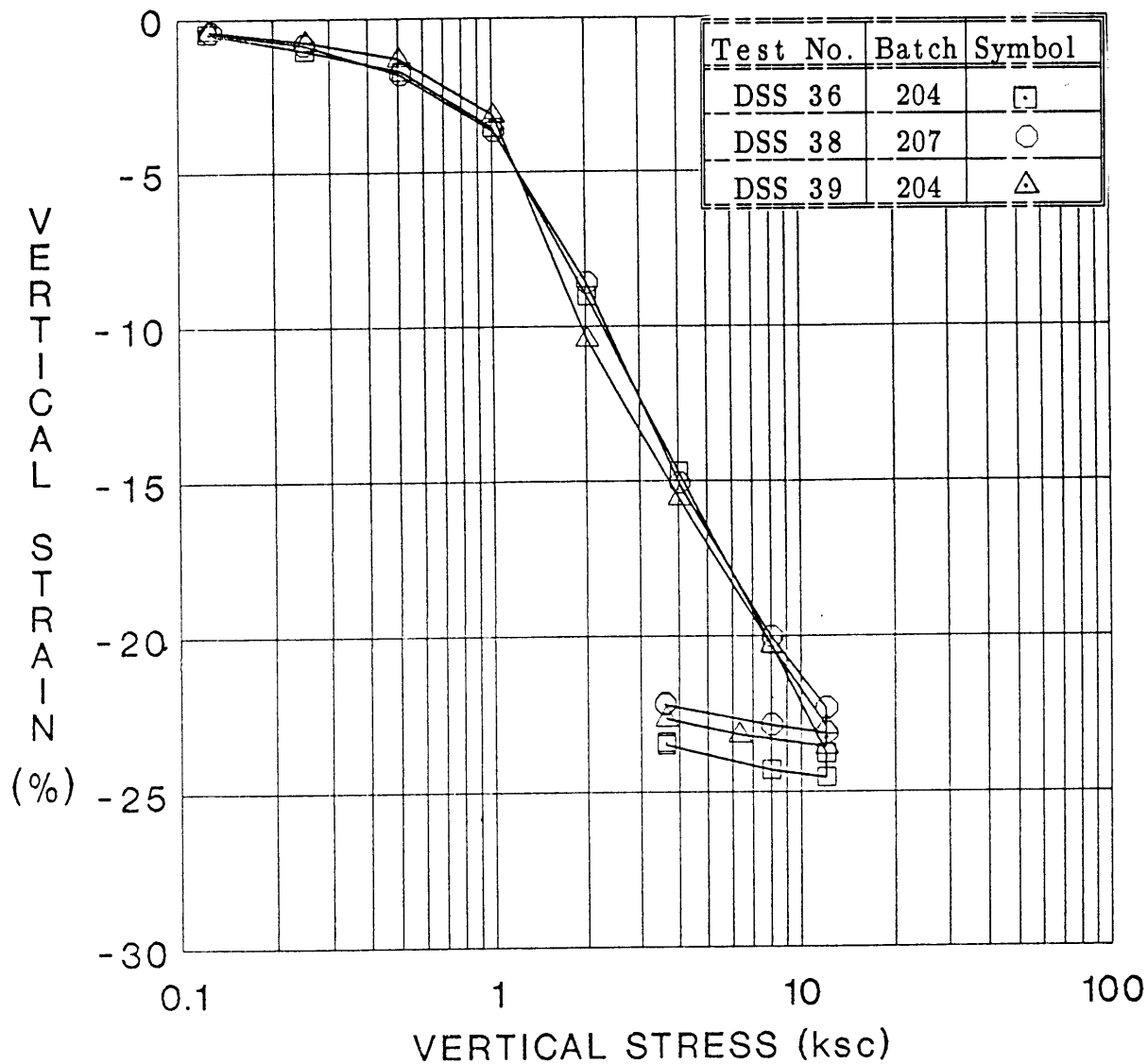


Figure 5.6: Compression Curves (ϵ_v versus $\log \sigma'_{vc}$) from DSS Tests on Batches 204 and 207 (From Werner, 1990).

OEDOMETER TESTS ON BBC III (Batches 204,205&207)

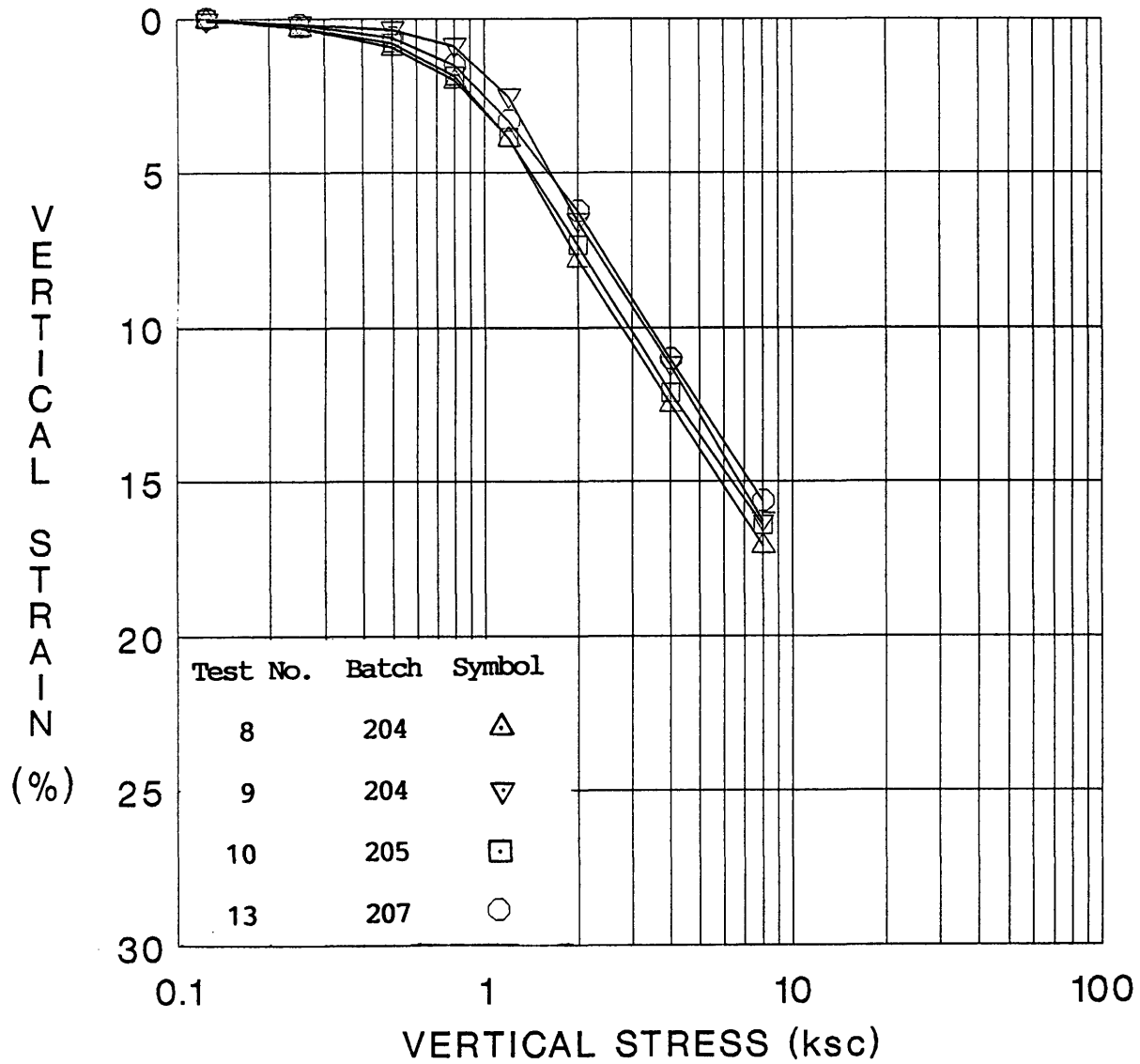


Figure 5.7 Compression Curves (ϵ_v versus $\log \sigma'_{vc}$) from Oedometer Tests on Batches 204, 205, and 207 (From Seah, 1990).

TESTS ON BATCH 204

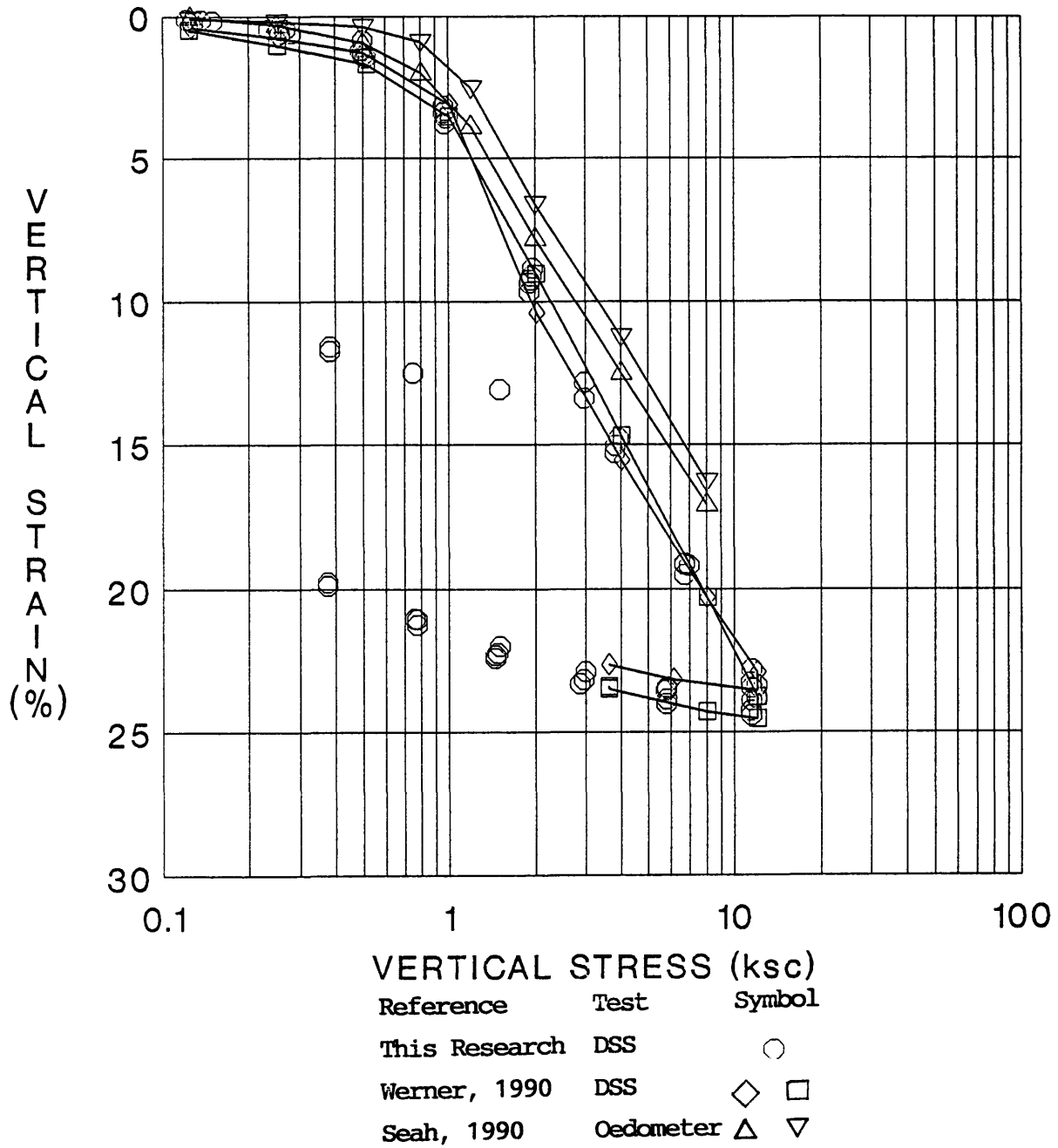
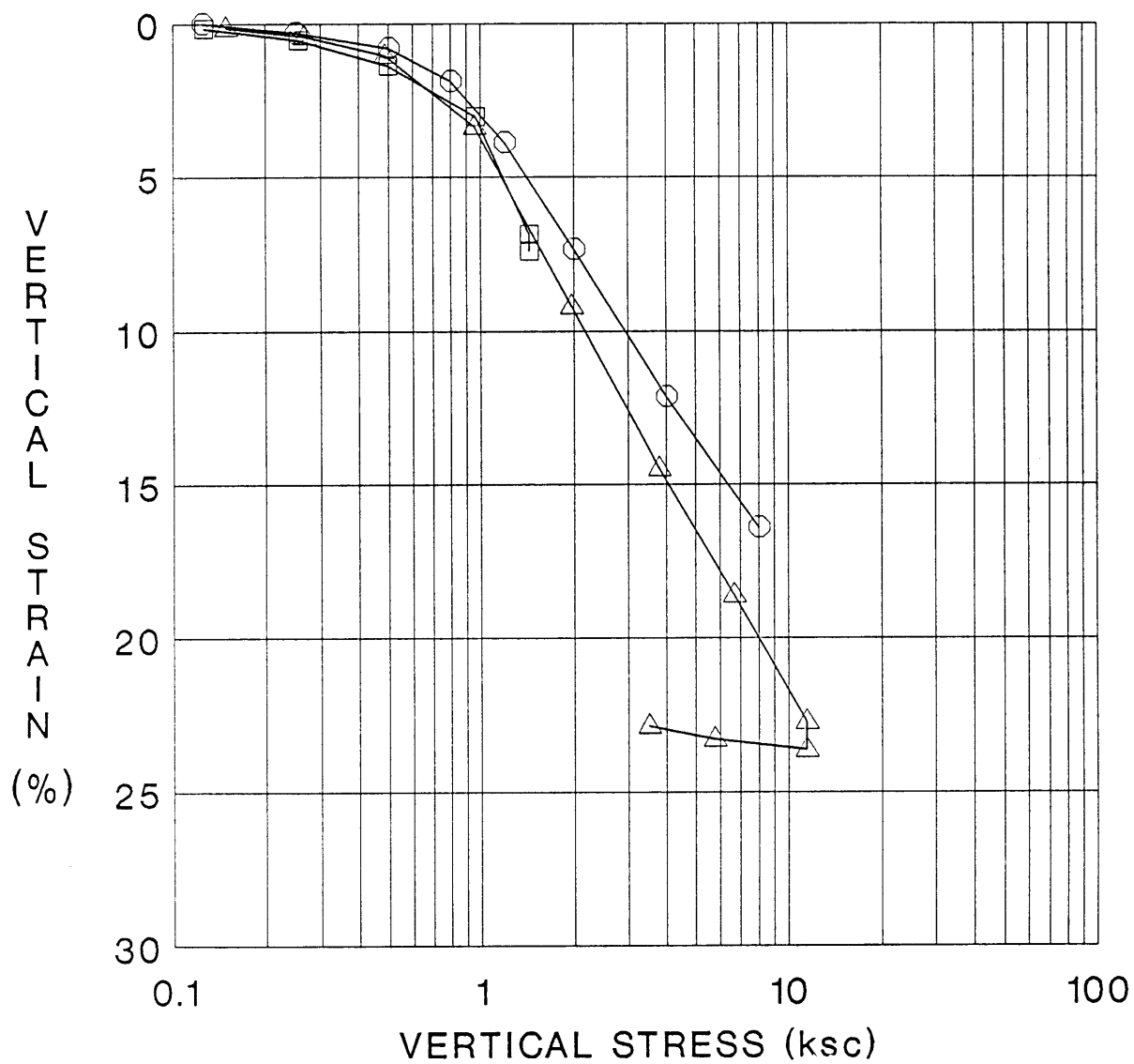


Figure 5.8: Comparison of Compression Curves (ϵ_v versus $\log \sigma'_{vc}$) from Tests on Batch 204 (Results from DSS and Oedometer Tests)

TESTS ON BATCH 205



Reference	Test	Symbol
This Research	DSS 31	□
	DSS 37	△
Seah, 1990	Oedometer 10	○

Figure 5.9 Comparison of Compression Curves (ϵ_v versus $\log \sigma'_{vc}$) from Tests on Batch 205 (Results from DSS and Oedometer Tests).

TESTS ON BATCH 207

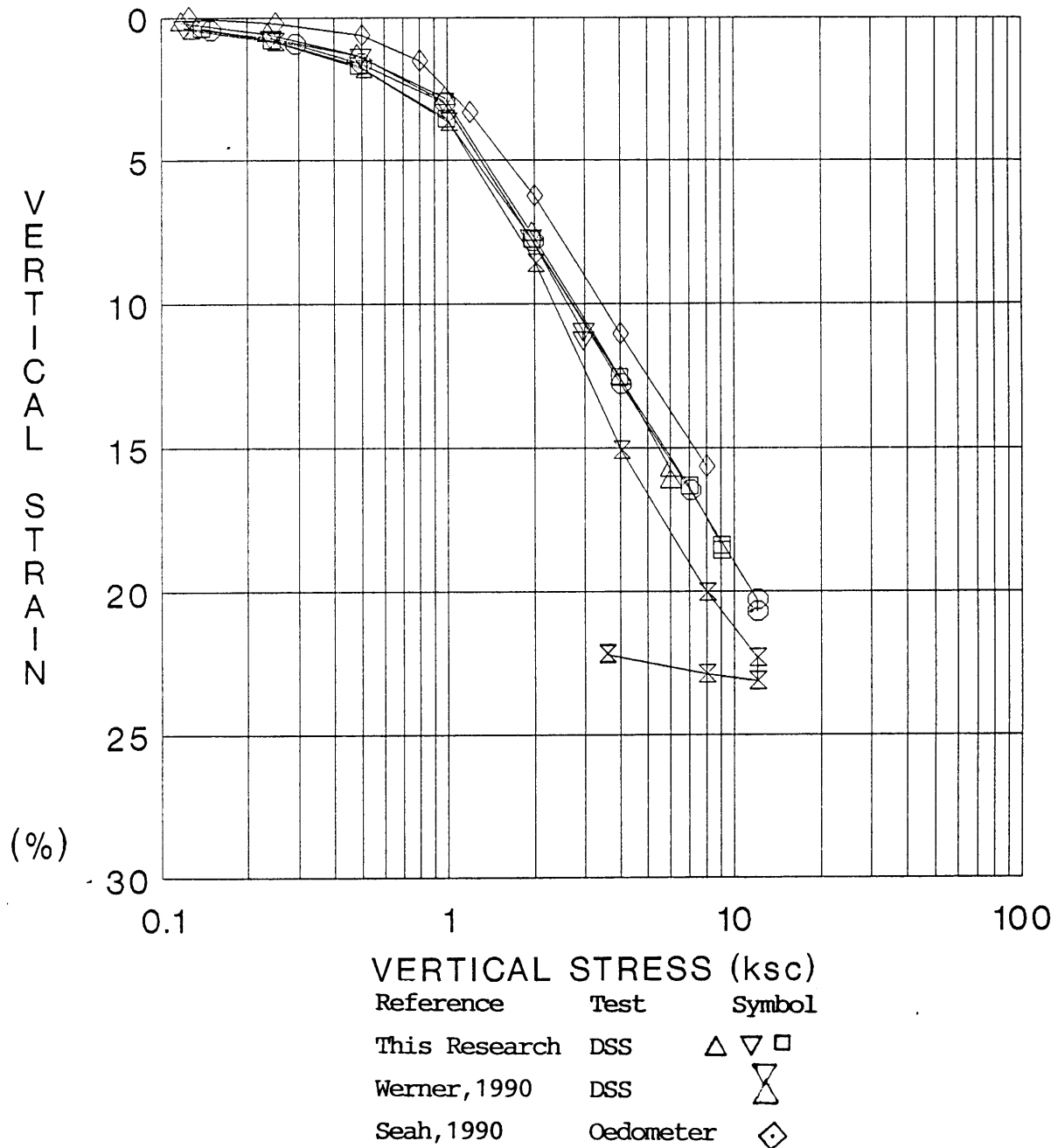


Figure 5.10 Comparison of Compression Curves (ϵ_v versus $\log \sigma'_{vc}$) from Tests on Batch 207 (Results from DSS and Oedometer Tests).

DSS TESTS ON BBC III

(Batches 204, 205 & 207)

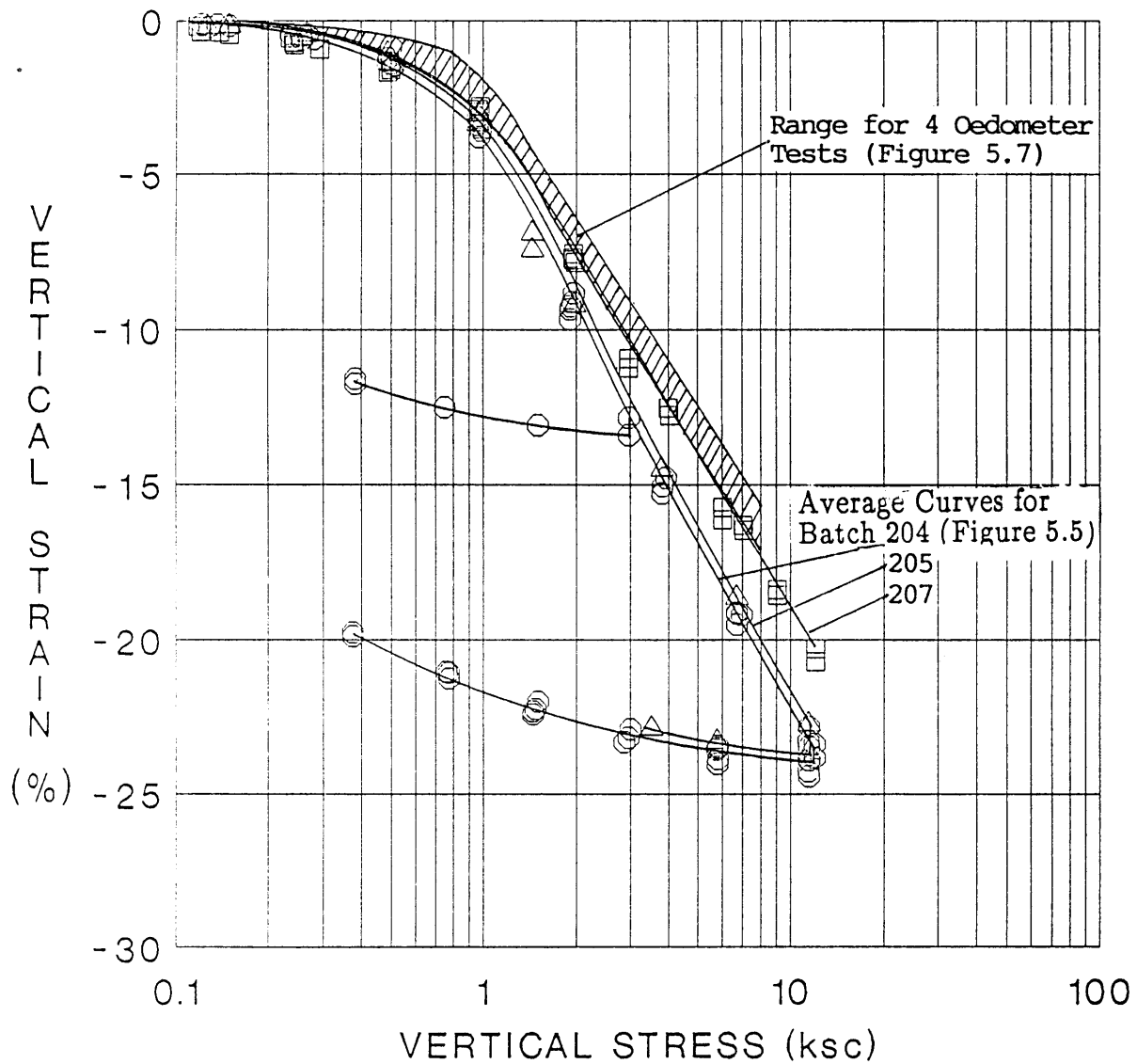
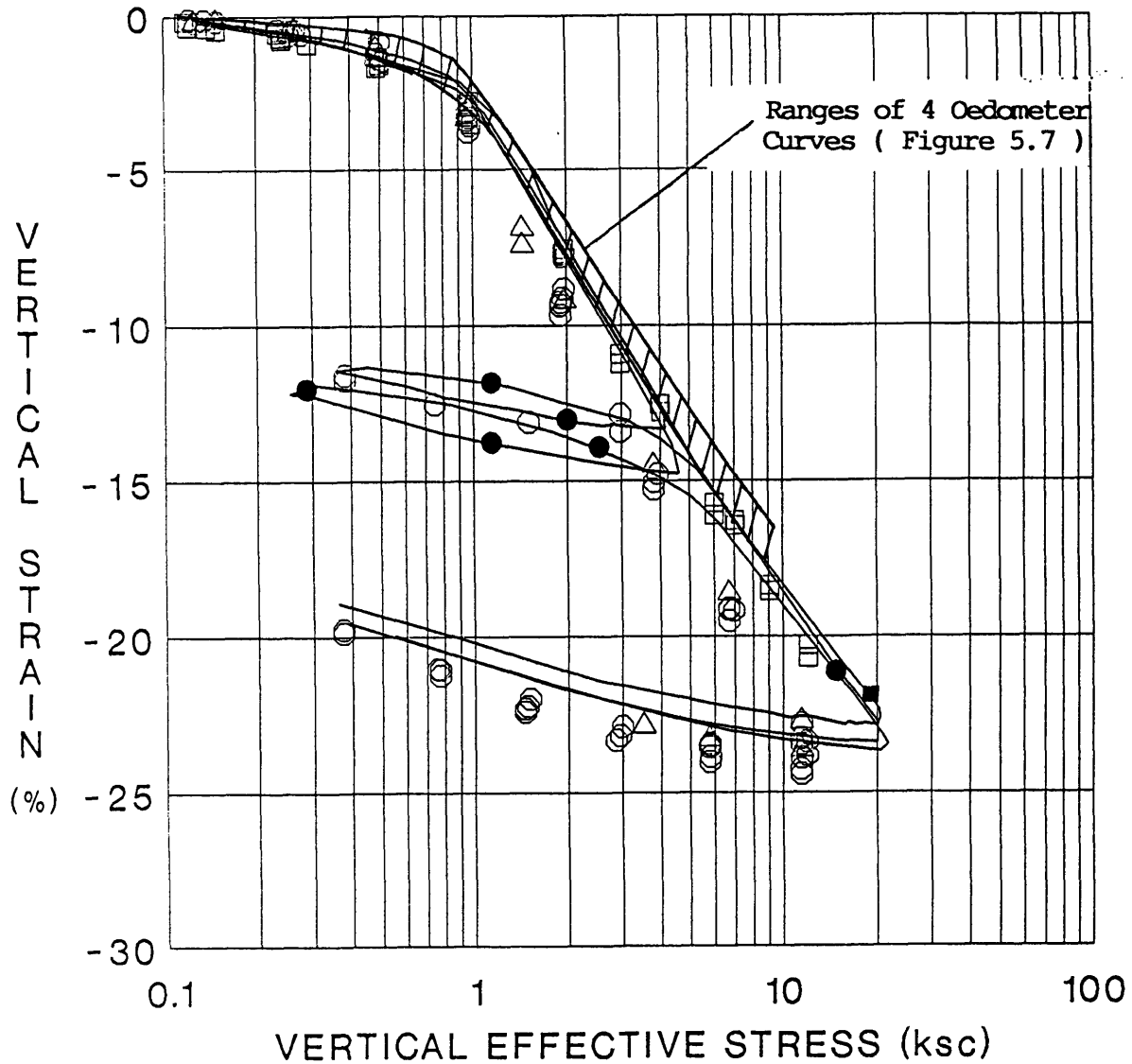


Figure 5.11: Comparison of Compression Curves (ϵ_v versus $\log \sigma'_{vc}$) from Tests on Batch 204, 205, and 207 of BBC III.

CONSOLIDATION BEHAVIOR OF BBC III (Batches 204,205&207)



Test	Batch	Symbol	Test	Batch	Symbol
DSS	204	○	CRS	204	●
DSS	205	△	DSS	207	■
DSS	207	□			

Figure 5.12: Comparison of Compression Curves (ϵ_v versus $\log \sigma'_{vr}$) from All the DSS, Oedometer, and CRS tests on Batches 204, 205, and 207 of BBC III.

TESTS ON BATCH 207

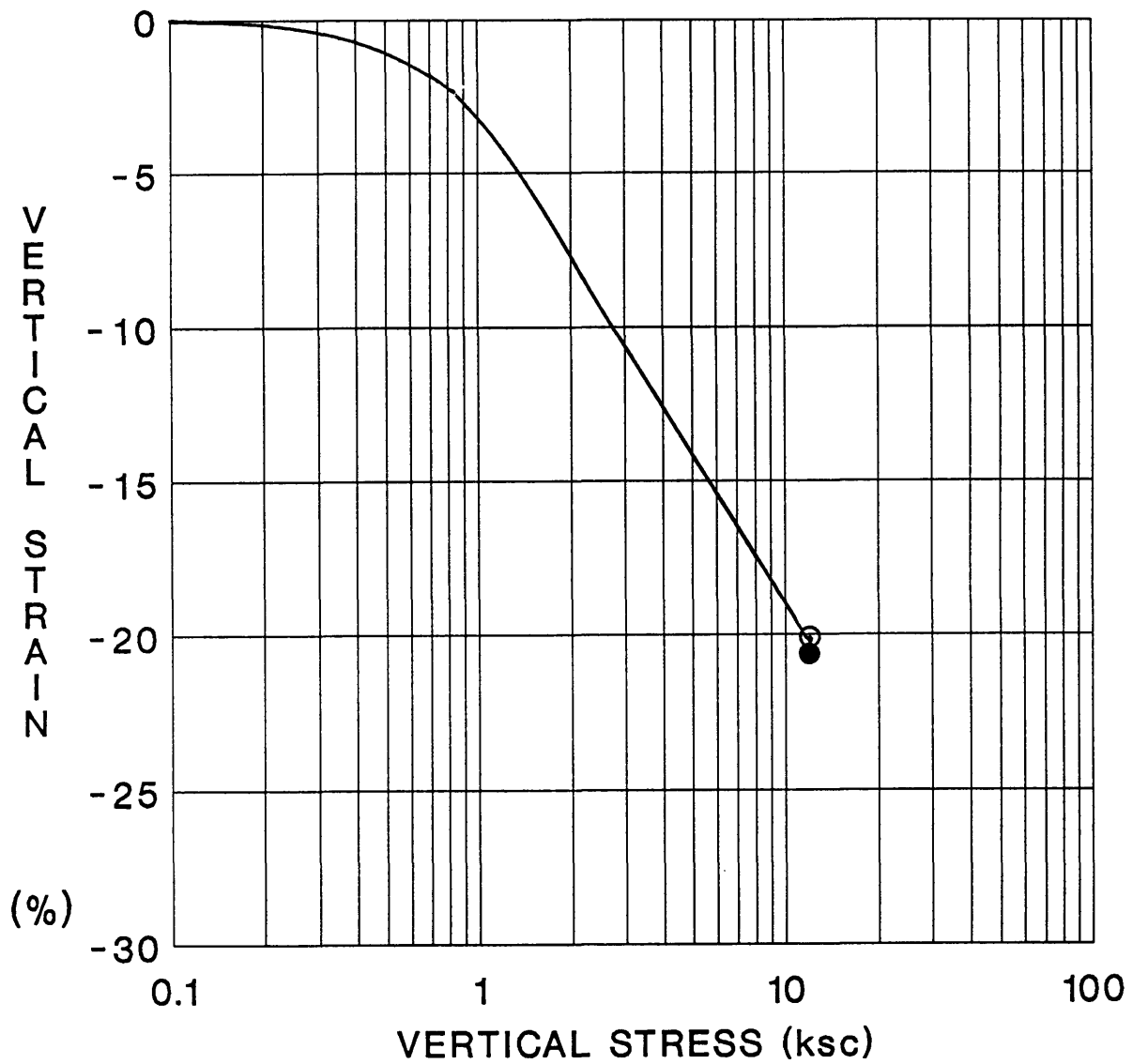


Figure 5.13: Typical Compression Curve for the BBC III in the Geonor DSS Test.

CHAPTER 6

UNDRAINED SHEAR BEHAVIOR OF NORMALLY CONSOLIDATED BBC

6.1 Introduction

This chapter presents the results and analysis of five CK_0 UDSS tests on normally consolidated specimens from batches of the new 200 series BBC. The tests were performed at different consolidation stress levels with the objective of investigating the normalized stress–strain–strength behavior of resedimented BBC in the Geonor DSS apparatus (see Chapter 2 for Normalized Soil Parameter concept). The tests were conducted following the procedures described in Chapter 3. The minimum consolidation stress was chosen as 1.5 times the estimated preconsolidation pressure as recommended by the SHANSEP procedure (Ladd and Foott, 1974) and the maximum stress of about 12 ksc was based on the capacity of the reinforced rubber membrane used in the Geonor DSS to prevent lateral straining of the specimen. To standardize the effects of secondary compression, the maximum consolidation stress was applied for approximately 24 hours to allow at least one cycle of secondary compression prior to undrained shear. All the specimens were sheared at a constant rate of strain of approximately 5% per hour.

The specimens for this phase of DSS testing came from Batches 205 and 207 of resedimented BBC. Chapter 4 summarizes the batching procedure and properties of the test soil. Chapter 5 discusses the results from the consolidation phase of the CK_0 UDSS tests. Based on the comparison and evaluation of the tests data in the preceding chapter, it has been found that significantly more consolidation strains were "measured" for DSS tests on Batch 205 than for Batch 207, most probably due to the bending of the metal porous stones used in the Geonor DSS. All the tests on the normally consolidated specimens were performed on Batch 207, with the exception of DSS Test 31 which had the minimum pre–shear consolidation stress.

The following section presents the data in graphical form and tabulated summaries of the results from all the tests. It also contains a brief discussion of the test data. Appendix B contains the tabulated undrained shear data from the individual tests.

Section 6.3 compares the results from tests conducted for this research with the published data for SHANSEP type undrained shear tests performed in the Geonor DSS and Section 6.4 discusses the effect of consolidation stress level on the normalized behavior for DSS tests on normally consolidated BBC. Finally, Section 6.5 summarizes the conclusions pertaining to normalized undrained shear behavior of normally consolidated resedimented BBC in the Geonor DSS.

6.2 Results of CK_0 UDSS Tests on Normally Consolidated BBC

6.2.1 Presentation of Results

Table 6.1 summarizes the results of five CK_0 UDSS tests conducted on normally consolidated specimens of BBC III at stress levels ranging from approximately 1.5 ksc to 12 ksc. The table presents the following information:

- The batch number of resedimented BBC from which the specimen was obtained, its water content and the pre-shear value of σ'_{vc} .
- Values at the peak horizontal shear stress (τ_{hmax}) of the shear strain (γ), normalized stresses (i.e., τ_h/σ'_{vc} and σ'_v/σ'_{vc}) and the ψ angle ($\psi = \arctan \tau_h/\sigma'_v$).
- Values of γ , τ_h/σ'_{vc} , σ'_v/σ'_{vc} and ψ angle at the maximum value of τ_h/σ'_v .
- Values of the normalized undrained Young's modulus at 50 % of the peak shear resistance, $E_u(50)/c_u$. This value is computed using the

following equation:

$$E_u = 2(1+\nu) G \quad (6.1)$$

where;

G = Shear modulus τ_h/γ

ν = Poisson's Ratio

Since the tests are undrained, $\nu = 0.5$ and Equation 6.1 reduces to :

$$E_u = 3(\tau_h/\gamma) \quad (6.2)$$

- Remarks pertaining to the test quality.

Figure 6.1 through 6.6 are the synthesized plots of the stress paths, normalized shear stress versus shear strain, applied shear stress ratio versus shear strain, pore pressure versus shear strain, vertical strain versus shear strain and normalized Young's modulus versus applied shear stress ratio, respectively.

6.2.2 Discussion of the Normally Consolidated CK_0 UDSS Results

The stress paths in Figure 6.1 plot the horizontal shear stress versus the vertical effective stress required to maintain constant volume, both normalized to the vertical consolidation stress. The data from the various tests (except for DSS 31) are quite consistent and plot within a narrow range, especially in the vicinity of the peak shear resistance. The plot shows that σ'_v decreases consistently throughout the test, which means that the material exhibits contractive behavior with continued straining. The peak undrained shear strength ratio, c_u/σ'_{vc} (where c_u is defined as the maximum value of the applied horizontal shear stress, τ_{hmax}), is 0.197 ± 0.004 SD, giving a coefficient of variation equal to 2 %. At the peak shear resistance, the value of $\sigma'_v/\sigma'_{vc} = 0.527 \pm 0.006$ SD and $\psi = \arctan (\tau_h/\sigma'_v)$ equals 20.4 ± 0.5 SD degrees

(excluding DSS Test 31 having a significantly lower value of σ'_v/σ'_{vc} compared to the other tests). The value of the ψ angle is not a material property since the Mohr's circle of stresses at this point is highly indeterminate because of the rapid rotation of principal stresses (see Chapter 2 for interpretation of stresses in the DSS). The values of the shear stress and normal stress ratios decrease with subsequent straining and at very large strains (i.e., $\gamma \approx 33\%$), the normalized shear stress decreases to a value of 0.092 ± 0.015 SD when σ'_v/σ'_{vc} is equal to 0.152 ± 0.035 SD. At this stage of the test, $\arctan(\tau_h/\sigma'_v)$ equaled $31.6^\circ \pm 3^\circ$ SD, which suggests that the horizontal plane is close to the plane of maximum obliquity (i.e., ψ is near to $\phi' = 34^\circ$ measured at large strains in CK₀UC tests, Sheahan, 1990). The data at maximum obliquity are much more scattered than at the peak shear strength.

The normalized stress–strain curves in Figure 6.2 show good agreement among the five CK₀UDSS tests performed at different consolidation stresses. The plot shows that the horizontal shear stress increases very rapidly, reaching a peak at an average shear strain of about 6%. However, there is an increase in the shear strain at failure with increase in the consolidation stress level. Figure 6.3 plots applied shear stress ratio (τ_h/c_u) versus shear strain. Both plots show that continued straining produces significant strain softening. The decrease in τ_h is relatively small until the shear strains become greater than about 12% and eventually drops to approximately 54% of the peak values at 30% shear strain.

Figure 6.4 is a plot of normalized pore pressure versus shear strain for all the DSS tests. The data demonstrate that significant positive pore pressures are developed during the tests. There is a constant increase in the value of $\Delta u/\sigma'_{vc}$ with increase in the shear strain, reaching a value of $0.82 \pm 0.02\%$ SD (excluding DSS 31) at a shear strain of about 30%. The curves indicate an increase in the values of $\Delta u/\sigma'_{vc}$ versus shear strain with decrease in the consolidation stress. However, the data in Figure 6.4 still fall within in a fairly narrow range, except for DSS 31 which yielded significantly

larger values of excess pore pressure beyond 1% shear strain. Figure 6.5, which plots variations in the vertical strain during shear versus shear strain, indicates some irregularity in the curve for DSS 31 at the very beginning of the test, which is probably due to some problem with the constant height DCDDT. It appears that during the initial about 2% shear strain the servo control system started unloading the sample more than the actual pore pressure developed in the specimen due to undrained shearing, which lead to this unusual behavior. By 2% strain, the controller recovered from the problem and returned the vertical strain to the value experience by the other specimens. However, the pore pressure does not recover from the problem but rather follows a path parallel to the other tests. As stated earlier, the consolidation data for DSS 31 were affected by the bending of porous stones used in the Geonor DSS. This may be another cause for the unusual behavior. However, this appears less likely since the effect of bent porous stones should be further enhanced with decrease in the vertical effective stress, whereas the subsequent data are consistent and follow the trends observed in the tests not affected by the bending of porous stones (i.e. see Figure 6.4).

The data from the measured sample deformation (Figure 6.5) indicate an average sample deflection of +0.095 % (a positive sign indicates compression) of the pre-shear height at the peak shear resistance. The undrained shearing in the Geonor DSS is performed under constant volume conditions by keeping the height of the specimen constant using a closed loop servo control system (see Chapter 3). The system activates on occurrence of small changes in the height due to development of the pore pressure during undrained shearing. Although the system is fairly efficient, some error in the pre-shear height is usually observed. The sample deflection with a positive sign indicates that the device has unloaded the specimen less than the actual pore pressures developed in the specimen during shear. However, the measured error in the pre-shear sample height is very small and it is expected to have little influence on

the measured undrained shear response for BBC. Hence, the assumption of maintaining constant volume during shear in the Geonor DSS is reasonably valid.

Figure 6.6 shows the logarithm of normalized undrained Young's modulus (E_u/c_u) versus applied shear stress ratio (τ_h/c_u) for all the DSS tests. The data are plotted as $\log E_u/c_u$ versus τ_h/c_u since E_u/c_u is a convenient ratio to use in undrained deformation analyses and it has been correlated with field data (D'Appolonia, Poulos and Ladd, 1971). The applied shear stress ratio can be roughly equated to the reciprocal of the factor of safety. Besides this, it is easier to compare these data with previous results from CK_0 UDSS tests since this plot has been widely used for comparison of data by many researchers at MIT in the past (e.g., Ladd and Edgers, 1972; Ladd et al. 1977; Walbaum, 1988; DeGroot, 1989). The plot in Figure 6.6 shows that the data are fairly consistent and demonstrate a continuous decrease in the modulus with increasing shear stress. The normalized modulus data for all the DSS tests, except DSS 31, plot on a fairly narrow range (Figure 6.6). DSS 31 yielded consistently higher modulus values compared to the other tests. Table 6.1 summarizes the values of normalized Young's modulus at 50 % of the peak shear resistance, $E_u(50)/c_u$, and reports a value of 687 ± 112 SD (excluding DSS 31). However, Figure 6.6 and Table 6.1 show that the modulus values decrease with increase in the consolidation stress level.

6.3 Comparison of CK_0 UDSS Tests With Published Data

Tables 6.2 and 6.3 summarize the results from CK_0 UDSS tests performed on different series of resedimented BBC in the Geonor DSS over the past two decades. The CK_0 UDSS tests, selected for comparison with the writer's DSS tests, were conducted using similar testing procedures and the same strain rate during undrained shearing. Figures 6.7 through 6.11 present plots of stress paths, normalized stress-strain curves, applied shear stress ratio versus shear strain, pore pressure versus

shear strain and normalized Young's modulus versus applied shear stress ratio, respectively, for three CK_0 UDSS tests performed by DeGroot (1989) at a consolidation stress of 3 ksc. The data are later compared using similar plots in Figures 12 to 17 with the writer's DSS tests performed at consolidation stresses ranging from 1.44 to 12 ksc. The three CK_0 UDSS tests selected for comparison with the writer's test data were conducted by DeGroot (1989) using SHANSEP procedures and under essentially identical test conditions on specimens from the new 200 series BBC and reportedly yielded satisfactory results. Tables 6.4 and 6.5 summarize the results from the CK_0 UDSS tests on specimens of BBC conducted during the various testing programs at $\sigma'_{vc} = 3$ and 12 ksc for comparison with the writer's tests at consolidation stresses ranging from 3 ksc to 12 ksc in order to evaluate the effect of consolidation stress on the normalized behavior of resedimented BBC in the Geonor DSS.

Figure 6.12 compares the stress paths from writer's DSS tests with those obtained from three CK_0 UDSS tests performed by DeGroot (1989) and shows good agreement in the shape of the curves. The curves from DeGroot's tests plot slightly above the writer's tests until the peak shear resistance, but show remarkable agreement subsequently, especially in the vicinity of maximum obliquity, with the exception of DSS 31. The results show significantly less scatter in the writer's tests at the peak strength (e.g., $c_u/\sigma'_{vc} = 0.197 \pm 0.004$ SD, COV = 2.0 % versus $c_u/\sigma'_{vc} = 0.203 \pm 0.011$ SD, COV = 5.5 %; Table 6.3).

The comparison of the stress-strain curves (Figure 6.13) show comparatively greater consistency in the data from tests performed for this research. DeGroot's tests show that the peak shear resistance was reached at somewhat smaller shear strains, which is in agreement with the findings from the analysis of the writer's tests in the preceding section, i.e., γ_f decreases with decrease in the consolidation stress. The stress-strain curves beyond the peak shear resistance for all the tests show similar strain softening behavior (Figure 6.14).

The normalized pore pressure data, plotted in Figure 6.15, show very good agreement in all the tests, with the exception of DSS 14 and especially DSS 31. Significantly greater pore pressures were measured during undrained shearing in DSS 31, which appear to have been caused due to some problem with the constant height DCDT (Section 6.2.2). DSS 14 had the highest consolidation stress (12 ksc) and the lowest pore pressure at strains less than about 16%. The data from all the CK_0 UDSS tests exhibit continuous increase in the excess pore pressure throughout the tests.

Figure 6.16 shows the normalized Young's modulus (E_u/c_u) versus applied shear stress ratio (τ_h/c_u) for the writer's DSS tests and the three CK_0 UDSS tests from DeGroot (1989). The data from all the tests show a fairly consistent trend of increase in the modulus value with decrease in the consolidation stress. However, DeGroot's tests yielded slightly higher values of modulus than writer's tests at $\sigma'_{vc} = 3$ ksc [e.g., $E_u(50)/c_u = 990 \pm 70$ versus 850].

Figure 6.17 is a plot of logarithm of Young' modulus normalized with respect to consolidation stress versus logarithm of shear stain. This plot shows less variation in normalized modulus than in the previous Figure 6.16. However, the results still confirm that lower consolidation stresses lead to higher values of modulus. The data from the writer's tests for shear strains less than 0.1% is generally inconsistent.

Table 6.4 summarizes the results of CK_0 UDSS tests performed on specimens from batches of BBC at consolidation stresses of 3 ksc and 12 ksc. The mean values of undrained shear parameters obtained at these two consolidation stress levels are then compared with the writer's tests performed at consolidation stresses ranging from 3 ksc to 12 ksc in Table 6.5. The normalized values at the peak shear resistance of undrained shear strength, c_u/σ'_{vc} ($c_u = \tau_{hmax}$), vertical effective stress (σ'_v/σ'_{vc}) and angle ψ ($\psi = \arctan \tau_h/\sigma'_v$) show very good agreement. The scatter observed in these parameters obtained from the writer's DSS tests at different consolidation stress levels is almost equal to that from Walbaum's three DSS tests having a consolidation stress of 12 ksc.

In contrast, the DSS tests conducted at a consolidation stress of 3 ksc indicate greater scatter in the values of these parameters than observed in the writer's tests at different consolidation stress levels. One might expect greater scatter since the results come from different sources of BBC and involved tests by several persons using both manual and automated height control. However, the three tests by DeGroot (1989) had more scatter in the normalized strength ($\text{COV} = 0.011/0.203 = 5.5\%$) than for the seven tests summarized in Table 6.5 ($\text{COV} = 4.0\%$).

6.4 Effect of Consolidation Stress Level on Normalized Behavior for DSS Tests on Normally Consolidated BBC

Figure 6.18 plots the normalized peak horizontal shear stress (τ_h/σ'_{vc}) versus consolidation stress (σ'_{vc}) for 23 CK_0UDSS tests on normally consolidated BBC. Although the data apparently show considerable scatter in the peak shear resistance, an in depth analysis of the results in Tables 6.2 and 6.3 and Figure 6.18 reveal following:

- The normalized shear strength, c_u/σ'_{vc} ($c_u = \tau_{h\max}$), from the writer's CK_0UDSS tests at stress levels ranging from 1.44 to 12 ksc is equal to 0.197 ± 0.004 SD ($\text{COV} = 2\%$), which is in excellent agreement with Ladd and Edgers, 1972 ($\tau_h/\sigma'_{vc} = 0.197 \pm 0.009$ SD from 5 CK_0UDSS tests at σ'_{vc} varying from 3 to 8 ksc) and Walbaum, 1988 ($\tau_h/\sigma'_{vc} = 0.197 \pm 0.003$ SD from one CK_0UDSS test at $\sigma'_{vc} = 3$ ksc and 3 tests at $\sigma'_{vc} \approx 12$ ksc). The tests performed by Malek (1987), DeGroot (1989) and Seah (1990) gave comparatively higher values of $\tau_h/\sigma'_{vc} = 0.201 \pm 0.010\text{SD}$, $0.203 \pm 0.011\text{SD}$, and $0.202 \pm 0.001\text{SD}$, respectively.
- Malek (1987) performed 5 CK_0UDSS tests on specimens from BBC II

which is a thixotropic material (O'Neill, 1985). The thixotropic material exhibits an increase in the preconsolidation pressure (and higher undrained shear strengths) with increase in the storage time. Hence, the small increase in the measured normalized peak shear resistance (i.e., a difference of 2% versus the author's tests) may have been caused by a difference in the material properties of this BBC (see Chapter 4). Thixotropy may have contributed to Malek's large scatter, although DeGroot (1989) obtained similar scatter with the non-thixotropic BBC III.

- An increase of about 2.5 to 3% in the measured normalized undrained shear strength reported by DeGroot (1989) and Seah (1990) may result from the fact that the tests were conducted at low consolidation stress levels.
- An analysis of the strength data from the writer's DSS tests at consolidation stresses ranging from 1.44 ksc to 12 ksc gave the following linear regression line ($r^2 = 0.69$):

- $$c_u/\sigma'_{vc} = 0.2016 - 0.00076\sigma'_{vc} \text{ (ksc)} \quad (6.3)$$

- The following relationship is obtained from linear regression analysis of strength data from all the CK_0 UDSS tests on BBC, conducted at consolidation stress ranging from 1.12 ksc to 12 ksc, plotted in Figure 6.18 ($r^2 = 0.09$):

- $$c_u/\sigma'_{vc} = 0.2017 - 0.00056\sigma'_{vc} \text{ (ksc)} \quad (6.4)$$

- Although the linear regression analyses of the strength data give almost

identical relationships (Equations 6.3 and 6.4), comparatively much less scatter is observed in the writer's test data compared to the combined analyses on all the test.

- The normalized undrained shear strength (c_u/σ'_{vc}) computed using Equation 6.2 varies from 0.201 to 0.195 for consolidation stress ranging from 1 ksc to 12 ksc.

The preceding analyses reveal that the variation in the mean strength (c_u/σ'_{vc}) for a wide range of consolidation stresses is not significant from a practical viewpoint, considering the multifarious factors which can influence the undrained shear strength of cohesive soils. Hence, it is concluded that normally consolidated resedimented BBC exhibits good normalized behavior with respect to the undrained shear strength, c_u/σ'_{vc} ($c_u = \tau_{hmax}$), in the Geonor DSS.

The plot of shear strain at the peak horizontal stress (γ_f) for all the CK_0 UDSS tests (Figure 6.19) shows that γ_f varies from approximately 3 to 8% for consolidation stress ranging from 1.3 to 12 ksc. The summarized values of γ_f for 23 CK_0 UDSS tests in Table 6.2 exhibit a definite trend of increase in γ_f with increase in the consolidation stress (linear regression shows $\gamma_f = 4.5 + 0.267\sigma'_{vc}$, $r^2 = 0.27$). The average value of γ_f is equal to approximately 6 % from the author's five DSS tests at variable consolidation stress levels, which falls between the average values obtained from other CK_0 UDSS tests conducted at $\sigma'_{vc} = 3$ ksc and 12 ksc (Table 6.5).

Figure 6.20, which is a plot of normalized vertical effective stress (σ'_v/σ'_{vc}) at the peak strength versus consolidation stress (σ'_{vc}), shows relatively large scatter in the values of σ'_v/σ'_{vc} at lower consolidation stress levels, i.e., $\sigma'_{vc} \leq 3$ ksc. The linear regression performed on 23 CK_0 UDSS tests suggests that the vertical effective stress ratio decreases slightly with an increase in the consolidation stress level ($\sigma'_v/\sigma'_{vc} = 0.560 - 0.002\sigma'_{vc}$, $r^2 = .04$), but is not significant from a practical viewpoint.

Figure 6.21 plots $(\Delta u/\sigma'_{vc})_f$ versus γ_f from 23 CK₀UDSS tests conducted on BBC during the various testing programs. The data in Figure 6.20 indicated little variation in the mean σ'_v/σ'_{vc} at the peak strength with increase in the consolidation stress. Hence $\Delta u/\sigma'_{vc} = 1 - \sigma'_v/\sigma'_{vc}$ also should remain fairly constant. The writer's data also indicated that increasing σ'_{vc} causes lower pore pressure versus shear strain (Figure 6.4), but an increase in the strain at failure (Table 6.1). Hence these two trends tend to cancel each other, but not completely since the data in Figure 6.21 show a general trend of increasing $\Delta u/\sigma'_{vc}$ with increasing γ_f . For the data with γ_f equal 4 to 9%, linear regression gives $\Delta u/\sigma'_{vc} = 0.366 + 0.015 \gamma$ (%) with $r^2 = 0.37$.

The plot of angle ψ ($\psi = \arctan \tau_h/\sigma'_{vc}$) at peak horizontal shear stress versus consolidation stress (Figure 6.22) shows a significant scatter in the values of ψ , especially at low consolidation stresses. The linear regression on the data from 23 DSS tests ($\psi = 20.01 + 0.009\sigma'_{vc}$ (°), $r^2 = 0.0005$) show a slight increase in the value of angle ψ with a large scatter in the results. Table 6.3 summarizes the mean values of angle ψ from tests reported by various researchers at MIT. The mean value of angle ψ at peak τ_h varies from 19.4° to 20.5° with the exception of the tests conducted by Seah (1990) at $\sigma'_{vc} = 1.12$ and 1.3 ksc (i.e., σ'_{vc} less than $1.5 \times \sigma'_p$). The mean value of angle ψ obtained from the writer's tests (i.e., $\psi = 20.4^\circ \pm 0.50^\circ$ SD; excluding DSS 31) falls within the range of average values from various tests. Figure 6.23, which is a plot of angle ψ at $(\tau_h/\sigma'_{vc})_{max}$ versus strain at failure, γ_f , demonstrates a general trend of increase in angle ψ with increase in the strain at failure ($\psi = 19.01 + 0.178\gamma_f$, $r^2 = 0.07$). DeGroot (1989) based on the analyses of data from 30 different normally consolidated soils tested in the Geonor DSS found that the vertical effective stress ratio lies within a narrow band ($\sigma'_v/\sigma'_{vc} = 0.598 \pm 0.051SD$) and as a result there is a strong correlation between angle ψ and $(\tau_h/\sigma'_{vc})_{max}$.

Figure 6.24 plots normalized undrained shear modulus at 50 % of the peak shear resistance, $E_u(50)/c_u$, versus consolidation stress from 23 CK₀UDSS tests. It shows a

fairly large scatter in the values of $E_u(50)/c_u$, especially at low consolidation stress levels. The summarized results in Tables 6.2 and 6.3 and Figure 6.24 demonstrate a strong trend of decrease in moduli with increase in the consolidation stress level (based on linear regression performed on the moduli data from 23 CK_0 UDSS tests on BBC, $E_u(50)/c_u = 943.7 - 43.6\sigma'_{vc}$, $r^2 = 0.48$). The stress-strain data in Figure 6.2 and the $\log(E_u(50)/\sigma'_{vc})$ versus σ'_{vc} plot in Figure 6.25 also demonstrate that the stiffness decreases with increase in the consolidation stress. Ladd and Edgers (1972) reported a value of $E_u(50)/c_u = 554 \pm 154$ SD from 5 CK_0 UDSS tests, which compares reasonably well with the writer's tests, i.e., $E_u(50)/c_u = 687 \pm 112$ SD (excluding DSS 31), and based on comparison with the other types of consolidated-undrained strength tests, they concluded that " In general, DSS tests yield more consistent stress strain moduli than were obtained with the plane strain and triaxial tests."

Tables 6.2 and 6.3 also compare the values of γ , τ_h/σ'_{vc} , σ'_v/σ'_{vc} and angle ψ at large strains, i.e., $\gamma > 25$ %. The stress-strain curves in Figure 6.13 exhibit significant strain softening with continued straining beyond the peak shear resistance. DeGroot (1989) investigated the strain softening behavior of the normally consolidated cohesive soils as measured in the Geonor CK_0 UDSS testing. Based on a thorough analyses of post peak behavior measured in 100 CK_0 UDSS tests on 30 different soils tested at MIT, he found that due to the nonuniformity of the vertical stresses in the Geonor DSS, the device "unloads" the specimen more than the actual pore pressure developed during undrained shearing with increasing large strains. Thus the influence of the device on the measured strain softening response of a DSS specimen is significant at large shear strains. However, the precise effect of the device on the measured strain softening response of normally consolidated specimens can not be quantified.

Table 6.3 reports that the mean angle ψ at strains greater than $\gamma = 25$ % varies from 28° to 33.5° . The angle ψ measured in the author's tests averaged $29.5^\circ \pm 1.6^\circ$ SD (excluding DSS 31) at shear strains of about 25 %, which compares well with the

results obtained by DeGroot (1989) from 3 DSS tests at the same shear strain (i.e., $\psi = 29.7^\circ \pm 2.0^\circ$ SD) and also shows good agreement with the results reported by Ladd and Edgers (1972) at maximum obliquity (i.e., $\psi = 31.8^\circ \pm 3.7^\circ$ SD versus $\psi = 31.6^\circ \pm 3.0^\circ$ SD from the writers tests). In many of the tests summarized in Table 6.2, it was reported that τ_h/σ'_v was still increasing even though the shear strain exceeded 25 %. The mean angle ψ at maximum obliquity from the CK_0 UDSS tests compares reasonably well with angle ϕ' in K_0 -consolidated-undrained triaxial compression tests at maximum obliquity ($\phi'_{m0} = 34^\circ \pm 0.5^\circ$ SD from the CK_0 UC tests on BBC, Sheahan, 1990). However, the influence of the membrane distortion, the rotation of principal stresses and the suspected influence of the device should be considered when using the parameters obtained from the CK_0 UDSS tests at large shear strains for design.

6.5 Summary and Conclusions

Five K_0 -consolidated-undrained shear tests were performed in MIT's Geonor DSS on specimens from batches of resedimented BBC III at consolidation stress levels ranging from 1.44 ksc to 12 ksc (Table 6.1). The tests yielded very consistent stress-strain-strength data, with the exception of DSS 31 ($\sigma'_{vc} = 3$ ksc), which presumably had a problem with the constant height DCDDT during undrained shearing. However, these data do indicate deviation from "perfect normalized behavior", especially regarding stiffness (modulus). A comparison of data from the writer's tests show excellent agreement with prior data from CK_0 UDSS tests on BBC.

Based on the experimental results and the analysis presented in the previous sections, the following conclusions are drawn regarding the normalized undrained shear behavior of resedimented BBC III in the Geonor CK_0 UDSS testing:

- The writer's tests at different consolidation stress levels demonstrate

good normalized behavior with respect to the undrained shear strength, ($c_u/\sigma'_{vc} = 0.197 \pm 0.004$ SD, COV = 2 %) and much less scatter in the undrained shear results compared to the prior data on BBC.

- Linear regression on the undrained shear strength ratio versus consolidation stress (Equation 6.4) based on 23 CK_0 UDSS tests on BBC in the Geonor DSS (Figure 6.18) show a variation in c_u/σ'_{vc} decreasing from 0.201 to 0.195 for consolidation stresses ranging from 1 ksc to 12 ksc. This small variation in the undrained shear strength ratio over a significant range of consolidation stresses is considered very small from a practical viewpoint.
- The measured data throughout the test program yielded very similar normalized stress–strain curves (Figure 6.2) and stress paths (Figure 6.1), despite substantial differences in the consolidation stresses. However, the strain at failure (γ_f) increases with increase in the consolidation stress, yielding a mean value of γ_f increasing from 4% to 8% for consolidation stress ranging from 1.44 to 12 ksc.
- The normally consolidated specimens develop positive excess pore pressures (Figure 6.4), which increase continuously with undrained shearing, i.e., the test material exhibits contractive behavior with continued straining. The data suggest that $\Delta u/\sigma'_{vc}$ versus shear strain decreases with increasing consolidation stress (although DSS 31 follows this trend, the pore pressures are believed to be too high due to problems with the height controller).
- A fairly constant value of σ'_v/σ'_{vc} at the peak shear resistance (Figure 6.20) supports DeGroot's (1989) conclusion that a strong correlation exists between the angle ψ ($= \arctan \tau_h/\sigma'_{vc}$) and $(\tau_h/\sigma'_{vc})_{max}$.

- The author's data show a definite trend of decreasing E_u/c_u versus applied shear stress ratio (τ_h/c_u) with increasing consolidation stress (Figure 6.6). This trend is supported by the collective, but more scattered, data previously obtained at MIT in terms of $E_u(50)/c_u$ (Figure 6.24). $E_u(50)/\sigma'_{vc}$ follows a similar trend (Figure 6.25)
- The values of the shear stress and vertical effective stress ratios (τ_h/σ'_{vc} and σ'_v/σ'_{vc}) decrease continuously with straining beyond the peak shear resistance and the value of angle ψ approaches approximately 32° at very large strains, i.e., $\gamma \simeq 33\%$, which compares well with the previous research. The value of angle ψ at maximum obliquity compares fairly well with the angle ϕ' at maximum obliquity from the K_o -consolidated- undrained triaxial compression tests ($\phi'_{m0} = 34^\circ \pm 0.5^\circ$ SD from CK_oUC tests on BBC, Sheahan, 1990).

The experimental study reveals that the data obtained from the Geonor DSS at the maximum obliquity is much more scattered than at the peak shear strength. In many of the tests (Table 6.2) it was found that τ_h/σ'_v was still increasing even though the shear strains exceeded 25%. A considerable distortion of the sample membrane and a large rotation of the principal stresses (see Chapter 2) occur at large shear strains. The experimental data show significant strain softening at large shear strains. DeGroot (1989) based on the analyses of 100 CK_oUDSS tests on 30 different normally consolidated soils and DSS tests on rubber specimens found that due to nonuniform vertical stress conditions in the Geonor DSS, the device "unloads" the specimen more than the actual pore pressure developed during the undrained shearing. Thus the influence of the device on the measured strain softening response increases with continued straining beyond the peak shear resistance. Although the undrained shear parameters at large shear strains from the Geonor DSS tests may appear reasonable,

the influence of sample membrane distortion, rotation of principal shear stresses, and the suspected influence of the device should be considered when using these parameters in design.

Table 6.1: Summary of Geonor CK₀UDSS Tests on Normally Consolidated BBC III

Test No.	Batch No. w _c (%)	σ' _{vc} (ksc)	At Peak τ _h				At τ _h /σ' _v max				<u>E_u(50)</u>	Remarks
			γ (%)	$\frac{\tau_h}{\sigma'_v}$	$\frac{\sigma'_v}{\sigma'_{vc}}$	$\frac{\tau_h}{\sigma'_v}$ ψ°	γ (%)	$\frac{\tau_h}{\sigma'_{vc}}$	$\frac{\sigma'_v}{\sigma'_{vc}}$	$\frac{\tau_h}{\sigma'_v}$ ψ°	C _u	
DSS14	207T 40.55	11.992	7.71	0.194	0.536	0.363 19.95	32.80	0.093	0.174	0.539 28.32	619	
DSS18	207MB 40.66	9.030	6.55	0.192	0.523	0.366 20.11	32.90	0.088	0.146	0.598 30.88	610	
DSS22	207MB 40.64	5.992	6.30	0.197	0.523	0.377 20.66	29.65	0.111	0.182	0.612 31.47	670	
DSS25	207B 40.78	2.955	5.61	0.202	0.526	0.385 21.06	36.71	0.075	0.105	0.715 35.56	850	
DSS31	205M 40.48	1.441	4.10	0.199	0.485	0.410 22.29	33.45	0.094	0.079	1.196 50.10	1240	low σ' _v /σ' _{vc} and high values of ψ
Mean ±1 SD	40.62 0.11		6.05 1.33	0.197 0.004	0.527 0.006	0.373 0.010 20.44 0.51	33.02 2.89	0.092 0.015	0.152 0.035	0.615 0.084 31.60 3.00	687 112	Mean values include only peak γ & τ _h /σ' _{vc} from DSS 31.

- Notes:
- 1 dγ/dt = 5% ± per hour.
 - 2 w_c = Initial water content.
 - 3 ψ = arctan (τ_h/σ' _v).

Table 6.2: Results of Geonor CK₀UDSS Tests on Different Series of Normally Consolidated BBC Sheet 1/2

Reference (Series)	Test No.	Batch No.	w _c (%)	σ'vc (ksc)	ε _v (%)	At Peak τ _h					At τ _h /σ'v Maximum					E _u (50) c _u	Remarks
						γ (%)	$\frac{\tau_h}{\sigma'_{vc}}$	$\frac{\sigma'_x}{\sigma'_{vc}}$	$\frac{\tau_h}{\sigma'_v}$	ψ (°)	γ (%)	$\frac{\tau_h}{\sigma'_{vc}}$	$\frac{\sigma'_x}{\sigma'_{vc}}$	$\frac{\tau_h}{\sigma'_v}$	ψ (°)		
Ladd & Edgers, 1972 (BBC Ib)	202	200	37.4	4.0	15.5	6.0	0.211	0.566	0.372	20.4	32.5	0.128	0.199	0.643	32.8	470	
	301	300	37.2	3.0	13.7	4.5	0.199	0.575	0.346	19.1	33.1	0.098	0.141	0.695	34.8	750	
	303	300	35.6	8.0	17.0	6.2	0.194	0.565	0.342	18.9	29.8	0.111	0.210	0.525	27.7	400	
	1301	1300	35.2	4.0	9.9	5.4	0.187	0.567	0.330	18.3	Not Reached					685	
	1303	1300	35.6	8.0	15.0	9.0	0.196	0.531	0.369	20.3	Not Reached					465	
	Mean ±S.D	-	-	36.2 1.0	-	-	6.2 1.7	0.197 0.009	0.561 0.017	0.352 0.018	19.4 0.9	31.8 1.8	0.112 0.015	0.184 0.037	0.621 0.087	31.8 3.7	554 154
Malek, 1987 (BBC II)	S1	111	39.8	3.1	10.1	2.4	0.201	0.592	0.340	18.8	Data Not Available					850	Low γ @ τ _{hmax}
	S2	111	39.7	3.1	10.1	10.7	0.192	0.447	0.430	23.2	Data Not Available					530	Good test
	S3	111	39.2	4.0	10.8	6.8	0.214	0.515	0.416	22.6	Data Not Available					700	Good test
	S4	111	39.5	4.0	10.0	6.8	0.195	0.505	0.386	21.1	Data Not Available					550	Good test
	S5	112	39.2	6.0	16.4	3.5	0.222	0.678	0.327	18.1	Data Not Available					680	High τ _{hmax}
	Mean ±S.D	-	-	39.6 0.3	-	-	6.7 3.4	0.201 0.010	0.515 0.060	0.393 0.040	21.4 2.0	Data Not Available					662 129

Table 6.2 (Continued)

Sheet 2/2

Reference (Series)	Test No.	Batch No.	w_c (%)	σ'_{vc} (ksc)	ϵ_v (%)	At Peak τ_h					At τ_h/σ'_v Maximum					$E_u(50)$ C_u	Remarks
						γ (%)	$\frac{\tau_h}{\sigma'_{vc}}$	$\frac{\sigma'_x}{\sigma'_{vc}}$	$\frac{\tau_h}{\sigma'_v}$	ψ (°)	γ (%)	$\frac{\tau_h}{\sigma'_{vc}}$	$\frac{\sigma'_x}{\sigma'_{vc}}$	$\frac{\tau_h}{\sigma'_v}$	ψ (°)		
Walbaum, 1988 (BBC III)	1	200	39.9	12.2	-	8.1	0.202	0.538	0.376	20.6	30.1	0.109	0.215	0.507	26.9	590	Incr. Consol.
	2	201	40.6	11.4	-	8.2	0.184	0.462	0.398	21.7	24.0	0.127	0.243	0.523	27.6	515	CRSC (low τ_f)
	3	201	41.5	11.6	-	6.0	0.195	0.543	0.359	19.8	27.4	0.114	0.219	0.521	27.2	420	CRSC
	4	201	40.9	11.4	-	6.8	0.194	0.545	0.356	19.6	27.5	0.104	0.202	0.515	27.2	370	Incr. Consol.
	5	202	41.1	3.0	11.7	4.9	0.195	0.600	0.325	18.0	31.0	0.105	0.176	0.597	30.8	830	
	Mean \pm S.D	-	-	40.9 0.6	-	-	6.4 1.3	0.197 0.003	0.556 0.029	0.354 0.021	19.5 1.1	29.0 1.8	0.108 0.005	0.203 0.019	0.525 0.042	28.1 1.8	553 208
DeGroot, 1989 (BBC III)	G1	200	41.1	3.0	14.6	4.7	0.191	0.561	0.340	18.8	24.9	0.133	0.252	0.516	27.8	930	Poor ϵ_v data.
	G2	200	40.8	3.0	15.3	5.4	0.213	0.528	0.403	22.0	25.0	0.132	0.214	0.627	31.7	970	Poor ϵ_v data.
	G4	200	41.0	3.0	15.2	5.5	0.205	0.542	0.379	20.7	24.4	0.134	0.237	0.593	29.5	1070	Poor ϵ_v data.
	Mean \pm S.D	-	-	41.0 0.2	3.0 0.4	15.0 0.4	5.2 0.4	0.203 0.011	0.544 0.017	0.374 0.032	20.5 1.6	24.8 0.3	0.133 0.001	0.234 0.019	0.579 0.057	29.7 2.0	990 72
Seah, 1990 (BBC III)	DSS6	203	40.5	1.12	5.1	2.5	0.201	0.667	0.301	16.8	24.2	0.095	0.153	0.621	31.8	925	Low σ'_{vc} .
	DSS7	204	40.1	1.30	5.2	3.1	0.202	0.606	0.333	18.4	26.2	0.111	0.158	0.702	35.1	876	Low σ'_{vc} .
	Mean \pm S.D	-	-	40.3 0.3	-	-	2.8 0.4	0.202 0.001	0.637 0.043	0.317 0.023	17.6 1.1	25.2 1.4	0.103 0.011	0.156 0.004	0.662 0.057	33.5 2.3	901 -

Table 6.3: Summary of Results from Geonor CK₀UDSS Tests on Normally consolidated BBC

Reference (Series)	Number of Tests Series	Stress Range (ksc)	At Peak τ_h					At τ_h/σ'_v Maximum					$E_u(50)$ C_u	Remarks
			γ (%)	$\frac{\tau_h}{\sigma'_{vc}}$	$\frac{\sigma'_x}{\sigma'_{vc}}$	$\frac{\tau_h}{\sigma'_v}$	ψ (°)	γ (%)	$\frac{\tau_h}{\sigma'_{vc}}$	$\frac{\sigma'_x}{\sigma'_{vc}}$	$\frac{\tau_h}{\sigma'_v}$	ψ (°)		
Ladd & Edgers (1972)	5 BBC Ib	3-8	6.2	0.197	0.561	0.352	19.4	31.8	0.112	0.184	0.621	31.8	554	
			1.7	0.009	0.017	0.018	0.9	1.8	0.015	0.037	0.087	3.7	154	
Malek (1987)	4 BBC II	3-4	6.7 3.4	0.201 0.010	0.515 0.060	0.393 0.040	21.4 2.0	33.1	0.098	0.141	0.695	34.8	750	
Walbaum (1988)	4 BBC III	3-12	6.4	0.197	0.556	0.354	19.5	29.8	0.108	0.203	0.535	28.1	553	
			1.3	0.003	0.029	0.021	1.1	1.8	0.005	0.019	0.042	1.8	208	
DeGroot (1989)	4 BBC III	3	5.2 0.4	0.203 0.011	0.554 0.017	0.374 0.032	20.5 1.6	24.8 0.3	0.133 0.001	0.234 0.019	0.579 0.057	29.7 2.0	990 72	
Seah (1990)	2 BBC III	1.1-1.3	2.8 0.4	0.202 0.001	0.637 0.043	0.317 0.023	17.6 1.1	25.2 1.4	0.103 0.011	0.156 0.004	0.662 0.057	33.5 2.3	901 30	Low σ'_v/σ'_{vc} . High angle ψ .
This Research	5 BBC III	1.5-12	6.1	0.197	0.527	0.373	20.4	33.0	0.092	0.152	0.615	31.6	798	From Table 6.1 *
			1.3	0.004	0.006	0.010	0.5	2.9	0.015	0.035	0.084	3.0	265	
	4 BBC III	3-12	-	-	-	-	-	25.0 0.1	0.133 0.006	0.239 0.015	0.560 0.044	29.5 1.6	687 112	@ $\gamma = 25\%$

- Notes:
1. Individual test data summarized in this Table can be found in Tables 6.1 and 6.2.
 2. Average for Malek (1987) and Walbaum (1988) exclude Test S5 and 2, respectively (Table 6.2).
 3. All values are average \pm one standard deviation.
- * Average values exclude DSS 31 except for peak γ and τ_h/σ'_{vc} .

Table 6.4: Results from Geonor CK_0 UDSS Tests at Various Stress Levels on Normally Consolidated BBC

Reference (Series)	Test No.	Batch No.	w_c (%)	σ'_{vc} (ksc)	At Peak τ_h					At τ_h/σ'_v Maximum					$E_u(50)$ C_u	Remarks
					γ (%)	$\frac{\tau_h}{\sigma'_{vc}}$	$\frac{\sigma'_y}{\sigma'_{vc}}$	$\frac{\tau_h}{\sigma'_v}$	ψ (°)	γ (%)	$\frac{\tau_h}{\sigma'_{vc}}$	$\frac{\sigma'_y}{\sigma'_{vc}}$	$\frac{\tau_h}{\sigma'_v}$	ψ (°)		
Walbaum, 1988 (BBC III)	1	200	39.9	12.2	8.1	0.202	0.538	0.376	20.6	30.1	0.109	0.215	0.507	26.9	590	Incr. Consol.
	3	201	41.5	11.6	6.0	0.195	0.543	0.359	19.8	27.4	0.114	0.219	0.521	27.2	420	CRSC
	4	201	40.9	11.4	6.8	0.194	0.545	0.356	19.6	27.5	0.104	0.202	0.515	27.2	370	Incr. Consol.
	Mean ±1 SD			40.8 0.8	11.7 0.4	7.0 1.1	0.197 0.004	0.542 0.004	0.364 0.010	20.0 0.5	28.3 1.5	0.109 0.005	0.212 0.009	0.514 0.007	27.1 0.2	460 115
L&E, 1972*	301	300	37.2	3.0	4.5	0.199	0.575	0.346	19.1	33.1	0.098	0.141	0.695	34.8	750	* (BBC Ib)
Malek, 1987 (BBC II)	S1	111	39.8	3.1	2.4	0.201	0.592	0.340	23.2	Data Not Available					850	Low γ @ τ_{hmax}
	S2	111	39.7	3.1	10.7	0.192	0.447	0.430	18.8	Data Not Available					530	Good Test
Walbaum†	5	202	41.1	3.0	4.9	0.195	0.600	0.325	18.0	31.0	0.105	0.176	0.597	30.8	830	† (BBC III)
DeGroot, 1989 (BBC III)	G1	200	41.1	3.0	4.7	0.191	0.561	0.340	18.8	24.9	0.133	0.252	0.516	27.8	930	Poor ϵ_v data.
	G2	200	40.8	3.0	5.4	0.213	0.528	0.403	22.0	25.0	0.132	0.214	0.627	31.7	970	Poor ϵ_v data.
	G4	200	41.0	3.0	5.5	0.205	0.542	0.379	20.7	24.4	0.134	0.237	0.593	29.5	1070	Poor ϵ_v data.
Mean ±1 SD			40.1 1.4	3.0 -	5.4 2.5	0.199 0.008	0.549 0.055	0.366 0.039	20.1 1.9	27.7 -	0.120 0.017	0.203 0.111	0.606 0.065	30.9 2.6	847 174	
This Research	Mean ±S.D	205 207	40.6 0.1	1.4to 12.0	6.1 1.3	0.197 0.004	0.527 0.006	0.373 0.010	33.0 2.9	20.4 0.5	0.092 0.015	0.152 0.035	0.615 0.084	31.6 3.0	687 112	From Table 6.1.

Note: The results from DeGroot (1989) reported under $(\tau_h/\sigma'_{vc})_{max}$ are at $\gamma \approx 25\%$.

Table 6.5: Comparison of Results with CK_0 UDSS Tests at Same σ'_{vc} on Normally Consolidated BBC

Reference	Number of Tests	w_c (%)	σ'_{vc} (ksc)	At Peak τ_h					$\frac{E_u(50)}{c_u}$	Remarks
				γ (%)	$\frac{\tau_h}{\sigma'_{vc}}$	COV \ddagger	$\frac{\sigma'_v}{\sigma'_{vc}}$	ψ ($^\circ$)		
Walbaum, 1988	3	40.8 0.8	11.7 0.4	7.0 1.1	0.197 0.003	2.0 -	0.542 0.004	20.0 0.5	460 115	Results from Table 6.4.
Table 6.4	7	40.1 1.4	3.0 -	5.4 2.5	0.199 0.008	4.0 -	0.549 0.055	20.1 1.9	847 174	Results from Table 6.4
This Research	4	40.7 0.1	12, 9 6, 3	6.5 1.3	0.196 0.004	2.0 -	0.527 0.006	20.4 0.5	687 112	Results from Table 6.1

- Notes: 1. All values are average \pm one standard deviation.
 2. Individual test data summarized in this Table can be found in Tables 6.1 and 6.4.
 \ddagger COV = Coefficient of Variation (τ_h/σ'_{vc}) = SD/Mean .

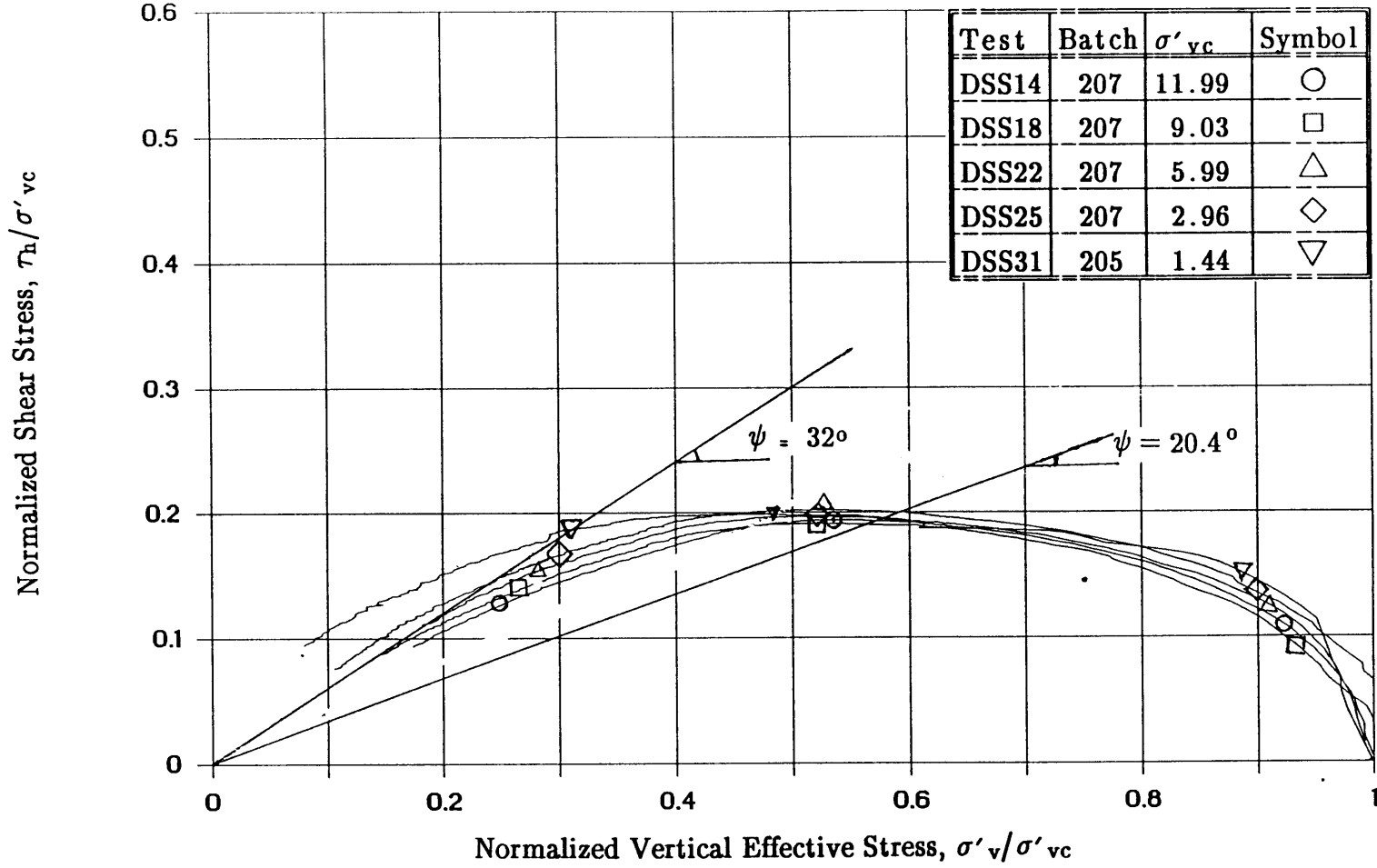


Figure 6.1: Normalized Stress Paths from CK_0 UDSS Tests on Normally Consolidated Boston Blue Clay.

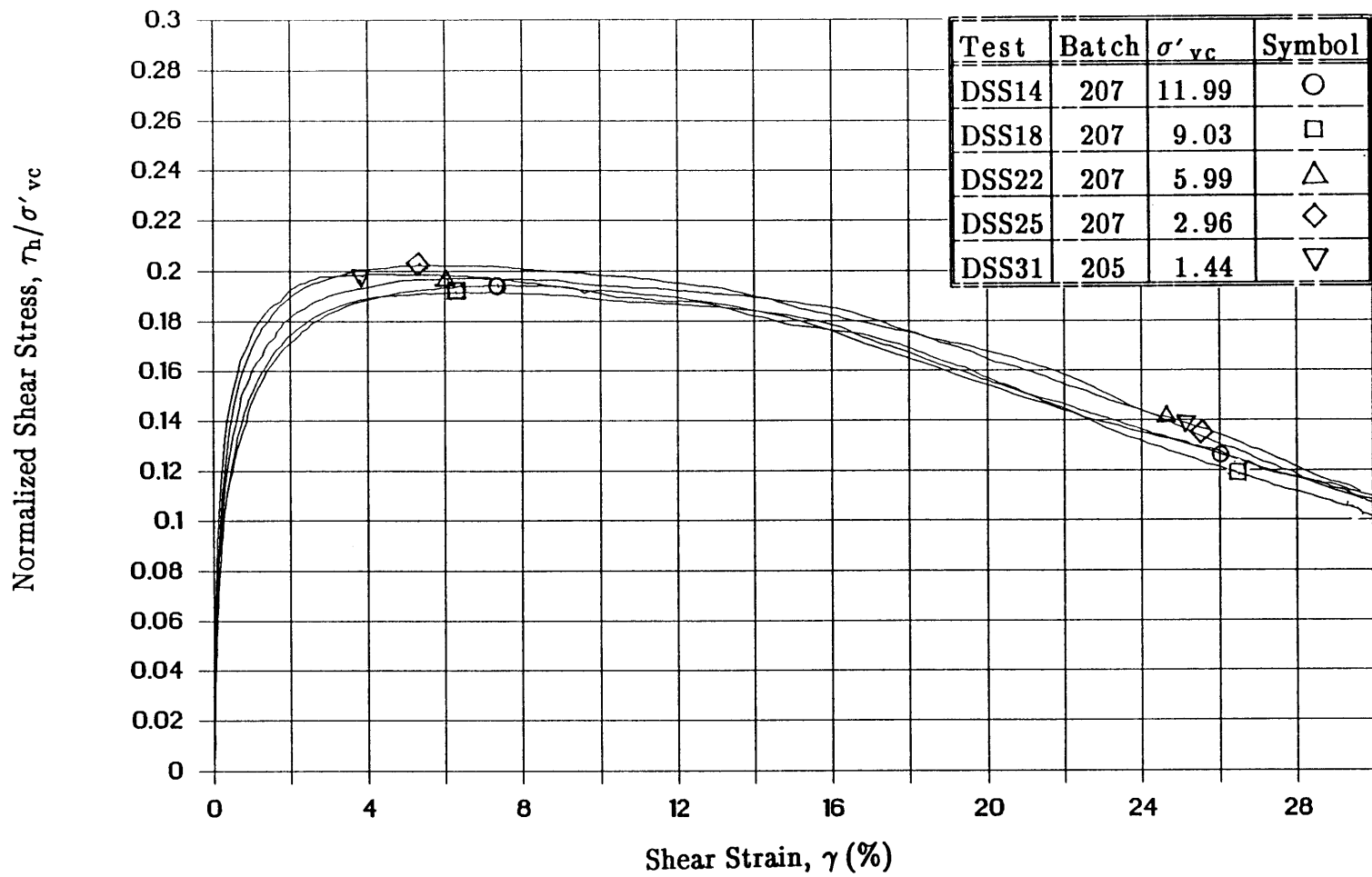


Figure 6.2: Normalized Shear Stress Versus Shear Strain from CK_0 UDSS Tests on Normally Consolidated Boston Blue Clay.

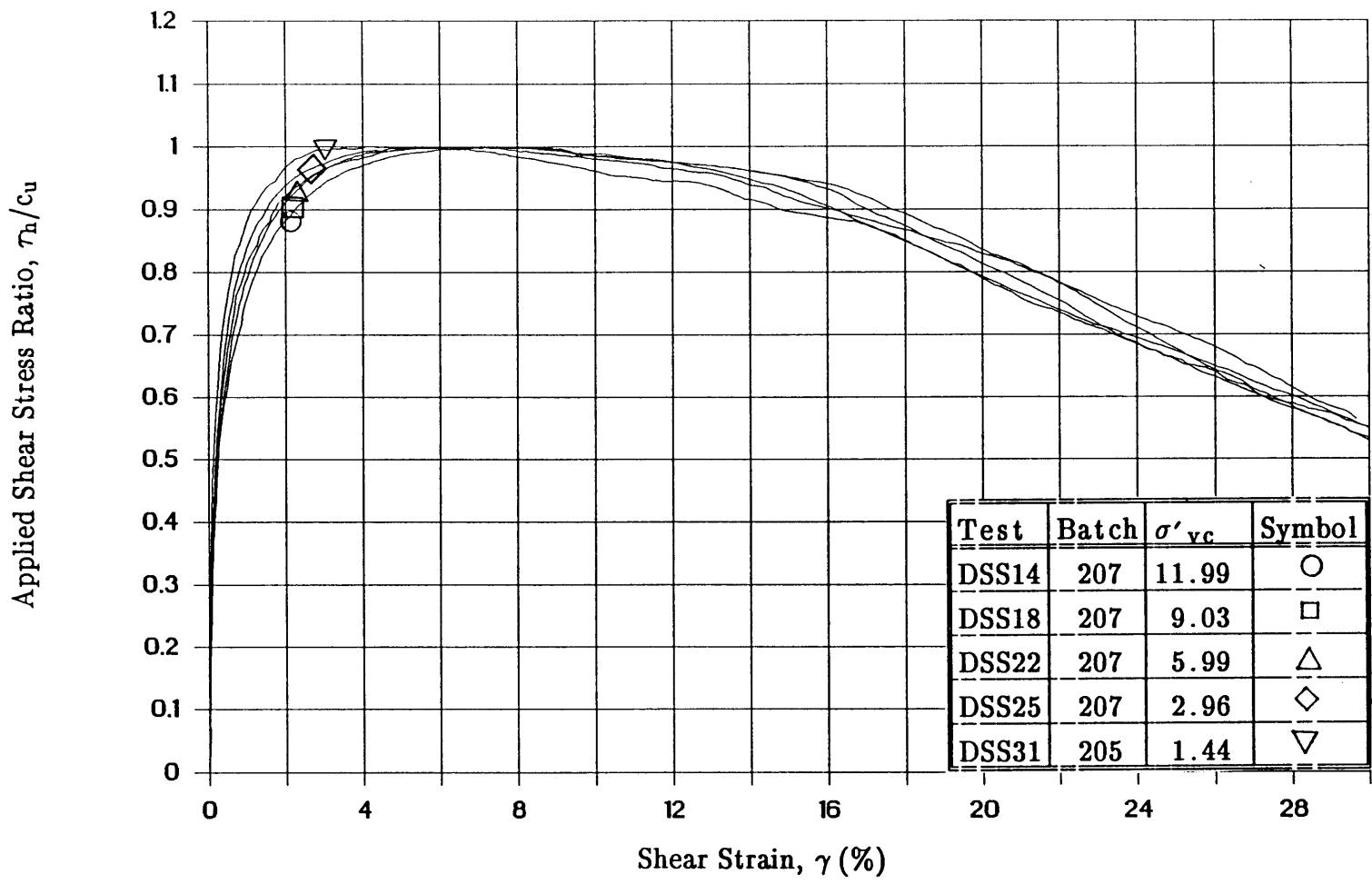


Figure 6.3: Applied Shear Stress Ratio Versus Shear Strain from CK_0 UDSS Tests on Normally Consolidated Boston Blue Clay.

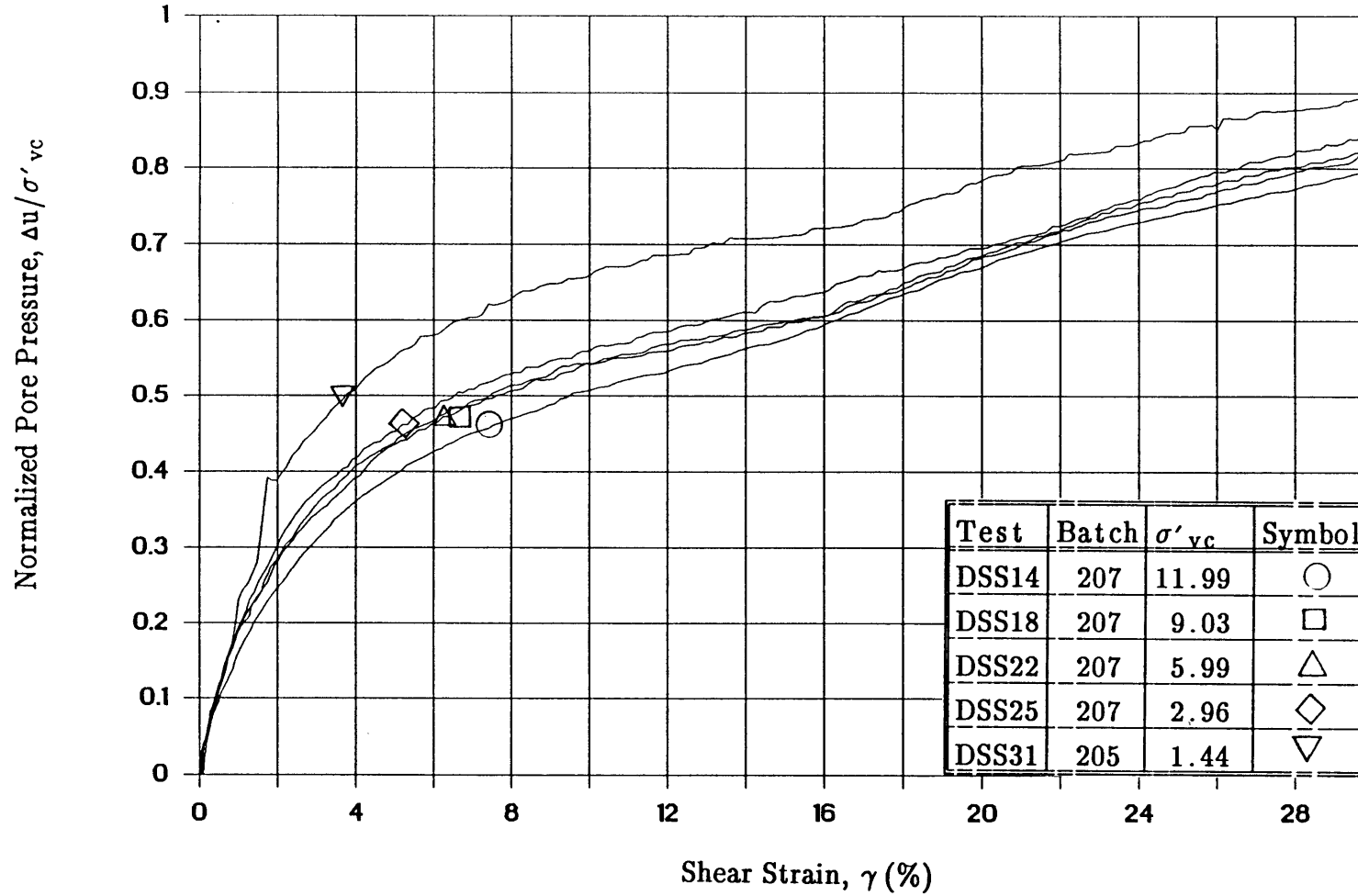


Figure 6.4: Normalized Pore Pressure Versus Shear Strain from CK_0 UDSS Tests on Normally Consolidated Boston Blue Clay.

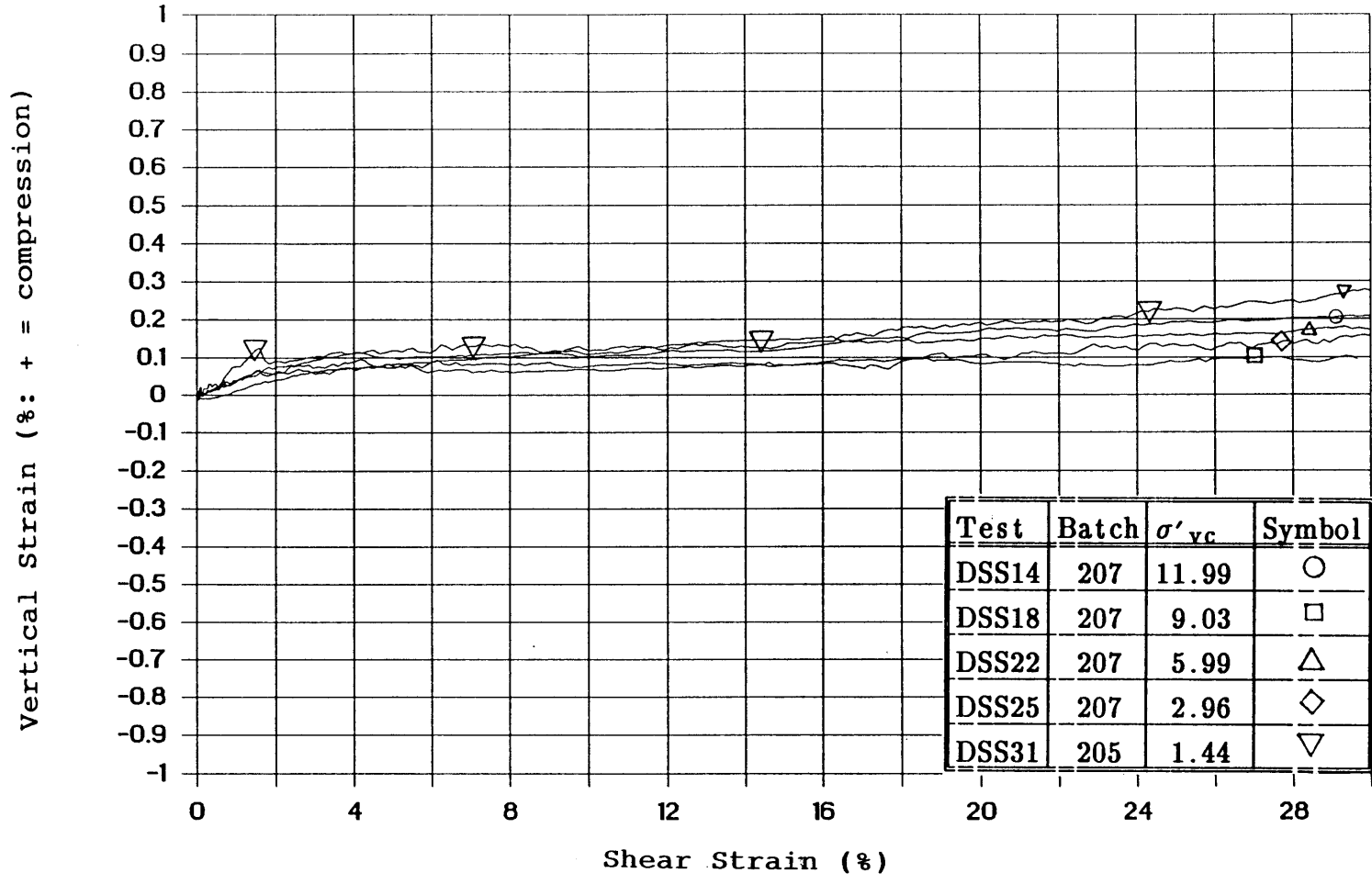


Figure 6.5: Vertical Strain Versus Shear Strain from CK_0 UDSS Tests on Normally Consolidated Boston Blue Clay.

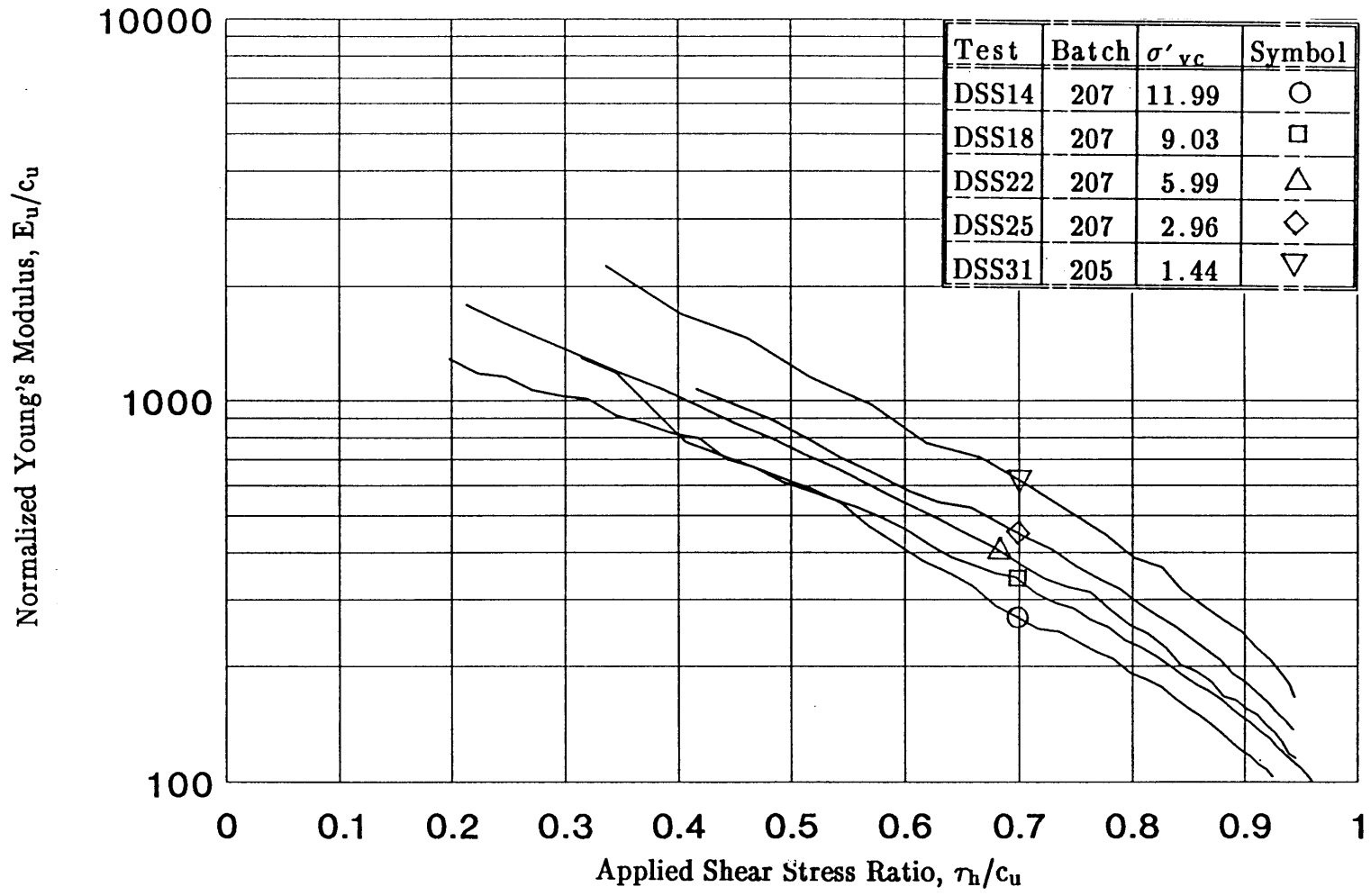


Figure 6.6: Normalized Undrained Young's Modulus Versus Applied Shear Stress Ratio from CK_0 UDSS Tests on Normally Consolidated Boston Blue Clay.

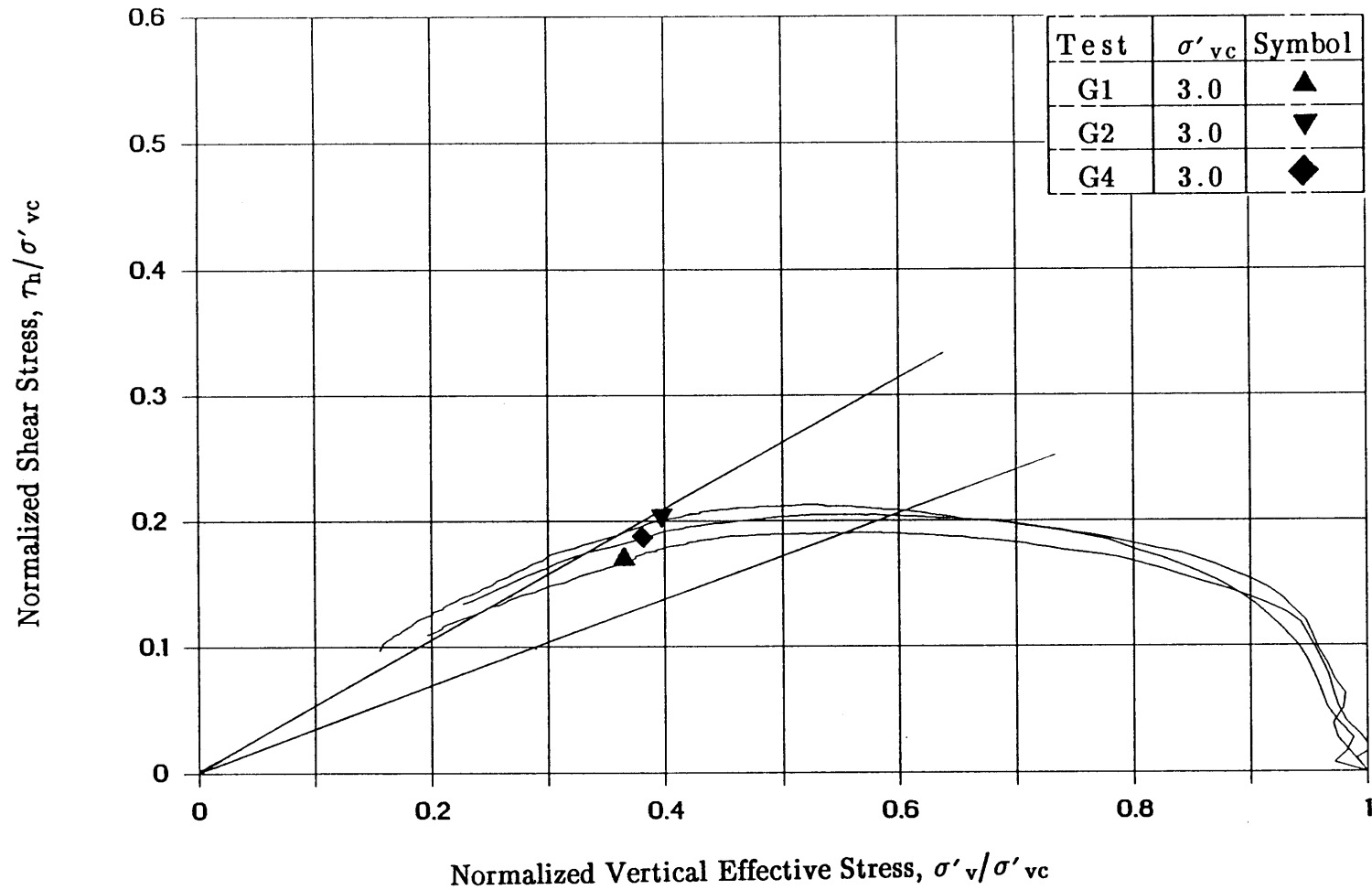


Figure 6.7: Normalized Stress Paths from CK_0 UDSS Tests on Normally Consolidated Boston Blue Clay (From DeGroot, 1989).

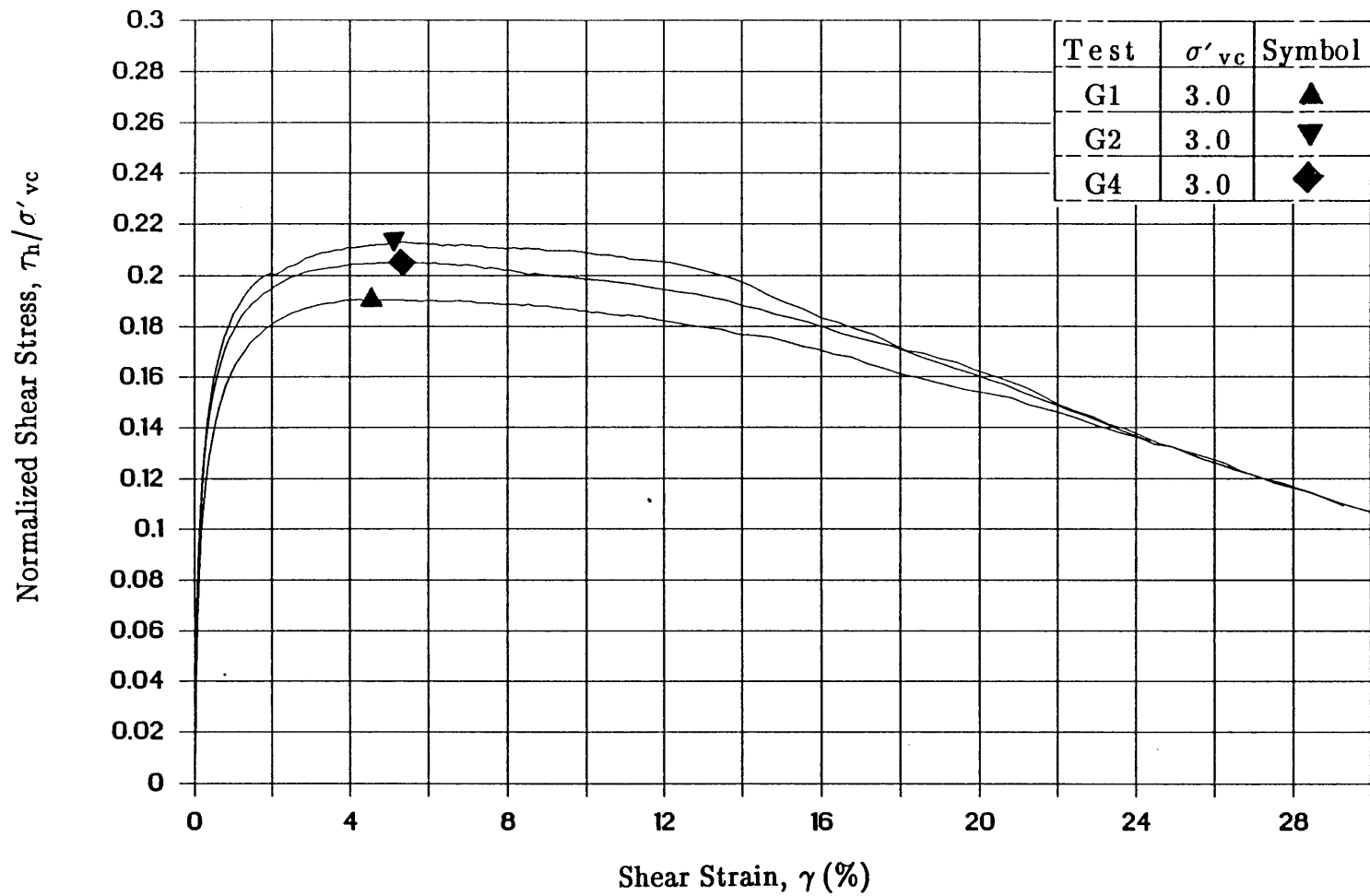


Figure 6.8: Normalized Shear Stress Versus Shear Strain from CK_0 UDSS Tests on Normally Consolidated BBC (From DeGroot, 1989).

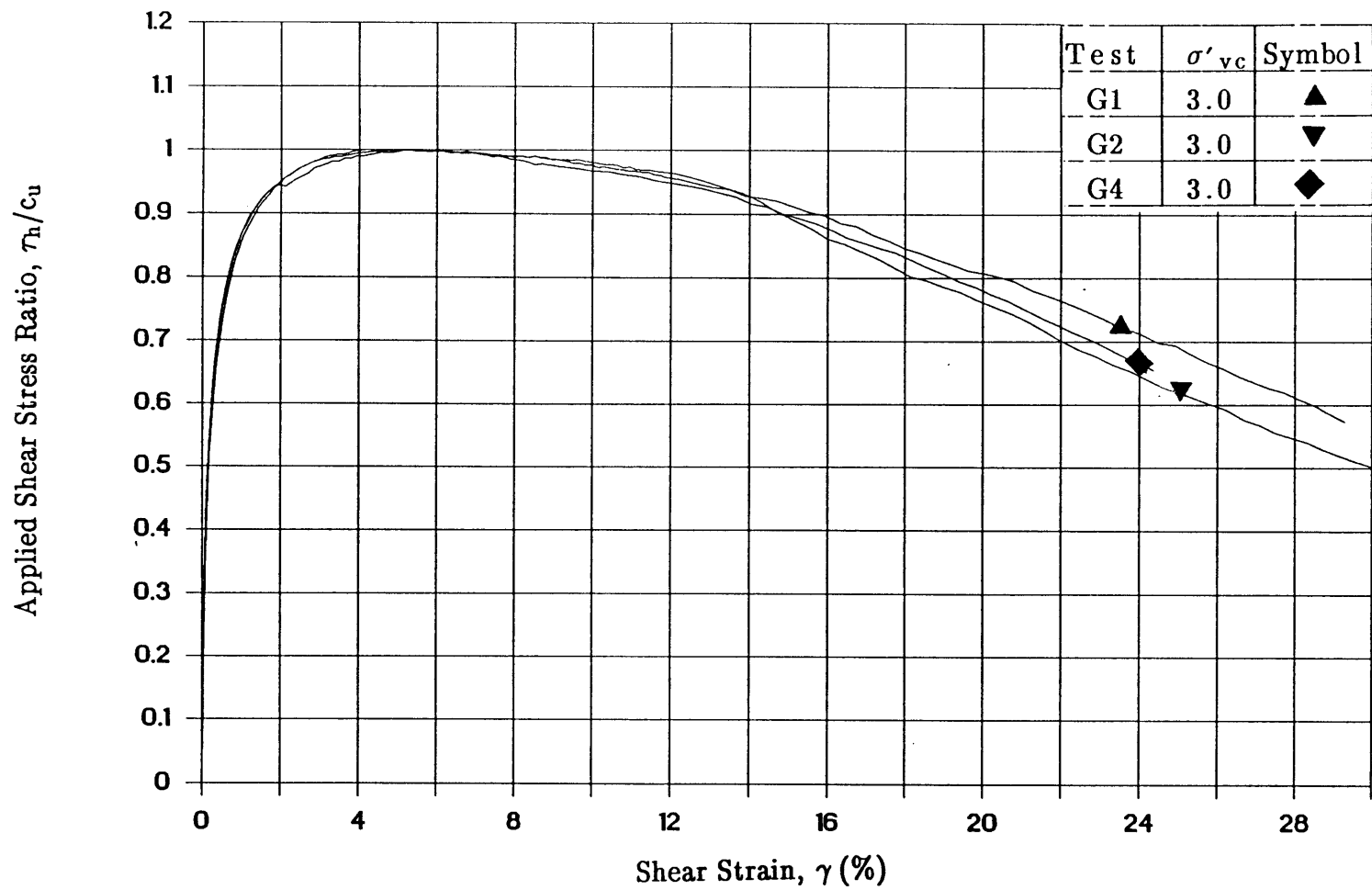


Figure 6.9: Applied Shear Stress Ratio Versus Shear Strain from CK_0 UDSS Tests on Normally Consolidated BBC (From DeGroot, 1989).

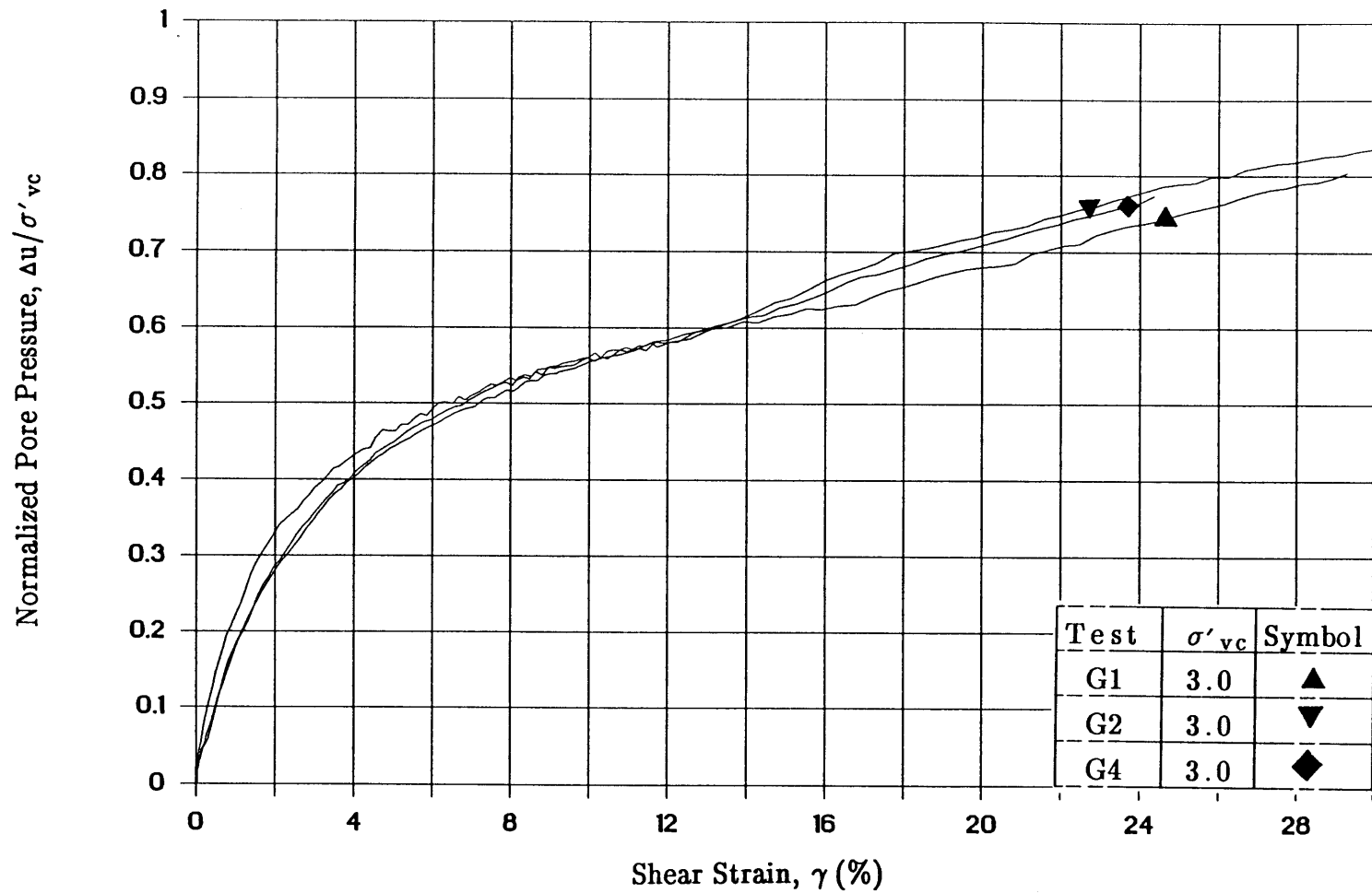


Figure 6.10: Normalized Pore Pressure Versus Shear Strain from CK_0 UDSS Tests on Normally Consolidated BBC (From DeGroot, 1989).

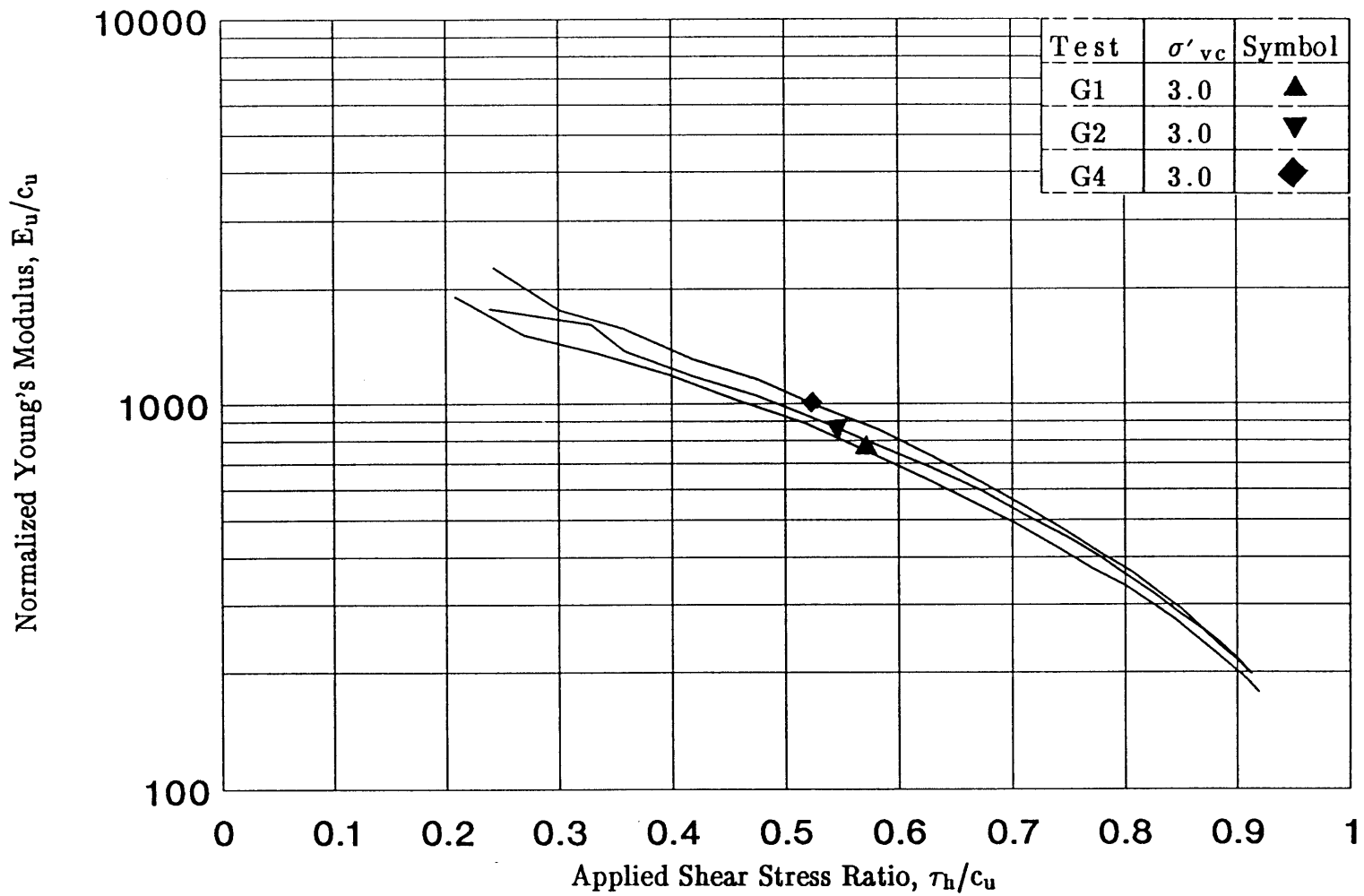


Figure 6.11: Normalized Undrained Young's Modulus Versus Applied Shear Stress Ratio from CK_0 UDSS Tests on Normally Consolidated BBC (From DeGroot, 1989).

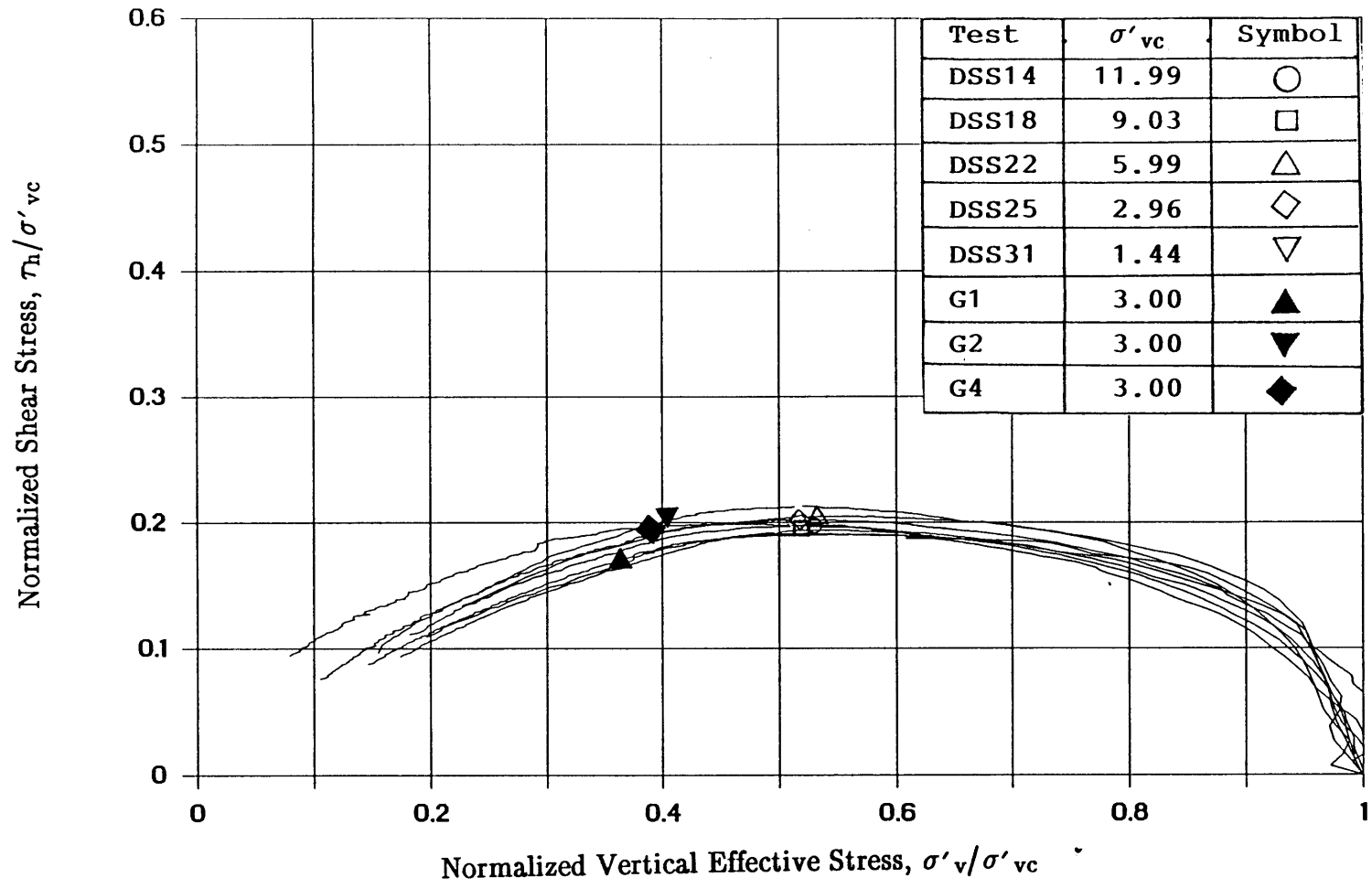


Figure 6.12: Stress Paths for CK_0 UDSS Tests on Normally Consolidated BBC (Curves from Figures 6.1 and 6.7).

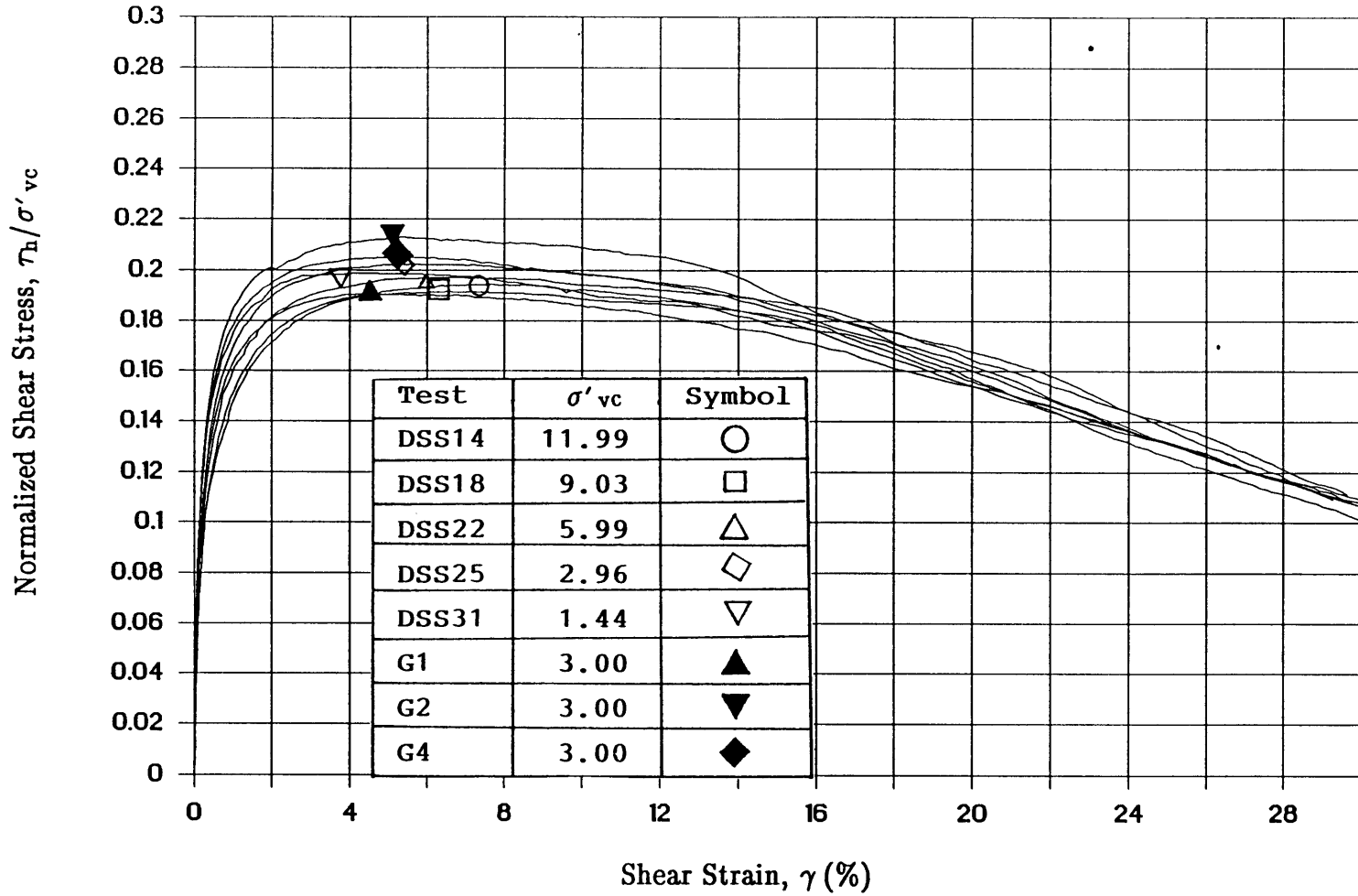


Figure 6.13: Normalized Shear Stress Versus Shear Strain for CK_0 UDSS Tests on Normally Consolidated BBC (Curves from Figures 6.2 and 6.8).

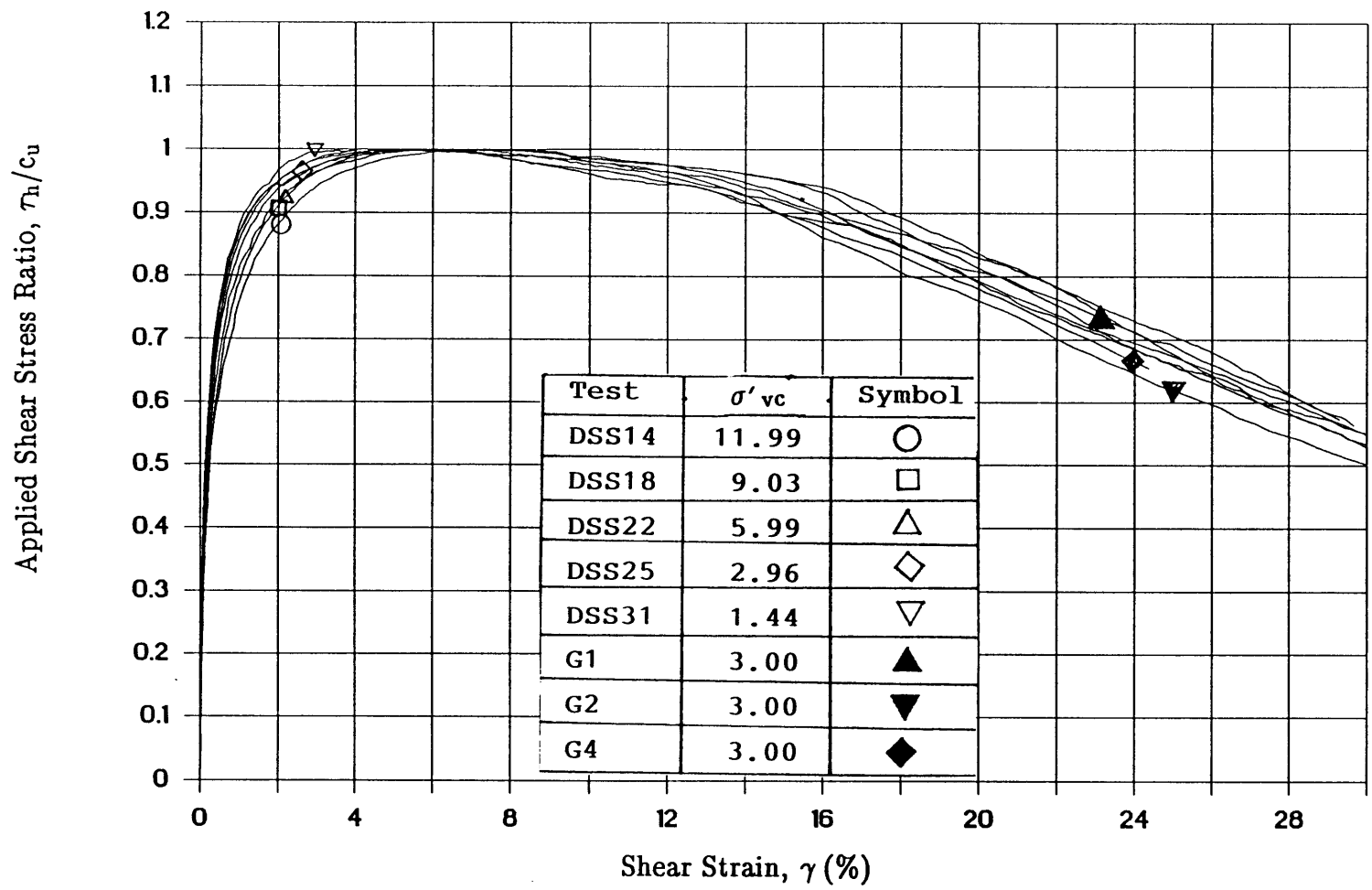


Figure 6.14: Applied Shear Stress Ratio Versus Shear Strain for CK_0 UDSS Tests on Normally Consolidated BBC (Curves from Figures 6.3 and 6.9).

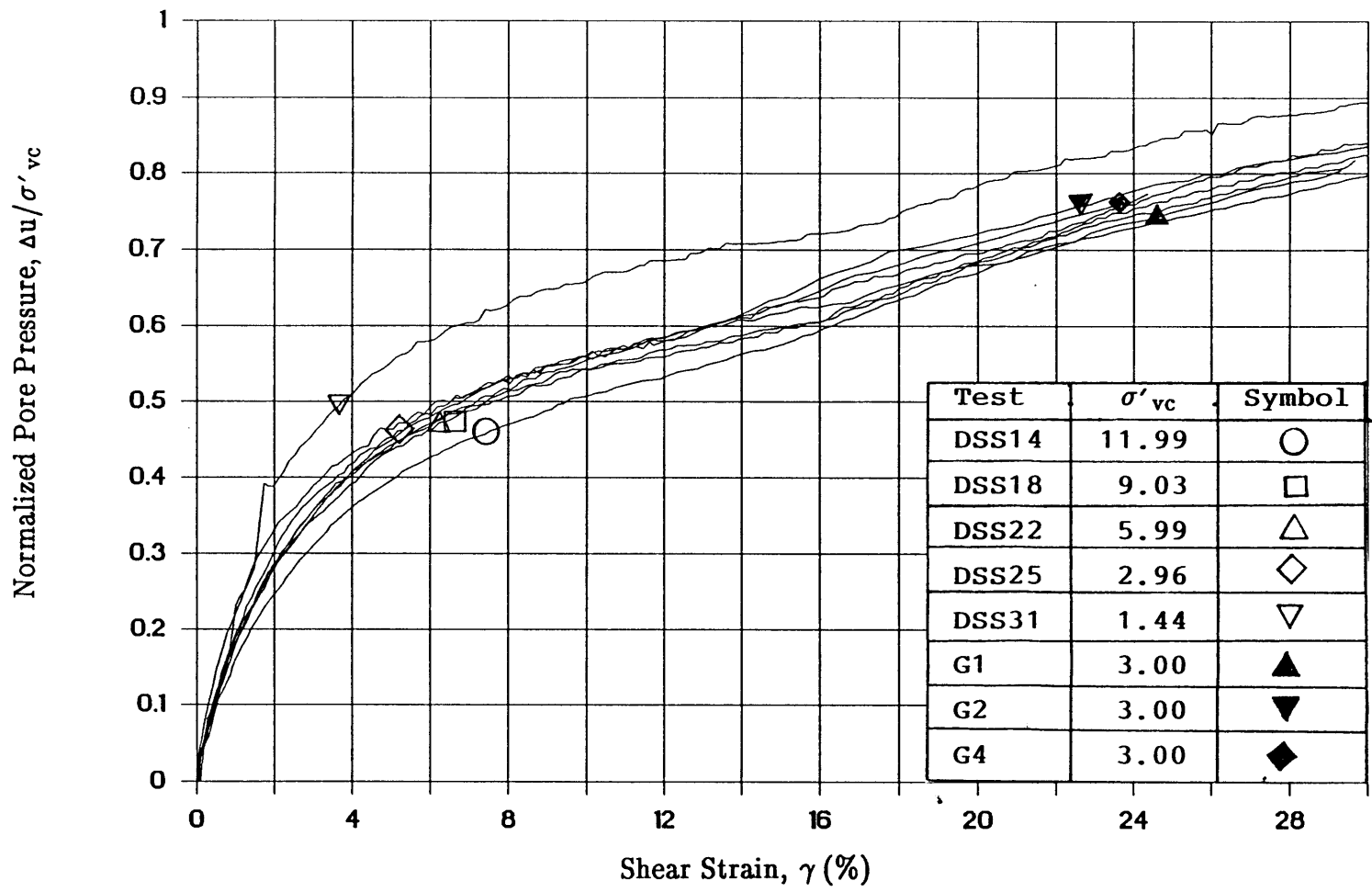


Figure 6.15: Pore Pressure Versus Shear Strain for CK_0 UDSS Tests on Normally Consolidated BBC (Curves from Figures 6.4 and 6.10)

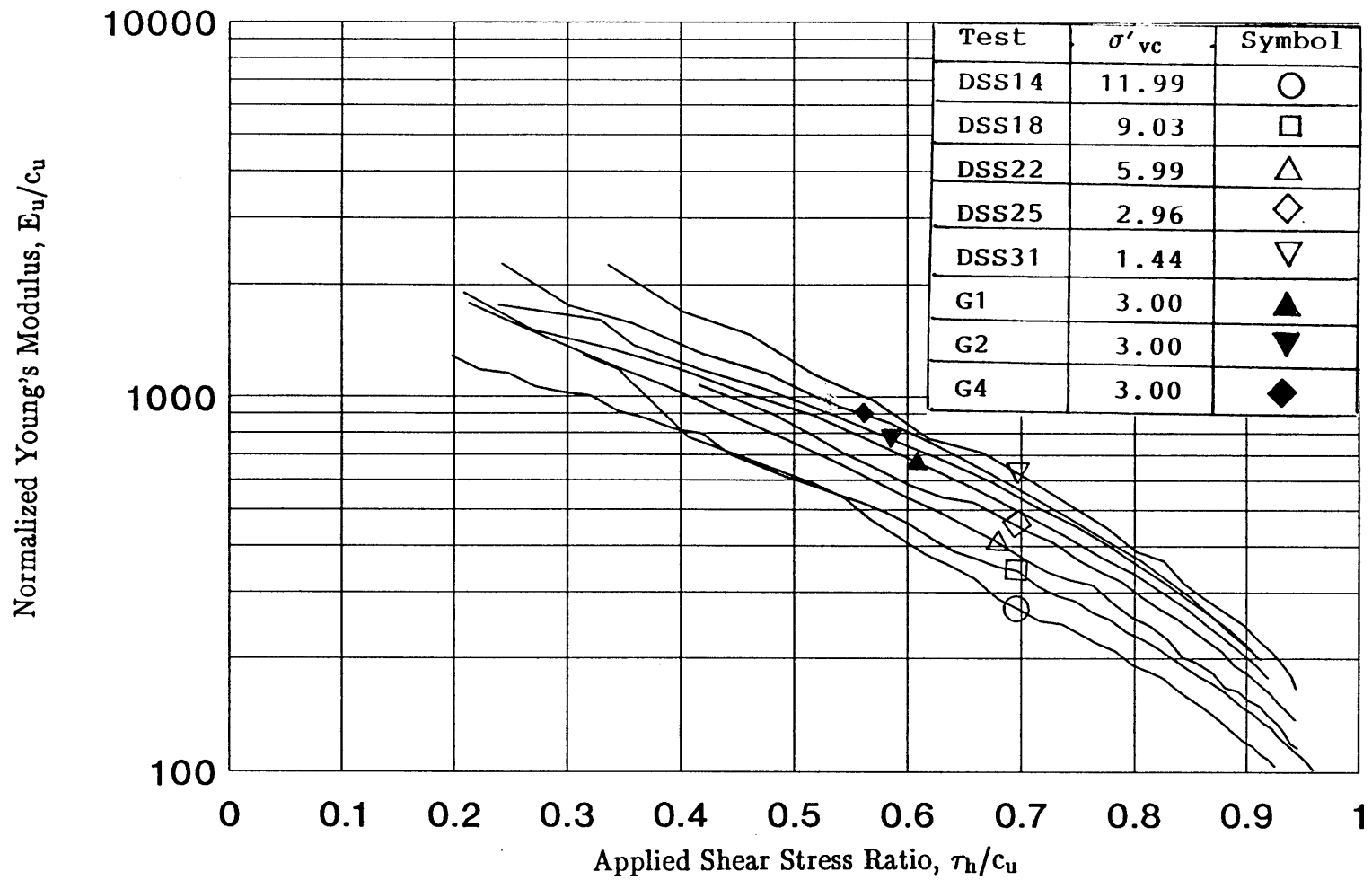


Figure 6.16: Young's Modulus Versus Applied Shear Stress Ratio for CK_0 UDSS Tests on Normally Consolidated BBC (Curves from Figures 6.6 and 6.11)

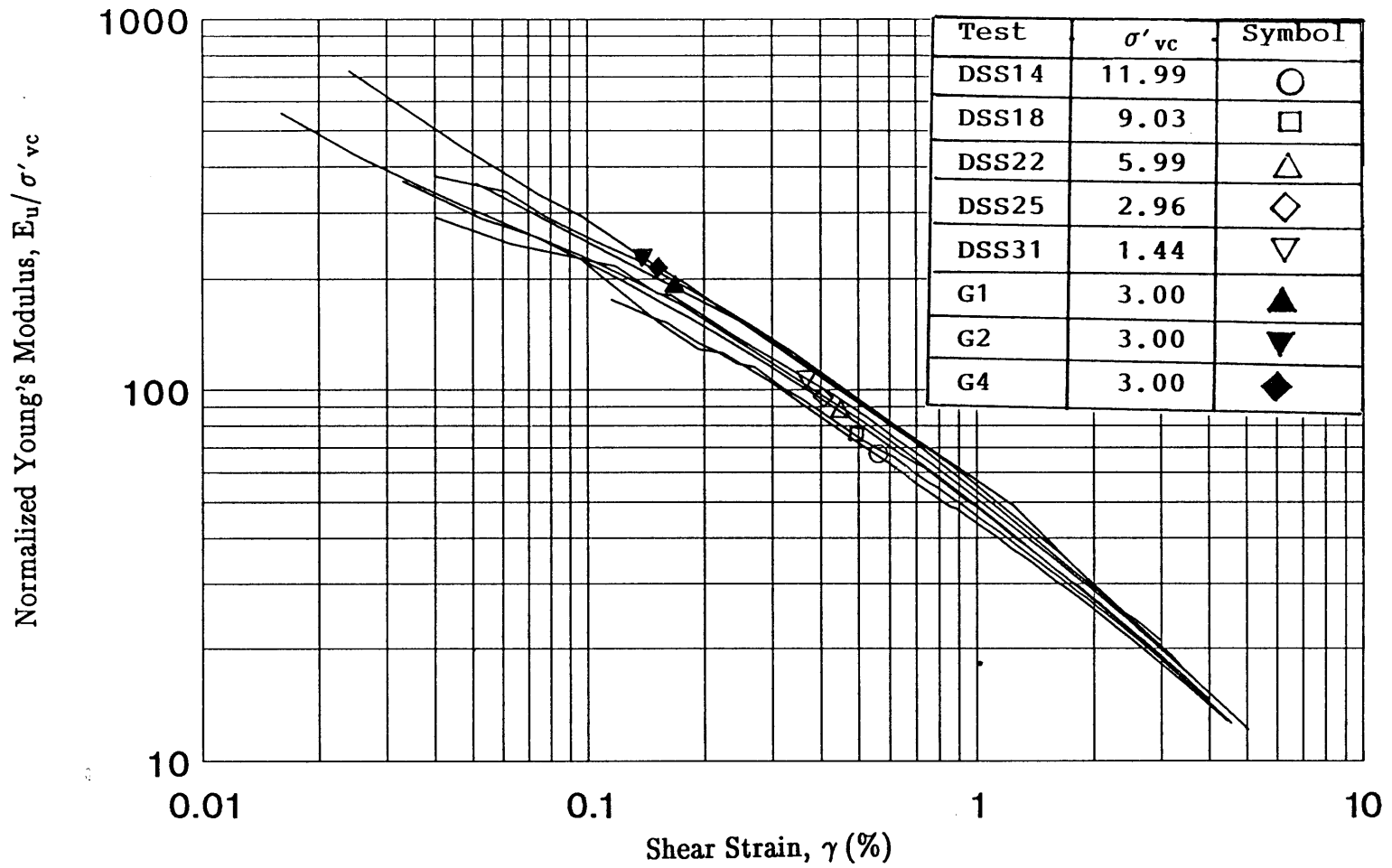


Figure 6.17: Young's Modulus (E_u/σ'_{vc}) versus Shear Strain (γ) for CK_0 UDSS Tests on BBC (Tests by Author and DeGroot, 1989).

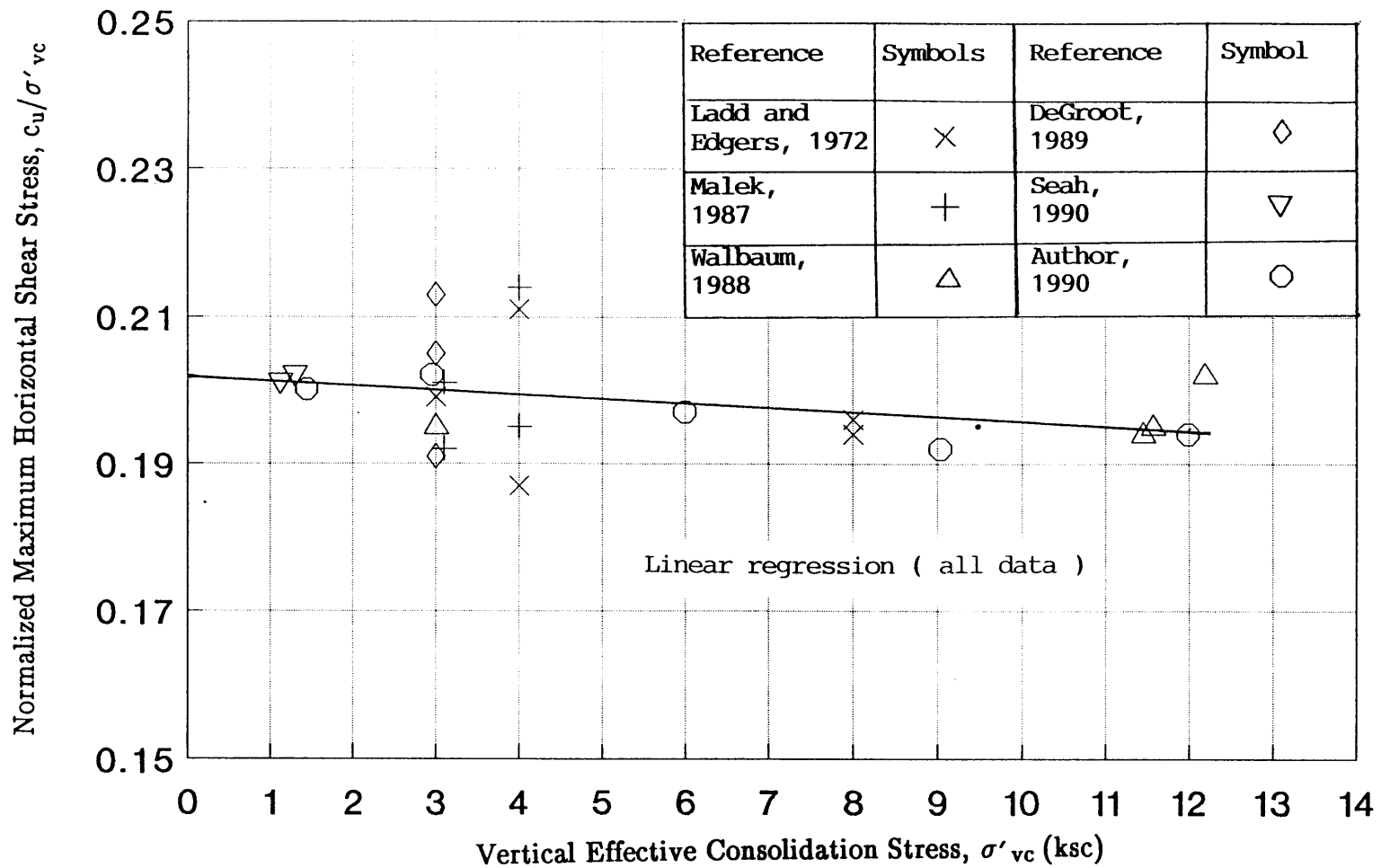


Figure 6.18: Maximum Normalized Shear Stress Versus Vertical Consolidation Stress for CK₀UDSS Tests on Normally Consolidated BBC (Data from Tables 6.1 and 6.2).

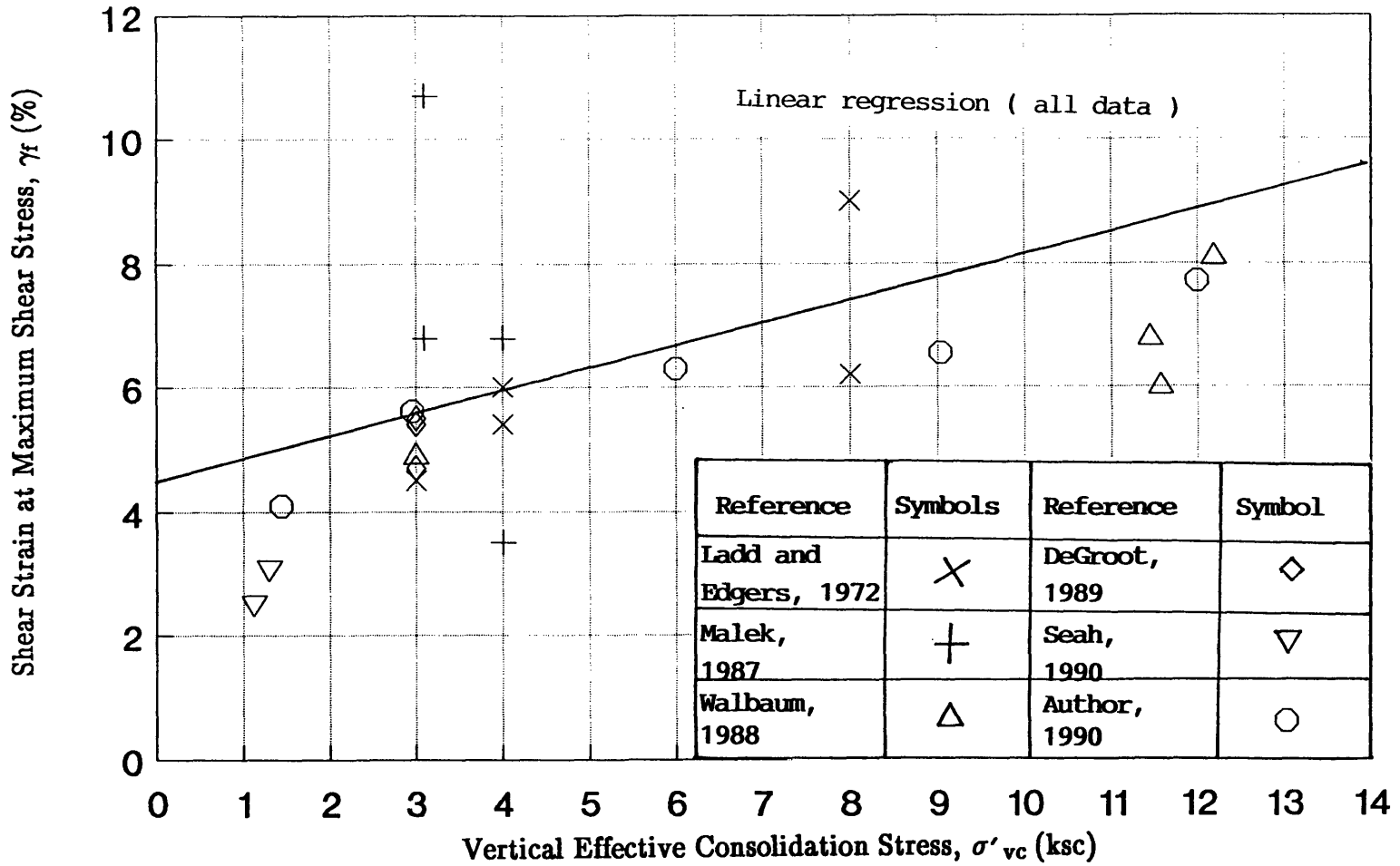


Figure 6.19: Shear Strain at Peak Shear Strength Versus Vertical Consolidation Stress for CK_0 UDSS Tests on Normally Consolidated BBC (Data from Tables 6.1 and 6.2).

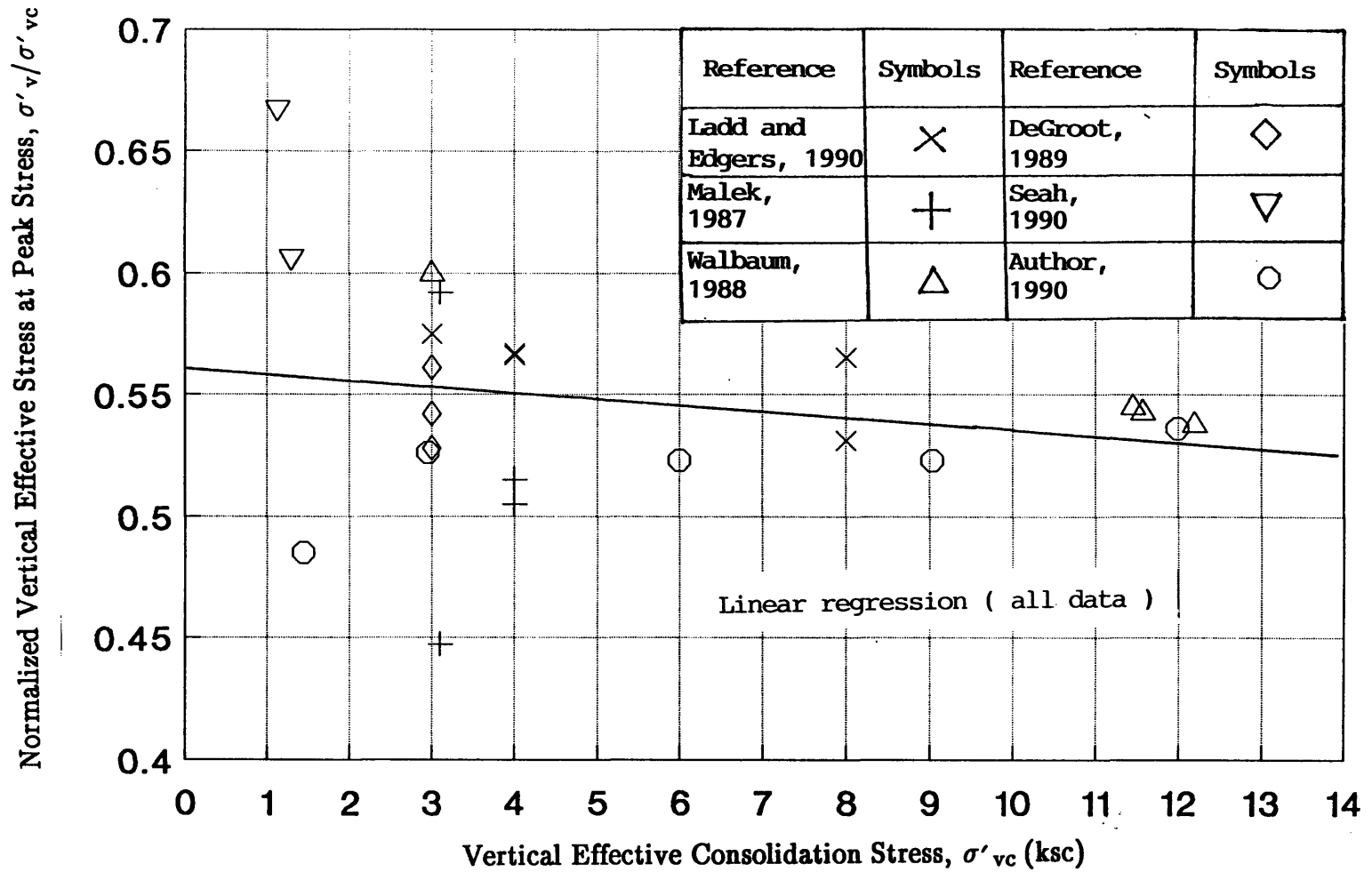


Figure 6.20: Normalized Vertical Effective Stress at Peak Strength Versus Consolidation Stress for CK_0 UDSS Tests on Normally Consolidated BBC (Data from Tables 6.1 and 6.2).

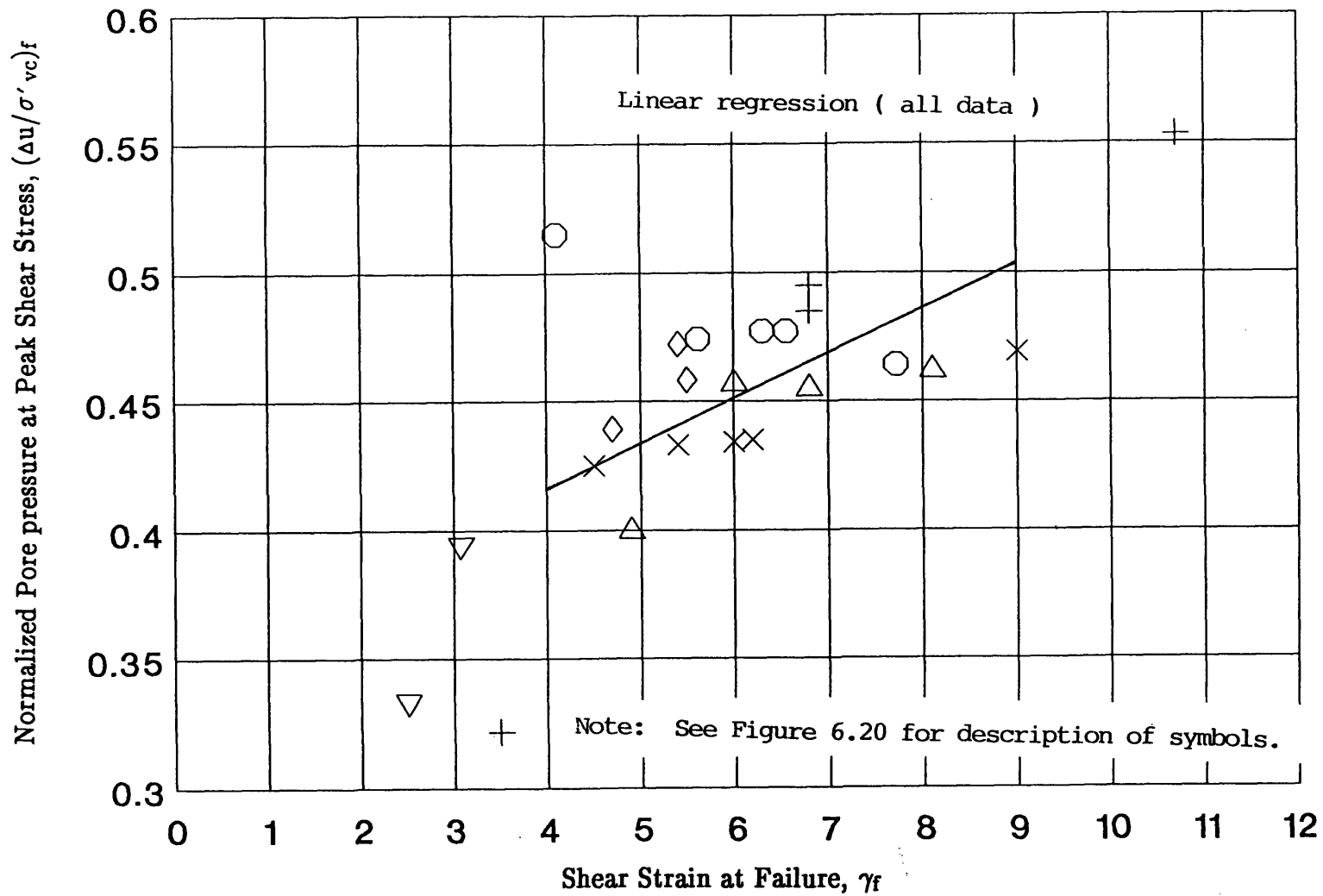


Figure 6.21: Normalized Pore Pressure at Peak Strength Versus Shear Strain at Failure for CK_0 UDSS Tests on Normally Consolidated BBC (Data from Tables 6.1 and 6.2).

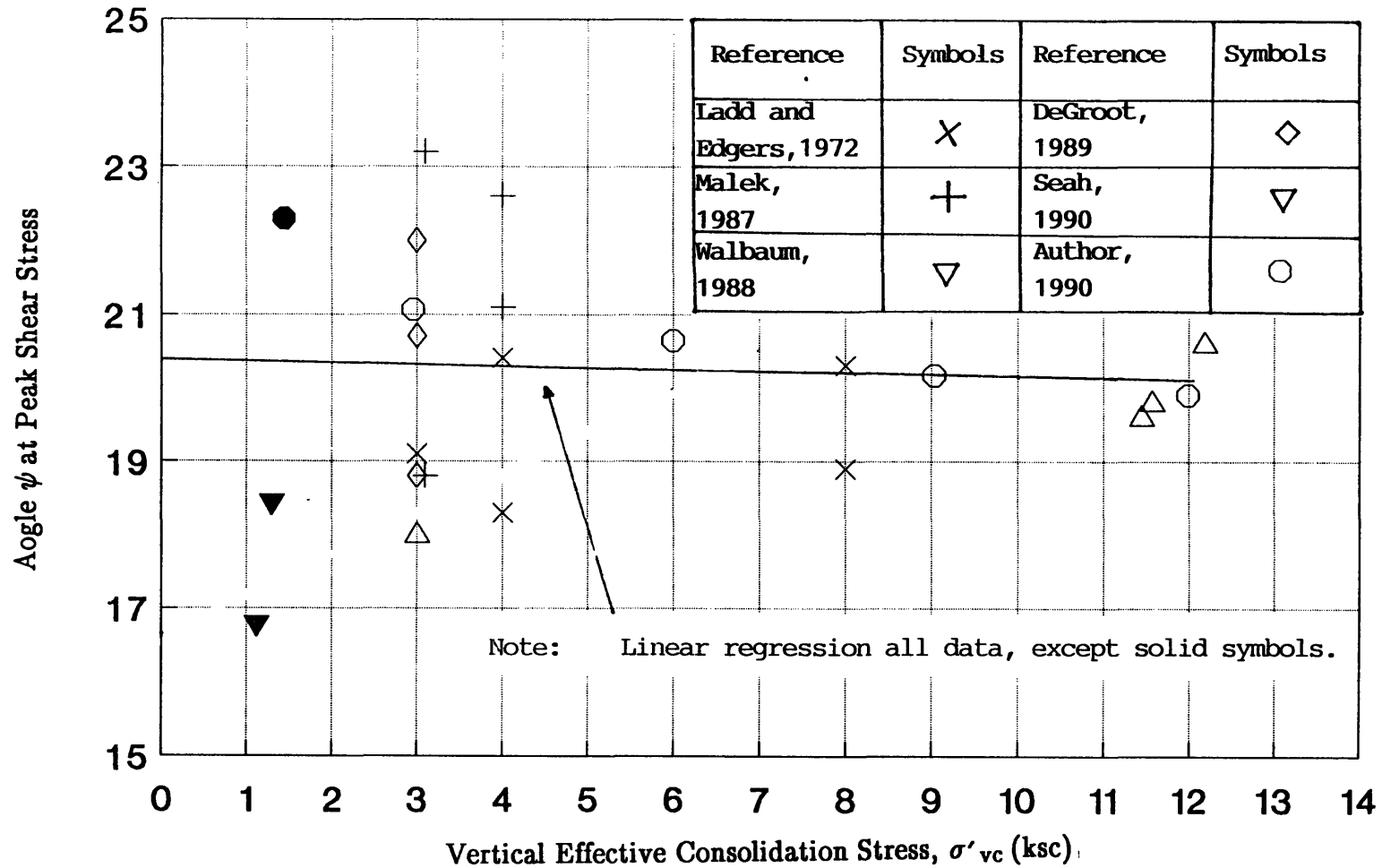


Figure 6.22: Angle ψ at Peak Shear Stress Versus Consolidation Stress for CK_0UDSS Tests on Normally Consolidated BBC (Data from Tables 6.1 and 6.2).

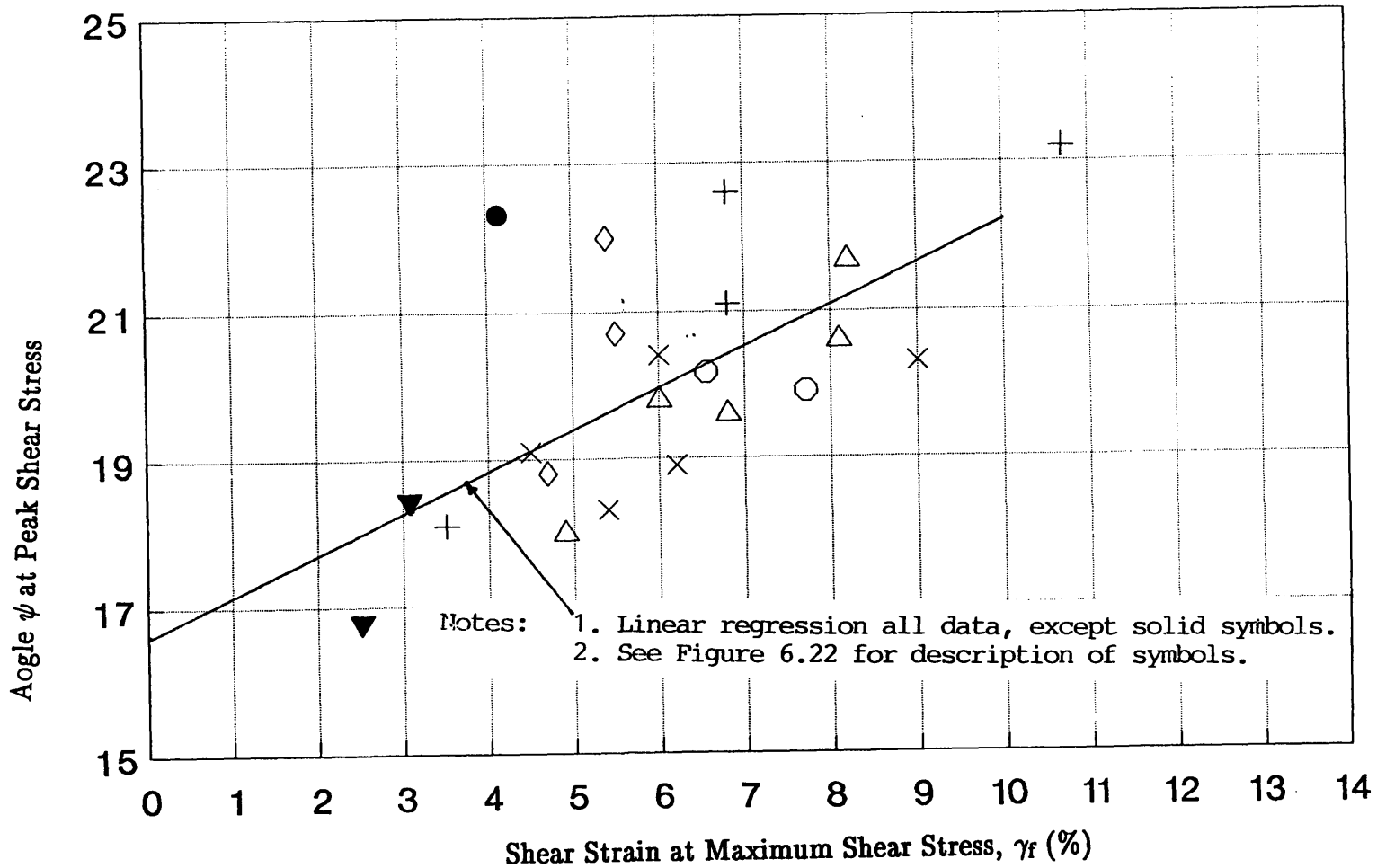


Figure 6.23: Angle ψ at Peak Shear Stress Versus Shear Strain at Failure for CK_0 UDSS Tests on Normally Consolidated BBC (Data from Tables 6.1 and 6.2)

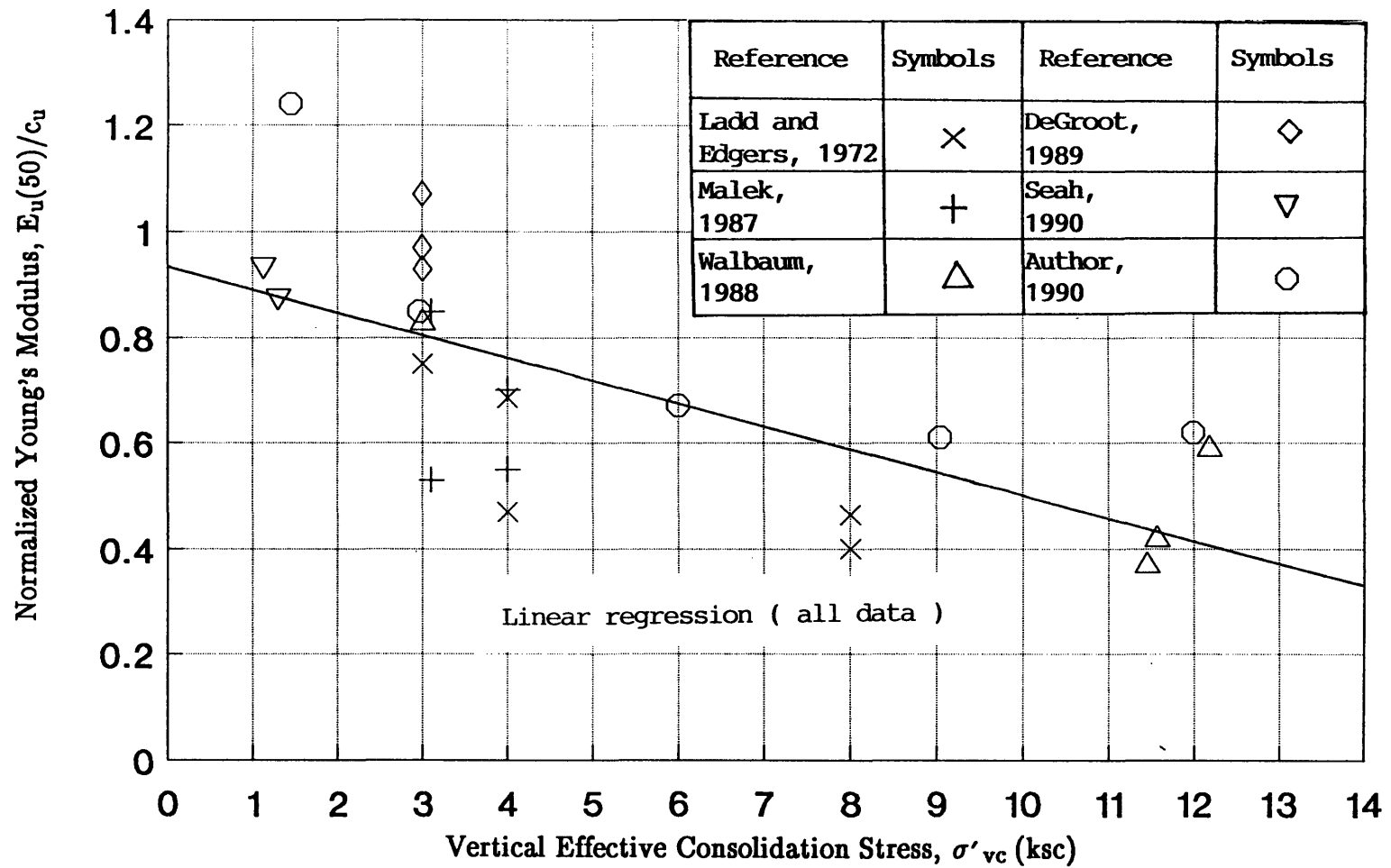


Figure 6.24: Normalized Undrained Young's Modulus Versus Vertical Consolidation Stress for CK₀UDSS Tests on Normally Consolidated BBC (Data from Tables 6.1 and 6.2).

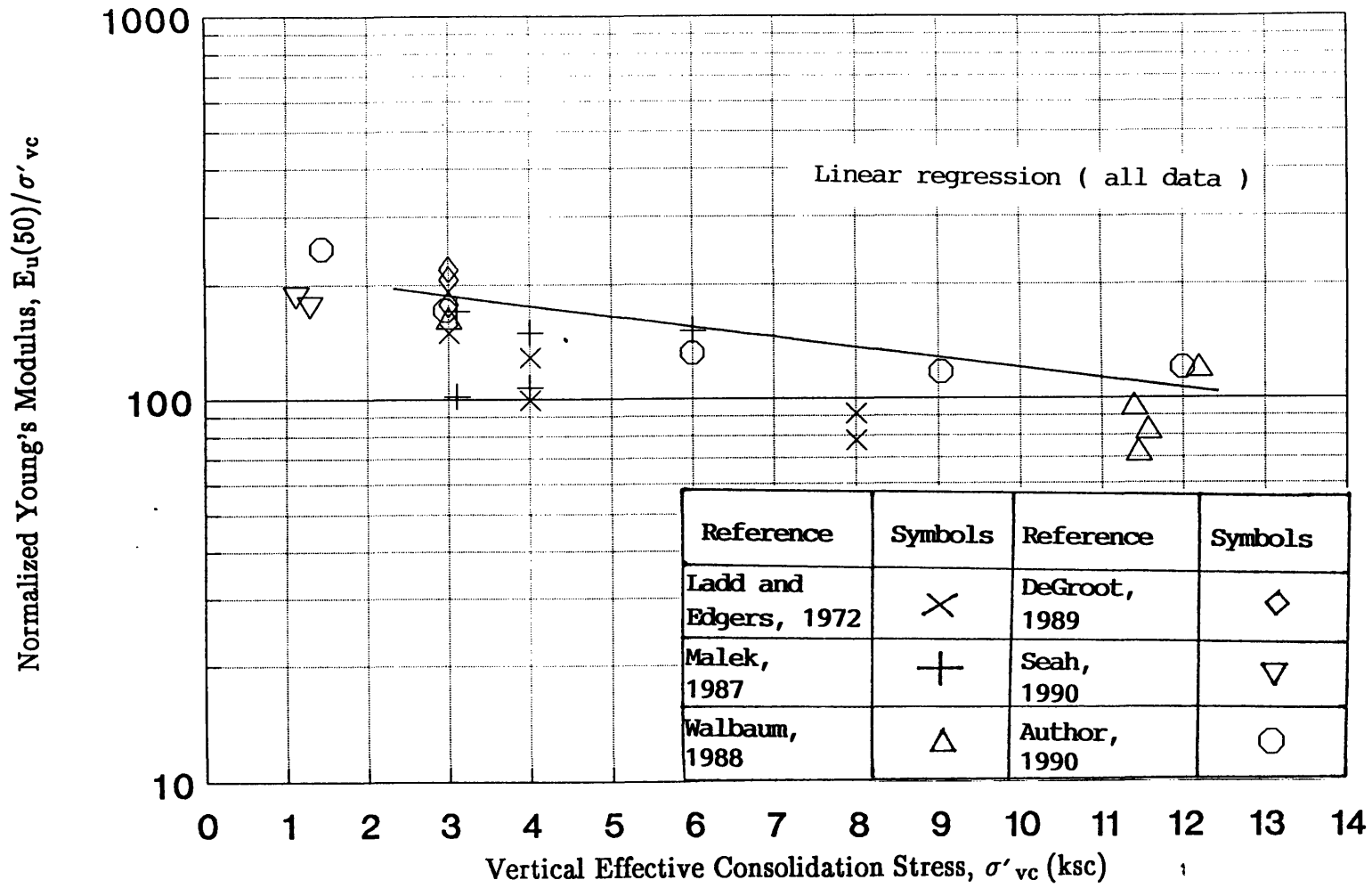


Figure 6.25: Young's Modulus (E_u/σ'_{vc}) Versus Vertical Consolidation Stress for CK_0 UDSS Tests on Normally Consolidated BBC (Data from Tables 6.1 and 6.2).

CHAPTER 7

UNDRAINED SHEAR BEHAVIOR OF OVERCONSOLIDATED BBC

7.1 Introduction

A testing program was conducted in the Geonor DSS with the objective of investigating the undrained shear behavior of overconsolidated resedimented BBC. The specimens were consolidated well beyond the batch preconsolidation pressure and then sheared undrained at different overconsolidation ratios (OCR's) along the swelling curve. Five CK_0 UDSS tests were performed with a maximum past pressure of approximately 12 ksc at OCR 's ranging from 1 to 32. The maximum OCR of 32 was selected keeping in view the minimum vertical stress required to prevent sliding between the top cap and the sample. One CK_0 UDSS test was performed at OCR of 8 with a maximum past pressure of 3 ksc to determine the influence of stress level on the undrained shear behavior of overconsolidated samples of BBC.

The tests were performed using procedures described in Chapter 3. As recommended by the SHANSEP procedure (Ladd and Foott, 1974), the maximum and also the final consolidation stresses were applied for approximately 24 hours to allow at least one cycle of secondary compression and then sheared undrained by keeping the volume of the sample constant. The undrained shear was applied at a constant rate of strain of approximately 5 % per hour. Table 4.8 gives an overview of the CK_0 UDSS testing program on overconsolidated specimens of resedimented BBC. The properties of the test soil are summarized in Chapter 4.

The results from the consolidation phase of the CK_0 UDSS tests on overconsolidated specimens are summarized in Chapter 5. The evaluation of consolidation data revealed that significantly larger consolidation strains were consistently measured for tests on Batch 204 and 205 versus Batch 207, most probably due to bending of porous stones used in the Geonor DSS.

All the specimens for this phase of DSS testing came from Batch 204 and 205. Variations in the vertical strains are observed during undrained shearing as plotted in Figure 7.5. The variations in ϵ_v were all within the absolute magnitude of those recorded for OCR = 1 BBC, except for DSS 37 with OCR 3.25 at large strains. There appears to be relatively little effect of these strains on the measured undrained shear behavior up to the peak shear (even for DSS 37), as the subsequent evaluation of the data will show.

The chapter begins with the presentation and discussion on the results from CK_0 UDSS tests on overconsolidated specimens. This is followed by comparison of writer's test data with the published research and evaluation of results. The chapter concludes with a summary and conclusions pertaining to the undrained shear behavior of overconsolidated resedimented BBC in the Geonor DSS.

7.2 Presentation and Discussion of Results from CK_0 UDSS Tests on Overconsolidated BBC

Table 7.1 summarizes the results of six CK_0 UDSS tests conducted on overconsolidated specimens of BBC III at OCR's ranging from 2 to 32, along with average values from normally consolidated CK_0 UDSS tests (from Table 6.1). Besides the information pertaining to the test specimens, i.e., batch number, water content (w_c) and stress history (σ'_{vc} , σ'_{vm} and $OCR = \sigma'_{vm}/\sigma'_{vc}$), the table contains the values of γ , τ_h/σ'_{vc} , σ'_v/σ'_{vc} , τ_h/σ'_v and angle ψ at peak τ_h and at the maximum value of τ_h/σ'_v . The Table also contains the normalized undrained Young's modulus values at 50% of peak shear resistance [$E_u(50)/c_u$]. The data are also presented in graphical form in Figures 7.1 through 7.13. Detailed tabulated data from each test are presented in Appendix B.

Figure 7.1 plots the effective stress paths, in which τ_h and σ'_v are divided by σ'_{vm} , from six CK_0 UDSS tests on overconsolidated specimens of BBC. The figure also

plots the curve from DSS 14 which was performed on a normally consolidated specimen tested at $\sigma'_{vc} = 12$ ksc (all the overconsolidated specimens have $\sigma'_{vm} \approx 12$ ksc except DSS 50 which has maximum past pressure of 3 ksc). If the normally consolidated effective stress path represents the State Boundary Surface for the DSS mode of shearing, then all the overconsolidated tests would be expected to hit this boundary and then follow it with subsequent straining. The curves from the overconsolidated tests in Figure 7.1 indeed follow this predicted behavior, i.e., all the curves climb up to the normally consolidated stress path, reaching the envelope at the peak shear resistance and then following the curve while strain softening and eventually reaching maximum obliquity.

The normalized shear stress versus shear strain data from all the tests are plotted in Figure 7.2. The plot indicates a consistent increase in the normalized undrained shear strength (c_u/σ'_{vc}) with increasing OCR. The primary reason for the increase in c_u/σ'_{vc} is the increase in the normalized effective stresses at peak shear resistance rather, than the increase in the obliquity of stresses (τ_h/σ'_{vc}). This fact is evident from Table 7.1, which shows that τ_h/σ'_{vc} increases from 0.197 to 1.84 with a corresponding increase in σ'_v/σ'_{vc} from 0.519 to 3.52, while the increase in τ_h/σ'_v is only from 0.373 to 0.523 with OCR increasing from 1 to 32. Of course, the increase in σ'_v is due to lower values of Δu as shown in Figure 7.4.

Figure 7.2 also demonstrates that the shear strain at failure, γ_f , generally increases with increase in the OCR. The applied shear stress ratio versus shear strain curves in Figure 7.3 show that higher OCR samples mobilize a lower fraction of their peak strength at "low" strains. Similar to normally consolidated specimens, significant strain softening is exhibited by all the overconsolidated specimens. If the degree of strain softening is defined as the ratio of τ_h/τ_{hmax} at $\gamma = 30\%$, the strain softening generally decreases with increasing OCR. However, DSS 37 (OCR = 3.25; which suffered from problems with servo control system during shear after the peak shear

strength) demonstrates inconsistency in its post peak undrained shear response compared to the other tests.

Figure 7.4 plots the normalized pore pressure ($\Delta u/\sigma'_{vc}$) versus the shear strain. The plot shows consistently positive pore pressures for $OCR < 2$ specimens, while more overconsolidated specimens initially develop negative pore pressures which gradually becomes less negative with straining, and even becomes positive in the case of moderately overconsolidated specimens (i.e., with OCR's up to 3.25). However, highly overconsolidated specimens develop large negative pore pressures which start becoming less negative in the vicinity of the peak shear resistance and remain negative even until very large strains, i.e., $\gamma = 30\%$.

Figure 7.5 plots the data for variations in the vertical height of the specimens during undrained shear compared to the pre-shear height. Ideally there should be no vertical strain for a constant volume test. However, the height control algorithm does not account for apparatus compressibility. Therefore, tests on low OCR specimen, which undergo a decrease in σ'_v , cause compression of the specimen due to expansion of the apparatus. Conversely, tests on higher OCR specimen, which undergo an increase in σ'_v , cause expansion of the specimen due to contraction of the apparatus. The measured dilation of the highly overconsolidated samples (i.e., $OCR > 3.25$), which increases with increase in the OCR, during undrained shearing compared to the pre-shear sample height demonstrates that the increase in the vertical stress acting on the sample is less than the actual negative pore pressures that would develop in the specimens if the tests were fully "undrained", i.e., at constant volume. However, this error is considered small and expected to have little influence on the measured undrained shear behavior of the soil, as the subsequent comparison of the tests data with the published results would show. The curve from DSS 37 (Figure 7.5) shows that the servo control system developed some problem in the vicinity of the shear strain at failure, which resulted in significant deviation of vertical strain compared to the other

tests. This discrepancy did influence the measured post peak undrained shear response of the specimen.

The normalized undrained Young's modulus, (E_u/c_u) , versus applied shear stress ratio, (τ_h/c_u) , are plotted in Figure 7.6 for the CK_oUDSS tests at OCR's ranging from 1 to 32. The data are fairly consistent and demonstrate a definite trend with change in OCR, i.e., decrease in moduli with increasing OCR. This trend is better illustrated by the curves for various "factors of safety" $(= \frac{1}{\tau_h/c_u})$ on a plot of E_u/c_u versus logarithm of OCR in Figure 7.8. Table 7.1 reports that the values of normalized undrained shear modulus at 50 % of peak shear resistance decrease from 619 to 49 for OCR's ranging from 1 to 32.

When E_u is normalized with respect to σ'_{vc} and plotted against shear strain, both on logarithm scale, a different pattern develops (Figure 7.7), i.e., increasing moduli with increasing OCR, which obviously decreases with increasing shear strains. The data on this plot display comparatively greater consistency and less spread in the curves for various OCR's.

Ladd et al. (1977) suggested an empirical relationship that assumes that the overconsolidated strength is related to the normally consolidated strength and OCR by:

$$c_u/\sigma'_{vc} = S (\text{OCR})^m \quad (7.1)$$

where;

$S = c_u/\sigma'_{vc}$ at OCR of one.

The data from the CK_oUDSS tests on overconsolidated specimens, along with the average results from normally consolidated specimens, are plotted on logarithm of normalized strength versus logarithm of OCR in Figure 7.9 to check the above relationship for resedimented BBC. Linear regression was used to compute the values

of m , based on above relationship, for various ranges of OCR's. The summarized results from linear regression in Table 7.4 show that the value of m decreases with increase in the OCR, i.e., m varies from 0.82 to 0.62 for OCR ranging from 3.25 to 32.

Critical State Soil Mechanics (i.e., the Modified Cam–Clay) predicts:

$$m = 1 - C_s/C_c \quad (7.2)$$

where C_s and C_c refer to the slopes of the swelling and virgin compression lines, respectively.

The computed values of m based on Equation 7.2 are contained in Table 7.4. The comparison of measured and predicted m values shows that the MCC overpredicts the m values for BBC, especially at high OCR's (the ratio of $m_{\text{measured}}/m_{\text{predicted}}$ varies from 0.91 to 0.74 for OCR ranging from 3 to 32; the predicted m values may be affected by the error in ϵ_v data due to bending of porous stones). However, the measured m values at OCR's greater than 8 do not fall within range suggested by Ladd et al. (1977) for typically DSS testing of clays (i.e., 0.8 ± 0.1) based on their tests up to OCR of 8.

The summary of results at $(\tau_h/\sigma'_v)_{\text{max}}$ in Table 7.1 demonstrates that CK₀UDSS tests do not show a definite trend regarding shear strain at maximum obliquity with change in OCR. However, overconsolidated specimens yield a higher average value of shear strain at $(\tau_h/\sigma'_v)_{\text{max}}$ compared to the normally consolidated specimens ($\gamma = 35\%$ versus 33% at OCR of one). The stress ratios (i.e., τ_h/σ'_{vc} and σ'_v/σ'_{vc}) show a significant decrease compared to the values at peak shear resistance. The strain softening generally decreases with increasing OCR. The average value of angle ψ at maximum obliquity for all the tests, summarized in Table 7.1, at OCR's ranging from 1 to 32 equals $30.7^\circ \pm 1.2^\circ$ SD (excluding DSS 37 and DSS 50). The distortion of the rubber membrane at large shear strains, along with continuous

rotation of the principal planes will effect, to some extent, the measured post peak undrained shear behavior of the overconsolidated specimens. DeGroot (1989) analyzed the strain softening behavior of undrained shear tests on normally consolidated cohesive soils in the Geonor DSS. Based on his analyses of the previous data on cohesive soils tested in the Geonor DSS and tests conducted on rubber specimens, he opined that the measured strain softening response of a DSS specimen in the Geonor is in part due to the nonuniform vertical stress caused by the device. Specifically, during undrained shear the DSS apparatus causes the vertical stress acting on the sample to decrease with increase in the shear strain. The substantial decrease in the shear stress ratio at large shear strains observed in the writer's test data from all the overconsolidated specimens may be partially due to the device causing more unloading than should have been observed.

7.3 Influence of Maximum Past Pressure on the Undrained Shear Behavior of BBC

The testing program on the overconsolidated specimens of BBC included two DSS tests (DSS 44 and DSS 50) conducted at approximately the same OCR but with different maximum past pressures (i.e., DSS 44 at OCR of 7.9 with $\sigma'_{vm} = 11.42$ and DSS 50 at OCR of 7.8 with $\sigma'_{vm} = 2.96$). This section discusses the influence of maximum past pressure on the undrained shear behavior of the overconsolidated specimens in the Geonor DSS.

Figure 7.10 plots the effective stress paths from DSS 44 and DSS 50. The curves from both the tests indeed overlap, suggesting that maximum past pressure does not significantly influence the normalized stress paths from CK_0 UDSS tests on the overconsolidated specimens of BBC III.

The stress–strain curves from DSS 44 and 50, plotted in Figure 7.11, exhibit some influence of maximum past pressure up to the peak shear strength on the undrained shear behavior of BBC III. The DSS test having a lower maximum past

pressure ($\sigma'_{vm} \approx 3$ ksc) gives a lower value of the shear strain at failure and slightly higher shear strength compared to the test at the same OCR but with a higher maximum past pressure ($\sigma'_{vm} \approx 12$ ksc). This is in conformity with the trend observed during the undrained shear tests on the normally consolidated specimens (Chapter 6), i.e., slight increase in the peak shear strength and more significant decrease in the strain at failure with decreasing stress levels. However, no significant influence of maximum past pressure is observed on the post peak stress–strain behavior of the soil.

Figure 7.12 plots the normalized pore pressure ($\Delta u/\sigma'_{vc}$) versus shear strain from the DSS tests at the same OCR but having different maximum past pressures. The plotted data demonstrate that the test with lower σ'_{vm} (DSS 50) develops a slightly larger negative pore pressure in the vicinity of the peak shear strength compared to the DSS test having higher σ'_{vm} (DSS 44). But the post peak curves for the two tests are essentially identical.

Figure 7.13 shows that DSS 50, with $\sigma'_{vm} = 3$ ksc, yields consistently higher undrained Young' modulus values compared to DSS 44, thus displaying some influence of maximum past pressure on the modulus values. This trend is consistent with undrained shear behavior observed in the tests on normally consolidated specimens of BBC (Chapter 6), i.e., stiffness increases with decreasing stress levels.

7.3 Comparison with the Previous Research

Seven CK_0 UDSS tests on overconsolidated specimens of BBC from Ladd and Edgers (1972) are selected for comparison with the data from the writer's tests. These tests were conducted under similar tests conditions and reportedly yielded satisfactory results. However, these tests were conducted at lower stress levels compared with the writer's tests. Table 7.2 summarizes the results of seven CK_0 UDSS tests on overconsolidated specimens of BBC along with average results from normally consolidated tests (from Table 6.2). Figures 7.14 to 7.19 are the plots of stress paths,

normalized stress-strain curves, applied shear stress ratio versus shear strain, normalized pore pressure versus shear strain, normalized Young's modulus (E_u/c_u) versus applied shear stress ratio and logarithm of E_u/σ'_{vc} versus logarithm of shear strain, respectively, for the CK_0 UDSS tests from Ladd and Edgers (1972). The range of data at OCR's of 2 and 8 from these tests are later compared with the writer's tests.

Figures 20 through 27 indicate that the data from the writer's tests at OCR's of 2 and 8 compare very well with the tests from Ladd and Edgers. The following comments are offered based on comparison of the results in Tables 7.3 and Figures 7.20 to 27:

- The tests from Ladd and Edgers yield slightly lower values of shear strain at failure compared to the writer's tests at OCR's of 2 and 8, which is consistent with the trend demonstrated by writer's tests data, i.e., strain at failure decreases with decreasing stress levels.
- The comparison of undrained shear strength ratios at OCR of 8 demonstrate a consistent trend of decreasing strength with increasing maximum past pressure (Tables 7.1 and 7.2).
- Figure 7.26 shows that the tests from Ladd and Edgers yielded comparatively higher normalized undrained Young's modulus (E_u/c_u) at the corresponding OCR's (i.e., OCR of 2 and 8). Their DSS test at an overconsolidation ratio of 8 having a lower σ'_{vm} ($\sigma'_{vm} = 4$ ksc) gives higher modulus values compared to the test with a higher σ'_{vm} ($\sigma'_{vm} = 8$ ksc), as observed from the writer's tests (Section 7.3). This is in conformity with the earlier findings from the stress-strain data for the writer's tests on the overconsolidated and normally consolidated specimens of BBC that the stiffness decreases with increase in the stress levels.

- The tests from Ladd and Edgers yielded comparatively higher value of m (the results computed based on Equation 7.1 are contained in Table 7.4) at OCR of 8 (i.e., $m = 0.75$ versus 0.72 from the writer's tests).

The data from the two testing programs are in good agreement, even though the tests from Ladd and Edgers were conducted on a different source of BBC (i.e., BBC-Ib versus BBC III; see Chapter 4 for comparison of properties of the two series). However, both test programs exhibit essentially similar trends up to OCR of 8, as discussed in the preceding section, pertaining to the undrained shear behavior of overconsolidated specimens in the Geonor DSS.

7.5 Summary and Conclusions

Five CK_0 UDSS tests were performed at OCR's ranging from 2 to 32 with a maximum past pressure of approximately 12 ksc on specimens from resedimented BBC III to investigate the undrained shear behavior of overconsolidated soil. One CK_0 UDSS test was performed at OCR of 8 with a different maximum past pressure (i.e., $\sigma'_{vm} = 3$ ksc) to determine the influence of maximum past pressure on the undrained shear behavior of the test soil. The tests yielded quite consistent and satisfactory data (except DSS 37 at large strains) which compared well with the previous data on BBC. In the case of DSS 37, the servo control system (used in the Geonor DSS to keep the height of the specimen constant during undrained shear) developed some problem in the vicinity of the shear strain at failure, which influenced the measured data beyond the peak shear resistance.

Based on the experimental results and the discussion presented in the preceding sections, the following conclusions are drawn regarding the normalized undrained shear behavior of the overconsolidated resedimented BBC in the Geonor DSS:

- The shear strain at failure, γ_f (i.e., γ at c_u/σ'_{vc} ; where $c_u = \tau_{hmax}$), increases with increase in the OCR (Figure 7.21).
- All the overconsolidated specimens develop negative pore pressures during undrained shearing at the beginning of the tests. The maximum negative pore pressure increased with increasing OCR and usually occurred at the peak undrained strength. The pore pressure become less negative during strain softening and even become positive at moderate OCR (see Figure 7.4).
- The normalized undrained shear strength, c_u/σ'_{vc} , increases with increase in the OCR. The primary reason for increase in c_u/σ'_{vc} is an increase in the vertical effective stress (σ'_v/σ'_{vc}) at the peak shear resistance (i.e., decrease in $\Delta u/\sigma'_{vc}$), rather than the increase in the obliquity of the stresses (i.e., τ_h/σ'_{vc}).
- The effective stress path from the normally consolidated sample forms an envelope for the paths of the overconsolidated samples (Figure 7.1). All the paths from the overconsolidated samples rise up to the normally consolidated stress path, reaching the envelope at the peak shear resistance and then following the curve while strain softening and eventually reaching maximum obliquity.
- The CK_0UDSS tests on the overconsolidated specimens yielded very consistent normalized Young's modulus data (E_u/c_u) and the moduli at various "factors of safety" ($= \frac{1}{\tau_h/c_u}$) decrease with increasing OCR's (Figure 7.6), which implies that the stiffness decreases with increasing OCR. However, when E_u is normalized with respect to σ'_{vc} and plotted against the shear strain (Figure 7.7), the trend reverses.
- The values of m , computed based on the empirical relationship suggested by Ladd et al.(1977) and given in Equation 7.1, decreases with increasing

OCR i.e., m varies from 0.82 to 0.62 for OCR's increasing from 3.25 to 32 (Table 7.4 and Figure 7.9). The typical range of m values suggested by Ladd et al. 1977 (i.e., 0.8 ± 0.1 , based on tests up to OCR of 8) does not hold for highly overconsolidated (i.e., $\text{OCR} > 8$) BBC III. The Modified Cam-Clay overpredicts the value of m (calculated based on Equation 7.2) for BBC, especially at higher OCR's (Table 7.4).

- The effective stress paths from all the overconsolidated specimens (Figure 7.1) reverse direction at the peak shear strength, c_u , and undergo a continuous decrease in the stress ratios (τ_h/σ'_{vc} and σ'_v/σ'_{vc}) with straining beyond the peak shear resistance. The value of angle ψ reaches $30.7^\circ \pm 1.2^\circ$ SD at very large shear strain, i.e., $\gamma \approx 35\%$.
- All the overconsolidated specimens exhibit significant strain softening, which generally decreases with increasing OCR (Figure 7.3). This strain softening is suspected to be partially due to device "unloading". The experimental data from the CK_0UDSS tests on overconsolidated specimens are consistent with DeGroot's (1989) finding about the post peak strain softening behavior of normally consolidated specimens in the Geonor DSS. Based on his analyses, he concluded that the measured strain softening response of a DSS specimen is partially due to the nonuniform state of stress imposed by the device.
- The CK_0UDSS tests at the same OCR ($\text{OCR} = 8$), but having different maximum past pressures ($\sigma'_{vm} = 3$ to 12 ksc), yield essentially similar stress paths (Figure 7.10), show an increase in the shear strain at failure with increasing stress level and demonstrate a definite trend of increase in the peak shear strength with decrease in the maximum past pressure (Figure 7.11). The overconsolidated specimens having lower σ'_{vm} develop comparatively greater negative pore pressure than specimens at the same

OCR having higher σ'_{vm} . (Figure 7.12). The data plotted in Figure 7.13 clearly demonstrate that the normalized Young's modulus (E_u/c_u) decreases with increasing maximum past pressure. The trends are consistent with the stress dependence behavior observed from the CK_0 UDSS tests on the normally consolidated specimens of BBC (Chapter 6), i.e., decrease in stress level results in decrease in the strain at failure, γ_f , slight increase in the peak shear strength ratio, c_u/σ'_{vc} , and increase in the normalized Young's modulus.

Table 7.1: Results from Geonor CK₀UDSS Tests on Overconsolidated BBC III

Test No.	Batch No w _c (%)	Stress History		At Peak τ_h				At τ_h/σ'_v Maximum				$E_u(50)$
		σ'_{vc} σ'_{vm}	OCR	γ (%)	τ_h/σ'_{vc} τ_h/σ'_{vm}	σ'_v/σ'_{vc} σ'_v/σ'_{vm}	τ_h/σ'_{vc} ψ°	γ (%)	τ_h/σ'_{vc} τ_h/σ'_{vm}	σ'_v/σ'_{vc} σ'_v/σ'_{vm}	τ_h/σ'_v ψ°	C_u
DSS14 to DSS31	205 to 207 40.62 ±0.11	1.44 to 11.99	1.00	6.05 ±1.33	0.197 ±0.004	0.527 ±0.006	0.373 ±0.010 20.40 ±0.50	33.02 ±2.89	0.092 ±0.015	0.152 ±0.035	0.615 ±0.084 31.60 ±3.0	619
DSS40	204T 40.12	5.798 11.394	1.97	7.64	0.362 0.184	0.917 0.467	0.394 21.50	36.56	0.189 0.096	0.338 0.172	0.560 29.25	469
DSS37	205B 39.70	3.512 11.407	3.25	10.55	0.515 0.159	1.20 0.269	0.429 23.22	32.93	0.335 0.103	0.676 0.208	0.496 26.38	331
DSS44	204M 39.75	1.447 11.420	7.89	13.32	0.881 0.112	1.811 0.229	0.486 25.92	39.72	0.399 0.050	0.637 0.081	0.627 32.09	128
DSS48	204T 40.21	0.772 11.342	14.69	12.96	1.108 0.075	2.325 0.152	0.476 25.45	35.03	0.572 0.039	0.977 0.066	0.586 30.37	86
DSS51	204B 39.80	0.379 11.897	31.90	15.38	1.840 0.058	3.520 0.110	0.523 27.61	31.29	1.270 0.040	2.202 0.069	0.577 29.98	49
DSS50	204B 40.00	0.379 2.956	7.82	10.73	0.909 0.116	1.988 0.254	0.457 24.56	Still Increasing				188

- Notes:
1. Mean ±1 SD from Table 6.1 (mean values include only peak γ and τ_h/σ'_{vc} from DSS 31; $E_u(50)/\sigma'_{vc}$ from DSS14 at $\sigma'_{vc} \approx 12$ ksc).
 2. Data from DSS 37 at maximum obliquity is unreliable due to servo control problem.
 3. Stresses in kg/cm²; strains in %.
 4. $d\gamma/dt = 5\% \pm$ per hour.

Table 7.2: Results of CK_0 UDSS Tests on Overconsolidated BBC (form Ladd and Edgers, 1972)

Test No.	w_c (%)	Stress History		At Peak τ_h				At τ_h/σ'_v Maximum			
		σ'_{vc}	OCR	γ	τ_h/σ'_{vc}	σ'_v/σ'_{vc}	τ_h/σ'_{vc}	γ	τ_h/σ'_{vc}	σ'_v/σ'_{vc}	τ_h/σ'_v
		σ'_{vm}		(%)	τ_h/σ'_{vm}	σ'_v/σ'_{vm}	ψ°	(%)	τ_h/σ'_{vm}	σ'_v/σ'_{vm}	ψ°
Mean ¹ ±1SD	- -	3 to 8	1.00	6.2 ±1.7	0.197 ±0.009	0.561 ±0.017	0.352 ±0.018 19.40 ±0.90	31.8 ±1.8	0.112 ±0.015	0.184 ±0.037	0.621 ±0.087 31.80 ±3.70
410 ²	35.5	2.0 4.0	2.00	7.1	0.382 0.191	0.915 0.458	0.417 22.64	32.3	0.239 0.120	0.387 0.193	0.619 31.76
1302	35.6	2.0 4.0	2.00	5.4	0.344 0.172	0.925 0.463	0.372 20.41	Not Reached			
611 ³	37.0	0.996 3.98	3.99	11.7	0.609 0.153	1.290 0.323	0.471 25.22	41.0	0.326 0.082	0.507 0.127	0.644 32.78
311	37.0	1.0 4.0	4.00	8.5	0.644 0.161	1.317 0.329	0.490 26.10	30.0	0.422 0.106	0.591 0.148	0.715 35.56
1304	35.8	1.0 4.0	4.00	7.7	0.555 0.139	1.230 0.305	0.451 24.28	Not Reached			
310	37.3	1.0 8.0	8.00	9.7	0.937 0.117	1.852 0.232	0.506 26.84	31.2	0.530 0.063	0.834 0.104	0.636 32.46
1001A	37.5	0.5 4.0	8.00	12.6	1.000 0.125	1.807 0.226	0.553 28.94	Not Reached			

Notes: 1. Average from 5 tests. 2. Top cap slipped.
 3. τ_h/σ'_v still increasing at $\gamma = 41\%$. 4. Stresses in kg/cm².
 5. $d\gamma/dt = 5\% \pm$ per hour.

Table 7.3: Comparison of Results from Geonor CK₀UDSS Tests on Overconsolidated BBC III

Reference (Series)	Number of Tests	OCR	At Peak τ_h				At τ_h/σ'_v Maximum				$E_u(50)$
			γ	τ_h/σ'_{vc}	σ'_v/σ'_{vc}	τ_h/σ'_{vc}	γ	τ_h/σ'_{vc}	σ'_v/σ'_{vc}	τ_h/σ'_v	c_u
			(%)	τ_h/σ'_{vm}	σ'_v/σ'_{vm}	ψ°	(%)	τ_h/σ'_{vm}	σ'_v/σ'_{vm}	ψ°	
Ladd and Edgers (1972)	2*	2	6.40	0.363 0.181	0.920 0.460	0.395 21.50	32.30	0.239 0.120	0.387 0.193	0.619 31.80	633
(BBC- Ib)	2	8	11.20	0.969 0.121	1.830 0.229	0.530 27.90	31.20	0.530 0.066	0.834 0.104	0.636 32.50	163
This Research	1	2	7.64	0.362 0.184	0.917 0.467	0.394 21.50	36.56	0.189 0.096	0.338 0.172	0.560 29.25	469
(BBC III)	2*	8	12.03	0.895 0.114	1.900 0.242	0.472 25.24	39.72	0.399 0.050	0.637 0.081	0.627 32.09	158

Note: * Data at $(\tau_h/\sigma'_v)_{max}$ only from one test.

Table 7.4: Comparison of m Values for CK_0 UDSS Tests on Overconsolidated BBC

Reference (Series)	No. of Tests	Range of OCR	m ¹ Measured	S ²	r^2 *	m ³ Predicted	$\frac{m_{\text{measured}}}{m_{\text{predicted}}}$
This Research (BBC III)	3	1-3.25	0.820	0.200	0.995	0.902	0.910
	5	1-7.89	0.719	0.210	0.992	0.873	0.824
	6	1-14.7	0.652	0.221	0.978	0.856	0.762
	7	1-31.9	0.624	0.227	0.983	0.845	0.738
Ladd & Edgers (1972) (BBC Ib)	6	1-4.0	0.791	0.203	0.981	-	-
	8	1-8.0	0.751	0.209	0.987	-	-

Notes:

1. Computed values of m from Equation 7.1 for BBC.
2. $S = c_u/\sigma'_{vc}$ at $OCR = 1$.
3. Values computed based on the relationship: $m = 1 - C_c/C_s$.
- *. r^2 is coefficient of determination for linear regression of $\log(c_u/\sigma'_{vc})$ on $\log OCR$.

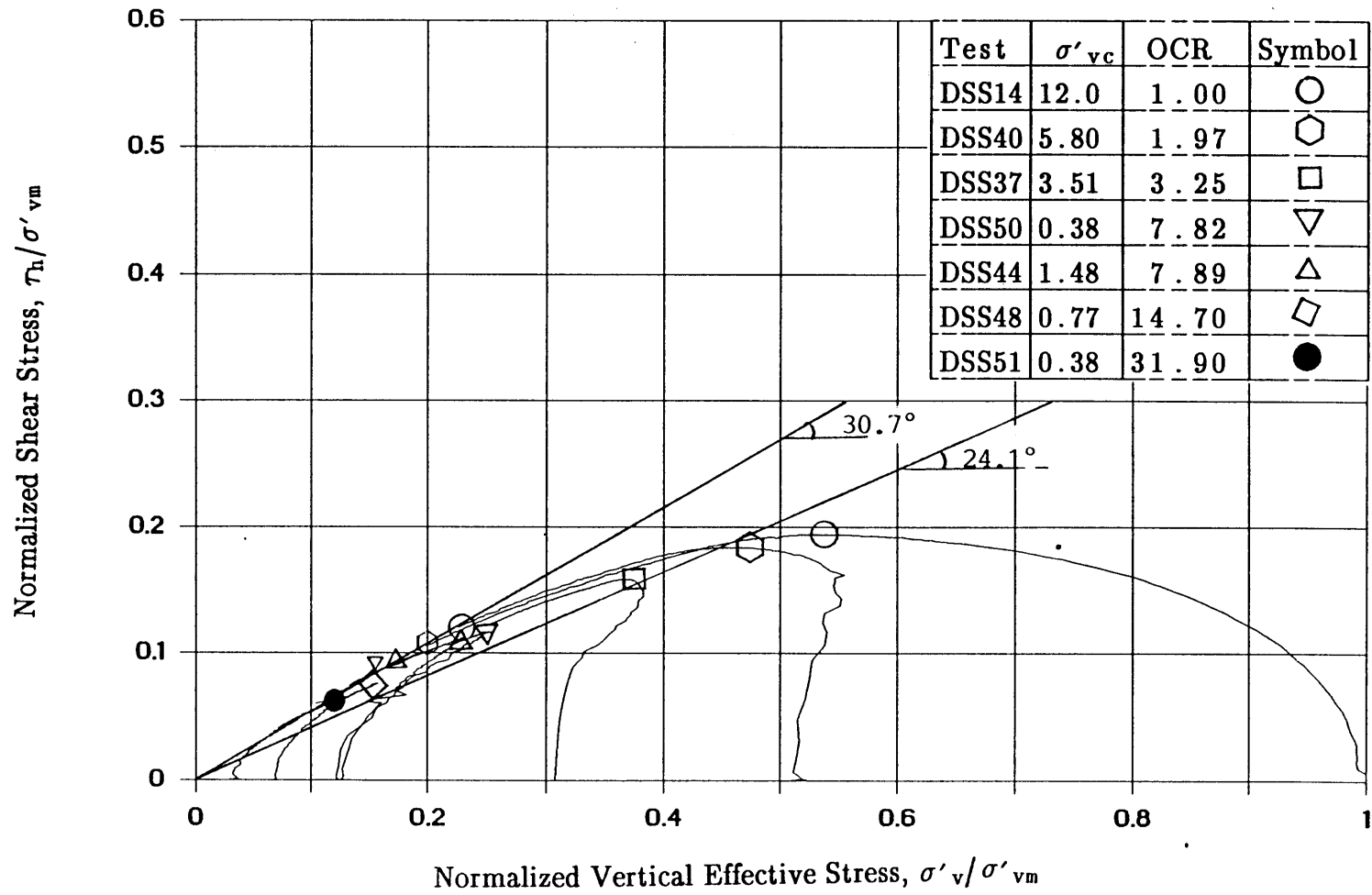


Figure 7.1: Normalized Stress Paths from CK_o UDSS Tests on Overconsolidated Boston Blue Clay.

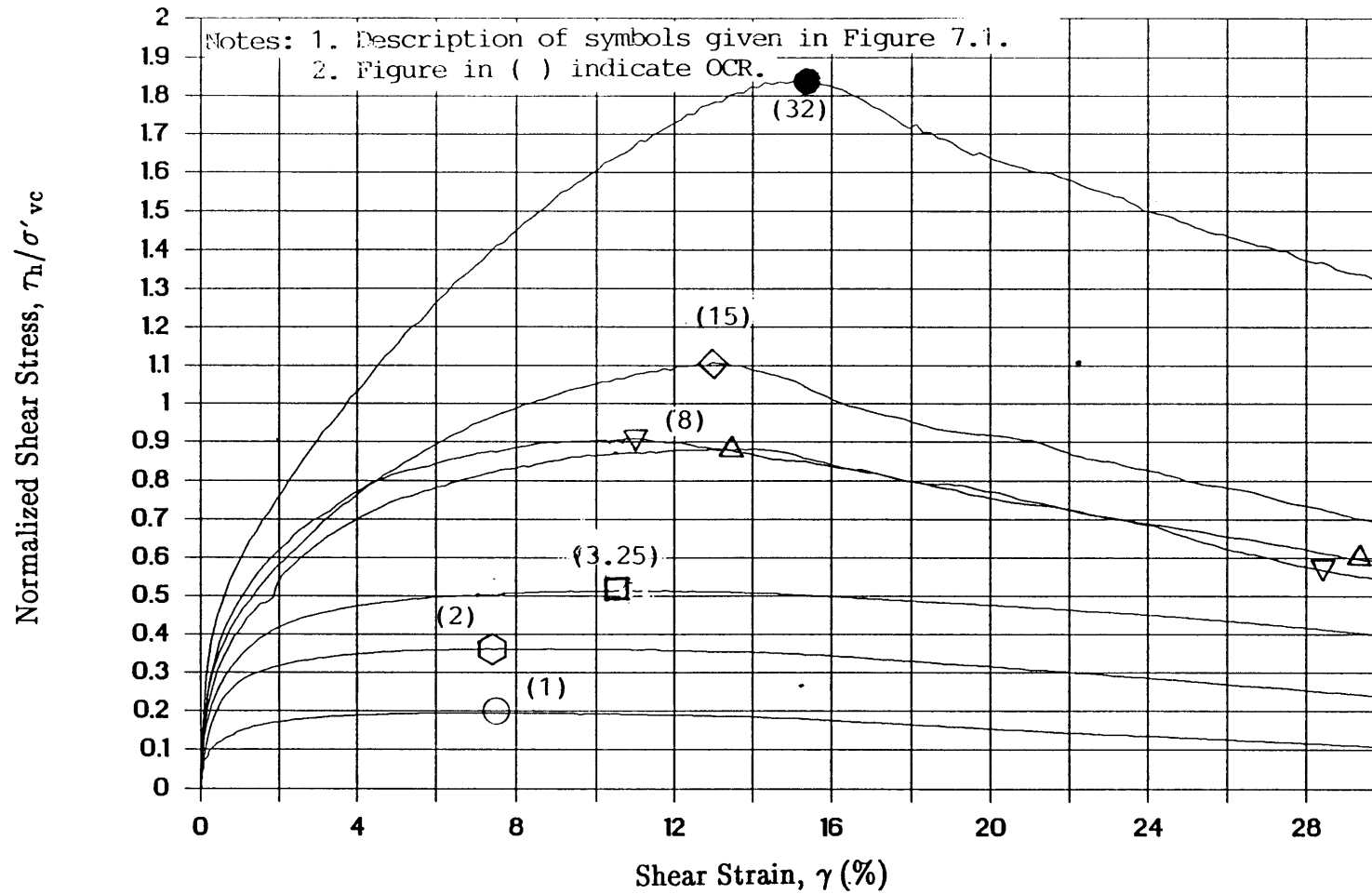


Figure 7.2: Normalized Shear Stress Versus Shear Strain from CK_0 UDSS Tests on Overconsolidated Boston Blue Clay.

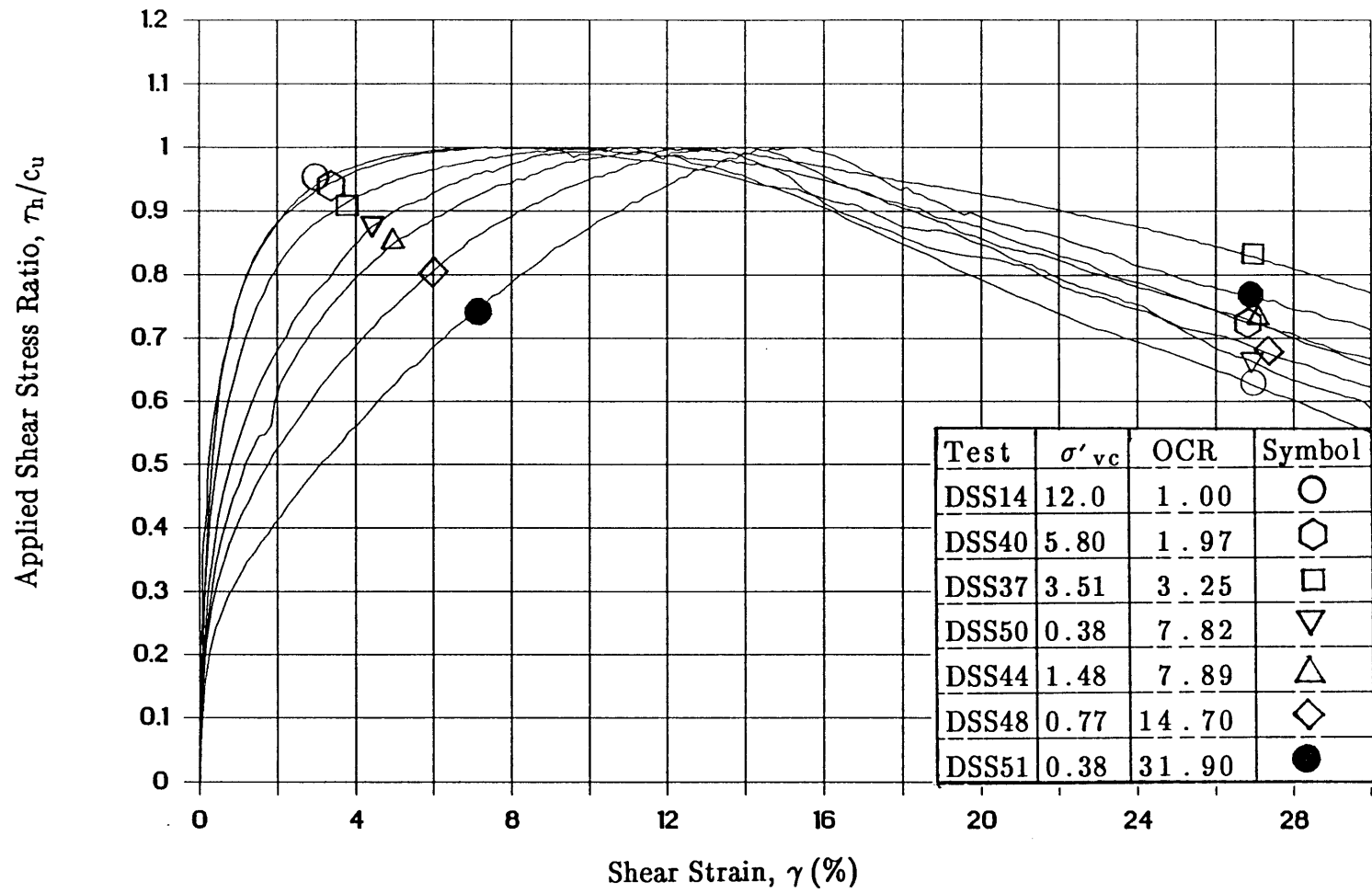


Figure 7.3: Applied Shear Stress Ratio Versus Shear Strain from CK_0 UDSS Tests on Overconsolidated Boston Blue Clay.

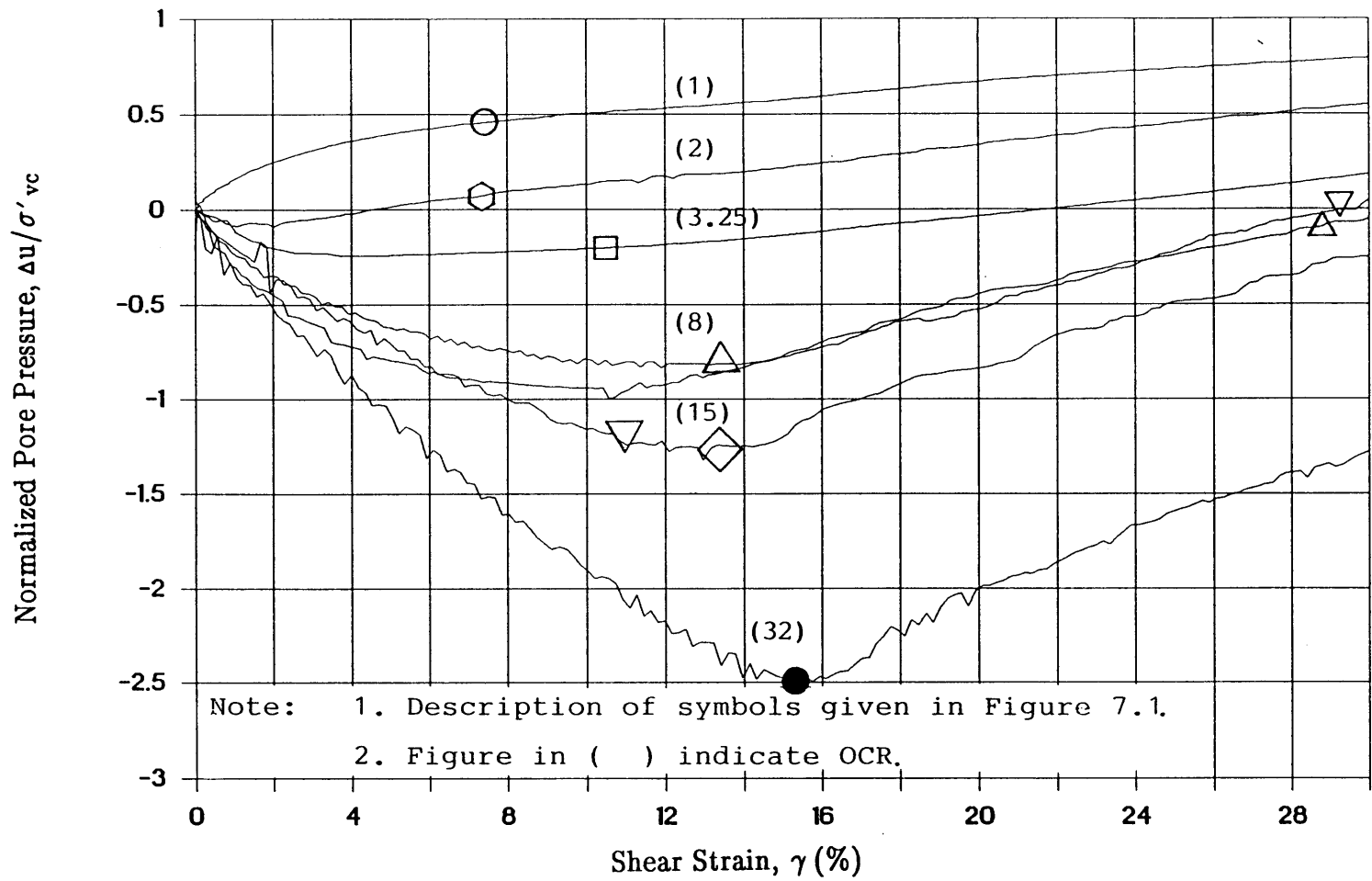


Figure 7.4: Normalized Pore Pressure Versus Shear Strain from CK_0 UDSS Tests on Overconsolidated Boston Blue Clay.

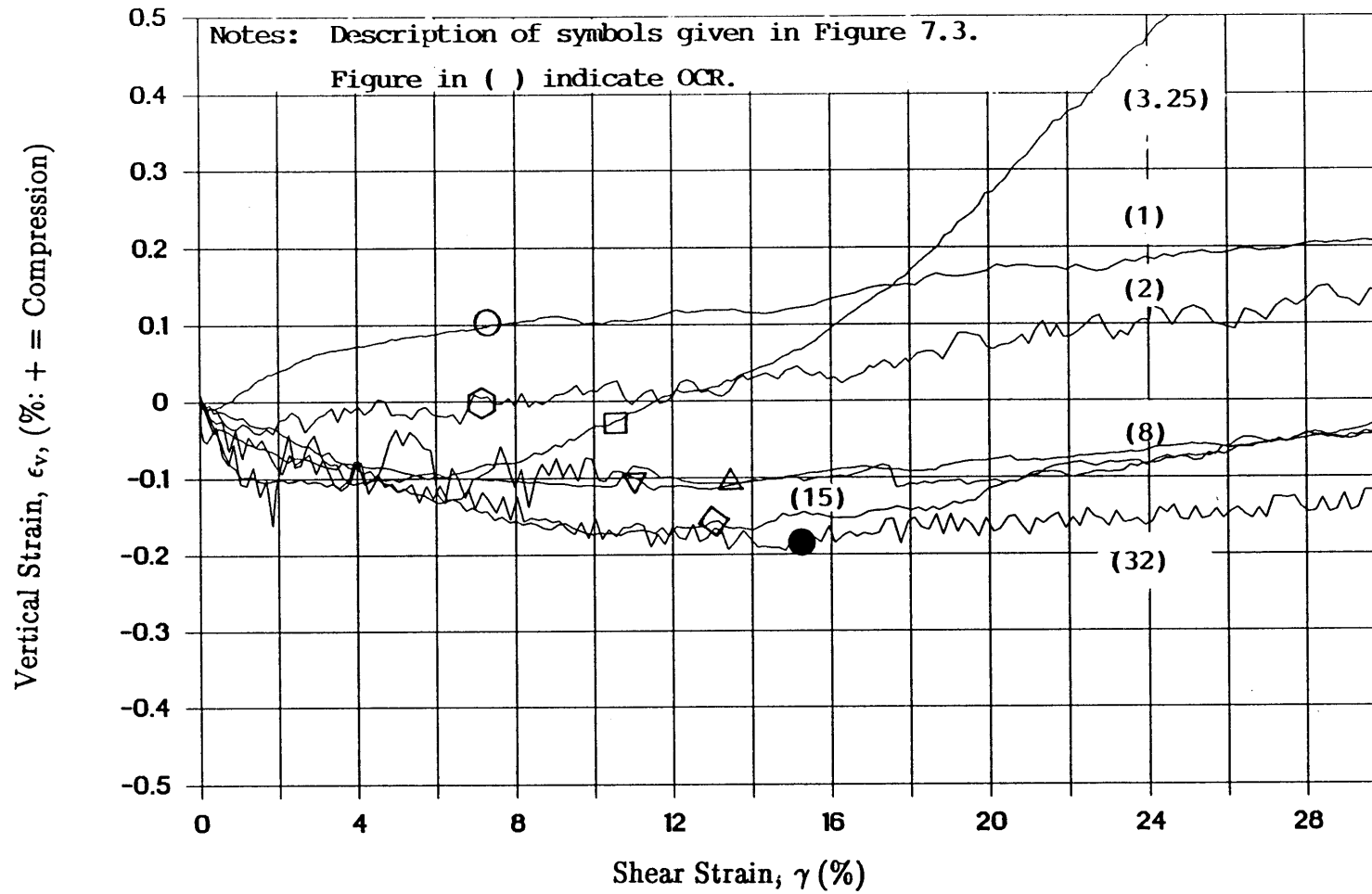


Figure 7.5: Vertical Strain Versus Shear Strain from CK_0 UDSS Tests on Overconsolidated Boston Blue Clay.

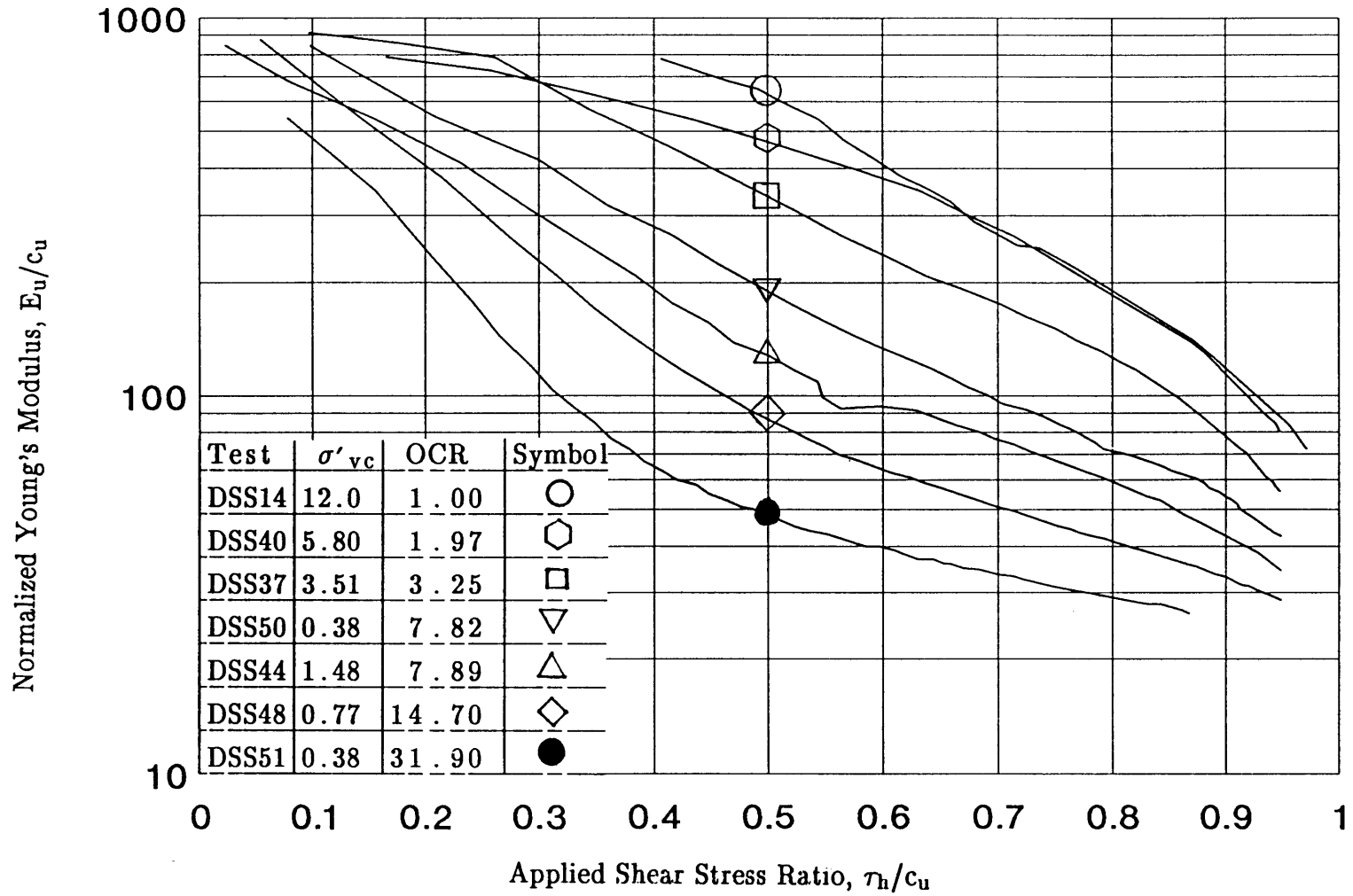


Figure 7.6: Normalized Undrained Young's Modulus Versus Applied Shear Stress Ratio from CK_0 UDSS Tests on Overconsolidated Boston Blue Clay.

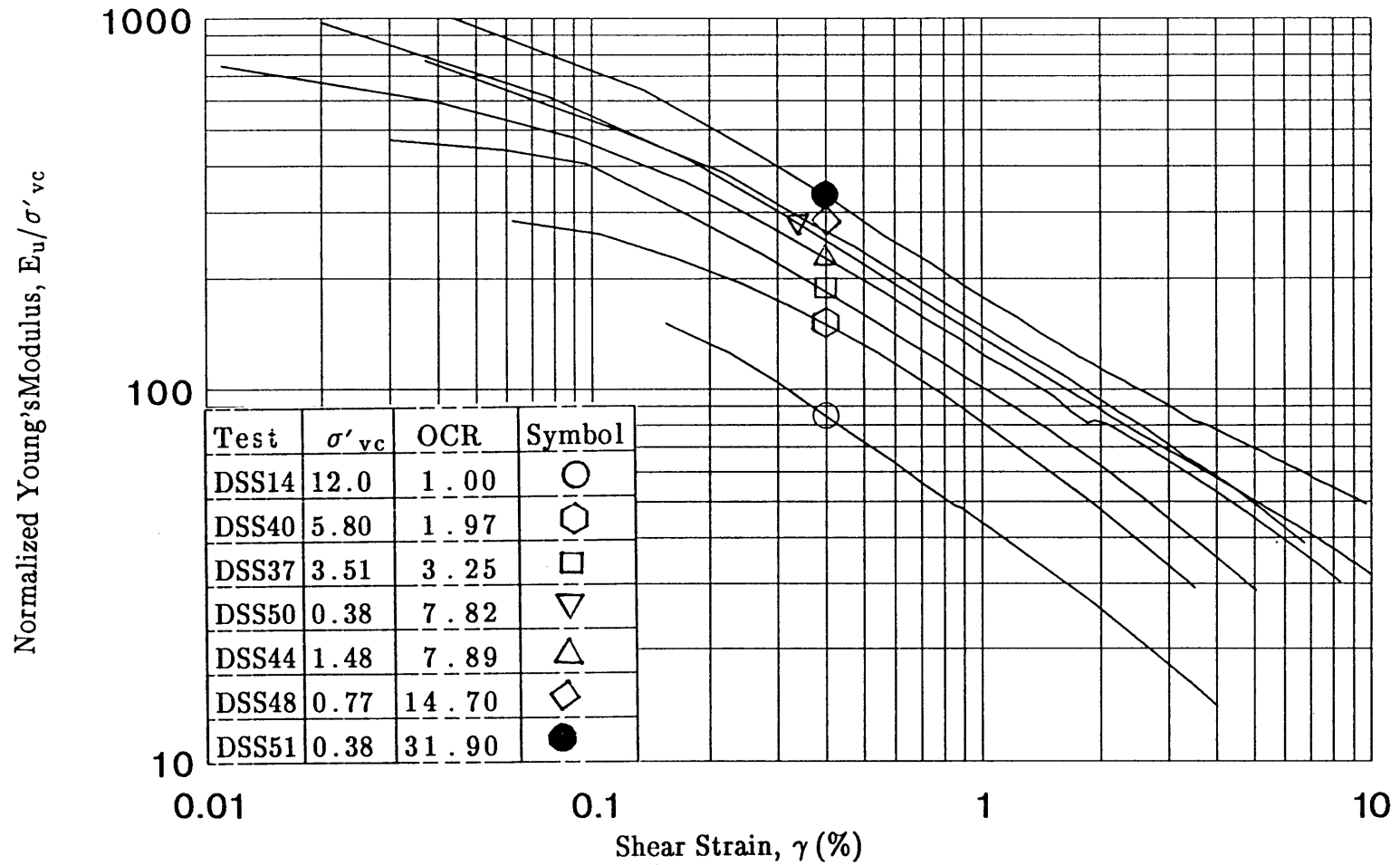


Figure 7.7: Normalized Undrained Young's Modulus (E_u/σ'_{vc}) Versus Shear Strain from CK₀UDSS Tests on Overconsolidated Boston Blue Clay.

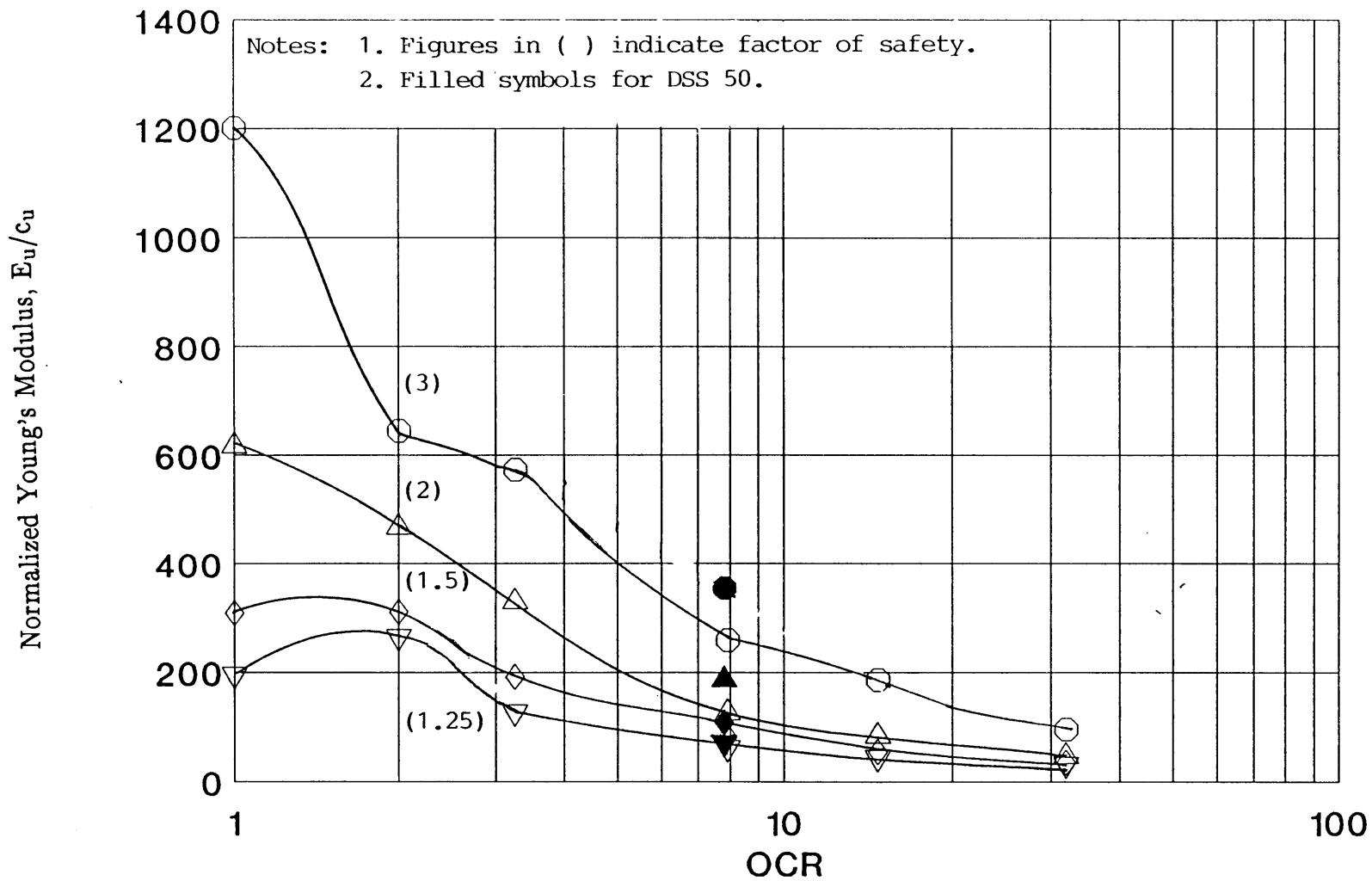


Figure 7.8: Normalized Young's Modulus Versus OCR from CK_o UDSS Tests on Overconsolidated Boston Blue Clay.

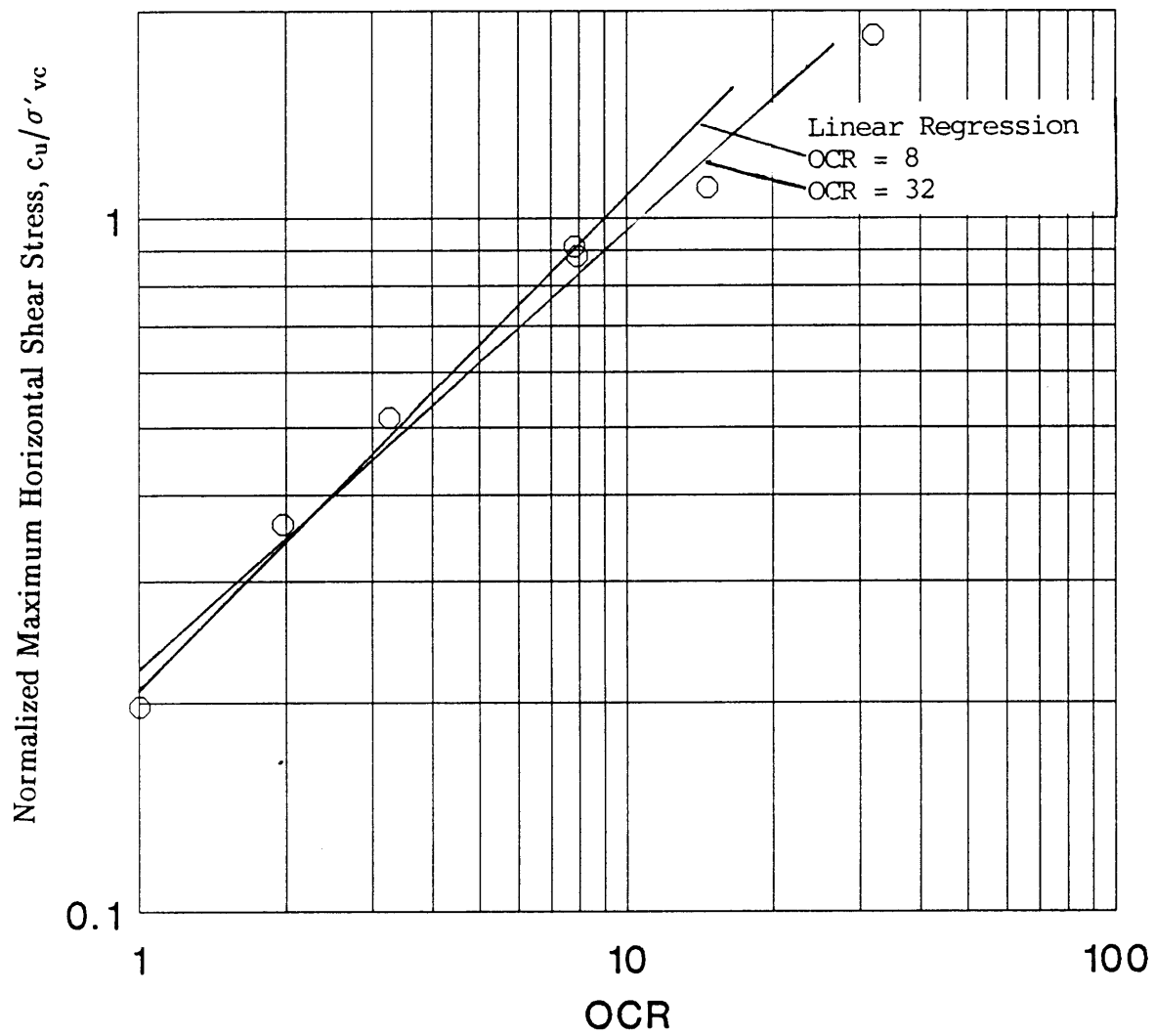


Figure 7.9: Undrained Shear Strength Ratio Versus OCR from CK_0 UDSS Test on Overconsolidated Boston Blue Clay.

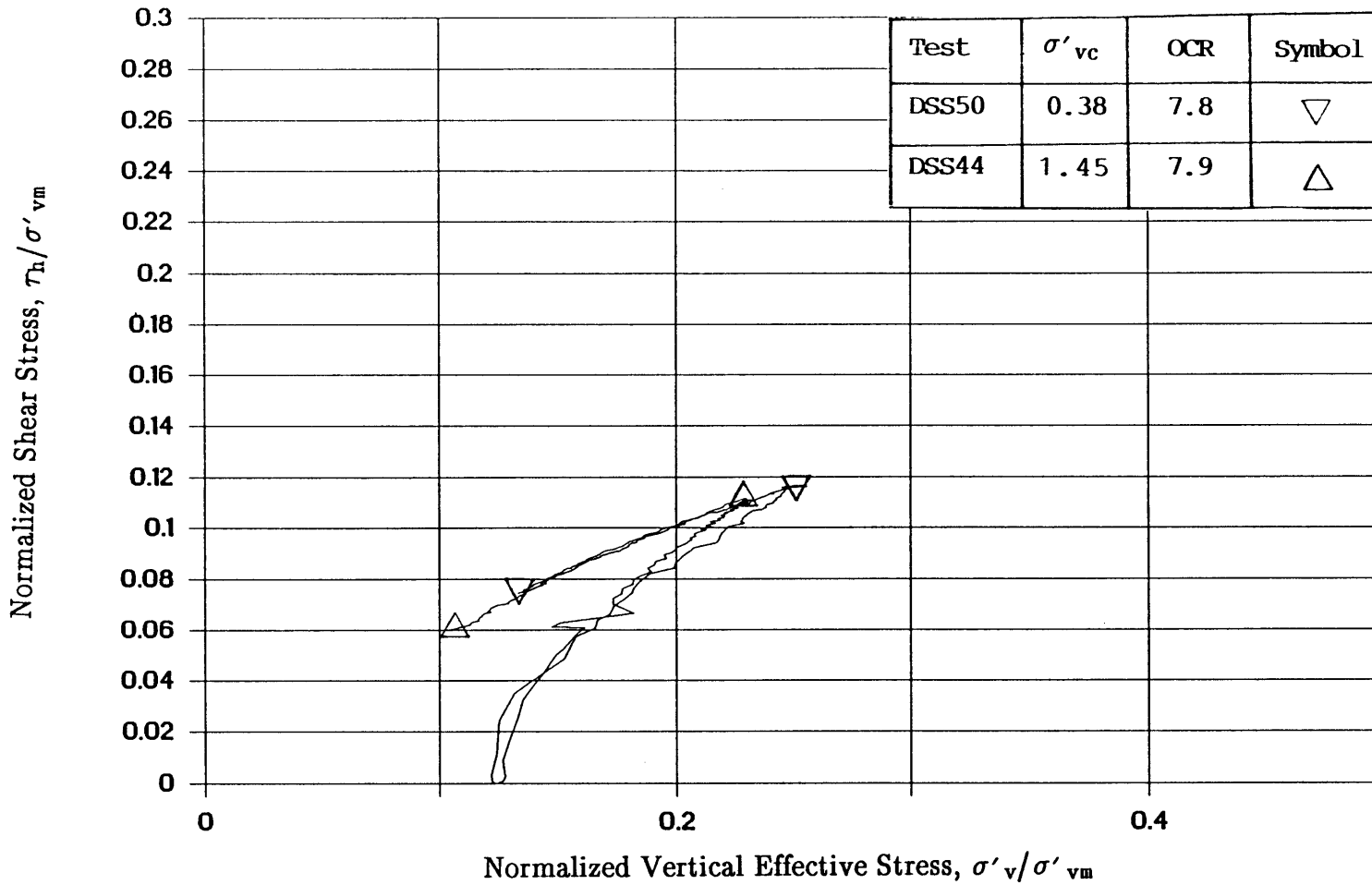


Figure 7.10: Comparison of Stress Paths from CK_0 UDSS Tests on BBC at the Same OCR with Different σ'_{vm} .

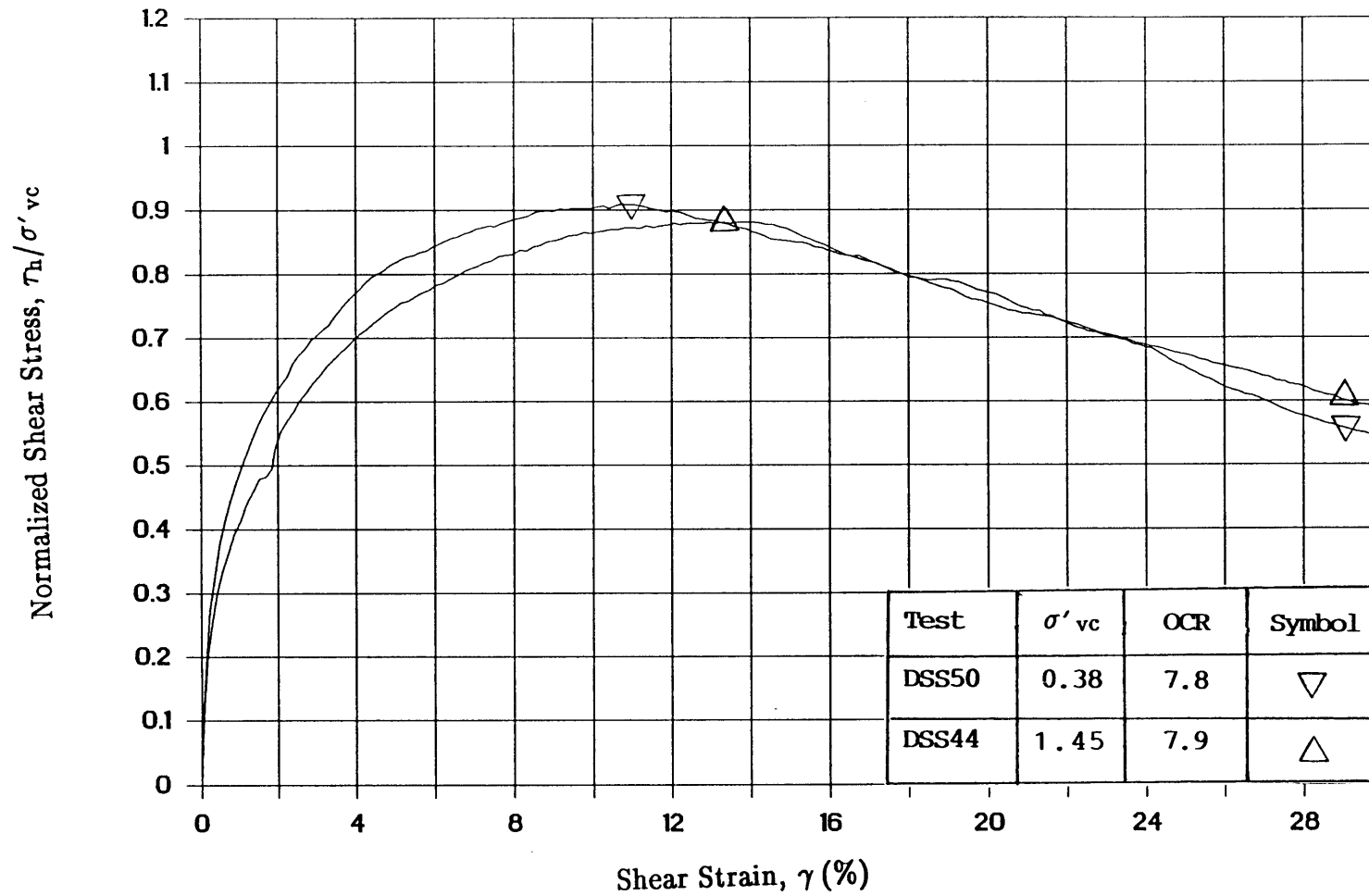


Figure 7.11: Normalized Shear Stress Versus Shear Strain from CK_0 UDSS Tests at the Same OCR with Different σ'_{vm} .

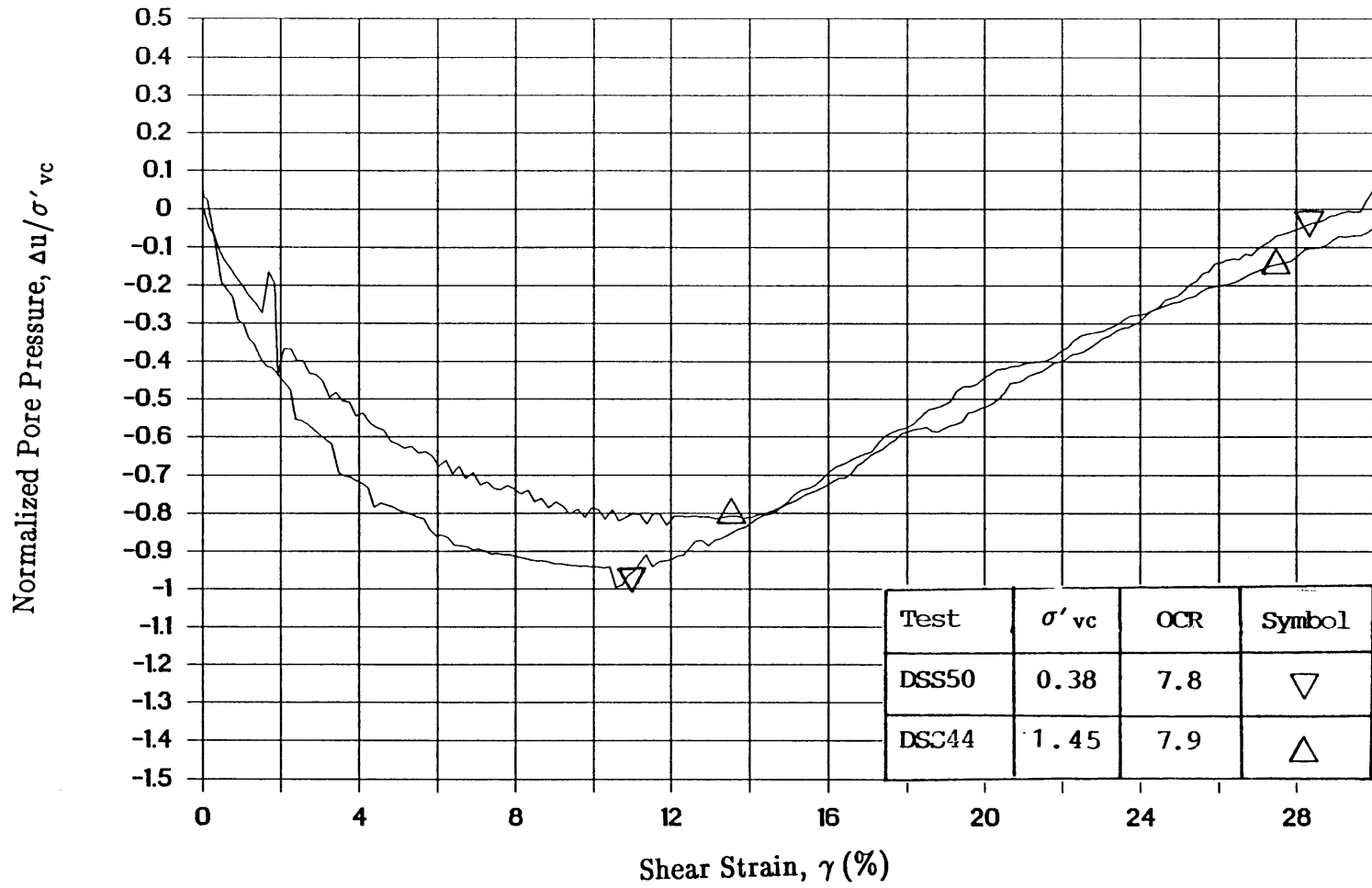


Figure 7.12: Normalized Pore Pressure Versus Shear Strain from CK_0 UDSS Tests at the Same OCR with σ'_{vm} .

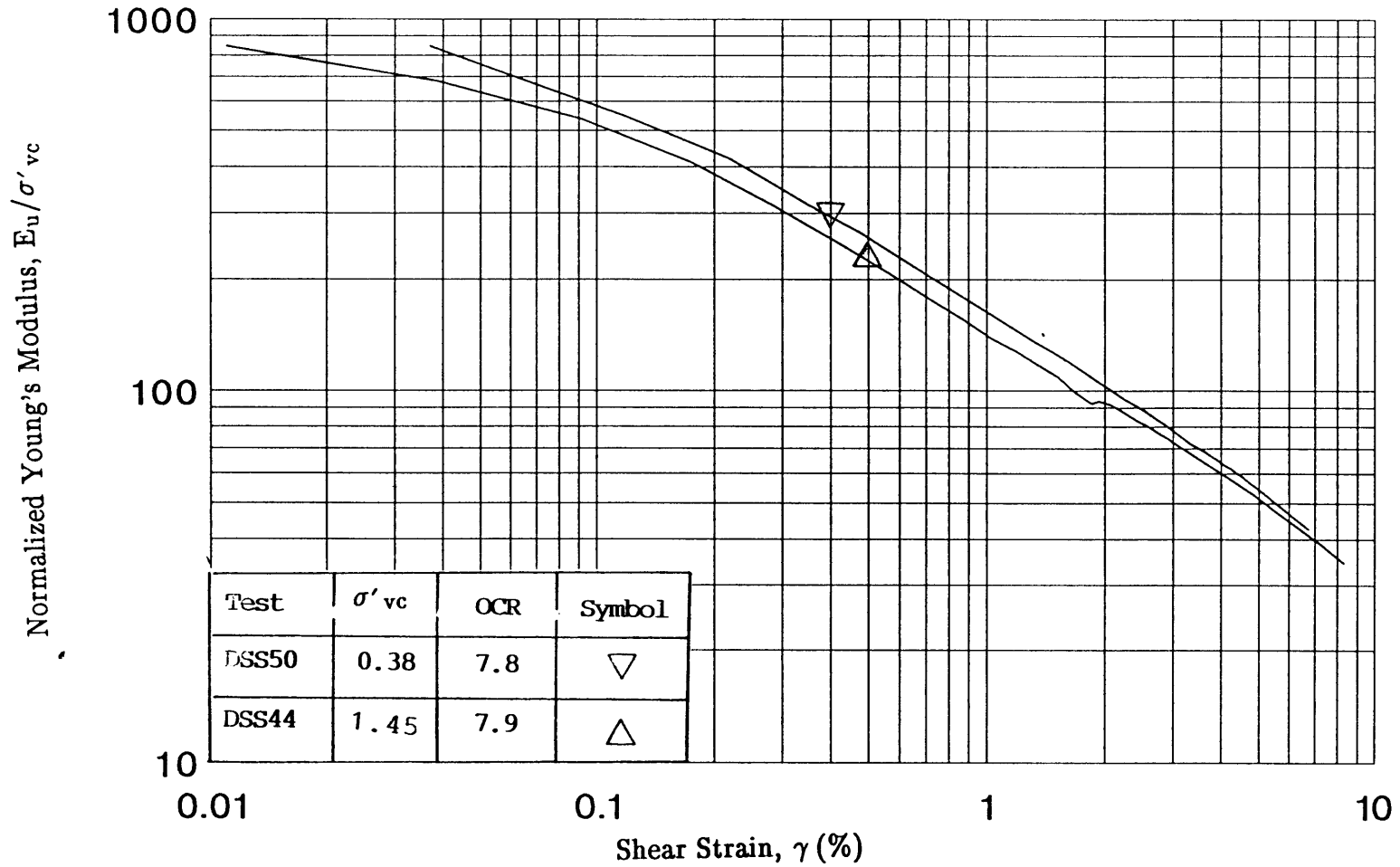


Figure 7.13: Normalized Undrained Young's Modulus (E_u/σ'_{vc}) Versus Shear Strain Ratio from CK_0 UDSS Tests on BBC at the Same OCR with Different σ'_{vm} .

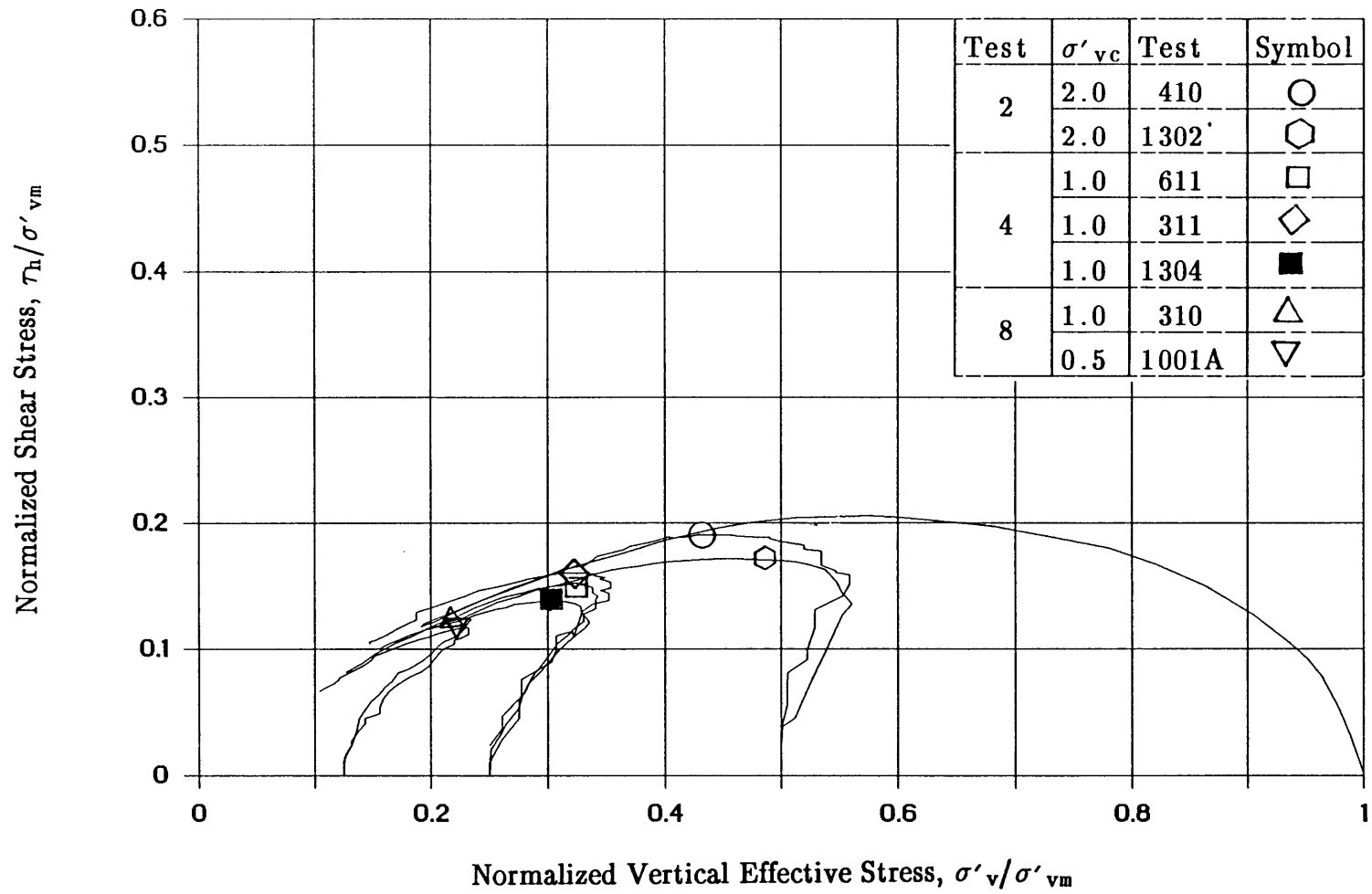


Figure 7.14: Normalized Stress Paths from CK_0 UDSS Tests on Overconsolidated Boston Blue Clay (from Ladd and Edgers, 1972).

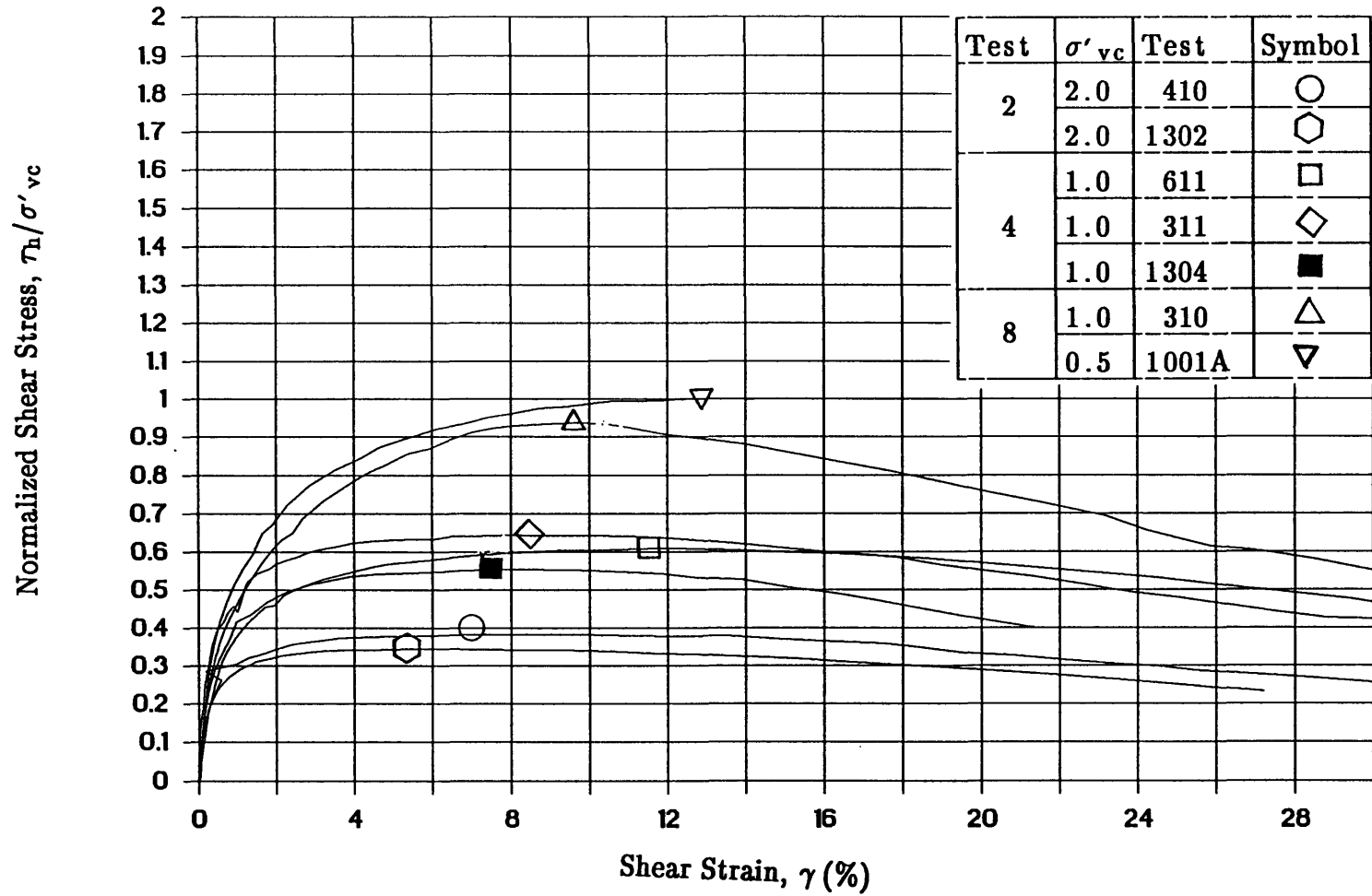


Figure 7.15: Normalized Shear Stress Versus Shear Strain from CK_0 UDSS Tests on Overconsolidated Boston Blue Clay (from Ladd and Edgers, 1972).

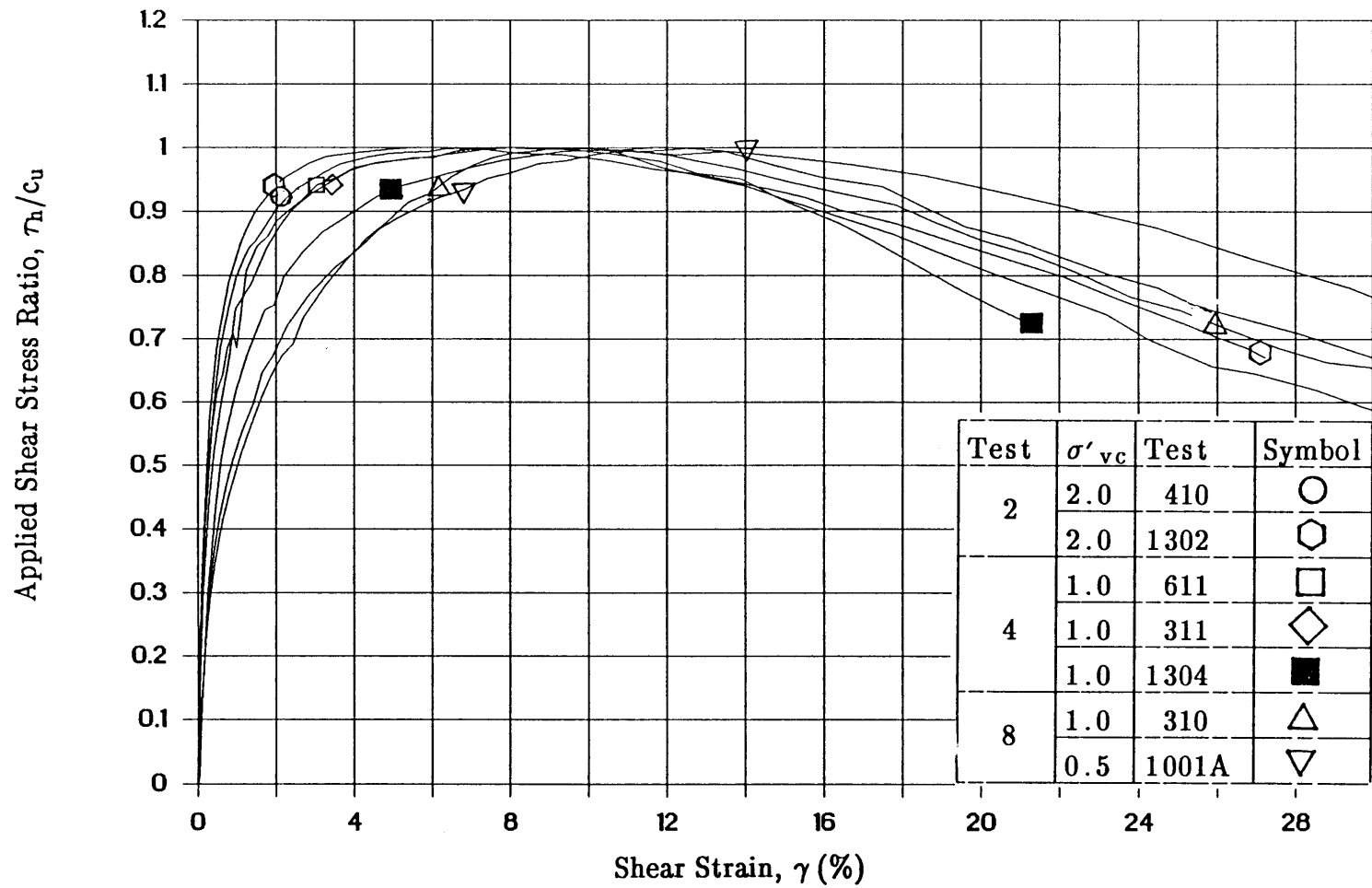


Figure 7.16: Applied Shear Stress Ratio Versus Shear Strain from CK_0 UDSS Tests on Overconsolidated Boston Blue Clay (from Ladd and Edgers, 1972).

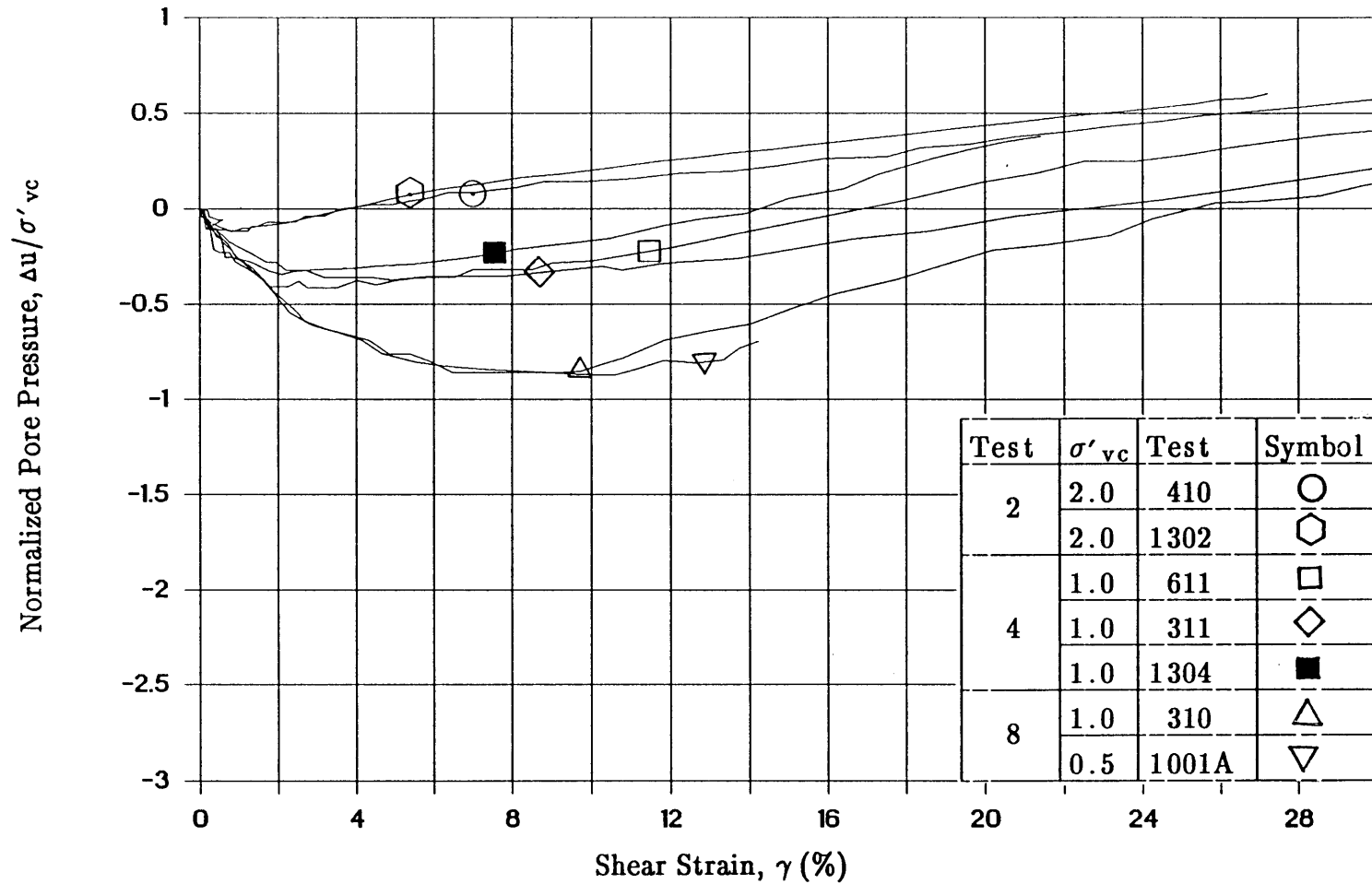


Figure 7.17: Normalized Pore Pressure Versus Shear Strain from CK_0 UDSS Tests on Overconsolidated Boston Blue Clay (from Ladd and Edgers, 1972).

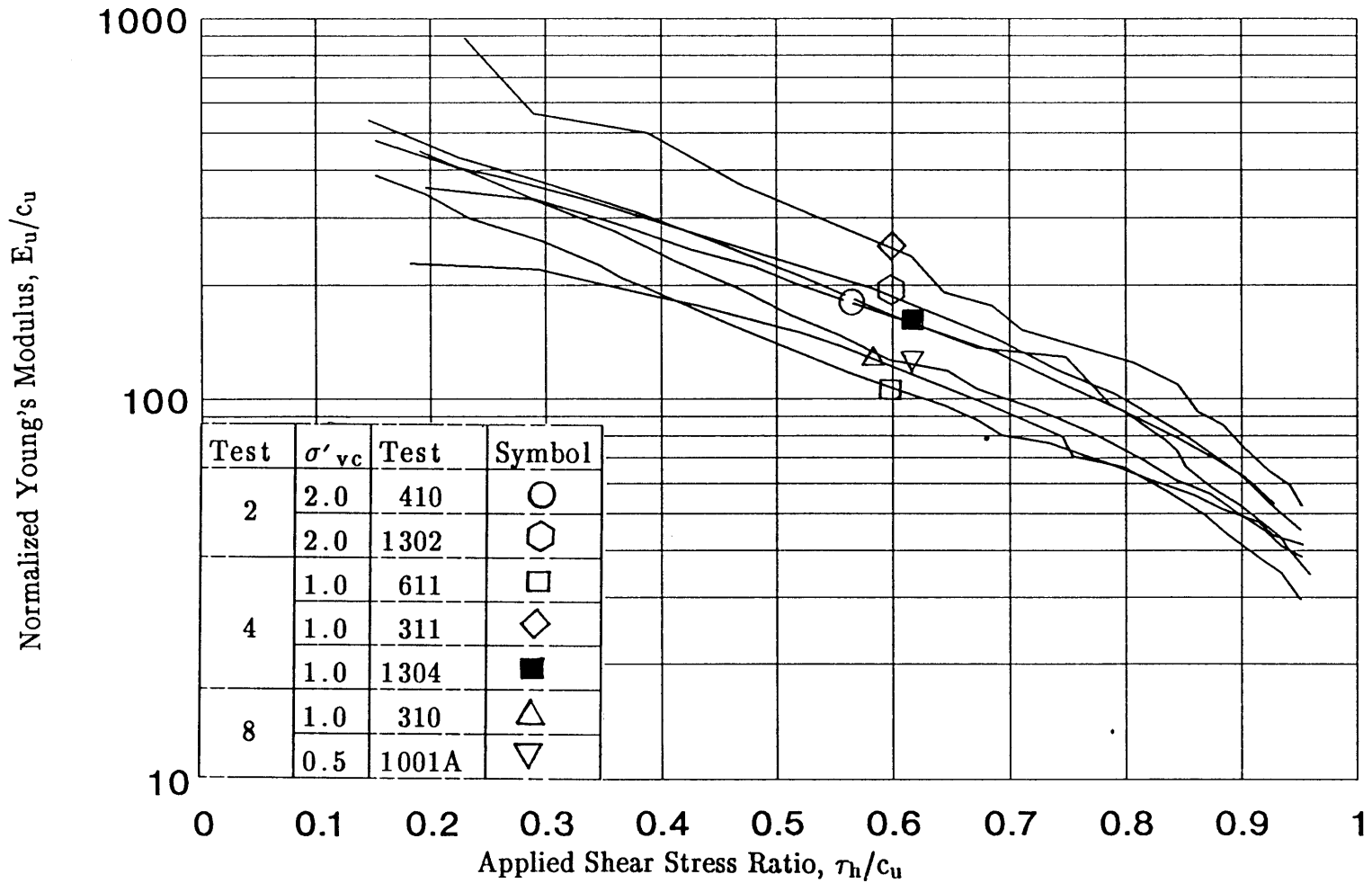


Figure 7.18: Normalized Undrained Young's Modulus Versus Applied Shear Stress Ratio from CK_0 UDSS Tests on Overconsolidated Boston Blue Clay (from Ladd and Edgers, 1972).

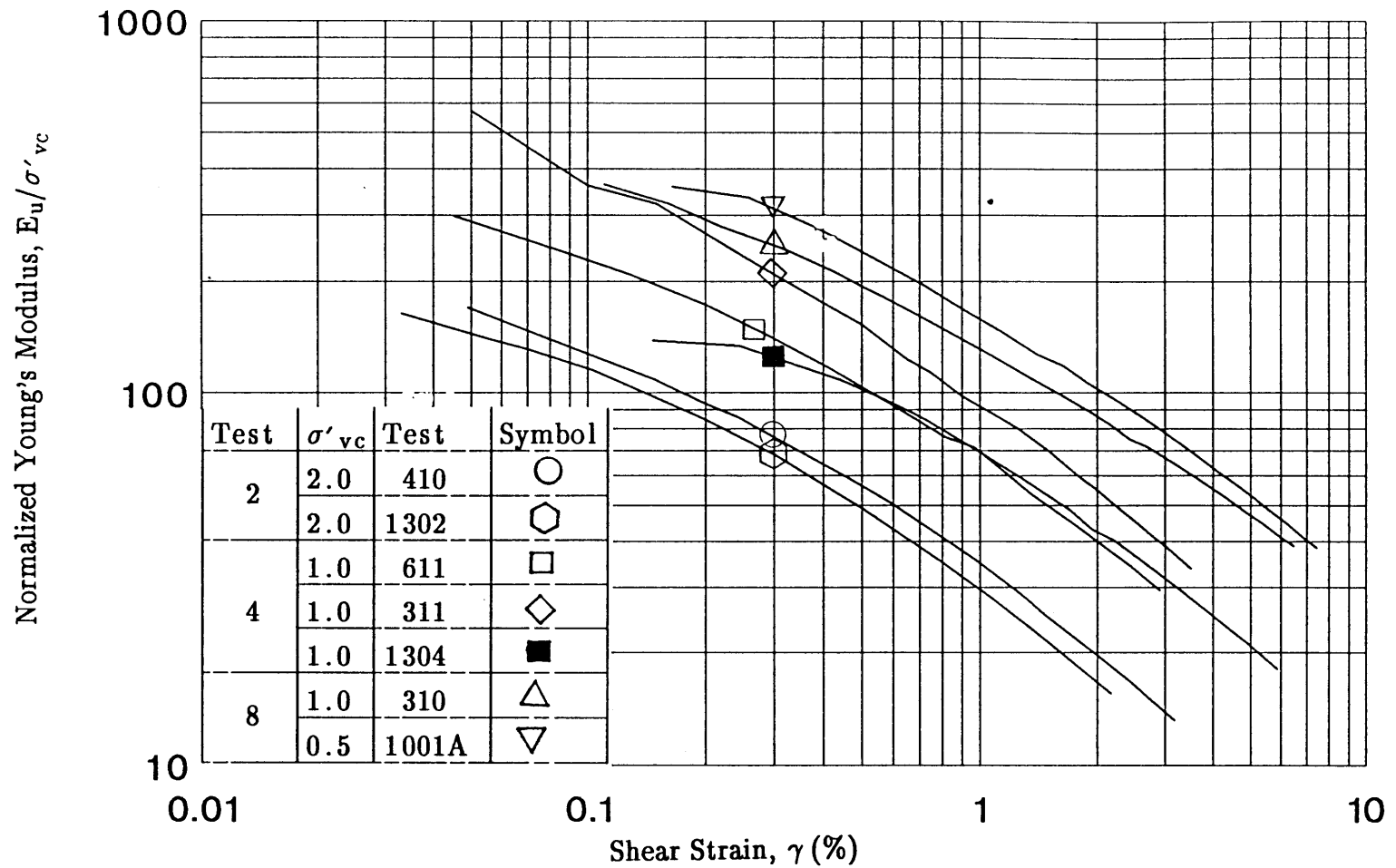


Figure 7.19: Normalized Undrained Young's Modulus (E_u/σ'_{vc}) Versus Shear Strain from CK_0 UDSS Tests on Overconsolidated Boston Blue Clay (from Ladd and Edgers, 1972).

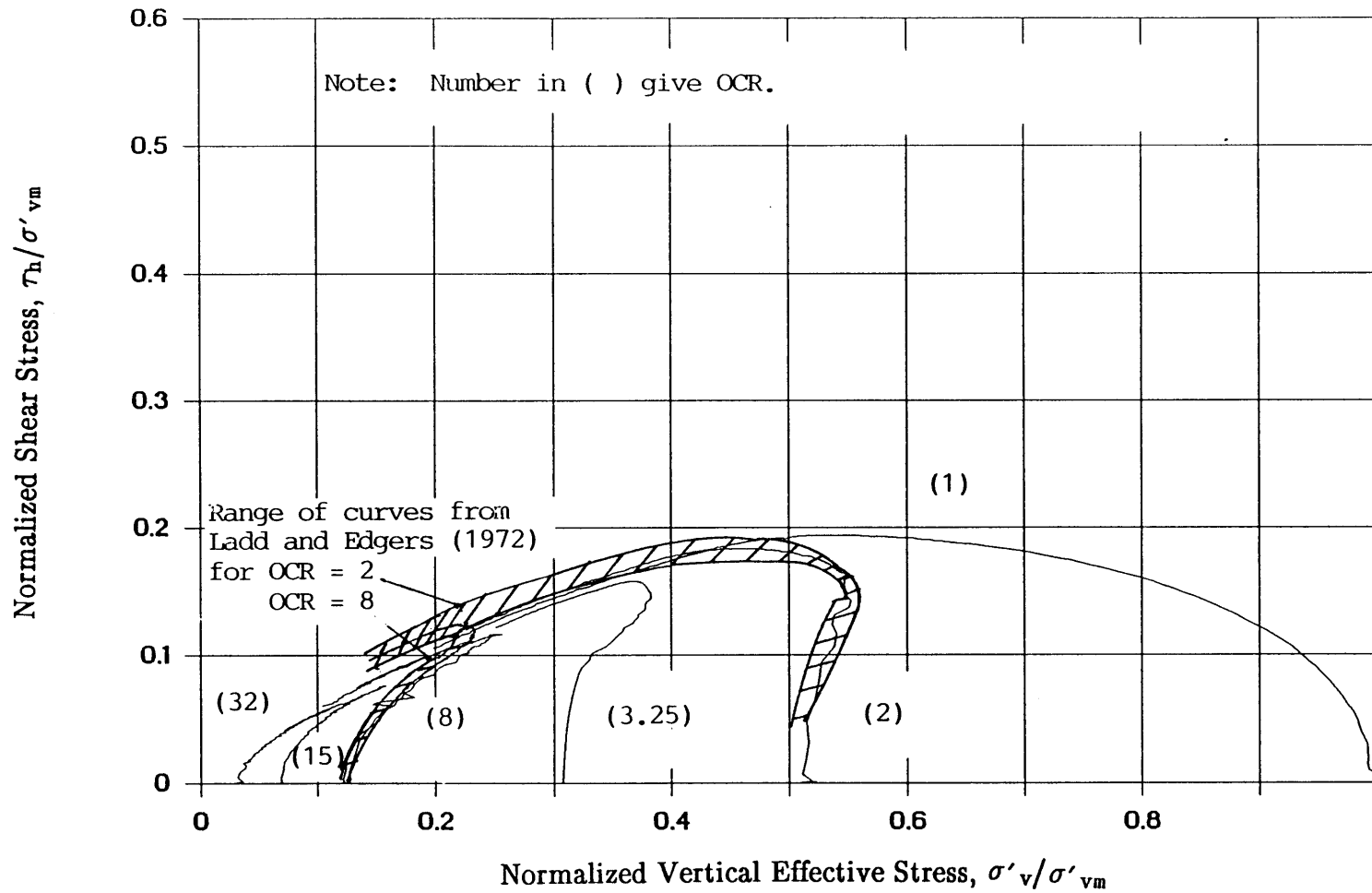


Figure 7.20: Normalized Stress Paths from CK_0 UDSS Tests on Overconsolidated Boston Blue Clay (Curves from Figures 7.1 and 7.14).

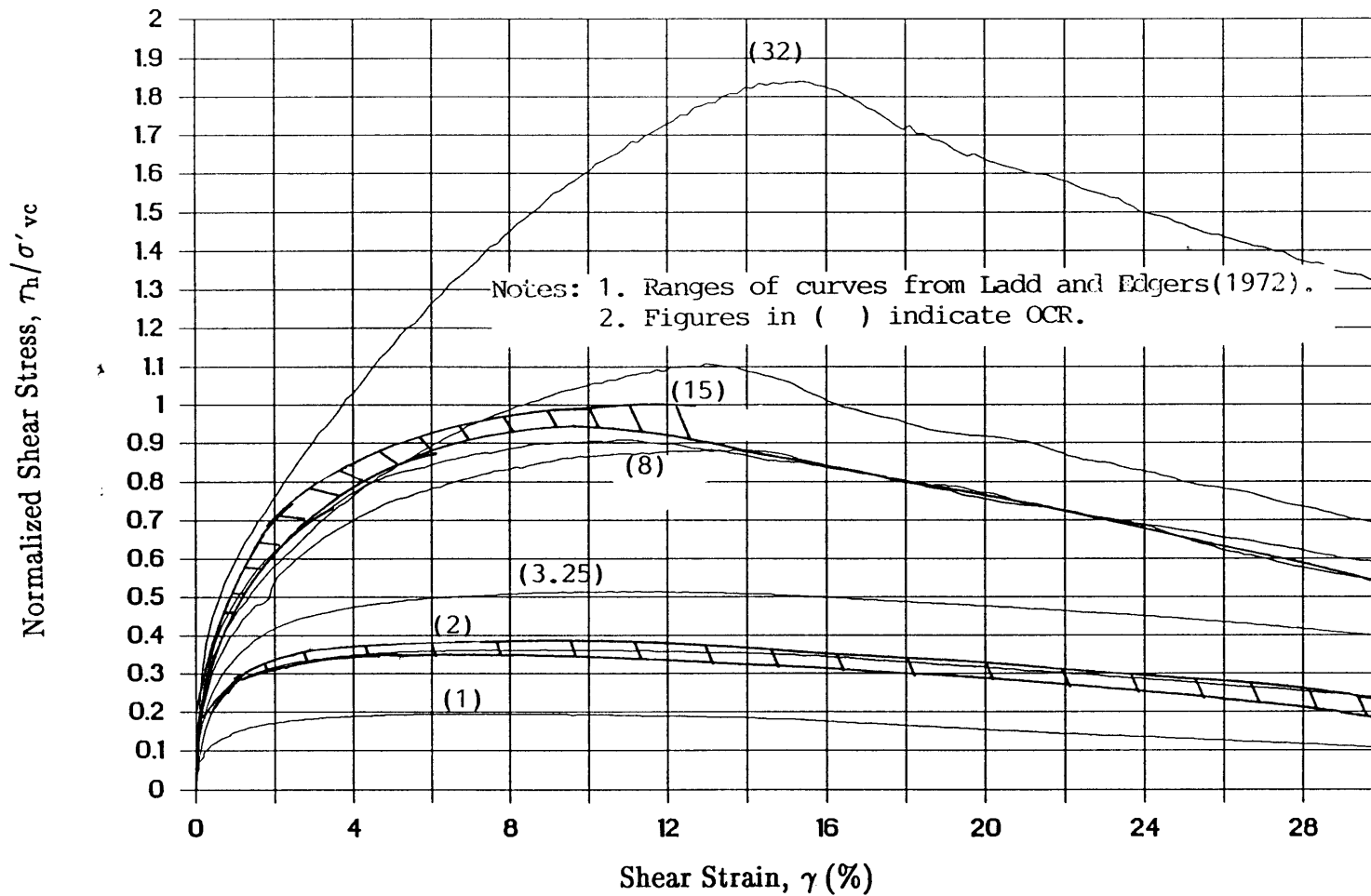


Figure 7.21: Normalized Shear Stress Versus Shear Strain from CK_o UDSS Tests on Overconsolidated Boston Blue Clay (Curves from Figures 7.2 and 7.15).

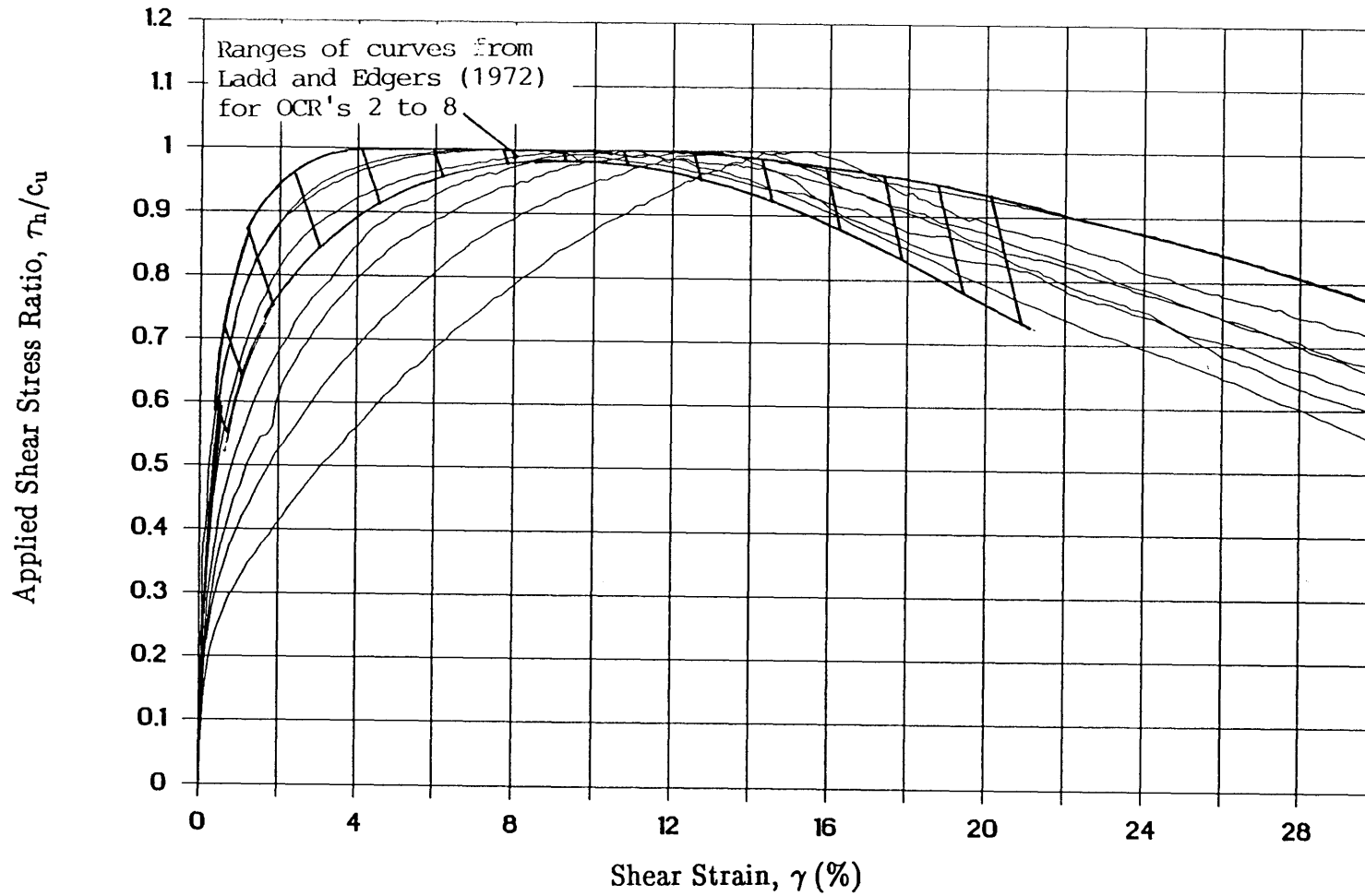


Figure 7.22: Applied Shear Stress Ratio Versus Shear Strain from CK_0 UDSS Tests on Overconsolidated Boston Blue Clay (Curves from Figures 7.3 and 7.16).

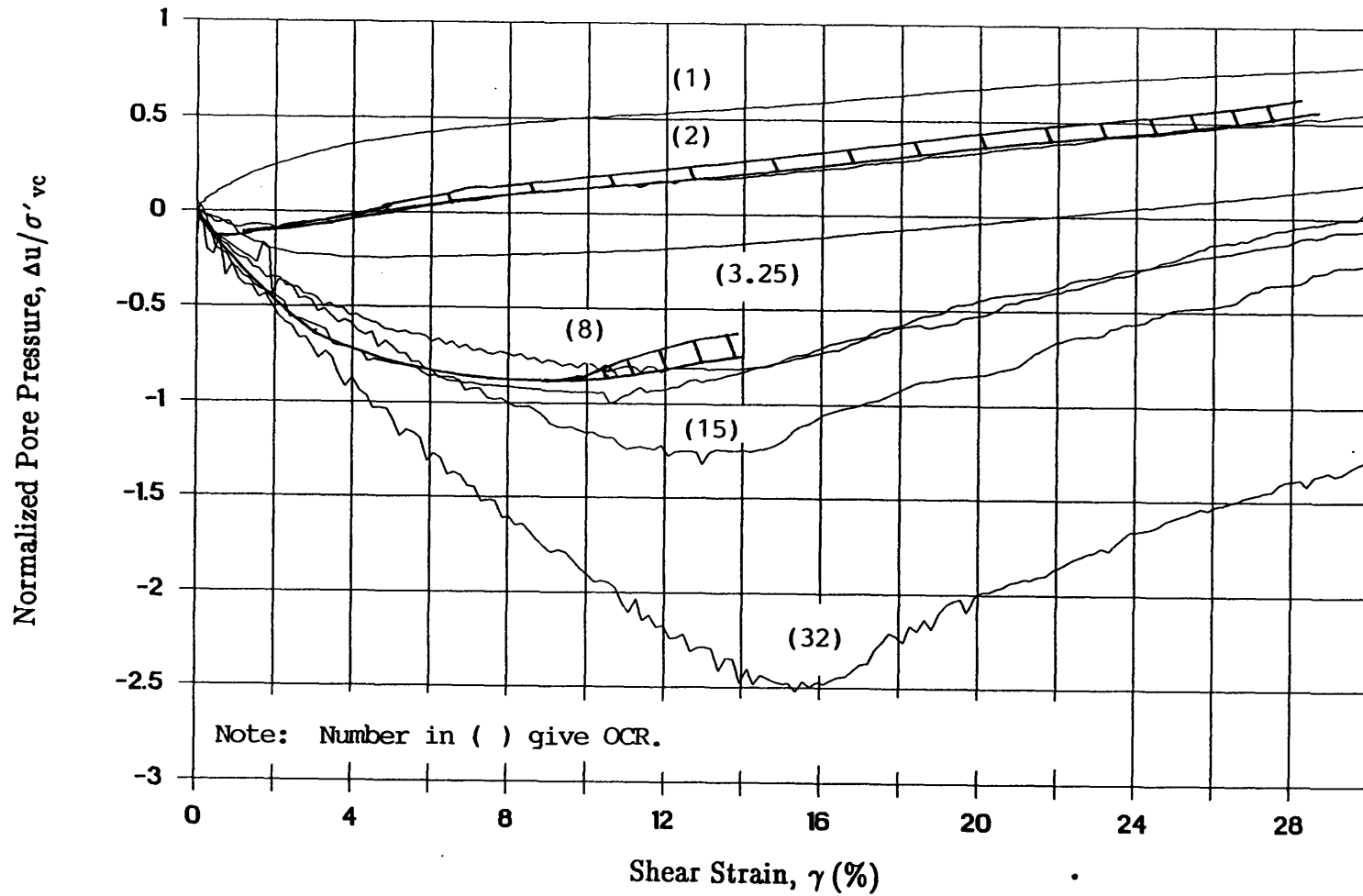


Figure 7.23: Normalized Pore Pressure Versus Shear Strain from CK_0 UDSS Tests on Overconsolidated Boston Blue Clay (Curves from Figures 7.4 and 7.17).

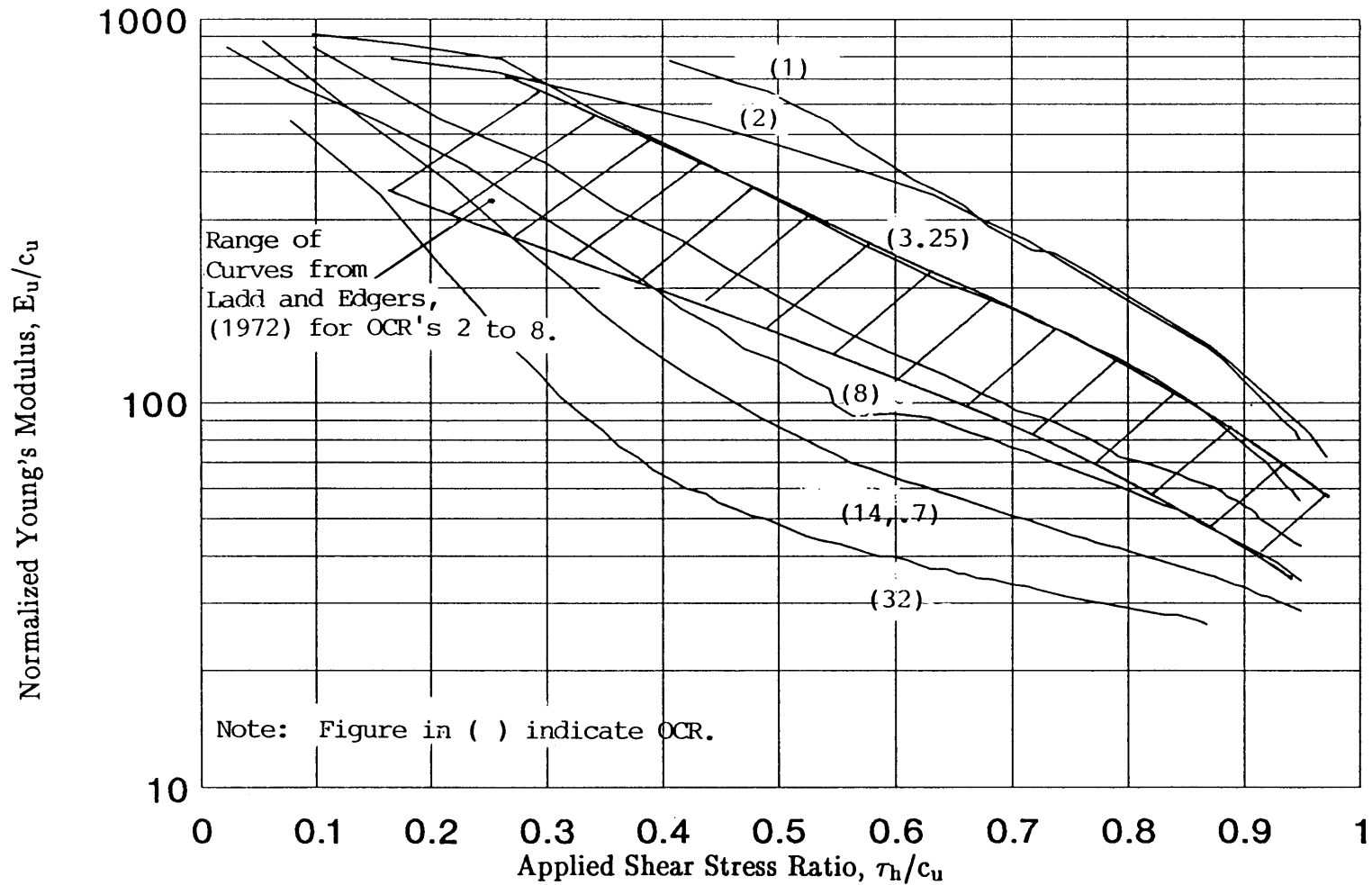


Figure 7.24: Normalized Undrained Young's Modulus Versus Applied Shear Stress Ratio from CK_0 UDSS Tests on Overconsolidated Boston Blue Clay (Curves from Figures 7.6 and 7.18).

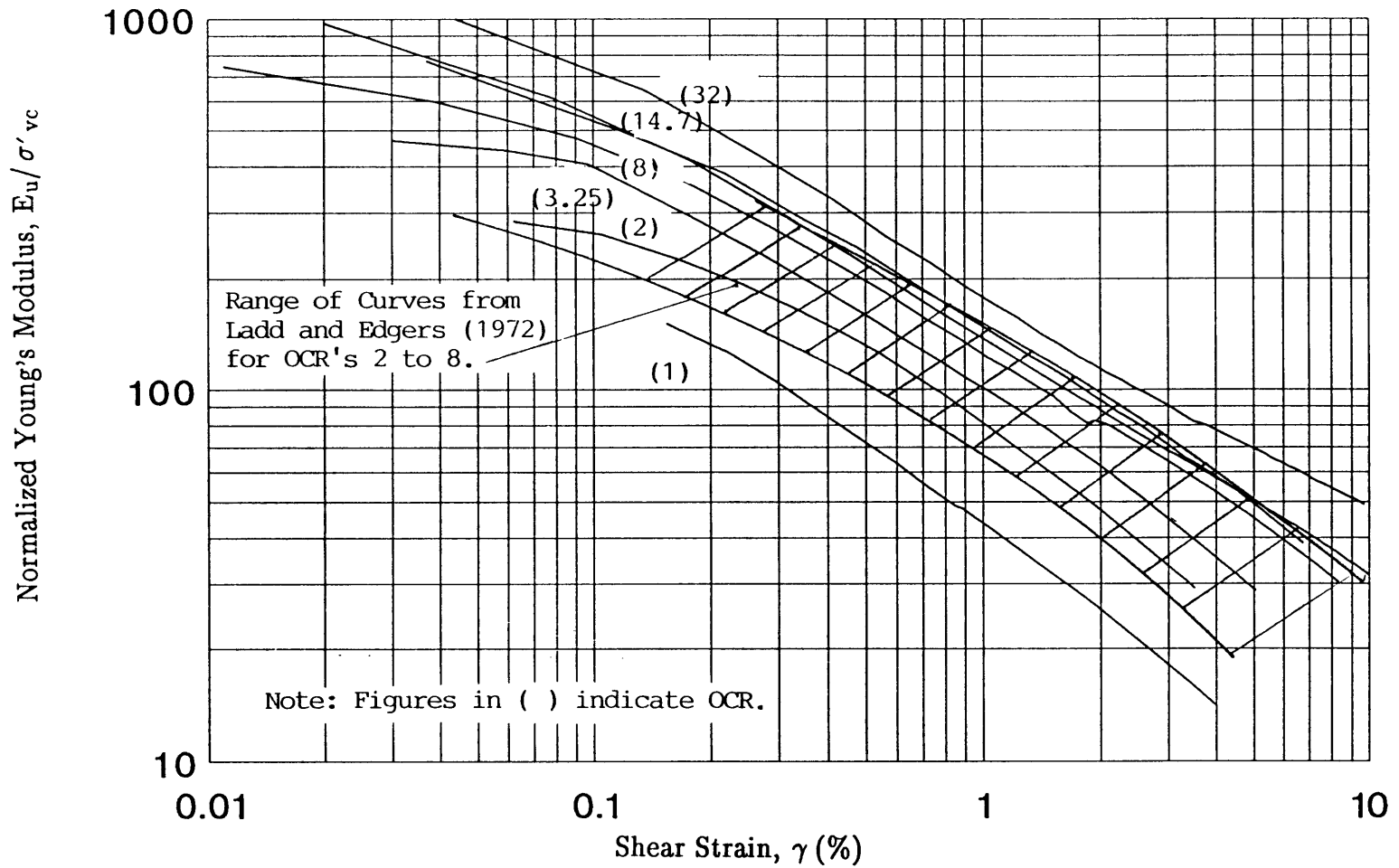


Figure 7.25: Normalized Undrained Young's Modulus (E_u/σ'_{vc}) Versus Shear Strain from CK_0 UDSS Tests on Overconsolidated Boston Blue Clay (Curves from Figures 7.7 and 7.19).

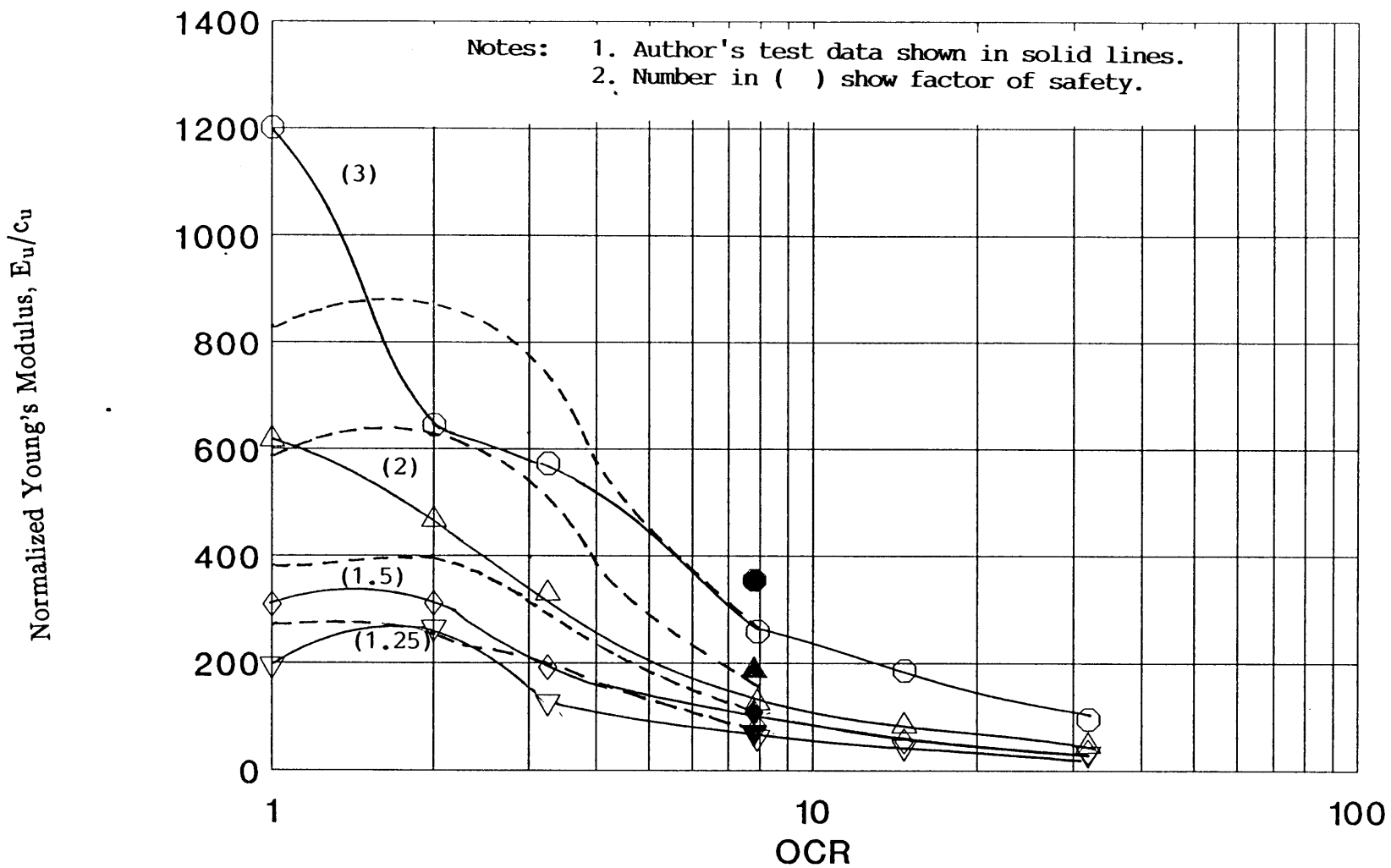


Figure 7.26: Normalized Young's Modulus Versus OCR from CK_0 UDSS Tests on Overconsolidated Boston Blue Clay (Tests by Author and from Ladd and Edgers, 1972).

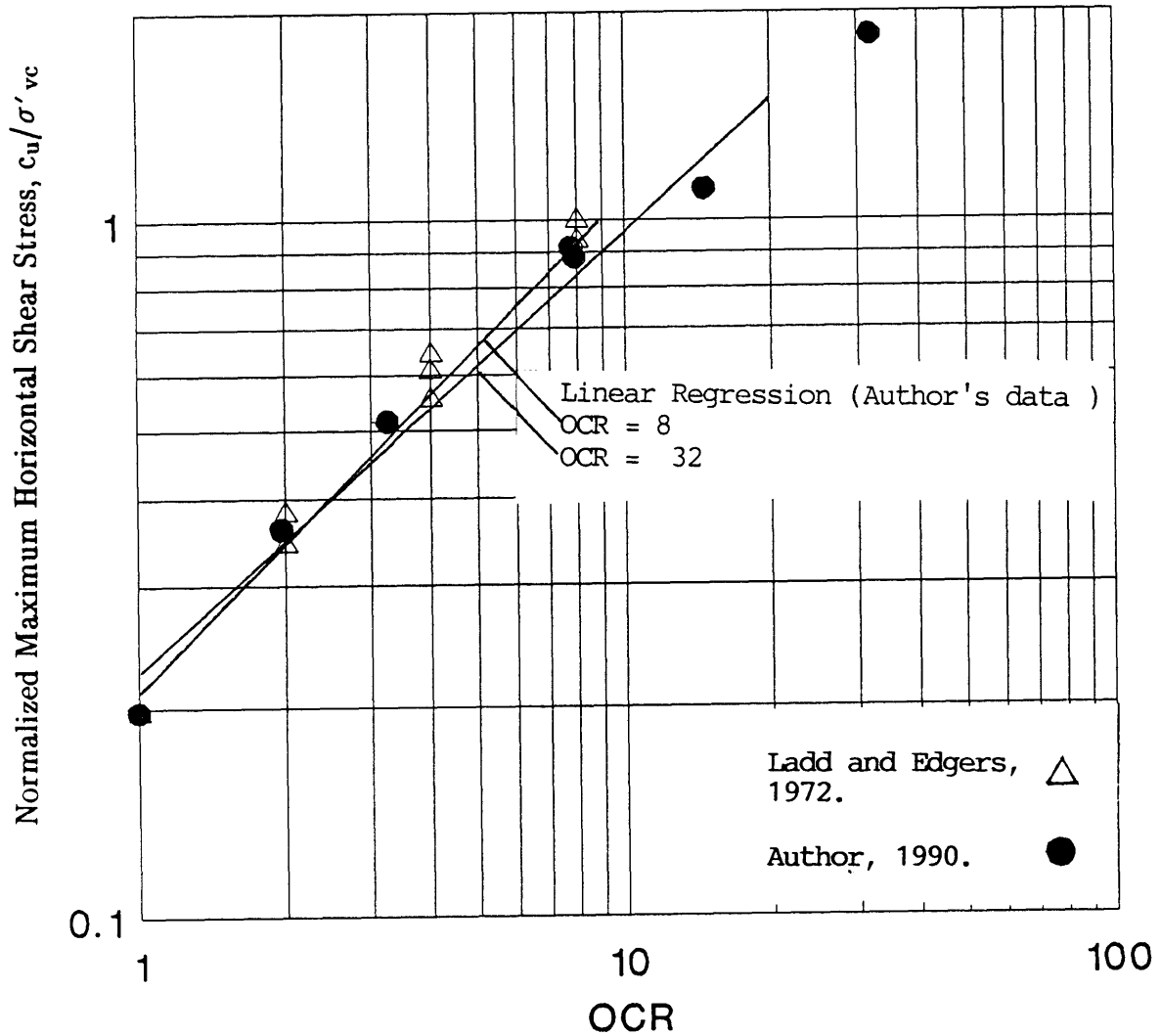


Figure 7.27: Normalized Undrained Shear Strength Ratio Versus OCR from CK_0 UDSS Tests on Boston Blue Clay (Results from Tables 7.1 and 7.2)

CHAPTER 8

SUMMARY , CONCLUSIONS AND RECOMMENDATIONS

8.1 Background

The objective of this thesis is to investigate the normalized undrained strength and stress–strain behavior of resedimented Boston Blue Clay (BBC) using the Geonor Direct Simple Shear (DSS) apparatus. This is accomplished by conducting a number of K_0 –consolidated–undrained tests in the Geonor DSS on specimens of normally consolidated BBC at different consolidation stress levels (Table 4.8) and also on specimens rebounded to different overconsolidation ratios (Table 4.9). In addition, a number of constant rate of strain consolidation (CRSC) tests were performed (Table 4.7) to obtain well defined compression curves for comparison with the data from the consolidation phase of the CK_0 UDSS tests.

Chapter 1 describes the research objectives and gives the organization of the thesis. Chapter 2 gives an overview of the Normalized Soil Parameter (NSP) concept along with an outline of the SHANSEP (an acronym for Stress History And Normalized Soil Engineering Properties) design method and the laboratory testing technique (Ladd and Foott, 1974). The NSP concept is based on the empirical observation that the results of laboratory tests on clay samples having the same OCR, but different consolidation stresses and therefore different maximum past (or preconsolidation) pressures (σ'_{vm} or σ'_p), exhibit very similar strength and stress–strain characteristics when normalized with respect to the consolidation stress. The NSP concept provides a powerful tool for evaluating and synthesizing experimental data. The concept has lead to the development of a very valuable design method, called SHANSEP, to estimate in–situ strength and stress–strain properties for stability analyses. The design method has been applied successfully in engineering practice to a variety of cohesive soils. However, the method is strictly applicable only

to mechanically overconsolidated and truly normally consolidated soils exhibiting normalized behavior (Ladd, 1988).

Chapter 2 also contains a review of existing simple shear devices and the state of stresses in DSS testing, with emphasis on the Geonor type DSS apparatus. The tests conducted for this research were performed in MIT's Geonor Model 4 DSS apparatus that has been extensively used for direct simple shear research and testing at MIT since 1965. It was designed for testing undisturbed cohesive soil samples in order to evaluate stress-strain behavior under simple shear strain conditions. It enables soil specimens to be tested wherein the major principal stress axis rotates during shear while the sample is kept under a condition of plane strain. Due to its inability to impose complementary shear stresses to the sides of the specimen, a condition of nonuniform stress and strain occurs within the specimen. However, many theoretical and experimental studies conducted in the DSS device reveal that for plastic soils the degree of uniformity of stress and strain in the device is acceptable up to the peak resistance. The description of DSS testing equipment and experimental procedures are described in Chapter 3.

This experimental study was conducted on resedimented Boston Blue Clay which has been chosen by MIT researchers to study clay behavior for many years. The initial researchers used undisturbed natural soil. The need for a large quantities of uniform soil specimens lead to the development of the resedimentation technique, which has been further refined and simplified over the years. Chapter 4 briefly describes the batching procedures and the properties of the test soil. The specimens for this research came from Batches 204, 205 and 207 of resedimented Boston Blue Clay III. Index properties of BBC III with 16 g/l of NaCl are: $w_1 = 45.20\% \pm 0.44\%$ SD, $I_p = 23.46\% \pm 0.42\%$ SD and clay fraction $< 2 \mu = 52.1\% + 4.1\%$ SD. The batches of Boston Blue Clay were consolidated to a maximum stress of 1.0 ksc and then rebounded to $\sigma'_{vc} = 0.25$ ksc. The resulting water content = 40.59 ± 0.57 SD and the

liquidity index was $= 0.82 \pm 0.02$ SD

8.2 Consolidation Behavior

The K_0 -consolidation response of resedimented BBC III in the Geonor DSS is evaluated in Chapter 5. The data from the consolidation phase of the CK_0 UDSS tests are presented (Table 5.1) and analyzed in the light of available consolidation data on BBC from the Geonor DSS, conventional incremental oedometer and constant rate of strain consolidation tests (Table 5.4). The analysis of the test data reveal that the porous stones used in the Geonor DSS were bent during DSS testing on samples from Batches 204 and 205, which resulted in larger vertical consolidation strains than those measured in the DSS tests on Batch 207 and from the oedometer tests on the same batches of clay (Figure 5.11). However, the consolidation data from Batch 207 compare very well with the data obtained from the oedometer and CRSC tests on BBC III (Figure 5.12). Hence, the conclusions given in the succeeding paragraphs are based on the consolidation results of the DSS tests on Batch 207 and are valid subject to the condition that the possibility of error in the consolidation data due to the bending of porous stones is eliminated.

The Geonor DSS test gives consistent and good estimates of the 1-D consolidation of BBC. The compression curves obtained from the DSS tests are in reasonable agreement with those obtained from the EOP incremental oedometer curves. Both types of tests gave Casagrande estimates of preconsolidation pressure that agree with the maximum stress applied to the clay batches. The consolidation results from the Geonor DSS show very good agreement with CRS consolidation at strain rates that result in the values of u_b/σ_v between 2% to 5% in the normally consolidated range. The compression data show (Tables 5.3 and 5.4) that the virgin compression ratio (CR) for resedimented BBC III decreases with increase in the stress level. The consolidation data (Tables 5.1 to 5.3) demonstrate that the new 200 series BBC

exhibits a lower rate of secondary compression than BBC II and that the ratio of $C\alpha\epsilon/CR$ for BBC III falls somewhat below the range found for most inorganic soft clays.

The results from the four CRSC tests performed on specimens of BBC III (Table 4.7) are presented and analyzed in Appendix C. Three CRSC tests were performed at standard strain rates recommended by Wissa et al. (1971) (i.e., the strain rates which result in values of u_b/σ_v between 2% to 5% in the normally consolidated range) and one CRSC test was run at an approximately 9 times faster strain rate (resulting in $u_b/\sigma'_{vc} > 25\%$ in the vicinity of σ'_p) than the standard tests. The consolidation data from the CRSC tests, performed at the standard strain rates, compare well with the incremental conventional oedometer tests and show a decrease in the compression ratio with increasing consolidation stress levels. The CRSC test performed at a faster strain rate show significant "rate effects" on the consolidation behavior of resedimented BBC (see Table C.1 and Figure C.6). The limited data show that a large increase in the strain rate results in a higher estimated preconsolidation pressure (e.g., 1.30 ksc versus 1.05 ± 0.05 ksc from the standard tests) and higher CR values at the corresponding stress levels.

8.3 Normally Consolidated Undrained Shear Behavior

The results of five CK_oUDSS tests on normally consolidated BBC are presented and analyzed in Chapter 6. The tests were conducted at consolidation stresses ranging from 1.44 to 12 ksc (Table 6.1). The tests yielded very consistent stress-strain-strength data, with the exception of one test (DSS 31 at $\sigma'_{vc} = 1.44$ ksc), which presumably had a problem with the constant height DCDDT during undrained shearing. However, these data do indicate deviation from "perfect normalized behavior", especially regarding stiffness (modulus). A comparison of data from the writer's tests show excellent overall agreement with prior data from

CK₀UDSS tests on BBC (Tables 6.3 and 6.4).

The writer's tests at different consolidation stress levels demonstrate good normalized behavior with respect to the undrained shear strength, ($c_u/\sigma'_{vc} = 0.197 \pm 0.004$ SD, COV = 2%) and much less scatter compared to the prior data on BBC (Figure 6.18). A linear regression on the undrained shear strength ratio versus consolidation stress based on 23 CK₀UDSS tests on BBC in the Geonor DSS (Figure 6.18) shows c_u/σ'_{vc} decreasing from 0.201 to 0.195 for consolidation stresses ranging from 1 to 12 ksc. This variation is considered very small from a practical viewpoint.

The plotted DSS data show very similar normalized stress strain curves (Figure 6.2) and stress paths (Figure 6.1), despite substantial differences in the consolidation stresses. However, the strain at failure (γ_f) increases with increase in the consolidation stress, e.g., γ_f increasing from 4% to 8% for consolidation stress levels ranging from 1.44 to 12 ksc (Figure 6.19).

The normally consolidated specimens develop positive excess pore pressures (Figure 6.4), which increase continuously with undrained shearing, i.e., BBC III exhibits contractive behavior with continued straining. The data suggests that $\Delta u/\sigma'_{vc}$ versus shear strain decreases with increasing consolidation stress (although DSS 31 follows this trend, the pore pressures are considered to be too high due to problem with the height controller).

The author's data show a definite trend of decreasing E_u/c_u versus applied shear stress ratio (τ_h/c_u) with increasing consolidation stress levels (see Figure 6.6). This trend is also supported by the collective, but more scattered, data previously obtained at MIT in terms of $E_u(50)/c_u$ (Figure 6.24). $E_u(50)/\sigma'_{vc}$ follows a similar trend (Figure 6.25).

The values of the shear stress and the vertical effective stress ratios (τ_h/σ'_{vc} and σ'_v/σ'_{vc}) decrease continuously with straining beyond the peak shear resistance and the value of angle ψ ($= \arctan(\tau_h/\sigma'_v)$) reaches approximately 32° at very large

strains (i.e., at $\gamma = 33\%$. in Table 6.1) This value of angle ψ compares fairly well with the angle ϕ' at maximum obliquity from the K_o -consolidated-undrained triaxial compression tests ($\phi'_{mo} = 34^\circ \pm 0.5^\circ$ SD from CK_oUC tests on BBC, Sheahan, 1990).

The experimental study reveals that the data obtained from the Geonor DSS at maximum obliquity are much more scattered than at the peak shear strength (Table 6.1) and all the normally consolidated specimens show significant strain softening, especially at large shear strains. The analysis of data supports DeGroot's (1989) finding that the DSS device "unloads" the specimen more than the actual pore pressure developed during undrained shearing. Thus the influence of the device on the measured strain softening response increases with continued straining beyond the peak shear resistance.

8.4 Overconsolidated Undrained Shear Behavior

The testing program was included tests to investigate the undrained shear behavior of overconsolidated BBC (Table 7.1). The specimens were consolidated well beyond the batch preconsolidation pressure and then sheared undrained at different overconsolidation ratios along the swelling curve. Five CK_oUDSS tests were performed with a maximum past pressure of approximately 12 ksc at OCR's ranging from 2 to 32. One CK_oUDSS test was performed at OCR of 8 with a maximum past pressure of 3 ksc to determine the influence of stress level on the normalized behavior of overconsolidated BBC. The tests yielded quite consistent and satisfactory data (except DSS 37, where the data beyond peak shear resistance were affected due to some problem with the height control system) which compared well with the previous data on BBC (Table 7.3).

The data from the CK_oUDSS tests show that all the overconsolidated specimens develop negative pore pressures during undrained shearing at the beginning of the tests (Figure 7.4). The maximum negative pore pressure increased with increasing OCR and

usually occurred at the peak undrained strength. The pore pressure become less negative during strain softening and even become positive at moderate OCR (i.e., $OCR \leq 3.25$; see Figure 7.4).

The stress–strain data show that the normalized undrained shear strength, c_u/σ'_{vc} , and the shear strain at failure increase with increasing OCR (Figure 7.2). The primary reason for the increase in c_u/σ'_{vc} is an increase in the vertical effective stress ratio (σ'_v/σ'_{vc}) at the peak shear resistance (i.e., decrease in $\Delta u/\sigma'_{vc}$), rather than the increase in the obliquity of the stresses (τ_h/σ'_v).

The effective stress path from the normally consolidated sample forms an envelope for the paths of the overconsolidated samples (Figure 7.1). All the paths from the overconsolidated samples rise up to the normally consolidated stress path, reaching the envelope at the peak shear resistance, and then follow the $OCR = 1$ curve while strain softening and eventually reaching maximum obliquity. The value of angle ψ reaches $30.7^\circ \pm 1.2^\circ$ SD at very large shear strains (i.e., $\gamma = 33\%$).

All the overconsolidated specimens exhibit significant strain softening, which generally decreases with increasing OCR (Figure 7.3). This strain softening is suspected to be partially due to device "unloading". The experimental data from the CK_0UDSS tests on overconsolidated specimens are consistent with DeGroot's (1989) finding about the measured post peak strain softening behavior of normally consolidated specimens in the Geonor DSS. His analysis revealed that the measured strain softening response of a DSS specimen is partially due to the nonuniform state of stress imposed by the device.

The CK_0UDSS tests on overconsolidated specimens yielded very consistent normalized Young's modulus data (E_u/c_u) plotted versus applied shear stress level (τ_h/c_u) that decrease with increasing OCR (Figure 7.6), which implies that the stiffness decreases with increasing OCR. However, when E_u is normalized with respect to σ'_{vc} and plotted against the shear strain (Figure 7.7), the trend reverses.

The values of m , computed based on the empirical relationship suggested by Ladd et al. (1977) and given in Equation 7.1, decrease with increasing OCR (i.e., m varies from 0.82 to 0.62 for OCR's increasing from 3.25 to 32 (see Table 7.4 and Figure 7.9). The typical range of m values suggested by Ladd et al. 1977 (i.e., 0.8 ± 0.1 , based on DSS tests up to OCR of 8) does not hold for highly overconsolidated (i.e., $\text{OCR} > 8$) BBC. The Modified Cam–Clay overpredicts the value of m (calculated based on Equation 7.2) for BBC, especially at higher OCR's (see Table 7.4).

Two CK_0UDSS tests at the same OCR ($\text{OCR} = 8$), but having different maximum past pressures ($\sigma'_{vm} = 3 \text{ ksc}$ versus 12 ksc), yielded very similar stress paths (Figure 7.10). However, the test with the higher σ'_{vm} shows: an increase in the strain at failure and slightly lower peak strength (Figure 7.11); less negative pore pressures prior to failure (Figure 7.12); and a lower E_u/σ'_{vc} versus shear strain (Figure 7.13). These trends are consistent with the stress dependent behavior observed from the CK_0UDSS tests on the normally consolidated specimens of BBC (Chapter 6), i.e., an increase in stress level results in an increase in the strain at failure, slight decrease in the peak shear strength ratio, and a decrease in the normalized Young's modulus.

The writer's tests at $\text{OCR} = 2$ and 8 agree quite well with those reported by Ladd and Edgers (1972) from prior testing on BBC of similar plasticity after accounting for differences in σ'_{vm} values (e.g., Table 7.3 and Figure 7.20 to 7.27).

8.5 Recommendations

The experimental study reveals that the data obtained from the Geonor DSS at maximum obliquity are much more scattered than at the peak shear strength. Although the undrained shear parameters at large shear strains from the Geonor DSS tests may appear reasonable, the influence of sample membrane distortion, rotation of principal shear stresses and especially the suspected influence of the device "unloading"

should be considered when using these parameters in design. An experimental study to quantify the influence of the DSS device on the measured strain softening response of normally consolidated and overconsolidated specimens of BBC will be very useful in understanding the undrained shear response in the Geonor DSS.

The porous stones used in the Geonor DSS were found to be bent during many of the DSS testing, which affected the consolidation data from the tests on specimens of Batches 204 and 205. It is recommended that the cindered bronze porous stones should either be flattened before each test, (based on a quality control standard to check the flatness), or preferably replaced with ceramic porous stones which will break instead of bending if accidentally dropped. This will reduce the possibility of a serious errors in the measured consolidation strains, thus improving the quality of data obtained from the Geonor DSS.

Ideally there should be no vertical strains for a constant volume test. However, the height control algorithm does not account for apparatus compressibility which leads to a small sample deflection during undrained shearing. It is, therefore, recommended that height control should be improved to account for apparatus compressibility during undrained shearing.

The testing program for this research included one CRSC test conducted at an approximately 9 times faster strain rate than the standard CRSC tests. The limited data show significant rate effects on the consolidation behavior of resedimented BBC. Hence, it would be worthwhile to run more CRSC tests at intermediate and fast strain rates for a better understanding of "rate effects" on the consolidation behavior of new 200 series BBC.

CHAPTER 9

REFERENCES

Note:	ASCE	= American Society of Civil Engineers
	ASTM	= American Society for Testing and Materials
	CGJ	= Canadian Geotechnical Journal
	GTJ	= Geotechnical Testing Journal
	ICSMFE	= International Conference on Soil Mechanics and Foundation Engineering
	ISSMFE	= International Society for Soil Mechanics and Foundation Engineering
	JGE	= Journal of Geotechnical Engineering
	JGED	= Journal of the Geotechnical Engineering Division
	JSMFD	= Journal of the Soil Mechanics and Foundations Division
	MIT	= Massachusetts Institute of Technology
	STP	= Special Technical Publication
	USGS	= United States Geological Survey

- Airey, D.W., Budhu, M. and Wood, D.M. (1985), "Some Aspects of the Behavior of Soils in Simple Shear," Developments in Soil Mechanics and Foundation Engineering, P.K. Banerjee and R. Butterfield, Eds., Vol. 2, Elsevier, London
- Airey, D.W. and Wood, D.M. (1987), "An Evaluation of Direct Simple Shear Tests on Clay," Géotechnique, Vol. 37, No. 1, pp. 25–25.
- Ansell, P. and Brown, S.F. (1978), "A Cyclic Simple Shear Apparatus for Dry Granular Material," GTJ, Vol. 1, No. 2, pp. 82–92.
- Bjerrum, L. (1973), "Problems of Soil Mechanics and Construction on Soft Clays: State-of-the-Art-Report," Proceedings 8th ICSMFE, Moscow, Vol. III.4, pp. 109–159
- Bjerrum, L., and Landva, A. (1966), "Direct Simple Shear Tests on Norwegian Quick Clay," Géotechnique, Vol. 16, No. 1, pp. 1–20.
- Budhu, M. (1985), "Lateral Stresses Observed in Two Simple Shear Apparatus," JGE, Vol. 111, No. 6, pp. 698–711.
- D'Appolonia, D.j., Poulos, H.G. and Ladd, C.C. (1971), "Initial Settlement of Structures on Clay," ASCE, JSMFD, Vol. 97 No. SM 10, pp. 1359–1377.
- Casagrande, A. (1936), "The Determination of the Preconsolidation Load and its Practical Significance," Proc. 1st ICSMFE, Cambridge, MA. pp. 60–64.
- DeGroot, D. J. (1989), "Multidirectional Direct Simple Shear Apparatus with Application to Design of Offshore Structures," Doctor of Science Thesis, Department of Civil Engineering, MIT, Cambridge, MA.

- de Josselin de Jong, G. (1971), Discussion: Session 2. Strain Strain Behaviour of Soils, Proc. Roscoe Memorial Symp., Ed. Parry, R.H.G, G.T. Foulis & Co., Henley-on-Thames, pp. 258-261.
- Duncan, J.M. and Dunlop, P. (1969), "Behavior of Soils in Simple Shear," Proc. 7th ICSMFE, Mexico, pp. 101-109.
- Franke, E., Kiekbusch, M. and Schuppener, B. (1979), "A New Direct Simple Shear Device," GTJ, Vol. 2, No. 4, pp. 190-199.
- Germaine, J.T. (1982), "Development of the Directional Shear Cell for Measuring Cross Anisotropic Clay Properties," Doctor of Science Thesis, Department of Civil Engineering, MIT, Cambridge, MA.
- Germaine, J.T. (1985), "Laboratory Measurements of Clay Behavior," in Recent Developments in Measurement and Modeling of Clay Behavior for Foundation Design, MIT Special Summer Course 1.60S, Department of Civil Engineering, MIT, Cambridge, MA.
- Hara, A. and Kiyota (1977), "Dynamic Shear Tests of Soils for Seismic Analysis," Proc. 9th ICSMFE, Tokyo, Vol. 2, pp. 247-250.
- Hill, R. (1950), Plasticity, Oxford University Press, 356p.
- Idriss, I.M., Moriwaki, Y., Wright, S.G., Doyle, E.H. and Ladd, R.S. (1980), "Behavior of Normally Consolidated Clay Under Simulated Earthquake and Ocean Wave Loading Conditions," Proc. Int. Symp. Soils Under Cyclic and Transient Loading, G.N. Pande and O.C. Zienkiewicz, Vol. 1, pp. 437-495, Balkema, Rotterdam
- Jamiolkowski, M., Ladd, C.C., Germaine, J.T., and Lancellotta, R. (1985), "New Developments in Field and Laboratory Testing of Soils," Proc. XI ICSMFE, San Francisco, Vol. I, pp. 57-153.
- Janbu, N. (1969), "The Resistance Concept Applied to Deformation of Soil," Proc. VII ICSMFE, Mexico City, Vol. 1, pp.191-196.
- Janbu, N. and Senneset, K. (1979), " Interpretation Procedures for Obtaining Soil Deformation Parameters," Proc. 7th ECSMFE, Brighton, V.1.
- Jonas, E. (1970), "Suggested Procedure for Determination of In-Situ Maximum Past Pressure," Draft Copy of proposed HRB Applications Bulletin (Unpublished).
- Kenny, T.C. (1964), "Sea-Level Movements and the Geologic Histories of the Post-Glacial Marine Soils at Boston, Nicolet, Ottawa and Oslo," Géotechnique, Vol. 14, No. 3, pp. 203-230.
- Kjellman, W. (1951), "Testing the Shear Strength of Clay in Sweden," Géotechnique, Vol. 2, No. 3, pp. 225-232.
- Koutsoftas, D. and Ladd, C.C. (1985), "Design Strengths for an Offshore Clay," ASCE, JGED, Vol. 111, No. 3, pp. 337-355.

- Ladd, C.C. (1973), Discussion, Proc. 8th ICSMFE, Moscow, Vol. 4, No. 2, pp. 108–115.
- Ladd, C.C. (1981), "Discussion of 'State of the Art: Laboratory Strength Testing of Soils'," Laboratory Shear Strength of Soils, ASTM STP 740, R.N. Yong and F.C. Townsend, Eds., ASTM, pp. 643–652.
- Ladd, C.C. (1985), "Stability Evaluation During Staged Construction," in Recent Developments in Measurement and Modeling of Clay Behavior for Foundation Design, MIT Special Summer Course 1.60S, Department of Civil Engineering, MIT, Cambridge, MA.
- Ladd, C.C. (1988), "Stability Evaluation During Staged Construction," 22nd Terzaghi Lecture, ASCE, draft version.
- Ladd, C. C. (1990), Personal Communication.
- Ladd, C.C. and Edgers, L. (1972), "Consolidated–Undrained Direct Simple Shear Tests on Saturated Clays," MIT Research Report R72–82, No. 284, Department of Civil Engineering, MIT, Cambridge, MA., 354p.
- Ladd, C.C. and Foott, R. (1974), "New Design Procedure for Stability of Soft Clays," ASCE, JGED, Vol. 100, No. GT7, pp. 763–786.
- Ladd, C.C. and Foott, R. (1980), "The Behavior of Embankments on Clay Foundations", Discussion, CGJ, No. 3.
- Ladd, C.C., Foott, R., Ishihara, K., Schlosser, F., and Poulos, H.G. (1977), "Stress–Deformation and Strength Characteristics, State-of-the-Art Report," Proc. 9th ICSMFE, Tokyo, Vol. 2, pp. 421–494.
- Ladd and Luscher, U. (1965), "Engineering Properties of the Soils Underlying the MIT Campus," Department of Civil Engineering, Research Report # R65–68, Soils Publication No. 181, MIT, Cambridge, MA.
- Leroueil, S., Kabbaj, M., Tavenas, F. and Bouchard, R. (1985), "Stress–Strain–Strain Rate Relation for the Compressibility of Sensitive Natural Clays," Geotechnique, 35, No.2, pp. 159–180.
- Leroueil, S., Tavenas, F., Samson, L. and Morin, P. (1983), "Preconsolidation Pressure of Champlain Clays," Part II, Laboratory Determination, CGJ, No. 4.
- Lucks, A.S., Christian, J.T., Brandow, G.E. and Høeg, K. (1972), "Stress Conditions in NGI Simple Shear Test," JSMFD, ASCE, Vol. 98, No. SM1, pp. 155–160.
- Malek, A.M. (1987), "Cyclic Behavior of Clay in Undrained Simple Shearing and Application to Offshore Tension Piles," Doctor of Science Thesis, Department of Civil Engineering, MIT, Cambridge, MA.
- Mesri, G. and Castro, A. (1987), " $C\alpha/C_c$ Concept and K_o During Secondary Compression," JGE, ASCE, pp. 230–247.

- Mesri, G. and Choi, Y.K. (1985), "The Uniqueness of End-of-Primary (EOP) Void Ratio Effective Stress Relationships," Proc. 11th ICSMFE, San Francisco 2, pp. 587-590.
- Mitchell, J. K. (1976), Fundamentals of Soil Behavior, John Wiley and Sons, New York, 422p.
- Ochiai, H. (1975), "The Behavior of Sands in Direct Shear Tests," Journal of JSSMFE, Vol. 15, No. 4, pp. 93-100.
- Ochiai, H. (1976a), "The Coefficient of Earth Pressure at Rest of Sands," Journal of JSSMFE, Vol. 16, No. 2, pp. 105-111.
- Ochiai, H. (1976b), "Discussion, On the Relation $\tau/\sigma_n = \kappa \tan\psi$ in the Simple Shear Test," Soils and Foundations, Vol. 16, No. 3, pp. 81-85.
- Ochiai, H. (1981), "A Method for Calculating the Undrained Strength Ratio, c_u/p , of Normally Consolidated Clay Measured in the Simple Shear Apparatus," Soils and Foundations, Vol. 21, No. 1, pp. 109-115.
- Oda, M. and Konishi, J. (1974), "Rotation of Principal Stresses in Granular Material During Simple Shear," Soils and Foundations, Vol. 14, No. 4, pp. 39-53.
- O'Neill, D.A. (1985), "Undrained Strength Anisotropy of an Overconsolidated Thixotropic Clay, S.M. Thesis, Dept. of Civil Eng., MIT, Cambridge, MA, 360p.
- Peacock, W.H. and Seed, H.B. (1968), "Sand Liquefaction Under Cyclic Loading Simple Shear Conditions," JSMFD, ASCE, Vol. 94, No. SM3, pp. 689-708.
- Randolph, M.F. and Wroth, C.P. (1981), "Application of the Failure State in Undrained Simple Shear to the Shaft Capacity of Driven Piles," Géotechnique, Vol. 31, No. 1, pp. 143-157.
- Roscoe, K.H. (1953), "An Apparatus for the Application of Simple Shear to Soil Samples," Proc. 3rd ICSMFE, London, Vol. 1, pp. 186-191.
- Roscoe, K.H., Bassett, R.H. and Cole, E.R.L. (1967), "Principal Axes Observed During Simple Shear of a Sand," Proc. Geotechnical Conf., Oslo, Vol. 1, pp. 231-237.
- Saada, A.S. and Townsend, F.C. (1981), "State of the Art: Laboratory Strength Testing of Soils," Laboratory Shear Strength of Soil, ASTM STP 740, R.N. Yong and F.C. Townsend, Eds., pp. 7-77.
- Schmertman, J.H. (1955), "The Undisturbed Consolidation Behavior of Clay," ASCE, Transactions Paper No. 2775, Vol. 120, pp. 1201-1233.
- Seah, T.H. (1990), "Anisotropy of Resedimented Boston Blue Clay," Doctor of Science Thesis, Department of Civil Engineering, MIT, Cambridge, MA.
- Sheahan, T. C. (1990), Personal Communication.

- Shen, C.K., Saligh, K. and Herrmann, L.R. (1978), "An Analysis of NGI Simple Shear Apparatus for Cyclic Soil Testing.," in Dynamic Geotechnical Testing, ASTM STP 654, ASTM, pp. 148–162.
- Sidney, R., Strom, J.A. and Pyke, R.M. (1978), "Discussion on Measurement of Dynamic Soil Properties," Proc. Specialty Conf. Earthquake and Soil Dynamics, Pasadena, Vol. 3, pp. 1478–1481.
- Silver, M.L., Tatsuoka, F., Phukunhaphan, A. and Avramidis, A.S. (1980), "Cyclic Undrained Strength of Sand by Triaxial Test and Simple Shear," Proc. 7th World Conference Earthquake Engineering, Istanbul, Vol. 3. pp. 281–288.
- Smith, R.E. and Wahls, H.E. (1969), "Consolidation Under Constant Rates of Strain," ASCE, JSMFD, Vol. 95, No. SM2, pp. 519–539.
- Tatsuoka, F. and Silver, M. (1981), "Undrained Stress–Strain Behavior of Sand Under Irregular Loading," Soils and Foundations, Vol. 21, No. 1, pp. 51–56.
- Tavenas, F., Leblond, P., Jean, P. and Leroueil, (1983), " The Permeability of Natural Soft Clays," Part I, Methods of Laboratory Measurement, CGJ, No. 4.
- Tavenas, F. and Leroueil, S. (1977), " Effect of Stresses and Time on Yielding of Clays", Proc. 9th ICSMF, Tokyo.
- Tavenas, F. and Leroueil, S. (1980), "The Behavior of Embankments on Clay Foundation", CGJ, No. 2.
- Taylor, D.W. (1948), Fundamentals of Soil Mechanics, Wiley, New York, p.700.
- Vucetic, M. (1984), "Discussion of 'An Evaluation of Laboratory Testing Techniques in Soil Mechanics'," Soils and Foundations, Vol. 24, No. 2 pp. 112–117.
- Vucetic, M. and Lacasse, S. (1982), "Specimen Size Effect in Simple Shear Test," JGED, Vol. 108, No. GT12, pp. 1567–1585.
- Vucetic, M. and Lacasse, S. (1984), "Specimen Size Effect in Simple Shear Test: Closure," JGE, Vol. 110, No. GT3, pp. 439–453.
- Walbaum, M. (1988), "Procedure for Investigation of Sample Disturbance Using the Direct Simple Shear Apparatus," Master's Thesis, Department of Civil Engineering, MIT, Cambridge, MA.
- Werner, R. J. (1990), Personal Communication.
- Wissa, A. E. Z. and Heiberg, S. (1969), "A New One Dimensional Consolidation Test," Research Report # 69–9, Soils Publication No. 10, Department of Civil Engineering, MIT, Cambridge, MA. pp. 1–161.
- Wissa, A. E. Z., Christian, J.T., Davis, E. H. and Heiberg, S. (1971), "Consolidation at Constant Rate of Strain," ASCE, JSMFD, ASCE, Vol. 79, No. SM10, PP. 1393–1413.

- Wood, D.M., Drescher, A. and Budhu, M. (1979), "On the Determination of the Stress State in the Simple Shear Apparatus," GTJ, ASTM, Vol. 2, No. 4, pp. 211-222.
- Wroth, C.P. (1984), "The Interpretation of In Situ Soil Tests," Géotechnique, Vol. 34, No. 4, pp. 449-489.
- Wroth, C.P. (1987), "The Behavior of Normally Consolidated Clay as Observed in Undrained Direct Simple Shear Tests," Géotechnique, Vol. 37, No.1, pp. 37-43.

APPENDIX A**K₀- CONSOLIDATION RESULTS FROM GEONOR DSS**

This Appendix Contains:

Table A.1: Tabulated Stress–Strain Data

Figures A.1 to A.11: Plots of ϵ_v Versus $\text{Log}(\sigma'_{vc})$

Figure A.12: Typical Settlement–Time Curve

Table A.1: Summary of Consolidation Results from CK_0 UDSS Tests on BBC III

Sheet 1/4

Incr. Number	DSS 14			DSS 18			DSS 22		
	σ'_{vc} , ksc	ϵ_{100} , (%)	ϵ_f , (%)	σ'_{vc} , ksc	ϵ_{100} , (%)	ϵ_f , (%)	σ'_{vc} , ksc	ϵ_{100} , (%)	ϵ_f , (%)
1	0.195	0.468		0.138	0.386		0.117	0.187	
2	0.292	0.956		0.242	0.798		0.235	0.594	
3	0.499	1.630		0.487	1.695		0.480	1.326	
4	0.980	3.005		0.990	3.552		0.976	2.820	
5	1.9800	7.840		1.961	7.760		1.960	7.560	
6	4.018	12.778		3.967	12.530		4.000	12.530	
7	7.057	16.460		6.970	16.300		5.992	15.720	16.123
8	11.992	20.288	20.714	9.030	18.390	18.567	-	-	-

Note: Excellent ϵ_v data.

Table A.1: (Continued)

Sheet2/4

Incr. Number	DSS 25			DSS 31			DSS 37		
	σ'_{vc} , ksc	ϵ_{100} , (%)	ϵ_f , (%)	σ'_{vc} , ksc	ϵ_{100} , (%)	ϵ_f , (%)	σ'_{vc} , ksc	ϵ_{100} , (%)	ϵ_f , (%)
1	0.120	0.373		0.126	0.160		0.149	0.150	
2	0.240	0.730		0.255	0.538		0.266	0.420	
3	0.494	1.360		0.499	1.388		0.486	1.051	
4	0.966	2.930		0.964	3.050		0.954	3.364	
5	1.941	7.720		1.441	6.868	7.412	1.967	9.182	
6	2.955	10.947	11.247	-	-	-	3.800	14.470	
7	-	-	-	-	-	-	6.668	18.610	
8	-	-	-	-	-	-	11.407	22.734	23.636
9	-	-	-	-	-	-	5.759	23.285	
10	-	-	-	-	-	-	3.512	22.880	22.843

Note: Data from DSS 31 and DSS 37 is affected by bent porous stones.

Table A.1: (Continued):

Sheet3/4

Incr. Number	DSS 40			DSS 44			DSS 48		
	σ'_{vc} , ksc	ϵ_{100} , (%)	ϵ_f , (%)	σ'_{vc} , ksc	ϵ_{100} , (%)	ϵ_f , (%)	σ'_{vc} , ksc	ϵ_{100} , (%)	ϵ_f , (%)
1	0.136	0.150		0.136	0.150		0.149	0.180	
2	0.266	0.480		0.253	0.515		0.279	0.629	
3	0.499	0.869		0.499	1.435		0.512	1.491	
4	0.954	3.200		0.967	3.823		0.954	3.440	
5	1.902	9.359		1.902	9.688		1.915	9.259	
6	3.811	15.053		3.798	15.300		¹		
7	6.668	19.130		6.668	19.510		6.668	19.170	
8	11.394	22.850	23.927	11.420	23.499	24.448	11.342	23.306	24.278
9	5.798	23.536	23.463	5.758	24.043		5.785	23.884	
10	-	-		2.850	23.340		2.944	23.206	
11	-	-	-	1.447	22.460	22.347	1.473	22.280	
12	-	-	-	-	-	-	0.772	21.285	21.076

Notes: ϵ_v Data affected by bent porous stones.¹ Consolidation data file deleted accidentally.

Table A.1: (Continued):

Sheet 4/4

Incr. Number	DSS 50			DSS 51		
	σ'_{vc} , ksc	ϵ_{100} , (%)	ϵ_f , (%)	σ'_{vc} , ksc	ϵ_{100} , (%)	ϵ_f , (%)
1	0.121	0.120		0.127	0.223	
2	0.2347	0.471		0.256	0.646	
3	0.488	1.243		0.505	1.531	
4	0.974	3.363		0.979	3.621	
5	1.958	8.850		1.942	9.115	
6	2.956	12.867	13.425	3.924	14.790	
7	1.498	13.092		6.916	19.205	
8	0.747	12.515		11.897	23.411	23.849
9	0.379	11.750	11.603	5.724	23.600	
10	-	-	-	2.981	22.939	
11	-	-	-	1.497	22.037	
12	-	-	-	0.757	21.048	
13	-	-	-	0.373	19.901	19.777

Note: ϵ_v data affected by bent porous stones.

DSS TEST 14

(Batch 207)

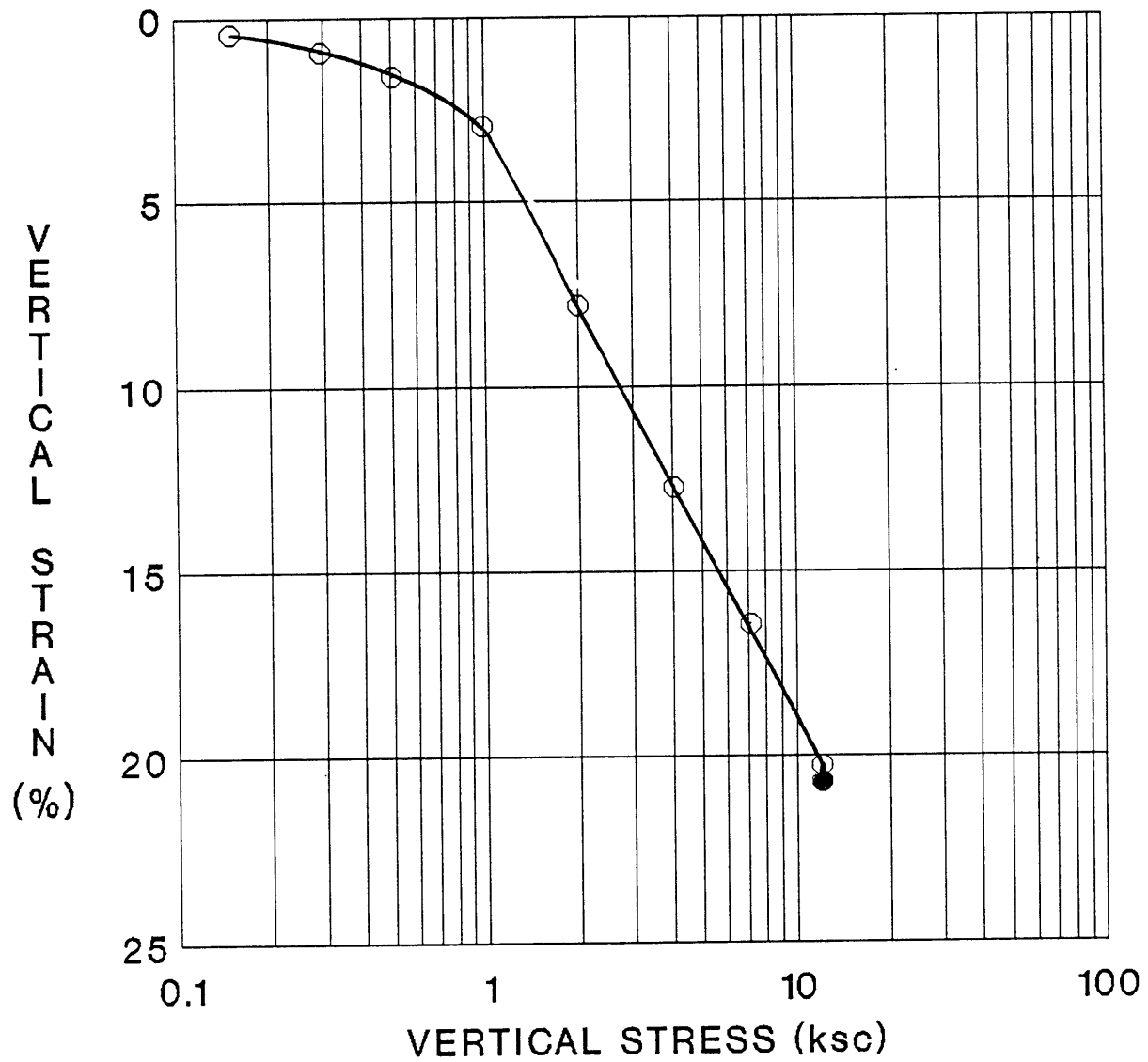


Figure A.1 Compression Curve (ϵ_v versus $\log \sigma'_{vc}$) from DSS Test 14.

DSS TEST 18

(Batch 207)

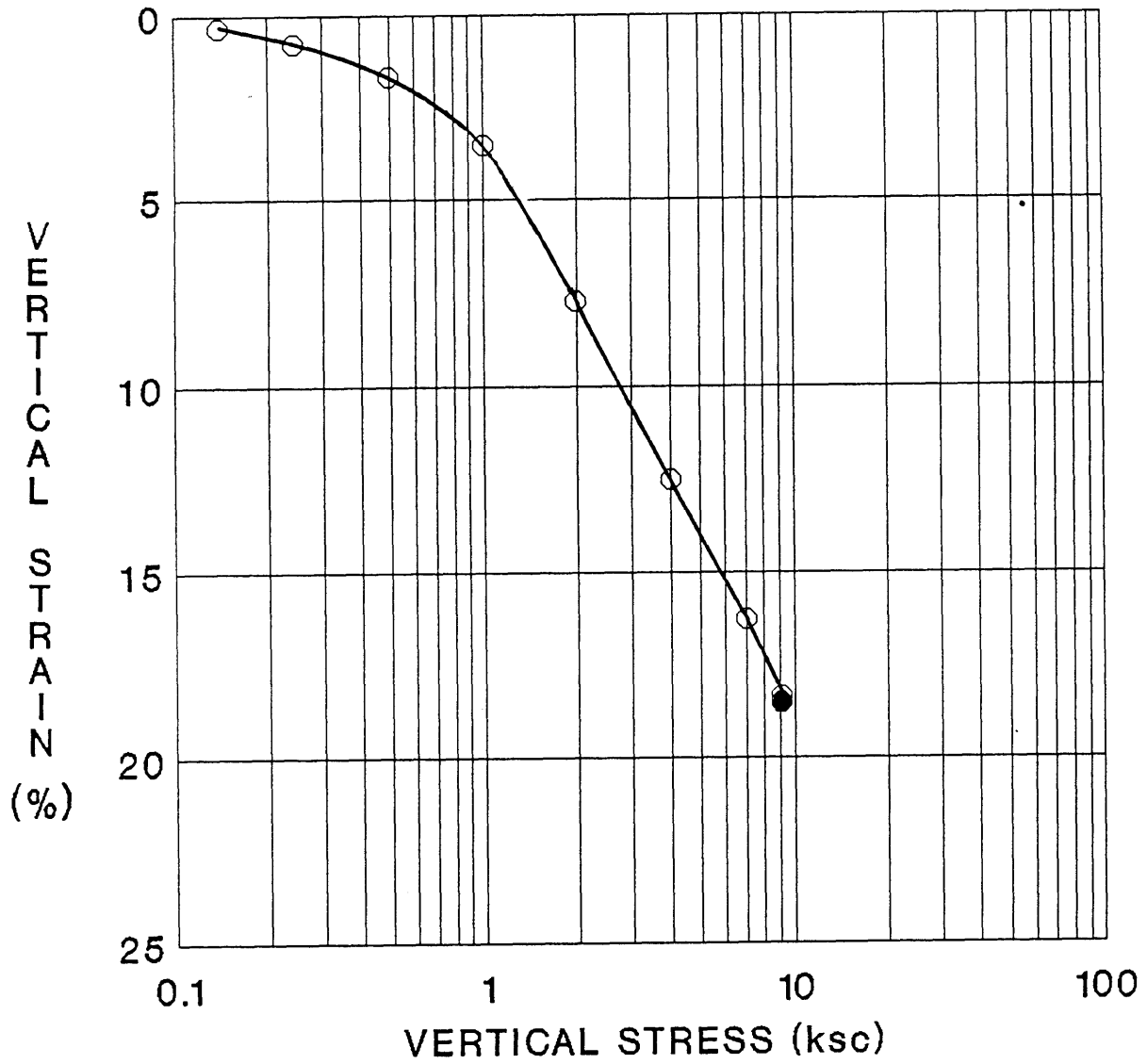


Figure A.2 Compression Curve (ϵ_v versus $\log \sigma'_{vc}$) from DSS Test 18.

DSS TEST 22

(Batch 207)

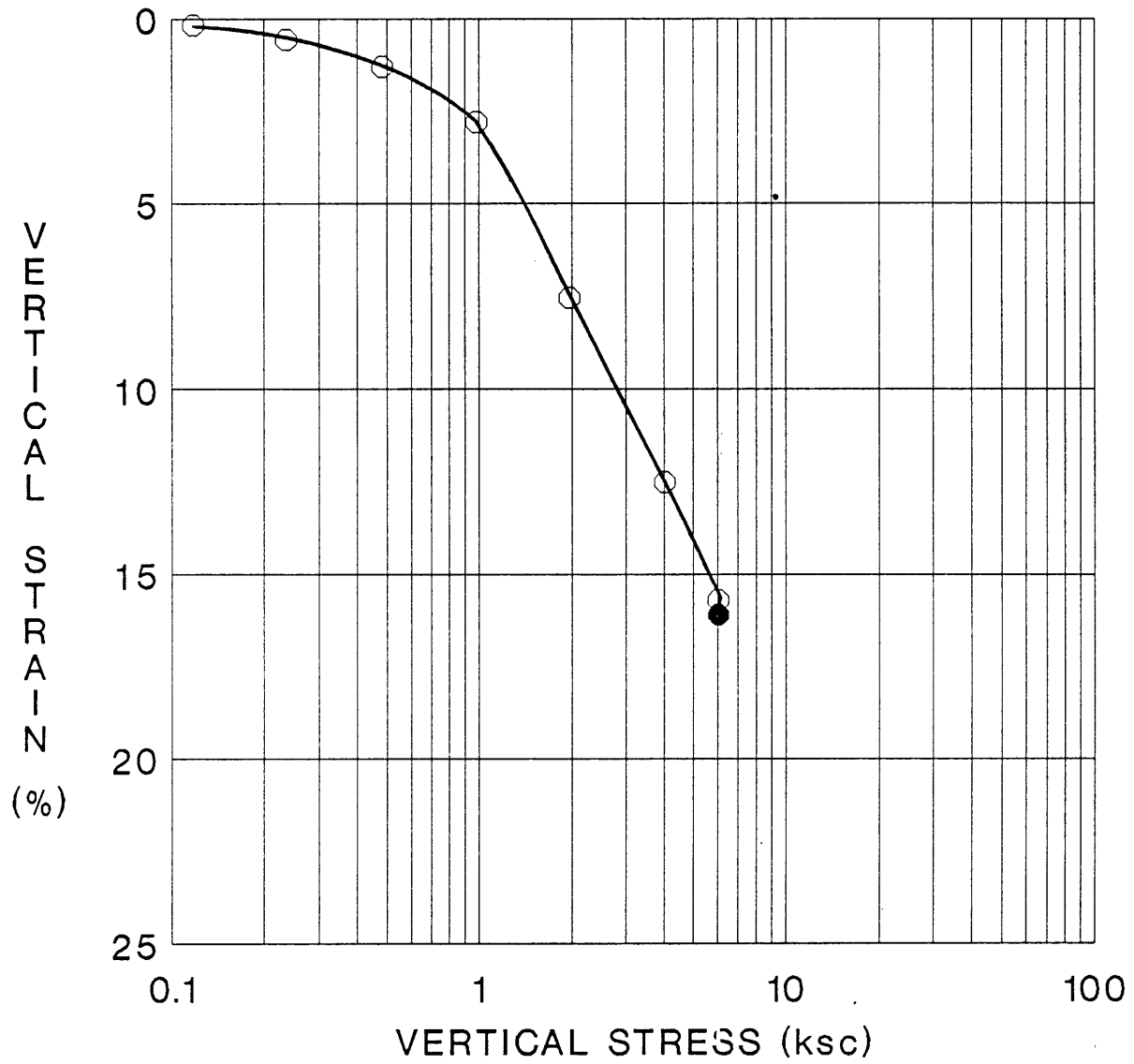


Figure A.3 Compression Curve (ϵ_v versus $\log \sigma'_{vc}$) from DSS Test 22.

DSS TEST 25

(Batch 207)

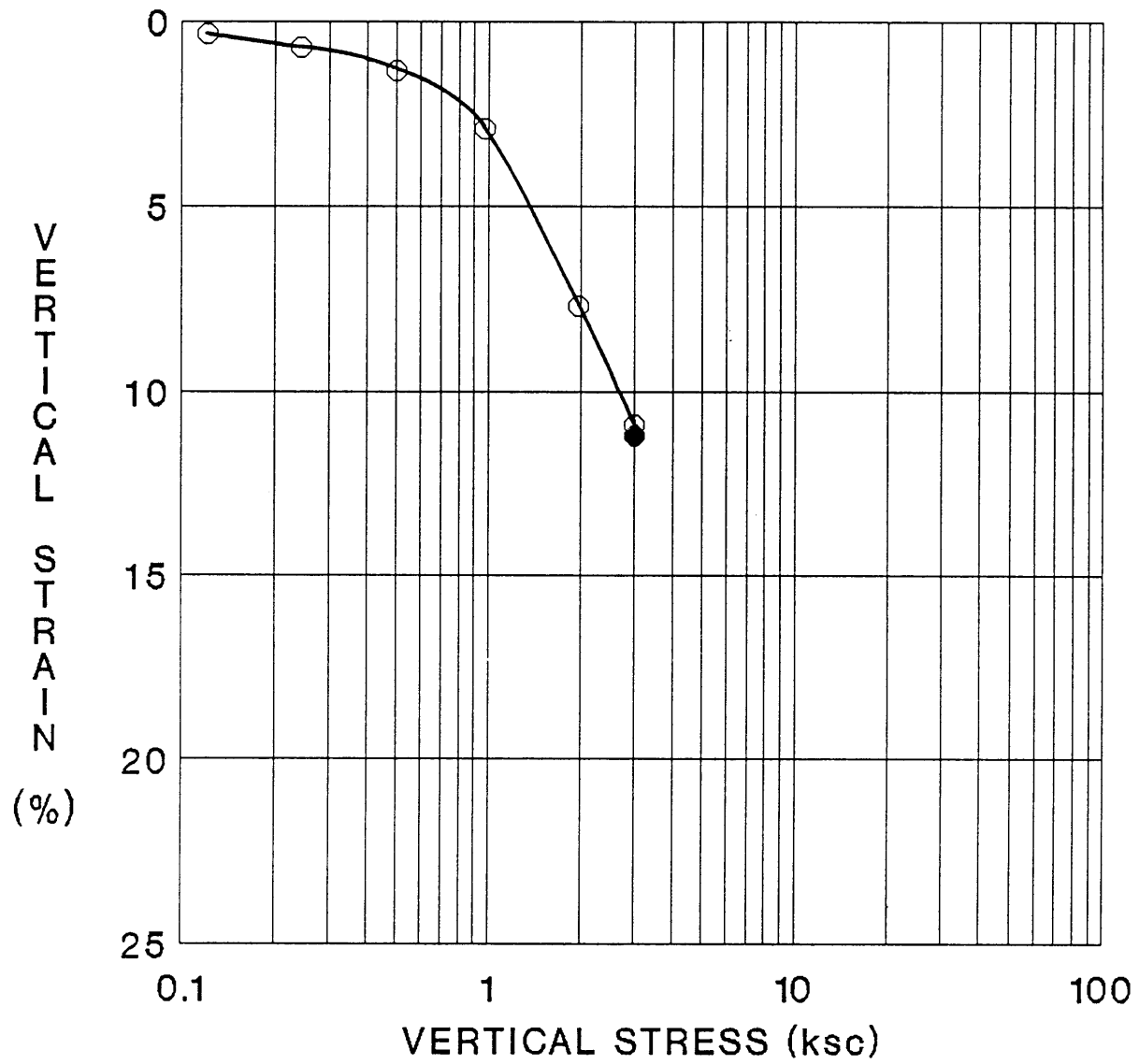


Figure A.4 Compression Curve (ϵ_v versus $\log \sigma'_{vc}$) from DSS Test 25.

DSS TEST 31

(Batch 205)

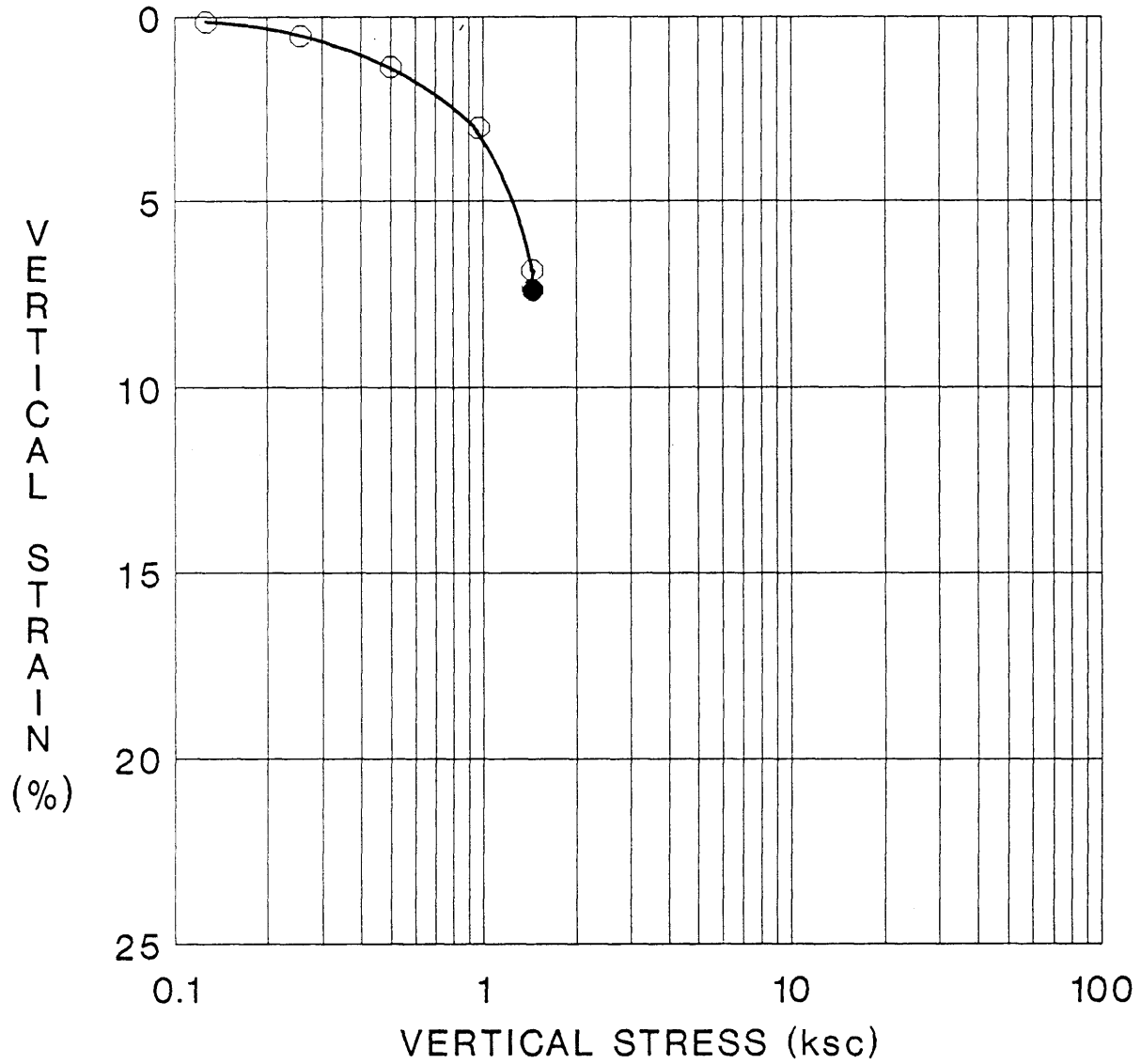


Figure A.5 Compression Curve (ϵ_v versus $\log \sigma'_{vc}$) from DSS Test 31.

DSS TEST 37

(Batch No 205)

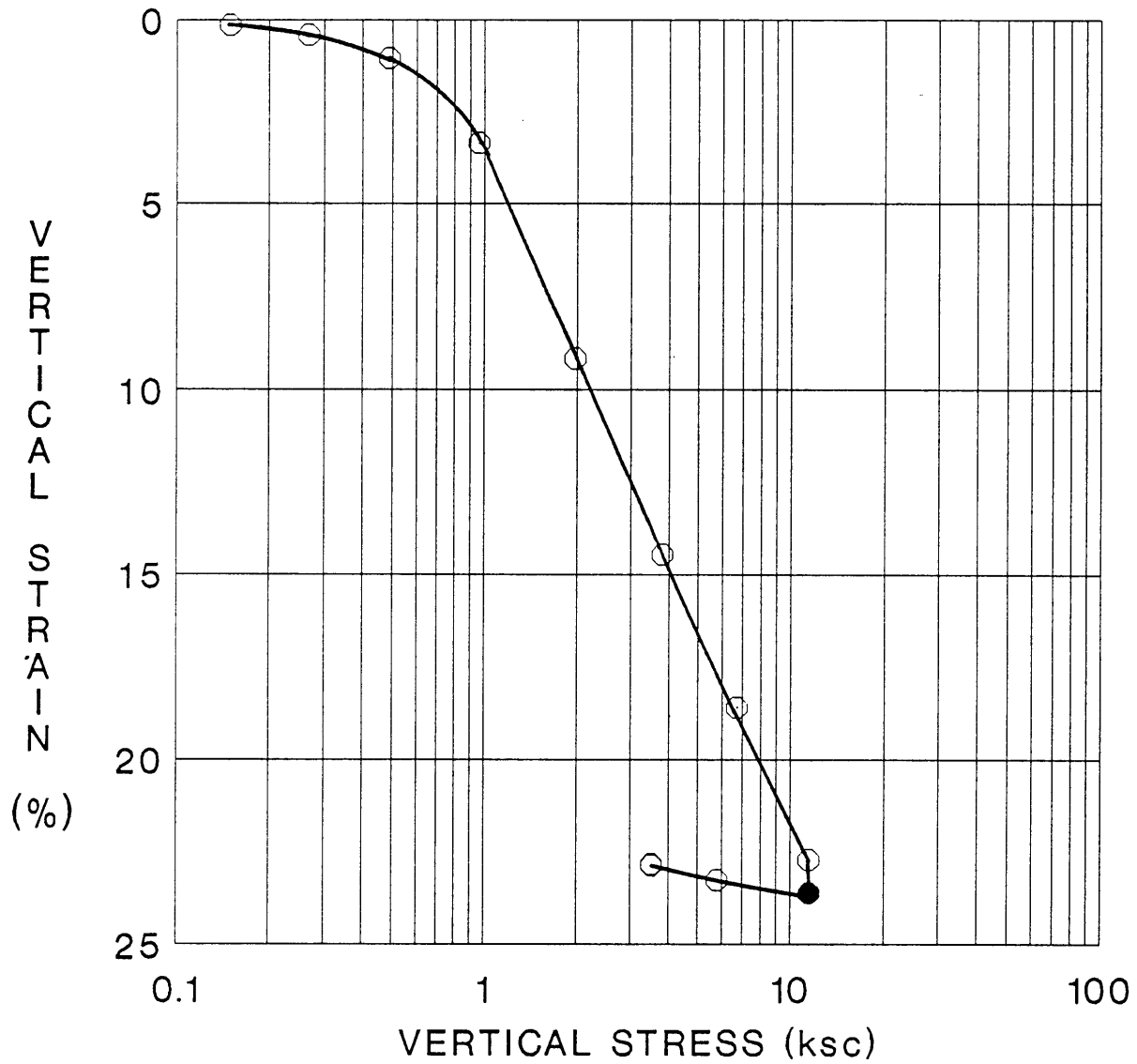


Figure A.6 Compression Curve (ϵ_v versus $\log \sigma'_{vc}$) from DSS Test 37.

DSS TEST 40

(Batch 204)

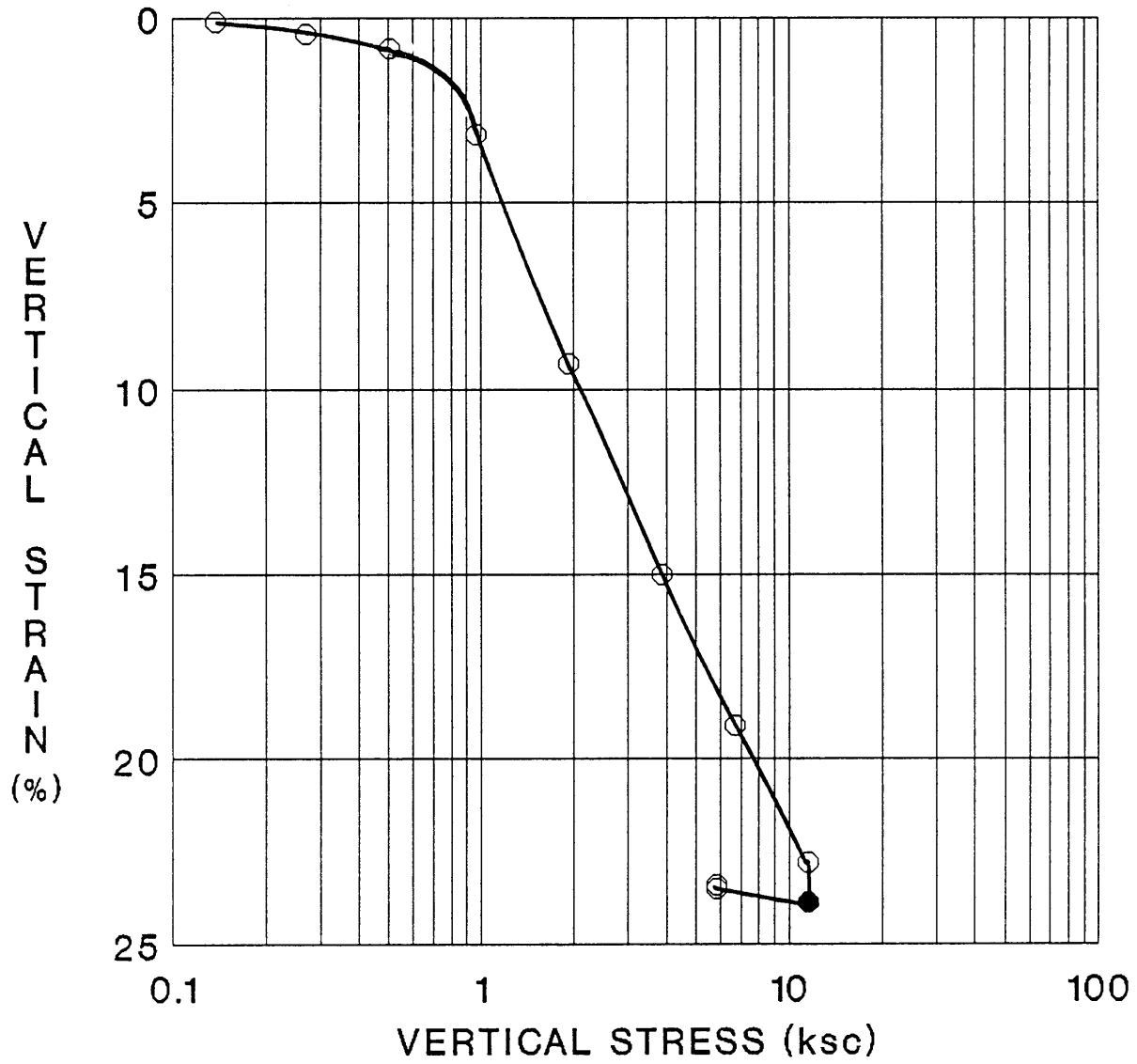


Figure A.7 Compression Curve (ϵ_v versus $\log \sigma'_{vc}$) from DSS Test 40.

DSS TEST 44

(Batch 204)

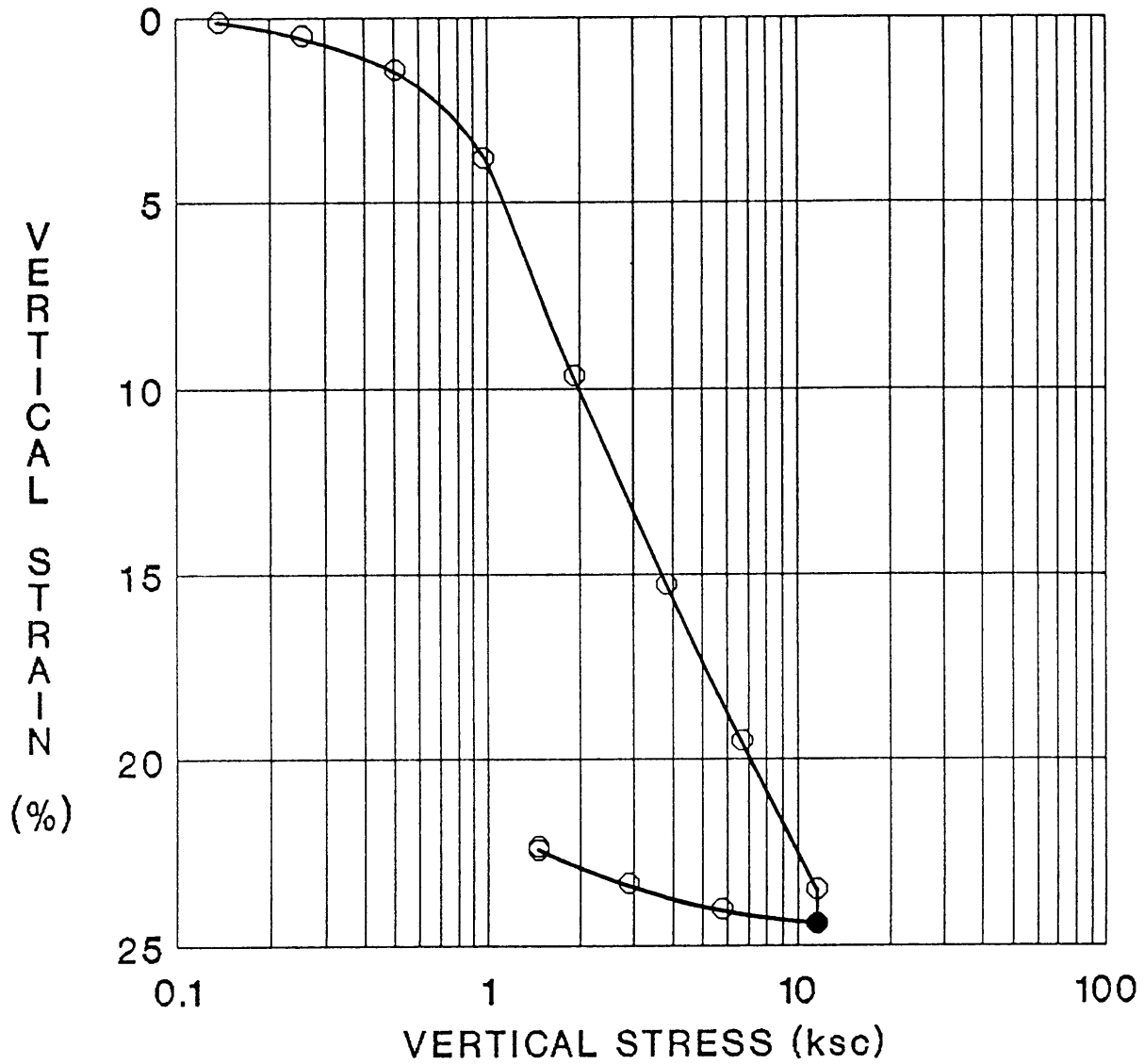


Figure A.8 Compression Curve (ϵ_v versus $\log \sigma'_{vc}$) from DSS Test 44.

DSS TEST 48

(Batch 204)

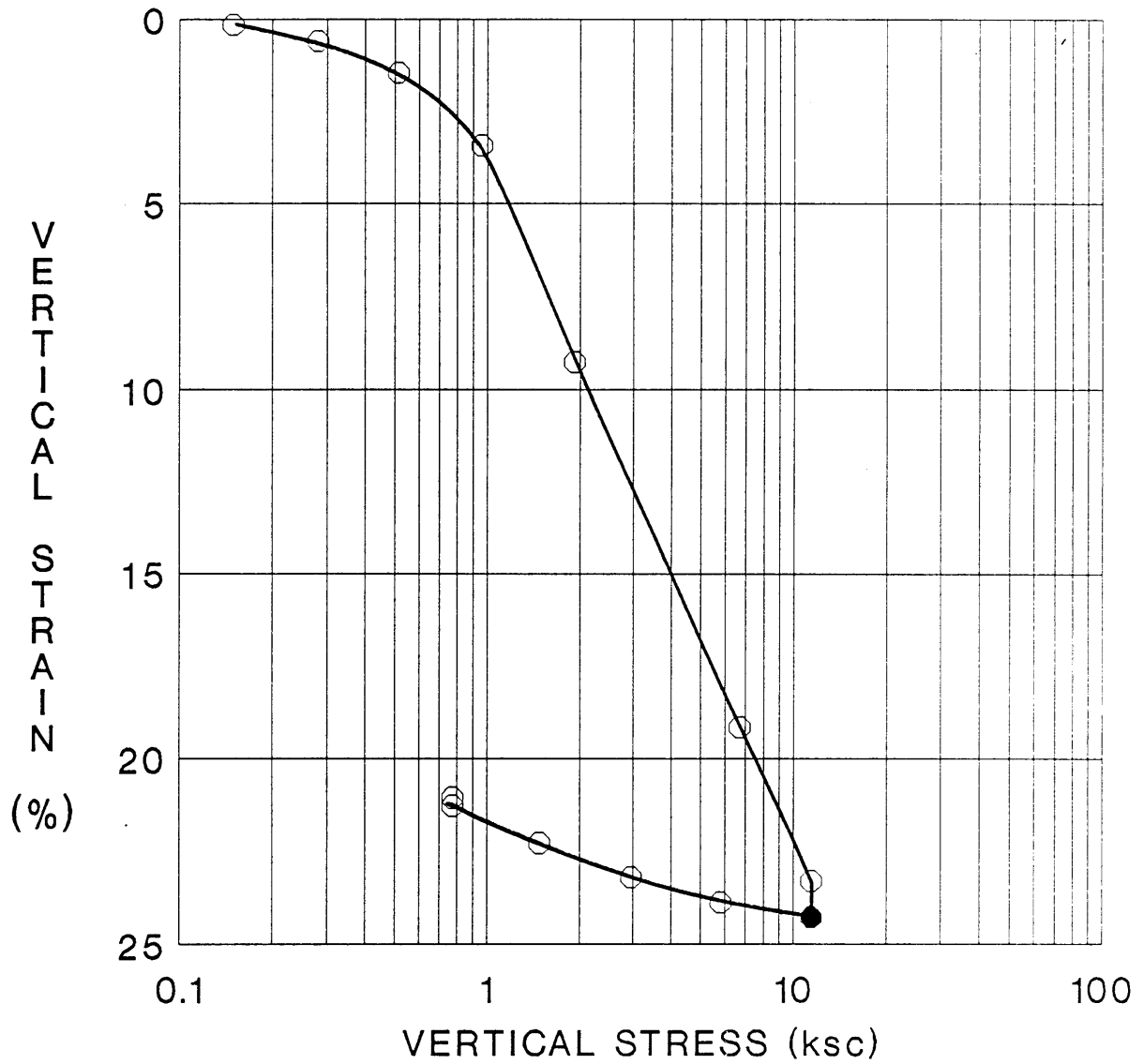


Figure A.9 Compression Curve (ϵ_v versus $\log \sigma'_{vc}$) from DSS Test 48.

DSS TEST 50

(Batch 204)

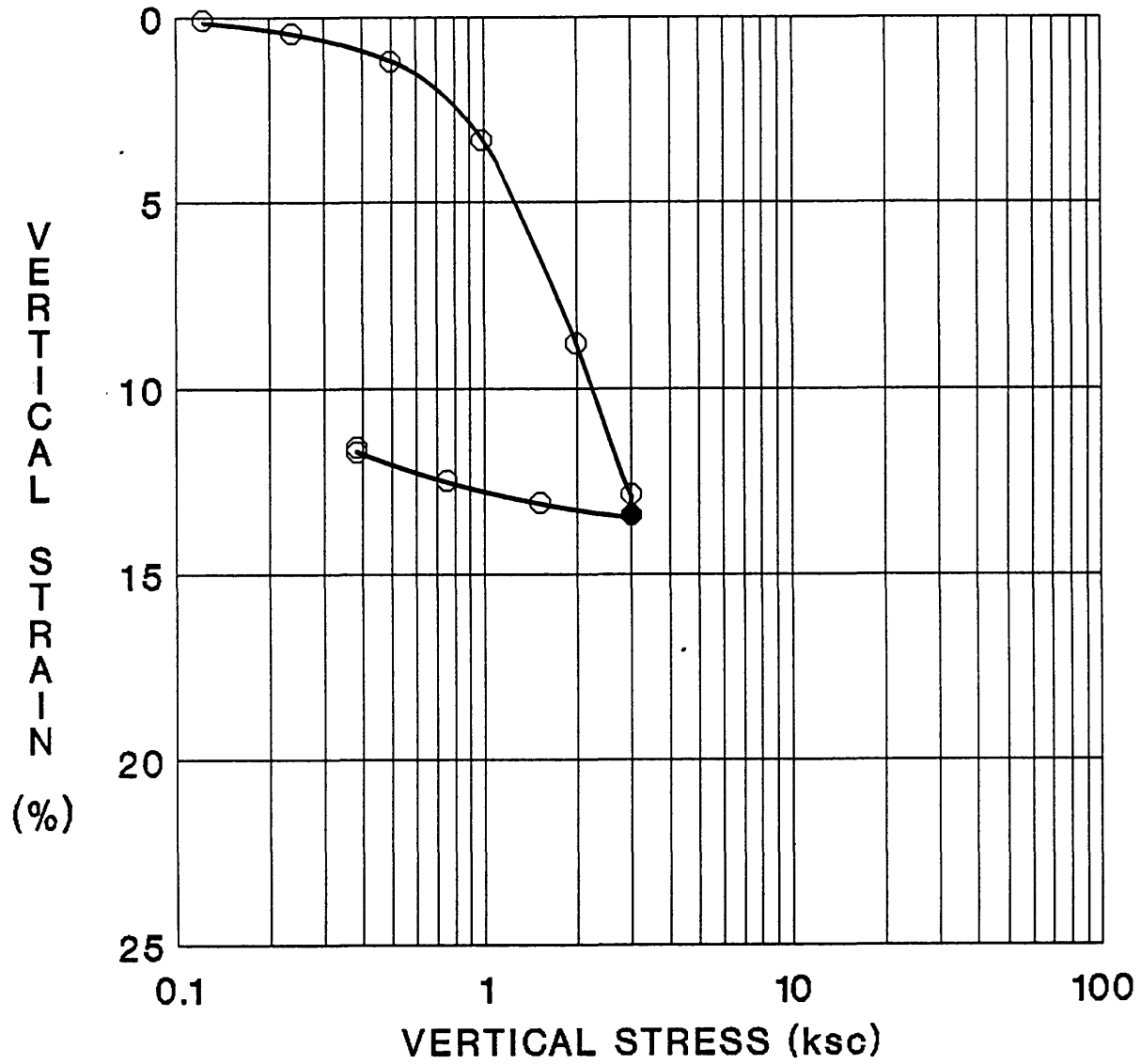


Figure A.10 Compression Curve (ϵ_v versus $\log \sigma'_{vc}$) from DSS Test 50.

DSS TEST 51

(Batch 204)

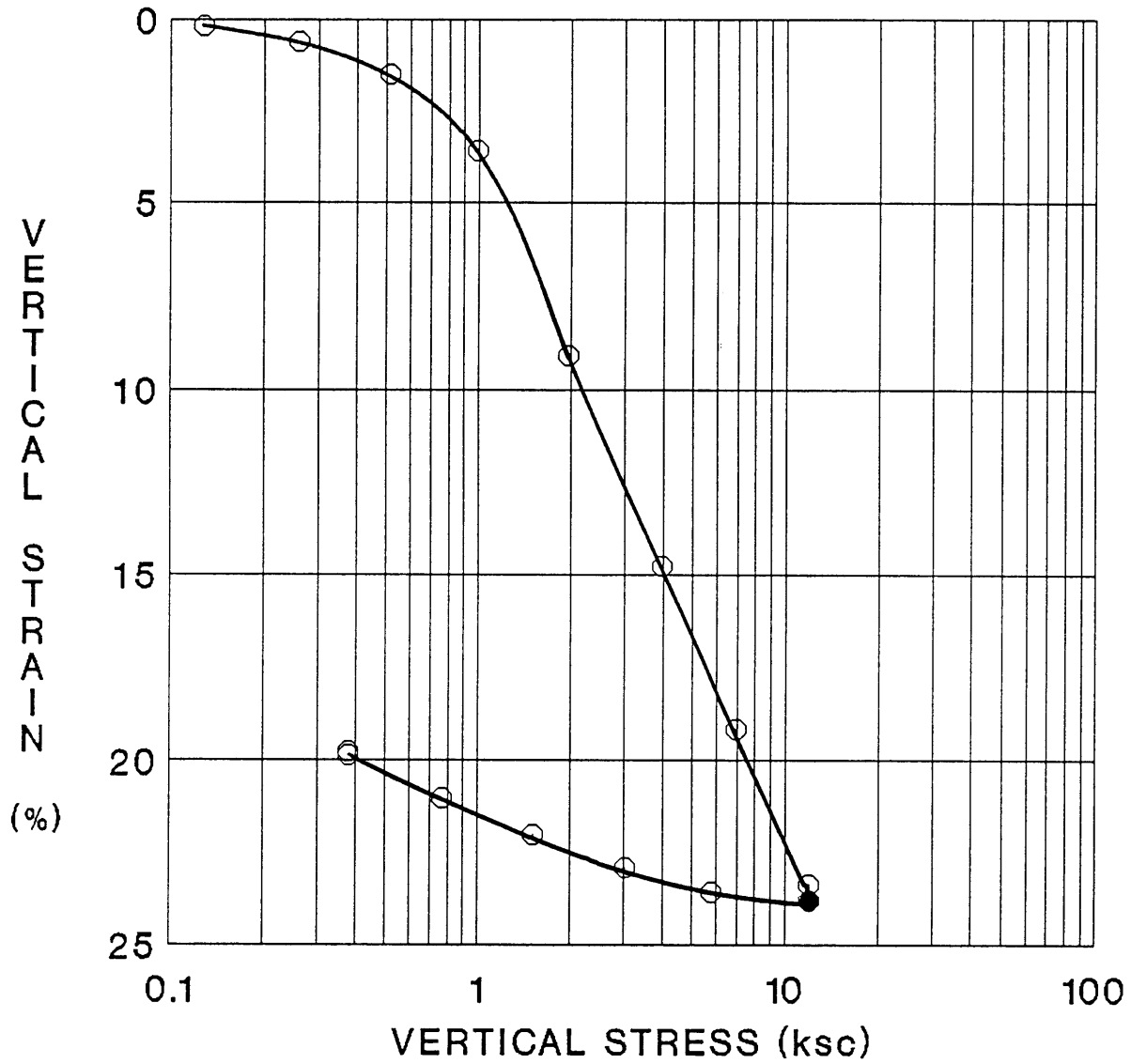


Figure A.11 Compression Curve (ϵ_v versus $\log \sigma'_{vc}$) from DSS Test 51.

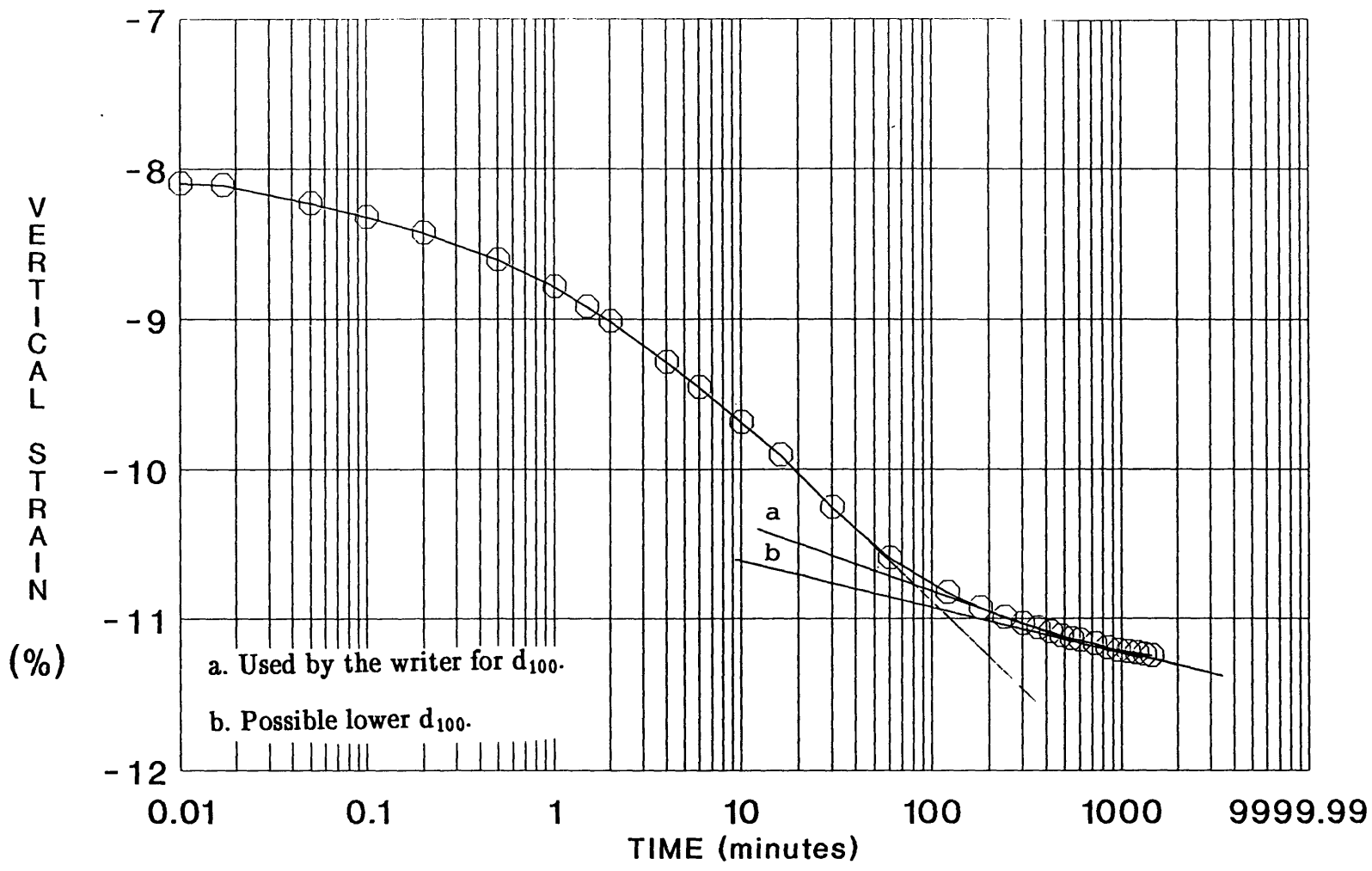


Figure A.12: Typical Settlement–Time Curve of a Consolidation Increment in the DSS.

APPENDIX B

UNDRAINED SHEAR RESULTS FROM GEONOR DSS

K0 CONSOLIDATED GEONOR DIRECT SIMPLE SHEAR TEST

MIT GEOTECHNICAL LAB

FILE NAME : DSS 14

REDUCTION DATA

UNITS: kg,cm,mVolts,Volts

1. Test Name : DSS 14
 2. Date : 2/7/89
 3. OCR : 1
 4. Ver. Consolidation Stress (ksc) :11.9917
 5. Pre-Shear Height (cm) :1.971199
 6. Horizontal Shear Load Cell: 7. Horizontal Displacement Transducer:
 Zero: 0.024804 Zero: 0.137151
 CF: -349.011 CF: 2.2815
 8. Vertical Stress Load Cell: 9. Vertical Height Transducer:
 Zero: 0.107548 Zero: 0.000913
 CF: -1188.86 CF: 2.0655

shr.stn	sh.sts.	ndelU.	nv.sts.	nsh./v.st	sh./su	eu/su	sh/mpp	v.sts/mpp	v.stn
0.000	0.001	0.000	1.001	0.001	0.005	9999.0	0.001	1.001	0.000
0.003	0.020	0.008	0.992	0.020	0.102	9999.0	0.020	0.992	-0.000
0.010	0.023	0.008	0.992	0.023	0.117	3375.1	0.023	0.992	-0.005
0.011	0.026	0.008	0.992	0.026	0.132	3388.6	0.026	0.992	-0.004
0.019	0.029	0.008	0.992	0.029	0.147	2186.7	0.029	0.992	-0.004
0.021	0.032	0.009	0.991	0.032	0.163	2279.6	0.032	0.991	-0.005
0.025	0.035	0.011	0.989	0.035	0.177	2036.1	0.035	0.989	-0.005
0.015	0.037	0.012	0.988	0.038	0.192	3724.1	0.037	0.988	-0.004
0.015	0.040	0.014	0.986	0.041	0.207	4090.6	0.040	0.986	-0.006
0.029	0.043	0.015	0.985	0.044	0.223	2252.4	0.043	0.985	-0.006
0.072	0.049	0.017	0.983	0.050	0.253	1035.5	0.049	0.983	-0.005
0.077	0.055	0.021	0.979	0.056	0.284	1088.9	0.055	0.979	-0.007
0.072	0.061	0.026	0.974	0.063	0.314	1294.6	0.061	0.974	-0.008
0.086	0.067	0.030	0.970	0.069	0.345	1184.5	0.067	0.970	-0.008
0.095	0.073	0.035	0.965	0.076	0.376	1170.9	0.073	0.965	-0.009
0.154	0.079	0.041	0.959	0.082	0.406	779.4	0.079	0.959	-0.009
0.194	0.085	0.046	0.954	0.089	0.436	664.9	0.085	0.954	-0.010
0.202	0.090	0.052	0.948	0.095	0.464	681.3	0.090	0.948	-0.009
0.224	0.095	0.059	0.941	0.101	0.491	649.1	0.095	0.941	-0.010
0.260	0.100	0.066	0.934	0.108	0.517	589.8	0.100	0.934	-0.009
0.299	0.106	0.072	0.928	0.114	0.544	540.4	0.106	0.928	-0.009
0.359	0.111	0.079	0.921	0.120	0.568	471.0	0.111	0.921	-0.009
0.418	0.115	0.087	0.913	0.126	0.593	422.2	0.115	0.913	-0.008
0.481	0.120	0.095	0.905	0.132	0.616	380.6	0.120	0.905	-0.006
0.535	0.124	0.105	0.895	0.139	0.638	354.5	0.124	0.895	-0.006
0.600	0.128	0.113	0.887	0.144	0.659	326.9	0.128	0.887	-0.004
0.698	0.132	0.121	0.879	0.150	0.679	289.9	0.132	0.879	-0.001
0.774	0.136	0.130	0.870	0.156	0.699	269.0	0.136	0.870	0.001
0.851	0.139	0.139	0.861	0.162	0.717	251.0	0.139	0.861	0.003
0.887	0.143	0.147	0.853	0.168	0.736	246.9	0.143	0.853	0.006
0.963	0.146	0.155	0.845	0.173	0.752	232.7	0.146	0.845	0.010

shr.stn	sh.sts.	ndelU.	nv.sts.	nsh./v.st	sh./su	eu/su	sh/mpp	v.sts/mpp	v.stn
1.047	0.149	0.165	0.835	0.179	0.768	218.5	0.149	0.835	0.012
1.115	0.152	0.174	0.826	0.184	0.783	209.3	0.152	0.826	0.015
1.238	0.155	0.183	0.817	0.190	0.798	192.1	0.155	0.817	0.017
1.311	0.158	0.191	0.809	0.195	0.812	184.7	0.158	0.809	0.022
1.387	0.160	0.200	0.800	0.200	0.825	177.2	0.160	0.800	0.025
1.506	0.163	0.209	0.791	0.206	0.837	165.6	0.163	0.791	0.029
1.612	0.165	0.218	0.782	0.211	0.848	156.7	0.165	0.782	0.031
1.725	0.167	0.227	0.773	0.216	0.860	148.6	0.167	0.773	0.036
1.838	0.169	0.236	0.764	0.221	0.870	141.0	0.169	0.764	0.035
1.965	0.171	0.245	0.755	0.226	0.880	133.5	0.171	0.755	0.039
2.095	0.173	0.253	0.747	0.231	0.889	126.5	0.173	0.747	0.041
2.217	0.174	0.260	0.740	0.236	0.897	120.7	0.174	0.740	0.043
2.308	0.176	0.268	0.732	0.240	0.905	116.9	0.176	0.732	0.046
2.445	0.177	0.276	0.724	0.245	0.912	111.2	0.177	0.724	0.051
2.537	0.179	0.283	0.717	0.249	0.919	108.1	0.179	0.717	0.053
2.666	0.180	0.291	0.709	0.254	0.925	103.5	0.180	0.709	0.056
2.789	0.181	0.298	0.702	0.258	0.932	99.7	0.181	0.702	0.058
2.913	0.182	0.305	0.695	0.262	0.937	96.0	0.182	0.695	0.062
3.049	0.184	0.313	0.687	0.267	0.944	92.3	0.184	0.687	0.063
3.191	0.184	0.320	0.680	0.271	0.948	88.7	0.184	0.680	0.065
3.338	0.185	0.328	0.672	0.276	0.953	85.2	0.185	0.672	0.067
3.445	0.186	0.336	0.664	0.281	0.957	82.9	0.186	0.664	0.067
3.577	0.187	0.342	0.658	0.284	0.961	80.1	0.187	0.658	0.069
3.738	0.188	0.349	0.651	0.288	0.965	77.0	0.188	0.651	0.069
3.873	0.188	0.356	0.644	0.292	0.967	74.5	0.188	0.644	0.071
4.014	0.189	0.361	0.639	0.295	0.971	72.2	0.189	0.639	0.072
4.152	0.189	0.367	0.633	0.299	0.972	69.9	0.189	0.633	0.073
4.295	0.190	0.371	0.629	0.302	0.976	67.8	0.190	0.629	0.074
4.436	0.190	0.376	0.624	0.305	0.978	65.8	0.190	0.624	0.076
4.579	0.191	0.381	0.619	0.308	0.981	63.9	0.191	0.619	0.078
4.714	0.191	0.386	0.614	0.311	0.983	62.2	0.191	0.614	0.078
4.856	0.192	0.391	0.609	0.315	0.985	60.5	0.192	0.609	0.082
5.009	0.192	0.395	0.605	0.318	0.988	58.8	0.192	0.605	0.082
5.155	0.192	0.400	0.600	0.321	0.988	57.2	0.192	0.600	0.084
5.298	0.192	0.407	0.593	0.325	0.990	55.7	0.192	0.593	0.084
5.462	0.193	0.411	0.589	0.327	0.991	54.1	0.193	0.589	0.085
5.611	0.193	0.415	0.585	0.330	0.992	52.8	0.193	0.585	0.086
5.756	0.193	0.419	0.581	0.332	0.992	51.4	0.193	0.581	0.086
5.902	0.193	0.423	0.577	0.335	0.994	50.3	0.193	0.577	0.088
6.050	0.194	0.427	0.573	0.338	0.996	49.1	0.194	0.573	0.088
6.196	0.194	0.430	0.570	0.339	0.995	47.9	0.194	0.570	0.091
6.346	0.194	0.435	0.565	0.343	0.997	46.9	0.194	0.565	0.092
6.496	0.194	0.438	0.562	0.345	0.997	45.8	0.194	0.562	0.093
6.645	0.194	0.442	0.558	0.348	0.998	44.8	0.194	0.558	0.094
6.798	0.194	0.446	0.554	0.350	0.998	43.8	0.194	0.554	0.093
6.946	0.194	0.450	0.550	0.353	0.999	42.9	0.194	0.550	0.095
7.103	0.194	0.452	0.548	0.354	0.999	42.0	0.194	0.548	0.096
7.261	0.194	0.454	0.546	0.356	0.999	41.1	0.194	0.546	0.097
7.409	0.194	0.457	0.543	0.358	0.999	40.3	0.194	0.543	0.101
7.562	0.194	0.461	0.539	0.361	0.999	39.4	0.194	0.539	0.101
7.712	0.194	0.464	0.536	0.363	1.000	38.7	0.194	0.536	0.102
7.868	0.194	0.468	0.532	0.365	0.999	37.9	0.194	0.532	0.103

shr.stn	sh.sts.	ndelU.	nv.sts.	nsh./v.st	sh./su	eu/su	sh/mpp	v.sts/mpp	v.stn
8.032	0.194	0.470	0.530	0.367	0.999	37.1	0.194	0.530	0.104
8.167	0.194	0.473	0.527	0.368	0.999	36.5	0.194	0.527	0.105
8.343	0.194	0.476	0.524	0.370	0.998	35.7	0.194	0.524	0.106
8.474	0.194	0.478	0.522	0.372	0.999	35.2	0.194	0.522	0.106
8.630	0.194	0.480	0.520	0.373	0.998	34.5	0.194	0.520	0.110
8.789	0.194	0.484	0.516	0.376	0.998	33.9	0.194	0.516	0.111
8.958	0.194	0.487	0.513	0.378	0.997	33.2	0.194	0.513	0.111
9.112	0.194	0.490	0.510	0.380	0.996	32.6	0.194	0.510	0.112
9.251	0.193	0.496	0.504	0.384	0.995	32.1	0.193	0.504	0.110
9.408	0.193	0.497	0.503	0.384	0.993	31.5	0.193	0.503	0.109
9.579	0.191	0.504	0.496	0.386	0.984	30.7	0.191	0.496	0.107
9.744	0.192	0.505	0.495	0.388	0.988	30.2	0.192	0.495	0.102
9.734	0.192	0.505	0.495	0.388	0.988	30.3	0.192	0.495	0.102
9.987	0.192	0.507	0.493	0.390	0.989	29.6	0.192	0.493	0.103
10.234	0.192	0.511	0.489	0.393	0.988	28.8	0.192	0.489	0.102
10.482	0.192	0.512	0.488	0.393	0.986	28.1	0.192	0.488	0.105
10.725	0.191	0.519	0.481	0.398	0.984	27.4	0.191	0.481	0.105
10.936	0.191	0.521	0.479	0.399	0.982	26.8	0.191	0.479	0.105
11.196	0.191	0.524	0.476	0.401	0.981	26.1	0.191	0.476	0.107
11.437	0.190	0.527	0.473	0.403	0.979	25.5	0.190	0.473	0.108
11.644	0.190	0.528	0.472	0.403	0.978	25.1	0.190	0.472	0.111
11.897	0.190	0.530	0.470	0.404	0.976	24.5	0.190	0.470	0.116
12.104	0.189	0.535	0.465	0.407	0.974	24.0	0.189	0.465	0.119
12.342	0.189	0.540	0.460	0.410	0.970	23.4	0.189	0.460	0.116
12.589	0.188	0.542	0.458	0.411	0.968	22.9	0.188	0.458	0.117
12.838	0.188	0.544	0.456	0.411	0.965	22.4	0.188	0.456	0.119
13.098	0.187	0.549	0.451	0.415	0.962	21.9	0.187	0.451	0.119
13.339	0.186	0.552	0.448	0.416	0.959	21.4	0.186	0.448	0.120
13.580	0.186	0.555	0.445	0.417	0.955	21.0	0.186	0.445	0.120
13.831	0.185	0.561	0.439	0.421	0.951	20.5	0.185	0.439	0.116
14.083	0.184	0.564	0.436	0.423	0.946	20.0	0.184	0.436	0.116
14.328	0.183	0.568	0.432	0.424	0.942	19.6	0.183	0.432	0.114
14.582	0.183	0.569	0.431	0.423	0.939	19.2	0.183	0.431	0.116
14.820	0.182	0.572	0.428	0.425	0.934	18.8	0.182	0.428	0.119
15.068	0.181	0.577	0.423	0.427	0.929	18.4	0.181	0.423	0.121
15.321	0.180	0.581	0.419	0.429	0.923	18.0	0.180	0.419	0.123
15.581	0.178	0.587	0.413	0.432	0.916	17.5	0.178	0.413	0.126
15.835	0.177	0.590	0.410	0.432	0.910	17.1	0.177	0.410	0.131
16.092	0.176	0.597	0.403	0.436	0.903	16.7	0.176	0.403	0.135
16.359	0.174	0.602	0.398	0.438	0.895	16.3	0.174	0.398	0.138
16.606	0.172	0.609	0.391	0.440	0.886	15.9	0.172	0.391	0.141
16.879	0.171	0.612	0.388	0.441	0.879	15.5	0.171	0.388	0.146
17.126	0.170	0.618	0.382	0.444	0.873	15.2	0.170	0.382	0.149
17.386	0.168	0.623	0.377	0.447	0.865	14.8	0.168	0.377	0.151
17.639	0.167	0.630	0.370	0.451	0.858	14.5	0.167	0.370	0.150
17.895	0.166	0.632	0.368	0.451	0.851	14.2	0.166	0.368	0.153
18.148	0.164	0.638	0.362	0.454	0.844	13.9	0.164	0.362	0.150
18.406	0.163	0.641	0.359	0.454	0.838	13.6	0.163	0.359	0.160
18.667	0.162	0.649	0.351	0.460	0.831	13.3	0.162	0.351	0.166
18.932	0.160	0.655	0.345	0.463	0.822	12.9	0.160	0.345	0.163
19.197	0.158	0.658	0.342	0.463	0.814	12.6	0.158	0.342	0.163
19.449	0.157	0.664	0.336	0.467	0.807	12.4	0.157	0.336	0.164

shr.stn	sh.sts.	ndelU.	nv.sts.	nsh./v.st	sh./su	eu/su	sh/mpp	v.sts/mpp	v.stn
19.700	0.156	0.666	0.334	0.466	0.801	12.1	0.156	0.334	0.166
19.945	0.155	0.669	0.331	0.467	0.795	11.9	0.155	0.331	0.169
20.199	0.153	0.675	0.325	0.471	0.788	11.6	0.153	0.325	0.177
20.450	0.152	0.681	0.319	0.476	0.781	11.4	0.152	0.319	0.174
20.708	0.150	0.684	0.316	0.476	0.773	11.1	0.150	0.316	0.176
20.960	0.149	0.688	0.312	0.478	0.767	10.9	0.149	0.312	0.177
21.207	0.148	0.691	0.309	0.478	0.761	10.7	0.148	0.309	0.174
21.454	0.147	0.696	0.304	0.482	0.755	10.5	0.147	0.304	0.174
21.706	0.145	0.699	0.301	0.484	0.748	10.3	0.145	0.301	0.174
21.957	0.144	0.703	0.297	0.485	0.741	10.1	0.144	0.297	0.170
22.204	0.143	0.707	0.293	0.488	0.735	9.9	0.143	0.293	0.176
22.454	0.142	0.711	0.289	0.490	0.728	9.7	0.142	0.289	0.171
22.701	0.141	0.715	0.285	0.494	0.723	9.5	0.141	0.285	0.169
22.948	0.139	0.716	0.284	0.491	0.716	9.3	0.139	0.284	0.169
23.189	0.139	0.718	0.282	0.492	0.712	9.1	0.139	0.282	0.177
23.428	0.138	0.722	0.278	0.496	0.708	9.0	0.138	0.278	0.182
23.677	0.136	0.726	0.274	0.498	0.702	8.8	0.136	0.274	0.180
23.918	0.135	0.728	0.272	0.498	0.696	8.7	0.135	0.272	0.186
24.157	0.135	0.731	0.269	0.499	0.692	8.5	0.135	0.269	0.184
24.389	0.134	0.734	0.266	0.502	0.687	8.4	0.134	0.266	0.189
24.630	0.133	0.736	0.264	0.502	0.682	8.2	0.133	0.264	0.187
24.873	0.132	0.739	0.261	0.504	0.677	8.1	0.132	0.261	0.192
25.118	0.131	0.743	0.257	0.507	0.671	8.0	0.131	0.257	0.192
25.359	0.129	0.744	0.256	0.506	0.666	7.8	0.129	0.256	0.194
25.604	0.128	0.747	0.253	0.507	0.660	7.7	0.128	0.253	0.191
25.843	0.127	0.750	0.250	0.508	0.654	7.5	0.127	0.250	0.191
26.090	0.126	0.753	0.247	0.510	0.648	7.4	0.126	0.247	0.193
26.327	0.125	0.755	0.245	0.510	0.643	7.3	0.125	0.245	0.198
26.572	0.124	0.758	0.242	0.513	0.637	7.1	0.124	0.242	0.197
26.819	0.122	0.762	0.238	0.513	0.629	7.0	0.122	0.238	0.195
27.060	0.121	0.763	0.237	0.512	0.623	6.8	0.121	0.237	0.196
27.301	0.120	0.768	0.232	0.517	0.617	6.7	0.120	0.232	0.196
27.546	0.119	0.769	0.231	0.515	0.611	6.6	0.119	0.231	0.197
27.786	0.118	0.770	0.230	0.513	0.606	6.5	0.118	0.230	0.201
28.013	0.117	0.773	0.227	0.515	0.602	6.4	0.117	0.227	0.204
28.256	0.116	0.778	0.222	0.522	0.595	6.3	0.116	0.222	0.205
28.502	0.114	0.780	0.220	0.520	0.588	6.1	0.114	0.220	0.204
28.738	0.113	0.782	0.218	0.520	0.582	6.0	0.113	0.218	0.206
28.986	0.112	0.786	0.214	0.524	0.575	5.9	0.112	0.214	0.204
29.221	0.111	0.788	0.212	0.524	0.570	5.8	0.111	0.212	0.206
29.457	0.110	0.792	0.208	0.528	0.564	5.7	0.110	0.208	0.208
29.705	0.108	0.795	0.205	0.527	0.556	5.6	0.108	0.205	0.207
29.935	0.107	0.796	0.204	0.526	0.551	5.5	0.107	0.204	0.209
30.178	0.106	0.801	0.199	0.532	0.543	5.3	0.106	0.199	0.207
30.417	0.104	0.803	0.197	0.529	0.537	5.2	0.104	0.197	0.209
30.694	0.103	0.808	0.192	0.535	0.528	5.1	0.103	0.192	0.203
30.905	0.102	0.809	0.191	0.532	0.523	5.0	0.102	0.191	0.204
31.163	0.101	0.810	0.190	0.531	0.518	4.9	0.101	0.190	0.207
31.368	0.100	0.812	0.188	0.531	0.513	4.9	0.100	0.188	0.209
31.630	0.099	0.813	0.187	0.527	0.508	4.8	0.099	0.187	0.212
31.847	0.098	0.816	0.184	0.532	0.503	4.7	0.098	0.184	0.215
32.099	0.097	0.818	0.182	0.531	0.498	4.6	0.097	0.182	0.217

shr.stn	sh.sts.	ndelU.	nv.sts.	nsh./v.st	sh./su	eu/su	sh/mpp	v.sts/mpp	v.stn
32.306	0.096	0.821	0.179	0.536	0.493	4.5	0.096	0.179	0.220
32.572	0.094	0.826	0.174	0.539	0.484	4.4	0.094	0.174	0.218
32.803	0.093	0.826	0.174	0.533	0.478	4.3	0.093	0.174	0.219

Ko CONSOLIDATED GEONOR DIRECT SIMPLE SHEAR TEST
MIT GEOTECHNICAL LAB

FILE NAME : DSS 18

REDUCTION DATA

UNITS: kg,cm,mVolts,Volts

1. Test Name : DSS 18
 2. Date : 3/1/89
 3. OCR : 1
 4. Ver. Consolidation Stress (ksc) :9.03
 5. Pre-Shear Height (cm) :1.979
 6. Horizontal Shear Load Cell: 7. Horizontal Displacement Transducer:
 Zero: 0.3592 Zero: 0.1571
 CF: -179.993 CF: 2.2815
 8. Vertical Stress Load Cell: 9. Vertical Height Transducer:
 Zero: 0.3718 Zero: -0.002
 CF: -636.571 CF: 2.0655

shr.stn	sh.sts.	ndelU.	nv.sts.	nsh./v.st	sh./su	eu/su	sh/mpp	v.sts/mppv.stn	
0.000	-0.001	0.000	1.000	-0.001	-0.006	9999.0	-0.001	1.000	0.000
0.006	0.015	0.000	1.000	0.015	0.078	3978.3	0.015	1.000	0.003
0.014	0.019	0.000	1.000	0.019	0.101	2263.3	0.019	1.000	0.005
0.024	0.024	0.000	1.000	0.024	0.125	1663.9	0.024	1.000	0.005
0.028	0.029	0.000	1.000	0.029	0.149	1673.2	0.029	1.000	0.004
0.040	0.033	0.001	0.999	0.033	0.174	1355.7	0.033	0.999	0.005
0.047	0.038	0.003	0.997	0.038	0.198	1290.0	0.038	0.997	0.005
0.058	0.043	0.006	0.994	0.043	0.223	1181.0	0.043	0.994	0.006
0.066	0.047	0.013	0.987	0.048	0.248	1157.1	0.047	0.987	0.005
0.078	0.052	0.020	0.980	0.053	0.272	1064.1	0.052	0.980	0.006
0.087	0.056	0.027	0.973	0.058	0.295	1031.7	0.056	0.973	0.004
0.097	0.061	0.033	0.967	0.063	0.320	1009.3	0.061	0.967	0.001
0.115	0.066	0.039	0.961	0.069	0.345	916.0	0.066	0.961	0.003
0.129	0.071	0.043	0.957	0.074	0.370	871.8	0.071	0.957	0.003
0.146	0.076	0.047	0.953	0.079	0.394	821.9	0.076	0.953	0.002
0.160	0.080	0.052	0.948	0.085	0.419	796.2	0.080	0.948	0.006
0.193	0.085	0.057	0.943	0.090	0.444	699.9	0.085	0.943	0.003
0.212	0.090	0.063	0.937	0.096	0.467	669.7	0.090	0.937	0.004
0.244	0.094	0.069	0.931	0.101	0.492	611.8	0.094	0.931	0.004
0.256	0.099	0.076	0.924	0.107	0.514	609.3	0.099	0.924	0.007
0.270	0.103	0.082	0.918	0.112	0.536	601.9	0.103	0.918	0.006
0.322	0.107	0.087	0.913	0.117	0.559	525.5	0.107	0.913	0.009
0.356	0.111	0.093	0.907	0.123	0.581	493.9	0.111	0.907	0.010
0.398	0.115	0.099	0.901	0.128	0.602	457.4	0.115	0.901	0.013
0.450	0.119	0.106	0.894	0.133	0.622	418.3	0.119	0.894	0.013
0.500	0.123	0.114	0.886	0.139	0.641	388.0	0.123	0.886	0.015
0.540	0.127	0.122	0.878	0.144	0.661	370.1	0.127	0.878	0.018
0.583	0.130	0.131	0.869	0.150	0.679	352.6	0.130	0.869	0.017
0.612	0.134	0.141	0.859	0.155	0.697	344.3	0.134	0.859	0.022
0.689	0.137	0.151	0.849	0.161	0.714	313.5	0.137	0.849	0.023
0.749	0.140	0.161	0.839	0.167	0.731	295.1	0.140	0.839	0.024

shr.stn	sh.sts.	ndelU.	nv.sts.	nsh./v.st	sh./su	eu/su	sh/mpp	v.sts/mppv.stn	
0.797	0.143	0.168	0.832	0.172	0.748	283.9	0.143	0.832	0.028
0.872	0.146	0.175	0.825	0.177	0.764	264.9	0.146	0.825	0.027
0.928	0.149	0.184	0.816	0.183	0.779	253.5	0.149	0.816	0.030
1.026	0.152	0.191	0.809	0.188	0.794	233.7	0.152	0.809	0.037
1.085	0.155	0.200	0.800	0.193	0.807	224.8	0.155	0.800	0.040
1.168	0.157	0.209	0.791	0.199	0.821	212.3	0.157	0.791	0.042
1.254	0.160	0.217	0.783	0.204	0.833	200.7	0.160	0.783	0.047
1.349	0.162	0.225	0.775	0.209	0.845	189.3	0.162	0.775	0.048
1.443	0.164	0.229	0.771	0.213	0.857	179.5	0.164	0.771	0.050
1.521	0.166	0.236	0.764	0.218	0.868	172.3	0.166	0.764	0.053
1.619	0.168	0.245	0.755	0.223	0.879	163.9	0.168	0.755	0.060
1.725	0.170	0.253	0.747	0.228	0.888	155.4	0.170	0.747	0.070
1.834	0.172	0.265	0.735	0.234	0.897	147.7	0.172	0.735	0.075
1.918	0.174	0.276	0.724	0.240	0.905	142.6	0.174	0.724	0.070
2.039	0.175	0.284	0.716	0.245	0.914	135.3	0.175	0.716	0.075
2.135	0.177	0.294	0.706	0.250	0.922	130.3	0.177	0.706	0.076
2.257	0.178	0.302	0.698	0.255	0.928	124.2	0.178	0.698	0.077
2.376	0.179	0.308	0.692	0.259	0.935	118.8	0.179	0.692	0.081
2.483	0.180	0.317	0.683	0.264	0.941	114.4	0.180	0.683	0.080
2.622	0.182	0.323	0.677	0.269	0.949	109.2	0.182	0.677	0.085
2.722	0.183	0.330	0.670	0.273	0.954	105.7	0.183	0.670	0.087
2.859	0.184	0.339	0.661	0.278	0.959	101.2	0.184	0.661	0.089
2.975	0.185	0.344	0.656	0.281	0.963	97.7	0.185	0.656	0.093
3.124	0.185	0.350	0.650	0.285	0.968	93.5	0.185	0.650	0.096
3.260	0.186	0.354	0.646	0.288	0.972	89.9	0.186	0.646	0.101
3.394	0.187	0.363	0.637	0.293	0.975	86.7	0.187	0.637	0.101
3.538	0.188	0.369	0.631	0.297	0.979	83.5	0.188	0.631	0.104
3.674	0.188	0.376	0.624	0.301	0.982	80.6	0.188	0.624	0.107
3.814	0.189	0.383	0.617	0.306	0.985	77.9	0.189	0.617	0.109
3.957	0.189	0.390	0.610	0.310	0.987	75.2	0.189	0.610	0.111
4.100	0.190	0.393	0.607	0.313	0.990	72.8	0.190	0.607	0.112
4.244	0.190	0.404	0.596	0.319	0.991	70.5	0.190	0.596	0.112
4.395	0.190	0.413	0.587	0.324	0.992	68.1	0.190	0.587	0.106
4.548	0.190	0.420	0.580	0.328	0.993	65.9	0.190	0.580	0.102
4.701	0.190	0.426	0.574	0.331	0.993	63.7	0.190	0.574	0.101
4.851	0.190	0.431	0.569	0.335	0.994	61.8	0.190	0.569	0.100
5.004	0.191	0.435	0.565	0.337	0.994	59.9	0.191	0.565	0.099
5.155	0.191	0.440	0.560	0.341	0.996	58.3	0.191	0.560	0.097
5.306	0.191	0.440	0.560	0.341	0.996	56.7	0.191	0.560	0.100
5.458	0.191	0.448	0.552	0.346	0.998	55.2	0.191	0.552	0.101
5.610	0.191	0.454	0.546	0.350	0.998	53.6	0.191	0.546	0.102
5.781	0.191	0.455	0.545	0.351	0.998	52.1	0.191	0.545	0.102
5.917	0.191	0.461	0.539	0.355	0.998	50.9	0.191	0.539	0.103
6.073	0.191	0.464	0.536	0.357	0.999	49.6	0.191	0.536	0.103
6.230	0.192	0.472	0.528	0.363	0.999	48.4	0.192	0.528	0.103
6.392	0.192	0.473	0.527	0.363	0.999	47.2	0.192	0.527	0.102
6.552	0.192	0.477	0.523	0.366	1.000	46.1	0.192	0.523	0.105
6.712	0.191	0.482	0.518	0.369	0.999	44.9	0.191	0.518	0.106
6.872	0.191	0.486	0.514	0.373	0.999	43.9	0.191	0.514	0.104
7.026	0.191	0.487	0.513	0.373	0.999	42.9	0.191	0.513	0.107
7.181	0.192	0.489	0.511	0.375	1.000	42.0	0.192	0.511	0.107
7.337	0.191	0.495	0.505	0.379	0.999	41.1	0.191	0.505	0.109

shr.stn	sh.sts.	ndelU.	nv.sts.	nsh./v.st	sh./su	eu/su	sh/mpp	v.sts/mpp	v.stn
7.509	0.191	0.496	0.504	0.380	0.999	40.1	0.191	0.504	0.107
7.652	0.191	0.501	0.499	0.384	0.999	39.4	0.191	0.499	0.109
7.812	0.191	0.502	0.498	0.384	0.998	38.6	0.191	0.498	0.111
7.970	0.191	0.506	0.494	0.387	0.998	37.8	0.191	0.494	0.111
8.124	0.191	0.507	0.493	0.388	0.997	37.0	0.191	0.493	0.113
8.279	0.191	0.510	0.490	0.390	0.998	36.4	0.191	0.490	0.113
8.437	0.191	0.516	0.484	0.394	0.997	35.6	0.191	0.484	0.113
8.604	0.191	0.521	0.479	0.398	0.995	34.9	0.191	0.479	0.110
8.765	0.191	0.521	0.479	0.398	0.994	34.2	0.191	0.479	0.110
8.928	0.190	0.521	0.479	0.398	0.994	33.6	0.190	0.479	0.114
9.085	0.190	0.522	0.478	0.399	0.994	33.0	0.190	0.478	0.118
9.246	0.190	0.529	0.471	0.404	0.993	32.4	0.190	0.471	0.118
9.412	0.190	0.532	0.468	0.406	0.991	31.8	0.190	0.468	0.115
9.571	0.190	0.532	0.468	0.405	0.989	31.2	0.190	0.468	0.117
9.732	0.189	0.538	0.462	0.410	0.989	30.7	0.189	0.462	0.115
9.905	0.189	0.543	0.457	0.413	0.986	30.0	0.189	0.457	0.110
10.068	0.189	0.542	0.458	0.412	0.984	29.5	0.189	0.458	0.109
10.229	0.189	0.544	0.456	0.413	0.984	29.0	0.189	0.456	0.111
10.395	0.188	0.546	0.454	0.415	0.983	28.5	0.188	0.454	0.112
10.559	0.188	0.549	0.451	0.417	0.982	28.1	0.188	0.451	0.113
10.724	0.188	0.550	0.450	0.418	0.980	27.6	0.188	0.450	0.112
10.883	0.188	0.550	0.450	0.418	0.980	27.2	0.188	0.450	0.114
11.040	0.188	0.552	0.448	0.418	0.979	26.8	0.188	0.448	0.118
11.199	0.188	0.552	0.448	0.419	0.978	26.4	0.188	0.448	0.121
11.356	0.187	0.554	0.446	0.420	0.978	26.0	0.187	0.446	0.125
11.515	0.187	0.557	0.443	0.423	0.977	25.6	0.187	0.443	0.126
11.676	0.187	0.558	0.442	0.424	0.976	25.2	0.187	0.442	0.127
11.837	0.187	0.559	0.441	0.424	0.975	24.9	0.187	0.441	0.130
11.996	0.187	0.560	0.440	0.424	0.975	24.5	0.187	0.440	0.133
12.155	0.187	0.562	0.438	0.426	0.974	24.2	0.187	0.438	0.134
12.314	0.187	0.565	0.435	0.429	0.973	23.9	0.187	0.435	0.135
12.472	0.186	0.567	0.433	0.430	0.972	23.5	0.186	0.433	0.135
12.631	0.186	0.568	0.432	0.431	0.971	23.2	0.186	0.432	0.137
12.790	0.186	0.569	0.431	0.432	0.971	22.9	0.186	0.431	0.140
12.949	0.186	0.572	0.428	0.434	0.970	22.6	0.186	0.428	0.140
13.110	0.186	0.572	0.428	0.434	0.969	22.3	0.186	0.428	0.142
13.271	0.185	0.575	0.425	0.436	0.967	22.0	0.185	0.425	0.142
13.435	0.185	0.578	0.422	0.439	0.967	21.7	0.185	0.422	0.144
13.598	0.185	0.578	0.422	0.438	0.964	21.4	0.185	0.422	0.143
13.763	0.185	0.579	0.421	0.439	0.964	21.1	0.185	0.421	0.144
13.921	0.184	0.583	0.417	0.442	0.962	20.9	0.184	0.417	0.145
14.090	0.184	0.585	0.415	0.443	0.960	20.6	0.184	0.415	0.145
14.251	0.184	0.586	0.414	0.443	0.959	20.3	0.184	0.414	0.145
14.412	0.183	0.586	0.414	0.443	0.957	20.1	0.183	0.414	0.147
14.578	0.183	0.592	0.408	0.449	0.956	19.8	0.183	0.408	0.146
14.741	0.183	0.592	0.408	0.447	0.953	19.5	0.183	0.408	0.146
14.907	0.182	0.592	0.408	0.447	0.952	19.3	0.182	0.408	0.148
15.075	0.182	0.598	0.402	0.452	0.948	19.0	0.182	0.402	0.149
15.243	0.181	0.598	0.402	0.451	0.946	18.7	0.181	0.402	0.147
15.407	0.181	0.599	0.401	0.450	0.944	18.5	0.181	0.401	0.148
15.570	0.180	0.602	0.398	0.453	0.941	18.2	0.180	0.398	0.150
15.743	0.180	0.606	0.394	0.455	0.937	18.0	0.180	0.394	0.149

shr.stn	sh.sts.	ndelU.	nv.sts.	nsh./v.st	sh./su	eu/su	sh/mpp	v.sts/mpp	v.stn
15.911	0.179	0.606	0.394	0.454	0.933	17.7	0.179	0.394	0.152
16.079	0.178	0.607	0.393	0.453	0.931	17.5	0.178	0.393	0.152
16.238	0.178	0.612	0.388	0.457	0.927	17.2	0.178	0.388	0.155
16.420	0.177	0.620	0.380	0.465	0.921	16.9	0.177	0.380	0.146
16.606	0.175	0.625	0.375	0.467	0.913	16.6	0.175	0.375	0.142
16.790	0.174	0.625	0.375	0.464	0.906	16.3	0.174	0.375	0.140
16.965	0.173	0.628	0.372	0.465	0.902	16.0	0.173	0.372	0.142
17.147	0.172	0.634	0.366	0.469	0.895	15.8	0.172	0.366	0.137
17.320	0.171	0.634	0.366	0.467	0.891	15.5	0.171	0.366	0.141
17.488	0.170	0.637	0.363	0.468	0.887	15.3	0.170	0.363	0.143
17.663	0.169	0.642	0.358	0.473	0.883	15.1	0.169	0.358	0.140
17.840	0.168	0.643	0.357	0.471	0.878	14.9	0.168	0.357	0.144
18.015	0.167	0.650	0.350	0.478	0.873	14.6	0.167	0.350	0.144
18.197	0.166	0.653	0.347	0.479	0.867	14.4	0.166	0.347	0.145
18.386	0.165	0.659	0.341	0.483	0.861	14.1	0.165	0.341	0.138
18.575	0.164	0.662	0.338	0.485	0.854	13.9	0.164	0.338	0.139
18.757	0.163	0.663	0.337	0.483	0.849	13.7	0.163	0.337	0.140
18.927	0.162	0.665	0.335	0.483	0.845	13.5	0.162	0.335	0.143
19.101	0.161	0.671	0.329	0.490	0.840	13.3	0.161	0.329	0.144
19.279	0.160	0.672	0.328	0.488	0.835	13.1	0.160	0.328	0.144
19.454	0.159	0.677	0.323	0.493	0.831	12.9	0.159	0.323	0.148
19.636	0.158	0.682	0.318	0.498	0.825	12.7	0.158	0.318	0.144
19.822	0.157	0.683	0.317	0.495	0.818	12.5	0.157	0.317	0.144
19.999	0.156	0.685	0.315	0.496	0.814	12.3	0.156	0.315	0.150
20.174	0.155	0.690	0.310	0.500	0.809	12.1	0.155	0.310	0.149
20.354	0.154	0.691	0.309	0.499	0.804	11.9	0.154	0.309	0.149
20.524	0.153	0.695	0.305	0.502	0.800	11.8	0.153	0.305	0.152
20.704	0.152	0.698	0.302	0.505	0.795	11.6	0.152	0.302	0.156
20.881	0.151	0.703	0.297	0.509	0.789	11.4	0.151	0.297	0.153
21.066	0.150	0.703	0.297	0.506	0.783	11.2	0.150	0.297	0.150
21.238	0.149	0.706	0.294	0.508	0.779	11.1	0.149	0.294	0.153
21.418	0.148	0.711	0.289	0.512	0.772	10.9	0.148	0.289	0.151
21.602	0.147	0.712	0.288	0.510	0.767	10.7	0.147	0.288	0.157
21.777	0.146	0.717	0.283	0.515	0.762	10.6	0.146	0.283	0.156
21.952	0.145	0.718	0.282	0.513	0.757	10.4	0.145	0.282	0.156
22.129	0.144	0.723	0.277	0.520	0.751	10.3	0.144	0.277	0.159
22.318	0.143	0.725	0.275	0.519	0.744	10.1	0.143	0.275	0.158
22.507	0.141	0.730	0.270	0.523	0.737	9.9	0.141	0.270	0.153
22.703	0.140	0.734	0.266	0.525	0.728	9.7	0.140	0.266	0.152
22.887	0.138	0.735	0.265	0.522	0.722	9.5	0.138	0.265	0.154
23.071	0.137	0.741	0.259	0.530	0.715	9.4	0.137	0.259	0.154
23.264	0.136	0.742	0.258	0.526	0.709	9.2	0.136	0.258	0.156
23.446	0.135	0.748	0.252	0.533	0.702	9.1	0.135	0.252	0.152
23.631	0.133	0.748	0.252	0.530	0.696	8.9	0.133	0.252	0.151
23.796	0.133	0.749	0.251	0.527	0.692	8.8	0.133	0.251	0.156
23.964	0.132	0.754	0.246	0.537	0.689	8.7	0.132	0.246	0.157
24.151	0.131	0.756	0.244	0.536	0.681	8.5	0.131	0.244	0.155
24.321	0.130	0.757	0.243	0.533	0.677	8.4	0.130	0.243	0.156
24.485	0.129	0.762	0.238	0.542	0.674	8.3	0.129	0.238	0.158
24.667	0.128	0.763	0.237	0.539	0.667	8.2	0.128	0.237	0.156
24.839	0.127	0.764	0.236	0.538	0.663	8.1	0.127	0.236	0.160
25.007	0.126	0.768	0.232	0.545	0.658	8.0	0.126	0.232	0.158

shr.stn	sh.sts.	ndelU.	nv.sts.	nsh./v.st	sh./su	eu/su	sh/mpp	v.sts/mpp	v.stn
25.183	0.125	0.769	0.231	0.543	0.653	7.9	0.125	0.231	0.159
25.346	0.125	0.771	0.229	0.545	0.650	7.8	0.125	0.229	0.162
25.526	0.123	0.776	0.224	0.551	0.644	7.6	0.123	0.224	0.158
25.701	0.122	0.777	0.223	0.549	0.639	7.5	0.122	0.223	0.156
25.865	0.122	0.777	0.223	0.546	0.635	7.4	0.122	0.223	0.160
26.028	0.121	0.780	0.220	0.552	0.633	7.4	0.121	0.220	0.162
26.201	0.120	0.784	0.216	0.557	0.627	7.2	0.120	0.216	0.159
26.381	0.119	0.785	0.215	0.553	0.622	7.1	0.119	0.215	0.160
26.544	0.118	0.785	0.215	0.551	0.618	7.1	0.118	0.215	0.163
26.717	0.118	0.791	0.209	0.562	0.614	7.0	0.118	0.209	0.163
26.894	0.116	0.791	0.209	0.558	0.608	6.8	0.116	0.209	0.161
27.053	0.116	0.791	0.209	0.555	0.605	6.8	0.116	0.209	0.163
27.221	0.115	0.797	0.203	0.566	0.601	6.7	0.115	0.203	0.163
27.401	0.114	0.798	0.202	0.563	0.594	6.6	0.114	0.202	0.162
27.567	0.113	0.798	0.202	0.560	0.591	6.5	0.113	0.202	0.161
27.728	0.112	0.801	0.199	0.566	0.587	6.4	0.112	0.199	0.163
27.898	0.112	0.802	0.198	0.563	0.583	6.3	0.112	0.198	0.165
28.057	0.111	0.802	0.198	0.562	0.580	6.3	0.111	0.198	0.167
28.216	0.111	0.803	0.197	0.562	0.578	6.2	0.111	0.197	0.172
28.379	0.110	0.808	0.192	0.572	0.574	6.1	0.110	0.192	0.172
28.550	0.109	0.808	0.192	0.567	0.568	6.0	0.109	0.192	0.174
28.704	0.108	0.808	0.192	0.565	0.566	6.0	0.108	0.192	0.175
28.858	0.108	0.812	0.188	0.574	0.563	5.9	0.108	0.188	0.178
29.033	0.107	0.814	0.186	0.575	0.557	5.8	0.107	0.186	0.175
29.194	0.106	0.814	0.186	0.570	0.553	5.7	0.106	0.186	0.178
29.353	0.106	0.816	0.184	0.573	0.551	5.7	0.106	0.184	0.181
29.531	0.104	0.821	0.179	0.582	0.543	5.6	0.104	0.179	0.174
29.699	0.103	0.821	0.179	0.577	0.538	5.5	0.103	0.179	0.176
29.869	0.102	0.824	0.176	0.581	0.533	5.4	0.102	0.176	0.174
30.028	0.101	0.824	0.176	0.576	0.529	5.3	0.101	0.176	0.172
30.185	0.101	0.825	0.175	0.578	0.526	5.3	0.101	0.175	0.176
30.350	0.100	0.830	0.170	0.586	0.521	5.2	0.100	0.170	0.174
30.514	0.099	0.829	0.171	0.581	0.517	5.1	0.099	0.171	0.176
30.668	0.099	0.830	0.170	0.579	0.515	5.1	0.099	0.170	0.178
30.827	0.098	0.832	0.168	0.585	0.511	5.0	0.098	0.168	0.180
30.986	0.097	0.834	0.166	0.586	0.506	5.0	0.097	0.166	0.180
31.152	0.096	0.836	0.164	0.587	0.502	4.9	0.096	0.164	0.184
31.320	0.095	0.839	0.161	0.590	0.497	4.8	0.095	0.161	0.183
31.481	0.094	0.839	0.161	0.584	0.492	4.7	0.094	0.161	0.185
31.634	0.094	0.839	0.161	0.583	0.490	4.7	0.094	0.161	0.188
31.784	0.093	0.840	0.160	0.584	0.487	4.6	0.093	0.160	0.192
31.945	0.093	0.842	0.158	0.587	0.483	4.6	0.093	0.158	0.200
32.108	0.092	0.844	0.156	0.589	0.479	4.5	0.092	0.156	0.200
32.274	0.091	0.846	0.154	0.588	0.473	4.5	0.091	0.154	0.200
32.431	0.090	0.847	0.153	0.589	0.470	4.4	0.090	0.153	0.202
32.587	0.089	0.848	0.152	0.586	0.465	4.3	0.089	0.152	0.208
32.737	0.089	0.849	0.151	0.587	0.463	4.3	0.089	0.151	0.209
32.900	0.088	0.854	0.146	0.599	0.457	4.2	0.088	0.146	0.209
33.085	0.086	0.856	0.144	0.596	0.449	4.1	0.086	0.144	0.204
33.239	0.085	0.856	0.144	0.591	0.445	4.1	0.085	0.144	0.205
33.388	0.085	0.856	0.144	0.589	0.442	4.0	0.085	0.144	0.207
33.547	0.084	0.859	0.141	0.593	0.437	4.0	0.084	0.141	0.208

Ko CONSOLIDATED GEONOR DIRECT SIMPLE SHEAR TEST
MIT GEOTECHNICAL LAB

FILE NAME : DSS 22

REDUCTION DATA

UNITS: kg,cm,mVolts,Volts

- | | |
|--|--|
| 1. Test Name : DSS 22 | |
| 2. Date : 3/11/89 | |
| 3. OCR : 1 | |
| 4. Ver. Consolidation Stress (ksc) :5.9916 | |
| 5. Pre-Shear Height (cm) :2.0362 | |
| 6. Horizontal Shear Load Cell: | 7. Horizontal Displacement Transducer: |
| Zero: 0.36192 | Zero: 0.1579 |
| CF: -175.993 | CF: 2.2815 |
| 8. Vertical Stress Load Cell: | 9. Vertical Height Transducer: |
| Zero: 0.37329 | Zero: -0.0273 |
| CF: -636.57 | CF: 2.0655 |

shr.stn	sh.sts.	ndelU.	nv.sts.	nsh./v.st	sh./su	eu/su	sh/mpp	v.sts/mpp	v.stn
0.000	-0.001	0.001	0.999	-0.001	-0.005	9999.0	-0.001	0.999	0.000
0.002	0.000	0.002	0.998	0.000	0.001	774.9	0.000	0.998	0.002
0.002	0.016	0.008	0.992	0.016	0.079	9999.0	0.016	0.992	-0.010
0.006	0.022	0.010	0.990	0.022	0.113	5716.4	0.022	0.990	-0.010
0.016	0.029	0.013	0.987	0.029	0.145	2835.2	0.029	0.987	-0.009
0.025	0.036	0.015	0.985	0.036	0.180	2178.6	0.036	0.985	-0.013
0.037	0.042	0.017	0.983	0.043	0.213	1789.1	0.042	0.983	-0.006
0.047	0.049	0.019	0.981	0.050	0.248	1597.1	0.049	0.981	-0.008
0.059	0.055	0.022	0.978	0.057	0.281	1446.5	0.055	0.978	-0.012
0.074	0.062	0.026	0.974	0.064	0.316	1305.6	0.062	0.974	-0.005
0.091	0.069	0.030	0.970	0.071	0.351	1177.8	0.069	0.970	0.000
0.109	0.076	0.033	0.967	0.079	0.386	1072.0	0.076	0.967	0.002
0.131	0.082	0.038	0.962	0.086	0.418	967.8	0.082	0.962	0.005
0.157	0.089	0.043	0.957	0.093	0.451	871.6	0.089	0.957	0.004
0.183	0.095	0.050	0.950	0.100	0.482	798.7	0.095	0.950	0.001
0.215	0.101	0.056	0.944	0.107	0.513	722.4	0.101	0.944	0.005
0.250	0.107	0.062	0.938	0.114	0.544	657.4	0.107	0.938	0.012
0.291	0.113	0.070	0.930	0.121	0.572	595.3	0.113	0.930	0.012
0.337	0.118	0.078	0.922	0.128	0.601	539.1	0.118	0.922	0.007
0.383	0.124	0.087	0.913	0.135	0.627	494.9	0.124	0.913	0.010
0.438	0.129	0.097	0.903	0.143	0.653	450.3	0.129	0.903	0.015
0.494	0.134	0.109	0.891	0.150	0.677	414.3	0.134	0.891	0.013
0.569	0.138	0.120	0.880	0.157	0.701	372.0	0.138	0.880	0.015
0.640	0.143	0.130	0.870	0.164	0.723	341.2	0.143	0.870	0.031
0.692	0.147	0.142	0.858	0.171	0.743	324.4	0.147	0.858	0.039
0.732	0.151	0.152	0.848	0.178	0.763	314.6	0.151	0.848	0.026
0.838	0.154	0.166	0.834	0.185	0.781	281.2	0.154	0.834	0.026
0.939	0.157	0.181	0.819	0.192	0.798	256.6	0.157	0.819	0.039
1.006	0.161	0.191	0.809	0.198	0.814	244.3	0.161	0.809	0.038
1.119	0.164	0.199	0.801	0.204	0.830	223.7	0.164	0.801	0.043
1.264	0.166	0.208	0.792	0.210	0.843	201.3	0.166	0.792	0.053

shr.stn	sh.sts.	ndelU.	nv.sts.	nsh./v.st	sh./su	eu/su	sh/mpp	v.sts/mpp	v.stn
1.330	0.169	0.221	0.779	0.217	0.856	194.2	0.169	0.779	0.053
1.436	0.172	0.232	0.768	0.223	0.870	182.6	0.172	0.768	0.057
1.592	0.174	0.243	0.757	0.229	0.881	166.8	0.174	0.757	0.067
1.644	0.176	0.254	0.746	0.236	0.892	163.6	0.176	0.746	0.058
1.748	0.178	0.265	0.735	0.242	0.901	155.4	0.178	0.735	0.052
1.838	0.180	0.275	0.725	0.248	0.911	149.5	0.180	0.725	0.053
1.970	0.181	0.282	0.718	0.253	0.919	140.6	0.181	0.718	0.059
2.078	0.183	0.292	0.708	0.258	0.927	134.4	0.183	0.708	0.064
2.206	0.184	0.303	0.697	0.264	0.933	127.5	0.184	0.697	0.058
2.378	0.185	0.313	0.687	0.269	0.939	119.1	0.185	0.687	0.077
2.461	0.186	0.320	0.680	0.274	0.945	115.7	0.186	0.680	0.077
2.585	0.187	0.330	0.670	0.280	0.950	110.8	0.187	0.670	0.078
2.709	0.188	0.337	0.663	0.284	0.955	106.3	0.188	0.663	0.078
2.836	0.189	0.346	0.654	0.289	0.959	102.0	0.189	0.654	0.081
2.956	0.190	0.354	0.646	0.294	0.964	98.3	0.190	0.646	0.074
3.103	0.191	0.362	0.638	0.299	0.967	94.0	0.191	0.638	0.075
3.266	0.191	0.370	0.630	0.304	0.971	89.6	0.191	0.630	0.073
3.465	0.192	0.377	0.623	0.308	0.974	84.8	0.192	0.623	0.083
3.573	0.193	0.386	0.614	0.313	0.976	82.4	0.193	0.614	0.077
3.755	0.193	0.393	0.607	0.318	0.979	78.6	0.193	0.607	0.087
3.854	0.193	0.400	0.600	0.322	0.980	76.6	0.193	0.600	0.086
3.984	0.194	0.406	0.594	0.326	0.982	74.3	0.194	0.594	0.089
4.157	0.194	0.411	0.589	0.329	0.984	71.3	0.194	0.589	0.096
4.263	0.195	0.415	0.585	0.332	0.986	69.7	0.195	0.585	0.094
4.367	0.195	0.419	0.581	0.336	0.988	68.2	0.195	0.581	0.084
4.504	0.195	0.423	0.577	0.339	0.990	66.3	0.195	0.577	0.080
4.668	0.196	0.429	0.571	0.343	0.993	64.1	0.196	0.571	0.074
4.828	0.196	0.433	0.567	0.346	0.995	62.1	0.196	0.567	0.083
4.980	0.196	0.437	0.563	0.349	0.996	60.3	0.196	0.563	0.080
5.079	0.196	0.443	0.557	0.353	0.996	59.1	0.196	0.557	0.073
5.252	0.197	0.449	0.551	0.357	0.997	57.2	0.197	0.551	0.081
5.411	0.197	0.455	0.545	0.361	0.997	55.5	0.197	0.545	0.080
5.640	0.197	0.459	0.541	0.364	0.998	53.3	0.197	0.541	0.079
5.743	0.197	0.461	0.539	0.365	0.998	52.4	0.197	0.539	0.073
5.846	0.197	0.463	0.537	0.367	0.999	51.5	0.197	0.537	0.080
6.009	0.197	0.467	0.533	0.370	1.000	50.1	0.197	0.533	0.089
6.155	0.197	0.473	0.527	0.374	1.000	49.0	0.197	0.527	0.093
6.303	0.197	0.477	0.523	0.377	1.000	47.8	0.197	0.523	0.083
6.456	0.197	0.482	0.518	0.381	1.000	46.7	0.197	0.518	0.081
6.606	0.197	0.483	0.517	0.382	1.000	45.6	0.197	0.517	0.087
6.767	0.197	0.485	0.515	0.382	1.000	44.5	0.197	0.515	0.080
6.911	0.197	0.490	0.510	0.387	1.000	43.6	0.197	0.510	0.082
7.063	0.197	0.494	0.506	0.389	0.999	42.6	0.197	0.506	0.081
7.213	0.197	0.494	0.506	0.390	0.999	41.8	0.197	0.506	0.082
7.356	0.197	0.497	0.503	0.392	0.999	40.9	0.197	0.503	0.084
7.504	0.197	0.503	0.497	0.396	0.999	40.1	0.197	0.497	0.085
7.656	0.197	0.506	0.494	0.399	0.999	39.3	0.197	0.494	0.084
7.808	0.197	0.510	0.490	0.402	0.999	38.6	0.197	0.490	0.083
7.958	0.197	0.513	0.487	0.404	0.998	37.8	0.197	0.487	0.081
8.106	0.197	0.514	0.486	0.405	0.998	37.1	0.197	0.486	0.082
8.256	0.197	0.515	0.485	0.406	0.998	36.4	0.197	0.485	0.083
8.393	0.197	0.519	0.481	0.409	0.997	35.8	0.197	0.481	0.080

shr.stn	sh.sts.	ndelU.	nv.sts.	nsh./v.st	sh./su	eu/su	sh/mpp	v.sts/mpp	v.stn
8.549	0.197	0.522	0.478	0.412	0.997	35.1	0.197	0.478	0.083
8.705	0.196	0.523	0.477	0.412	0.996	34.5	0.196	0.477	0.084
8.859	0.196	0.525	0.475	0.413	0.995	33.9	0.196	0.475	0.086
9.007	0.196	0.529	0.471	0.417	0.995	33.3	0.196	0.471	0.086
9.167	0.196	0.536	0.464	0.421	0.992	32.6	0.196	0.464	0.081
9.321	0.195	0.539	0.461	0.424	0.991	32.0	0.195	0.461	0.078
9.475	0.195	0.540	0.460	0.424	0.989	31.5	0.195	0.460	0.076
9.629	0.195	0.543	0.457	0.426	0.988	30.9	0.195	0.457	0.074
9.779	0.194	0.543	0.457	0.425	0.986	30.4	0.194	0.457	0.074
9.930	0.194	0.543	0.457	0.426	0.986	29.9	0.194	0.457	0.076
10.082	0.194	0.544	0.456	0.426	0.985	29.4	0.194	0.456	0.078
10.230	0.194	0.546	0.454	0.428	0.985	29.0	0.194	0.454	0.079
10.380	0.194	0.549	0.451	0.431	0.984	28.6	0.194	0.451	0.081
10.532	0.194	0.551	0.449	0.432	0.983	28.1	0.194	0.449	0.080
10.680	0.194	0.553	0.447	0.433	0.983	27.7	0.194	0.447	0.081
10.832	0.193	0.555	0.445	0.435	0.981	27.3	0.193	0.445	0.081
10.983	0.194	0.556	0.444	0.435	0.981	26.9	0.194	0.444	0.081
11.131	0.193	0.556	0.444	0.435	0.981	26.6	0.193	0.444	0.084
11.279	0.193	0.557	0.443	0.436	0.980	26.2	0.193	0.443	0.084
11.427	0.193	0.560	0.440	0.439	0.980	25.9	0.193	0.440	0.085
11.577	0.193	0.564	0.436	0.443	0.979	25.5	0.193	0.436	0.086
11.733	0.193	0.566	0.434	0.445	0.978	25.1	0.193	0.434	0.083
11.885	0.192	0.569	0.431	0.446	0.976	24.8	0.192	0.431	0.083
12.036	0.192	0.569	0.431	0.446	0.975	24.4	0.192	0.431	0.082
12.186	0.192	0.570	0.430	0.447	0.974	24.1	0.192	0.430	0.082
12.340	0.192	0.574	0.426	0.451	0.973	23.8	0.192	0.426	0.080
12.492	0.192	0.574	0.426	0.450	0.972	23.5	0.192	0.426	0.080
12.645	0.191	0.575	0.425	0.450	0.971	23.1	0.191	0.425	0.080
12.795	0.191	0.575	0.425	0.450	0.971	22.9	0.191	0.425	0.081
12.943	0.191	0.577	0.423	0.452	0.970	22.6	0.191	0.423	0.082
13.099	0.191	0.580	0.420	0.454	0.968	22.3	0.191	0.420	0.082
13.241	0.191	0.580	0.420	0.454	0.967	22.0	0.191	0.420	0.082
13.397	0.191	0.580	0.420	0.454	0.967	21.8	0.191	0.420	0.086
13.536	0.191	0.582	0.418	0.456	0.966	21.5	0.191	0.418	0.086
13.690	0.190	0.586	0.414	0.459	0.965	21.2	0.190	0.414	0.085
13.844	0.190	0.587	0.413	0.460	0.963	21.0	0.190	0.413	0.083
13.994	0.190	0.587	0.413	0.460	0.962	20.7	0.190	0.413	0.084
14.150	0.190	0.590	0.410	0.462	0.961	20.5	0.190	0.410	0.083
14.304	0.189	0.593	0.407	0.464	0.959	20.2	0.189	0.407	0.082
14.458	0.189	0.595	0.405	0.466	0.957	20.0	0.189	0.405	0.080
14.610	0.188	0.596	0.404	0.466	0.955	19.7	0.188	0.404	0.086
14.760	0.188	0.596	0.404	0.466	0.954	19.5	0.188	0.404	0.079
14.907	0.188	0.597	0.403	0.467	0.953	19.3	0.188	0.403	0.081
15.059	0.188	0.600	0.400	0.469	0.952	19.0	0.188	0.400	0.080
15.211	0.187	0.601	0.399	0.469	0.950	18.8	0.187	0.399	0.080
15.362	0.187	0.603	0.397	0.470	0.947	18.6	0.187	0.397	0.080
15.512	0.187	0.603	0.397	0.471	0.946	18.4	0.187	0.397	0.080
15.664	0.186	0.604	0.396	0.470	0.945	18.2	0.186	0.396	0.081
15.814	0.186	0.604	0.396	0.470	0.943	18.0	0.186	0.396	0.084
15.960	0.186	0.605	0.395	0.470	0.941	17.8	0.186	0.395	0.087
16.120	0.185	0.608	0.392	0.473	0.940	17.6	0.185	0.392	0.089
16.270	0.185	0.610	0.390	0.474	0.937	17.4	0.185	0.390	0.090

shr.stn	sh.sts.	ndelU.	nv.sts.	nsh./v.st	sh./su	eu/su	sh/mpp	v.sts/mpp	v.stn
16.422	0.184	0.612	0.388	0.475	0.934	17.1	0.184	0.388	0.093
16.573	0.184	0.618	0.382	0.481	0.931	16.9	0.184	0.382	0.092
16.729	0.183	0.621	0.379	0.482	0.926	16.7	0.183	0.379	0.090
16.883	0.182	0.624	0.376	0.484	0.922	16.5	0.182	0.376	0.091
17.048	0.181	0.625	0.375	0.483	0.918	16.2	0.181	0.375	0.091
17.201	0.180	0.627	0.373	0.484	0.915	16.0	0.180	0.373	0.093
17.366	0.179	0.632	0.368	0.488	0.909	15.8	0.179	0.368	0.091
17.527	0.178	0.636	0.364	0.489	0.903	15.5	0.178	0.364	0.089
17.686	0.177	0.636	0.364	0.487	0.899	15.3	0.177	0.364	0.090
17.847	0.177	0.638	0.362	0.488	0.896	15.1	0.177	0.362	0.093
17.999	0.176	0.642	0.358	0.492	0.893	15.0	0.176	0.358	0.096
18.157	0.175	0.646	0.354	0.494	0.888	14.8	0.175	0.354	0.095
18.311	0.174	0.650	0.350	0.499	0.885	14.6	0.174	0.350	0.094
18.471	0.173	0.652	0.348	0.499	0.879	14.4	0.173	0.348	0.096
18.640	0.172	0.657	0.343	0.503	0.874	14.1	0.172	0.343	0.097
18.794	0.171	0.658	0.342	0.501	0.869	14.0	0.171	0.342	0.090
18.952	0.171	0.659	0.341	0.502	0.867	13.8	0.171	0.341	0.091
19.104	0.170	0.666	0.334	0.509	0.863	13.6	0.170	0.334	0.092
19.278	0.169	0.667	0.333	0.508	0.859	13.4	0.169	0.333	0.091
19.424	0.169	0.670	0.330	0.511	0.855	13.3	0.169	0.330	0.093
19.584	0.168	0.674	0.326	0.515	0.850	13.1	0.168	0.326	0.089
19.748	0.167	0.680	0.320	0.520	0.845	12.9	0.167	0.320	0.085
19.907	0.165	0.682	0.318	0.519	0.838	12.7	0.165	0.318	0.083
20.072	0.164	0.685	0.315	0.522	0.834	12.5	0.164	0.315	0.083
20.228	0.163	0.686	0.314	0.520	0.828	12.4	0.163	0.314	0.084
20.386	0.163	0.687	0.313	0.520	0.826	12.2	0.163	0.313	0.085
20.533	0.162	0.690	0.310	0.523	0.823	12.1	0.162	0.310	0.086
20.687	0.162	0.692	0.308	0.526	0.820	12.0	0.162	0.308	0.088
20.839	0.161	0.695	0.305	0.529	0.817	11.8	0.161	0.305	0.088
20.993	0.160	0.699	0.301	0.533	0.813	11.7	0.160	0.301	0.088
21.155	0.159	0.703	0.297	0.536	0.809	11.5	0.159	0.297	0.087
21.311	0.158	0.704	0.296	0.535	0.803	11.4	0.158	0.296	0.086
21.473	0.158	0.707	0.293	0.538	0.800	11.2	0.158	0.293	0.087
21.625	0.157	0.711	0.289	0.543	0.795	11.1	0.157	0.289	0.085
21.785	0.156	0.713	0.287	0.543	0.790	10.9	0.156	0.287	0.083
21.937	0.155	0.715	0.285	0.545	0.786	10.8	0.155	0.285	0.083
22.095	0.154	0.719	0.281	0.547	0.781	10.7	0.154	0.281	0.080
22.251	0.153	0.719	0.281	0.546	0.777	10.5	0.153	0.281	0.081
22.400	0.153	0.722	0.278	0.549	0.774	10.4	0.153	0.278	0.075
22.555	0.152	0.725	0.275	0.553	0.770	10.3	0.152	0.275	0.082
22.708	0.151	0.729	0.271	0.557	0.764	10.2	0.151	0.271	0.079
22.870	0.150	0.731	0.269	0.557	0.760	10.0	0.150	0.269	0.079
23.018	0.149	0.733	0.267	0.557	0.755	9.9	0.149	0.267	0.079
23.182	0.148	0.737	0.263	0.562	0.750	9.8	0.148	0.263	0.076
23.332	0.147	0.738	0.262	0.561	0.746	9.7	0.147	0.262	0.075
23.487	0.147	0.739	0.261	0.560	0.743	9.5	0.147	0.261	0.076
23.630	0.146	0.741	0.259	0.562	0.740	9.4	0.146	0.259	0.077
23.806	0.145	0.743	0.257	0.563	0.735	9.3	0.145	0.257	0.079
23.938	0.144	0.744	0.256	0.565	0.732	9.2	0.144	0.256	0.079
24.087	0.143	0.747	0.253	0.567	0.727	9.1	0.143	0.253	0.079
24.241	0.143	0.748	0.252	0.566	0.724	9.0	0.143	0.252	0.080
24.399	0.142	0.748	0.252	0.563	0.720	8.9	0.142	0.252	0.080

shr.stn	sh.sts.	ndelU.	nv.sts.	nsh./v.st	sh./su	eu/su	sh/mpp	v.sts/mpp	v.stn
24.551	0.141	0.749	0.251	0.563	0.717	8.8	0.141	0.251	0.084
24.703	0.141	0.751	0.249	0.567	0.715	8.7	0.141	0.249	0.086
24.855	0.140	0.755	0.245	0.573	0.711	8.6	0.140	0.245	0.090
25.006	0.139	0.757	0.243	0.574	0.706	8.5	0.139	0.243	0.086
25.163	0.138	0.758	0.242	0.573	0.702	8.4	0.138	0.242	0.088
25.312	0.138	0.760	0.240	0.574	0.698	8.3	0.138	0.240	0.088
25.460	0.137	0.760	0.240	0.571	0.694	8.2	0.137	0.240	0.090
25.603	0.136	0.761	0.239	0.572	0.692	8.2	0.136	0.239	0.095
25.755	0.136	0.767	0.233	0.581	0.688	8.1	0.136	0.233	0.087
25.911	0.135	0.768	0.232	0.581	0.683	8.0	0.135	0.232	0.096
26.057	0.134	0.771	0.229	0.585	0.679	7.9	0.134	0.229	0.096
26.215	0.133	0.774	0.226	0.587	0.674	7.8	0.133	0.226	0.096
26.363	0.132	0.774	0.226	0.583	0.669	7.7	0.132	0.226	0.096
26.513	0.131	0.776	0.224	0.585	0.665	7.6	0.131	0.224	0.097
26.648	0.130	0.780	0.220	0.591	0.660	7.5	0.130	0.220	0.097
26.814	0.129	0.780	0.220	0.585	0.653	7.4	0.129	0.220	0.095
26.997	0.128	0.781	0.219	0.585	0.649	7.3	0.128	0.219	0.097
27.134	0.127	0.783	0.217	0.587	0.645	7.2	0.127	0.217	0.098
27.299	0.126	0.787	0.213	0.591	0.639	7.1	0.126	0.213	0.098
27.407	0.125	0.787	0.213	0.589	0.635	7.0	0.125	0.213	0.098
27.545	0.124	0.789	0.211	0.589	0.631	6.9	0.124	0.211	0.099
27.711	0.123	0.791	0.209	0.592	0.626	6.8	0.123	0.209	0.100
27.873	0.122	0.793	0.207	0.590	0.619	6.7	0.122	0.207	0.095
28.023	0.121	0.796	0.204	0.593	0.614	6.6	0.121	0.204	0.093
28.175	0.120	0.797	0.203	0.592	0.609	6.5	0.120	0.203	0.091
28.327	0.119	0.801	0.199	0.598	0.604	6.4	0.119	0.199	0.090
28.483	0.118	0.803	0.197	0.597	0.597	6.3	0.118	0.197	0.087
28.637	0.117	0.803	0.197	0.592	0.592	6.3	0.117	0.197	0.086
28.780	0.116	0.803	0.197	0.591	0.589	6.2	0.116	0.197	0.089
28.924	0.115	0.804	0.196	0.590	0.586	6.1	0.115	0.196	0.092
29.067	0.115	0.805	0.195	0.589	0.583	6.1	0.115	0.195	0.096
29.204	0.114	0.806	0.194	0.590	0.580	6.0	0.114	0.194	0.099
29.340	0.114	0.807	0.193	0.590	0.577	6.0	0.114	0.193	0.102
29.484	0.113	0.810	0.190	0.596	0.573	5.9	0.113	0.190	0.103
29.653	0.111	0.818	0.182	0.612	0.564	5.8	0.111	0.182	0.093
29.823	0.110	0.818	0.182	0.603	0.556	5.6	0.110	0.182	0.086
29.958	0.109	0.819	0.181	0.601	0.551	5.6	0.109	0.181	0.085
30.079	0.108	0.819	0.181	0.597	0.548	5.5	0.108	0.181	0.087
30.246	0.107	0.820	0.180	0.595	0.545	5.4	0.107	0.180	0.089
30.397	0.107	0.820	0.180	0.594	0.542	5.4	0.107	0.180	0.092
30.536	0.106	0.821	0.179	0.593	0.539	5.3	0.106	0.179	0.095
30.742	0.106	0.822	0.178	0.596	0.537	5.3	0.106	0.178	0.100

Ko CONSOLIDATED GEONOR DIRECT SIMPLE SHEAR TEST
MIT GEOTECHNICAL LAB

FILE NAME : DSS 25

REDUCTION DATA

UNITS: kg,cm,mVolts,Volts

- 1. Test Name : DSS 25
- 2. Date : 3/18/89
- 3. OCR : 1
- 4. Ver. Consolidation Stress (ksc) :2.955
- 5. Pre-Shear Height (cm) :2.1009
- 6. Horizontal Shear Load Cell:
 - Zero: 0.03997
 - CF: -80.2
- 7. Horizontal Displacement Transducer:
 - Zero: 0.11258
 - CF: 2.2815
- 8. Vertical Stress Load Cell:
 - Zero: 0.12055
 - CF: -348.57
- 9. Vertical Height Transducer:
 - Zero: -0.11276
 - CF: 2.0655

shr.stn	sh.sts.	ndelU.	nv.sts.	nsh./v.st	sh./su	eu/su	sh/mpp	v.sts/mpp	v.stn
-0.009	0.000	0.005	0.995	0.000	-0.002	-202.9	0.000	0.995	-0.005
0.017	0.012	-0.009	1.009	0.011	0.057	1132.5	0.012	1.009	-0.003
0.016	0.017	-0.009	1.009	0.017	0.086	1775.6	0.017	1.009	0.004
0.024	0.024	-0.009	1.009	0.024	0.118	1549.1	0.024	1.009	0.010
0.030	0.030	-0.009	1.009	0.030	0.151	1594.4	0.030	1.009	0.008
0.040	0.037	-0.009	1.009	0.037	0.185	1451.8	0.037	1.009	0.008
0.051	0.044	-0.009	1.009	0.044	0.218	1329.5	0.044	1.009	0.010
0.063	0.051	-0.007	1.007	0.051	0.251	1230.0	0.051	1.007	0.003
0.060	0.058	-0.005	1.005	0.057	0.284	1464.1	0.058	1.005	0.014
0.091	0.064	0.000	1.000	0.064	0.319	1072.4	0.064	1.000	0.021
0.104	0.071	0.009	0.991	0.072	0.350	1038.6	0.071	0.991	0.020
0.107	0.078	0.010	0.990	0.078	0.384	1097.1	0.078	0.990	0.007
0.118	0.084	0.020	0.980	0.086	0.416	1074.0	0.084	0.980	0.005
0.152	0.091	0.030	0.970	0.094	0.449	902.7	0.091	0.970	0.009
0.164	0.098	0.038	0.962	0.101	0.482	896.7	0.098	0.962	0.016
0.197	0.104	0.048	0.952	0.109	0.514	796.4	0.104	0.952	0.017
0.236	0.110	0.054	0.946	0.117	0.546	703.0	0.110	0.946	0.016
0.271	0.116	0.064	0.936	0.124	0.574	643.1	0.116	0.936	0.019
0.316	0.122	0.074	0.926	0.132	0.603	580.2	0.122	0.926	0.030
0.353	0.128	0.082	0.918	0.139	0.630	543.0	0.128	0.918	0.030
0.381	0.133	0.096	0.904	0.147	0.658	524.8	0.133	0.904	0.023
0.432	0.138	0.107	0.893	0.154	0.682	479.2	0.138	0.893	0.027
0.489	0.143	0.117	0.883	0.162	0.706	438.7	0.143	0.883	0.029
0.541	0.147	0.122	0.878	0.168	0.729	408.7	0.147	0.878	0.021
0.616	0.152	0.134	0.866	0.175	0.750	369.1	0.152	0.866	0.021
0.686	0.156	0.145	0.855	0.183	0.771	340.6	0.156	0.855	0.028
0.745	0.160	0.158	0.842	0.189	0.789	321.1	0.160	0.842	0.036
0.834	0.163	0.171	0.829	0.197	0.806	293.0	0.163	0.829	0.031
0.922	0.167	0.183	0.817	0.204	0.823	270.4	0.167	0.817	0.034
1.001	0.170	0.194	0.806	0.211	0.839	253.8	0.170	0.806	0.039
1.099	0.173	0.205	0.795	0.217	0.854	235.2	0.173	0.795	0.041

shr.stn	sh.sts.	ndelU.	nv.sts.	nsh./v.st	sh./su	eu/su	sh/mpp	v.sts/mpp	v.stn
1.194	0.175	0.217	0.783	0.224	0.867	219.7	0.175	0.783	0.048
1.276	0.178	0.230	0.770	0.231	0.878	208.1	0.178	0.770	0.052
1.405	0.180	0.241	0.759	0.237	0.889	191.4	0.180	0.759	0.056
1.501	0.182	0.254	0.746	0.244	0.901	181.6	0.182	0.746	0.066
1.604	0.184	0.262	0.738	0.250	0.910	171.8	0.184	0.738	0.064
1.733	0.186	0.274	0.726	0.257	0.921	160.8	0.186	0.726	0.060
1.845	0.188	0.286	0.714	0.263	0.928	152.1	0.188	0.714	0.058
1.964	0.189	0.298	0.702	0.270	0.936	144.2	0.189	0.702	0.055
2.081	0.191	0.312	0.688	0.277	0.943	137.1	0.191	0.688	0.060
2.202	0.192	0.323	0.677	0.284	0.949	130.3	0.192	0.677	0.061
2.325	0.193	0.332	0.668	0.289	0.954	124.2	0.193	0.668	0.057
2.452	0.194	0.341	0.659	0.295	0.958	118.3	0.194	0.659	0.062
2.581	0.195	0.351	0.649	0.300	0.963	112.9	0.195	0.649	0.070
2.715	0.196	0.359	0.641	0.305	0.966	107.7	0.196	0.641	0.065
2.850	0.196	0.365	0.635	0.309	0.970	102.9	0.196	0.635	0.065
2.982	0.197	0.373	0.627	0.314	0.972	98.6	0.197	0.627	0.057
3.114	0.198	0.380	0.620	0.319	0.977	94.9	0.198	0.620	0.058
3.244	0.198	0.385	0.615	0.322	0.979	91.3	0.198	0.615	0.061
3.378	0.199	0.390	0.610	0.326	0.982	88.0	0.199	0.610	0.056
3.507	0.199	0.394	0.606	0.329	0.985	84.9	0.199	0.606	0.064
3.643	0.200	0.403	0.597	0.334	0.987	82.0	0.200	0.597	0.071
3.781	0.200	0.405	0.595	0.337	0.989	79.1	0.200	0.595	0.073
3.915	0.200	0.415	0.585	0.343	0.990	76.5	0.200	0.585	0.073
4.052	0.201	0.418	0.582	0.345	0.993	74.1	0.201	0.582	0.067
4.195	0.201	0.429	0.571	0.352	0.993	71.6	0.201	0.571	0.073
4.340	0.201	0.433	0.567	0.355	0.994	69.3	0.201	0.567	0.074
4.478	0.201	0.438	0.562	0.358	0.994	67.1	0.201	0.562	0.071
4.617	0.202	0.438	0.562	0.359	0.996	65.2	0.202	0.562	0.074
4.751	0.202	0.446	0.554	0.364	0.998	63.5	0.202	0.554	0.075
4.895	0.202	0.451	0.549	0.368	0.998	61.7	0.202	0.549	0.072
5.036	0.202	0.452	0.548	0.369	0.999	60.0	0.202	0.548	0.072
5.178	0.202	0.461	0.539	0.375	1.000	58.4	0.202	0.539	0.076
5.319	0.202	0.461	0.539	0.376	1.000	56.8	0.202	0.539	0.072
5.461	0.202	0.470	0.530	0.382	1.000	55.4	0.202	0.530	0.078
5.609	0.202	0.474	0.526	0.385	1.000	53.9	0.202	0.526	0.073
5.754	0.202	0.481	0.519	0.390	1.000	52.6	0.202	0.519	0.065
5.900	0.202	0.483	0.517	0.391	0.999	51.2	0.202	0.517	0.060
6.040	0.202	0.483	0.517	0.392	1.000	50.1	0.202	0.517	0.062
6.184	0.202	0.493	0.507	0.399	1.000	48.9	0.202	0.507	0.066
6.329	0.202	0.494	0.506	0.400	1.000	47.8	0.202	0.506	0.066
6.474	0.202	0.496	0.504	0.401	0.999	46.7	0.202	0.504	0.065
6.618	0.202	0.505	0.495	0.408	0.999	45.6	0.202	0.495	0.068
6.759	0.202	0.504	0.496	0.407	0.998	44.7	0.202	0.496	0.068
6.908	0.202	0.509	0.491	0.412	0.999	43.7	0.202	0.491	0.066
7.049	0.202	0.509	0.491	0.411	0.998	42.8	0.202	0.491	0.060
7.195	0.202	0.515	0.485	0.416	0.998	42.0	0.202	0.485	0.063
7.340	0.202	0.517	0.483	0.418	0.998	41.1	0.202	0.483	0.062
7.484	0.202	0.519	0.481	0.419	0.997	40.3	0.202	0.481	0.066
7.633	0.202	0.522	0.478	0.422	0.997	39.5	0.202	0.478	0.064
7.781	0.201	0.527	0.473	0.425	0.995	38.7	0.201	0.473	0.062
7.928	0.201	0.529	0.471	0.427	0.994	37.9	0.201	0.471	0.063
8.074	0.201	0.531	0.469	0.428	0.992	37.2	0.201	0.469	0.061

shr.stn	sh.sts.	ndelU.	nv.sts.	nsh./v.st	sh./su	eu/su	sh/mpp	v.sts/mpp	v.stn
8.223	0.201	0.531	0.469	0.428	0.992	36.5	0.201	0.469	0.062
8.368	0.200	0.538	0.462	0.434	0.990	35.8	0.200	0.462	0.063
8.517	0.200	0.538	0.462	0.434	0.990	35.2	0.200	0.462	0.062
8.660	0.200	0.538	0.462	0.434	0.989	34.5	0.200	0.462	0.063
8.805	0.200	0.541	0.459	0.436	0.988	34.0	0.200	0.459	0.063
8.953	0.200	0.546	0.454	0.440	0.988	33.4	0.200	0.454	0.065
9.099	0.200	0.548	0.452	0.442	0.986	32.8	0.200	0.452	0.065
9.245	0.199	0.549	0.451	0.443	0.986	32.2	0.199	0.451	0.065
9.392	0.199	0.550	0.450	0.442	0.984	31.7	0.199	0.450	0.065
9.540	0.199	0.550	0.450	0.443	0.984	31.2	0.199	0.450	0.067
9.686	0.199	0.556	0.444	0.448	0.983	30.7	0.199	0.444	0.069
9.824	0.199	0.559	0.441	0.450	0.982	30.2	0.199	0.441	0.068
9.975	0.198	0.559	0.441	0.450	0.980	29.7	0.198	0.441	0.067
10.126	0.198	0.564	0.436	0.455	0.979	29.2	0.198	0.436	0.068
10.292	0.198	0.567	0.433	0.457	0.978	28.8	0.198	0.433	0.066
10.443	0.198	0.566	0.434	0.456	0.978	28.3	0.198	0.434	0.065
10.600	0.198	0.568	0.432	0.458	0.977	27.9	0.198	0.432	0.066
10.754	0.197	0.570	0.430	0.459	0.976	27.4	0.197	0.430	0.067
10.907	0.197	0.570	0.430	0.459	0.975	27.0	0.197	0.430	0.068
11.051	0.197	0.571	0.429	0.459	0.974	26.7	0.197	0.429	0.070
11.202	0.197	0.577	0.423	0.466	0.973	26.3	0.197	0.423	0.071
11.361	0.197	0.578	0.422	0.466	0.972	25.9	0.197	0.422	0.071
11.510	0.196	0.583	0.417	0.471	0.969	25.5	0.196	0.417	0.071
11.648	0.196	0.584	0.416	0.471	0.968	25.1	0.196	0.416	0.070
11.793	0.195	0.584	0.416	0.470	0.966	24.8	0.195	0.416	0.070
11.941	0.195	0.585	0.415	0.471	0.965	24.5	0.195	0.415	0.071
12.086	0.195	0.586	0.414	0.472	0.964	24.1	0.195	0.414	0.072
12.245	0.195	0.591	0.409	0.477	0.963	23.8	0.195	0.409	0.073
12.404	0.194	0.593	0.407	0.478	0.961	23.4	0.194	0.407	0.072
12.556	0.194	0.594	0.406	0.479	0.959	23.1	0.194	0.406	0.075
12.705	0.194	0.594	0.406	0.479	0.959	22.8	0.194	0.406	0.072
12.838	0.194	0.595	0.405	0.478	0.958	22.6	0.194	0.405	0.073
12.992	0.194	0.599	0.401	0.483	0.957	22.3	0.194	0.401	0.076
13.143	0.193	0.602	0.398	0.486	0.955	22.0	0.193	0.398	0.077
13.286	0.193	0.603	0.397	0.486	0.953	21.7	0.193	0.397	0.078
13.436	0.192	0.604	0.396	0.485	0.950	21.4	0.192	0.396	0.078
13.605	0.192	0.607	0.393	0.487	0.947	21.1	0.192	0.393	0.078
13.774	0.191	0.609	0.391	0.489	0.944	20.7	0.191	0.391	0.075
13.937	0.190	0.611	0.389	0.489	0.940	20.4	0.190	0.389	0.076
14.089	0.190	0.612	0.388	0.489	0.938	20.1	0.190	0.388	0.080
14.246	0.190	0.611	0.389	0.487	0.937	19.9	0.190	0.389	0.080
14.407	0.189	0.620	0.380	0.498	0.935	19.6	0.189	0.380	0.082
14.592	0.188	0.625	0.375	0.501	0.928	19.2	0.188	0.375	0.076
14.744	0.187	0.625	0.375	0.499	0.925	19.0	0.187	0.375	0.077
14.897	0.186	0.626	0.374	0.498	0.921	18.7	0.186	0.374	0.077
15.041	0.186	0.628	0.372	0.500	0.919	18.5	0.186	0.372	0.078
15.184	0.185	0.632	0.368	0.503	0.915	18.2	0.185	0.368	0.079
15.345	0.185	0.632	0.368	0.502	0.912	18.0	0.185	0.368	0.080
15.497	0.184	0.633	0.367	0.501	0.910	17.8	0.184	0.367	0.082
15.660	0.184	0.635	0.365	0.503	0.907	17.5	0.184	0.365	0.083
15.819	0.183	0.637	0.363	0.505	0.905	17.3	0.183	0.363	0.081
15.975	0.182	0.638	0.362	0.504	0.901	17.1	0.182	0.362	0.082

shr.stn	sh.sts.	ndelU.	nv.sts.	nsh./v.st	sh./su	eu/su	sh/mpp	v.sts/mpp	v.stn
16.120	0.182	0.641	0.359	0.507	0.900	16.9	0.182	0.359	0.083
16.287	0.181	0.648	0.352	0.516	0.896	16.7	0.181	0.352	0.084
16.448	0.181	0.651	0.349	0.517	0.893	16.4	0.181	0.349	0.078
16.580	0.180	0.653	0.347	0.519	0.890	16.2	0.180	0.347	0.079
16.743	0.180	0.655	0.345	0.521	0.888	16.1	0.180	0.345	0.076
16.896	0.179	0.659	0.341	0.526	0.886	15.9	0.179	0.341	0.074
17.060	0.179	0.659	0.341	0.524	0.883	15.7	0.179	0.341	0.070
17.195	0.178	0.659	0.341	0.524	0.881	15.5	0.178	0.341	0.079
17.370	0.177	0.666	0.334	0.531	0.877	15.3	0.177	0.334	0.077
17.524	0.177	0.665	0.335	0.529	0.874	15.1	0.177	0.335	0.071
17.671	0.176	0.665	0.335	0.527	0.871	14.9	0.176	0.335	0.069
17.825	0.176	0.666	0.334	0.527	0.870	14.8	0.176	0.334	0.080
17.980	0.176	0.668	0.332	0.529	0.868	14.6	0.176	0.332	0.087
18.133	0.175	0.673	0.327	0.536	0.865	14.5	0.175	0.327	0.092
18.290	0.174	0.675	0.325	0.537	0.861	14.3	0.174	0.325	0.096
18.448	0.173	0.677	0.323	0.537	0.857	14.1	0.173	0.323	0.098
18.605	0.173	0.677	0.323	0.536	0.855	13.9	0.173	0.323	0.102
18.762	0.172	0.679	0.321	0.538	0.852	13.8	0.172	0.321	0.107
18.912	0.172	0.683	0.317	0.543	0.850	13.6	0.172	0.317	0.109
19.061	0.171	0.683	0.317	0.541	0.847	13.5	0.171	0.317	0.110
19.212	0.171	0.686	0.314	0.544	0.845	13.3	0.171	0.314	0.097
19.366	0.171	0.688	0.312	0.547	0.844	13.2	0.171	0.312	0.100
19.521	0.170	0.692	0.308	0.553	0.841	13.0	0.170	0.308	0.102
19.674	0.169	0.695	0.305	0.555	0.837	12.9	0.169	0.305	0.103
19.831	0.168	0.695	0.305	0.553	0.832	12.7	0.168	0.305	0.103
19.987	0.168	0.696	0.304	0.552	0.830	12.6	0.168	0.304	0.107
20.138	0.167	0.696	0.304	0.551	0.827	12.4	0.167	0.304	0.107
20.295	0.167	0.700	0.300	0.556	0.824	12.3	0.167	0.300	0.100
20.441	0.166	0.702	0.298	0.558	0.821	12.2	0.166	0.298	0.099
20.597	0.166	0.703	0.297	0.558	0.819	12.0	0.166	0.297	0.093
20.748	0.165	0.707	0.293	0.563	0.816	11.9	0.165	0.293	0.097
20.907	0.164	0.708	0.292	0.563	0.810	11.7	0.164	0.292	0.102
21.056	0.163	0.711	0.289	0.565	0.807	11.6	0.163	0.289	0.110
21.212	0.162	0.712	0.288	0.565	0.803	11.5	0.162	0.288	0.110
21.337	0.162	0.713	0.287	0.564	0.800	11.4	0.162	0.287	0.116
21.494	0.161	0.715	0.285	0.565	0.797	11.2	0.161	0.285	0.112
21.636	0.161	0.716	0.284	0.566	0.794	11.1	0.161	0.284	0.109
21.791	0.160	0.725	0.275	0.580	0.790	11.0	0.160	0.275	0.111
21.952	0.159	0.724	0.276	0.575	0.783	10.8	0.159	0.276	0.112
22.107	0.158	0.726	0.274	0.576	0.780	10.7	0.158	0.274	0.112
22.266	0.157	0.730	0.270	0.580	0.774	10.5	0.157	0.270	0.108
22.426	0.156	0.734	0.266	0.586	0.770	10.4	0.156	0.266	0.111
22.585	0.154	0.736	0.264	0.584	0.763	10.2	0.154	0.264	0.119
22.745	0.153	0.737	0.263	0.583	0.758	10.1	0.153	0.263	0.127
22.895	0.152	0.742	0.258	0.590	0.752	10.0	0.152	0.258	0.134
23.059	0.151	0.746	0.254	0.593	0.745	9.8	0.151	0.254	0.126
23.212	0.150	0.747	0.253	0.593	0.740	9.7	0.150	0.253	0.131
23.381	0.149	0.753	0.247	0.601	0.734	9.5	0.149	0.247	0.124
23.554	0.147	0.754	0.246	0.598	0.727	9.4	0.147	0.246	0.125
23.712	0.146	0.756	0.244	0.597	0.720	9.2	0.146	0.244	0.128
23.871	0.145	0.759	0.241	0.601	0.716	9.1	0.145	0.241	0.120
24.028	0.144	0.759	0.241	0.597	0.710	9.0	0.144	0.241	0.119

shr.stn	sh.sts.	ndelU.	nv.sts.	nsh./v.st	sh./su	eu/su	sh/mpp	v.sts/mpp	v.stn
24.182	0.143	0.765	0.235	0.607	0.706	8.9	0.143	0.235	0.131
24.333	0.142	0.767	0.233	0.610	0.701	8.7	0.142	0.233	0.136
24.496	0.141	0.771	0.229	0.616	0.695	8.6	0.141	0.229	0.136
24.659	0.139	0.773	0.227	0.615	0.689	8.5	0.139	0.227	0.129
24.815	0.138	0.775	0.225	0.614	0.683	8.4	0.138	0.225	0.132
24.972	0.137	0.777	0.223	0.615	0.679	8.3	0.137	0.223	0.133
25.131	0.136	0.782	0.218	0.624	0.673	8.1	0.136	0.218	0.130
25.291	0.135	0.784	0.216	0.626	0.667	8.0	0.135	0.216	0.130
25.444	0.134	0.787	0.213	0.628	0.662	7.9	0.134	0.213	0.132
25.611	0.133	0.790	0.210	0.633	0.656	7.8	0.133	0.210	0.126
25.762	0.132	0.791	0.209	0.630	0.650	7.7	0.132	0.209	0.120
25.914	0.131	0.796	0.204	0.640	0.647	7.6	0.131	0.204	0.118
26.071	0.130	0.795	0.205	0.634	0.642	7.5	0.130	0.205	0.126
26.216	0.129	0.796	0.204	0.632	0.638	7.4	0.129	0.204	0.131
26.369	0.129	0.798	0.202	0.638	0.635	7.3	0.129	0.202	0.139
26.520	0.128	0.799	0.201	0.635	0.630	7.2	0.128	0.201	0.135
26.675	0.127	0.805	0.195	0.651	0.626	7.1	0.127	0.195	0.139
26.835	0.125	0.809	0.191	0.655	0.619	7.0	0.125	0.191	0.127
26.992	0.124	0.809	0.191	0.649	0.613	6.9	0.124	0.191	0.125
27.143	0.123	0.809	0.191	0.645	0.609	6.8	0.123	0.191	0.132
27.295	0.123	0.812	0.188	0.650	0.605	6.7	0.123	0.188	0.134
27.442	0.122	0.815	0.185	0.656	0.601	6.7	0.122	0.185	0.137
27.593	0.121	0.816	0.184	0.654	0.596	6.6	0.121	0.184	0.133
27.747	0.120	0.816	0.184	0.651	0.592	6.5	0.120	0.184	0.141
27.896	0.119	0.817	0.183	0.651	0.588	6.4	0.119	0.183	0.142
28.055	0.118	0.823	0.177	0.668	0.582	6.3	0.118	0.177	0.135
28.208	0.117	0.823	0.177	0.659	0.576	6.2	0.117	0.177	0.142
28.350	0.116	0.824	0.176	0.660	0.574	6.2	0.116	0.176	0.146
28.497	0.115	0.826	0.174	0.662	0.570	6.1	0.115	0.174	0.136
28.646	0.115	0.826	0.174	0.660	0.567	6.0	0.115	0.174	0.135
28.792	0.114	0.832	0.168	0.680	0.564	6.0	0.114	0.168	0.147
28.945	0.113	0.831	0.169	0.669	0.557	5.9	0.113	0.169	0.137
29.082	0.113	0.832	0.168	0.668	0.556	5.8	0.113	0.168	0.145
29.224	0.112	0.833	0.167	0.672	0.553	5.8	0.112	0.167	0.153
29.381	0.111	0.839	0.161	0.688	0.548	5.7	0.111	0.161	0.155
29.532	0.110	0.838	0.162	0.678	0.542	5.6	0.110	0.162	0.151
29.678	0.109	0.839	0.161	0.678	0.540	5.5	0.109	0.161	0.156
29.816	0.109	0.839	0.161	0.676	0.537	5.5	0.109	0.161	0.158
29.961	0.108	0.840	0.160	0.677	0.535	5.4	0.108	0.160	0.156
30.113	0.107	0.845	0.155	0.690	0.530	5.4	0.107	0.155	0.158
30.263	0.106	0.845	0.155	0.684	0.525	5.3	0.106	0.155	0.151
30.397	0.106	0.845	0.155	0.682	0.524	5.2	0.106	0.155	0.145
30.535	0.105	0.845	0.155	0.680	0.521	5.2	0.105	0.155	0.151
30.680	0.105	0.845	0.155	0.679	0.520	5.2	0.105	0.155	0.155
30.826	0.104	0.848	0.152	0.685	0.514	5.1	0.104	0.152	0.161
30.977	0.103	0.848	0.152	0.681	0.510	5.0	0.103	0.152	0.165
31.114	0.103	0.847	0.153	0.670	0.506	5.0	0.103	0.153	0.165
31.275	0.101	0.854	0.146	0.691	0.499	4.9	0.101	0.146	0.170
31.413	0.101	0.855	0.145	0.694	0.497	4.8	0.101	0.145	0.168
31.554	0.100	0.855	0.145	0.688	0.493	4.8	0.100	0.145	0.166
31.695	0.099	0.855	0.145	0.688	0.491	4.7	0.099	0.145	0.163
31.839	0.098	0.858	0.142	0.693	0.485	4.7	0.098	0.142	0.162

shr.stn	sh.sts.	ndelU.	nv.sts.	nsh./v.st	sh./su	eu/su	sh/mpp	v.sts/mpp	v.stn
31.974	0.098	0.859	0.141	0.696	0.484	4.6	0.098	0.141	0.169
32.127	0.096	0.861	0.139	0.692	0.476	4.5	0.096	0.139	0.163
32.271	0.096	0.861	0.139	0.689	0.474	4.5	0.096	0.139	0.166
32.406	0.095	0.861	0.139	0.686	0.472	4.4	0.095	0.139	0.169
32.541	0.095	0.862	0.138	0.690	0.470	4.4	0.095	0.138	0.167
32.697	0.094	0.863	0.137	0.691	0.467	4.4	0.094	0.137	0.170
32.822	0.094	0.864	0.136	0.691	0.463	4.3	0.094	0.136	0.179
32.962	0.093	0.867	0.133	0.697	0.459	4.3	0.093	0.133	0.181
33.103	0.092	0.867	0.133	0.692	0.455	4.2	0.092	0.133	0.176
33.244	0.091	0.868	0.132	0.695	0.452	4.2	0.091	0.132	0.187
33.384	0.091	0.869	0.131	0.694	0.448	4.1	0.091	0.131	0.184
33.531	0.090	0.870	0.130	0.692	0.445	4.1	0.090	0.130	0.188
33.672	0.089	0.870	0.130	0.690	0.442	4.0	0.089	0.130	0.186
33.830	0.089	0.872	0.128	0.694	0.439	4.0	0.089	0.128	0.190
33.945	0.088	0.872	0.128	0.693	0.437	3.9	0.088	0.128	0.186
34.088	0.088	0.874	0.126	0.695	0.434	3.9	0.088	0.126	0.183
34.228	0.087	0.876	0.124	0.703	0.429	3.8	0.087	0.124	0.191
34.371	0.086	0.876	0.124	0.699	0.426	3.8	0.086	0.124	0.184
34.516	0.085	0.878	0.122	0.702	0.422	3.7	0.085	0.122	0.186
34.643	0.085	0.879	0.121	0.701	0.419	3.7	0.085	0.121	0.187
34.809	0.084	0.879	0.121	0.698	0.416	3.7	0.084	0.121	0.185
34.948	0.083	0.882	0.118	0.705	0.412	3.6	0.083	0.118	0.185
35.084	0.082	0.883	0.117	0.703	0.407	3.6	0.082	0.117	0.186
35.211	0.082	0.884	0.116	0.705	0.406	3.5	0.082	0.116	0.188
35.361	0.081	0.884	0.116	0.702	0.401	3.5	0.081	0.116	0.183
35.486	0.081	0.885	0.115	0.699	0.399	3.4	0.081	0.115	0.181
35.599	0.080	0.886	0.114	0.705	0.396	3.4	0.080	0.114	0.187
35.775	0.079	0.887	0.113	0.703	0.393	3.4	0.079	0.113	0.194
35.906	0.079	0.888	0.112	0.703	0.389	3.3	0.079	0.112	0.196
36.039	0.078	0.888	0.112	0.698	0.387	3.3	0.078	0.112	0.201
36.169	0.078	0.888	0.112	0.696	0.386	3.3	0.078	0.112	0.200
36.300	0.078	0.888	0.112	0.694	0.383	3.2	0.078	0.112	0.205
36.426	0.077	0.889	0.111	0.696	0.382	3.2	0.077	0.111	0.207
36.563	0.077	0.890	0.110	0.699	0.378	3.2	0.077	0.110	0.193
36.708	0.075	0.895	0.105	0.715	0.372	3.1	0.075	0.105	0.203
36.846	0.074	0.896	0.104	0.714	0.367	3.1	0.074	0.104	0.203
36.983	0.074	0.896	0.104	0.708	0.365	3.0	0.074	0.104	0.196
37.113	0.074	0.896	0.104	0.710	0.363	3.0	0.074	0.104	0.198
37.252	0.073	0.897	0.103	0.707	0.360	3.0	0.073	0.103	0.199

 Ko CONSOLIDATED GEONOR DIRECT SIMPLE SHEAR TEST
 MIT GEOTECHNICAL LAB

FILE NAME : DSS 31

 REDUCTION DATA
 UNITS: kg,cm,mVolts,Volts

1. Test Name : DSS 31
 2. Date : 4/2/89
 3. OCR : 1
 4. Ver. Consolidation Stress (ksc) :1.441
 5. Pre-Shear Height (cm) :2.1
 6. Horizontal Shear Load Cell: 7. Horizontal Displacement Transducer:
 Zero: 0.0359 Zero: 0.1164
 CF: -80.2 CF: 2.2815
 8. Vertical Stress Load Cell: 9. Vertical Height Transducer:
 Zero: 0.1149 Zero: -0.1271
 CF: -348.5 CF: 2.0655

shr.stn	sh.sts.	ndelU.	nv.sts.	nsh./v.st	sh./su	eu/su	sh/mpp	v.sts/mpp	v.stn
0.000	-0.003	0.001	0.999	-0.003	-0.015	9999.0	-0.003	0.999	0.000
0.024	0.055	0.029	0.971	0.057	0.277	3651.3	0.055	0.971	-0.004
0.047	0.067	0.029	0.971	0.069	0.336	2263.6	0.067	0.971	-0.002
0.074	0.080	0.036	0.964	0.083	0.402	1695.0	0.080	0.964	0.000
0.097	0.092	0.041	0.959	0.096	0.461	1469.2	0.092	0.959	0.000
0.138	0.103	0.045	0.955	0.108	0.517	1153.2	0.103	0.955	-0.005
0.180	0.114	0.049	0.951	0.120	0.571	976.3	0.114	0.951	0.001
0.246	0.123	0.062	0.938	0.131	0.619	774.9	0.123	0.938	0.006
0.288	0.133	0.077	0.923	0.144	0.666	710.7	0.133	0.923	0.009
0.356	0.140	0.091	0.909	0.154	0.705	607.5	0.140	0.909	0.013
0.440	0.148	0.106	0.894	0.165	0.743	516.9	0.148	0.894	0.017
0.531	0.154	0.120	0.880	0.175	0.776	447.1	0.154	0.880	0.023
0.632	0.159	0.133	0.867	0.184	0.802	387.8	0.159	0.867	0.032
0.689	0.164	0.149	0.851	0.193	0.826	366.2	0.164	0.851	0.047
0.812	0.168	0.166	0.834	0.201	0.844	317.5	0.168	0.834	0.061
0.908	0.171	0.195	0.805	0.213	0.862	289.5	0.171	0.805	0.074
1.009	0.175	0.231	0.769	0.228	0.880	266.3	0.175	0.769	0.076
1.110	0.178	0.244	0.756	0.236	0.897	246.5	0.178	0.756	0.077
1.241	0.181	0.253	0.747	0.242	0.910	223.8	0.181	0.747	0.091
1.359	0.184	0.267	0.733	0.250	0.923	207.1	0.184	0.733	0.105
1.478	0.186	0.281	0.719	0.258	0.932	192.3	0.186	0.719	0.118
1.599	0.187	0.330	0.670	0.279	0.940	179.3	0.187	0.670	0.126
1.730	0.188	0.392	0.608	0.309	0.944	166.3	0.188	0.608	0.092
1.841	0.190	0.388	0.612	0.310	0.955	158.1	0.190	0.612	0.084
1.988	0.192	0.388	0.612	0.314	0.967	148.2	0.192	0.612	0.090
2.111	0.194	0.397	0.603	0.321	0.973	140.4	0.194	0.603	0.090
2.251	0.195	0.407	0.593	0.329	0.980	132.6	0.195	0.593	0.087
2.366	0.195	0.420	0.580	0.337	0.982	126.4	0.195	0.580	0.092
2.537	0.196	0.428	0.572	0.344	0.987	118.5	0.196	0.572	0.094
2.655	0.197	0.439	0.561	0.351	0.990	113.6	0.197	0.561	0.096
2.783	0.198	0.445	0.555	0.356	0.994	108.8	0.198	0.555	0.099

shr.stn	sh.sts.	ndelU.	nv.sts.	nsh./v.st	sh./su	eu/su	sh/mpp	v.sts/mpp	v.stn
2.946	0.198	0.453	0.547	0.362	0.995	102.9	0.198	0.547	0.103
3.072	0.198	0.462	0.538	0.368	0.994	98.6	0.198	0.538	0.104
3.234	0.198	0.470	0.530	0.374	0.997	93.9	0.198	0.530	0.102
3.381	0.198	0.481	0.519	0.382	0.996	89.7	0.198	0.519	0.110
3.504	0.198	0.487	0.513	0.387	0.997	86.7	0.198	0.513	0.113
3.670	0.198	0.495	0.505	0.393	0.997	82.7	0.198	0.505	0.114
3.789	0.198	0.503	0.497	0.399	0.997	80.1	0.198	0.497	0.110
3.960	0.199	0.506	0.494	0.402	0.998	76.8	0.199	0.494	0.111
4.098	0.199	0.515	0.485	0.410	1.000	74.3	0.199	0.485	0.114
4.239	0.199	0.523	0.477	0.417	1.000	71.8	0.199	0.477	0.113
4.385	0.199	0.530	0.470	0.423	0.999	69.4	0.199	0.470	0.118
4.506	0.199	0.537	0.463	0.429	0.999	67.5	0.199	0.463	0.120
4.665	0.199	0.539	0.461	0.432	0.999	65.2	0.199	0.461	0.110
4.808	0.199	0.544	0.456	0.436	0.999	63.3	0.199	0.456	0.114
4.960	0.199	0.550	0.450	0.442	0.998	61.3	0.199	0.450	0.119
5.107	0.199	0.558	0.442	0.449	0.999	59.6	0.199	0.442	0.119
5.239	0.199	0.561	0.439	0.453	0.998	58.0	0.199	0.439	0.116
5.388	0.199	0.564	0.436	0.455	0.999	56.5	0.199	0.436	0.124
5.524	0.199	0.569	0.431	0.461	0.998	55.0	0.199	0.431	0.125
5.667	0.199	0.579	0.421	0.471	0.998	53.6	0.199	0.421	0.116
5.805	0.198	0.579	0.421	0.472	0.997	52.3	0.198	0.421	0.114
5.956	0.198	0.580	0.420	0.472	0.997	51.0	0.198	0.420	0.112
6.112	0.198	0.582	0.418	0.474	0.997	49.7	0.198	0.418	0.122
6.246	0.198	0.587	0.413	0.480	0.996	48.6	0.198	0.413	0.133
6.380	0.198	0.593	0.407	0.487	0.996	47.5	0.198	0.407	0.130
6.524	0.198	0.598	0.402	0.493	0.995	46.5	0.198	0.402	0.120
6.679	0.198	0.600	0.400	0.495	0.995	45.4	0.198	0.400	0.128
6.835	0.198	0.603	0.397	0.498	0.994	44.3	0.198	0.397	0.134
6.957	0.198	0.604	0.396	0.499	0.993	43.5	0.198	0.396	0.130
7.123	0.198	0.604	0.396	0.499	0.993	42.4	0.198	0.396	0.129
7.244	0.197	0.607	0.393	0.502	0.991	41.7	0.197	0.393	0.136
7.412	0.197	0.622	0.378	0.521	0.990	40.7	0.197	0.378	0.132
7.539	0.197	0.620	0.380	0.518	0.988	39.9	0.197	0.380	0.129
7.694	0.197	0.622	0.378	0.520	0.988	39.1	0.197	0.378	0.135
7.814	0.196	0.624	0.376	0.521	0.985	38.4	0.196	0.376	0.132
7.978	0.196	0.627	0.373	0.526	0.984	37.6	0.196	0.373	0.131
8.121	0.195	0.635	0.365	0.535	0.982	36.8	0.195	0.365	0.136
8.283	0.195	0.639	0.361	0.540	0.981	36.1	0.195	0.361	0.127
8.419	0.195	0.639	0.361	0.541	0.981	35.5	0.195	0.361	0.128
8.567	0.195	0.640	0.360	0.541	0.979	34.8	0.195	0.360	0.124
8.710	0.194	0.645	0.355	0.547	0.977	34.2	0.194	0.355	0.116
8.839	0.194	0.647	0.353	0.549	0.974	33.6	0.194	0.353	0.113
8.978	0.194	0.648	0.352	0.551	0.974	33.0	0.194	0.352	0.115
9.135	0.193	0.648	0.352	0.550	0.971	32.4	0.193	0.352	0.114
9.282	0.193	0.649	0.351	0.551	0.971	31.9	0.193	0.351	0.116
9.442	0.193	0.655	0.345	0.558	0.968	31.3	0.193	0.345	0.122
9.583	0.192	0.655	0.345	0.557	0.967	30.7	0.192	0.345	0.125
9.740	0.192	0.656	0.344	0.558	0.966	30.2	0.192	0.344	0.129
9.874	0.191	0.656	0.344	0.557	0.962	29.7	0.191	0.344	0.123
10.007	0.191	0.658	0.342	0.560	0.961	29.3	0.191	0.342	0.119
10.159	0.191	0.665	0.335	0.570	0.958	28.7	0.191	0.335	0.121
10.314	0.190	0.668	0.332	0.573	0.956	28.2	0.190	0.332	0.120

shr.stn	sh.sts.	ndelU.	nv.sts.	nsh./v.st	sh./su	eu/su	sh/mpp	v.sts/mpp	v.stn
10.428	0.190	0.671	0.329	0.576	0.953	27.9	0.190	0.329	0.120
10.597	0.190	0.671	0.329	0.576	0.953	27.4	0.190	0.329	0.126
10.733	0.190	0.671	0.329	0.576	0.953	27.1	0.190	0.329	0.129
10.891	0.189	0.671	0.329	0.576	0.952	26.6	0.189	0.329	0.131
11.017	0.189	0.671	0.329	0.576	0.951	26.3	0.189	0.329	0.127
11.172	0.189	0.675	0.325	0.581	0.950	25.9	0.189	0.325	0.131
11.327	0.189	0.679	0.321	0.589	0.949	25.5	0.189	0.321	0.130
11.472	0.188	0.679	0.321	0.587	0.947	25.2	0.188	0.321	0.129
11.618	0.188	0.685	0.315	0.598	0.946	24.8	0.188	0.315	0.128
11.763	0.188	0.686	0.314	0.598	0.944	24.5	0.188	0.314	0.121
11.924	0.188	0.686	0.314	0.599	0.944	24.1	0.188	0.314	0.120
12.082	0.188	0.686	0.314	0.599	0.945	23.8	0.188	0.314	0.125
12.239	0.188	0.687	0.313	0.599	0.944	23.5	0.188	0.313	0.123
12.385	0.188	0.687	0.313	0.600	0.944	23.2	0.188	0.313	0.128
12.536	0.188	0.688	0.312	0.601	0.943	22.9	0.188	0.312	0.132
12.683	0.187	0.695	0.305	0.616	0.942	22.6	0.187	0.305	0.136
12.833	0.187	0.695	0.305	0.613	0.940	22.3	0.187	0.305	0.132
12.982	0.187	0.697	0.303	0.615	0.938	22.0	0.187	0.303	0.135
13.132	0.186	0.702	0.298	0.624	0.934	21.7	0.186	0.298	0.134
13.285	0.185	0.701	0.299	0.621	0.932	21.4	0.185	0.299	0.134
13.430	0.185	0.701	0.299	0.618	0.928	21.1	0.185	0.299	0.130
13.582	0.184	0.708	0.292	0.630	0.924	20.7	0.184	0.292	0.128
13.735	0.183	0.708	0.292	0.627	0.921	20.4	0.183	0.292	0.127
13.885	0.182	0.708	0.292	0.624	0.916	20.1	0.182	0.292	0.131
14.034	0.182	0.708	0.292	0.623	0.915	19.9	0.182	0.292	0.128
14.181	0.182	0.708	0.292	0.622	0.913	19.6	0.182	0.292	0.125
14.335	0.181	0.708	0.292	0.620	0.910	19.4	0.181	0.292	0.126
14.484	0.181	0.709	0.291	0.620	0.908	19.1	0.181	0.291	0.126
14.640	0.180	0.709	0.291	0.618	0.903	18.8	0.180	0.291	0.124
14.789	0.179	0.710	0.290	0.617	0.900	18.6	0.179	0.290	0.127
14.938	0.178	0.711	0.289	0.616	0.897	18.3	0.178	0.289	0.130
15.084	0.178	0.711	0.289	0.618	0.896	18.1	0.178	0.289	0.138
15.227	0.178	0.712	0.288	0.618	0.894	17.9	0.178	0.288	0.137
15.377	0.178	0.713	0.287	0.619	0.893	17.7	0.178	0.287	0.137
15.520	0.177	0.714	0.286	0.620	0.892	17.5	0.177	0.286	0.137
15.671	0.177	0.720	0.280	0.634	0.891	17.3	0.177	0.280	0.139
15.821	0.177	0.721	0.279	0.634	0.888	17.1	0.177	0.279	0.141
15.968	0.176	0.721	0.279	0.633	0.887	16.9	0.176	0.279	0.143
16.122	0.176	0.722	0.278	0.633	0.886	16.8	0.176	0.278	0.143
16.274	0.176	0.722	0.278	0.633	0.884	16.6	0.176	0.278	0.143
16.420	0.176	0.723	0.277	0.634	0.882	16.4	0.176	0.277	0.153
16.564	0.175	0.724	0.276	0.635	0.881	16.2	0.175	0.276	0.160
16.712	0.175	0.725	0.275	0.637	0.880	16.1	0.175	0.275	0.158
16.857	0.175	0.728	0.272	0.642	0.877	15.9	0.175	0.272	0.164
17.008	0.174	0.732	0.268	0.649	0.875	15.7	0.174	0.268	0.161
17.156	0.173	0.733	0.267	0.649	0.870	15.5	0.173	0.267	0.159
17.305	0.173	0.734	0.266	0.649	0.868	15.3	0.173	0.266	0.157
17.452	0.172	0.735	0.265	0.648	0.864	15.1	0.172	0.265	0.166
17.598	0.171	0.737	0.263	0.651	0.862	14.9	0.171	0.263	0.170
17.748	0.171	0.742	0.258	0.663	0.859	14.8	0.171	0.258	0.173
17.899	0.170	0.743	0.257	0.660	0.854	14.6	0.170	0.257	0.171
18.054	0.169	0.750	0.250	0.675	0.849	14.4	0.169	0.250	0.179

shr.stn	sh.sts.	ndelU.	nv.sts.	nsh./v.st	sh./su	eu/su	sh/mpp	v.sts/mpp	v.stn
18.207	0.168	0.754	0.246	0.681	0.843	14.1	0.168	0.246	0.181
18.359	0.167	0.755	0.245	0.683	0.840	14.0	0.167	0.245	0.178
18.505	0.166	0.759	0.241	0.691	0.835	13.8	0.166	0.241	0.182
18.658	0.165	0.761	0.239	0.691	0.830	13.6	0.165	0.239	0.177
18.809	0.164	0.761	0.239	0.689	0.826	13.4	0.164	0.239	0.175
18.959	0.164	0.766	0.234	0.698	0.822	13.2	0.164	0.234	0.179
19.106	0.163	0.767	0.233	0.700	0.818	13.1	0.163	0.233	0.186
19.246	0.162	0.768	0.232	0.697	0.814	12.9	0.162	0.232	0.181
19.397	0.162	0.769	0.231	0.700	0.812	12.8	0.162	0.231	0.183
19.548	0.160	0.778	0.222	0.721	0.806	12.6	0.160	0.222	0.188
19.704	0.159	0.780	0.220	0.724	0.800	12.4	0.159	0.220	0.186
19.853	0.158	0.780	0.220	0.719	0.794	12.2	0.158	0.220	0.190
20.005	0.157	0.785	0.215	0.730	0.789	12.1	0.157	0.215	0.192
20.156	0.156	0.789	0.211	0.740	0.785	11.9	0.156	0.211	0.185
20.309	0.155	0.791	0.209	0.740	0.779	11.7	0.155	0.209	0.188
20.453	0.154	0.792	0.208	0.740	0.776	11.6	0.154	0.208	0.192
20.604	0.154	0.792	0.208	0.738	0.772	11.5	0.154	0.208	0.197
20.758	0.153	0.794	0.206	0.743	0.768	11.3	0.153	0.206	0.194
20.909	0.152	0.803	0.197	0.768	0.762	11.1	0.152	0.197	0.190
21.062	0.151	0.804	0.196	0.766	0.756	11.0	0.151	0.196	0.190
21.212	0.150	0.804	0.196	0.762	0.752	10.9	0.150	0.196	0.192
21.357	0.149	0.804	0.196	0.760	0.749	10.7	0.149	0.196	0.195
21.499	0.149	0.805	0.195	0.760	0.747	10.6	0.149	0.195	0.194
21.644	0.148	0.806	0.194	0.760	0.743	10.5	0.148	0.194	0.197
21.794	0.147	0.807	0.193	0.765	0.741	10.4	0.147	0.193	0.193
21.939	0.147	0.810	0.190	0.773	0.737	10.3	0.147	0.190	0.195
22.088	0.146	0.811	0.189	0.774	0.734	10.2	0.146	0.189	0.194
22.232	0.145	0.819	0.181	0.802	0.730	10.1	0.145	0.181	0.201
22.381	0.144	0.819	0.181	0.795	0.724	9.9	0.144	0.181	0.196
22.531	0.144	0.819	0.181	0.795	0.721	9.8	0.144	0.181	0.193
22.680	0.143	0.820	0.180	0.791	0.717	9.7	0.143	0.180	0.189
22.831	0.142	0.820	0.180	0.790	0.714	9.6	0.142	0.180	0.190
22.971	0.141	0.821	0.179	0.790	0.711	9.5	0.141	0.179	0.196
23.118	0.141	0.822	0.178	0.793	0.709	9.4	0.141	0.178	0.205
23.264	0.140	0.822	0.178	0.789	0.704	9.3	0.140	0.178	0.204
23.413	0.139	0.830	0.170	0.817	0.700	9.2	0.139	0.170	0.208
23.558	0.138	0.830	0.170	0.812	0.696	9.1	0.138	0.170	0.208
23.708	0.138	0.830	0.170	0.809	0.692	8.9	0.138	0.170	0.206
23.851	0.137	0.830	0.170	0.809	0.689	8.9	0.137	0.170	0.209
24.003	0.136	0.834	0.166	0.819	0.685	8.8	0.136	0.166	0.217
24.150	0.135	0.837	0.163	0.830	0.681	8.6	0.135	0.163	0.224
24.288	0.135	0.837	0.163	0.823	0.676	8.5	0.135	0.163	0.219
24.433	0.134	0.841	0.159	0.843	0.675	8.5	0.134	0.159	0.226
24.572	0.134	0.843	0.157	0.853	0.672	8.4	0.134	0.157	0.226
24.722	0.133	0.846	0.154	0.862	0.667	8.3	0.133	0.154	0.225
24.861	0.132	0.847	0.153	0.866	0.665	8.2	0.132	0.153	0.225
25.009	0.132	0.847	0.153	0.863	0.662	8.1	0.132	0.153	0.229
25.154	0.131	0.847	0.153	0.861	0.660	8.1	0.131	0.153	0.227
25.300	0.130	0.857	0.143	0.905	0.652	7.9	0.130	0.143	0.225
25.445	0.130	0.856	0.144	0.900	0.651	7.9	0.130	0.144	0.221
25.586	0.129	0.856	0.144	0.897	0.648	7.8	0.129	0.144	0.227
25.728	0.129	0.857	0.143	0.898	0.647	7.7	0.129	0.143	0.233

shr.stn	sh.sts.	ndelU.	nv.sts.	nsh./v.st	sh./su	eu/su	sh/mpp	v.sts/mpp	v.stn
25.871	0.128	0.858	0.142	0.901	0.644	7.6	0.128	0.142	0.229
26.019	0.127	0.852	0.148	0.860	0.640	7.6	0.127	0.148	0.227
26.166	0.126	0.866	0.134	0.941	0.633	7.4	0.126	0.134	0.233
26.308	0.125	0.866	0.134	0.933	0.628	7.3	0.125	0.134	0.231
26.451	0.124	0.866	0.134	0.926	0.625	7.3	0.124	0.134	0.234
26.594	0.124	0.866	0.134	0.922	0.621	7.2	0.124	0.134	0.238
26.736	0.123	0.865	0.135	0.917	0.620	7.1	0.123	0.135	0.242
26.875	0.122	0.869	0.131	0.936	0.615	7.0	0.122	0.131	0.246
27.031	0.121	0.875	0.125	0.964	0.607	6.9	0.121	0.125	0.246
27.168	0.120	0.876	0.124	0.964	0.602	6.8	0.120	0.124	0.245
27.312	0.119	0.876	0.124	0.961	0.599	6.7	0.119	0.124	0.244
27.451	0.119	0.876	0.124	0.954	0.597	6.7	0.119	0.124	0.240
27.588	0.118	0.876	0.124	0.952	0.594	6.6	0.118	0.124	0.244
27.732	0.118	0.876	0.124	0.953	0.593	6.6	0.118	0.124	0.248
27.869	0.117	0.877	0.123	0.953	0.590	6.5	0.117	0.123	0.249
28.015	0.117	0.878	0.122	0.959	0.589	6.5	0.117	0.122	0.250
28.148	0.116	0.878	0.122	0.956	0.586	6.4	0.116	0.122	0.244
28.296	0.116	0.879	0.121	0.962	0.584	6.3	0.116	0.121	0.245
28.427	0.116	0.880	0.120	0.960	0.581	6.3	0.116	0.120	0.248
28.567	0.115	0.880	0.120	0.963	0.579	6.2	0.115	0.120	0.250
28.706	0.115	0.881	0.119	0.965	0.577	6.2	0.115	0.119	0.256
28.841	0.115	0.882	0.118	0.971	0.576	6.1	0.115	0.118	0.259
28.979	0.114	0.883	0.117	0.975	0.574	6.1	0.114	0.117	0.264
29.120	0.114	0.884	0.116	0.976	0.571	6.0	0.114	0.116	0.265
29.264	0.113	0.889	0.111	1.016	0.567	6.0	0.113	0.111	0.267
29.403	0.112	0.890	0.110	1.015	0.562	5.9	0.112	0.110	0.270
29.545	0.111	0.891	0.109	1.026	0.560	5.8	0.111	0.109	0.275
29.682	0.111	0.893	0.107	1.031	0.556	5.8	0.111	0.107	0.274
29.822	0.110	0.893	0.107	1.032	0.554	5.7	0.110	0.107	0.279
29.957	0.110	0.894	0.106	1.036	0.552	5.7	0.110	0.106	0.276
30.094	0.109	0.894	0.106	1.029	0.549	5.6	0.109	0.106	0.273
30.228	0.109	0.896	0.104	1.044	0.547	5.6	0.109	0.104	0.272
30.375	0.108	0.899	0.101	1.062	0.541	5.5	0.108	0.101	0.275
30.511	0.107	0.899	0.101	1.060	0.538	5.4	0.107	0.101	0.279
30.648	0.106	0.899	0.101	1.055	0.535	5.4	0.106	0.101	0.282
30.782	0.106	0.900	0.100	1.057	0.532	5.3	0.106	0.100	0.284
30.913	0.106	0.901	0.099	1.068	0.531	5.3	0.106	0.099	0.280
31.053	0.105	0.904	0.096	1.091	0.528	5.2	0.105	0.096	0.283
31.192	0.104	0.904	0.096	1.091	0.524	5.2	0.104	0.096	0.286
31.322	0.104	0.905	0.095	1.086	0.521	5.1	0.104	0.095	0.283
31.457	0.103	0.905	0.095	1.084	0.519	5.1	0.103	0.095	0.288
31.588	0.103	0.905	0.095	1.087	0.517	5.0	0.103	0.095	0.286
31.726	0.102	0.906	0.094	1.081	0.513	5.0	0.102	0.094	0.291
31.859	0.102	0.906	0.094	1.084	0.511	5.0	0.102	0.094	0.295
31.995	0.101	0.909	0.091	1.107	0.509	4.9	0.101	0.091	0.298
32.126	0.101	0.911	0.089	1.126	0.506	4.9	0.101	0.089	0.292
32.262	0.100	0.911	0.089	1.119	0.503	4.8	0.100	0.089	0.288
32.395	0.100	0.911	0.089	1.116	0.501	4.8	0.100	0.089	0.287
32.529	0.099	0.911	0.089	1.114	0.498	4.7	0.099	0.089	0.287
32.658	0.098	0.912	0.088	1.124	0.495	4.7	0.098	0.088	0.294
32.792	0.098	0.912	0.088	1.116	0.491	4.6	0.098	0.088	0.295
32.925	0.097	0.915	0.085	1.148	0.488	4.6	0.097	0.085	0.303

shr.stn	sh.sts.	ndelU.	nv.sts.	nsh./v.st	sh./su	eu/su	sh/mpp	v.sts/mpp	v.stn
33.053	0.096	0.916	0.084	1.150	0.485	4.5	0.096	0.084	0.308
33.190	0.096	0.919	0.081	1.184	0.482	4.5	0.096	0.081	0.313
33.322	0.095	0.920	0.080	1.184	0.477	4.4	0.095	0.080	0.313
33.453	0.094	0.921	0.079	1.196	0.475	4.4	0.094	0.079	0.314
33.579	0.094	0.921	0.079	1.195	0.474	4.4	0.094	0.079	0.317
33.710	0.094	0.921	0.079	1.192	0.473	4.3	0.094	0.079	0.314
33.838	0.094	0.921	0.079	1.190	0.472	4.3	0.094	0.079	0.318
33.969	0.093	0.921	0.079	1.188	0.469	4.3	0.093	0.079	0.320
34.096	0.093	0.922	0.078	1.186	0.467	4.2	0.093	0.078	0.316
34.226	0.092	0.922	0.078	1.183	0.464	4.2	0.092	0.078	0.315
34.361	0.092	0.923	0.077	1.186	0.461	4.2	0.092	0.077	0.312
34.486	0.091	0.923	0.077	1.184	0.458	4.1	0.091	0.077	0.312
34.614	0.091	0.926	0.074	1.222	0.456	4.1	0.091	0.074	0.319
34.743	0.090	0.927	0.073	1.244	0.454	4.0	0.090	0.073	0.323
34.871	0.090	0.929	0.071	1.257	0.451	4.0	0.090	0.071	0.330
35.003	0.089	0.929	0.071	1.250	0.449	4.0	0.089	0.071	0.332
35.131	0.089	0.929	0.071	1.242	0.446	3.9	0.089	0.071	0.337
35.257	0.088	0.929	0.071	1.242	0.444	3.9	0.088	0.071	0.338

Ko CONSOLIDATED GEONOR DIRECT SIMPLE SHEAR TEST
MIT GEOTECHNICAL LAB

FILE NAME : DSS 37

REDUCTION DATA

UNITS: kg,cm,mVolts,Volts

- | | |
|---|--|
| 1. Test Name : DSS 37 | 7. Horizontal Displacement Transducer: |
| 2. Date : 6/11/89 | Zero: -0.12234 |
| 3. OCR : 3.248 | CF: 2.2815 |
| 4. Ver. Consolidation Stress (ksc) :3.512 | |
| 5. Pre-Shear Height (cm) :1.777 | |
| 6. Horizontal Shear Load Cell: | |
| Zero: 0.000092 | |
| CF: 7065.518 | |
| 8. Vertical Stress Load Cell: | 9. Vertical Height Transducer: |
| Zero: 0.2103 | Zero: 0.05873 |
| CF: -1188.86 | CF: 2.0655 |

shr.stn	sh.sts.	ndelU.	nv.sts.	nsh./v.st	sh./su	eu/su	sh/mpp	v.sts/mpp	v.stn
0.000	0.003	0.001	0.999	0.003	0.006	9999.0	0.001	0.308	0.000
0.005	0.002	0.002	0.998	0.002	0.004	-146.5	0.001	0.307	-0.005
0.006	0.003	0.003	0.997	0.003	0.005	-49.9	0.001	0.307	0.001
2.000	0.003	0.003	0.997	0.003	0.006	-3.8	0.001	0.307	-0.003
0.017	0.003	0.003	0.997	0.003	0.006	7.3	0.001	0.307	-0.003
0.017	0.020	0.001	0.999	0.020	0.039	578.0	0.006	0.308	0.002
0.030	0.050	-0.001	1.001	0.050	0.097	913.0	0.015	0.308	0.000
0.060	0.092	-0.004	1.004	0.092	0.179	857.8	0.028	0.309	-0.002
0.097	0.134	-0.008	1.008	0.133	0.261	787.5	0.041	0.310	-0.002
0.179	0.178	-0.015	1.015	0.175	0.346	568.9	0.055	0.312	-0.015
0.274	0.215	-0.022	1.022	0.210	0.418	450.8	0.066	0.315	-0.025
0.388	0.246	-0.031	1.031	0.239	0.478	364.6	0.076	0.317	-0.038
0.514	0.272	-0.040	1.040	0.262	0.528	305.1	0.084	0.320	-0.052
0.639	0.292	-0.048	1.048	0.278	0.567	263.2	0.090	0.323	-0.068
0.772	0.312	-0.071	1.071	0.291	0.606	233.2	0.096	0.330	-0.082
0.907	0.328	-0.077	1.077	0.304	0.637	208.9	0.101	0.332	-0.087
1.044	0.346	-0.117	1.117	0.310	0.672	191.4	0.106	0.344	-0.099
1.184	0.361	-0.134	1.134	0.318	0.701	176.0	0.111	0.349	-0.098
1.334	0.374	-0.149	1.149	0.325	0.726	161.9	0.115	0.354	-0.098
1.482	0.386	-0.164	1.164	0.332	0.751	150.7	0.119	0.359	-0.103
1.634	0.396	-0.168	1.168	0.339	0.769	140.0	0.122	0.360	-0.105
1.787	0.407	-0.193	1.193	0.341	0.790	131.6	0.125	0.367	-0.104
1.937	0.414	-0.197	1.197	0.346	0.805	123.8	0.128	0.368	-0.103
2.097	0.423	-0.207	1.207	0.350	0.822	116.7	0.130	0.372	-0.102
2.251	0.429	-0.208	1.208	0.355	0.834	110.3	0.132	0.372	-0.105
2.415	0.435	-0.217	1.217	0.358	0.846	104.4	0.134	0.375	-0.104
2.571	0.441	-0.225	1.225	0.360	0.857	99.3	0.136	0.377	-0.100
2.735	0.446	-0.226	1.226	0.364	0.867	94.4	0.137	0.378	-0.106
2.897	0.451	-0.227	1.227	0.367	0.876	90.1	0.139	0.378	-0.104
3.059	0.454	-0.229	1.229	0.370	0.883	86.0	0.140	0.378	-0.105
3.225	0.459	-0.229	1.229	0.373	0.891	82.4	0.141	0.378	-0.110

shr.stn	sh.sts.	ndelU.	nv.sts.	nsh./v.st	sh./su	eu/su	sh/mpp	v.sts/mpp	v.stn
3.386	0.461	-0.230	1.230	0.375	0.896	78.9	0.142	0.379	-0.107
3.554	0.465	-0.235	1.235	0.377	0.904	75.8	0.143	0.380	-0.112
3.716	0.469	-0.243	1.243	0.377	0.911	73.0	0.144	0.383	-0.105
3.887	0.472	-0.243	1.243	0.380	0.918	70.4	0.145	0.383	-0.108
4.051	0.475	-0.243	1.243	0.382	0.923	67.9	0.146	0.383	-0.106
4.218	0.477	-0.243	1.243	0.384	0.927	65.5	0.147	0.383	-0.105
4.383	0.480	-0.243	1.243	0.386	0.933	63.4	0.148	0.383	-0.103
4.550	0.481	-0.242	1.242	0.387	0.935	61.3	0.148	0.382	-0.101
4.722	0.484	-0.242	1.242	0.390	0.941	59.4	0.149	0.382	-0.103
4.888	0.486	-0.241	1.241	0.391	0.944	57.6	0.150	0.382	-0.100
5.058	0.488	-0.238	1.238	0.394	0.948	55.9	0.150	0.381	-0.104
5.227	0.490	-0.237	1.237	0.396	0.952	54.3	0.151	0.381	-0.100
5.398	0.492	-0.237	1.237	0.397	0.955	52.8	0.151	0.381	-0.096
5.561	0.493	-0.236	1.236	0.399	0.958	51.4	0.152	0.380	-0.095
5.733	0.494	-0.235	1.235	0.400	0.960	49.9	0.152	0.380	-0.095
5.903	0.496	-0.234	1.234	0.402	0.964	48.7	0.153	0.380	-0.093
6.074	0.497	-0.233	1.233	0.403	0.965	47.4	0.153	0.380	-0.095
6.250	0.499	-0.232	1.232	0.405	0.969	46.2	0.154	0.379	-0.099
6.417	0.499	-0.231	1.231	0.405	0.970	45.1	0.154	0.379	-0.094
6.590	0.501	-0.230	1.230	0.407	0.973	44.0	0.154	0.379	-0.094
6.757	0.502	-0.230	1.230	0.408	0.975	43.0	0.154	0.379	-0.091
6.931	0.502	-0.228	1.228	0.409	0.976	42.0	0.155	0.378	-0.088
7.099	0.504	-0.227	1.227	0.411	0.979	41.1	0.155	0.378	-0.084
7.269	0.504	-0.226	1.226	0.411	0.980	40.2	0.155	0.378	-0.082
7.440	0.506	-0.225	1.225	0.413	0.983	39.4	0.156	0.377	-0.082
7.611	0.506	-0.224	1.224	0.413	0.983	38.5	0.156	0.377	-0.080
7.783	0.507	-0.223	1.223	0.415	0.986	37.8	0.156	0.377	-0.081
7.952	0.508	-0.222	1.222	0.416	0.987	37.0	0.156	0.376	-0.081
8.127	0.509	-0.221	1.221	0.417	0.990	36.3	0.157	0.376	-0.078
8.299	0.510	-0.220	1.220	0.418	0.991	35.6	0.157	0.376	-0.074
8.477	0.510	-0.218	1.218	0.419	0.992	34.9	0.157	0.375	-0.068
8.654	0.511	-0.217	1.217	0.420	0.994	34.2	0.157	0.375	-0.069
8.827	0.511	-0.215	1.215	0.420	0.993	33.5	0.157	0.374	-0.064
8.999	0.512	-0.214	1.214	0.422	0.995	33.0	0.158	0.374	-0.057
9.169	0.512	-0.213	1.213	0.422	0.994	32.3	0.158	0.373	-0.059
9.343	0.513	-0.211	1.211	0.423	0.997	31.8	0.158	0.373	-0.050
9.510	0.513	-0.210	1.210	0.424	0.996	31.2	0.158	0.373	-0.050
9.689	0.513	-0.209	1.209	0.425	0.997	30.7	0.158	0.372	-0.044
9.859	0.513	-0.207	1.207	0.425	0.998	30.2	0.158	0.372	-0.037
10.035	0.513	-0.205	1.205	0.426	0.997	29.6	0.158	0.371	-0.032
10.207	0.514	-0.204	1.204	0.427	0.999	29.2	0.158	0.371	-0.032
10.379	0.513	-0.202	1.202	0.427	0.998	28.7	0.158	0.370	-0.031
10.550	0.515	-0.200	1.200	0.429	1.000	28.3	0.158	0.370	-0.026
10.720	0.514	-0.199	1.199	0.428	0.998	27.8	0.158	0.369	-0.024
10.892	0.514	-0.197	1.197	0.430	1.000	27.4	0.158	0.369	-0.016
11.061	0.514	-0.196	1.196	0.430	0.999	26.9	0.158	0.368	-0.014
11.237	0.514	-0.194	1.194	0.431	0.999	26.5	0.158	0.368	-0.010
11.406	0.514	-0.192	1.192	0.431	0.999	26.1	0.158	0.367	-0.006
11.581	0.514	-0.190	1.190	0.432	0.998	25.7	0.158	0.366	0.000
11.753	0.514	-0.188	1.188	0.433	0.999	25.4	0.158	0.366	0.006
11.928	0.513	-0.185	1.185	0.433	0.997	24.9	0.158	0.365	0.007
12.103	0.514	-0.182	1.182	0.434	0.998	24.6	0.158	0.364	0.014

shr.stn	sh.sts.	ndelU.	nv.sts.	nsh./v.st	sh./su	eu/su	sh/mpp	v.sts/mpp	v.stn
12.277	0.512	-0.180	1.180	0.434	0.996	24.2	0.158	0.363	0.011
12.454	0.513	-0.177	1.177	0.436	0.997	23.9	0.158	0.362	0.013
12.630	0.513	-0.175	1.175	0.436	0.996	23.5	0.158	0.362	0.014
12.814	0.513	-0.172	1.172	0.437	0.997	23.2	0.158	0.361	0.015
12.993	0.512	-0.169	1.169	0.438	0.995	22.8	0.158	0.360	0.018
13.166	0.511	-0.167	1.167	0.438	0.993	22.5	0.157	0.359	0.019
13.354	0.511	-0.164	1.164	0.439	0.994	22.2	0.157	0.358	0.027
13.516	0.510	-0.161	1.161	0.439	0.991	21.9	0.157	0.357	0.026
13.696	0.511	-0.159	1.159	0.441	0.992	21.6	0.157	0.357	0.033
13.867	0.509	-0.156	1.156	0.440	0.989	21.3	0.157	0.356	0.037
14.027	0.509	-0.153	1.153	0.442	0.990	21.0	0.157	0.355	0.039
14.216	0.508	-0.150	1.150	0.442	0.988	20.7	0.157	0.354	0.044
14.368	0.508	-0.147	1.147	0.443	0.986	20.5	0.156	0.353	0.047
14.550	0.507	-0.144	1.144	0.443	0.986	20.2	0.156	0.352	0.050
14.743	0.506	-0.141	1.141	0.443	0.982	19.9	0.156	0.351	0.057
14.916	0.505	-0.138	1.138	0.444	0.982	19.6	0.156	0.350	0.061
15.068	0.504	-0.135	1.135	0.444	0.979	19.4	0.155	0.349	0.066
15.243	0.503	-0.131	1.131	0.445	0.978	19.1	0.155	0.348	0.068
15.424	0.502	-0.128	1.128	0.445	0.976	18.9	0.155	0.347	0.074
15.612	0.501	-0.124	1.124	0.446	0.973	18.6	0.154	0.346	0.078
15.792	0.500	-0.121	1.121	0.446	0.972	18.4	0.154	0.345	0.088
15.944	0.499	-0.117	1.117	0.447	0.970	18.1	0.154	0.344	0.093
16.130	0.498	-0.114	1.114	0.448	0.969	17.9	0.153	0.343	0.101
16.294	0.497	-0.110	1.110	0.447	0.965	17.7	0.153	0.342	0.107
16.474	0.496	-0.106	1.106	0.449	0.964	17.4	0.153	0.341	0.113
16.637	0.494	-0.102	1.102	0.448	0.961	17.2	0.152	0.339	0.119
16.821	0.494	-0.099	1.099	0.450	0.960	17.0	0.152	0.338	0.126
16.973	0.493	-0.095	1.095	0.450	0.958	16.8	0.152	0.337	0.131
17.181	0.492	-0.091	1.091	0.451	0.956	16.6	0.151	0.336	0.139
17.332	0.491	-0.088	1.088	0.452	0.955	16.4	0.151	0.335	0.143
17.510	0.490	-0.084	1.084	0.452	0.952	16.2	0.151	0.334	0.148
17.707	0.489	-0.080	1.080	0.453	0.951	16.0	0.151	0.333	0.158
17.875	0.488	-0.077	1.077	0.453	0.947	15.8	0.150	0.332	0.162
18.035	0.487	-0.074	1.074	0.453	0.947	15.6	0.150	0.331	0.171
18.192	0.486	-0.072	1.072	0.454	0.944	15.5	0.150	0.330	0.179
18.366	0.486	-0.069	1.069	0.454	0.944	15.3	0.150	0.329	0.187
18.551	0.484	-0.065	1.065	0.455	0.941	15.1	0.149	0.328	0.193
18.722	0.484	-0.062	1.062	0.455	0.940	15.0	0.149	0.327	0.202
18.894	0.483	-0.059	1.059	0.456	0.939	14.8	0.149	0.326	0.215
19.066	0.482	-0.056	1.056	0.456	0.937	14.6	0.148	0.325	0.219
19.237	0.482	-0.053	1.053	0.457	0.936	14.5	0.148	0.324	0.231
19.408	0.480	-0.050	1.050	0.457	0.933	14.3	0.148	0.323	0.238
19.581	0.480	-0.047	1.047	0.458	0.932	14.2	0.148	0.322	0.245
19.752	0.478	-0.043	1.043	0.458	0.929	14.0	0.147	0.321	0.254
19.925	0.477	-0.040	1.040	0.459	0.928	13.9	0.147	0.320	0.270
20.093	0.476	-0.036	1.036	0.459	0.925	13.7	0.147	0.319	0.271
20.265	0.475	-0.033	1.033	0.460	0.923	13.6	0.146	0.318	0.281
20.435	0.474	-0.029	1.029	0.461	0.922	13.4	0.146	0.317	0.289
20.610	0.473	-0.026	1.026	0.461	0.920	13.3	0.146	0.316	0.303
20.779	0.472	-0.022	1.022	0.462	0.918	13.2	0.145	0.315	0.311
20.954	0.471	-0.018	1.018	0.462	0.915	13.0	0.145	0.314	0.317
21.125	0.470	-0.015	1.015	0.463	0.914	12.9	0.145	0.312	0.329

shr.stn	sh.sts.	ndelU.	nv.sts.	nsh./v.st	sh./su	eu/su	sh/mpp	v.sts/mpp	v.stn
21.298	0.469	-0.011	1.011	0.463	0.911	12.7	0.144	0.311	0.341
21.477	0.468	-0.007	1.007	0.465	0.909	12.6	0.144	0.310	0.350
21.648	0.466	-0.004	1.004	0.465	0.906	12.5	0.144	0.309	0.364
21.824	0.466	0.000	1.000	0.466	0.905	12.4	0.143	0.308	0.365
21.994	0.464	0.004	0.996	0.466	0.902	12.2	0.143	0.307	0.376
22.171	0.463	0.008	0.992	0.466	0.899	12.1	0.142	0.305	0.380
22.343	0.461	0.012	0.988	0.467	0.897	12.0	0.142	0.304	0.383
22.515	0.460	0.016	0.984	0.467	0.893	11.8	0.142	0.303	0.397
22.689	0.460	0.019	0.981	0.468	0.893	11.7	0.141	0.302	0.405
22.862	0.458	0.023	0.977	0.468	0.889	11.6	0.141	0.301	0.417
23.034	0.457	0.026	0.974	0.469	0.888	11.5	0.141	0.300	0.423
23.205	0.456	0.030	0.970	0.470	0.886	11.4	0.140	0.299	0.433
23.381	0.455	0.033	0.967	0.471	0.884	11.3	0.140	0.298	0.445
23.551	0.454	0.036	0.964	0.471	0.882	11.2	0.140	0.297	0.453
23.725	0.452	0.040	0.960	0.471	0.879	11.0	0.139	0.296	0.460
23.896	0.452	0.043	0.957	0.472	0.878	10.9	0.139	0.295	0.463
24.070	0.450	0.048	0.952	0.472	0.874	10.8	0.138	0.293	0.477
24.242	0.449	0.051	0.949	0.473	0.873	10.7	0.138	0.292	0.488
24.412	0.447	0.055	0.945	0.473	0.868	10.6	0.138	0.291	0.493
24.588	0.446	0.058	0.942	0.474	0.868	10.5	0.137	0.290	0.500
24.758	0.444	0.062	0.938	0.474	0.864	10.4	0.137	0.289	0.510
24.934	0.443	0.066	0.934	0.474	0.861	10.3	0.136	0.288	0.520
25.105	0.442	0.069	0.931	0.475	0.859	10.2	0.136	0.287	0.525
25.277	0.440	0.073	0.927	0.475	0.855	10.1	0.135	0.285	0.533
25.449	0.439	0.076	0.924	0.476	0.854	10.0	0.135	0.284	0.539
25.624	0.437	0.080	0.920	0.475	0.850	9.9	0.135	0.283	0.546
25.799	0.437	0.084	0.916	0.477	0.849	9.8	0.135	0.282	0.553
25.974	0.435	0.088	0.912	0.477	0.844	9.7	0.134	0.281	0.564
26.152	0.433	0.092	0.908	0.478	0.842	9.6	0.133	0.279	0.576
26.321	0.431	0.096	0.904	0.477	0.838	9.5	0.133	0.278	0.584
26.499	0.430	0.100	0.900	0.478	0.836	9.4	0.132	0.277	0.597
26.670	0.429	0.104	0.896	0.478	0.833	9.3	0.132	0.276	0.602
26.844	0.427	0.108	0.892	0.478	0.829	9.2	0.131	0.275	0.613
27.019	0.426	0.112	0.888	0.480	0.828	9.1	0.131	0.273	0.624
27.192	0.423	0.116	0.884	0.479	0.823	9.0	0.130	0.272	0.634
27.365	0.423	0.120	0.880	0.480	0.821	8.9	0.130	0.271	0.639
27.538	0.420	0.124	0.876	0.480	0.817	8.8	0.129	0.270	0.646
27.715	0.419	0.128	0.872	0.481	0.815	8.8	0.129	0.269	0.654
27.884	0.418	0.132	0.868	0.481	0.811	8.7	0.129	0.267	0.666
28.061	0.416	0.136	0.864	0.481	0.808	8.6	0.128	0.266	0.673
28.234	0.414	0.140	0.860	0.482	0.805	8.5	0.128	0.265	0.685
28.411	0.412	0.144	0.856	0.482	0.801	8.4	0.127	0.263	0.695
28.583	0.411	0.148	0.852	0.483	0.799	8.3	0.127	0.262	0.704
28.758	0.409	0.153	0.847	0.482	0.794	8.2	0.126	0.261	0.714
28.931	0.408	0.157	0.843	0.484	0.792	8.2	0.126	0.260	0.724
29.103	0.405	0.160	0.840	0.483	0.788	8.1	0.125	0.259	0.729
29.282	0.404	0.164	0.836	0.484	0.786	8.0	0.125	0.257	0.736
29.452	0.402	0.169	0.831	0.484	0.782	7.9	0.124	0.256	0.749
29.629	0.401	0.173	0.827	0.484	0.779	7.8	0.123	0.255	0.760
29.800	0.399	0.177	0.823	0.485	0.776	7.8	0.123	0.253	0.769
29.980	0.397	0.181	0.819	0.485	0.772	7.7	0.122	0.252	0.778
30.152	0.396	0.185	0.815	0.486	0.770	7.6	0.122	0.251	0.790

shr.stn	sh.sts.	ndelU.	nv.sts.	nsh./v.st	sh./su	eu/su	sh/mpp	v.sts/mpp	v.stn
30.327	0.393	0.189	0.811	0.485	0.765	7.5	0.121	0.250	0.797
30.502	0.392	0.194	0.806	0.487	0.763	7.4	0.121	0.248	0.802
30.673	0.390	0.198	0.802	0.486	0.758	7.4	0.120	0.247	0.812
30.851	0.389	0.202	0.798	0.487	0.756	7.3	0.120	0.246	0.819
31.021	0.387	0.206	0.794	0.487	0.752	7.2	0.119	0.244	0.832
31.201	0.385	0.210	0.790	0.488	0.748	7.1	0.119	0.243	0.840
31.370	0.383	0.214	0.786	0.488	0.745	7.1	0.118	0.242	0.853
31.547	0.381	0.218	0.782	0.487	0.741	7.0	0.117	0.241	0.856
31.718	0.380	0.223	0.777	0.488	0.738	6.9	0.117	0.239	0.864
31.894	0.377	0.227	0.773	0.488	0.733	6.8	0.116	0.238	0.872
32.070	0.376	0.231	0.769	0.489	0.730	6.8	0.116	0.237	0.879
32.241	0.373	0.235	0.765	0.488	0.726	6.7	0.115	0.236	0.896
32.420	0.372	0.239	0.761	0.489	0.723	6.6	0.115	0.234	0.906
32.593	0.370	0.243	0.757	0.489	0.718	6.6	0.114	0.233	0.919
32.771	0.368	0.248	0.752	0.489	0.715	6.5	0.113	0.232	0.925
32.943	0.366	0.252	0.748	0.489	0.711	6.4	0.113	0.230	0.933
33.121	0.364	0.256	0.744	0.489	0.707	6.3	0.112	0.229	0.942
33.293	0.362	0.261	0.739	0.490	0.704	6.3	0.112	0.228	0.949
33.467	0.360	0.265	0.735	0.490	0.699	6.2	0.111	0.226	0.964
33.644	0.359	0.269	0.731	0.491	0.697	6.2	0.110	0.225	0.972
33.815	0.357	0.273	0.727	0.491	0.693	6.1	0.110	0.224	0.980
33.992	0.356	0.278	0.722	0.492	0.691	6.0	0.109	0.222	0.989
34.165	0.354	0.282	0.718	0.493	0.688	6.0	0.109	0.221	1.002
34.345	0.352	0.286	0.714	0.493	0.684	5.9	0.108	0.220	1.010
34.517	0.350	0.291	0.709	0.494	0.681	5.9	0.108	0.218	1.024
34.694	0.348	0.295	0.705	0.494	0.676	5.8	0.107	0.217	1.031
34.868	0.347	0.299	0.701	0.494	0.674	5.7	0.107	0.216	1.046
35.044	0.344	0.303	0.697	0.494	0.669	5.7	0.106	0.215	1.048
35.222	0.343	0.307	0.693	0.495	0.666	5.6	0.106	0.213	1.061
35.395	0.341	0.311	0.689	0.495	0.662	5.6	0.105	0.212	1.067
35.575	0.339	0.315	0.685	0.495	0.659	5.5	0.104	0.211	1.076
35.745	0.337	0.320	0.680	0.495	0.655	5.4	0.104	0.209	1.087
35.926	0.335	0.324	0.676	0.496	0.652	5.4	0.103	0.208	1.101
36.098	0.333	0.328	0.672	0.496	0.648	5.3	0.103	0.207	1.107
36.279	0.331	0.333	0.667	0.496	0.643	5.3	0.102	0.205	1.115
36.456	0.329	0.337	0.663	0.496	0.639	5.2	0.101	0.204	1.128
36.637	0.327	0.341	0.659	0.495	0.635	5.1	0.101	0.203	1.131
36.815	0.325	0.345	0.655	0.496	0.631	5.1	0.100	0.202	1.141
36.991	0.322	0.349	0.651	0.495	0.626	5.0	0.099	0.201	1.150
37.171	0.320	0.353	0.647	0.495	0.623	5.0	0.099	0.199	1.164
37.344	0.318	0.357	0.643	0.495	0.618	4.9	0.098	0.198	1.169
37.524	0.316	0.361	0.639	0.494	0.614	4.9	0.097	0.197	1.182
37.698	0.314	0.365	0.635	0.495	0.611	4.8	0.097	0.196	1.191
37.875	0.312	0.369	0.631	0.494	0.606	4.8	0.096	0.194	1.202
38.053	0.310	0.373	0.627	0.494	0.603	4.7	0.095	0.193	1.209
38.228	0.308	0.376	0.624	0.493	0.598	4.6	0.095	0.192	1.220
38.408	0.306	0.381	0.619	0.494	0.595	4.6	0.094	0.191	1.234
38.579	0.304	0.384	0.616	0.494	0.591	4.5	0.094	0.190	1.243
38.758	0.302	0.389	0.611	0.494	0.587	4.5	0.093	0.188	1.250
38.928	0.300	0.393	0.607	0.494	0.583	4.4	0.092	0.187	1.259
39.103	0.297	0.397	0.603	0.493	0.578	4.4	0.092	0.186	1.272
39.272	0.296	0.401	0.599	0.494	0.574	4.3	0.091	0.184	1.271

shr.stn	sh.sts.	ndelU.	nv.sts.	nsh./v.st	sh./su	eu/su	sh/mpp	v.sts/mpp	v.stn
39.445	0.293	0.406	0.594	0.493	0.569	4.3	0.090	0.183	1.277
39.617	0.291	0.410	0.590	0.494	0.566	4.2	0.090	0.182	1.288
39.789	0.289	0.415	0.585	0.493	0.561	4.2	0.089	0.180	1.291
39.965	0.287	0.419	0.581	0.493	0.557	4.1	0.088	0.179	1.295
40.127	0.280	0.423	0.577	0.486	0.545	4.0	0.086	0.178	1.304

 Ko CONSOLIDATED GEONOR DIRECT SIMPLE SHEAR TEST
 MIT GEOTECHNICAL LAB

FILE NAME : DSS 40

 REDUCTION DATA
 UNITS: kg,cm,mVolts,Volts

- 1. Test Name : DSS 40
- 2. Date : 5/29/89
- 3. OCR : 1.965
- 4. Ver. Consolidation Stress (ksc) :5.7975
- 5. Pre-Shear Height (cm) :1.737
- 6. Horizontal Shear Load Cell:
 - Zero: 0.000092
 - CF: 7065.518
- 7. Horizontal Displacement Transducer:
 - Zero: -0.12312
 - CF: 2.2815
- 8. Vertical Stress Load Cell:
 - Zero: 0.2085
 - CF: -1188.86
- 9. Vertical Height Transducer:
 - Zero: 0.071488
 - CF: 2.0655

shr.stn	sh.sts.	ndelU.	nv.sts.	nsh./v.st	sh./su	eu/su	sh/mpp	v.sts/mpp	v.stn
0.000	0.001	-0.003	1.003	0.001	0.003	9999.0	0.001	0.510	0.000
-0.002	0.001	-0.015	1.015	0.001	0.003	2.3	0.001	0.516	0.002
0.000	0.001	-0.026	1.026	0.001	0.004	606.0	0.001	0.522	0.008
0.005	0.001	-0.010	1.010	0.001	0.003	14.2	0.001	0.514	0.001
0.010	0.001	-0.012	1.012	0.001	0.003	10.1	0.001	0.515	0.004
0.010	0.002	-0.021	1.021	0.002	0.005	54.6	0.001	0.520	0.009
0.010	0.003	-0.021	1.021	0.003	0.007	141.0	0.001	0.519	0.004
0.014	0.012	-0.005	1.005	0.012	0.034	688.2	0.006	0.511	0.006
0.035	0.033	-0.009	1.009	0.033	0.092	762.6	0.017	0.514	0.008
0.062	0.060	-0.014	1.014	0.059	0.166	788.1	0.031	0.516	0.000
0.105	0.093	-0.012	1.012	0.092	0.258	728.0	0.047	0.515	0.000
0.166	0.126	-0.025	1.025	0.123	0.349	624.6	0.064	0.521	-0.006
0.241	0.157	-0.032	1.032	0.152	0.435	537.4	0.080	0.525	-0.004
0.331	0.185	-0.036	1.036	0.178	0.510	459.5	0.094	0.527	-0.014
0.433	0.208	-0.057	1.057	0.197	0.576	397.4	0.106	0.538	-0.013
0.544	0.229	-0.061	1.061	0.216	0.633	347.6	0.116	0.540	-0.021
0.669	0.244	-0.055	1.055	0.231	0.674	301.1	0.124	0.537	-0.031
0.804	0.258	-0.057	1.057	0.244	0.714	265.5	0.131	0.538	-0.036
0.939	0.270	-0.082	1.082	0.250	0.747	238.0	0.138	0.551	-0.035
1.086	0.281	-0.085	1.085	0.259	0.778	214.3	0.143	0.552	-0.028
1.234	0.290	-0.076	1.076	0.269	0.801	194.0	0.147	0.548	-0.032
1.385	0.296	-0.073	1.073	0.276	0.820	177.0	0.151	0.546	-0.041
1.540	0.303	-0.073	1.073	0.282	0.837	162.6	0.154	0.546	-0.042
1.701	0.308	-0.074	1.074	0.287	0.852	149.8	0.157	0.547	-0.036
1.858	0.314	-0.074	1.074	0.292	0.868	139.7	0.160	0.547	-0.041
2.020	0.318	-0.090	1.090	0.292	0.881	130.4	0.162	0.555	-0.024
2.180	0.323	-0.075	1.075	0.300	0.893	122.5	0.164	0.547	-0.022
2.341	0.326	-0.066	1.066	0.305	0.900	115.0	0.166	0.542	-0.014
2.514	0.329	-0.060	1.060	0.310	0.910	108.2	0.167	0.540	-0.019
2.675	0.331	-0.056	1.056	0.314	0.917	102.5	0.169	0.537	-0.040
2.842	0.334	-0.053	1.053	0.317	0.924	97.3	0.170	0.536	-0.029

shr.stn	sh.sts.	ndelU.	nv.sts.	nsh./v.st	sh./su	eu/su	sh/mpp	v.sts/mpp	v.stn
3.014	0.337	-0.050	1.050	0.321	0.932	92.5	0.172	0.534	-0.020
3.175	0.339	-0.046	1.046	0.324	0.936	88.2	0.172	0.532	-0.017
3.344	0.341	-0.042	1.042	0.327	0.944	84.5	0.174	0.530	-0.008
3.512	0.342	-0.036	1.036	0.330	0.947	80.7	0.174	0.527	-0.026
3.677	0.345	-0.030	1.030	0.335	0.954	77.6	0.176	0.524	-0.007
3.846	0.346	-0.025	1.025	0.338	0.958	74.5	0.176	0.522	-0.014
4.019	0.348	-0.023	1.023	0.340	0.962	71.6	0.177	0.521	-0.006
4.179	0.349	-0.016	1.016	0.344	0.966	69.2	0.178	0.517	-0.017
4.355	0.350	-0.006	1.006	0.348	0.969	66.5	0.178	0.512	-0.010
4.521	0.352	-0.001	1.001	0.351	0.972	64.3	0.179	0.509	0.003
4.694	0.353	0.004	0.996	0.354	0.975	62.2	0.179	0.507	0.000
4.873	0.354	0.009	0.991	0.357	0.979	60.1	0.180	0.504	-0.017
5.039	0.355	0.014	0.986	0.360	0.981	58.2	0.180	0.502	-0.017
5.215	0.356	0.019	0.981	0.363	0.985	56.5	0.181	0.499	-0.017
5.389	0.356	0.027	0.973	0.366	0.985	54.7	0.181	0.495	-0.023
5.559	0.357	0.030	0.970	0.368	0.988	53.2	0.182	0.494	-0.010
5.733	0.358	0.034	0.966	0.371	0.990	51.7	0.182	0.492	-0.007
5.907	0.358	0.040	0.960	0.373	0.991	50.2	0.182	0.489	-0.017
6.078	0.359	0.045	0.955	0.376	0.993	48.9	0.183	0.486	-0.019
6.250	0.359	0.049	0.951	0.377	0.992	47.5	0.183	0.484	-0.020
6.425	0.360	0.054	0.946	0.380	0.995	46.3	0.183	0.481	-0.017
6.598	0.360	0.056	0.944	0.381	0.995	45.1	0.183	0.480	-0.029
6.776	0.360	0.058	0.942	0.383	0.996	44.0	0.183	0.479	-0.012
6.943	0.361	0.060	0.940	0.384	0.997	43.0	0.183	0.478	0.008
7.117	0.361	0.064	0.936	0.385	0.998	42.0	0.184	0.476	0.005
7.291	0.361	0.070	0.930	0.388	0.999	41.0	0.184	0.473	0.006
7.462	0.361	0.075	0.925	0.390	0.999	40.0	0.184	0.471	-0.003
7.635	0.362	0.083	0.917	0.394	1.000	39.2	0.184	0.467	-0.003
7.812	0.361	0.090	0.910	0.396	0.998	38.2	0.184	0.463	0.005
7.985	0.361	0.092	0.908	0.398	0.999	37.4	0.184	0.462	-0.006
8.156	0.361	0.098	0.902	0.400	0.997	36.6	0.184	0.459	0.011
8.338	0.361	0.101	0.899	0.401	0.998	35.8	0.184	0.458	-0.007
8.504	0.361	0.103	0.897	0.403	0.999	35.1	0.184	0.456	0.001
8.680	0.361	0.106	0.894	0.404	0.999	34.4	0.184	0.455	-0.004
8.853	0.361	0.109	0.891	0.406	0.999	33.8	0.184	0.453	0.001
9.031	0.361	0.115	0.885	0.407	0.997	33.0	0.184	0.451	0.009
9.204	0.361	0.117	0.883	0.409	0.999	32.5	0.184	0.449	0.010
9.378	0.361	0.120	0.880	0.410	0.998	31.8	0.184	0.448	0.014
9.556	0.361	0.124	0.876	0.412	0.999	31.3	0.184	0.446	0.022
9.728	0.361	0.127	0.873	0.413	0.997	30.7	0.183	0.444	0.009
9.905	0.361	0.130	0.870	0.415	0.998	30.1	0.184	0.443	0.014
10.075	0.360	0.134	0.866	0.416	0.997	29.6	0.183	0.441	0.012
10.255	0.360	0.141	0.859	0.419	0.995	29.0	0.183	0.437	0.021
10.429	0.360	0.146	0.854	0.421	0.995	28.5	0.183	0.434	0.024
10.607	0.359	0.150	0.850	0.422	0.993	28.0	0.183	0.432	0.027
10.789	0.359	0.150	0.850	0.423	0.993	27.5	0.183	0.432	0.004
10.967	0.358	0.152	0.848	0.423	0.991	27.0	0.182	0.432	-0.005
11.147	0.359	0.153	0.847	0.424	0.993	26.6	0.183	0.431	0.004
11.320	0.359	0.142	0.858	0.419	0.994	26.3	0.183	0.437	0.012
11.497	0.359	0.156	0.844	0.426	0.994	25.9	0.183	0.429	0.015
11.671	0.357	0.172	0.828	0.432	0.989	25.3	0.182	0.421	-0.003
11.849	0.357	0.175	0.825	0.432	0.986	24.9	0.181	0.420	0.000

shr.stn	sh.sts.	ndelU.	nv.sts.	nsh./v.st	sh./su	eu/su	sh/mpp	v.sts/mpp	v.stn
12.017	0.357	0.175	0.825	0.432	0.987	24.6	0.182	0.420	0.007
12.197	0.357	0.161	0.839	0.426	0.988	24.2	0.182	0.427	0.024
12.373	0.357	0.178	0.822	0.434	0.987	23.9	0.182	0.418	0.027
12.547	0.355	0.184	0.816	0.435	0.982	23.4	0.181	0.415	0.025
12.727	0.355	0.185	0.815	0.436	0.982	23.1	0.181	0.415	0.011
12.899	0.354	0.187	0.813	0.436	0.980	22.7	0.180	0.414	0.013
13.079	0.354	0.187	0.813	0.436	0.980	22.4	0.180	0.414	0.008
13.252	0.354	0.188	0.812	0.436	0.979	22.1	0.180	0.413	0.006
13.433	0.354	0.190	0.810	0.436	0.978	21.8	0.180	0.412	0.012
13.632	0.354	0.192	0.808	0.438	0.979	21.5	0.180	0.411	0.029
13.790	0.353	0.193	0.807	0.437	0.976	21.2	0.180	0.410	0.033
13.896	0.353	0.197	0.803	0.440	0.977	21.0	0.180	0.409	0.028
14.133	0.352	0.200	0.800	0.440	0.973	20.6	0.179	0.407	0.033
14.353	0.352	0.205	0.795	0.443	0.973	20.3	0.179	0.404	0.036
14.458	0.351	0.210	0.790	0.444	0.970	20.1	0.178	0.402	0.034
14.649	0.350	0.212	0.788	0.444	0.968	19.8	0.178	0.401	0.028
14.857	0.349	0.215	0.785	0.445	0.966	19.5	0.178	0.400	0.041
14.996	0.348	0.217	0.783	0.445	0.964	19.2	0.177	0.398	0.042
15.151	0.348	0.221	0.779	0.447	0.963	19.0	0.177	0.396	0.046
15.333	0.346	0.229	0.771	0.449	0.958	18.7	0.176	0.392	0.037
15.518	0.346	0.232	0.768	0.450	0.956	18.4	0.176	0.391	0.032
15.722	0.345	0.235	0.765	0.450	0.953	18.1	0.175	0.389	0.038
15.896	0.343	0.238	0.762	0.451	0.950	17.9	0.175	0.388	0.028
16.084	0.342	0.245	0.755	0.453	0.947	17.6	0.174	0.384	0.031
16.275	0.341	0.248	0.752	0.454	0.943	17.3	0.174	0.383	0.023
16.505	0.340	0.249	0.751	0.453	0.941	17.1	0.173	0.382	0.031
16.621	0.339	0.252	0.748	0.453	0.937	16.9	0.172	0.380	0.032
16.810	0.338	0.258	0.742	0.456	0.936	16.7	0.172	0.378	0.036
16.980	0.336	0.268	0.732	0.459	0.929	16.4	0.171	0.373	0.045
17.077	0.335	0.271	0.729	0.459	0.926	16.2	0.170	0.371	0.043
17.336	0.333	0.274	0.726	0.459	0.922	15.9	0.170	0.369	0.053
17.497	0.332	0.279	0.721	0.461	0.919	15.7	0.169	0.367	0.049
17.617	0.331	0.284	0.716	0.463	0.916	15.5	0.169	0.364	0.042
17.882	0.330	0.287	0.713	0.463	0.913	15.3	0.168	0.363	0.055
17.967	0.329	0.289	0.711	0.463	0.911	15.2	0.168	0.362	0.050
18.190	0.328	0.292	0.708	0.463	0.907	14.9	0.167	0.360	0.062
18.414	0.327	0.297	0.703	0.465	0.905	14.7	0.167	0.358	0.065
18.584	0.325	0.307	0.693	0.469	0.899	14.5	0.165	0.353	0.065
18.715	0.323	0.314	0.686	0.471	0.894	14.3	0.165	0.349	0.060
18.827	0.322	0.316	0.684	0.470	0.890	14.1	0.164	0.348	0.054
19.065	0.321	0.317	0.683	0.470	0.888	13.9	0.163	0.347	0.074
19.238	0.320	0.319	0.681	0.471	0.886	13.8	0.163	0.346	0.089
19.418	0.319	0.322	0.678	0.471	0.883	13.6	0.163	0.345	0.089
19.593	0.319	0.325	0.675	0.472	0.882	13.5	0.162	0.344	0.086
19.767	0.317	0.329	0.671	0.473	0.878	13.3	0.162	0.341	0.085
19.942	0.317	0.333	0.667	0.474	0.876	13.1	0.161	0.340	0.070
20.116	0.315	0.339	0.661	0.476	0.871	12.9	0.160	0.336	0.068
20.293	0.314	0.348	0.652	0.481	0.867	12.8	0.160	0.332	0.073
20.468	0.312	0.352	0.648	0.481	0.862	12.6	0.159	0.330	0.073
20.647	0.310	0.358	0.642	0.484	0.858	12.4	0.158	0.327	0.078
20.822	0.309	0.362	0.638	0.484	0.854	12.3	0.157	0.324	0.086
21.004	0.307	0.365	0.635	0.484	0.850	12.1	0.156	0.323	0.074

shr.stn	sh.sts.	ndelU.	nv.sts.	nsh./v.st	sh./su	eu/su	sh/mpp	v.sts/mpp	v.stn
21.175	0.306	0.367	0.633	0.484	0.848	12.0	0.156	0.322	0.092
21.354	0.305	0.369	0.631	0.484	0.844	11.8	0.155	0.321	0.104
21.527	0.304	0.372	0.628	0.485	0.842	11.7	0.155	0.319	0.083
21.702	0.303	0.379	0.621	0.488	0.838	11.5	0.154	0.316	0.098
21.881	0.302	0.385	0.615	0.490	0.835	11.4	0.154	0.313	0.083
22.055	0.300	0.388	0.612	0.490	0.830	11.2	0.153	0.311	0.084
22.234	0.299	0.391	0.609	0.491	0.827	11.1	0.152	0.310	0.090
22.408	0.298	0.392	0.608	0.490	0.824	11.0	0.152	0.309	0.099
22.589	0.297	0.395	0.605	0.490	0.821	10.9	0.151	0.308	0.108
22.762	0.296	0.403	0.597	0.495	0.818	10.7	0.150	0.304	0.111
22.943	0.293	0.411	0.589	0.498	0.811	10.6	0.149	0.300	0.093
23.121	0.291	0.417	0.583	0.500	0.806	10.4	0.148	0.297	0.079
23.298	0.290	0.421	0.579	0.500	0.801	10.3	0.147	0.294	0.091
23.478	0.288	0.424	0.576	0.500	0.797	10.2	0.147	0.293	0.085
23.652	0.287	0.427	0.573	0.500	0.793	10.0	0.146	0.292	0.100
23.833	0.286	0.428	0.572	0.500	0.791	9.9	0.146	0.291	0.106
24.008	0.285	0.431	0.569	0.501	0.789	9.8	0.145	0.290	0.105
24.074	0.285	0.433	0.567	0.502	0.788	9.8	0.145	0.289	0.123
24.338	0.283	0.438	0.562	0.503	0.782	9.6	0.144	0.286	0.119
24.600	0.281	0.443	0.557	0.503	0.776	9.4	0.143	0.284	0.098
24.864	0.278	0.450	0.550	0.506	0.770	9.3	0.142	0.280	0.118
25.133	0.276	0.454	0.546	0.506	0.764	9.1	0.141	0.278	0.124
25.395	0.274	0.463	0.537	0.510	0.758	8.9	0.139	0.273	0.118
25.659	0.272	0.467	0.533	0.510	0.753	8.8	0.138	0.271	0.100
25.921	0.270	0.474	0.526	0.513	0.746	8.6	0.137	0.268	0.097
26.185	0.267	0.478	0.522	0.512	0.740	8.4	0.136	0.266	0.093
26.452	0.265	0.487	0.513	0.517	0.733	8.3	0.135	0.261	0.119
26.718	0.263	0.489	0.511	0.515	0.728	8.1	0.134	0.260	0.114
26.979	0.262	0.490	0.510	0.514	0.724	8.0	0.133	0.259	0.104
27.239	0.260	0.494	0.506	0.514	0.720	7.9	0.132	0.258	0.124
27.502	0.258	0.499	0.501	0.516	0.715	7.8	0.132	0.255	0.132
27.769	0.255	0.512	0.488	0.523	0.706	7.6	0.130	0.248	0.123
28.033	0.253	0.515	0.485	0.522	0.699	7.5	0.129	0.247	0.133
28.302	0.250	0.525	0.475	0.527	0.693	7.3	0.127	0.242	0.148
28.565	0.248	0.526	0.474	0.524	0.687	7.2	0.126	0.241	0.149
28.829	0.247	0.529	0.471	0.524	0.683	7.1	0.126	0.240	0.134
29.090	0.245	0.534	0.466	0.527	0.678	7.0	0.125	0.237	0.131
29.356	0.242	0.543	0.457	0.530	0.670	6.8	0.123	0.233	0.121
29.626	0.240	0.547	0.453	0.529	0.663	6.7	0.122	0.231	0.144
29.890	0.238	0.550	0.450	0.529	0.659	6.6	0.121	0.229	0.140
30.156	0.236	0.556	0.444	0.532	0.654	6.5	0.120	0.226	0.160
30.421	0.234	0.561	0.439	0.533	0.647	6.4	0.119	0.223	0.159
30.682	0.232	0.562	0.438	0.531	0.643	6.3	0.118	0.223	0.142
30.943	0.231	0.565	0.435	0.531	0.639	6.2	0.118	0.221	0.159
31.207	0.229	0.574	0.426	0.537	0.632	6.1	0.116	0.217	0.170
31.479	0.226	0.580	0.420	0.537	0.624	5.9	0.115	0.214	0.167
31.747	0.224	0.584	0.416	0.537	0.619	5.8	0.114	0.212	0.171
32.014	0.222	0.591	0.409	0.543	0.613	5.7	0.113	0.208	0.178
32.283	0.219	0.594	0.406	0.540	0.606	5.6	0.112	0.207	0.158
32.554	0.218	0.598	0.402	0.542	0.602	5.5	0.111	0.204	0.153
32.819	0.215	0.603	0.397	0.542	0.596	5.4	0.110	0.202	0.148
33.089	0.213	0.609	0.391	0.545	0.590	5.3	0.108	0.199	0.153

shr.stn	sh.sts.	ndelU.	nv.sts.	nsh./v.st	sh./su	eu/su	sh/mpp	v.sts/mpp	v.stn
33.355	0.211	0.612	0.388	0.545	0.585	5.2	0.108	0.197	0.143
33.622	0.210	0.615	0.385	0.545	0.581	5.2	0.107	0.196	0.135
33.884	0.208	0.621	0.379	0.548	0.575	5.1	0.106	0.193	0.150
34.152	0.205	0.626	0.374	0.550	0.568	5.0	0.105	0.190	0.148
34.418	0.204	0.628	0.372	0.547	0.563	4.9	0.104	0.189	0.143
34.689	0.202	0.632	0.368	0.549	0.559	4.8	0.103	0.187	0.161
34.953	0.201	0.634	0.366	0.549	0.555	4.7	0.102	0.186	0.168
35.217	0.200	0.634	0.366	0.546	0.553	4.7	0.102	0.186	0.153
35.481	0.198	0.639	0.361	0.549	0.548	4.6	0.101	0.184	0.147
35.748	0.196	0.646	0.354	0.554	0.543	4.5	0.100	0.180	0.145
36.016	0.194	0.649	0.351	0.552	0.536	4.4	0.099	0.179	0.143
36.288	0.192	0.651	0.349	0.550	0.531	4.4	0.098	0.178	0.150
36.560	0.189	0.662	0.338	0.560	0.524	4.3	0.096	0.172	0.150
36.832	0.187	0.665	0.335	0.558	0.517	4.2	0.095	0.171	0.140
37.098	0.185	0.668	0.332	0.557	0.511	4.1	0.094	0.169	0.154
37.365	0.183	0.669	0.331	0.553	0.505	4.0	0.093	0.168	0.142
37.634	0.181	0.675	0.325	0.555	0.500	4.0	0.092	0.166	0.156
37.907	0.179	0.677	0.323	0.553	0.494	3.9	0.091	0.164	0.165
38.175	0.177	0.678	0.322	0.550	0.489	3.8	0.090	0.164	0.156
38.439	0.176	0.680	0.320	0.549	0.486	3.8	0.089	0.163	0.160
38.703	0.174	0.683	0.317	0.549	0.481	3.7	0.089	0.161	0.175
38.972	0.172	0.689	0.311	0.552	0.475	3.6	0.087	0.158	0.176
39.246	0.169	0.694	0.306	0.551	0.467	3.6	0.086	0.156	0.184
39.512	0.167	0.696	0.304	0.549	0.462	3.5	0.085	0.155	0.177
39.782	0.165	0.701	0.299	0.553	0.457	3.4	0.084	0.152	0.184
40.057	0.163	0.709	0.291	0.558	0.450	3.3	0.083	0.148	0.174
40.337	0.160	0.711	0.289	0.555	0.444	3.3	0.082	0.147	0.181
40.602	0.159	0.712	0.288	0.552	0.439	3.2	0.081	0.146	0.182
40.868	0.157	0.716	0.284	0.552	0.434	3.2	0.080	0.145	0.180
41.140	0.155	0.724	0.276	0.561	0.429	3.1	0.079	0.141	0.168
41.419	0.152	0.730	0.270	0.563	0.421	3.0	0.077	0.138	0.177
41.697	0.150	0.734	0.266	0.564	0.415	3.0	0.076	0.135	0.168
41.966	0.148	0.734	0.266	0.557	0.410	2.9	0.075	0.135	0.164

Ko CONSOLIDATED GEONOR DIRECT SIMPLE SHEAR TEST
MIT GEOTECHNICAL LAB

FILE NAME : DSS 44

REDUCTION DATA

UNITS: kg,cm,mVolts,Volts

- 1. Test Name : DSS 44
- 2. Date : 6/12/89
- 3. OCR : 7.892
- 4. Ver. Consolidation Stress (ksc) :1.447
- 5. Pre-Shear Height (cm) :1.7024
- 6. Horizontal Shear Load Cell:
 - Zero: 0.000092
 - CF: 7065.518
- 7. Horizontal Displacement Transducer:
 - Zero: -0.1127
 - CF: 2.2815
- 8. Vertical Stress Load Cell:
 - Zero: 0.2099
 - CF: -1188.86
- 9. Vertical Height Transducer:
 - Zero: 0.08546
 - CF: 2.0655

shr.stn	sh.sts.	ndelU.	nv.sts.	nsh./v.st	sh./su	eu/su	sh/mpp	v.sts/mpp	v.stn
0.000	0.000	0.000	1.000	0.000	0.000	9999.0	0.000	0.127	0.000
0.004	0.003	0.006	0.994	0.003	0.003	679.7	0.000	0.126	0.001
0.011	0.020	-0.009	1.009	0.020	0.023	846.5	0.003	0.128	-0.024
0.039	0.071	-0.002	1.002	0.071	0.080	678.4	0.009	0.127	-0.038
0.091	0.138	-0.026	1.026	0.134	0.156	538.1	0.017	0.130	-0.050
0.174	0.204	-0.051	1.051	0.194	0.232	411.6	0.026	0.133	-0.053
0.287	0.257	-0.068	1.068	0.241	0.292	312.5	0.033	0.135	-0.043
0.420	0.302	-0.105	1.105	0.273	0.343	249.8	0.038	0.140	-0.032
0.563	0.339	-0.137	1.137	0.298	0.384	208.6	0.043	0.144	-0.071
0.717	0.367	-0.157	1.157	0.317	0.416	177.2	0.046	0.147	-0.082
0.870	0.394	-0.178	1.178	0.335	0.448	156.7	0.050	0.149	-0.056
1.030	0.414	-0.202	1.202	0.345	0.470	138.9	0.052	0.152	-0.107
1.189	0.441	-0.227	1.227	0.359	0.501	128.0	0.056	0.156	-0.110
1.349	0.460	-0.246	1.246	0.369	0.522	117.6	0.058	0.158	-0.085
1.519	0.480	-0.271	1.271	0.377	0.544	108.9	0.061	0.161	-0.123
1.681	0.483	-0.164	1.164	0.415	0.548	99.0	0.061	0.147	-0.103
1.851	0.496	-0.194	1.194	0.415	0.563	92.3	0.063	0.151	-0.161
1.931	0.526	-0.438	1.438	0.366	0.597	93.8	0.067	0.182	-0.116
2.082	0.554	-0.367	1.367	0.405	0.629	91.6	0.070	0.173	-0.080
2.265	0.572	-0.367	1.367	0.418	0.649	86.9	0.072	0.173	-0.042
2.411	0.585	-0.397	1.397	0.419	0.664	83.5	0.074	0.177	-0.085
2.577	0.602	-0.397	1.397	0.431	0.683	80.3	0.076	0.177	-0.083
2.740	0.614	-0.433	1.433	0.429	0.697	77.1	0.078	0.182	-0.056
2.910	0.629	-0.436	1.436	0.438	0.714	74.4	0.080	0.182	-0.044
3.074	0.640	-0.453	1.453	0.441	0.727	71.6	0.081	0.184	-0.069
3.245	0.655	-0.495	1.495	0.438	0.743	69.4	0.083	0.189	-0.088
3.414	0.665	-0.483	1.483	0.449	0.755	67.0	0.084	0.188	-0.108
3.581	0.675	-0.506	1.506	0.448	0.766	64.8	0.086	0.191	-0.115
3.754	0.686	-0.508	1.508	0.455	0.778	62.8	0.087	0.191	-0.109
3.924	0.696	-0.546	1.546	0.450	0.790	60.9	0.088	0.196	-0.078
4.097	0.706	-0.537	1.537	0.459	0.801	59.2	0.089	0.195	-0.079

shr.stn	sh.sts.	ndelU.	nv.sts.	nsh./v.st	sh./su	eu/su	sh/mpp	v.sts/mpp	v.stn
4.272	0.714	-0.563	1.563	0.457	0.810	57.4	0.090	0.198	-0.119
4.451	0.724	-0.577	1.577	0.459	0.822	55.9	0.092	0.200	-0.104
4.628	0.731	-0.582	1.582	0.462	0.830	54.3	0.093	0.200	-0.084
4.806	0.742	-0.613	1.613	0.460	0.842	53.0	0.094	0.204	-0.052
4.982	0.748	-0.619	1.619	0.462	0.849	51.6	0.095	0.205	-0.037
5.158	0.755	-0.630	1.630	0.463	0.857	50.2	0.096	0.207	-0.057
5.336	0.759	-0.624	1.624	0.467	0.861	48.8	0.096	0.206	-0.040
5.509	0.765	-0.642	1.642	0.466	0.868	47.7	0.097	0.208	-0.048
5.689	0.771	-0.640	1.640	0.471	0.876	46.5	0.098	0.208	-0.061
5.863	0.775	-0.650	1.650	0.470	0.880	45.4	0.098	0.209	-0.063
6.036	0.783	-0.677	1.677	0.467	0.889	44.5	0.099	0.212	-0.121
6.207	0.786	-0.661	1.661	0.473	0.892	43.4	0.100	0.210	-0.132
6.382	0.793	-0.695	1.695	0.468	0.900	42.6	0.100	0.215	-0.086
6.553	0.798	-0.678	1.678	0.475	0.905	41.8	0.101	0.213	-0.100
6.732	0.803	-0.710	1.710	0.470	0.912	40.9	0.102	0.217	-0.125
6.914	0.808	-0.693	1.693	0.477	0.917	40.1	0.102	0.215	-0.102
7.085	0.813	-0.726	1.726	0.471	0.922	39.3	0.103	0.219	-0.097
7.263	0.818	-0.718	1.718	0.476	0.928	38.6	0.104	0.218	-0.093
7.438	0.821	-0.735	1.735	0.473	0.932	37.9	0.104	0.220	-0.086
7.619	0.827	-0.739	1.739	0.476	0.939	37.2	0.105	0.220	-0.058
7.789	0.829	-0.729	1.729	0.480	0.941	36.5	0.105	0.219	-0.081
7.968	0.830	-0.738	1.738	0.478	0.943	35.8	0.105	0.220	-0.112
8.138	0.837	-0.750	1.750	0.478	0.950	35.3	0.106	0.222	-0.089
8.317	0.836	-0.741	1.741	0.480	0.949	34.5	0.106	0.221	-0.138
8.495	0.843	-0.771	1.771	0.476	0.957	34.0	0.107	0.224	-0.101
8.662	0.845	-0.761	1.761	0.480	0.959	33.4	0.107	0.223	-0.082
8.846	0.851	-0.786	1.786	0.476	0.966	33.0	0.108	0.226	-0.096
9.019	0.852	-0.771	1.771	0.481	0.967	32.4	0.108	0.224	-0.074
9.201	0.856	-0.781	1.781	0.481	0.971	31.9	0.108	0.226	-0.098
9.382	0.860	-0.801	1.801	0.478	0.977	31.5	0.109	0.228	-0.082
9.571	0.861	-0.789	1.789	0.481	0.977	30.8	0.109	0.227	-0.105
9.756	0.865	-0.811	1.811	0.477	0.981	30.4	0.110	0.229	-0.074
9.937	0.864	-0.785	1.785	0.484	0.980	29.8	0.109	0.226	-0.076
10.115	0.866	-0.791	1.791	0.484	0.983	29.4	0.110	0.227	-0.103
10.288	0.867	-0.816	1.816	0.478	0.985	28.9	0.110	0.230	-0.104
10.473	0.869	-0.792	1.792	0.485	0.986	28.4	0.110	0.227	-0.092
10.646	0.870	-0.821	1.821	0.478	0.987	28.0	0.110	0.231	-0.092
10.832	0.872	-0.811	1.811	0.482	0.990	27.6	0.111	0.229	-0.094
11.002	0.871	-0.801	1.801	0.484	0.989	27.2	0.110	0.228	-0.084
11.189	0.871	-0.803	1.803	0.483	0.989	26.7	0.110	0.228	-0.087
11.364	0.875	-0.829	1.829	0.478	0.993	26.4	0.111	0.232	-0.087
11.539	0.872	-0.801	1.801	0.484	0.990	25.9	0.111	0.228	-0.093
11.715	0.875	-0.803	1.803	0.485	0.993	25.6	0.111	0.228	-0.101
11.890	0.876	-0.833	1.833	0.478	0.994	25.3	0.111	0.232	-0.099
12.070	0.879	-0.810	1.810	0.486	0.998	25.0	0.111	0.229	-0.101
12.236	0.877	-0.809	1.809	0.485	0.996	24.6	0.111	0.229	-0.104
12.419	0.879	-0.810	1.810	0.486	0.997	24.3	0.111	0.229	-0.106
12.594	0.879	-0.809	1.809	0.486	0.998	23.9	0.111	0.229	-0.107
12.775	0.878	-0.810	1.810	0.485	0.997	23.6	0.111	0.229	-0.107
12.954	0.880	-0.811	1.811	0.486	0.999	23.3	0.111	0.229	-0.107
13.131	0.879	-0.815	1.815	0.484	0.997	22.9	0.111	0.230	-0.108
13.315	0.881	-0.811	1.811	0.486	1.000	22.7	0.112	0.229	-0.108

shr.stn	sh.sts.	ndelU.	nv.sts.	nsh./v.st	sh./su	eu/su	sh/mpp	v.sts/mpp	v.stn
13.490	0.879	-0.809	1.809	0.486	0.998	22.3	0.111	0.229	-0.107
13.675	0.881	-0.810	1.810	0.487	1.000	22.1	0.112	0.229	-0.106
13.849	0.880	-0.814	1.814	0.485	0.999	21.8	0.112	0.230	-0.106
14.034	0.880	-0.811	1.811	0.486	0.999	21.5	0.112	0.229	-0.104
14.214	0.880	-0.804	1.804	0.488	0.999	21.2	0.112	0.229	-0.104
14.396	0.877	-0.800	1.800	0.487	0.996	20.9	0.111	0.228	-0.103
14.579	0.876	-0.793	1.793	0.489	0.994	20.6	0.111	0.227	-0.102
14.757	0.873	-0.787	1.787	0.489	0.991	20.3	0.111	0.226	-0.102
14.940	0.870	-0.774	1.774	0.491	0.988	20.0	0.110	0.225	-0.100
15.119	0.865	-0.753	1.753	0.494	0.982	19.6	0.110	0.222	-0.100
15.301	0.859	-0.740	1.740	0.493	0.975	19.2	0.109	0.221	-0.105
15.480	0.856	-0.736	1.736	0.493	0.971	19.0	0.108	0.220	-0.103
15.663	0.851	-0.727	1.727	0.493	0.966	18.6	0.108	0.219	-0.101
15.847	0.847	-0.710	1.710	0.495	0.961	18.3	0.107	0.217	-0.100
16.023	0.840	-0.692	1.692	0.497	0.954	18.0	0.106	0.214	-0.099
16.203	0.836	-0.679	1.679	0.498	0.949	17.7	0.106	0.213	-0.098
16.380	0.831	-0.672	1.672	0.497	0.943	17.4	0.105	0.212	-0.099
16.563	0.827	-0.662	1.662	0.497	0.939	17.1	0.105	0.211	-0.096
16.736	0.824	-0.654	1.654	0.498	0.935	16.9	0.104	0.210	-0.094
16.918	0.821	-0.646	1.646	0.499	0.932	16.6	0.104	0.209	-0.091
17.097	0.819	-0.639	1.639	0.499	0.929	16.4	0.104	0.208	-0.087
17.282	0.814	-0.614	1.614	0.504	0.923	16.2	0.103	0.204	-0.084
17.466	0.809	-0.595	1.595	0.507	0.918	15.9	0.102	0.202	-0.087
17.641	0.803	-0.588	1.588	0.506	0.911	15.6	0.102	0.201	-0.113
17.813	0.801	-0.581	1.581	0.507	0.909	15.4	0.101	0.200	-0.113
17.995	0.797	-0.577	1.577	0.506	0.905	15.2	0.101	0.200	-0.108
18.175	0.795	-0.565	1.565	0.508	0.902	15.0	0.101	0.198	-0.110
18.354	0.791	-0.547	1.547	0.511	0.898	14.8	0.100	0.196	-0.107
18.539	0.786	-0.528	1.528	0.514	0.892	14.5	0.100	0.194	-0.109
18.721	0.782	-0.524	1.524	0.513	0.888	14.3	0.099	0.193	-0.105
18.902	0.778	-0.518	1.518	0.513	0.883	14.1	0.099	0.192	-0.105
19.080	0.776	-0.508	1.508	0.515	0.881	14.0	0.098	0.191	-0.105
19.259	0.770	-0.479	1.479	0.521	0.874	13.7	0.098	0.187	-0.105
19.440	0.764	-0.467	1.467	0.521	0.868	13.5	0.097	0.186	-0.110
19.617	0.761	-0.467	1.467	0.519	0.863	13.3	0.096	0.186	-0.108
19.799	0.759	-0.461	1.461	0.520	0.862	13.2	0.096	0.185	-0.106
19.972	0.755	-0.445	1.445	0.523	0.857	13.0	0.096	0.183	-0.106
20.158	0.752	-0.434	1.434	0.524	0.853	12.8	0.095	0.182	-0.104
20.335	0.748	-0.421	1.421	0.526	0.848	12.6	0.095	0.180	-0.107
20.517	0.744	-0.419	1.419	0.524	0.844	12.4	0.094	0.180	-0.106
20.692	0.742	-0.413	1.413	0.525	0.842	12.3	0.094	0.179	-0.107
20.876	0.739	-0.411	1.411	0.524	0.839	12.2	0.094	0.179	-0.102
21.054	0.739	-0.406	1.406	0.525	0.838	12.0	0.094	0.178	-0.098
21.233	0.735	-0.403	1.403	0.524	0.835	11.9	0.093	0.178	-0.097
21.413	0.735	-0.401	1.401	0.525	0.834	11.8	0.093	0.177	-0.090
21.587	0.733	-0.397	1.397	0.524	0.832	11.7	0.093	0.177	-0.087
21.772	0.730	-0.389	1.389	0.526	0.829	11.5	0.093	0.176	-0.085
21.951	0.726	-0.373	1.373	0.529	0.824	11.4	0.092	0.174	-0.084
22.130	0.724	-0.363	1.363	0.531	0.821	11.2	0.092	0.173	-0.082
22.308	0.720	-0.344	1.344	0.536	0.817	11.1	0.091	0.170	-0.080
22.491	0.715	-0.332	1.332	0.537	0.811	10.9	0.091	0.169	-0.084
22.672	0.712	-0.327	1.327	0.537	0.808	10.8	0.090	0.168	-0.086

shr.stn	sh.sts.	ndelU.	nv.sts.	nsh./v.st	sh./su	eu/su	sh/mpp	v.sts/mpp	v.stn
22.847	0.708	-0.324	1.324	0.535	0.804	10.6	0.090	0.168	-0.083
23.028	0.706	-0.319	1.319	0.535	0.802	10.5	0.089	0.167	-0.081
23.205	0.703	-0.311	1.311	0.536	0.798	10.4	0.089	0.166	-0.082
23.382	0.701	-0.304	1.304	0.537	0.795	10.3	0.089	0.165	-0.081
23.564	0.697	-0.290	1.290	0.540	0.791	10.2	0.088	0.163	-0.079
23.747	0.692	-0.279	1.279	0.541	0.786	10.0	0.088	0.162	-0.079
23.925	0.690	-0.276	1.276	0.541	0.783	9.9	0.087	0.162	-0.085
24.099	0.687	-0.274	1.274	0.539	0.780	9.8	0.087	0.161	-0.079
24.280	0.686	-0.267	1.267	0.541	0.778	9.7	0.087	0.161	-0.076
24.457	0.682	-0.260	1.260	0.542	0.774	9.6	0.086	0.160	-0.073
24.641	0.679	-0.252	1.252	0.542	0.771	9.5	0.086	0.159	-0.076
24.815	0.676	-0.246	1.246	0.543	0.768	9.4	0.086	0.158	-0.074
25.002	0.673	-0.242	1.242	0.542	0.764	9.3	0.085	0.157	-0.072
25.177	0.671	-0.232	1.232	0.544	0.761	9.2	0.085	0.156	-0.074
25.356	0.667	-0.228	1.228	0.543	0.757	9.0	0.085	0.156	-0.072
25.533	0.665	-0.216	1.216	0.547	0.754	8.9	0.084	0.154	-0.073
25.713	0.660	-0.207	1.207	0.547	0.749	8.8	0.084	0.153	-0.068
25.897	0.658	-0.202	1.202	0.547	0.747	8.7	0.083	0.152	-0.071
26.072	0.654	-0.199	1.199	0.546	0.743	8.6	0.083	0.152	-0.067
26.252	0.653	-0.195	1.195	0.546	0.741	8.5	0.083	0.151	-0.062
26.431	0.651	-0.190	1.190	0.547	0.739	8.5	0.082	0.151	-0.062
26.612	0.647	-0.181	1.181	0.548	0.735	8.4	0.082	0.150	-0.062
26.788	0.644	-0.170	1.170	0.550	0.731	8.3	0.082	0.148	-0.057
26.968	0.640	-0.163	1.163	0.550	0.726	8.2	0.081	0.147	-0.057
27.147	0.638	-0.156	1.156	0.551	0.724	8.1	0.081	0.146	-0.055
27.326	0.632	-0.149	1.149	0.550	0.718	8.0	0.080	0.146	-0.053
27.507	0.631	-0.144	1.144	0.552	0.716	7.9	0.080	0.145	-0.055
27.683	0.627	-0.142	1.142	0.549	0.712	7.8	0.079	0.145	-0.050
27.867	0.626	-0.136	1.136	0.551	0.710	7.7	0.079	0.144	-0.047
28.042	0.622	-0.122	1.122	0.554	0.706	7.6	0.079	0.142	-0.043
28.227	0.616	-0.106	1.106	0.557	0.699	7.5	0.078	0.140	-0.042
28.399	0.613	-0.103	1.103	0.555	0.695	7.4	0.078	0.140	-0.043
28.581	0.609	-0.101	1.101	0.554	0.692	7.3	0.077	0.139	-0.048
28.761	0.608	-0.096	1.096	0.555	0.690	7.3	0.077	0.139	-0.050
28.935	0.603	-0.082	1.082	0.557	0.684	7.2	0.076	0.137	-0.052
29.116	0.600	-0.072	1.072	0.559	0.681	7.1	0.076	0.136	-0.046
29.293	0.596	-0.073	1.073	0.556	0.677	7.0	0.076	0.136	-0.047
29.478	0.595	-0.070	1.070	0.556	0.675	6.9	0.075	0.136	-0.042
29.654	0.593	-0.070	1.070	0.554	0.673	6.9	0.075	0.136	-0.043
29.839	0.591	-0.062	1.062	0.556	0.670	6.8	0.075	0.135	-0.039
30.017	0.588	-0.052	1.052	0.559	0.668	6.7	0.075	0.133	-0.035
30.200	0.582	-0.037	1.037	0.561	0.660	6.6	0.074	0.131	-0.039
30.381	0.579	-0.034	1.034	0.560	0.658	6.6	0.073	0.131	-0.035
30.556	0.575	-0.027	1.027	0.560	0.653	6.5	0.073	0.130	-0.036
30.733	0.573	-0.021	1.021	0.561	0.650	6.4	0.073	0.129	-0.039
30.914	0.569	-0.013	1.013	0.561	0.645	6.3	0.072	0.128	-0.039
31.098	0.565	-0.002	1.002	0.564	0.642	6.3	0.072	0.127	-0.034
31.274	0.561	0.005	0.995	0.564	0.637	6.2	0.071	0.126	-0.037
31.456	0.559	0.008	0.992	0.563	0.634	6.1	0.071	0.126	-0.032
31.634	0.556	0.011	0.989	0.563	0.631	6.1	0.070	0.125	-0.030
31.816	0.552	0.020	0.980	0.564	0.627	6.0	0.070	0.124	-0.032
31.995	0.550	0.026	0.974	0.565	0.625	5.9	0.070	0.123	-0.032

shr.stn	sh.sts.	ndelU.	nv.sts.	nsh./v.st	sh./su	eu/su	sh/mpp	v.sts/mpp	v.stn
32.174	0.546	0.035	0.965	0.566	0.620	5.8	0.069	0.122	-0.027
32.353	0.543	0.041	0.959	0.567	0.617	5.8	0.069	0.122	-0.024
32.530	0.539	0.047	0.953	0.566	0.612	5.7	0.068	0.121	-0.022
32.715	0.537	0.054	0.946	0.567	0.609	5.6	0.068	0.120	-0.025
32.891	0.534	0.058	0.942	0.567	0.606	5.6	0.068	0.119	-0.023
33.077	0.529	0.071	0.929	0.570	0.601	5.5	0.067	0.118	-0.025
33.247	0.527	0.072	0.928	0.567	0.598	5.5	0.067	0.118	-0.023
33.432	0.524	0.076	0.924	0.567	0.594	5.4	0.066	0.117	-0.018
33.607	0.520	0.083	0.917	0.567	0.591	5.3	0.066	0.116	-0.018
33.789	0.516	0.095	0.905	0.570	0.586	5.3	0.065	0.115	-0.016
33.968	0.514	0.097	0.903	0.569	0.583	5.2	0.065	0.114	-0.016
34.142	0.511	0.098	0.902	0.567	0.580	5.2	0.065	0.114	-0.019
34.327	0.510	0.102	0.898	0.567	0.578	5.1	0.065	0.114	-0.012
34.503	0.507	0.108	0.892	0.568	0.575	5.1	0.064	0.113	-0.007
34.689	0.503	0.119	0.881	0.571	0.571	5.0	0.064	0.112	-0.009
34.864	0.500	0.126	0.874	0.573	0.568	4.9	0.063	0.111	-0.003
35.047	0.497	0.128	0.872	0.570	0.564	4.9	0.063	0.110	-0.003
35.228	0.495	0.130	0.870	0.570	0.562	4.8	0.063	0.110	-0.001
35.404	0.493	0.134	0.866	0.569	0.559	4.8	0.062	0.110	0.005
35.583	0.491	0.141	0.859	0.572	0.557	4.8	0.062	0.109	0.008
35.753	0.488	0.150	0.850	0.575	0.554	4.7	0.062	0.108	0.011
35.932	0.486	0.159	0.841	0.578	0.552	4.7	0.062	0.107	0.015
36.092	0.483	0.173	0.827	0.584	0.548	4.6	0.061	0.105	0.024
36.265	0.479	0.196	0.804	0.596	0.544	4.6	0.061	0.102	0.030
36.434	0.473	0.214	0.786	0.602	0.537	4.5	0.060	0.100	0.025
36.624	0.468	0.221	0.779	0.601	0.531	4.4	0.059	0.099	0.023
36.803	0.463	0.235	0.765	0.606	0.526	4.3	0.059	0.097	0.022
36.981	0.459	0.244	0.756	0.607	0.521	4.3	0.058	0.096	0.027
37.162	0.456	0.253	0.747	0.610	0.517	4.2	0.058	0.095	0.024
37.348	0.450	0.264	0.736	0.612	0.511	4.2	0.057	0.093	0.027
37.530	0.445	0.270	0.730	0.610	0.505	4.1	0.056	0.092	0.024
37.714	0.442	0.275	0.725	0.609	0.502	4.0	0.056	0.092	0.022
37.897	0.439	0.274	0.726	0.606	0.499	4.0	0.056	0.092	0.023
38.074	0.437	0.280	0.720	0.606	0.495	4.0	0.055	0.091	0.027
38.261	0.433	0.284	0.716	0.605	0.492	3.9	0.055	0.091	0.025
38.441	0.430	0.291	0.709	0.606	0.488	3.9	0.055	0.090	0.026
38.623	0.427	0.297	0.703	0.607	0.484	3.8	0.054	0.089	0.028
38.810	0.424	0.300	0.700	0.605	0.481	3.8	0.054	0.089	0.034
38.986	0.421	0.306	0.694	0.606	0.478	3.7	0.053	0.088	0.038
39.168	0.418	0.311	0.689	0.608	0.475	3.7	0.053	0.087	0.044
39.346	0.413	0.326	0.674	0.613	0.469	3.6	0.052	0.085	0.044
39.535	0.406	0.346	0.654	0.621	0.461	3.5	0.051	0.083	0.047
39.723	0.399	0.363	0.637	0.626	0.452	3.5	0.050	0.081	0.043
39.906	0.393	0.370	0.630	0.625	0.447	3.4	0.050	0.080	0.037
40.088	0.392	0.370	0.630	0.622	0.445	3.4	0.050	0.080	0.041
40.268	0.390	0.368	0.632	0.617	0.443	3.3	0.049	0.080	0.037
40.452	0.388	0.371	0.629	0.616	0.440	3.3	0.049	0.080	0.039
40.624	0.386	0.375	0.625	0.617	0.438	3.3	0.049	0.079	0.040
40.806	0.383	0.380	0.620	0.617	0.434	3.2	0.048	0.079	0.050
40.985	0.380	0.385	0.615	0.619	0.432	3.2	0.048	0.078	0.049
41.176	0.377	0.395	0.605	0.623	0.427	3.2	0.048	0.077	0.056
41.364	0.373	0.403	0.597	0.624	0.423	3.1	0.047	0.076	0.060

shr.stn	sh.sts.	ndelU.	nv.sts.	nsh./v.st	sh./su	eu/su	sh/mpp	v.sts/mpp	v.stn
41.553	0.369	0.408	0.592	0.623	0.419	3.1	0.047	0.075	0.061
41.737	0.366	0.416	0.584	0.626	0.415	3.0	0.046	0.074	0.062
41.915	0.363	0.420	0.580	0.626	0.412	3.0	0.046	0.073	0.066
42.099	0.359	0.430	0.570	0.630	0.408	3.0	0.045	0.072	0.065
42.280	0.356	0.437	0.563	0.631	0.404	2.9	0.045	0.071	0.068

Ko CONSOLIDATED GEONOR DIRECT SIMPLE SHEAR TEST
MIT GEOTECHNICAL LAB

FILE NAME : DSS 48

REDUCTION DATA

UNITS: kg,cm,mVolts,Volts

- | | |
|---|--|
| 1. Test Name : DSS 48 | |
| 2. Date : 6/20/89 | |
| 3. OCR : 14.962 | |
| 4. Ver. Consolidation Stress (ksc) :0.772 | |
| 5. Pre-Shear Height (cm) :1.706 | |
| 6. Horizontal Shear Load Cell: | 7. Horizontal Displacement Transducer: |
| Zero: 0.0001 | Zero: -0.1134 |
| CF: 7065.518 | CF: 2.2815 |
| 8. Vertical Stress Load Cell: | 9. Vertical Height Transducer: |
| Zero: 0.2122 | Zero: 0.07545 |
| CF: -1188.86 | CF: 2.0655 |

shr.stn	sh.sts.	ndelU.	nv.sts.	nsh./v.st	sh./su	eu/su	sh/mpp	v.sts/mpp	v.stn
0.000	0.002	0.004	0.996	0.002	0.002	8907.6	0.000	0.068	0.007
0.007	0.013	-0.016	1.016	0.013	0.012	664.4	0.001	0.069	0.006
0.020	0.060	-0.005	1.005	0.060	0.054	877.4	0.004	0.068	0.008
0.078	0.154	-0.038	1.038	0.149	0.139	554.1	0.011	0.071	-0.002
0.177	0.239	-0.047	1.047	0.229	0.216	375.8	0.016	0.071	-0.010
0.317	0.304	-0.103	1.103	0.275	0.274	264.6	0.021	0.075	-0.007
0.461	0.350	-0.118	1.118	0.313	0.316	208.4	0.024	0.076	-0.012
0.619	0.386	-0.165	1.165	0.331	0.348	171.2	0.026	0.079	-0.015
0.776	0.416	-0.180	1.180	0.353	0.376	147.3	0.028	0.080	-0.019
0.936	0.444	-0.222	1.222	0.363	0.401	130.1	0.030	0.083	-0.022
1.099	0.469	-0.246	1.246	0.377	0.424	117.0	0.032	0.085	-0.021
1.265	0.490	-0.255	1.255	0.391	0.443	106.2	0.033	0.085	-0.030
1.429	0.515	-0.296	1.296	0.397	0.465	98.6	0.035	0.088	-0.032
1.597	0.535	-0.303	1.303	0.411	0.483	91.7	0.036	0.089	-0.034
1.770	0.556	-0.352	1.352	0.411	0.502	85.9	0.038	0.092	-0.032
1.930	0.575	-0.347	1.347	0.427	0.519	81.5	0.039	0.092	-0.036
2.098	0.591	-0.348	1.348	0.439	0.534	77.0	0.040	0.092	-0.044
2.268	0.609	-0.391	1.391	0.438	0.550	73.4	0.041	0.095	-0.048
2.438	0.623	-0.392	1.392	0.448	0.562	69.8	0.042	0.095	-0.054
2.608	0.642	-0.456	1.456	0.441	0.579	67.2	0.044	0.099	-0.058
2.779	0.658	-0.455	1.455	0.452	0.594	64.7	0.045	0.099	-0.058
2.944	0.673	-0.467	1.467	0.459	0.608	62.5	0.046	0.100	-0.066
3.107	0.691	-0.526	1.526	0.453	0.624	60.7	0.047	0.104	-0.070
3.280	0.705	-0.510	1.510	0.467	0.637	58.7	0.048	0.103	-0.066
3.450	0.721	-0.546	1.546	0.466	0.651	57.0	0.049	0.105	-0.077
3.624	0.736	-0.585	1.585	0.464	0.665	55.4	0.050	0.108	-0.080
3.795	0.746	-0.566	1.566	0.476	0.674	53.6	0.051	0.107	-0.086
3.968	0.760	-0.587	1.587	0.479	0.686	52.3	0.052	0.108	-0.086
4.142	0.774	-0.626	1.626	0.476	0.699	51.0	0.053	0.111	-0.095
4.310	0.787	-0.644	1.644	0.479	0.711	49.8	0.054	0.112	-0.090
4.486	0.797	-0.630	1.630	0.489	0.720	48.5	0.054	0.111	-0.099

shr.stn	sh.sts.	ndelU.	nv.sts.	nsh./v.st	sh./su	eu/su	sh/mpp	v.sts/mpp	v.stn
4.654	0.813	-0.709	1.709	0.476	0.734	47.6	0.055	0.116	-0.106
4.834	0.822	-0.674	1.674	0.491	0.742	46.4	0.056	0.114	-0.109
5.002	0.832	-0.703	1.703	0.488	0.751	45.3	0.057	0.116	-0.117
5.180	0.845	-0.740	1.740	0.485	0.763	44.5	0.057	0.118	-0.113
5.350	0.854	-0.740	1.740	0.491	0.771	43.5	0.058	0.118	-0.120
5.517	0.864	-0.786	1.786	0.484	0.780	42.7	0.059	0.122	-0.120
5.701	0.877	-0.786	1.786	0.491	0.792	41.9	0.060	0.122	-0.123
5.874	0.885	-0.824	1.824	0.485	0.799	41.1	0.060	0.124	-0.128
6.050	0.896	-0.825	1.825	0.491	0.809	40.3	0.061	0.124	-0.132
6.219	0.905	-0.868	1.868	0.485	0.817	39.7	0.062	0.127	-0.131
6.395	0.916	-0.865	1.865	0.491	0.827	39.0	0.062	0.127	-0.128
6.573	0.925	-0.867	1.867	0.496	0.835	38.4	0.063	0.127	-0.132
6.745	0.932	-0.878	1.878	0.496	0.841	37.6	0.063	0.128	-0.142
6.917	0.945	-0.932	1.932	0.489	0.853	37.2	0.064	0.131	-0.138
7.095	0.951	-0.924	1.924	0.494	0.859	36.5	0.065	0.131	-0.144
7.282	0.959	-0.923	1.923	0.498	0.866	35.9	0.065	0.131	-0.143
7.462	0.967	-0.972	1.972	0.491	0.874	35.3	0.066	0.134	-0.154
7.650	0.974	-0.980	1.980	0.492	0.880	34.7	0.066	0.135	-0.150
7.823	0.981	-0.974	1.974	0.497	0.886	34.2	0.067	0.134	-0.158
8.004	0.987	-1.005	2.005	0.492	0.891	33.6	0.067	0.136	-0.156
8.183	0.997	-1.021	2.021	0.493	0.900	33.2	0.068	0.138	-0.161
8.359	1.000	-1.019	2.019	0.496	0.903	32.6	0.068	0.137	-0.158
8.537	1.008	-1.019	2.019	0.499	0.910	32.2	0.069	0.137	-0.161
8.715	1.011	-1.043	2.043	0.495	0.913	31.6	0.069	0.139	-0.165
8.898	1.020	-1.066	2.066	0.493	0.921	31.2	0.069	0.141	-0.167
9.072	1.025	-1.108	2.108	0.486	0.925	30.8	0.070	0.143	-0.161
9.255	1.033	-1.126	2.126	0.486	0.933	30.4	0.070	0.145	-0.159
9.430	1.038	-1.130	2.130	0.487	0.937	30.0	0.071	0.145	-0.164
9.612	1.042	-1.125	2.125	0.490	0.940	29.5	0.071	0.145	-0.168
9.789	1.046	-1.144	2.144	0.488	0.945	29.1	0.071	0.146	-0.171
9.967	1.051	-1.159	2.159	0.487	0.949	28.7	0.072	0.147	-0.174
10.142	1.057	-1.155	2.155	0.490	0.954	28.4	0.072	0.147	-0.171
10.323	1.056	-1.176	2.176	0.485	0.953	27.8	0.072	0.148	-0.172
10.496	1.064	-1.185	2.185	0.487	0.960	27.6	0.072	0.149	-0.173
10.668	1.065	-1.185	2.185	0.488	0.962	27.2	0.072	0.149	-0.175
10.848	1.071	-1.220	2.220	0.483	0.967	26.9	0.073	0.151	-0.170
11.021	1.078	-1.243	2.243	0.481	0.973	26.6	0.073	0.153	-0.169
11.201	1.078	-1.233	2.233	0.483	0.974	26.2	0.073	0.152	-0.168
11.374	1.083	-1.232	2.232	0.485	0.978	25.9	0.074	0.152	-0.169
11.554	1.084	-1.241	2.241	0.484	0.979	25.5	0.074	0.153	-0.172
11.736	1.091	-1.245	2.245	0.486	0.985	25.3	0.074	0.153	-0.165
11.905	1.086	-1.220	2.220	0.489	0.981	24.8	0.074	0.151	-0.176
12.094	1.098	-1.279	2.279	0.482	0.991	24.7	0.075	0.155	-0.163
12.254	1.098	-1.256	2.256	0.487	0.992	24.4	0.075	0.154	-0.165
12.436	1.100	-1.253	2.253	0.488	0.993	24.1	0.075	0.153	-0.165
12.611	1.101	-1.253	2.253	0.488	0.994	23.8	0.075	0.153	-0.164
12.810	1.100	-1.255	2.255	0.488	0.994	23.4	0.075	0.153	-0.163
12.962	1.108	-1.325	2.325	0.476	1.000	23.3	0.075	0.158	-0.158
13.158	1.106	-1.261	2.261	0.489	0.999	22.9	0.075	0.154	-0.157
13.310	1.103	-1.242	2.242	0.492	0.996	22.6	0.075	0.153	-0.164
13.505	1.100	-1.247	2.247	0.489	0.993	22.2	0.075	0.153	-0.166
13.696	1.098	-1.250	2.250	0.488	0.992	21.8	0.075	0.153	-0.165

shr.stn	sh.sts.	ndelU.	nv.sts.	nsh./v.st	sh./su	eu/su	sh/mpp	v.sts/mpp	v.stn
13.846	1.094	-1.249	2.249	0.486	0.988	21.5	0.074	0.153	-0.167
14.034	1.088	-1.246	2.246	0.484	0.982	21.1	0.074	0.153	-0.168
14.222	1.083	-1.253	2.253	0.481	0.978	20.7	0.074	0.153	-0.163
14.417	1.078	-1.243	2.243	0.481	0.973	20.4	0.073	0.153	-0.158
14.583	1.074	-1.237	2.237	0.480	0.970	20.0	0.073	0.152	-0.156
14.771	1.068	-1.224	2.224	0.480	0.965	19.7	0.073	0.151	-0.147
14.925	1.063	-1.208	2.208	0.481	0.960	19.4	0.072	0.150	-0.150
15.110	1.057	-1.185	2.185	0.484	0.954	19.0	0.072	0.149	-0.149
15.309	1.046	-1.139	2.139	0.489	0.944	18.6	0.071	0.146	-0.145
15.501	1.034	-1.114	2.114	0.489	0.934	18.2	0.070	0.144	-0.149
15.676	1.027	-1.103	2.103	0.488	0.927	17.8	0.070	0.143	-0.147
15.838	1.020	-1.082	2.082	0.490	0.921	17.5	0.069	0.142	-0.150
16.031	1.009	-1.055	2.055	0.491	0.911	17.1	0.069	0.140	-0.153
16.214	1.003	-1.040	2.040	0.492	0.906	16.8	0.068	0.139	-0.153
16.411	0.994	-1.027	2.027	0.490	0.898	16.5	0.068	0.138	-0.153
16.586	0.990	-1.020	2.020	0.490	0.894	16.3	0.067	0.138	-0.153
16.768	0.986	-1.014	2.014	0.489	0.890	16.0	0.067	0.137	-0.149
16.948	0.980	-1.005	2.005	0.489	0.885	15.8	0.067	0.136	-0.145
17.135	0.975	-0.987	1.987	0.491	0.881	15.5	0.066	0.135	-0.143
17.302	0.970	-0.978	1.978	0.490	0.876	15.3	0.066	0.135	-0.143
17.469	0.967	-0.970	1.970	0.491	0.873	15.1	0.066	0.134	-0.141
17.661	0.963	-0.954	1.954	0.493	0.869	14.8	0.066	0.133	-0.138
17.849	0.958	-0.932	1.932	0.496	0.865	14.6	0.065	0.132	-0.141
18.026	0.951	-0.916	1.916	0.496	0.858	14.4	0.065	0.130	-0.143
18.208	0.946	-0.899	1.899	0.498	0.854	14.2	0.064	0.129	-0.140
18.386	0.941	-0.884	1.884	0.500	0.850	13.9	0.064	0.128	-0.144
18.565	0.936	-0.874	1.874	0.499	0.845	13.7	0.064	0.128	-0.140
18.742	0.933	-0.872	1.872	0.498	0.842	13.6	0.063	0.127	-0.143
18.923	0.929	-0.867	1.867	0.498	0.839	13.4	0.063	0.127	-0.138
19.100	0.927	-0.860	1.860	0.499	0.837	13.2	0.063	0.127	-0.133
19.275	0.925	-0.852	1.852	0.499	0.835	13.1	0.063	0.126	-0.135
19.452	0.922	-0.846	1.846	0.499	0.832	12.9	0.063	0.126	-0.131
19.626	0.920	-0.844	1.844	0.499	0.830	12.8	0.063	0.126	-0.132
19.801	0.919	-0.841	1.841	0.499	0.830	12.6	0.063	0.125	-0.123
19.976	0.918	-0.836	1.836	0.500	0.829	12.5	0.062	0.125	-0.115
20.156	0.916	-0.831	1.831	0.500	0.827	12.4	0.062	0.125	-0.113
20.330	0.914	-0.823	1.823	0.501	0.826	12.3	0.062	0.124	-0.110
20.511	0.912	-0.809	1.809	0.504	0.823	12.1	0.062	0.123	-0.106
20.685	0.908	-0.805	1.805	0.503	0.820	12.0	0.062	0.123	-0.105
20.863	0.904	-0.798	1.798	0.503	0.816	11.8	0.062	0.122	-0.102
21.034	0.904	-0.785	1.785	0.507	0.816	11.7	0.062	0.121	-0.096
21.214	0.899	-0.756	1.756	0.512	0.812	11.6	0.061	0.120	-0.093
21.394	0.892	-0.721	1.721	0.518	0.806	11.4	0.061	0.117	-0.094
21.571	0.885	-0.703	1.703	0.520	0.799	11.2	0.060	0.116	-0.093
21.756	0.879	-0.681	1.681	0.523	0.794	11.0	0.060	0.114	-0.094
21.930	0.873	-0.661	1.661	0.526	0.789	10.9	0.059	0.113	-0.098
22.111	0.865	-0.651	1.651	0.524	0.781	10.7	0.059	0.112	-0.100
22.291	0.862	-0.642	1.642	0.525	0.778	10.5	0.059	0.112	-0.097
22.469	0.856	-0.631	1.631	0.525	0.773	10.4	0.058	0.111	-0.096
22.650	0.854	-0.630	1.630	0.524	0.771	10.3	0.058	0.111	-0.093
22.823	0.850	-0.628	1.628	0.522	0.767	10.1	0.058	0.111	-0.093
23.001	0.850	-0.627	1.627	0.522	0.767	10.1	0.058	0.111	-0.094

shr.stn	sh.sts.	ndelU.	nv.sts.	nsh./v.st	sh./su	eu/su	sh/mpp	v.sts/mpp	v.stn
23.175	0.846	-0.618	1.618	0.523	0.764	10.0	0.058	0.110	-0.093
23.356	0.841	-0.586	1.586	0.530	0.759	9.8	0.057	0.108	-0.093
23.532	0.836	-0.581	1.581	0.529	0.755	9.7	0.057	0.108	-0.084
23.715	0.831	-0.565	1.565	0.531	0.750	9.6	0.057	0.107	-0.087
23.889	0.829	-0.564	1.564	0.530	0.748	9.5	0.056	0.106	-0.082
24.070	0.825	-0.563	1.563	0.528	0.745	9.3	0.056	0.106	-0.082
24.247	0.823	-0.550	1.550	0.531	0.743	9.3	0.056	0.106	-0.082
24.422	0.816	-0.523	1.523	0.536	0.737	9.1	0.056	0.104	-0.077
24.607	0.812	-0.519	1.519	0.534	0.733	9.0	0.055	0.103	-0.076
24.783	0.806	-0.498	1.498	0.538	0.728	8.9	0.055	0.102	-0.073
24.965	0.800	-0.485	1.485	0.539	0.723	8.7	0.054	0.101	-0.075
25.141	0.795	-0.481	1.481	0.537	0.718	8.6	0.054	0.101	-0.079
25.319	0.791	-0.479	1.479	0.535	0.714	8.5	0.054	0.101	-0.078
25.497	0.789	-0.477	1.477	0.534	0.713	8.4	0.054	0.101	-0.069
25.675	0.787	-0.474	1.474	0.534	0.710	8.4	0.054	0.100	-0.071
25.857	0.784	-0.470	1.470	0.533	0.708	8.3	0.053	0.100	-0.061
26.033	0.781	-0.469	1.469	0.532	0.705	8.2	0.053	0.100	-0.061
26.213	0.779	-0.461	1.461	0.533	0.704	8.1	0.053	0.099	-0.053
26.391	0.775	-0.451	1.451	0.534	0.700	8.0	0.053	0.099	-0.049
26.573	0.772	-0.442	1.442	0.536	0.697	7.9	0.053	0.098	-0.049
26.746	0.767	-0.412	1.412	0.543	0.693	7.8	0.052	0.096	-0.051
26.925	0.761	-0.387	1.387	0.548	0.687	7.7	0.052	0.094	-0.053
27.103	0.756	-0.384	1.384	0.546	0.682	7.6	0.051	0.094	-0.057
27.283	0.751	-0.357	1.357	0.553	0.678	7.5	0.051	0.092	-0.050
27.462	0.746	-0.353	1.353	0.551	0.673	7.4	0.051	0.092	-0.053
27.637	0.741	-0.353	1.353	0.547	0.669	7.3	0.050	0.092	-0.053
27.816	0.739	-0.349	1.349	0.547	0.667	7.2	0.050	0.092	-0.047
27.994	0.734	-0.348	1.348	0.545	0.663	7.2	0.050	0.092	-0.044
28.174	0.732	-0.342	1.342	0.545	0.661	7.1	0.050	0.091	-0.046
28.350	0.728	-0.327	1.327	0.549	0.658	7.0	0.050	0.090	-0.047
28.532	0.722	-0.293	1.293	0.558	0.652	6.9	0.049	0.088	-0.049
28.710	0.718	-0.287	1.287	0.558	0.648	6.8	0.049	0.088	-0.048
28.887	0.713	-0.284	1.284	0.555	0.644	6.7	0.049	0.087	-0.049
29.071	0.709	-0.261	1.261	0.563	0.641	6.7	0.048	0.086	-0.051
29.246	0.703	-0.259	1.259	0.559	0.635	6.6	0.048	0.086	-0.051
29.427	0.701	-0.258	1.258	0.557	0.633	6.5	0.048	0.086	-0.046
29.603	0.697	-0.257	1.257	0.554	0.629	6.4	0.047	0.086	-0.045
29.785	0.693	-0.253	1.253	0.553	0.626	6.4	0.047	0.085	-0.045
29.960	0.690	-0.249	1.249	0.553	0.623	6.3	0.047	0.085	-0.035
30.140	0.686	-0.239	1.239	0.554	0.620	6.2	0.047	0.084	-0.029
30.318	0.682	-0.217	1.217	0.561	0.616	6.1	0.046	0.083	-0.033
30.497	0.675	-0.206	1.206	0.560	0.610	6.0	0.046	0.082	-0.037
30.678	0.673	-0.203	1.203	0.560	0.608	6.0	0.046	0.082	-0.036
30.854	0.669	-0.201	1.201	0.557	0.604	5.9	0.046	0.082	-0.029
31.036	0.667	-0.198	1.198	0.557	0.602	5.9	0.045	0.082	-0.033
31.206	0.663	-0.190	1.190	0.557	0.599	5.8	0.045	0.081	-0.026
31.392	0.659	-0.164	1.164	0.566	0.595	5.7	0.045	0.079	-0.028
31.571	0.649	-0.133	1.133	0.573	0.586	5.6	0.044	0.077	-0.038
31.756	0.642	-0.129	1.129	0.569	0.580	5.5	0.044	0.077	-0.034
31.934	0.638	-0.115	1.115	0.572	0.576	5.5	0.043	0.076	-0.035
32.113	0.632	-0.103	1.103	0.573	0.571	5.4	0.043	0.075	-0.043
32.295	0.629	-0.104	1.104	0.569	0.568	5.3	0.043	0.075	-0.043

shr.stn	sh.sts.	ndelU.	nv.sts.	nsh./v.st	sh./su	eu/su	sh/mpp	v.sts/mpp	v.stn
32.469	0.627	-0.102	1.102	0.568	0.566	5.3	0.043	0.075	-0.037
32.657	0.623	-0.100	1.100	0.567	0.563	5.2	0.042	0.075	-0.034
32.836	0.621	-0.097	1.097	0.566	0.561	5.2	0.042	0.075	-0.027
33.025	0.618	-0.099	1.099	0.562	0.558	5.1	0.042	0.075	-0.026
33.204	0.616	-0.097	1.097	0.562	0.556	5.1	0.042	0.075	-0.028
33.389	0.613	-0.087	1.087	0.564	0.554	5.0	0.042	0.074	-0.023
33.567	0.609	-0.069	1.069	0.570	0.550	5.0	0.041	0.073	-0.018
33.746	0.604	-0.060	1.060	0.570	0.545	4.9	0.041	0.072	-0.022
33.930	0.600	-0.058	1.058	0.567	0.542	4.8	0.041	0.072	-0.026
34.117	0.598	-0.056	1.056	0.567	0.540	4.8	0.041	0.072	-0.027
34.301	0.596	-0.050	1.050	0.567	0.538	4.7	0.041	0.071	-0.016
34.481	0.593	-0.048	1.048	0.566	0.535	4.7	0.040	0.071	-0.021
34.660	0.589	-0.034	1.034	0.569	0.532	4.6	0.040	0.070	-0.024
34.841	0.583	-0.011	1.011	0.577	0.527	4.6	0.040	0.069	-0.017
35.027	0.572	0.023	0.977	0.586	0.517	4.5	0.039	0.066	-0.025
35.198	0.567	0.018	0.982	0.578	0.512	4.4	0.039	0.067	-0.026
35.377	0.563	0.018	0.982	0.573	0.508	4.3	0.038	0.067	-0.030
35.557	0.561	-0.006	1.006	0.557	0.506	4.3	0.038	0.068	-0.032
35.736	0.560	0.002	0.998	0.562	0.506	4.3	0.038	0.068	-0.025
35.921	0.555	0.032	0.968	0.574	0.501	4.2	0.038	0.066	-0.021

 Ko CONSOLIDATED GEONOR DIRECT SIMPLE SHEAR TEST
 MIT GEOTECHNICAL LAB

FILE NAME : DSS 50

 REDUCTION DATA
 UNITS: kg,cm,mVolts,Volts

1. Test Name : DSS 50
 2. Date : 6/28/89
 3. OCR : 7.799
 4. Ver. Consolidation Stress (ksc) :0.379
 5. Pre-Shear Height (cm) :1.9315
 6. Horizontal Shear Load Cell: 7. Horizontal Displacement Transducer:
 Zero: 0.0001 Zero: -0.124
 CF: 7065.518 CF: 2.2815
 8. Vertical Stress Load Cell: 9. Vertical Height Transducer:
 Zero: -0.00053 Zero: -0.1338
 CF: 13674.89 CF: 2.0655

shr.stn	sh.sts.	ndelU.	nv.sts.	nsh./v.st	sh./su	eu/su	sh/mpp	v.sts/mpp	v.stn
0.000	-0.006	0.003	0.997	-0.006	-0.007	9999.0	-0.001	0.128	0.000
0.001	-0.006	0.021	0.979	-0.006	-0.007	48.8	-0.001	0.125	0.002
0.003	0.001	0.037	0.963	0.001	0.002	782.8	0.000	0.123	0.001
0.004	0.003	0.044	0.956	0.004	0.004	714.9	0.000	0.123	0.001
0.012	0.024	0.048	0.952	0.025	0.026	794.6	0.003	0.122	-0.001
0.037	0.089	0.031	0.969	0.092	0.098	847.3	0.011	0.124	-0.003
0.118	0.189	0.022	0.978	0.194	0.208	547.6	0.024	0.125	-0.011
0.219	0.273	-0.027	1.027	0.266	0.300	420.4	0.035	0.132	-0.024
0.346	0.328	-0.110	1.110	0.295	0.360	318.6	0.042	0.142	-0.041
0.475	0.378	-0.191	1.191	0.318	0.416	267.2	0.049	0.153	-0.035
0.617	0.414	-0.210	1.210	0.342	0.456	224.8	0.053	0.155	-0.037
0.764	0.447	-0.229	1.229	0.364	0.492	196.1	0.057	0.158	-0.041
0.898	0.473	-0.291	1.291	0.366	0.520	176.1	0.061	0.166	-0.046
1.037	0.497	-0.301	1.301	0.382	0.546	160.1	0.064	0.167	-0.049
1.176	0.518	-0.340	1.340	0.387	0.570	147.1	0.066	0.172	-0.055
1.328	0.541	-0.354	1.354	0.399	0.595	135.9	0.069	0.174	-0.057
1.477	0.562	-0.391	1.391	0.404	0.618	127.0	0.072	0.178	-0.061
1.626	0.581	-0.413	1.413	0.411	0.639	119.2	0.075	0.181	-0.061
1.776	0.597	-0.418	1.418	0.421	0.657	112.1	0.077	0.182	-0.064
1.929	0.612	-0.435	1.435	0.426	0.673	105.7	0.078	0.184	-0.067
2.088	0.628	-0.456	1.456	0.431	0.691	100.2	0.081	0.187	-0.073
2.240	0.640	-0.475	1.475	0.434	0.704	95.2	0.082	0.189	-0.078
2.391	0.659	-0.554	1.554	0.424	0.725	91.8	0.085	0.199	-0.074
2.541	0.673	-0.557	1.557	0.432	0.740	88.1	0.086	0.200	-0.073
2.699	0.684	-0.569	1.569	0.436	0.752	84.4	0.088	0.201	-0.075
2.853	0.696	-0.581	1.581	0.440	0.765	81.2	0.089	0.203	-0.077
3.007	0.705	-0.595	1.595	0.442	0.775	78.0	0.090	0.205	-0.081
3.164	0.714	-0.609	1.609	0.444	0.785	75.1	0.092	0.206	-0.085
3.315	0.720	-0.619	1.619	0.445	0.792	72.3	0.092	0.208	-0.087
3.469	0.736	-0.693	1.693	0.434	0.809	70.6	0.094	0.217	-0.088
3.615	0.746	-0.703	1.703	0.438	0.821	68.7	0.096	0.218	-0.080

shr.stn	sh.sts.	ndelU.	nv.sts.	nsh./v.st	sh./su	eu/su	sh/mpp	v.sts/mpp	v.stn
3.771	0.757	-0.706	1.706	0.444	0.833	66.8	0.097	0.219	-0.080
3.924	0.767	-0.715	1.715	0.447	0.844	65.0	0.098	0.220	-0.082
4.080	0.776	-0.723	1.723	0.450	0.853	63.2	0.099	0.221	-0.083
4.236	0.786	-0.733	1.733	0.453	0.864	61.7	0.101	0.222	-0.085
4.384	0.795	-0.785	1.785	0.445	0.874	60.3	0.102	0.229	-0.086
4.543	0.801	-0.773	1.773	0.452	0.881	58.6	0.103	0.227	-0.085
4.698	0.805	-0.778	1.778	0.453	0.885	57.0	0.103	0.228	-0.086
4.858	0.813	-0.784	1.784	0.456	0.894	55.6	0.104	0.229	-0.088
5.013	0.818	-0.793	1.793	0.456	0.899	54.2	0.105	0.230	-0.090
5.170	0.824	-0.798	1.798	0.458	0.906	53.0	0.106	0.231	-0.092
5.328	0.827	-0.804	1.804	0.459	0.910	51.6	0.106	0.231	-0.094
5.485	0.829	-0.810	1.810	0.458	0.912	50.3	0.106	0.232	-0.095
5.641	0.834	-0.815	1.815	0.459	0.917	49.1	0.107	0.233	-0.098
5.795	0.836	-0.843	1.843	0.453	0.919	47.9	0.107	0.236	-0.101
5.951	0.843	-0.860	1.860	0.453	0.927	47.1	0.108	0.238	-0.098
6.106	0.846	-0.857	1.857	0.456	0.931	46.1	0.109	0.238	-0.099
6.266	0.852	-0.863	1.863	0.457	0.937	45.2	0.109	0.239	-0.099
6.422	0.856	-0.884	1.884	0.454	0.941	44.3	0.110	0.242	-0.100
6.582	0.858	-0.886	1.886	0.455	0.943	43.3	0.110	0.242	-0.101
6.738	0.863	-0.886	1.886	0.457	0.949	42.5	0.111	0.242	-0.100
6.895	0.865	-0.894	1.894	0.457	0.952	41.7	0.111	0.243	-0.101
7.049	0.870	-0.893	1.893	0.460	0.957	41.0	0.112	0.243	-0.101
7.205	0.871	-0.899	1.899	0.459	0.958	40.2	0.112	0.243	-0.102
7.366	0.875	-0.908	1.908	0.459	0.963	39.5	0.112	0.245	-0.103
7.520	0.874	-0.907	1.907	0.458	0.961	38.6	0.112	0.244	-0.102
7.683	0.878	-0.909	1.909	0.460	0.966	38.0	0.113	0.245	-0.104
7.844	0.882	-0.909	1.909	0.462	0.970	37.3	0.113	0.245	-0.104
8.022	0.885	-0.913	1.913	0.463	0.973	36.7	0.113	0.245	-0.105
8.185	0.887	-0.916	1.916	0.463	0.976	36.0	0.114	0.246	-0.105
8.350	0.891	-0.921	1.921	0.464	0.980	35.4	0.114	0.246	-0.106
8.512	0.896	-0.925	1.925	0.465	0.985	35.0	0.115	0.247	-0.105
8.672	0.897	-0.926	1.926	0.466	0.987	34.4	0.115	0.247	-0.106
8.833	0.899	-0.929	1.929	0.466	0.989	33.8	0.115	0.247	-0.107
8.988	0.898	-0.934	1.934	0.464	0.988	33.2	0.115	0.248	-0.107
9.149	0.901	-0.933	1.933	0.466	0.991	32.7	0.116	0.248	-0.107
9.302	0.901	-0.936	1.936	0.465	0.991	32.2	0.115	0.248	-0.108
9.465	0.902	-0.938	1.938	0.466	0.992	31.7	0.116	0.248	-0.109
9.623	0.902	-0.939	1.939	0.465	0.992	31.2	0.116	0.249	-0.110
9.779	0.902	-0.940	1.940	0.465	0.992	30.6	0.116	0.249	-0.110
9.937	0.903	-0.940	1.940	0.465	0.993	30.2	0.116	0.249	-0.110
10.096	0.904	-0.941	1.941	0.466	0.994	29.8	0.116	0.249	-0.111
10.259	0.906	-0.943	1.943	0.466	0.996	29.3	0.116	0.249	-0.112
10.412	0.903	-0.942	1.942	0.465	0.993	28.8	0.116	0.249	-0.111
10.573	0.906	-0.995	1.995	0.454	0.996	28.5	0.116	0.256	-0.110
10.726	0.909	-0.988	1.988	0.457	1.000	28.2	0.117	0.255	-0.097
10.884	0.908	-0.964	1.964	0.462	0.998	27.7	0.116	0.252	-0.097
11.037	0.908	-0.952	1.952	0.465	0.999	27.3	0.116	0.250	-0.100
11.197	0.906	-0.929	1.929	0.470	0.997	26.9	0.116	0.247	-0.104
11.359	0.904	-0.911	1.911	0.473	0.994	26.4	0.116	0.245	-0.111
11.518	0.901	-0.941	1.941	0.464	0.991	26.0	0.116	0.249	-0.116
11.679	0.900	-0.928	1.928	0.467	0.990	25.6	0.115	0.247	-0.111
11.836	0.897	-0.926	1.926	0.466	0.986	25.2	0.115	0.247	-0.111

shr.stn	sh.sts.	ndelU.	nv.sts.	nsh./v.st	sh./su	eu/su	sh/mpp	v.sts/mpp	v.stn
11.999	0.897	-0.924	1.924	0.467	0.987	24.9	0.115	0.247	-0.111
12.159	0.897	-0.913	1.913	0.469	0.986	24.5	0.115	0.245	-0.111
12.320	0.894	-0.911	1.911	0.468	0.983	24.1	0.115	0.245	-0.112
12.474	0.891	-0.892	1.892	0.471	0.980	23.7	0.114	0.243	-0.113
12.638	0.886	-0.873	1.873	0.473	0.975	23.3	0.114	0.240	-0.115
12.799	0.885	-0.871	1.871	0.473	0.973	23.0	0.113	0.240	-0.115
12.961	0.883	-0.885	1.885	0.469	0.972	22.6	0.113	0.242	-0.116
13.106	0.883	-0.872	1.872	0.472	0.971	22.4	0.113	0.240	-0.114
13.259	0.880	-0.867	1.867	0.471	0.968	22.1	0.113	0.239	-0.113
13.428	0.878	-0.858	1.858	0.472	0.965	21.7	0.113	0.238	-0.111
13.575	0.874	-0.850	1.850	0.473	0.962	21.4	0.112	0.237	-0.109
13.730	0.872	-0.841	1.841	0.473	0.959	21.1	0.112	0.236	-0.108
13.895	0.871	-0.837	1.837	0.474	0.958	20.8	0.112	0.235	-0.107
14.055	0.866	-0.825	1.825	0.474	0.952	20.5	0.111	0.234	-0.105
14.214	0.863	-0.813	1.813	0.476	0.949	20.2	0.111	0.232	-0.104
14.378	0.859	-0.806	1.806	0.476	0.945	19.9	0.110	0.232	-0.103
14.529	0.854	-0.803	1.803	0.474	0.939	19.5	0.110	0.231	-0.103
14.696	0.854	-0.792	1.792	0.476	0.939	19.3	0.109	0.230	-0.102
14.858	0.852	-0.781	1.781	0.478	0.937	19.1	0.109	0.228	-0.099
15.004	0.851	-0.775	1.775	0.480	0.936	18.9	0.109	0.228	-0.098
15.156	0.849	-0.768	1.768	0.480	0.934	18.6	0.109	0.227	-0.097
15.322	0.850	-0.758	1.758	0.483	0.934	18.4	0.109	0.225	-0.095
15.476	0.846	-0.750	1.750	0.484	0.931	18.2	0.108	0.224	-0.094
15.646	0.842	-0.742	1.742	0.483	0.926	17.9	0.108	0.223	-0.095
15.805	0.841	-0.734	1.734	0.485	0.925	17.7	0.108	0.222	-0.093
15.962	0.837	-0.727	1.727	0.485	0.920	17.4	0.107	0.221	-0.091
16.105	0.834	-0.718	1.718	0.486	0.917	17.2	0.107	0.220	-0.090
16.266	0.831	-0.709	1.709	0.486	0.914	17.0	0.107	0.219	-0.089
16.435	0.830	-0.708	1.708	0.486	0.913	16.8	0.106	0.219	-0.089
16.584	0.828	-0.695	1.695	0.488	0.910	16.6	0.106	0.217	-0.088
16.727	0.829	-0.675	1.675	0.495	0.911	16.5	0.106	0.215	-0.086
16.885	0.825	-0.668	1.668	0.495	0.908	16.3	0.106	0.214	-0.087
17.065	0.819	-0.651	1.651	0.496	0.901	16.0	0.105	0.212	-0.088
17.217	0.816	-0.640	1.640	0.498	0.898	15.8	0.105	0.210	-0.089
17.376	0.812	-0.633	1.633	0.497	0.893	15.5	0.104	0.209	-0.090
17.534	0.809	-0.619	1.619	0.500	0.890	15.3	0.104	0.208	-0.090
17.695	0.803	-0.606	1.606	0.500	0.884	15.1	0.103	0.206	-0.090
17.851	0.800	-0.592	1.592	0.503	0.880	14.9	0.103	0.204	-0.092
18.008	0.795	-0.586	1.586	0.501	0.874	14.7	0.102	0.203	-0.092
18.165	0.794	-0.581	1.581	0.502	0.874	14.5	0.102	0.203	-0.092
18.321	0.792	-0.578	1.578	0.502	0.871	14.4	0.102	0.202	-0.092
18.482	0.791	-0.574	1.574	0.503	0.870	14.2	0.101	0.202	-0.091
18.631	0.790	-0.586	1.586	0.498	0.869	14.1	0.101	0.203	-0.092
18.788	0.792	-0.588	1.588	0.499	0.871	14.0	0.102	0.204	-0.086
18.941	0.791	-0.577	1.577	0.502	0.870	13.9	0.101	0.202	-0.084
19.099	0.789	-0.571	1.571	0.502	0.867	13.7	0.101	0.201	-0.083
19.255	0.787	-0.566	1.566	0.503	0.866	13.6	0.101	0.201	-0.082
19.412	0.784	-0.559	1.559	0.503	0.862	13.4	0.101	0.200	-0.080
19.570	0.780	-0.537	1.537	0.507	0.858	13.3	0.100	0.197	-0.079
19.726	0.776	-0.532	1.532	0.506	0.853	13.1	0.099	0.196	-0.079
19.885	0.773	-0.526	1.526	0.507	0.851	12.9	0.099	0.196	-0.078
20.038	0.771	-0.522	1.522	0.506	0.847	12.8	0.099	0.195	-0.077

shr.stn	sh.sts.	ndelU.	nv.sts.	nsh./v.st	sh./su	eu/su	sh/mpp	v.sts/mpp	v.stn
20.202	0.768	-0.512	1.512	0.508	0.845	12.6	0.099	0.194	-0.077
20.356	0.764	-0.501	1.501	0.509	0.840	12.5	0.098	0.193	-0.076
20.517	0.759	-0.482	1.482	0.512	0.835	12.3	0.097	0.190	-0.074
20.674	0.754	-0.457	1.457	0.517	0.829	12.1	0.097	0.187	-0.079
20.833	0.749	-0.455	1.455	0.515	0.824	12.0	0.096	0.187	-0.079
20.989	0.747	-0.451	1.451	0.515	0.822	11.8	0.096	0.186	-0.079
21.144	0.744	-0.438	1.438	0.517	0.818	11.7	0.095	0.184	-0.077
21.305	0.743	-0.432	1.432	0.519	0.817	11.6	0.095	0.184	-0.078
21.457	0.737	-0.428	1.428	0.516	0.810	11.4	0.094	0.183	-0.078
21.619	0.735	-0.416	1.416	0.519	0.808	11.3	0.094	0.182	-0.077
21.772	0.729	-0.405	1.405	0.519	0.802	11.1	0.093	0.180	-0.076
21.935	0.725	-0.400	1.400	0.518	0.797	11.0	0.093	0.180	-0.076
22.091	0.721	-0.394	1.394	0.517	0.793	10.9	0.092	0.179	-0.075
22.248	0.717	-0.382	1.382	0.519	0.788	10.7	0.092	0.177	-0.073
22.404	0.714	-0.378	1.378	0.518	0.785	10.6	0.092	0.177	-0.073
22.561	0.710	-0.374	1.374	0.517	0.781	10.5	0.091	0.176	-0.072
22.723	0.709	-0.363	1.363	0.520	0.780	10.4	0.091	0.175	-0.071
22.876	0.705	-0.352	1.352	0.522	0.776	10.3	0.090	0.173	-0.071
23.033	0.703	-0.338	1.338	0.525	0.773	10.2	0.090	0.172	-0.070
23.190	0.701	-0.332	1.332	0.526	0.771	10.1	0.090	0.171	-0.070
23.352	0.697	-0.321	1.321	0.528	0.767	9.9	0.089	0.169	-0.069
23.510	0.696	-0.312	1.312	0.530	0.765	9.9	0.089	0.168	-0.067
23.673	0.690	-0.310	1.310	0.527	0.759	9.7	0.088	0.168	-0.068
23.836	0.688	-0.302	1.302	0.528	0.757	9.6	0.088	0.167	-0.067
23.992	0.686	-0.294	1.294	0.530	0.754	9.5	0.088	0.166	-0.065
24.151	0.683	-0.277	1.277	0.535	0.752	9.4	0.088	0.164	-0.062
24.307	0.678	-0.265	1.265	0.536	0.745	9.3	0.087	0.162	-0.061
24.470	0.671	-0.255	1.255	0.535	0.738	9.1	0.086	0.161	-0.061
24.624	0.665	-0.238	1.238	0.537	0.731	9.0	0.085	0.159	-0.060
24.786	0.660	-0.232	1.232	0.535	0.726	8.9	0.085	0.158	-0.059
24.943	0.656	-0.226	1.226	0.535	0.721	8.8	0.084	0.157	-0.058
25.100	0.651	-0.215	1.215	0.536	0.716	8.6	0.083	0.156	-0.057
25.261	0.645	-0.197	1.197	0.539	0.710	8.5	0.083	0.153	-0.058
25.418	0.640	-0.189	1.189	0.538	0.704	8.4	0.082	0.152	-0.058
25.577	0.636	-0.169	1.169	0.544	0.700	8.3	0.082	0.150	-0.059
25.733	0.631	-0.163	1.163	0.543	0.694	8.2	0.081	0.149	-0.059
25.894	0.626	-0.142	1.142	0.548	0.688	8.1	0.080	0.146	-0.061
26.049	0.621	-0.140	1.140	0.545	0.683	7.9	0.080	0.146	-0.063
26.209	0.618	-0.133	1.133	0.545	0.679	7.9	0.079	0.145	-0.061
26.361	0.615	-0.130	1.130	0.544	0.677	7.8	0.079	0.145	-0.060
26.523	0.610	-0.131	1.131	0.539	0.671	7.7	0.078	0.145	-0.060
26.680	0.609	-0.116	1.116	0.546	0.670	7.6	0.078	0.143	-0.058
26.834	0.606	-0.121	1.121	0.540	0.666	7.5	0.078	0.144	-0.058
26.992	0.602	-0.107	1.107	0.544	0.662	7.4	0.077	0.142	-0.055
27.153	0.597	-0.095	1.095	0.545	0.657	7.3	0.077	0.140	-0.054
27.314	0.593	-0.085	1.085	0.546	0.652	7.2	0.076	0.139	-0.053
27.472	0.588	-0.071	1.071	0.549	0.647	7.1	0.075	0.137	-0.053
27.634	0.584	-0.066	1.066	0.548	0.642	7.0	0.075	0.137	-0.054
27.789	0.580	-0.062	1.062	0.546	0.638	7.0	0.074	0.136	-0.051
27.945	0.577	-0.056	1.056	0.546	0.635	6.9	0.074	0.135	-0.051
28.099	0.575	-0.050	1.050	0.547	0.632	6.8	0.074	0.135	-0.049
28.257	0.571	-0.044	1.044	0.547	0.628	6.7	0.073	0.134	-0.048

shr.stn	sh.sts.	ndelU.	nv.sts.	nsh./v.st	sh./su	eu/su	sh/mpp	v.sts/mpp	v.stn
28.413	0.568	-0.038	1.038	0.548	0.625	6.7	0.073	0.133	-0.047
28.568	0.565	-0.035	1.035	0.546	0.621	6.6	0.072	0.133	-0.046
28.729	0.563	-0.030	1.030	0.546	0.619	6.5	0.072	0.132	-0.045
28.886	0.560	-0.020	1.020	0.549	0.616	6.5	0.072	0.131	-0.042
29.044	0.557	-0.016	1.016	0.548	0.613	6.4	0.071	0.130	-0.041
29.197	0.555	-0.010	1.010	0.549	0.610	6.3	0.071	0.129	-0.039
29.356	0.552	-0.007	1.007	0.548	0.607	6.3	0.071	0.129	-0.038
29.513	0.550	-0.009	1.009	0.545	0.605	6.2	0.071	0.129	-0.036
29.665	0.548	-0.007	1.007	0.544	0.603	6.2	0.070	0.129	-0.033
29.824	0.544	0.024	0.976	0.557	0.598	6.1	0.070	0.125	-0.030
29.984	0.535	0.047	0.953	0.562	0.589	6.0	0.069	0.122	-0.037
30.143	0.532	0.051	0.949	0.561	0.585	5.9	0.068	0.122	-0.038
30.298	0.529	0.055	0.945	0.559	0.581	5.8	0.068	0.121	-0.039
30.456	0.525	0.058	0.942	0.557	0.577	5.8	0.067	0.121	-0.039
30.609	0.523	0.060	0.940	0.557	0.576	5.7	0.067	0.120	-0.038
30.765	0.522	0.050	0.950	0.549	0.574	5.7	0.067	0.122	-0.037
30.921	0.519	0.069	0.931	0.557	0.571	5.6	0.067	0.119	-0.034
31.081	0.515	0.075	0.925	0.556	0.566	5.5	0.066	0.119	-0.034
31.241	0.512	0.077	0.923	0.555	0.563	5.5	0.066	0.118	-0.033
31.391	0.510	0.079	0.921	0.553	0.561	5.4	0.065	0.118	-0.032
31.552	0.506	0.084	0.916	0.552	0.556	5.4	0.065	0.117	-0.032
31.709	0.503	0.086	0.914	0.550	0.553	5.3	0.064	0.117	-0.031
31.865	0.500	0.088	0.912	0.548	0.550	5.2	0.064	0.117	-0.029
32.026	0.499	0.091	0.909	0.549	0.549	5.2	0.064	0.117	-0.027
32.178	0.496	0.088	0.912	0.544	0.545	5.1	0.064	0.117	-0.025
32.340	0.495	0.092	0.908	0.545	0.545	5.1	0.064	0.116	-0.022
32.495	0.493	0.102	0.898	0.549	0.542	5.1	0.063	0.115	-0.020
32.655	0.489	0.115	0.885	0.553	0.538	5.0	0.063	0.114	-0.019
32.810	0.489	0.116	0.884	0.552	0.537	5.0	0.063	0.113	-0.019
32.968	0.485	0.116	0.884	0.549	0.534	4.9	0.062	0.113	-0.018
33.125	0.483	0.117	0.883	0.547	0.531	4.9	0.062	0.113	-0.018
33.297	0.468	0.186	0.814	0.575	0.515	4.7	0.060	0.104	-0.021

 Ko CONSOLIDATED GEONOR DIRECT SIMPLE SHEAR TEST
 MIT GEOTECHNICAL LAB

FILE NAME : DSS 51

 REDUCTION DATA
 UNITS: kg,cm,mVolts,Volts

1. Test Name : DSS 51
 2. Date : 7/2/89
 3. OCR : 31.904
 4. Ver. Consolidation Stress (ksc) :0.3729
 5. Pre-Shear Height (cm) :1.697
 6. Horizontal Shear Load Cell: 7. Horizontal Displacement Transducer:
 Zero: 0.0001 Zero: -0.1273
 CF: 7065.518 CF: 2.2815
 8. Vertical Stress Load Cell: 9. Vertical Height Transducer:
 Zero: -0.00053 Zero: -0.01435
 CF: 13674.89 CF: 2.0655

shr.stn	sh.sts.	ndelU.	nv.sts.	nsh./v.st	sh./su	eu/su	sh/mpp	v.sts/mpp	v.stn
0.000	-0.002	0.007	0.993	-0.002	-0.001	9999.0	0.000	0.031	0.000
0.004	0.001	0.078	0.922	0.001	0.000	126.6	0.000	0.029	0.011
0.005	0.009	0.068	0.932	0.010	0.005	351.6	0.000	0.029	0.003
0.005	0.036	-0.135	1.135	0.031	0.019	1141.1	0.001	0.036	-0.033
0.044	0.143	0.001	0.999	0.143	0.078	542.2	0.004	0.031	0.003
0.135	0.286	-0.052	1.052	0.272	0.156	349.3	0.009	0.033	-0.005
0.266	0.379	-0.205	1.205	0.314	0.206	233.7	0.012	0.038	-0.021
0.410	0.446	-0.229	1.229	0.363	0.242	178.3	0.014	0.039	-0.027
0.570	0.490	-0.141	1.141	0.430	0.266	140.8	0.015	0.036	-0.025
0.733	0.539	-0.340	1.340	0.402	0.293	120.4	0.017	0.042	-0.065
0.900	0.573	-0.277	1.277	0.449	0.311	104.1	0.018	0.040	-0.037
1.067	0.607	-0.357	1.357	0.448	0.330	93.1	0.019	0.043	-0.074
1.230	0.641	-0.389	1.389	0.461	0.348	85.3	0.020	0.044	-0.046
1.410	0.666	-0.394	1.394	0.478	0.362	77.3	0.021	0.044	-0.059
1.576	0.697	-0.453	1.453	0.480	0.379	72.3	0.022	0.046	-0.049
1.753	0.719	-0.435	1.435	0.501	0.391	67.0	0.023	0.045	-0.068
1.922	0.750	-0.488	1.488	0.504	0.408	63.8	0.024	0.047	-0.084
2.092	0.772	-0.549	1.549	0.499	0.420	60.3	0.024	0.049	-0.094
2.268	0.804	-0.581	1.581	0.508	0.437	57.9	0.025	0.050	-0.069
2.437	0.825	-0.598	1.598	0.516	0.448	55.3	0.026	0.050	-0.081
2.611	0.852	-0.664	1.664	0.512	0.463	53.4	0.027	0.052	-0.075
2.784	0.876	-0.658	1.658	0.529	0.476	51.5	0.027	0.052	-0.069
2.959	0.899	-0.712	1.712	0.525	0.488	49.6	0.028	0.054	-0.095
3.122	0.926	-0.769	1.769	0.523	0.503	48.5	0.029	0.055	-0.075
3.300	0.943	-0.729	1.729	0.545	0.512	46.7	0.030	0.054	-0.082
3.478	0.963	-0.766	1.766	0.546	0.524	45.3	0.030	0.055	-0.081
3.646	0.985	-0.854	1.854	0.531	0.536	44.2	0.031	0.058	-0.099
3.822	1.015	-0.918	1.918	0.529	0.552	43.4	0.032	0.060	-0.106
3.996	1.031	-0.871	1.871	0.551	0.560	42.2	0.032	0.059	-0.077
4.174	1.053	-0.938	1.938	0.543	0.572	41.2	0.033	0.061	-0.107
4.347	1.077	-0.963	1.963	0.548	0.585	40.5	0.034	0.062	-0.103

shr.stn	sh.sts.	ndelU.	nv.sts.	nsh./v.st	sh./su	eu/su	sh/mpp	v.sts/mpp	v.stn
4.520	1.099	-1.031	2.031	0.541	0.597	39.7	0.034	0.064	-0.094
4.691	1.122	-1.028	2.028	0.553	0.610	39.1	0.035	0.064	-0.110
4.866	1.139	-1.034	2.034	0.560	0.619	38.3	0.036	0.064	-0.107
5.042	1.158	-1.096	2.096	0.553	0.630	37.5	0.036	0.066	-0.118
5.212	1.183	-1.179	2.179	0.543	0.643	37.1	0.037	0.068	-0.114
5.390	1.201	-1.146	2.146	0.560	0.653	36.4	0.038	0.067	-0.108
5.567	1.211	-1.162	2.162	0.560	0.658	35.5	0.038	0.068	-0.131
5.744	1.232	-1.189	2.189	0.563	0.670	35.0	0.039	0.069	-0.109
5.914	1.257	-1.313	2.313	0.543	0.683	34.7	0.039	0.073	-0.126
6.091	1.274	-1.268	2.268	0.562	0.692	34.2	0.040	0.071	-0.109
6.273	1.288	-1.294	2.294	0.562	0.700	33.6	0.040	0.072	-0.128
6.440	1.312	-1.382	2.382	0.551	0.713	33.3	0.041	0.075	-0.126
6.620	1.327	-1.371	2.371	0.560	0.721	32.7	0.042	0.074	-0.126
6.794	1.341	-1.387	2.387	0.562	0.729	32.2	0.042	0.075	-0.114
6.973	1.356	-1.443	2.443	0.555	0.737	31.8	0.043	0.077	-0.139
7.150	1.371	-1.444	2.444	0.561	0.745	31.3	0.043	0.077	-0.118
7.321	1.390	-1.523	2.523	0.551	0.756	31.0	0.044	0.079	-0.130
7.500	1.410	-1.515	2.515	0.561	0.766	30.7	0.044	0.079	-0.145
7.678	1.417	-1.520	2.520	0.563	0.771	30.2	0.044	0.079	-0.123
7.856	1.438	-1.612	2.612	0.550	0.781	29.9	0.045	0.082	-0.154
8.032	1.452	-1.605	2.605	0.558	0.789	29.5	0.046	0.082	-0.124
8.209	1.470	-1.647	2.647	0.555	0.799	29.2	0.046	0.083	-0.156
8.383	1.482	-1.641	2.641	0.561	0.806	28.9	0.046	0.083	-0.151
8.566	1.497	-1.684	2.684	0.558	0.814	28.5	0.047	0.084	-0.154
8.739	1.510	-1.727	2.727	0.554	0.821	28.2	0.047	0.085	-0.153
8.920	1.530	-1.761	2.761	0.554	0.831	28.0	0.048	0.087	-0.157
9.105	1.548	-1.791	2.791	0.555	0.842	27.8	0.049	0.087	-0.156
9.295	1.556	-1.777	2.777	0.560	0.846	27.3	0.049	0.087	-0.167
9.480	1.572	-1.792	2.792	0.563	0.854	27.1	0.049	0.087	-0.173
9.662	1.582	-1.830	2.830	0.559	0.860	26.7	0.050	0.089	-0.157
9.846	1.596	-1.876	2.876	0.555	0.867	26.5	0.050	0.090	-0.178
10.021	1.607	-1.907	2.907	0.553	0.874	26.2	0.050	0.091	-0.153
10.203	1.626	-1.944	2.944	0.552	0.884	26.0	0.051	0.092	-0.179
10.376	1.633	-1.934	2.934	0.556	0.888	25.7	0.051	0.092	-0.167
10.558	1.642	-1.947	2.947	0.557	0.893	25.4	0.051	0.092	-0.176
10.735	1.652	-1.972	2.972	0.556	0.898	25.1	0.052	0.093	-0.165
10.910	1.665	-2.057	3.057	0.545	0.905	24.9	0.052	0.096	-0.164
11.085	1.682	-2.103	3.103	0.542	0.914	24.8	0.053	0.097	-0.159
11.262	1.681	-2.032	3.032	0.555	0.914	24.4	0.053	0.095	-0.162
11.444	1.698	-2.148	3.148	0.539	0.923	24.2	0.053	0.099	-0.189
11.618	1.707	-2.114	3.114	0.548	0.928	24.0	0.054	0.098	-0.173
11.799	1.717	-2.179	3.179	0.540	0.933	23.8	0.054	0.100	-0.187
11.975	1.728	-2.174	3.174	0.544	0.939	23.6	0.054	0.099	-0.164
12.148	1.736	-2.239	3.239	0.536	0.944	23.3	0.054	0.102	-0.178
12.325	1.751	-2.235	3.235	0.541	0.952	23.2	0.055	0.101	-0.181
12.506	1.753	-2.219	3.219	0.545	0.953	22.9	0.055	0.101	-0.161
12.681	1.770	-2.310	3.310	0.535	0.962	22.8	0.055	0.104	-0.183
12.860	1.776	-2.287	3.287	0.540	0.965	22.5	0.056	0.103	-0.178
13.040	1.783	-2.288	3.288	0.542	0.969	22.3	0.056	0.103	-0.166
13.214	1.785	-2.290	3.290	0.542	0.970	22.1	0.056	0.103	-0.168
13.398	1.802	-2.412	3.412	0.528	0.979	22.0	0.056	0.107	-0.194
13.578	1.808	-2.343	3.343	0.541	0.983	21.7	0.057	0.105	-0.183

shr.stn	sh.sts.	ndelU.	nv.sts.	nsh./v.st	sh./su	eu/su	sh/mpp	v.sts/mpp	v.stn
13.769	1.807	-2.347	3.347	0.540	0.983	21.4	0.057	0.105	-0.169
13.947	1.824	-2.477	3.477	0.525	0.991	21.4	0.057	0.109	-0.179
14.135	1.822	-2.397	3.397	0.536	0.991	21.0	0.057	0.106	-0.190
14.304	1.834	-2.483	3.483	0.527	0.997	20.9	0.057	0.109	-0.189
14.497	1.830	-2.430	3.430	0.533	0.995	20.6	0.057	0.108	-0.192
14.672	1.836	-2.450	3.450	0.532	0.998	20.4	0.058	0.108	-0.191
14.845	1.832	-2.467	3.467	0.529	0.996	20.2	0.057	0.109	-0.195
15.045	1.837	-2.480	3.480	0.528	0.999	19.9	0.058	0.109	-0.174
15.195	1.838	-2.477	3.477	0.529	0.999	19.7	0.058	0.109	-0.189
15.378	1.840	-2.520	3.520	0.523	1.000	19.5	0.058	0.110	-0.189
15.558	1.838	-2.464	3.464	0.531	0.999	19.3	0.058	0.109	-0.177
15.733	1.830	-2.495	3.495	0.524	0.995	19.0	0.057	0.110	-0.184
15.930	1.826	-2.465	3.465	0.527	0.993	18.7	0.057	0.109	-0.163
16.088	1.820	-2.479	3.479	0.523	0.989	18.5	0.057	0.109	-0.185
16.276	1.815	-2.459	3.459	0.525	0.987	18.2	0.057	0.108	-0.176
16.460	1.805	-2.441	3.441	0.525	0.981	17.9	0.057	0.108	-0.171
16.652	1.796	-2.438	3.438	0.522	0.976	17.6	0.056	0.108	-0.177
16.823	1.785	-2.405	3.405	0.524	0.971	17.3	0.056	0.107	-0.172
17.010	1.771	-2.372	3.372	0.525	0.963	17.0	0.056	0.106	-0.175
17.188	1.766	-2.370	3.370	0.524	0.960	16.8	0.055	0.106	-0.172
17.374	1.752	-2.292	3.292	0.532	0.952	16.5	0.055	0.103	-0.155
17.565	1.740	-2.255	3.255	0.535	0.946	16.2	0.055	0.102	-0.154
17.741	1.726	-2.206	3.206	0.538	0.938	15.9	0.054	0.100	-0.185
17.928	1.715	-2.221	3.221	0.532	0.932	15.6	0.054	0.101	-0.158
18.101	1.725	-2.254	3.254	0.530	0.938	15.6	0.054	0.102	-0.153
18.281	1.706	-2.167	3.167	0.539	0.927	15.2	0.053	0.099	-0.165
18.461	1.704	-2.196	3.196	0.533	0.926	15.1	0.053	0.100	-0.169
18.654	1.689	-2.133	3.133	0.539	0.918	14.8	0.053	0.098	-0.149
18.826	1.685	-2.181	3.181	0.530	0.916	14.6	0.053	0.100	-0.174
19.019	1.677	-2.102	3.102	0.541	0.912	14.4	0.053	0.097	-0.148
19.203	1.664	-2.055	3.055	0.545	0.904	14.1	0.052	0.096	-0.171
19.373	1.654	-2.034	3.034	0.545	0.899	13.9	0.052	0.095	-0.154
19.561	1.645	-2.024	3.024	0.544	0.894	13.7	0.052	0.095	-0.163
19.722	1.651	-2.095	3.095	0.533	0.898	13.7	0.052	0.097	-0.177
19.909	1.642	-2.011	3.011	0.545	0.892	13.5	0.051	0.094	-0.154
20.098	1.633	-1.985	2.985	0.547	0.888	13.3	0.051	0.094	-0.171
20.278	1.627	-1.981	2.981	0.546	0.884	13.1	0.051	0.093	-0.167
20.459	1.621	-1.967	2.967	0.546	0.881	12.9	0.051	0.093	-0.153
20.633	1.617	-1.957	2.957	0.547	0.879	12.8	0.051	0.093	-0.150
20.817	1.611	-1.936	2.936	0.549	0.876	12.6	0.050	0.092	-0.164
20.997	1.606	-1.929	2.929	0.548	0.873	12.5	0.050	0.092	-0.175
21.177	1.600	-1.916	2.916	0.549	0.870	12.3	0.050	0.091	-0.154
21.357	1.599	-1.918	2.918	0.548	0.869	12.2	0.050	0.091	-0.161
21.538	1.596	-1.901	2.901	0.550	0.868	12.1	0.050	0.091	-0.152
21.720	1.590	-1.897	2.897	0.549	0.864	12.0	0.050	0.091	-0.147
21.898	1.584	-1.870	2.870	0.552	0.861	11.8	0.050	0.090	-0.167
22.080	1.579	-1.849	2.849	0.554	0.858	11.7	0.049	0.089	-0.153
22.259	1.570	-1.831	2.831	0.554	0.853	11.5	0.049	0.089	-0.164
22.442	1.562	-1.810	2.810	0.556	0.849	11.4	0.049	0.088	-0.141
22.623	1.556	-1.796	2.796	0.556	0.846	11.2	0.049	0.088	-0.152
22.809	1.550	-1.782	2.782	0.557	0.842	11.1	0.049	0.087	-0.155
22.985	1.545	-1.770	2.770	0.558	0.840	11.0	0.048	0.087	-0.165

shr.stn	sh.sts.	ndelU.	nv.sts.	nsh./v.st	sh./su	eu/su	sh/mpp	v.sts/mpp	v.stn
23.173	1.537	-1.752	2.752	0.558	0.835	10.8	0.048	0.086	-0.145
23.350	1.535	-1.767	2.767	0.555	0.835	10.7	0.048	0.087	-0.159
23.532	1.524	-1.727	2.727	0.559	0.828	10.6	0.048	0.085	-0.158
23.715	1.515	-1.694	2.694	0.562	0.823	10.4	0.047	0.084	-0.154
23.898	1.502	-1.663	2.663	0.564	0.816	10.3	0.047	0.083	-0.163
24.079	1.496	-1.663	2.663	0.562	0.813	10.1	0.047	0.083	-0.159
24.256	1.491	-1.653	2.653	0.562	0.811	10.0	0.047	0.083	-0.140
24.439	1.489	-1.645	2.645	0.563	0.809	9.9	0.047	0.083	-0.146
24.615	1.483	-1.631	2.631	0.564	0.806	9.8	0.046	0.082	-0.137
24.798	1.474	-1.605	2.605	0.566	0.801	9.7	0.046	0.082	-0.155
24.979	1.468	-1.590	2.590	0.567	0.798	9.6	0.046	0.081	-0.156
25.162	1.459	-1.577	2.577	0.566	0.793	9.5	0.046	0.081	-0.139
25.341	1.454	-1.568	2.568	0.566	0.790	9.4	0.046	0.080	-0.155
25.523	1.446	-1.553	2.553	0.566	0.786	9.3	0.045	0.080	-0.153
25.704	1.441	-1.537	2.537	0.568	0.784	9.2	0.045	0.080	-0.142
25.879	1.441	-1.548	2.548	0.566	0.784	9.1	0.045	0.080	-0.155
26.064	1.432	-1.526	2.526	0.567	0.779	9.0	0.045	0.079	-0.145
26.240	1.428	-1.521	2.521	0.566	0.776	8.9	0.045	0.079	-0.140
26.425	1.421	-1.505	2.505	0.567	0.772	8.8	0.045	0.079	-0.148
26.604	1.417	-1.496	2.496	0.568	0.771	8.7	0.044	0.078	-0.154
26.785	1.411	-1.480	2.480	0.569	0.767	8.6	0.044	0.078	-0.141
26.967	1.408	-1.470	2.470	0.570	0.766	8.5	0.044	0.077	-0.154
27.145	1.404	-1.462	2.462	0.570	0.763	8.4	0.044	0.077	-0.126
27.328	1.397	-1.449	2.449	0.570	0.759	8.3	0.044	0.077	-0.127
27.503	1.397	-1.447	2.447	0.571	0.759	8.3	0.044	0.077	-0.128
27.687	1.385	-1.408	2.408	0.575	0.753	8.2	0.043	0.075	-0.126
27.865	1.377	-1.392	2.392	0.576	0.748	8.1	0.043	0.075	-0.140
28.045	1.371	-1.388	2.388	0.574	0.745	8.0	0.043	0.075	-0.146
28.225	1.367	-1.383	2.383	0.574	0.743	7.9	0.043	0.075	-0.144
28.401	1.368	-1.418	2.418	0.566	0.744	7.9	0.043	0.076	-0.128
28.584	1.362	-1.365	2.365	0.576	0.740	7.8	0.043	0.074	-0.146
28.766	1.349	-1.352	2.352	0.574	0.734	7.7	0.042	0.074	-0.142
28.950	1.344	-1.342	2.342	0.574	0.730	7.6	0.042	0.073	-0.121
29.125	1.341	-1.359	2.359	0.568	0.729	7.5	0.042	0.074	-0.145
29.307	1.339	-1.349	2.349	0.570	0.728	7.5	0.042	0.074	-0.141
29.482	1.336	-1.327	2.327	0.574	0.726	7.4	0.042	0.073	-0.117
29.662	1.327	-1.309	2.309	0.575	0.721	7.3	0.042	0.072	-0.118
29.844	1.321	-1.292	2.292	0.576	0.718	7.2	0.041	0.072	-0.133
30.026	1.311	-1.278	2.278	0.575	0.712	7.1	0.041	0.071	-0.138
30.209	1.308	-1.278	2.278	0.574	0.711	7.1	0.041	0.071	-0.124
30.384	1.313	-1.296	2.296	0.572	0.714	7.1	0.041	0.072	-0.115
30.570	1.304	-1.265	2.265	0.575	0.709	7.0	0.041	0.071	-0.135
30.747	1.298	-1.260	2.260	0.574	0.706	6.9	0.041	0.071	-0.133
30.930	1.290	-1.243	2.243	0.575	0.701	6.8	0.040	0.070	-0.113
31.106	1.284	-1.232	2.232	0.576	0.698	6.7	0.040	0.070	-0.117
31.291	1.270	-1.202	2.202	0.577	0.690	6.6	0.040	0.069	-0.148
31.466	1.280	-1.255	2.255	0.568	0.696	6.6	0.040	0.071	-0.140
31.646	1.276	-1.233	2.233	0.571	0.694	6.6	0.040	0.070	-0.136
31.828	1.275	-1.234	2.234	0.571	0.693	6.5	0.040	0.070	-0.119
32.006	1.267	-1.213	2.213	0.573	0.689	6.5	0.040	0.069	-0.138
32.189	1.264	-1.212	2.212	0.571	0.687	6.4	0.040	0.069	-0.117
32.361	1.271	-1.261	2.261	0.562	0.691	6.4	0.040	0.071	-0.128

shr.stn	sh.sts.	ndelU.	nv.sts.	nsh./v.st	sh./su	eu/su	sh/mpp	v.sts/mpp	v.stn
32.549	1.262	-1.212	2.212	0.570	0.686	6.3	0.040	0.069	-0.127
32.724	1.268	-1.252	2.252	0.563	0.689	6.3	0.040	0.071	-0.105
32.911	1.251	-1.198	2.198	0.569	0.680	6.2	0.039	0.069	-0.104
33.088	1.251	-1.209	2.209	0.566	0.680	6.2	0.039	0.069	-0.122
33.267	1.244	-1.191	2.191	0.567	0.676	6.1	0.039	0.069	-0.130
33.451	1.241	-1.182	2.182	0.569	0.674	6.1	0.039	0.068	-0.108
33.631	1.226	-1.155	2.155	0.569	0.667	6.0	0.038	0.068	-0.130
33.813	1.224	-1.154	2.154	0.568	0.665	5.9	0.038	0.068	-0.107
33.986	1.235	-1.186	2.186	0.565	0.672	5.9	0.039	0.069	-0.104
34.173	1.217	-1.145	2.145	0.568	0.662	5.8	0.038	0.067	-0.113
34.349	1.215	-1.146	2.146	0.566	0.661	5.8	0.038	0.067	-0.115
34.536	1.206	-1.131	2.131	0.566	0.656	5.7	0.038	0.067	-0.131
34.714	1.214	-1.158	2.158	0.562	0.660	5.7	0.038	0.068	-0.117
34.896	1.204	-1.134	2.134	0.564	0.655	5.6	0.038	0.067	-0.113
35.075	1.204	-1.133	2.133	0.565	0.654	5.6	0.038	0.067	-0.130
35.259	1.199	-1.122	2.122	0.565	0.651	5.6	0.038	0.067	-0.107
35.449	1.194	-1.112	2.112	0.566	0.649	5.5	0.037	0.066	-0.118
35.630	1.192	-1.110	2.110	0.565	0.648	5.5	0.037	0.066	-0.132
35.820	1.188	-1.105	2.105	0.565	0.646	5.4	0.037	0.066	-0.106
36.000	1.186	-1.099	2.099	0.565	0.645	5.4	0.037	0.066	-0.124
36.184	1.183	-1.098	2.098	0.564	0.643	5.3	0.037	0.066	-0.129
36.366	1.180	-1.089	2.089	0.565	0.641	5.3	0.037	0.065	-0.117
36.545	1.174	-1.081	2.081	0.564	0.638	5.2	0.037	0.065	-0.103
36.726	1.173	-1.080	2.080	0.564	0.638	5.2	0.037	0.065	-0.108
36.902	1.172	-1.078	2.078	0.564	0.637	5.2	0.037	0.065	-0.131
37.088	1.168	-1.072	2.072	0.564	0.635	5.1	0.037	0.065	-0.117
37.267	1.164	-1.066	2.066	0.564	0.633	5.1	0.036	0.065	-0.120

APPENDIX C

CONSOLIDATION AT CONSTANT RATE OF STRAIN

- C.1 Introduction**
- C.2 CRSC Testing Procedures**
- C.3 Presentation and Discussion of Test Results**
 - C.3.1 Preconsolidation Pressure.**
 - C.3.2 Compression CurveS**
 - C.3.3 Coefficient of Permeability**
- C.4 Conclusions**

Tables

Figures

Reference and Reduction Data from CRSC Tests

APPENDIX C

CONSOLIDATION AT CONSTANT RATE OF STRAIN

C.1 Introduction

The constant Rate of Strain (CRS) Consolidometer was first developed by Smith and Wahls (1969) with the objective of performing quicker consolidation tests. Soon after, Wissa et. al. (1971) developed a more versatile general purpose one dimensional consolidometer at MIT, which is shown schematically in Figure C.1. The apparatus is designed to load the specimen, by incremental loads, at constant rate of strain, or at a constant rate of stress. The equipment has high initial cost and is more complicated than conventional consolidation devices. An expert operator is needed to set-up the test. However, the constant rate of strain consolidation (CRSC) test is reported to have several advantages over the standard incremental test (Wissa et al., 1971; Germaine, 1985; Ladd, 1985), which are summarized below:

- A continuous curve corresponding to the end of primary consolidation is easily obtained.
- The duration of the test is reduced from several weeks to a few days for Boston Blue Clay.
- One can obtain continuous data on the rate of consolidation.
- The specimen can be saturated at constant volume under a back pressure.
- There is no loss of soil due to squeezing near the preconsolidation pressure with soft clays.
- Data are easily collected with data acquisition system.

MIT's general purpose consolidometer was used to perform all the CRSC tests

for this research. The tests were performed on samples of resedimented BBC with the intended purpose of obtaining well defined compression curves for comparison of general consolidation characteristics of the soil with CK_0 UDSS consolidation results. This appendix presents an outline of the testing procedures, the tests results, and a brief discussion on the consolidation behavior of resedimented BBC III. The reader is referred to Wissa and Heiberg (1969) for detail description of the apparatus, operating and testing procedures, and analysis of conditions in the CRSC test.

C.2 CRSC Testing Procedures

The test specimen is trimmed directly into a smooth and greased stainless steel ring by placing a knife-edged shoe adapter on the ring and alternately pressing the cutting edge into the soil and trimming the excess soil ahead of the ring with a surgical knife. This minimizes disturbance and results in a tight fit between the ring and the sample, which is required to ensure that no lateral strain occurs during testing. The shoe is then removed and the top and bottom of the test specimen are trimmed level with a thin wire saw.

The stainless steel ring containing the specimen is then located in the test chamber. A tight fit exists between the sample ring and the test chamber in order to prevent lateral strain during loading. The piston head, with the loading cap containing the porous stone, is brought in contact with the specimen. The clearance between the loading cap and the test chamber wall is small in order to apply a uniform displacement to the top surface and to prevent soil from squeezing out during loading. At this stage, distilled de-aired water is added to the test chamber and the sample is allowed to sit overnight under the back pressure for complete saturation.

On the following day, the specimen is loaded at a constant rate of strain by a gear-driven load frame that forces the cell piston to move down at a constant velocity. The load required to maintain constant piston velocity is monitored with the load cell,

and the excess pore water pressure at the impervious sample base is measured with the pore pressure transducer. The movement of the piston is monitored as a function of time with a DCDT, throughout the test, to ensure that the cell piston velocity is constant. The DCDT versus time readings are subsequently used to compute strain rates (the selection of strain rates for CRSC tests is discussed under Sub Section C.3.1) and also for data interpretation. All of the transducer readings are taken during the test by MIT's central data acquisition system at specified time intervals.

C.3 Presentation and Discussion of Test Results

The clay samples for this research came from Batch No. 204, 205, and 207 of resedimented BBC III. Chapter 4 summarizes the batching procedures and properties of the test soil. Four CRSC tests were performed for this thesis. All the samples were loaded at a constant rate of strain to a maximum vertical consolidation stress of about 20 ksc, and then unloaded to about 0.4 ksc. CRSC Test No. 1 and 2 were also rebounded from a vertical stress of about 4 ksc to 0.30 ksc before reloading to the maximum vertical consolidation stress. At the end of each loading/unloading, all the samples were equilibrated for about 24 hours at a constant vertical stress before they were rebounded/reloaded (CRSC Test No. 1 was also stopped for about 18 hours at a vertical stress of 1.5 ksc during the first loading. Some fluctuations in vertical stress occurred due to a defective Bellofram and variations in the temperature during this period). CRSC Test No. 1, 2, and 3 were loaded at the average strain rate of about 2.27×10^{-6} per second, where as CRSC Tests No. 8 was run at the strain rate of 2.018×10^{-5} per second. The loading program of each test is given in Table 4.7.

The tabulated data from all the tests are attached at the end of this appendix. The following Figures present the selected test data in graphical form:

C.2 to C.7 – ϵ_v versus $\log(\sigma'_v)$;

C.8 to C.11 – Constrained Modulus, D , versus $\log(\sigma'_v)$;

C.12 to C.16 – void ratio, e , versus $\log(\sigma'_v)$;

C.17 to C.21 – e versus \log of coefficient of permeability, k ;

C.22 to C.26 – $\log(e)$ versus $\log(k)$;

C.27 to C.30 – Normalized excess pore pressure, u_b/σ_v , versus σ'_v ;

Table C.1 summarizes the results of the CRSC tests performed on samples from batches of resedimented BBC III. The subsequent sub sections present a discussion of the experimental results.

C.3.1 Preconsolidation pressure

Figures C.2 through C.5 are the plots of vertical strain versus logarithm of vertical effective stress for the four CRSC tests. The preconsolidation pressures, determined by Casagrande's (1936) construction method, are given in Tables C.1. The values of preconsolidation pressures for the three CRSC tests (CRSC Test No. 1, 2, and 3) performed at slower rates of strain (i.e., the normalized excess pore pressures, $u_b/\sigma_v \approx 2$ to 5 %; see plots of u_b/σ_v versus σ'_v in Figures C.27 to C.29) are fairly close to the applied loads during batch consolidation (computed σ'_p from batch consolidometer tests are given in Table 4.2). Table C.3 compares the average values of σ'_p from CRSC tests with average results from 14 oedometer tests (from Table 4.3) on samples of BBC III and shows good agreement in the values of σ'_p . However, preconsolidation pressure determined from compression curve for CRSC Test No. 8 (which was performed approximately 9 times faster than the other CRSC tests, at a displacement rate that resulted in normalized excess pore pressures $u_b/\sigma_v \approx 25$ % in the vicinity of preconsolidation pressure; Figure C.30) yielded a value of σ'_p which is approximately 25% higher than the other tests. This increase in the preconsolidation pressure may have been caused by a number of factors which are discussed in the

succeeding paragraphs.

It has been reported that the Casagrande's construction method is only accurate to 5 percent of the true value of σ'_p for resedimented BBC (Seah, 1990) and that reconstruction of the laboratory curve by Schmertmann (1955) may increase the preconsolidation pressure by 10 to 15 % compared to Casagrande's method (Germaine, 1985). However, an increase of 25 % in the preconsolidation pressure can not be attributed to the error in the method used for determining the preconsolidation pressure in this case.

The side friction of the wall on the stainless steel ring may effect the stress distribution, thus influencing the preconsolidation pressure. This effect is more pronounced when the ratio of sample height to diameter is large. The sample height to sample diameter ratio of about 0.37, application of grease on the smooth walls of stainless steel ring, and reasonable and consistent values of σ'_p obtained from the other CRSC tests, eliminate the possibility of side friction as the cause of such a large increase in the preconsolidation pressure.

Thixotropic soil (reported by O' Neill , 1985 and discussed in Chapter 4) may exhibit increases in the apparent σ'_p with storage time. Seah (1990) verified by extensive laboratory testing that BBC III is a non-thixotropic material. Furthermore, this test specimen had less storage time than the specimens used for CRSC Tests No. 1 and 2 (Table 4.7).

It is well documented in the literature that the rate of loading can have significant effect on the value of preconsolidation pressure determined from the CRS consolidation curves (e.g. Ladd, 1973; Leroueil et al., 1983; Leroueil et al., 1985; Jamiolkowski et al., 1985). Leroueil et al. (1983) reported experimental results for 11 clays which typically show a 10 % increase in σ'_p per log cycle increase in rate of strain. Germaine (1985) and Jamiolkowski et al. (1985) opined that the $d\epsilon/dt$ should not effect σ'_p at a strain rate equal to or greater than that required to prevent

secondary compression, if the EOP curve is independent of drainage height. They offered two possible explanations for the experimental evidence of increase in σ'_p with increase in the strain rate, which are in agreement with Mesri (1985):—

- "1. ...CRS tests run at "fast" rate have significant pore pressure (effective stress) gradients across the specimen such that resultant variations in compressibility and permeability may invalidate Terzaghi's theory used to interpret the results.
2. At strain rates faster than occur near the end of primary consolidation in conventional incremental tests, many clays may indeed exhibit a structural viscosity."

It is evident from the above discussion that there are many factors which may influence the preconsolidation pressure. However, such a large increase in the preconsolidation pressure seems to have been caused mainly due to the substantial increase in the rate of loading. The writer concurs with the explanation given by Germaine (1985) and Jamiolkowski et al. (1985) for increases in σ'_p with increase in the rate of strain. The test data reveal that large excess pore pressures were developed at the base of the specimen, which subject the specimen to high hydraulic gradients. The data also indicate significant transient effects for stress—strain distribution during initial stages of the test. Although the theoretical solutions presented by Wissa et al. (1971) for a linear (constant m_v) and a non—linear material (constant C_c) include transient behavior, the results of the tests have been analyzed assuming steady state conditions. Furthermore, results are interpreted using the linear theory which is only valid for small values of u_b/σ_v (i.e. $u_b/\sigma_v \simeq 2$ to 5 %). The results obtained from two theories diverge significantly at the larger values of u_b/σ_v (Wissa et al., 1971). Hence the results of the test may be viewed qualitatively only, i.e., preconsolidation pressure

increases with increase in the strain rate. However, it is not confirmed that the increase in σ'_p is due to high effective stress gradients or to structural viscosity.

Mesri and Castro, (1987) suggests the following relationship to select the strain rate to be used in CRS tests in order to obtain the same σ'_p as obtained from end of EOP incremental oedometer curves:

$$\frac{d\epsilon}{dt} = \frac{k_0}{2(C_c/C_k) \times H_d^2} \times \frac{\sigma'_p}{\gamma_w} \times \frac{C_{\alpha e}}{C_c} \quad (C.1)$$

where

$$C_c = -de/d\log(\sigma'_{vc})$$

k_0 = Initial coefficient of permeability at the in-situ void ratio.

γ_w = Unit weight of water.

H_d = Drainage height.

$$C_{\alpha e} = -de/d\log(t)$$

$$C_k = de/d\log(k)$$

The strain rate calculated based on the average parameters for resedimented BBC III [i.e. $C_c = 0.31$, $k_0 = 4.0 \times 10^{-8}$ cm/s, and $C_k = 0.425$, (from Seah, 1990); $H_d = 2.35$ cm (average of the three CRSC tests performed for this research); $C_{\alpha e} / C_c = 0.04$ (Mesri and Choi,1985)] yielded an approximate value of 2×10^{-7} per second. Wissa et al. (1971) conducted CRSC tests on samples of resedimented BBC at strain rates ranging from 10^{-6} to 8×10^{-6} per second and reported that their consolidation data compared well with the incremental tests. Walbaum (1988) performed three CRSC tests (Table C.2) on samples from batches of resedimented BBC III with average strain rates falling in the range reported by Wissa et al.(1971) and ensuring that the value of u_b/σ_v remains between 2% to 5%, obtained compression data which showed good

agreement with the results from EOP incremental consolidation tests. Wissa et al. (1971) suggested that the optimum strain rate for determining a well defined e versus $\log \sigma'_{vc}$ curve is that which results in u_b/σ_v values of 2% to 5%. Based on the reported data and the test performed for this research, the writer is of the opinion that the test conducted on resedimented BBC at a strain rate calculated based on Equation C.1 will yield lower value of σ'_p than that obtained for EOP incremental oedometer compression curves. Hence, it is concluded that for resedimented BBC the strain rate in CRSC test that results in the value of u_b/σ_v between 2% to 5% is more likely to yield the same value of σ'_p as obtained from EOP incremental oedometer compression curves. The initial rate of deformation can be selected from the range of values reported by Wissa et al. (1971).

Janbu (1969) has suggested that a plot of constrained modulus ($D = 1/m_v$; $m_v =$ coefficient of volume change) versus σ'_{vc} (natural scale) can be used to determine the preconsolidation pressure since D often undergoes a marked drop in the vicinity of σ'_p . The constrained modulus versus vertical effective stress is plotted in Figure C.8 through C.11 for the four CRSC tests to observe the behavior of resedimented BBC in the light of the proposed method. Significant scatter is observed in the plotted data for CRSC Test No. 1 and 2. However, the arithmetic plots of D versus σ'_v for CRSC Test No. 3 and 8 indicate a sharp drop in D around the preconsolidation pressure, which then increases linearly with stress. Linear regression analysis for D on σ'_{vc} in the normally consolidated range results in a straight line passing approximately through the origin (Figures C.8 through C.11). The preconsolidation pressure is better defined by the lowest point on the curve, as proposed by Janbu and Senneset (1979), but yield higher values of σ'_p than expected (i.e., based on applied pressures from the large consolidometer tests and that obtained from incremental/CRSC tests by Casagrande's construction method). The values of σ'_p obtained by using Jonas's (1970) technique, who suggested that σ'_p equals the midpoint between points 1 and 2 in Figure C.11, are

closer to the expected values. However, scatter in the test data for the overconsolidated range makes it difficult to determine the value of σ'_p precisely by this method.

C.3.2 Compression Curves

Figure C.12 through C.15 are plots of void ratio versus logarithm of vertical effective stress for the CRSC tests. The variation observed between the different tests (Figure C.16) is partly due to the errors in measuring the water content which contributes to the error in void ratios (the void ratio is calculated based on $G_s w = S e$ relationship; $G_s = 2.785$, $S = 100\%$, w is the measured water content of the specimen). Plots of vertical strain versus logarithm of vertical effective stress (Figure C.6) for the four CRSC tests show much smaller variation in the curves for tests performed at the same strain rate. However, the compression curve for CRSC Test No. 8, run at a fast strain rate, indicate a large variation, specially in the normally consolidated zone.

Figure C.2 through C.5 are the plots of the vertical strain versus logarithm of vertical effective stress for CRSC Test No. 1, 2, ,3 and 8. The slope of the virgin compression line is concave upwards, i.e., the slope decreases with increase in the vertical consolidation stress. Table C.1 summarizes the values of the virgin compression ratio (CR) and swelling ratio (SR).

Table C.3 compares the results of CRSC tests with average values obtained for 13 incremental consolidation tests performed on batches of resedimented BBC III. Figure C.7 is a plot of the compression curves for CRSC Tests No. 1, 2, and 3 and the range of results for the four oedometer tests performed on samples from the same batches (i.e. Batches 204, 205, and 207) of resedimented BBC III. Table C.3 and Figure C.7 indicate that the CRSC and incremental oedometer tests compare very well (the oedometer tests give slightly lower virgin compression ratios). Table C.3 and Figure C.6 show that the virgin compression ratios increase with increase in the strain rate for resedimented BBC.

The time dependent deformation behavior of soil can be suitably analyzed based on the continuous data obtained in the CRSC testing. However, reliable data on the creep effects under constant stress could not be obtained during this research due to a faulty air pressure system and fluctuations in the temperature which resulted in small variations in the vertical stress.

Further discussion on the consolidation behavior of resedimented BBC III and comparison of CRSC data with CK_0 UDSS results is done in Chapter 5.

C.3.3 Coefficient of Permeability

The coefficient of permeability in the CRSC tests can be calculated directly using the relationship derived by Wissa et al. (1971) based on the linear theory analysis, as follows:

$$k = \frac{\dot{\epsilon} H_d^2 \gamma_w}{2 u_b} \quad (C.2)$$

where

$$\dot{\epsilon} = d\epsilon/dt$$

H_d = Length of drainage path.

u_b = Excess pore water pressure at the base of the specimen.

γ_w = Unit weight of water.

The coefficient of permeability is generally expressed as a function of the void ratio. The most widely used empirical linear relationship between the logarithm of k and the void ratio is given by Taylor (1948), which is expressed by the following equation:

$$\log(k/k_0) = (e_0 - e/C) \quad (C.3)$$

where

C is a constant, which is latter defined as the permeability change index, C_k .

k_0 is the initial coefficient of permeability at the initial void ratio, e_0 .

The Equation C.3 can also be expressed as,

$$C_k = \frac{\Delta e}{\Delta \log(k)} \quad (C.4)$$

In engineering practice, C_k is usually assumed to be constant over the typical range of void ratios. Tavenas et al. (1983) concluded that $C_k = 0.50 e_0$ is a reasonable practical approximation for clays having an initial void ratio between 0.8 and 3.0. Ladd (1.322 Soil Behavior Course at MIT) suggests C_k falls within a range of $0.33 e_0$ to $0.5 e_0$ (Figure C.31).

Mesri and Olson (1971) presented another empirical relationship, this time between logarithm of k and logarithm of e ,

$$\log(k) = A \log(e) + B \quad (C.5)$$

Where A and B are constants.

Equation C.5 can be written in terms of e as, follows:

$$\log(e) = \frac{2.303}{A} (\log k + B) \quad (C.6)$$

Seah (1990) derived the following expression by differentiating Equation C.6 and then combining it with Equation C.4 to express C_k as a function of e , for a $\log(e)$ – $\log(k)$ relationship,

$$C_k = \frac{2.303 e}{A} \quad (C.7)$$

The void ratio versus coefficient of permeability data are plotted on semi-log and log-log scales in Figures C.17 through C.26 for analysis and comparison in the light of above discussed empirical relationships. Linear regression is used to compute the constants C_k and A from Equations C.4 and C.6. Table C.4 summarizes the results obtained from linear regression analyses on CRSC tests conducted for this research and the incremental consolidation tests performed on samples of resedimented BBC III, reported by Seah (1990).

Table C.4 indicates that the CRSC tests give higher k values than incremental consolidation tests. The variation is partly due to errors in computing the initial void ratios. However, a variation of approximately 25% may be attributed to the methods of testing and interpretation of results. It is added that the explanation put forth by Seah (1990) for higher values of k in the CRSC tests (i.e. the actual void ratios are higher than those reported since the compressibility corrections are not made on the CRSC data), is not valid since the test data presented for this research have been appropriately corrected for the apparatus compressibility based on the measured load deflection relationship of the apparatus.

The values of C_k (calculated based on Equation C.4), when plotted on Figure C.31, fall within the typical range of C_k values (i.e. $C_k \simeq 0.33 e_0$ to $0.50 e_0$) for clays given by Tavenas et al. (1983). Figure C.32 is a plot of C_k versus e_0 for BBC. The values of C_k , computed based on Equations C.4 and C.6, are compared with the consolidation tests done on the 200 series BBC (3 CRSC, 11 oedometer, 2 DSS, and 8 large consolidometer tests). Figure C.32 shows that the C_k values computed using Equation C.6 (i.e., $\log e - \log k$) are closer to $0.50e_0$ than C_k calculated based on Equation C.4 ($e - \log k$).

C.4 Conclusions

Based on the experimental results, the following conclusions are drawn:—

- The strain rate best suited for resedimented BBC to be used in CRSC tests in order to obtain the same preconsolidation pressure as obtained from EOP incremental tests is that which results in u_b/σ_v values between 2% to 5%.
- CRS consolidation performed at significantly faster strain rates that result in u_b/σ_v values greater than 5% can result in value of σ'_p which is higher than obtained from oedometer EOP curves.
- Janbu's (1969) method for determining preconsolidation pressure yields much higher values compared to Casagrande's (1936) construction method. It is difficult to find precise value of σ'_p using the technique suggested by Jonas (1970).
- The values of virgin compression ratio obtained from CRSC tests on resedimented BBC III decrease significantly with increase in the consolidation stress and compare very well with values obtained from EOP oedometer curves at high stresses. The compression ratio increased with an the increase in the strain rate.
- The CRSC tests give coefficient of permeability which are approximately 25% higher than those obtained from incremental consolidation tests.

The CRSC results are analyzed using the linear theory solution for steady state conditions presented by Wissa et al. (1971). It is reported (Wissa and Heiberg, 1969; Wissa et al., 1971) that the difference between the results obtained using the linear or non-linear theory is not significant if the rate of strain is slow enough to keep the hydraulic gradients relatively small ($u_b/\sigma_{vc} < 5\%$) and the transient component of the

strain distribution for the linear material is small for time after non-dimensional time, T_v , is equal to 0.35 and becomes negligible for values of T_v greater than 0.5 (Wissa and Heiberg, 1969). Hence, the analysis is justified for CRSC Test No. 1, 2, and 3 as the ratio of pore pressure to the applied total vertical stress remained generally within 2% to 5% in the normally consolidated range. The strain rate was sufficiently low so that the transient state could be ignored. However, it would have been more appropriate to also evaluate the data for CRSC Test No. 8, which was performed at a fast strain rate resulting in u_b/σ_v value greater than 5%, using non-linear theory and also considering the transient effects.

The strain rate effects have been evaluated qualitatively only. The limited data show significant rate effects on the consolidation behavior of resedimented BBC. Hence, it is considered a worthwhile effort to run more CRSC tests at intermediate strain rates for a better understanding of rate effects on the consolidation behavior of new 200 series BBC.

Table C.1: Results of CRSC Tests on Boston Blue Clay III

Test No.	Batch No. w_c (%)	σ'_p (ksc)	Strain Rate (per sec)	CR (Stress Range in ksc)				SR (Stress Range in ksc)					C_k , from e -logk
				1.2-2	2-4	4-8	8-20	20-10	20-5	20-2.5	20-1.25	20-.625	
CRSC1	204 39.58	0.98	2.26×10^{-6}	0.1885	0.1730	-	0.134	0.011	0.014	0.018	0.021	0.023	0.375
CRSC2	204 39.55	1.08	2.27×10^{-6}	0.1888	0.1670	0.140	0.132	0.011	0.013	0.016	0.020	0.022	0.421
CRSC3	207 41.02	1.08	2.29×10^{-6}	0.1750	0.1680	0.156	0.136	0.009	0.012	0.015	0.019	0.023	0.521
Mean ± 1 SD	40.05 0.84	1.05 0.05	2.27×10^{-6} -	0.1841 0.0079	0.1693 0.0032	0.148 -	0.134 0.002	0.010 0.001	0.013 0.001	0.016 0.002	0.020 0.001	0.023 0.001	0.440 0.070
CRSC8	205 39.59	1.30	2.02×10^{-5}	0.2210	0.2090	0.182	0.158	0.007	0.010	0.016	0.019	-	0.490

Table C.2: Results of CRSC Tests on BBC III (after Walbaum, 1988)

Test No. Batch	w_i (%) e_i ¹	σ'_p (ksc)	σ'_{vc} (ksc) OCR	CR ²	RR	C_k ³
2 201	40.60 1.131	1.05	3.82 1.00	0.165	-	0.45
3 201	41.50 1.156	0.97	0.62 3.94	0.174	0.0125	0.47
4 201	40.90 1.140	1.05	3.81 1.00	0.177	-	0.52

- Notes:
1. Initial void ratio based on $G_s w = S e$; where $G_s = 2.785$ and $S = 100\%$.
 2. Average values of CR.
 3. Gives best estimates of C_k . Linear regression was not performed.
 4. The test were performed at variable strain rates ensuring $u_b/\sigma_v \approx 2-5\%$.

Table C.3: Summary of Consolidation Results from CRS and Oedometer Tests on BBC III

Type of Tests Number of Tests	Batch	w _c (%)	σ' _p (ksc)	CR (Stress Range in ksc)				SR (Stress Range in ksc)				C _k , from e-logk	
				1.2-2	2-4	4-8	8-20	20-10	20-5	20-2.5	20-1.25		
CRSC 1 3	204 and 207	40.05 ±0.84	1.05 ±0.05	0.184 ±0.008	0.169 ±0.003	0.148 -	0.134 ±0.002	0.010 ±0.001	0.013 ±0.001	0.016 ±0.002	0.020 ±0.001	0.440 ±0.070	
CRSC 2 1	205	39.59	1.30	0.221	0.209	0.182	0.158	0.070	0.010	0.016	0.019	0.490	
Oedometer 3 14	200 to 207	41.03 ±0.73	1.00 ±0.02	0.160 ±0.020	0.164 ±0.011	0.146 ±0.009	- -	- -	- -	- -	⁴ 0.016 ±0.002	- -	0.470 ±0.008

- Notes:
1. Average rate of strain $\approx 2.27 \times 10^{-6}$ per second.
 2. Rate of strain $\approx 2.02 \times 10^{-5}$ per second.
 3. Results of the tests given in Table 4.3. From Seah, 1990.
 4. SR taken from 16-2 ksc load increment.

Table C.4: Linear Regression Results for e-k Relationship for Tests on BBC III

Source	Type of Relation	Number of Observations	e_0	k_0 (cm/s)	A	C_k (e)	r^2	Initial void Ratio, e_i
CRSC1	e vs lg(k)	87	1.05	11.68×10^{-8}		0.375	0.85	1.12
	lg(e) vs lg(k)	87	1.05	11.02×10^{-8}	5.293	0.435e	0.86	1.12
CRSC2	e vs lg(k)	87	1.05	11.08×10^{-8}		0.421	0.87	1.12
	lg(e) vs lg(k)	87	1.05	11.15×10^{-8}	4.693	0.491e	0.88	1.12
CRSC3	e vs lg(k)	103	1.08	11.25×10^{-8}		0.521	0.85	1.14
	lg(e) vs lg(k)	103	1.08	11.72×10^{-8}	3.920	0.588e	0.85	1.14
CRSC8	e vs lg(k)	76	1.06	11.28×10^{-8}		0.458	0.99	1.10
	lg(e) vs lg(k)	76	1.06	11.68×10^{-8}	3.920	0.588e	0.97	1.10
Oedometer	e vs lg(k)	79	0.90	4.00×10^{-8}		0.425	0.73	≈ 1.10
	lg(e) vs lg(k)	79	0.90	4.10×10^{-8}	5.056	0.455e	0.73	≈ 1.10
Oedometer and Batch	e vs lg(k)	111	1.00	6.10×10^{-8}		0.565	0.91	$\approx 1.1-2$
	lg(e) vs (k)	111	1.00	6.50×10^{-8}	4.855	0.474e	0.94	$\approx 1.1-2$

Note: Results from oedometer and batch tests from Seah (1990).

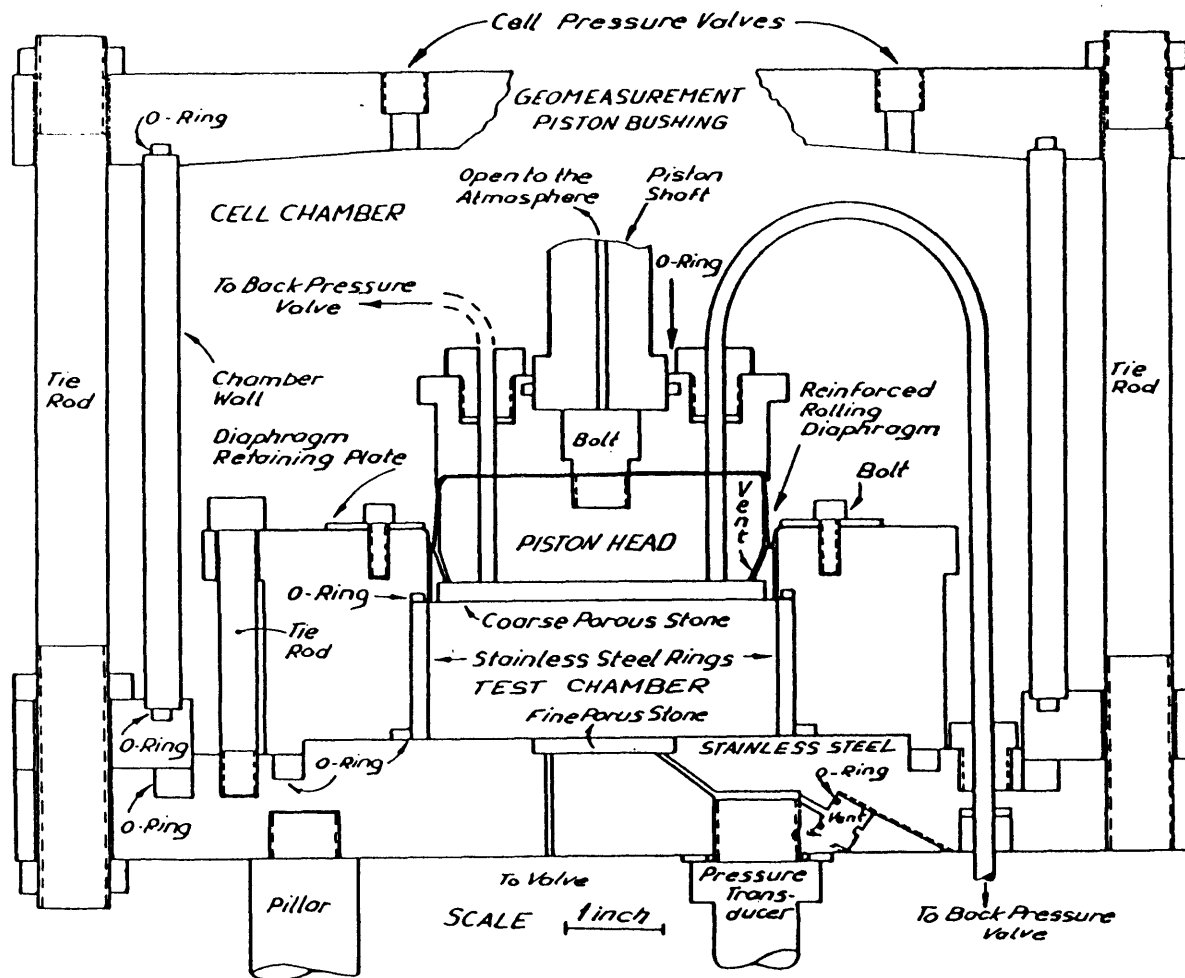


Figure C.1: Schematic of MIT General Purpose Consolidometer. (from Wissa and Heiberg, 1969).

CRSC TEST NO. 1

(Batch 204)

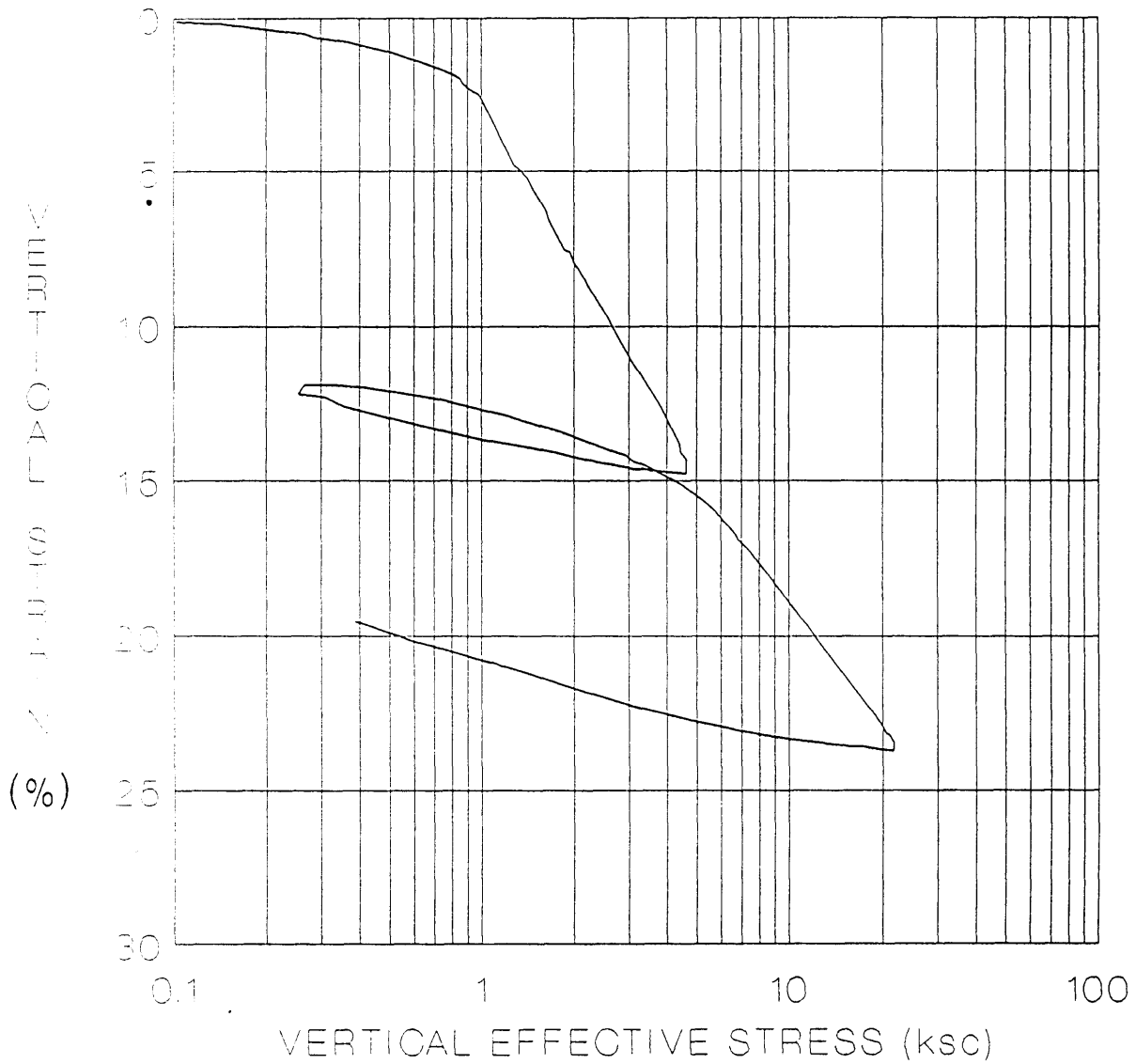


Figure C.2: Compression Curve (ϵ_v Vs. $\log \sigma'_{vc}$) from CRSC TEST No. 1.

CRSC TEST NO. 2 (Batch 204)

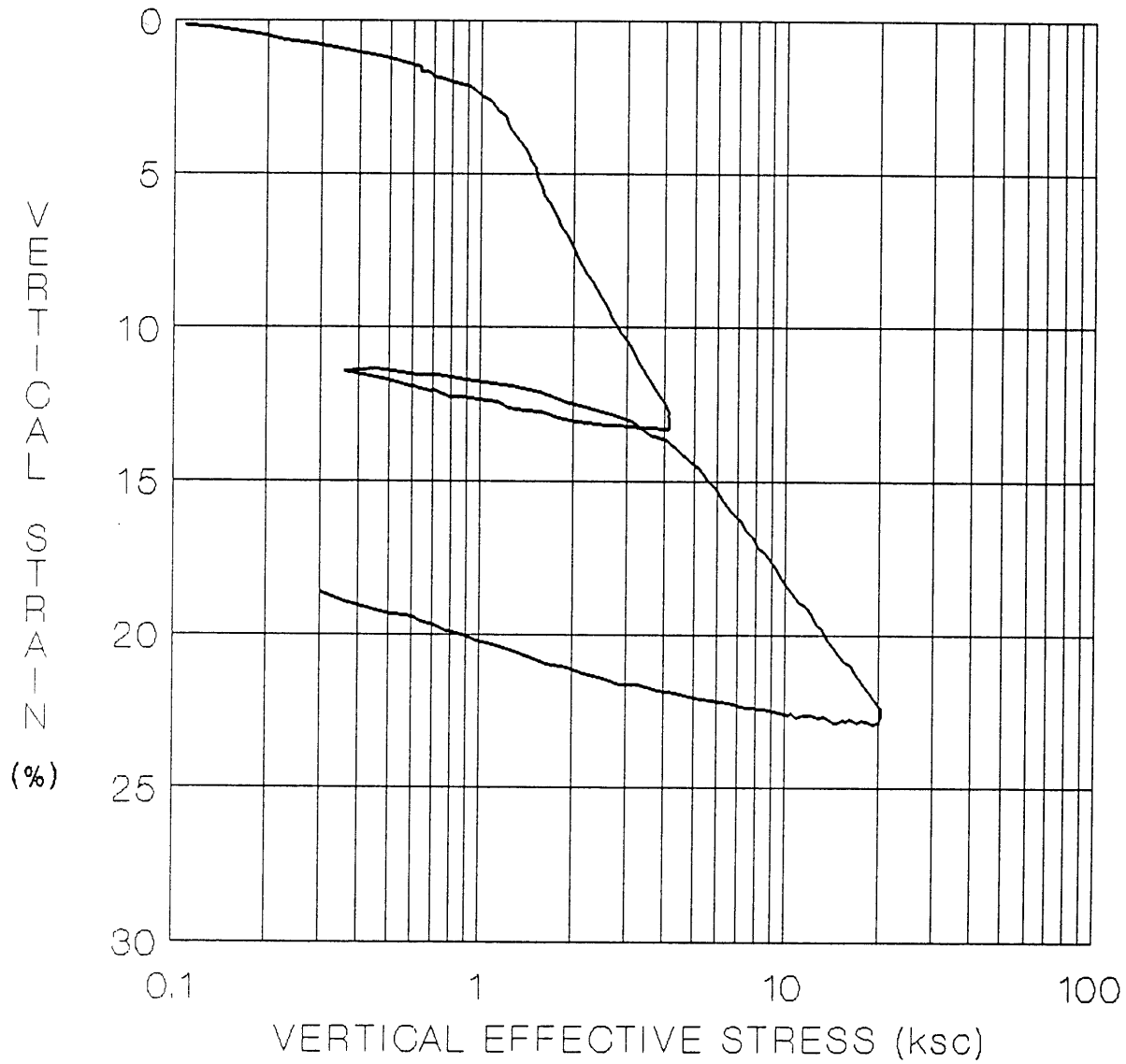


Figure C.3: Compression Curve (ϵ_v Vs. $\log \sigma'_{vc}$) from CRSC TEST No. 2.

CRSC TEST NO. 3 (Batch 207)

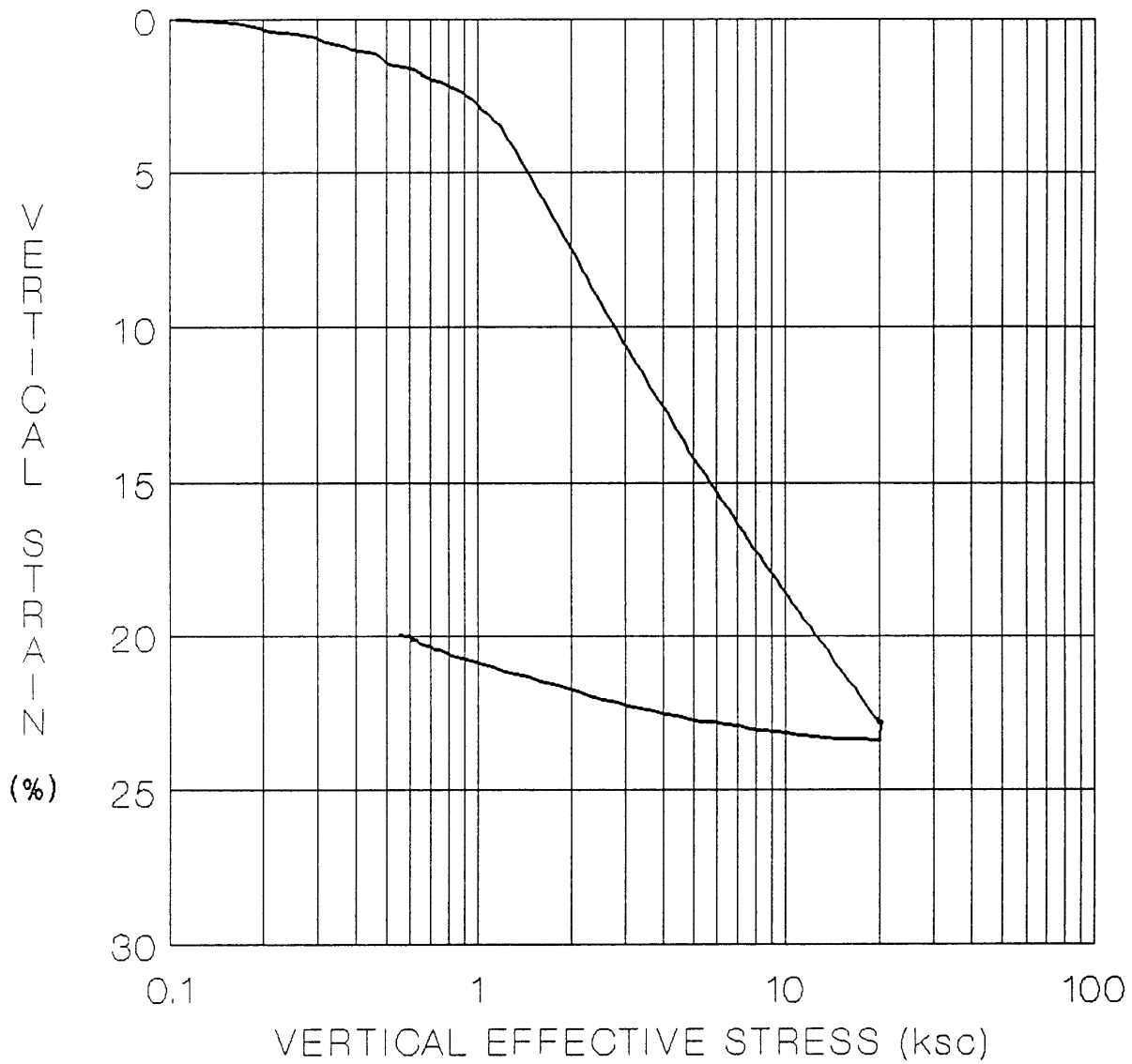


Figure C.4: Compression Curve (ϵ_v Vs. $\log \sigma'_{vc}$) from CRSC TEST No. 3.

CRSC TEST NO. 8

(Batch 205)

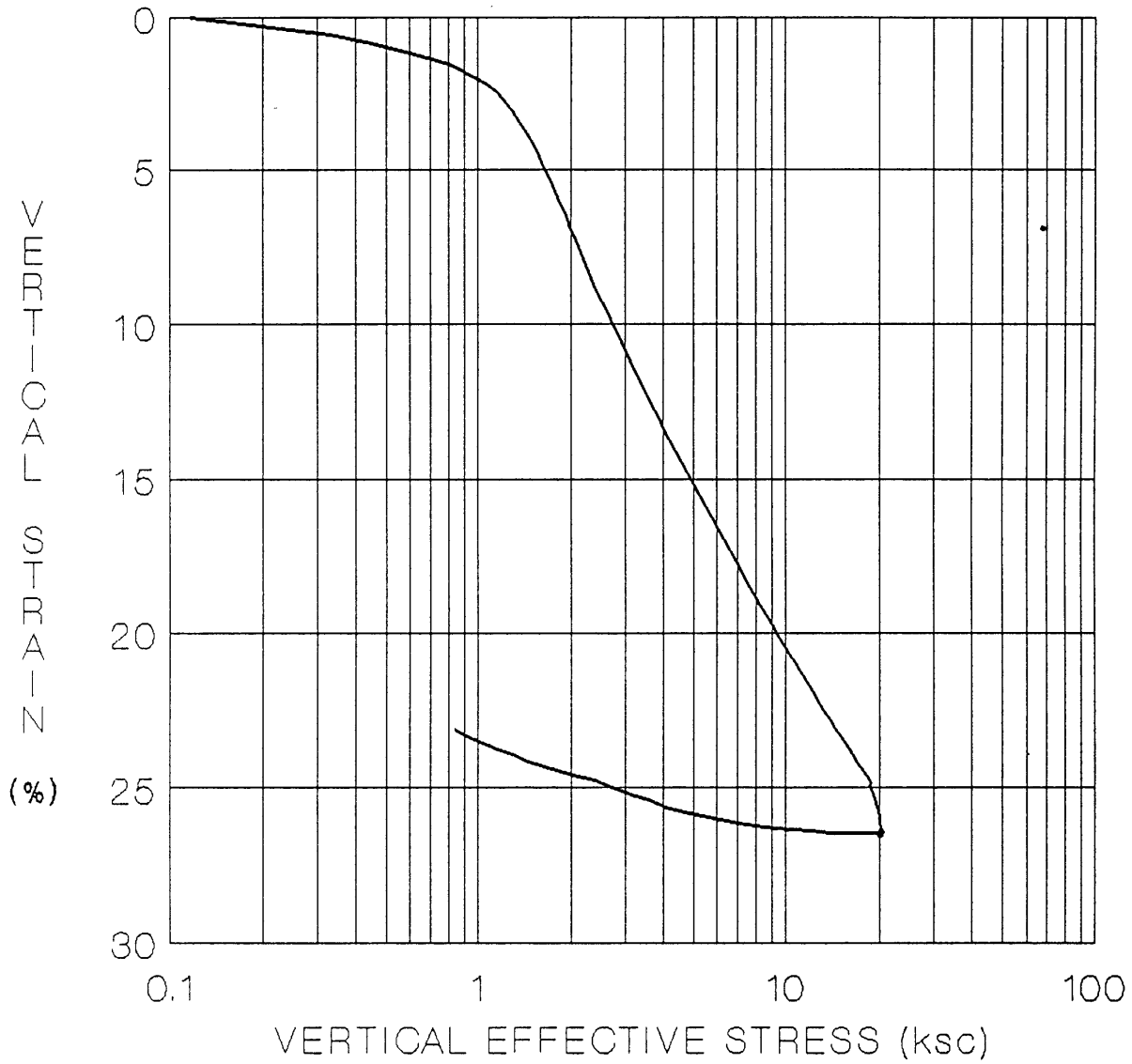


Figure C.5: Compression Curve (ϵ_v Vs. $\log \sigma'_{vc}$) from CRSC TEST No. 8.

BLANK PAGE

CRSC TESTS ON BBC III (CRS 1,2,3&8)

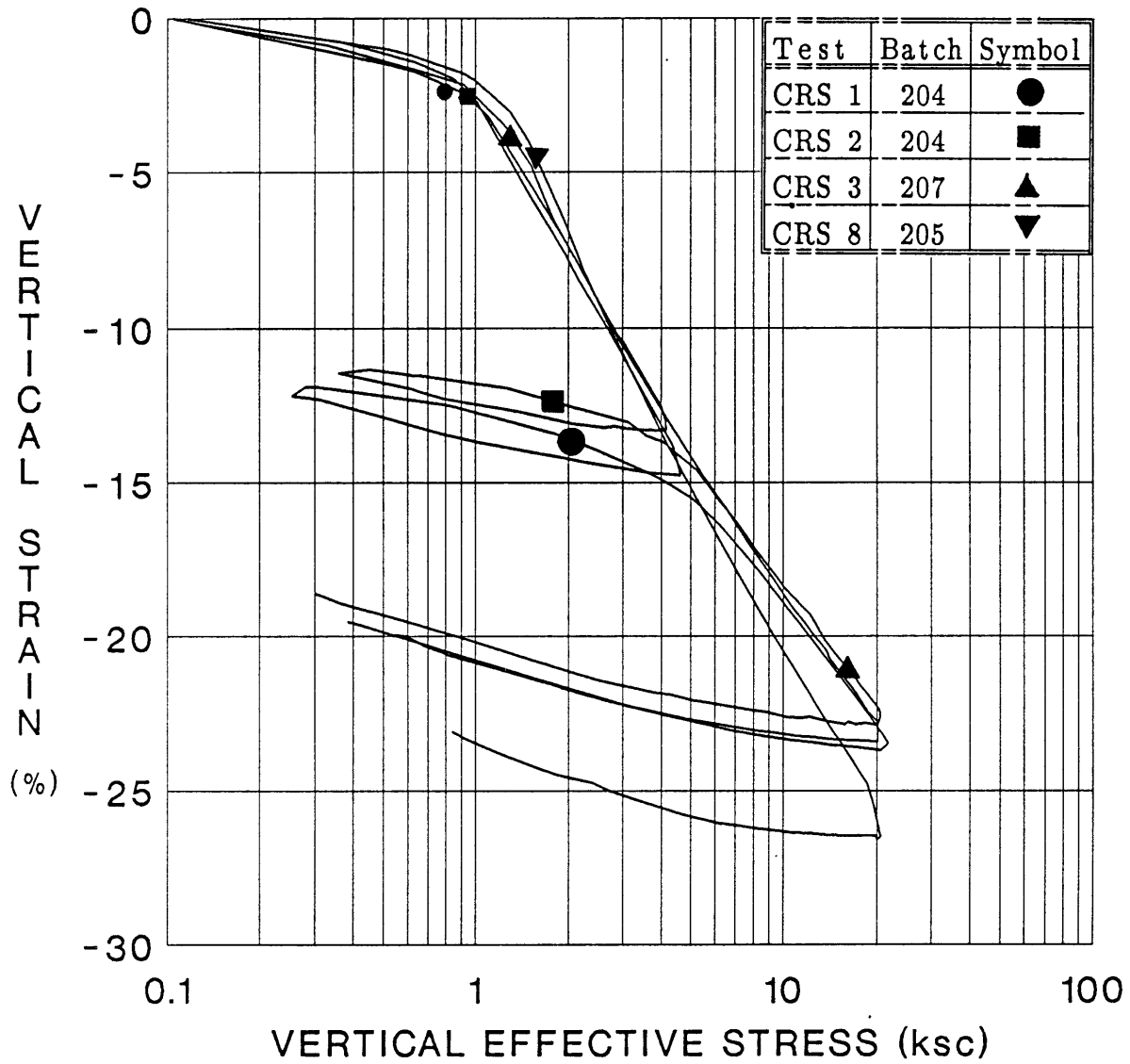


Figure C.6: Comparison of Compression Curves (ϵ_v Vs. $\log \sigma'_{vc}$) from All CRS Tests.

CRSC TESTS ON BBC III (CRSC 1,2&3)

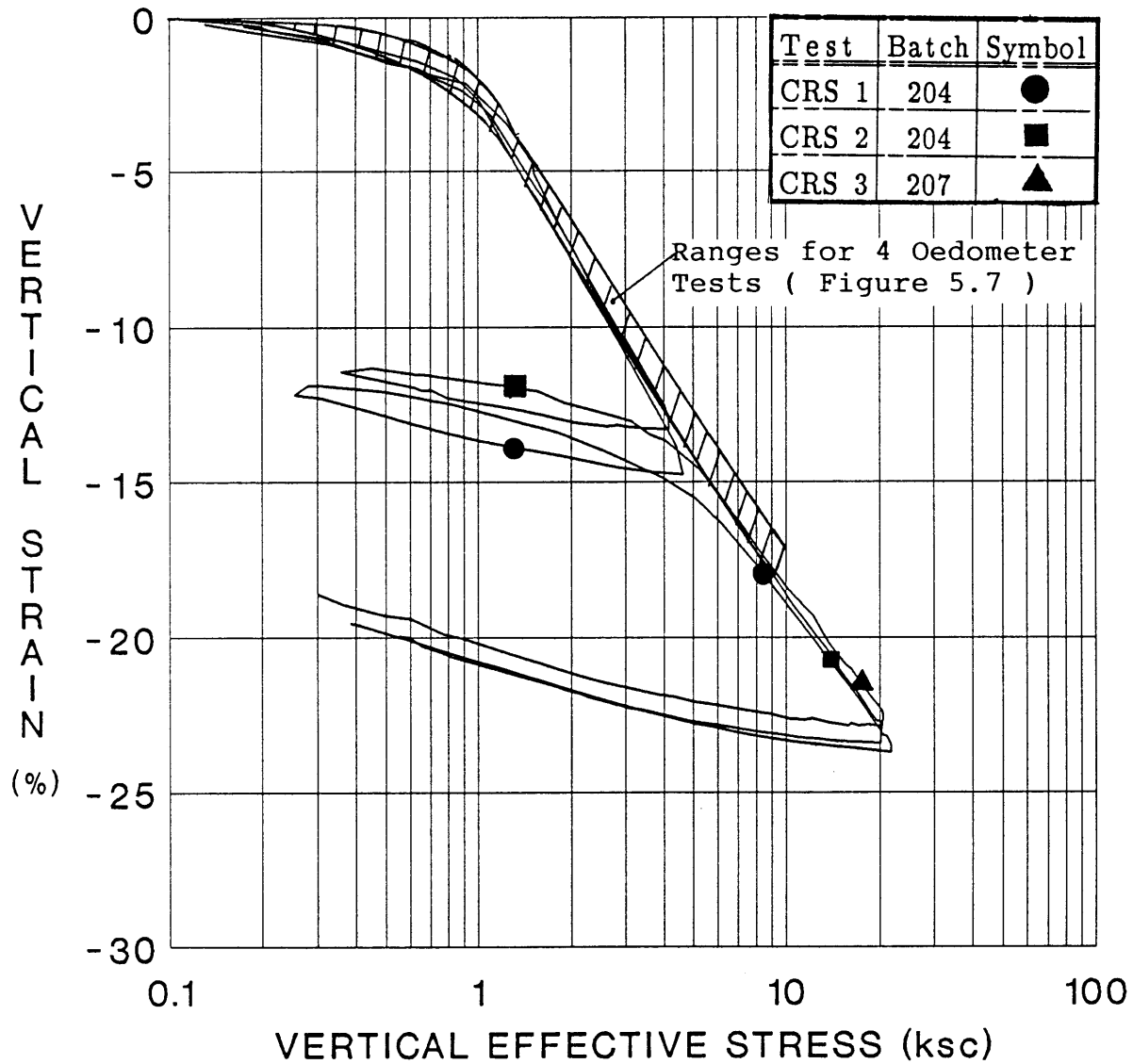


Figure C.7: Comparison of Compression Curves (ϵ_v Vs. $\log \sigma'_{vc}$) from CRS and Oedometer Tests.

CRSC TEST NO. 1

(Batch 204)

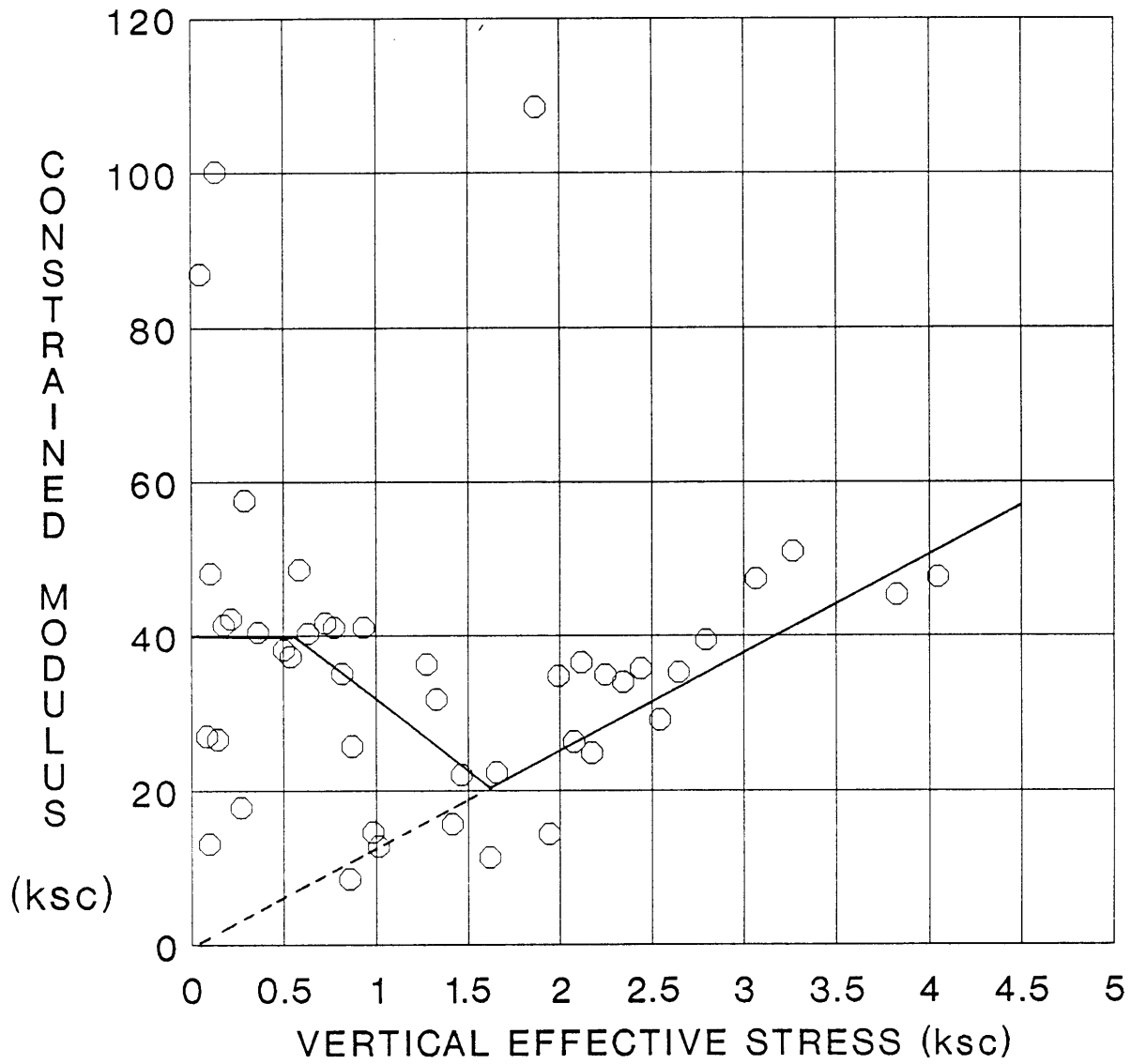


Figure C.8: Plot of Constrained Modulus (D) Vs. Vertical Effective Stress (σ'_{vc}) for CRSC Test No. 1.

CRSC TEST NO. 2

(Batch 204)

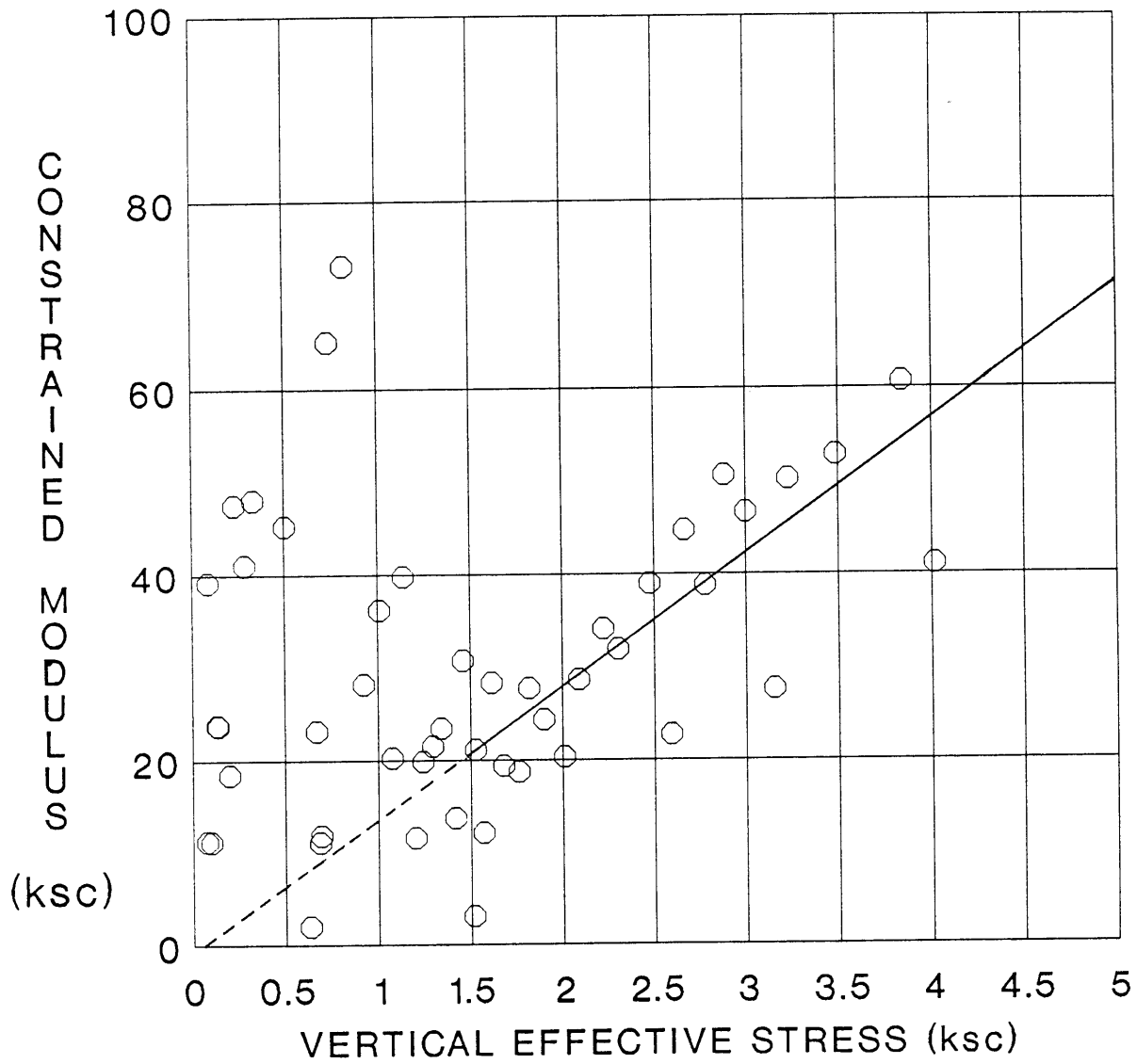


Figure C.9: Plot of Constrained Modulus (D) Vs. Vertical Effective Stress (σ'_{vc}) for CRSC Test No. 2.

CRSC TEST NO. 3 (Batch 207)

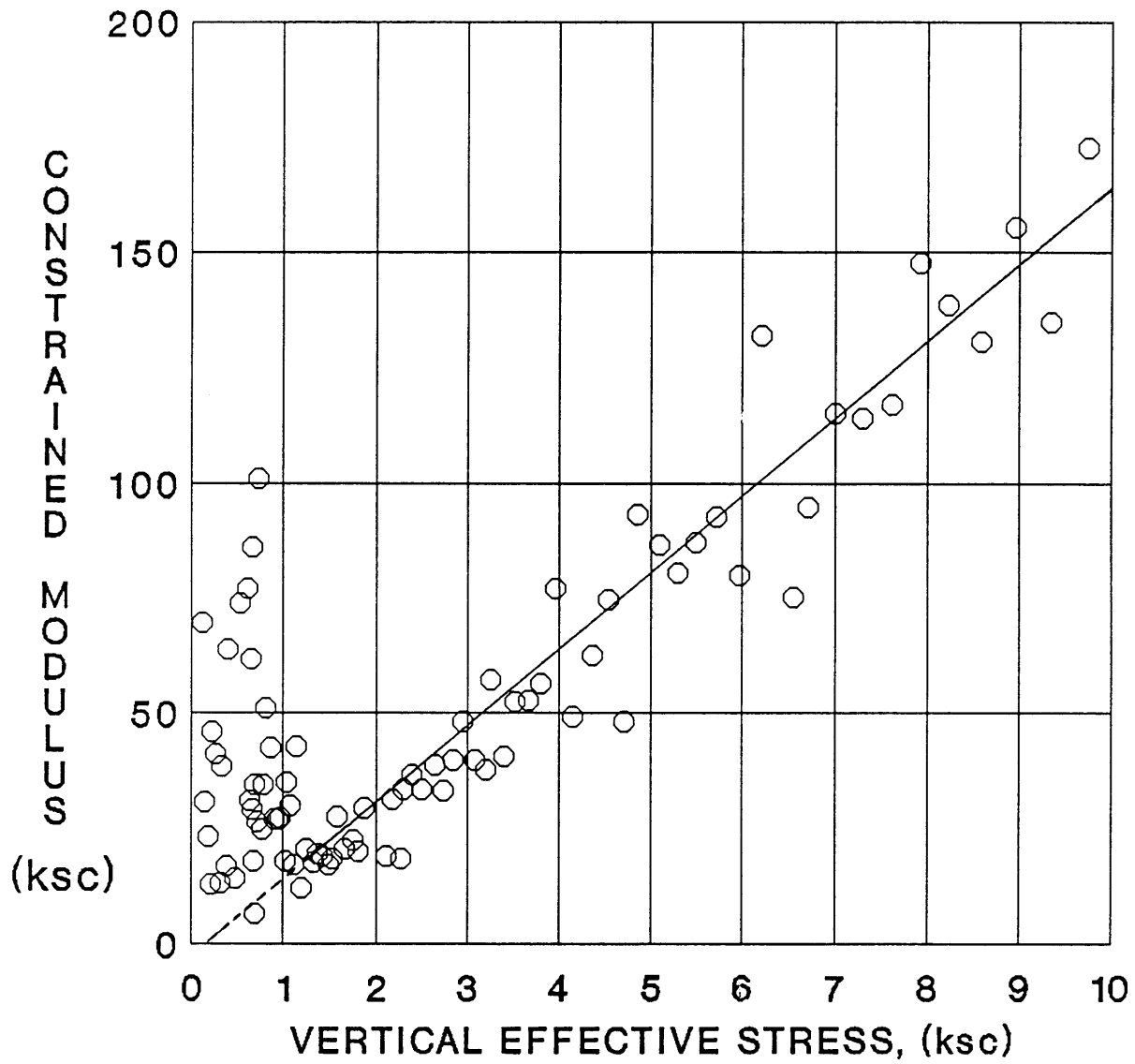


Figure C.10: Plot of Constrained Modulus (D) Vs. Vertical Effective Stress (σ'_{vc}) for CRSC Test No. 3.

CRSC TEST NO. 8

(Batch 205)

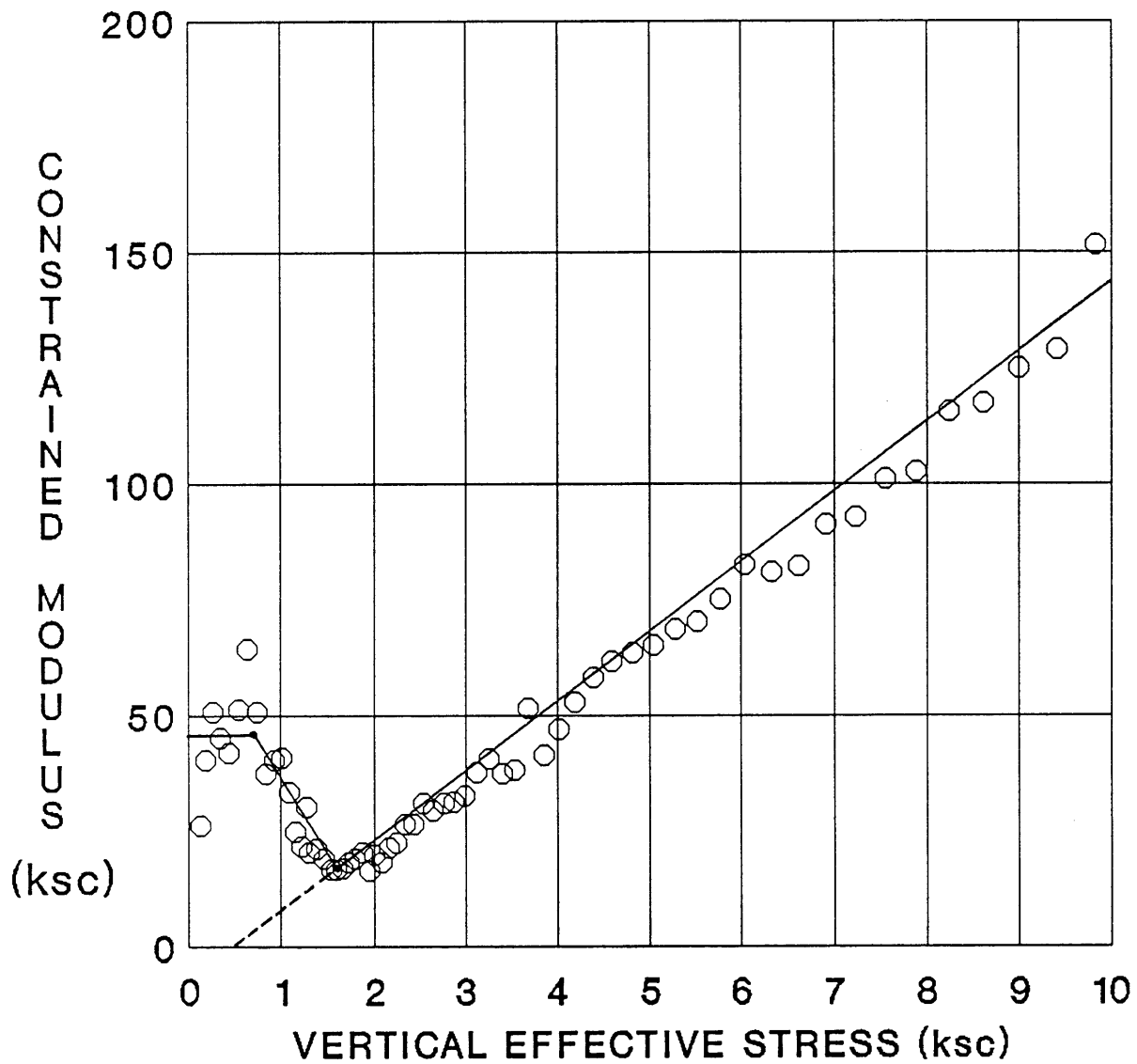


Figure C.11: Plot of Constrained Modulus (D) Vs. Vertical Effective Stress (σ'_{vc}) for CRSC Test No. 8.

CRS TEST NO. 1

(Batch 204)

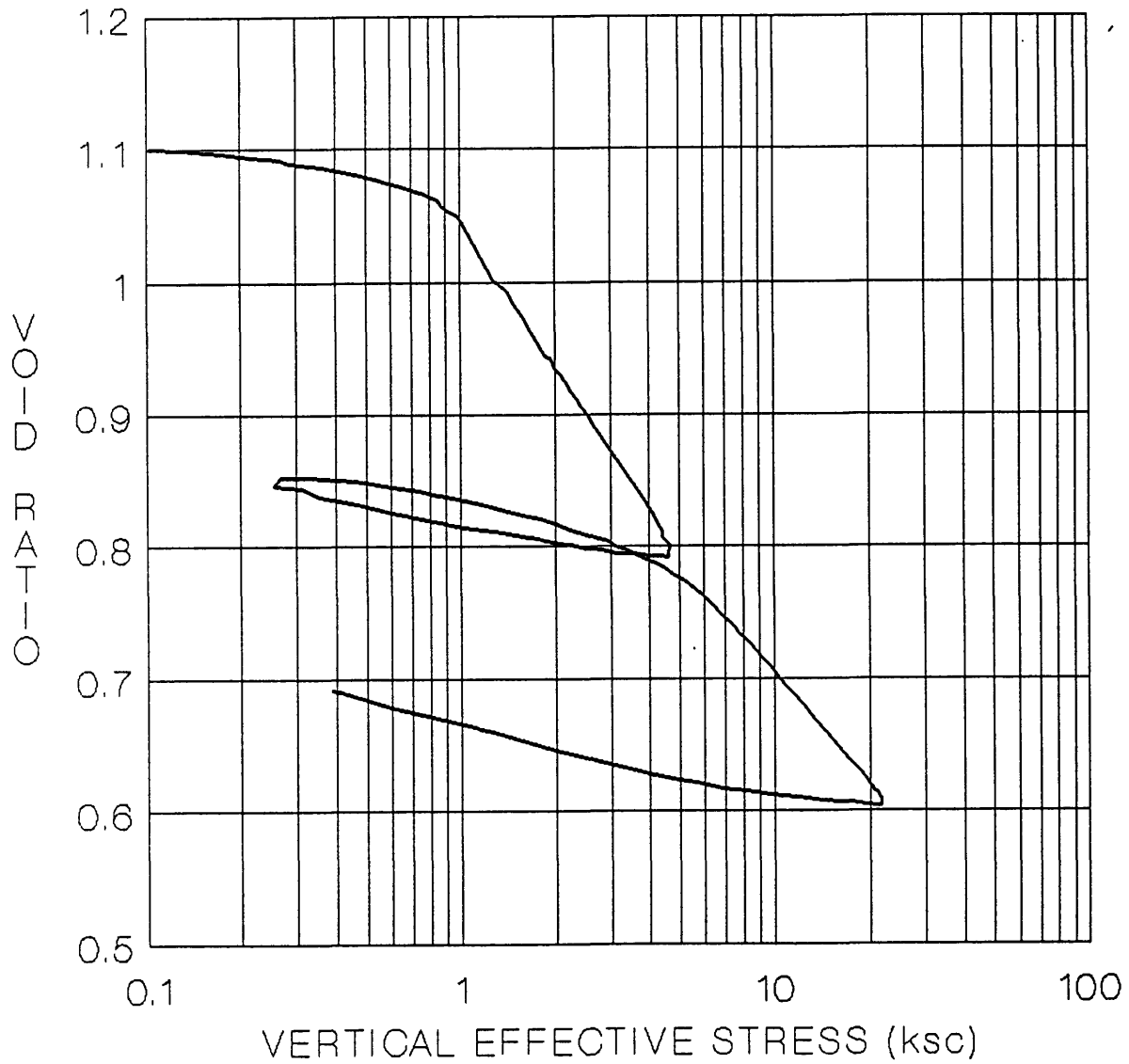


Figure C.12: Compression Curve (e Vs. $\log \sigma'_{vc}$) from CRS TEST No. 1.

CRSC TEST NO. 2 (Batch 204)

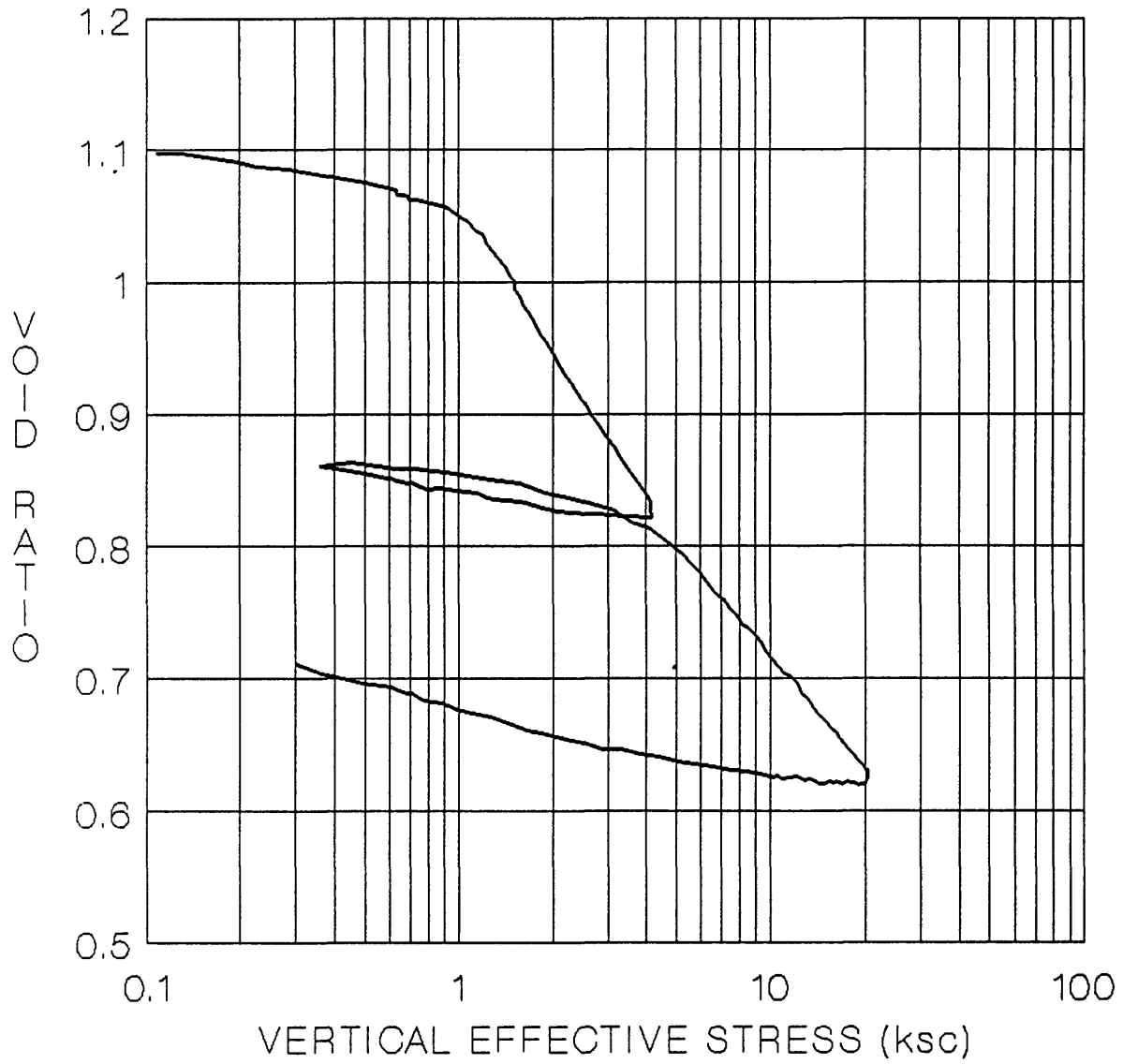


Figure C.13: Compression Curve (e Vs. $\log \sigma'_{vc}$) from CRSC TEST No. 2.

CRSC TEST NO. 3

(Batch 207)

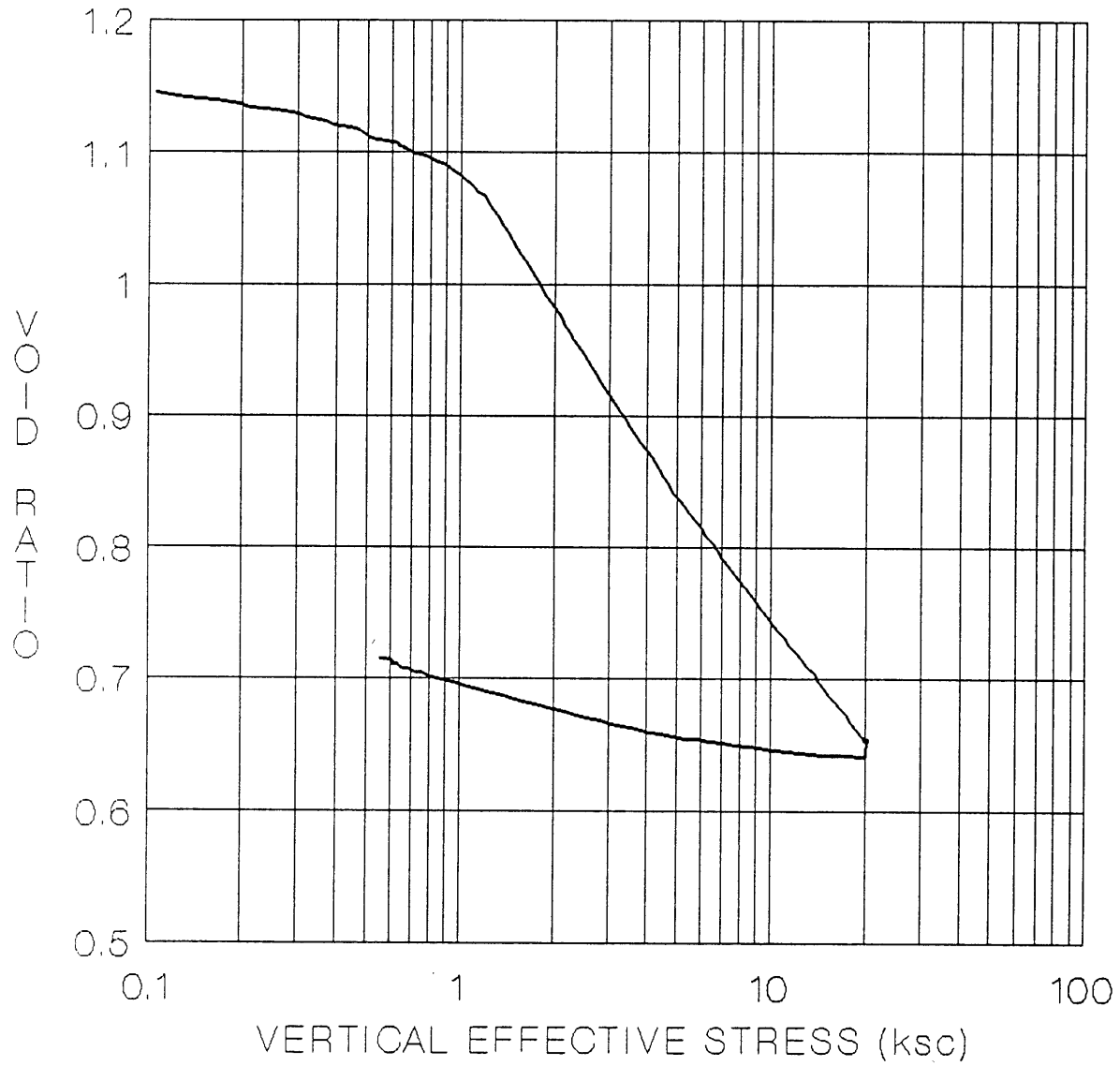


Figure C.14: Compression Curve (e Vs. $\log \sigma'_{vc}$) from CRSC TEST No. 3.

CRSC TEST NO. 8

(Batch 205)

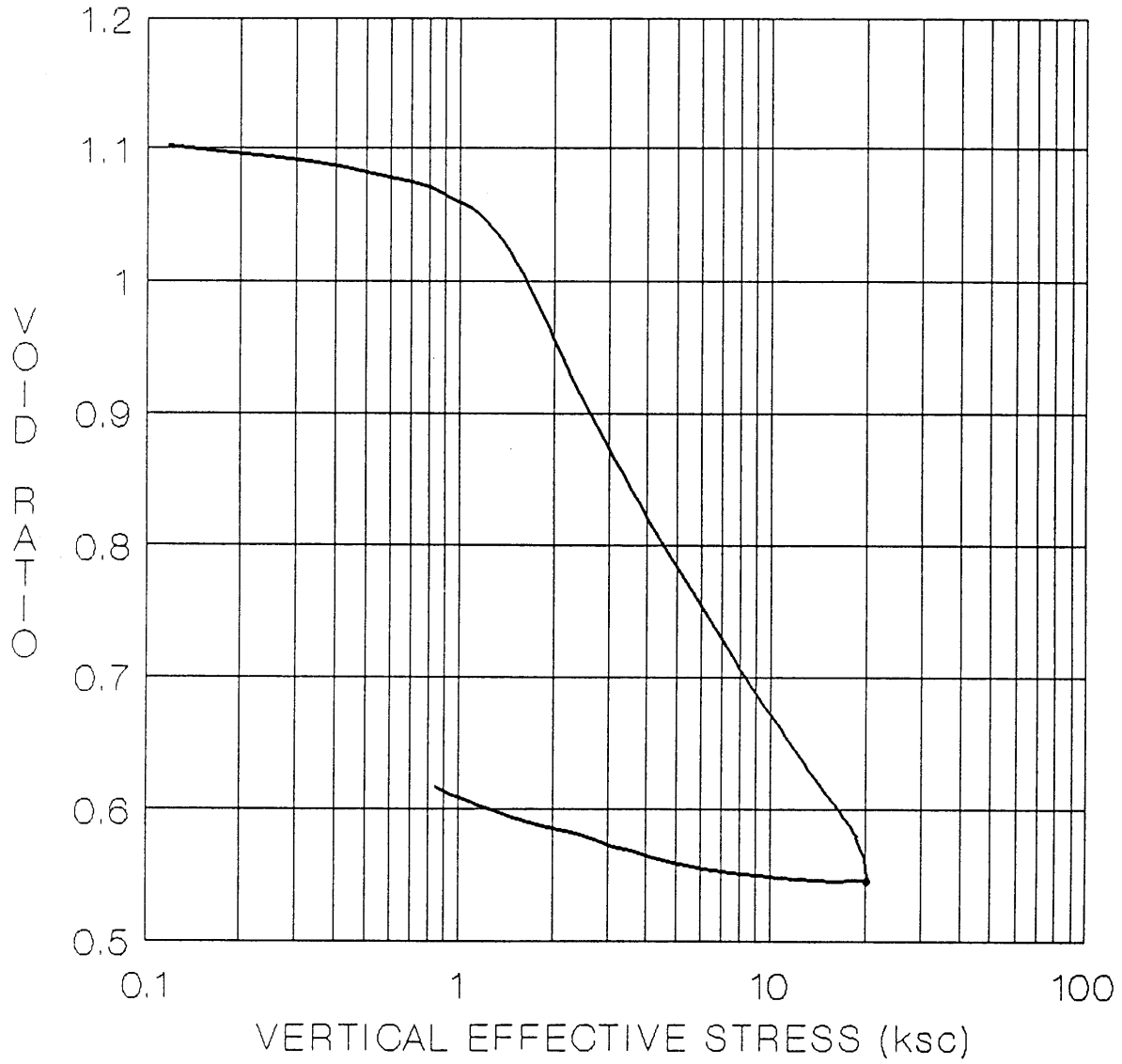


Figure C.15: Compression Curve (e Vs. $\log \sigma'_{vc}$) from CRSC TEST No. 8.

CRSC TESTS ON BBC III (CRS 1,2,3&8)

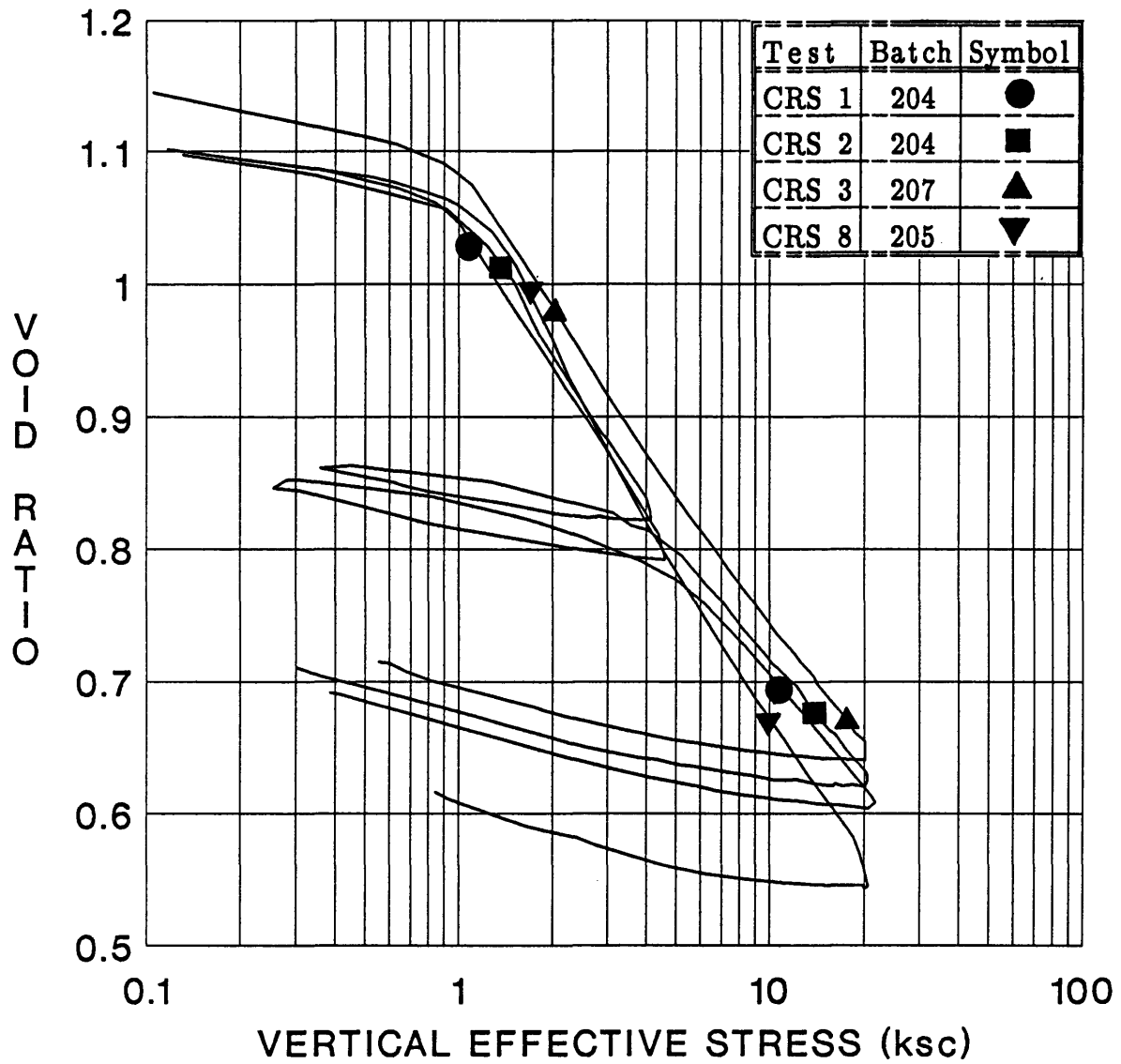


Figure C.16: Comparison of Compression Curves (e Vs. $\log \sigma'_{vc}$) from All the CRS Tests.

CRSC TEST NO. 1

(Batch 204)

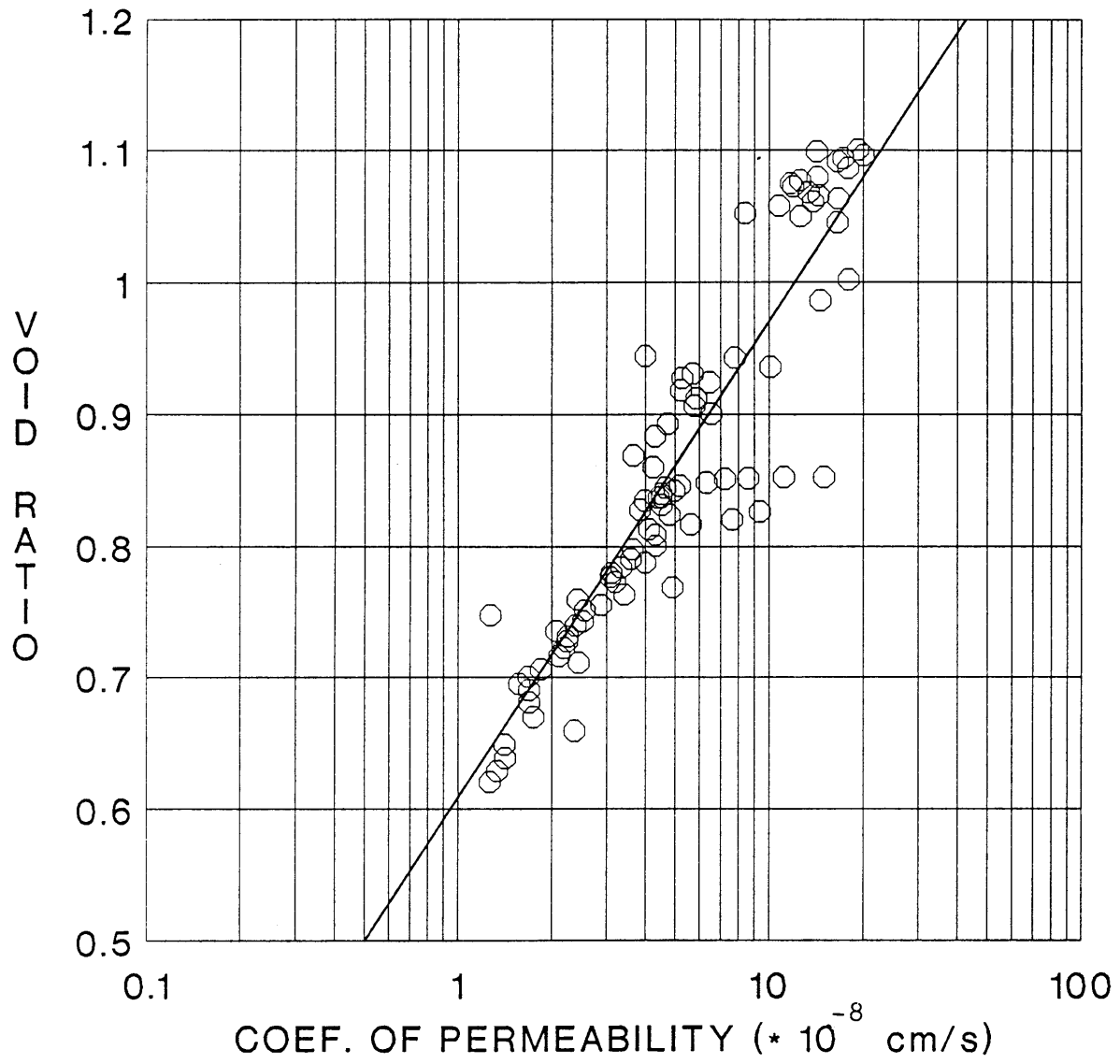


Figure C.17: Graph of Void Ratio (e) Vs. Logarithm of Coefficient of Permeability (k) for CRSC Test No. 1.

CRSC TEST NO. 2

(Batch 204)

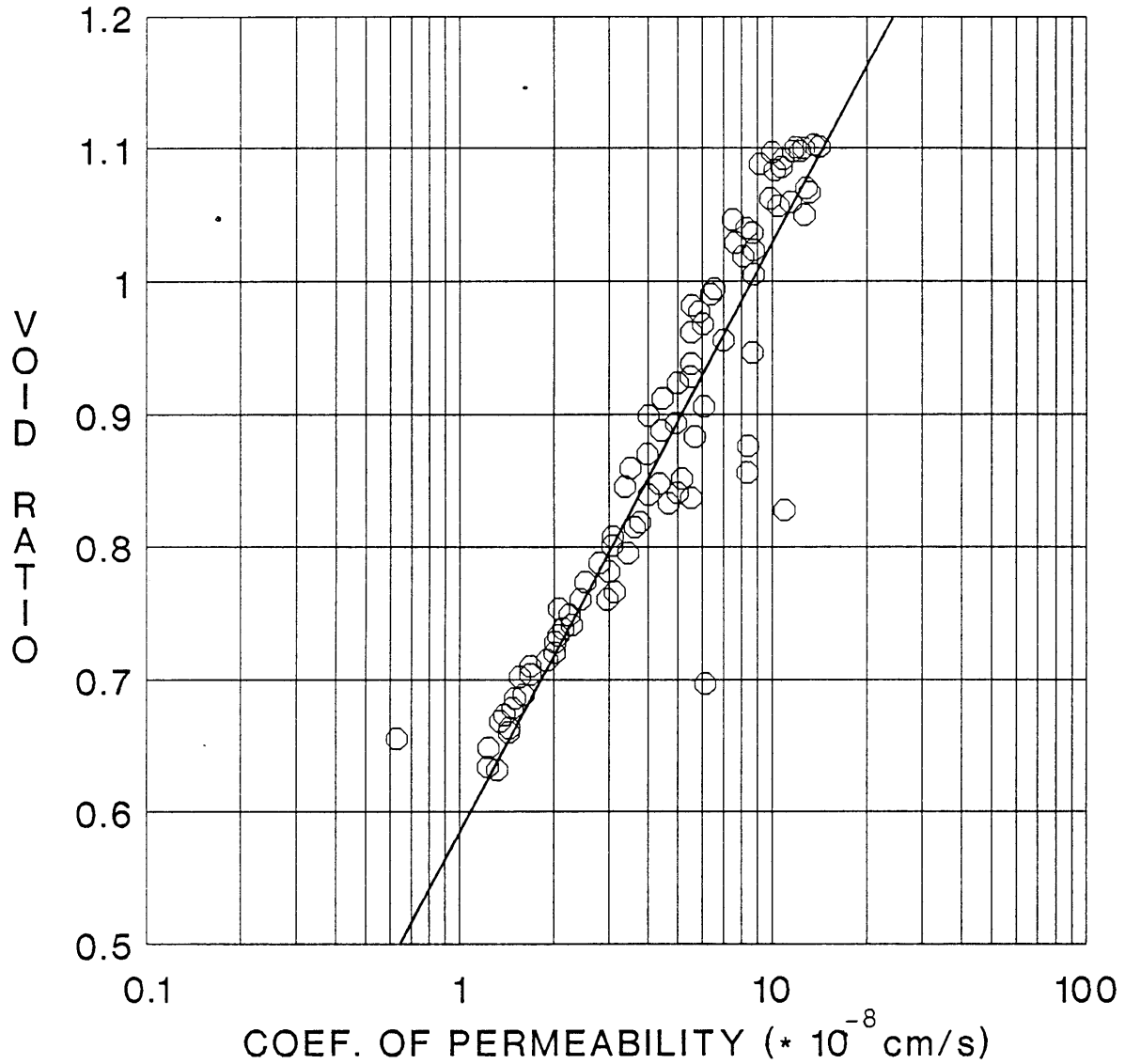


Figure C.18: Graph of Void Ratio (e) Vs. Logarithm of Coefficient of Permeability (k) for CRSC Test No. 2.

CRSC TEST NO. 3 (Batch 207)

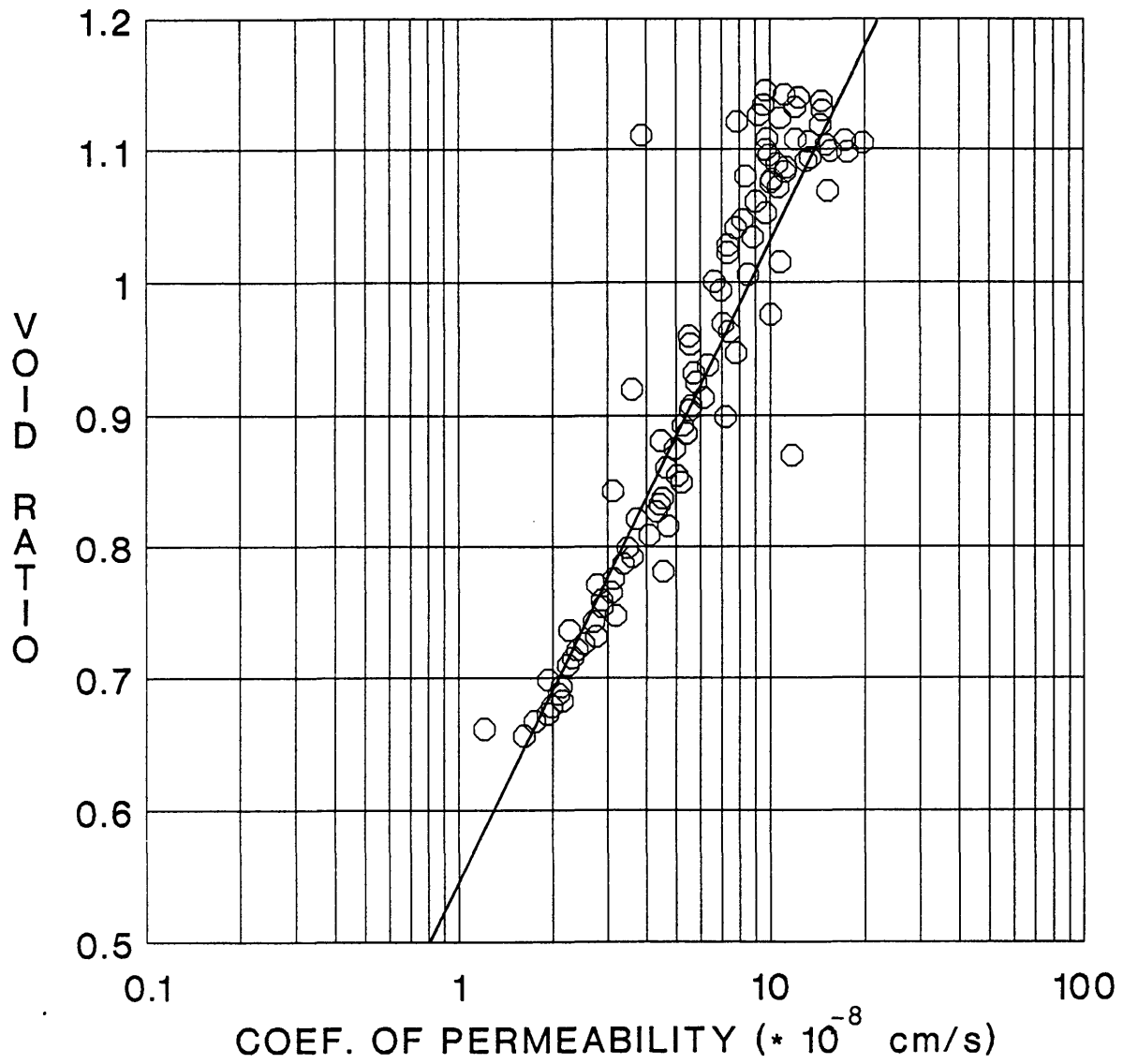


Figure C.19: Graph of Void Ratio (e) Vs. Logarithm of Coefficient of Permeability (k) for CRSC Test No. 3.

CRSC TEST NO. 8 (Batch 205)

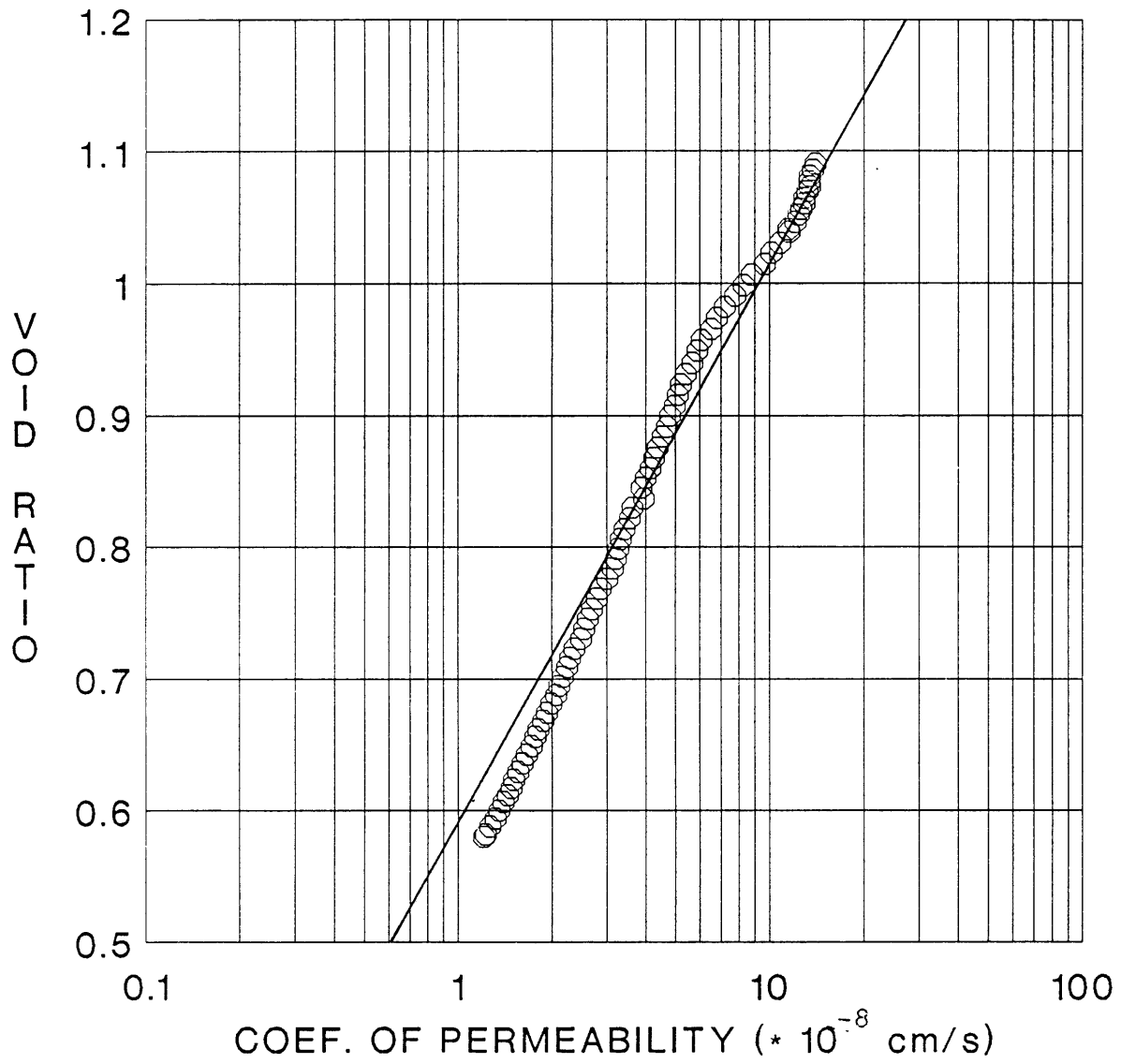


Figure C.20: Graph of Void Ratio (e) Vs. Logarithm of Coefficient of Permeability (k) for CRSC Test No. 8.

CRSC TESTS ON BBC III (Batches 204,205&207)

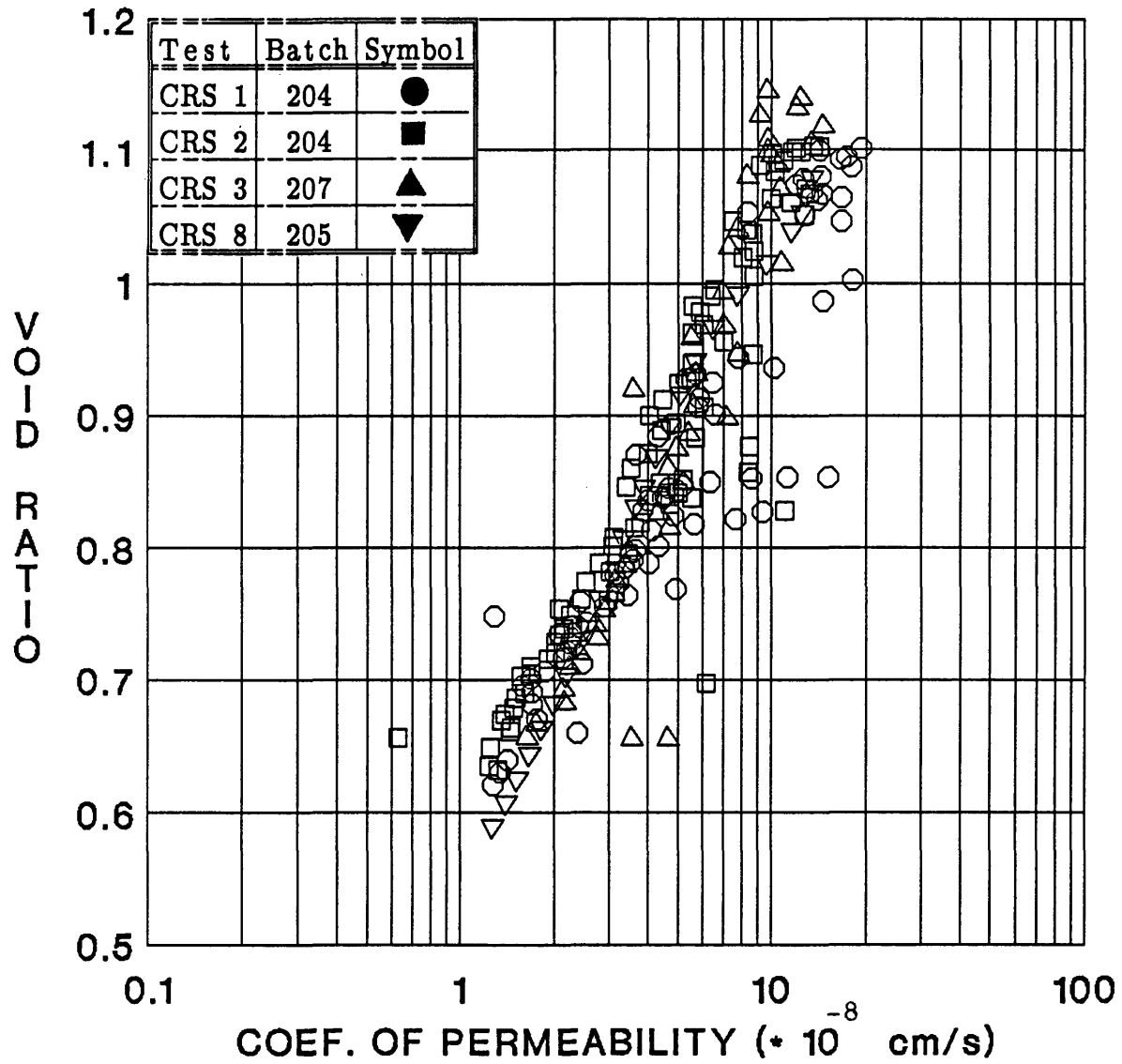


Figure C.21: Graph of Void Ratio (e) Vs. Logarithm of Coefficient of Permeability (k) for All the CRS Tests.

CRSC TEST NO. 1

(Batch 204)

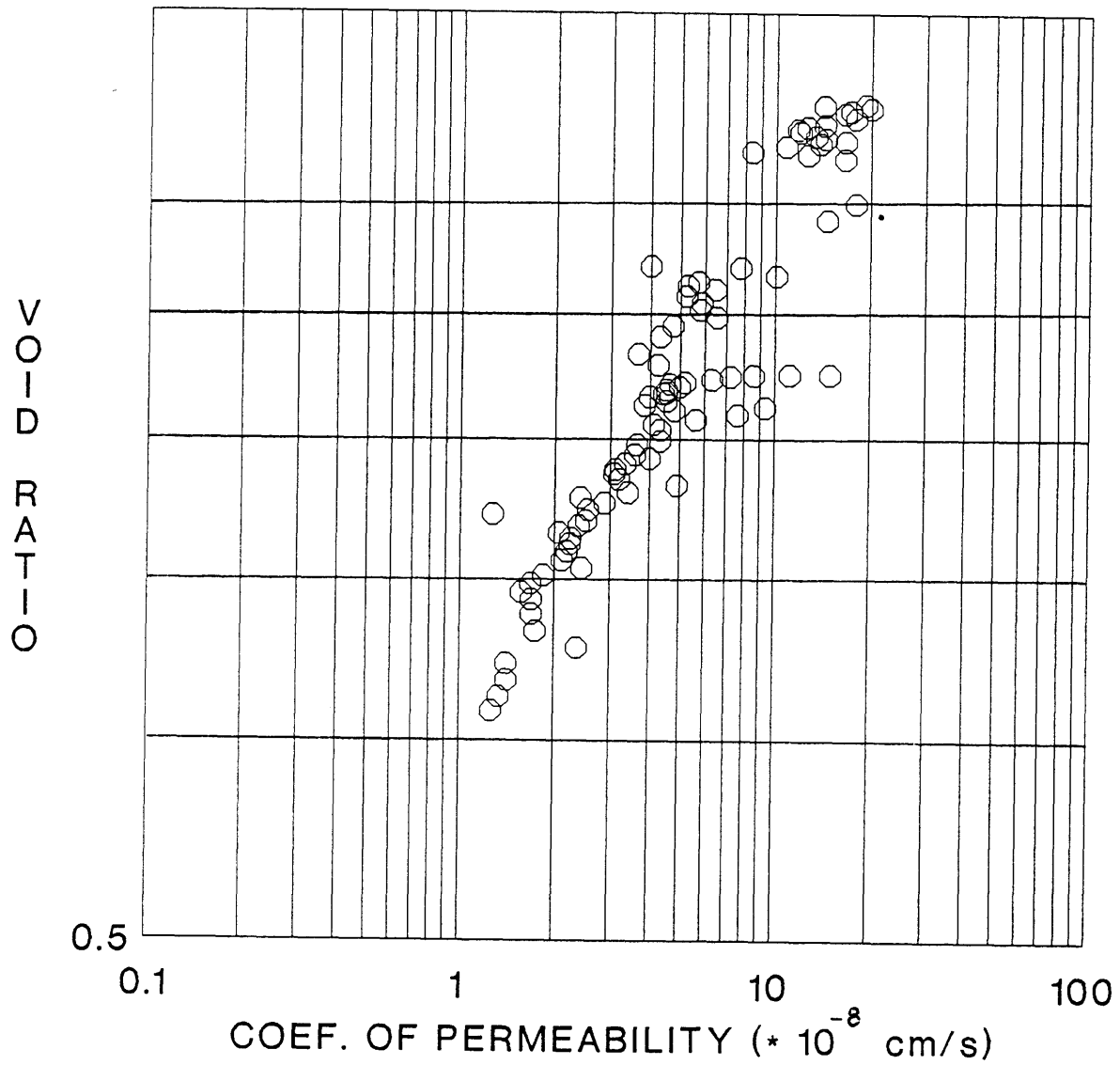


Figure C.22: Graph of Logarithm of Void Ratio (e) Vs. Logarithm of Coefficient of Permeability (k) for CRSC Test No. 1.

CRSC TEST NO. 2

(Batch 204)

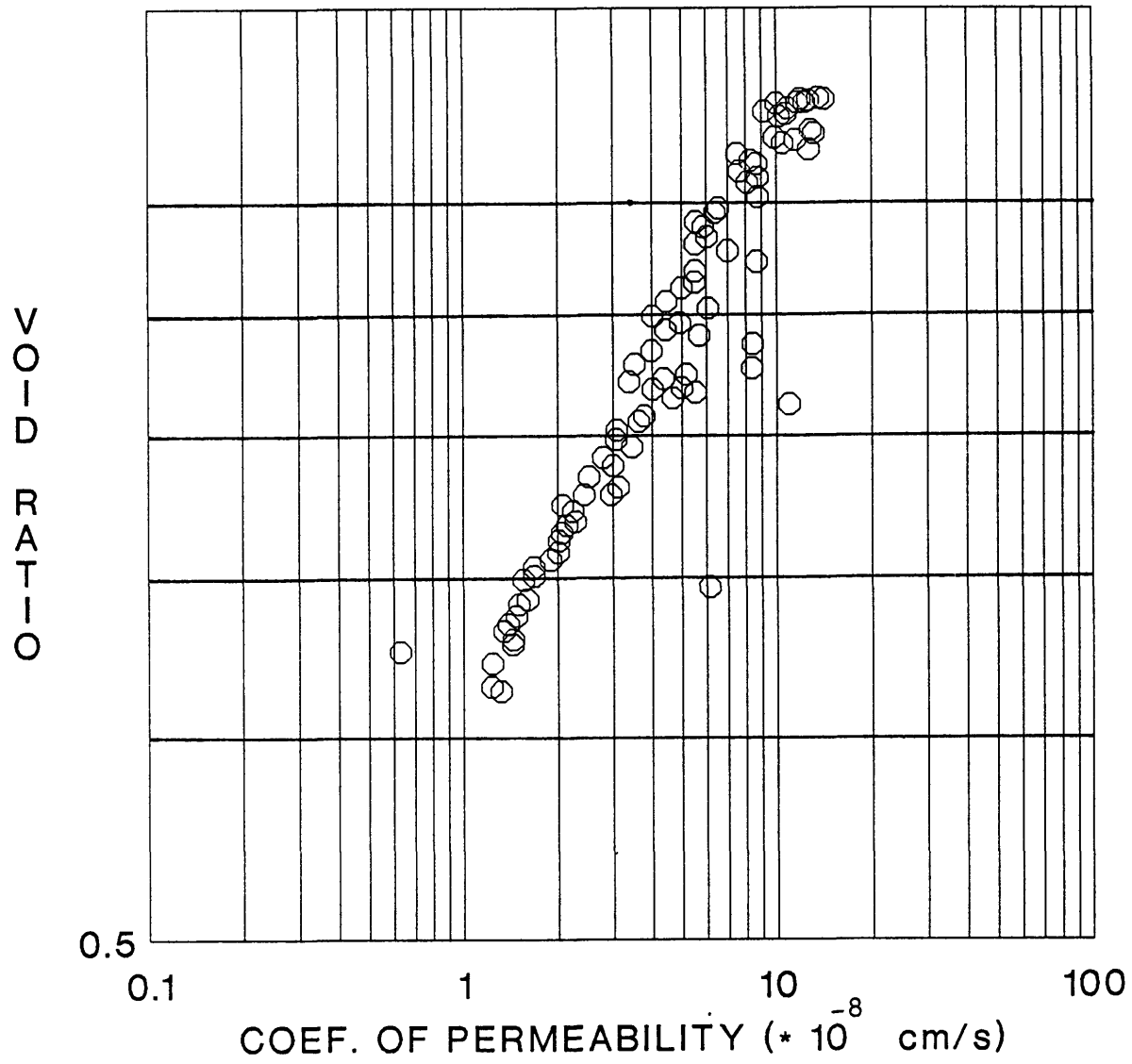


Figure C.23: Graph of Logarithm of Void Ratio (e) Vs. Logarithm of Coefficient of Permeability (k) for CRSC Test No. 2.

CRSC TEST NO. 3
(Batch 207)

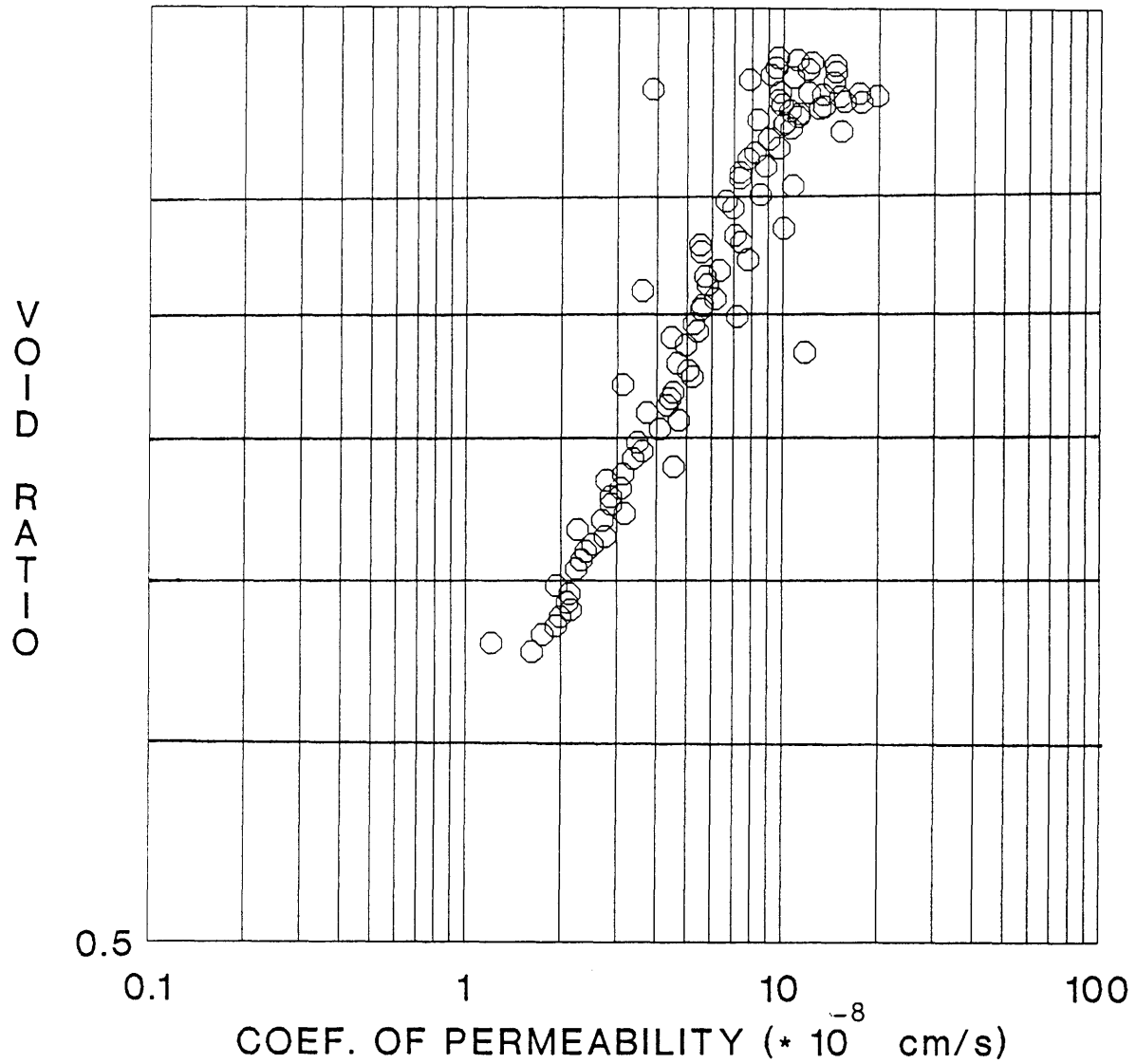


Figure C.24: Graph of Logarithm of Void Ratio (e) Vs. Logarithm of Coefficient of Permeability (k) for CRSC Test No. 3.

CRSC TEST NO. 8

(Batch 205)

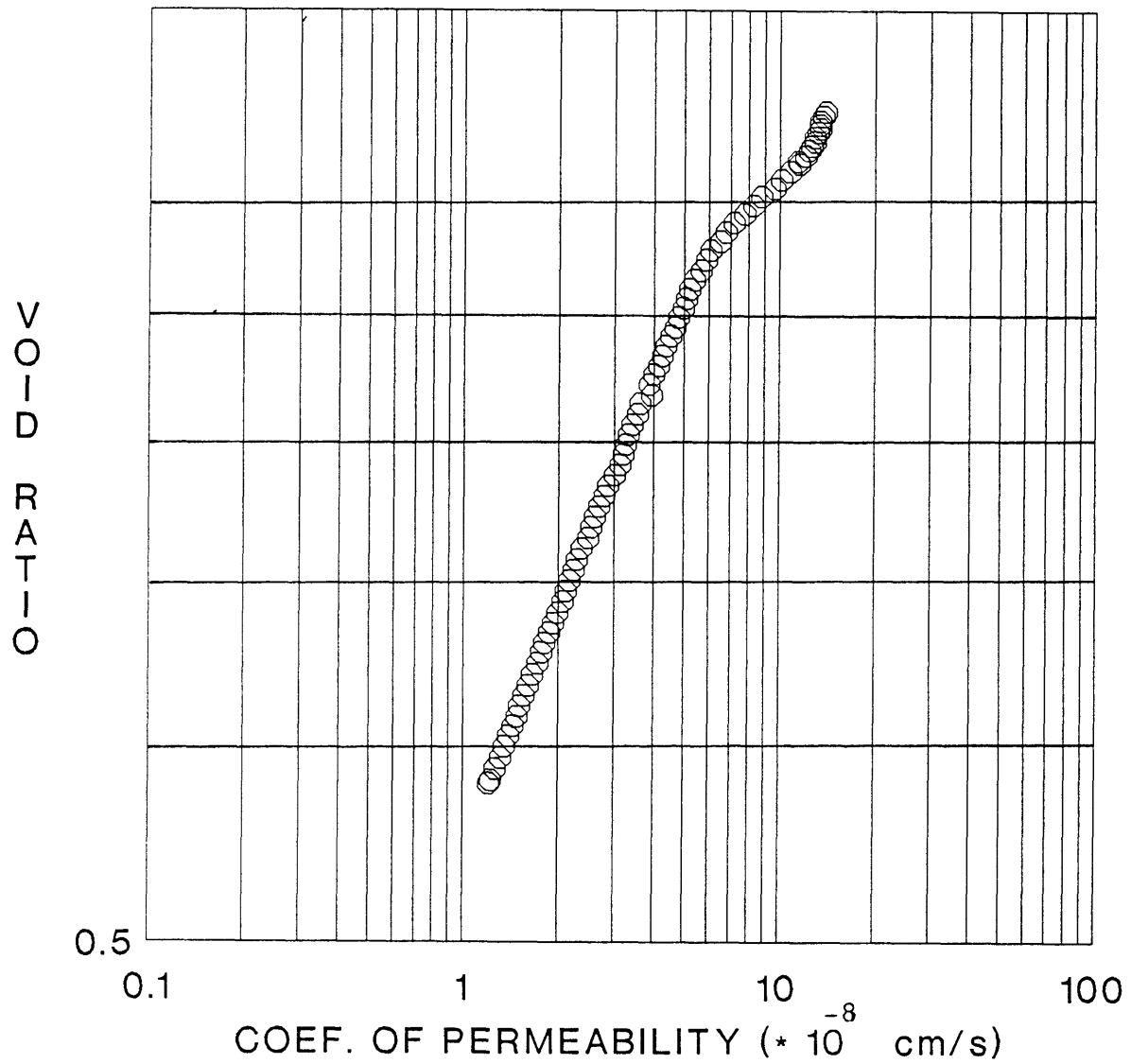


Figure C.25: Graph of Logarithm of Void Ratio (e) Vs. Logarithm of Coefficient of Permeability (k) for CRSC Test No. 8.

CRSC TESTS ON BBC III (Batches 204,205&207)

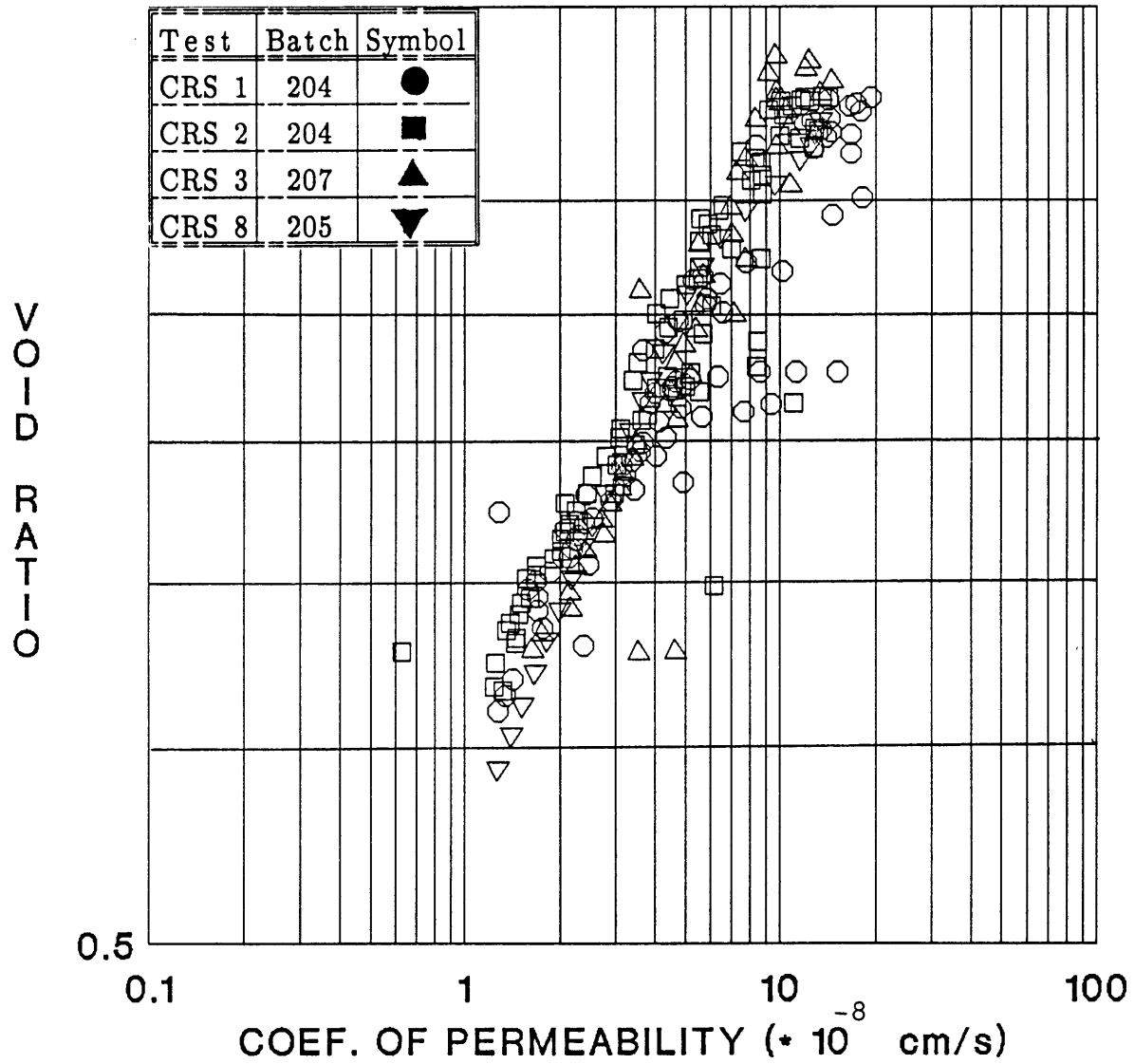


Figure C.26: Graph of Logarithm of Void Ratio (e) Vs. Logarithm of Coefficient Permeability (k) for All the CRS Tests.

CRSC TEST NO. 1
(Batch 204)

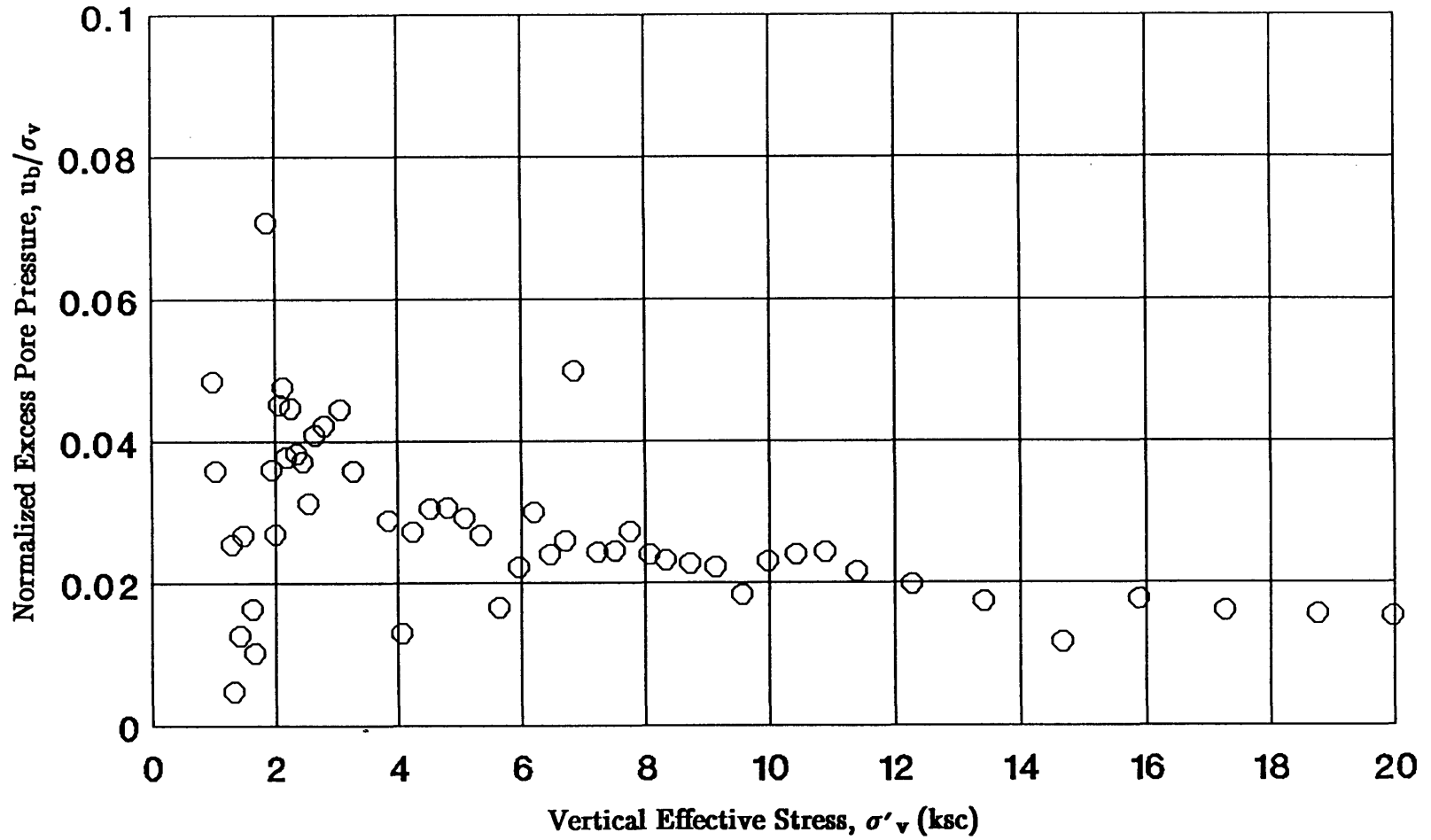


Figure C.27: Plot of Normalized Excess Pore Pressure (u_b/σ_v) versus Vertical Effective Stress (σ'_v) for CRSC Test No. 1.

CRSC TEST NO. 2
(Batch 204)

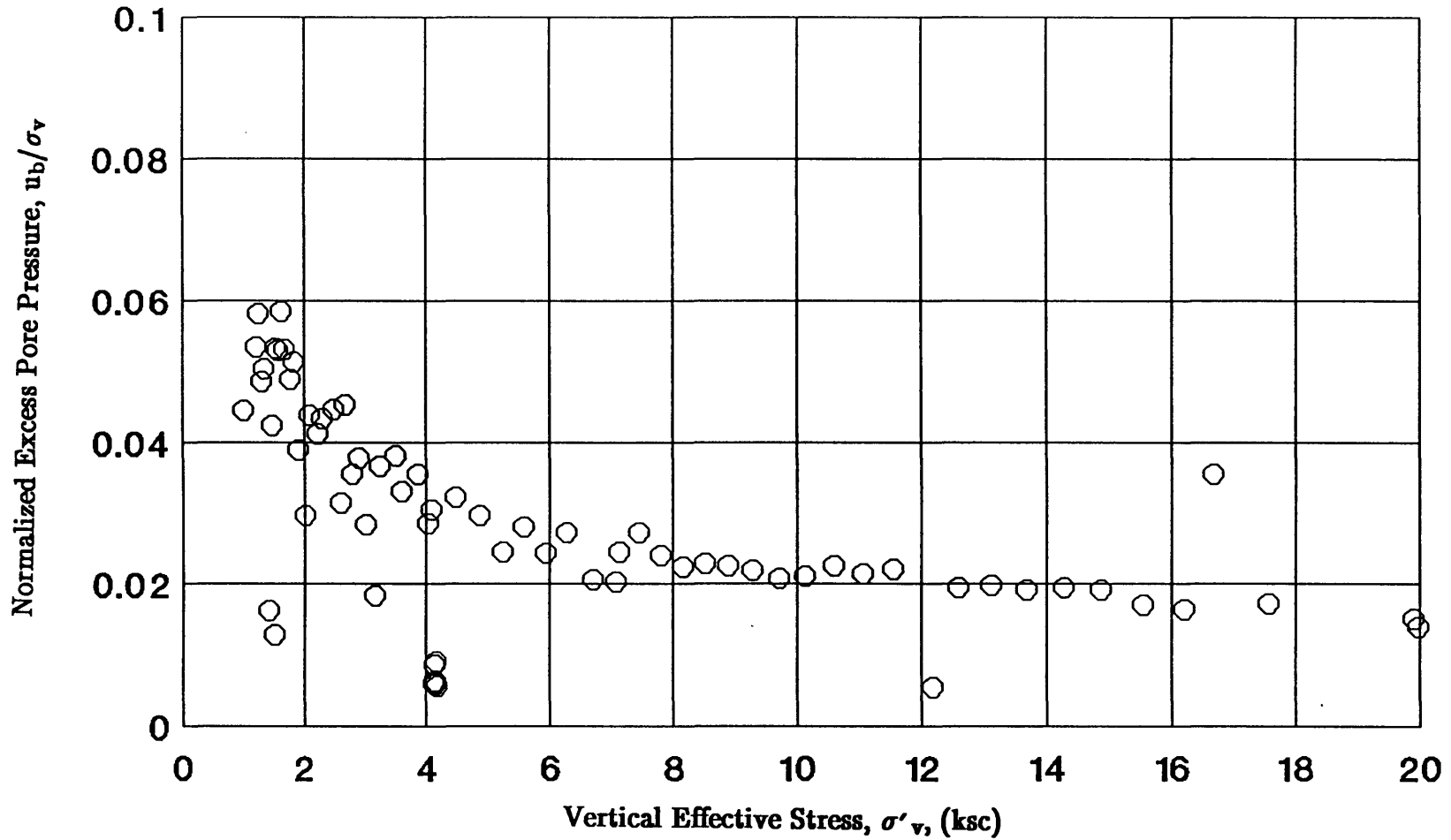


Figure C.28: Plot of Normalized Excess Pore Pressure (u_b/σ_v) versus Vertical Effective Stress (σ'_v) for CRSC Test No. 2.

CRSC TEST NO. 3
(Batch 207)

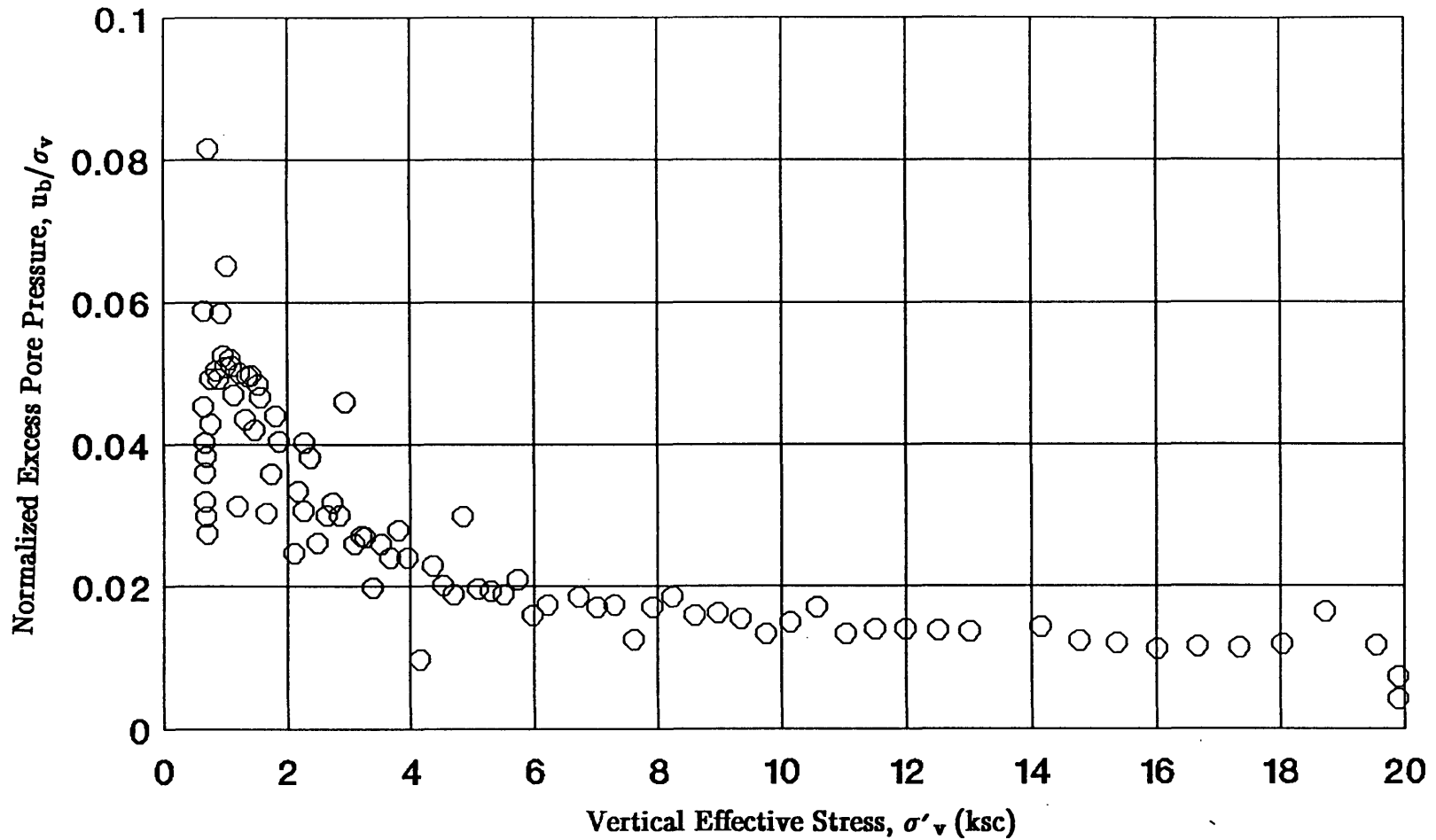


Figure C.29: Plot of Normalized Excess Pore Pressure (u_b/σ_v) versus Vertical Effective Stress (σ'_v) for CRSC Test No. 3.

CRSC TEST NO. 8
(Batch 205)

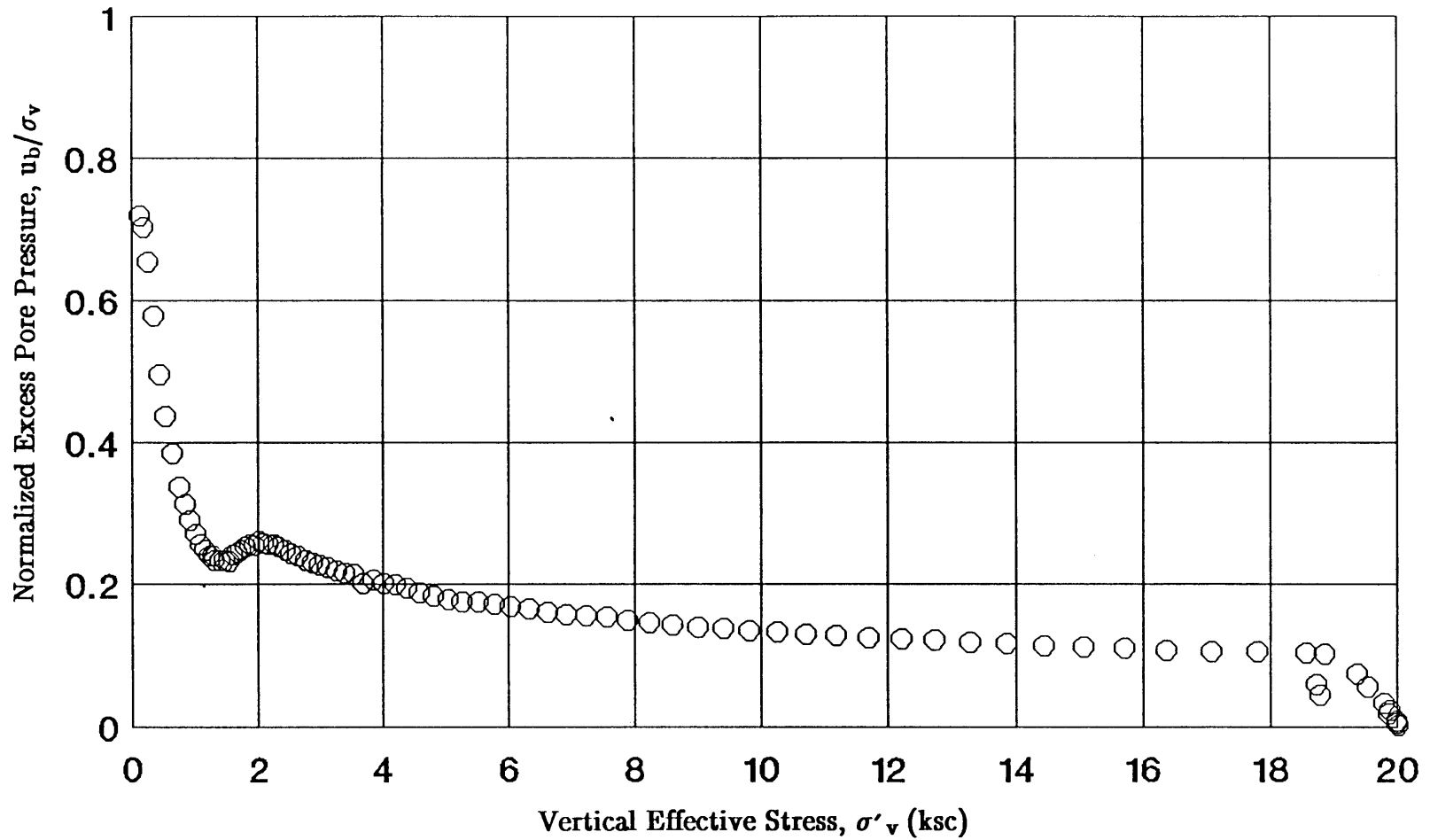
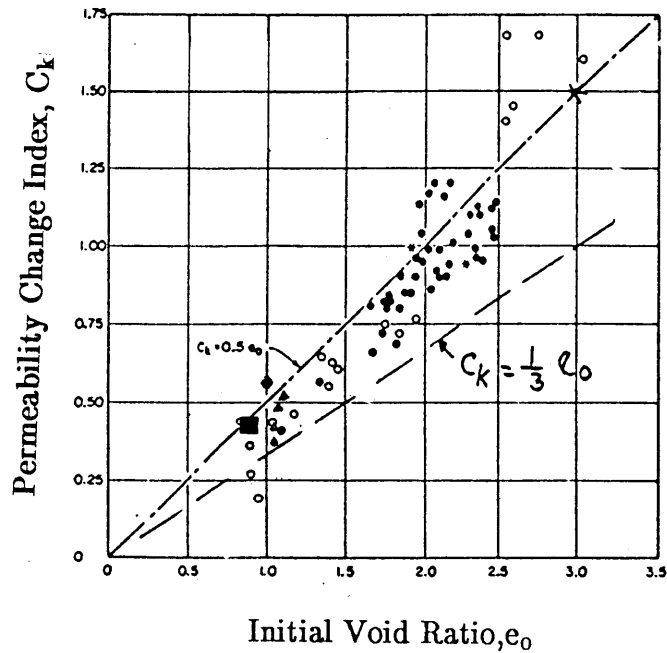


Figure C.30: Plot of Normalized Excess Pore Pressure (u_b/σ'_v) versus Vertical Effective Stress (σ'_v) for CRSC Test No. 8.

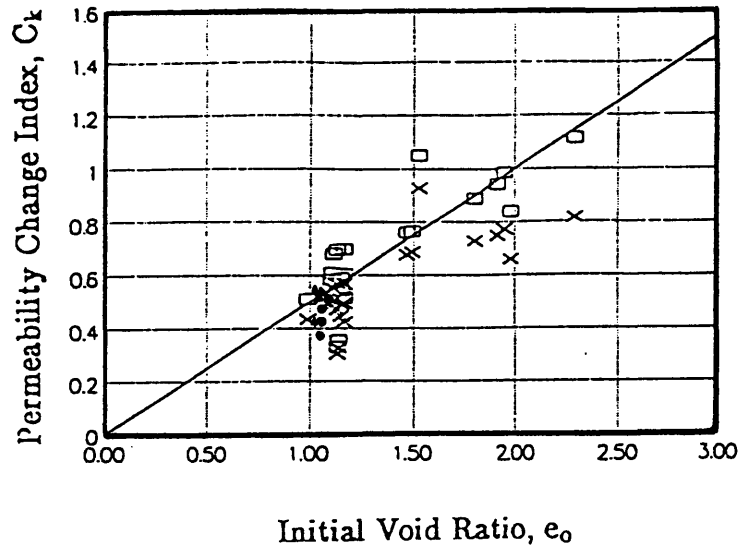
COEFFICIENT OF PERMEABILITY



Type of Soil	Symbol
Champlain Clays	●
Other Canadian Clays	○
Other Clays	✱
Resedimented BBC III	
CRS	▲
Oedometer	■
Oedometer and Batch	◆

Figure C.31: Graph of Permeability Change Index, C_k , Versus Void Ratio, e_0 , for All Clays Tested (after Tavenas et al., 1983).

COEFFICIENT OF PERMEABILITY



Relationship	Reference	Symbol
$\log(e) - \log(k)$	Seah, 1990	×
	This Research	Δ
$e - \log(k)$	Seah, 1990	□
	This Research	•

Figure C.32: Graph of Permeability Change Index, C_k , Versus Void Ratio, e_0 , for BBC III.

 CONSOLIDATION AT CONSTANT RATE OF STRAIN
 MIT GEOTECHNICAL LAB

File Name: CRS01.PRN

1. Test Name: CRS 01
 2. Date: 1/7/89
 3. Initial Height of Sample (cm): 2.357
 4. Initial Water Content of Sample (%): 39.58
 5. Area of Sample (sq cm): 31.64
 6. DCDT
 Zero: 0.38024
 CF: -1.8526 cm/V/V
 7. Cell Pressure
 Zero: -0.00006
 CF: 705.735 ksc/V/V
 8. Vertical Load Cell
 Zero: 0.00006
 CF: 27013.98 kg/V/V
 9. Pore Pressure
 Zero: -0.0010
 CF: 965.359 ksc/V/V

TIME (secs)	STRAIN (%)	CELL (ksc)	V.STS (ksc)	PORE P (ksc)	V.E.STS (ksc)	VOID RATIO,e	DEL U (ksc)	DEL K (*10 cm/(*10 cm/s))	TOT. K	D (ksc)	Ub/Ov
600	0.002	2.040	0.094	2.061	0.080	1.102	0.021	-29.032	30.960	26.928	0.222
780	-0.059	2.040	0.111	2.062	0.096	1.101	0.022	-1.251	28.706	13.043	0.202
960	-0.103	2.040	0.125	2.073	0.102	1.100	0.034	35.496	19.102	48.077	0.271
1260	-0.160	2.039	0.147	2.065	0.130	1.099	0.025	8.162	25.411	100.113	0.173
1560	-0.172	2.041	0.172	2.086	0.142	1.099	0.046	-51.839	14.109	26.550	0.265
1860	-0.295	2.037	0.196	2.069	0.174	1.096	0.032	56.433	19.902	41.325	0.165
2460	-0.397	2.037	0.241	2.075	0.216	1.094	0.037	-46.170	17.115	42.149	0.155
3060	-0.514	2.036	0.292	2.075	0.266	1.091	0.039	-33.775	16.444	17.725	0.133
3660	-0.628	2.036	0.335	2.109	0.286	1.089	0.073	-11.570	8.686	57.569	0.219
4260	-0.759	2.035	0.385	2.071	0.361	1.086	0.036	20.750	17.810	40.420	0.093
6060	-1.099	2.037	0.529	2.082	0.499	1.079	0.045	-16.493	14.172	38.058	0.084
6600	-1.197	2.036	0.570	2.087	0.536	1.077	0.051	-7.766	12.477	37.239	0.089
7200	-1.320	2.039	0.618	2.093	0.582	1.074	0.054	0.599	11.656	48.530	0.087
7800	-1.422	2.053	0.667	2.106	0.631	1.072	0.053	13.132	11.875	40.224	0.079
9000	-1.650	2.052	0.754	2.099	0.723	1.068	0.047	-17.513	13.312	41.627	0.062
9600	-1.757	2.052	0.797	2.096	0.768	1.065	0.044	8.116	14.292	41.021	0.055
10200	-1.869	2.052	0.838	2.090	0.813	1.063	0.038	-11.081	16.525	35.019	0.045
10800	-1.978	2.052	0.882	2.097	0.852	1.061	0.045	-7.959	13.776	8.447	0.051
11400	-2.136	2.052	0.903	2.109	0.865	1.057	0.058	27.547	10.732	25.674	0.064
12600	-2.389	2.052	0.979	2.126	0.930	1.052	0.074	19.717	8.356	41.063	0.075
13200	-2.506	2.052	1.010	2.101	0.978	1.050	0.049	45.729	12.569	14.550	0.048
14400	-2.725	2.052	1.034	2.089	1.010	1.045	0.037	17.725	16.484	12.704	0.036
32110	-4.799	2.049	1.295	2.081	1.273	1.001	0.033	0.278	17.867	36.209	0.025
37510	-4.944	2.048	1.330	2.054	1.326	0.998	0.006	17.738	93.858	31.657	0.005
42010	-5.212	2.048	1.422	2.066	1.410	0.993	0.018	8.810	32.706	15.583	0.012
46510	-5.540	2.047	1.488	2.086	1.462	0.986	0.040	3.087	14.482	21.981	0.027
51010	-6.249	2.045	1.635	2.072	1.617	0.971	0.027	10.121	21.290	11.311	0.016
56410	-6.576	2.043	1.666	2.060	1.654	0.964	0.017	8.444	33.327	22.277	0.010
600	-7.527	2.054	1.959	2.192	1.866	0.944	0.138	-1.018	3.988	108.367	0.071
780	-7.596	2.054	1.989	2.125	1.941	0.943	0.071	3.589	7.731	14.343	0.036
1260	-7.931	2.057	2.025	2.112	1.989	0.935	0.054	-5.587	10.088	34.629	0.027
2414	-8.174	2.056	2.137	2.152	2.073	0.930	0.096	7.364	5.662	26.179	0.045
3014	-8.325	2.056	2.182	2.159	2.113	0.927	0.103	5.476	5.248	36.423	0.047
3614	-8.481	2.056	2.226	2.140	2.170	0.924	0.084	10.919	6.428	24.789	0.038
4864	-8.782	2.048	2.313	2.151	2.244	0.918	0.103	5.864	5.212	34.837	0.045
6064	-9.055	2.049	2.400	2.140	2.339	0.912	0.092	4.423	5.824	33.887	0.038
7264	-9.337	2.046	2.497	2.138	2.435	0.906	0.092	4.837	5.742	35.593	0.037
8464	-9.630	2.046	2.593	2.127	2.539	0.900	0.081	4.573	6.512	29.028	0.031

TIME (secs)	STRAIN (%)	CELL (ksc)	V.STS (ksc)	PORE P (ksc)	V.E.STS (ksc)	VOID RATIO,e	DEL U (ksc)	DEL K (*10 cm/(*10 cm/s)	TOT. K	D (ksc)	Ub/Ov
9913	-9.976	2.042	2.713	2.153	2.640	0.893	0.111	4.609	4.722	35.175	0.041
11713	-10.409	2.046	2.873	2.167	2.792	0.883	0.121	4.012	4.281	39.388	0.042
14713	-11.095	2.032	3.156	2.172	3.062	0.869	0.140	2.799	3.643	47.372	0.044
16513	-11.519	2.031	3.343	2.151	3.263	0.860	0.119	4.469	4.235	50.946	0.036
21313	-12.618	2.031	3.897	2.143	3.823	0.837	0.112	5.158	4.407	45.275	0.029
24061	-13.109	2.031	4.080	2.084	4.045	0.827	0.052	6.682	9.323	47.551	0.013
27661	-13.544	2.032	4.275	2.066	4.252	0.817	0.034	5.160	14.178	50.574	0.008
35761	-13.837	2.033	4.417	2.059	4.400	0.811	0.026	2.970	18.400	4.824	0.006
46561	-14.055	2.036	4.414	2.041	4.411	0.807	0.005	5.590	97.125	85.879	0.001
52861	-14.104	2.039	4.460	2.049	4.453	0.806	0.010	3.640	45.755	91.859	0.002
64561	-14.294	2.041	4.636	2.055	4.627	0.802	0.013	1.568	35.515	ERR	0.003
840	-14.707	2.045	3.962	1.966	4.014	0.793	-0.079	0.752	-5.959	773.364	-0.020
1080	-14.674	2.046	3.708	1.970	3.758	0.794	-0.075	2.021	-6.229	727.232	-0.020
1320	-14.643	2.046	3.475	1.953	3.536	0.794	-0.092	0.140	-5.092	ERR	-0.027
1800	-14.603	2.046	3.067	1.961	3.123	0.795	-0.085	-7.596	-5.549	343.891	-0.028
2040	-14.550	2.047	2.883	1.959	2.942	0.796	-0.088	-2.273	-5.337	318.001	-0.031
2280	-14.507	2.047	2.721	1.920	2.805	0.797	-0.126	7.417	-3.732	411.770	-0.046
2520	-14.462	2.047	2.563	1.965	2.618	0.798	-0.082	12.423	-5.773	376.102	-0.032
2760	-14.426	2.047	2.422	1.954	2.484	0.799	-0.093	8.485	-5.084	262.280	-0.038
3000	-14.369	2.047	2.291	1.980	2.335	0.800	-0.067	5.268	-7.076	223.321	-0.029
3240	-14.321	2.047	2.166	1.955	2.227	0.801	-0.092	13.617	-5.149	277.575	-0.042
3420	-14.299	2.047	2.082	1.922	2.165	0.802	-0.125	1.959	-3.789	292.197	-0.060
3540	-14.273	2.047	2.029	1.956	2.090	0.802	-0.091	10.014	-5.195	187.732	-0.045
3780	-14.215	2.045	1.920	1.954	1.981	0.803	-0.091	15.568	-5.193	203.671	-0.048
4080	-14.158	2.048	1.805	1.959	1.865	0.805	-0.090	8.948	-5.311	164.169	-0.050
4380	-14.102	2.049	1.684	1.915	1.773	0.806	-0.134	2.386	-3.556	181.494	-0.080
4680	-14.033	2.049	1.582	1.948	1.649	0.807	-0.100	14.492	-4.749	181.477	-0.064
5677	-13.873	2.049	1.292	1.952	1.357	0.811	-0.097	3.221	-4.921	167.312	-0.075
7177	-13.673	2.049	0.961	1.956	1.023	0.815	-0.093	2.866	-5.163	96.007	-0.097
8677	-13.425	2.049	0.723	1.956	0.785	0.820	-0.093	4.407	-5.195	64.801	-0.129
10177	-13.147	2.050	0.542	1.956	0.605	0.826	-0.094	5.198	-5.160	50.787	-0.174
11677	-12.871	2.045	0.399	1.947	0.465	0.832	-0.098	2.946	-5.013	38.631	-0.245
13177	-12.584	2.050	0.284	1.946	0.354	0.838	-0.104	4.169	-4.743	14.794	-0.366
14677	-12.281	2.048	0.193	1.874	0.309	0.844	-0.173	0.996	-2.864	55.038	-0.897
14977	-12.181	2.047	0.188	1.949	0.254	0.846	-0.098	7.301	-5.068	-4.208	-0.522
23377	-11.878	2.044	0.268	2.046	0.266	0.853	0.002	*****	295.061	1545.899	0.006
28177	-11.879	2.044	0.279	2.047	0.277	0.853	0.002	8.615	212.553	-199.476	0.008
47077	-11.877	2.059	0.280	2.060	0.280	0.853	0.001	21.126	477.871	-4.453	0.004
47377	-11.870	2.059	0.280	2.060	0.280	0.853	0.001	-67.546	622.004	186.570	0.003
480	-11.883	2.059	0.327	2.092	0.305	0.852	0.034	-10.706	14.929	700.004	0.103
600	-11.888	2.059	0.366	2.104	0.336	0.852	0.045	-9.028	11.111	93.320	0.123
720	-11.912	2.058	0.398	2.117	0.359	0.852	0.059	13.202	8.545	131.472	0.147
1057	-11.954	2.060	0.461	2.129	0.415	0.851	0.069	7.040	7.217	68.546	0.150
1657	-12.071	2.058	0.548	2.138	0.495	0.848	0.079	7.440	6.309	64.268	0.144
2257	-12.184	2.060	0.632	2.157	0.567	0.846	0.097	5.633	5.154	96.981	0.153
2857	-12.262	2.059	0.715	2.166	0.643	0.844	0.107	4.285	4.628	96.218	0.150
3457	-12.360	2.059	0.805	2.159	0.738	0.842	0.100	1.633	4.950	64.739	0.124
4057	-12.480	2.059	0.889	2.169	0.816	0.840	0.110	4.297	4.515	83.584	0.123
4657	-12.583	2.059	0.975	2.169	0.902	0.838	0.110	4.310	4.504	92.616	0.112
5557	-12.722	2.059	1.113	2.183	1.030	0.835	0.124	1.872	3.963	117.731	0.111
6457	-12.876	2.059	1.284	2.168	1.212	0.832	0.109	2.840	4.501	87.605	0.085
7357	-13.057	2.060	1.455	2.187	1.370	0.828	0.127	3.512	3.837	114.643	0.087
8257	-13.240	2.060	1.647	2.161	1.579	0.824	0.102	3.487	4.787	144.982	0.062
9157	-13.394	2.060	1.845	2.124	1.803	0.821	0.064	3.498	7.597	109.507	0.035
10057	-13.579	2.060	2.063	2.147	2.006	0.817	0.086	2.397	5.588	122.789	0.042
10957	-13.761	2.060	2.307	2.178	2.229	0.813	0.117	2.682	4.097	145.322	0.051
11857	-13.956	2.061	2.586	2.172	2.512	0.809	0.111	1.948	4.310	204.227	0.043
12757	-14.168	2.061	2.871	1.949	2.945	0.804	-0.112	-4.570	-4.252	78.530	-0.039

TIME (secs)	STRAIN (%)	CELL (ksc)	V.STS (ksc)	PORE P (ksc)	V.E.STS (ksc)	VOID RATIO,e	DEL U (ksc)	DEL K (*10 cm/(*10 cm/s)	TOT. K (*10 cm/s)	D (ksc)	Ub/Ov
13657	-14.354	2.069	3.165	2.179	3.091	0.800	0.110	3.416	4.299	214.641	0.035
14557	-14.495	2.061	3.482	2.192	3.395	0.797	0.130	1.810	3.620	151.167	0.037
16057	-14.835	2.062	3.997	2.193	3.909	0.790	0.131	2.934	3.573	219.723	0.033
16957	-14.978	2.062	4.301	2.179	4.223	0.787	0.117	2.128	3.991	154.267	0.027
17857	-15.154	2.062	4.588	2.202	4.495	0.784	0.140	2.776	3.331	140.326	0.030
18757	-15.354	2.062	4.875	2.211	4.775	0.779	0.149	3.392	3.099	175.583	0.031
19657	-15.513	2.062	5.155	2.212	5.054	0.776	0.150	2.271	3.067	142.645	0.029
20557	-15.697	2.062	5.412	2.206	5.316	0.772	0.144	1.372	3.187	156.723	0.027
21457	-15.888	2.062	5.679	2.156	5.616	0.768	0.093	4.514	4.888	122.813	0.016
22657	-16.150	2.063	6.026	2.196	5.937	0.763	0.133	3.597	3.401	136.231	0.022
23557	-16.329	2.062	6.307	2.250	6.181	0.759	0.188	1.766	2.402	136.774	0.030
24457	-16.515	2.064	6.541	2.221	6.437	0.755	0.157	1.681	2.870	115.677	0.024
25357	-16.735	2.063	6.808	2.239	6.691	0.750	0.176	3.369	2.537	92.821	0.026
26257	-16.895	2.063	7.074	2.415	6.839	0.747	0.352	1.344	1.267	168.612	0.050
27157	-17.116	2.063	7.330	2.240	7.212	0.742	0.177	3.407	2.501	168.472	0.024
28057	-17.277	2.062	7.606	2.248	7.482	0.739	0.186	1.853	2.376	114.686	0.024
28957	-17.486	2.062	7.866	2.276	7.723	0.735	0.214	1.480	2.054	159.395	0.027
29857	-17.686	2.064	8.171	2.259	8.041	0.730	0.195	2.997	2.242	164.382	0.024
30757	-17.855	2.061	8.449	2.257	8.318	0.727	0.195	1.788	2.229	153.120	0.023
31957	-18.105	2.061	8.834	2.260	8.701	0.722	0.199	1.818	2.174	146.631	0.023
33157	-18.383	2.060	9.246	2.265	9.110	0.716	0.205	2.098	2.102	176.309	0.022
34357	-18.630	2.061	9.661	2.237	9.544	0.711	0.176	2.588	2.430	167.457	0.018
35557	-18.877	2.062	10.112	2.293	9.958	0.705	0.231	1.155	1.839	176.196	0.023
36757	-19.133	2.064	10.578	2.316	10.410	0.700	0.252	0.767	1.675	175.256	0.024
37957	-19.397	2.065	11.051	2.334	10.872	0.694	0.268	0.921	1.563	220.166	0.024
39157	-19.628	2.064	11.545	2.311	11.380	0.690	0.248	1.420	1.684	198.353	0.021
41203	-20.074	2.064	12.428	2.309	12.265	0.680	0.245	1.598	1.681	216.233	0.020
43603	-20.601	2.063	13.559	2.297	13.403	0.669	0.234	1.599	1.742	251.291	0.017
46003	-21.093	2.062	14.755	2.233	14.641	0.659	0.171	1.527	2.352	252.134	0.012
48403	-21.576	2.063	16.047	2.345	15.859	0.649	0.282	1.264	1.407	288.978	0.018
50803	-22.058	2.060	17.437	2.338	17.252	0.639	0.278	1.233	1.410	320.098	0.016
53203	-22.523	2.062	18.933	2.354	18.739	0.629	0.291	1.242	1.330	301.021	0.015
55067	-22.930	2.060	20.168	2.365	19.965	0.620	0.305	1.362	1.259	252.578	0.015
65520	-23.142	2.061	20.521	2.091	20.501	0.616	0.030	0.927	12.839	392.193	0.001
66420	-23.157	2.061	20.586	2.101	20.559	0.615	0.040	0.676	9.601	1334.659	0.002
67320	-23.177	2.061	20.882	2.143	20.828	0.615	0.082	0.445	4.626	639.532	0.004
68220	-23.220	2.061	21.140	2.120	21.101	0.614	0.059	1.310	6.416	256.061	0.003
79920	-23.423	2.060	21.637	2.086	21.620	0.610	0.026	1.318	14.473	212.255	0.001
80820	-23.437	2.060	21.670	2.090	21.650	0.610	0.030	0.863	12.636	358.752	0.001
81720	-23.450	2.059	21.716	2.087	21.697	0.609	0.028	0.853	13.586	-180.865	0.001
82620	-23.459	2.059	21.695	2.082	21.680	0.609	0.022	0.744	16.811	-472.019	0.001
83520	-23.466	2.059	21.670	2.088	21.651	0.609	0.030	0.384	12.776	445.290	0.001
84420	-23.478	2.058	21.720	2.078	21.707	0.609	0.020	1.177	19.324	-29.355	0.001
85320	-23.486	2.058	21.716	2.074	21.705	0.608	0.016	0.804	23.049	-80.945	0.001
87120	-23.499	2.058	21.704	2.073	21.694	0.608	0.015	0.566	24.637	108.213	0.001
90720	-23.519	2.057	21.733	2.082	21.716	0.608	0.025	0.980	15.131	26.142	0.001
91620	-23.526	2.057	21.726	2.070	21.718	0.608	0.013	0.872	28.702	-984.926	0.001
92520	-23.528	2.057	21.700	2.071	21.691	0.608	0.014	0.345	26.620	292.088	0.001
93420	-23.534	2.056	21.718	2.070	21.708	0.607	0.014	0.768	27.043	1.690	0.001
126168	-23.632	2.060	21.714	2.066	21.710	0.605	0.006	2.725	66.465	-33.543	0.000
1	-23.704	2.061	21.691	2.068	21.686	0.604	0.007	*****	53.857	-709.801	0.000
241	-23.716	2.061	21.605	2.068	21.600	0.604	0.006	-37.904	61.036	1837.673	0.000
601	-23.685	2.061	21.001	2.020	21.029	0.604	-0.041	12.960	-9.183	*****	-0.002
661	-23.685	2.061	20.814	2.011	20.848	0.604	-0.050	-0.067	-7.448	*****	-0.002
721	-23.687	2.062	20.628	2.010	20.662	0.604	-0.051	-0.954	-7.340	*****	-0.002
781	-23.697	2.062	20.451	1.965	20.516	0.604	-0.097	-2.724	-3.874	2415.679	-0.005
841	-23.688	2.061	20.267	2.000	20.308	0.604	-0.062	3.773	-6.111	1211.916	-0.003
901	-23.673	2.061	20.086	1.996	20.129	0.605	-0.065	6.143	-5.800	4108.347	-0.003

TIME (secs)	STRAIN (%)	CELL (ksc)	V.STS (ksc)	PORE P (ksc)	V.E.STS (ksc)	VOID RATIO,e	DEL U (ksc)	DEL K (*10 cm/(*10 cm/s)	TOT. K (*10 cm/s)	D (ksc)	Ub/Ov
1081	-23.661	2.058	19.566	1.981	19.617	0.605	-0.077	3.505	-4.892	5980.399	-0.004
1261	-23.652	2.058	19.055	1.979	19.108	0.605	-0.079	-1.698	-4.755	2835.711	-0.004
1502	-23.629	2.061	18.387	1.964	18.452	0.605	-0.097	1.750	-3.901	2105.435	-0.005
1982	-23.571	2.060	17.159	1.947	17.235	0.607	-0.114	2.905	-3.309	*****	-0.007
2342	-23.578	2.061	16.298	1.934	16.383	0.607	-0.127	-2.672	-2.967	4639.265	-0.008
2702	-23.561	2.061	15.479	1.898	15.588	0.607	-0.163	0.027	-2.318	2846.992	-0.011
3062	-23.532	2.061	14.686	1.916	14.783	0.608	-0.145	0.721	-2.601	4913.976	-0.010
3422	-23.517	2.061	13.928	1.903	14.034	0.608	-0.159	1.386	-2.375	2114.374	-0.011
3782	-23.483	2.061	13.211	1.906	13.315	0.609	-0.156	0.818	-2.429	797.753	-0.012
3785	-23.482	2.062	13.204	1.906	13.308	0.609	-0.156	3.092	-2.425	1681.422	-0.012
4085	-23.447	2.061	12.627	1.926	12.717	0.609	-0.135	1.415	-2.806	2553.828	-0.011
5285	-23.367	2.061	10.546	1.882	10.665	0.611	-0.179	0.375	-2.120	1509.304	-0.017
5885	-23.306	2.061	9.640	1.903	9.745	0.612	-0.158	1.423	-2.402	1433.892	-0.016
7085	-23.192	2.062	8.025	1.939	8.107	0.615	-0.123	1.118	-3.098	992.122	-0.015
8285	-23.061	2.062	6.683	1.874	6.809	0.617	-0.189	1.080	-2.023	598.828	-0.028
9185	-22.914	2.062	5.817	1.894	5.929	0.621	-0.168	1.100	-2.280	688.178	-0.029
10385	-22.774	2.063	4.811	1.833	4.964	0.623	-0.230	0.896	-1.677	414.685	-0.048
11585	-22.575	2.063	3.982	1.824	4.142	0.628	-0.239	1.512	-1.618	334.790	-0.060
13345	-22.288	2.063	3.011	1.812	3.179	0.634	-0.251	1.278	-1.553	224.390	-0.083
15145	-21.942	2.064	2.242	1.822	2.403	0.641	-0.242	1.013	-1.627	162.375	-0.108
16345	-21.690	2.063	1.819	1.801	1.993	0.646	-0.262	1.212	-1.511	116.901	-0.144
18745	-21.172	2.065	1.220	1.812	1.388	0.657	-0.253	1.164	-1.588	101.307	-0.207
19589	-21.010	2.065	1.057	1.814	1.224	0.661	-0.251	1.800	-1.605	126.344	-0.238
19634	-20.994	2.066	1.048	1.832	1.204	0.661	-0.234	-0.961	-1.723	114.496	-0.223
19964	-20.950	2.065	0.985	1.813	1.153	0.662	-0.252	-2.066	-1.598	64.987	-0.256
20294	-20.879	2.066	0.947	1.826	1.107	0.663	-0.240	11.160	-1.685	95.633	-0.253
21239	-20.748	2.066	0.817	1.820	0.982	0.666	-0.246	1.426	-1.646	66.463	-0.301
23714	-20.272	2.067	0.512	1.836	0.666	0.676	-0.231	5.709	-1.777	69.679	-0.451
24344	-20.166	2.065	0.446	1.846	0.592	0.678	-0.219	-4.344	-1.881	33.126	-0.491
25274	-19.981	2.068	0.378	1.839	0.530	0.682	-0.228	-3.957	-1.810	31.825	-0.604
25799	-19.851	2.068	0.336	1.839	0.489	0.685	-0.229	2.233	-1.810	31.265	-0.681
0	-19.616	2.068	0.266	1.843	0.416	0.690	-0.224	*****	-1.858	26.081	-0.844
120	-19.592	2.069	0.260	1.845	0.409	0.690	-0.224	1.984	-1.867	32.097	-0.859
240	-19.569	2.069	0.253	1.846	0.402	0.691	-0.223	3.958	-1.871	73.719	-0.882
276.2	-19.544	2.069	0.248	1.864	0.384	0.691	-0.204	5.928	-2.044	1.964	-0.826

 CONSOLIDATION AT CONSTANT RATE OF STRAIN
 MIT GEOTECHNICAL LAB

File Name: CRS02.PRN

1. Test Name: CRS 02
 2. Date: 1/17/89
 3. Initial Height of Sample (cm): 2.354
 4. Initial Water Content of Sample (%): 39.55
 5. Area of Sample (sq cm): 31.62
 6. DCDT
 Zero: 0.37518
 CF: -1.8526 cm/V/V
 7. Cell Pressure
 Zero: -0.00006
 CF: 705.735 ksc/V/V
 8. Vertical Load Cell
 Zero: 0.00005
 CF: 27013.98 kg/V/V
 9. Pore Pressure
 Zero: -0.0010
 CF: 965.359 ksc/V/V

TIME (secs)	STRAIN (%)	CELL (ksc)	V.STS (ksc)	PORE P (ksc)	V.E.STS (ksc)	VOID RATIO,e	DEL U (ksc)	DEL K (*10 cm/(*10 cm/s)	TOT. K	D (ksc)	Ub/Ov
900	-0.032	2.009	0.098	2.053	0.069	1.101	0.043	2.309	14.083	-9.817	0.442
960	0.026	2.009	0.105	2.055	0.075	1.102	0.045	-59.836	13.492	11.168	0.431
1117	-0.053	2.009	0.118	2.061	0.083	1.100	0.051	-0.431	11.848	39.104	0.436
1357	-0.090	2.008	0.130	2.057	0.098	1.100	0.048	-11.121	12.537	11.153	0.373
1597	-0.187	2.008	0.143	2.061	0.108	1.098	0.052	31.168	11.561	122.533	0.366
1837	-0.204	2.008	0.163	2.058	0.130	1.097	0.050	-4.820	12.247	23.739	0.303
2077	-0.237	2.007	0.179	2.068	0.138	1.096	0.061	-13.186	9.961	23.723	0.340
3060	-0.484	2.007	0.234	2.063	0.197	1.091	0.056	7.374	10.807	18.384	0.238
3660	-0.661	2.006	0.273	2.072	0.229	1.088	0.066	3.237	9.133	47.453	0.241
4260	-0.778	2.006	0.322	2.063	0.285	1.085	0.056	15.536	10.690	40.964	0.174
4860	-0.887	2.006	0.369	2.065	0.330	1.083	0.059	11.595	10.180	47.987	0.159
6360	-1.242	2.003	0.502	2.005	0.500	1.075	0.002	273.608	271.353	45.152	0.004
8160	-1.531	2.002	0.662	2.049	0.631	1.069	0.046	5.594	12.765	1.972	0.070
9360	-1.682	2.002	0.664	2.047	0.634	1.066	0.045	8.515	13.062	406.059	0.068
10560	-1.690	2.007	0.686	2.034	0.668	1.066	0.027	0.911	21.743	23.111	0.039
12360	-1.756	2.001	0.700	2.027	0.683	1.065	0.026	0.127	22.615	11.066	0.037
13560	-1.825	2.000	0.709	2.027	0.691	1.063	0.027	1.853	21.565	11.791	0.038
14760	-1.860	2.001	0.713	2.027	0.695	1.062	0.027	10.567	21.979	111.139	0.037
15960	-1.895	2.002	0.774	2.061	0.734	1.062	0.059	2.710	9.856	65.016	0.077
17760	-2.025	2.000	0.853	2.051	0.819	1.059	0.051	6.550	11.405	73.122	0.060
18960	-2.162	2.001	0.956	2.057	0.918	1.056	0.056	1.481	10.442	28.179	0.058
20160	-2.465	2.001	1.034	2.047	1.004	1.050	0.046	18.289	12.594	36.156	0.044
21360	-2.657	2.000	1.125	2.077	1.073	1.046	0.077	4.557	7.484	20.180	0.069
22560	-2.972	2.001	1.183	2.071	1.137	1.039	0.070	8.462	8.238	39.703	0.059
23760	-3.126	2.000	1.242	2.066	1.198	1.036	0.066	4.602	8.631	11.536	0.053
24960	-3.465	2.000	1.287	2.075	1.237	1.029	0.075	12.124	7.601	19.743	0.058
26160	-3.746	2.001	1.336	2.065	1.293	1.023	0.065	9.854	8.724	21.466	0.048
27360	-3.959	1.999	1.385	2.069	1.338	1.018	0.070	4.941	8.062	23.376	0.050
28560	-4.289	2.001	1.431	2.024	1.416	1.011	0.023	32.618	24.130	13.655	0.016
30360	-4.609	2.002	1.502	2.066	1.459	1.005	0.064	8.005	8.712	30.678	0.042
30960	-4.785	2.000	1.526	2.020	1.513	1.001	0.019	38.045	28.605	3.008	0.013
32160	-5.102	2.001	1.579	2.085	1.523	0.994	0.084	6.262	6.535	21.007	0.053
33360	-5.317	2.001	1.625	2.086	1.568	0.990	0.086	2.557	6.362	12.041	0.053
34560	-5.701	2.002	1.679	2.100	1.614	0.982	0.098	10.061	5.523	28.262	0.058
35760	-5.924	2.001	1.738	2.093	1.677	0.977	0.092	7.064	5.841	19.298	0.053
37560	-6.363	2.001	1.821	2.090	1.762	0.968	0.089	7.258	6.000	18.634	0.049

TIME (secs)	STRAIN (%)	CELL (ksc)	V.STS (ksc)	PORE P (ksc)	V.E.STS (ksc)	VOID RATIO,e	DEL U (ksc)	DEL K (*10 cm/(*10 cm/s)	TOT. K (*10 cm/s)	D (ksc)	Ub/Ov
38760	-6.662	1.991	1.882	2.088	1.817	0.961	0.096	4.243	5.498	27.694	0.051
39960	-6.950	2.001	1.948	2.077	1.897	0.955	0.076	7.676	6.978	24.312	0.039
41760	-7.397	2.001	2.046	2.062	2.006	0.946	0.061	16.019	8.628	20.253	0.030
42960	-7.787	2.002	2.148	2.096	2.085	0.938	0.094	11.608	5.504	28.635	0.044
45360	-8.253	2.003	2.281	2.097	2.218	0.928	0.094	6.294	5.471	34.092	0.041
46560	-8.486	2.004	2.366	2.106	2.298	0.923	0.102	5.038	4.980	31.897	0.043
48960	-9.036	2.002	2.549	2.115	2.473	0.912	0.113	4.065	4.441	38.920	0.044
50160	-9.328	2.004	2.642	2.086	2.587	0.905	0.083	3.927	6.043	22.600	0.031
51360	-9.652	2.004	2.743	2.128	2.660	0.899	0.124	4.262	4.011	44.640	0.045
52560	-9.910	2.006	2.843	2.107	2.775	0.893	0.101	4.431	4.899	38.703	0.035
53760	-10.183	2.005	2.955	2.116	2.881	0.887	0.111	3.924	4.405	50.501	0.038
54960	-10.412	2.015	3.054	2.101	2.997	0.883	0.086	2.698	5.653	46.583	0.028
56160	-10.741	2.007	3.188	2.065	3.150	0.876	0.058	10.081	8.376	27.575	0.018
57360	-11.023	2.009	3.308	2.130	3.228	0.870	0.121	5.584	3.979	50.097	0.037
59760	-11.533	2.006	3.574	2.143	3.483	0.859	0.136	2.918	3.500	52.681	0.038
62760	-12.209	2.010	3.932	2.150	3.839	0.845	0.139	3.199	3.365	60.619	0.035
63960	-12.495	2.011	4.090	2.127	4.013	0.839	0.116	5.741	4.012	41.015	0.028
72960	-12.773	2.017	4.150	2.052	4.127	0.833	0.035	1.286	13.083	-4.951	0.009
84360	-12.913	2.023	4.137	2.049	4.120	0.830	0.026	2.856	17.627	50.016	0.006
88861	-12.937	2.024	4.149	2.049	4.132	0.830	0.025	2.263	18.107	-82.000	0.006
0	-12.938	2.024	4.156	2.061	4.131	0.830	0.037	*****	12.392	-800.735	0.009
900	-12.941	2.024	4.127	2.048	4.111	0.830	0.024	0.238	19.234	198.770	0.006
2700	-12.949	2.025	4.144	2.050	4.127	0.829	0.025	-0.034	18.442	-0.119	0.006
5400	-12.959	2.025	4.144	2.050	4.127	0.829	0.025	-0.177	18.630	-67.041	0.006
7200	-12.961	2.026	4.141	2.049	4.125	0.829	0.024	-0.488	19.494	3.023	0.006
9000	-12.979	2.026	4.142	2.050	4.126	0.829	0.023	0.507	19.622	-4.202	0.006
10800	-12.981	2.027	4.142	2.051	4.126	0.829	0.024	0.774	19.116	58.301	0.006
12600	-12.988	2.028	4.146	2.052	4.130	0.829	0.024	0.321	19.391	8.564	0.006
14256	-13.289	2.029	4.171	2.052	4.155	0.822	0.023	35.561	19.963	3200.559	0.005
900	-13.266	2.029	3.453	2.050	3.440	0.823	0.020	*****	22.374	909.521	0.006
1380	-13.219	2.030	2.988	1.995	3.011	0.824	-0.034	55.333	-13.399	311.998	-0.011
1620	-13.161	2.030	2.799	1.982	2.831	0.825	-0.048	88.523	-9.636	-704.422	-0.017
1920	-13.194	2.030	2.576	1.990	2.603	0.824	-0.040	27.028	-11.506	438.415	-0.015
2881	-13.069	2.032	2.029	1.988	2.058	0.827	-0.044	2.203	-10.496	177.576	-0.022
3481	-12.926	2.031	1.768	1.979	1.803	0.830	-0.052	7.317	-8.862	114.691	-0.029
4081	-12.735	2.031	1.547	1.976	1.584	0.834	-0.055	12.209	-8.368	476.452	-0.036
4681	-12.695	2.032	1.358	1.973	1.397	0.835	-0.058	-2.596	-7.977	163.271	-0.043
5281	-12.597	2.030	1.201	1.977	1.237	0.837	-0.054	-0.477	-8.640	52.208	-0.045
5881	-12.434	2.032	1.063	1.900	1.151	0.840	-0.132	7.044	-3.540	210.766	-0.124
6481	-12.353	2.032	0.955	1.994	0.980	0.842	-0.038	5.591	-12.232	105.886	-0.040
7081	-12.256	2.033	0.850	1.990	0.878	0.844	-0.042	23.841	-11.051	-549.992	-0.050
7681	-12.271	2.035	0.756	1.976	0.796	0.844	-0.059	-0.376	-7.949	41.466	-0.078
8581	-12.107	2.033	0.719	2.021	0.727	0.847	-0.013	36.142	-37.030	32.149	-0.018
9481	-12.028	2.033	0.699	2.028	0.702	0.849	-0.005	-4.996	-100.488	-116.950	-0.007
10381	-12.047	2.033	0.680	2.034	0.679	0.848	0.001	*****	423.300	252.470	0.002
11281	-12.038	2.033	0.656	2.036	0.655	0.849	0.002	-53.133	209.475	38.511	0.003
12181	-11.931	2.027	0.636	2.060	0.614	0.851	0.033	-15.724	14.148	14.439	0.052
14881	-11.879	2.034	0.629	2.069	0.606	0.852	0.035	-12.831	13.579	-634.925	0.055
16681	-11.882	2.034	0.598	2.051	0.586	0.852	0.017	-5.672	27.718	52.684	0.029
18481	-11.711	2.035	0.480	2.010	0.496	0.855	-0.025	41.221	-19.082	49.102	-0.052
20281	-11.430	2.035	0.319	1.975	0.358	0.861	-0.060	11.708	-8.001	-91.532	-0.187
22081	-11.327	2.036	0.506	2.115	0.453	0.863	0.079	-3.028	6.066	86.837	0.156
23881	-11.528	2.035	0.658	2.081	0.627	0.859	0.046	10.056	10.353	*****	0.070
29281	-11.527	2.034	0.679	2.065	0.658	0.859	0.031	-8.056	15.543	465.255	0.045
31081	-11.540	2.034	0.735	2.057	0.720	0.859	0.023	-13.040	20.614	126.944	0.031
32881	-11.686	2.035	0.943	2.092	0.905	0.856	0.057	1.934	8.321	155.856	0.061

TIME (secs)	STRAIN (%)	CELL (ksc)	V.STS (ksc)	PORE P (ksc)	V.E.STS (ksc)	VOID RATIO,e	DEL U (ksc)	DEL K (*10 cm/(*10 cm/s)	TOT. K (*10 cm/s)	D (ksc)	Ub/Ov
34681	-11.919	2.035	1.330	2.127	1.268	0.851	0.092	3.309	5.139	185.369	0.069
35881	-12.082	2.035	1.642	2.143	1.570	0.848	0.108	3.931	4.348	96.056	0.066
37081	-12.431	2.036	1.967	2.130	1.905	0.840	0.094	12.833	4.966	208.634	0.048
38281	-12.602	2.035	2.320	2.120	2.263	0.837	0.085	-3.152	5.491	202.095	0.037
39481	-12.806	2.033	2.741	2.132	2.674	0.832	0.099	-1.337	4.655	199.372	0.036
40681	-13.039	2.035	3.168	2.077	3.140	0.827	0.042	2.435	10.916	100.256	0.013
42181	-13.480	2.034	3.662	2.155	3.581	0.818	0.121	5.719	3.767	258.869	0.033
43681	-13.666	2.034	4.148	2.160	4.064	0.814	0.126	2.387	3.607	120.350	0.030
45181	-13.996	2.035	4.559	2.181	4.461	0.807	0.147	3.455	3.073	119.244	0.032
46681	-14.320	2.034	4.945	2.180	4.848	0.801	0.146	-0.082	3.058	140.660	0.030
48181	-14.585	2.026	5.306	2.155	5.220	0.795	0.129	-1.668	3.441	91.570	-0.024
49681	-14.954	2.041	5.664	2.200	5.558	0.787	0.159	1.924	2.777	123.647	0.028
51181	-15.251	2.035	6.022	2.181	5.924	0.781	0.146	0.264	2.992	87.970	0.024
52681	-15.632	2.035	6.375	2.208	6.260	0.773	0.173	2.795	2.500	115.738	0.027
54181	-15.989	2.034	6.766	2.173	6.674	0.765	0.138	4.384	3.105	147.297	0.020
55681	-16.256	2.034	7.163	2.179	7.066	0.760	0.145	5.171	2.946	*****	0.020
55981	-16.254	2.034	7.235	2.211	7.117	0.760	0.177	-0.079	2.413	93.572	0.024
57181	-16.594	2.041	7.573	2.246	7.436	0.753	0.205	4.283	2.061	159.138	0.027
58381	-16.814	2.035	7.911	2.225	7.785	0.748	0.189	3.783	2.224	103.959	0.024
59581	-17.158	2.034	8.265	2.218	8.143	0.741	0.184	5.062	2.269	275.621	0.022
60781	-17.287	2.034	8.629	2.230	8.499	0.738	0.196	-0.248	2.125	153.135	0.023
61981	-17.532	2.033	9.009	2.235	8.874	0.733	0.202	-0.621	2.053	156.887	0.022
63181	-17.785	2.034	9.408	2.239	9.271	0.728	0.205	1.812	2.007	109.530	0.022
64381	-18.168	2.032	9.827	2.235	9.691	0.720	0.204	5.609	2.003	162.669	0.021
65581	-18.421	2.034	10.245	2.249	10.102	0.714	0.214	2.274	1.891	197.440	0.021
66781	-18.657	2.032	10.729	2.273	10.568	0.709	0.241	0.908	1.673	179.833	0.022
67981	-18.925	2.031	11.208	2.270	11.049	0.704	0.239	3.219	1.676	440.556	0.021
69181	-19.034	2.031	11.701	2.288	11.530	0.701	0.258	1.265	1.550	262.867	0.022
70381	-19.273	2.031	12.203	2.096	12.160	0.696	0.065	-4.158	6.104	108.221	0.005
71581	-19.657	2.030	12.740	2.276	12.575	0.688	0.246	4.421	1.595	356.801	0.019
72781	-19.806	2.030	13.280	2.292	13.106	0.685	0.262	0.370	1.496	157.953	0.020
73981	-20.160	2.030	13.841	2.294	13.665	0.678	0.264	2.290	1.469	238.717	0.019
75181	-20.405	2.030	14.434	2.309	14.249	0.673	0.278	3.322	1.386	278.289	0.019
76381	-20.621	2.031	15.041	2.316	14.851	0.668	0.285	0.861	1.345	270.172	0.019
77581	-20.871	2.030	15.703	2.295	15.526	0.663	0.265	2.705	1.438	467.446	0.017
78781	-21.011	2.030	16.360	2.295	16.183	0.660	0.266	-0.957	1.430	200.830	0.016
79981	-21.242	2.029	17.048	2.633	16.645	0.655	0.603	-0.548	0.626	272.539	0.035
81181	-21.575	2.030	17.756	2.333	17.554	0.648	0.304	2.146	1.234	338.952	0.017
84815.	-22.263	2.030	20.086	2.330	19.886	0.634	0.300	-11.242	1.226	61.431	0.015
85081	-22.372	2.029	20.140	2.309	19.953	0.631	0.280	2.446	1.311	2777.308	0.014
90391	-22.387	2.031	20.442	2.114	20.386	0.631	0.083	0.569	4.427	37.531	0.004
101191	-22.517	2.031	20.461	2.070	20.435	0.628	0.039	0.724	9.485	7.741	0.002
147391	-22.650	2.031	20.461	2.055	20.445	0.625	0.024	0.185	15.043	*****	0.001
150391	-22.656	2.030	20.387	2.054	20.371	0.625	0.023	0.113	15.537	-743.902	0.001
150991	-22.658	2.030	20.375	2.054	20.359	0.625	0.024	0.193	15.463	-114.921	0.001
0	-22.869	2.025	20.130	2.045	20.117	0.621	0.020	*****	18.240	-162.615	0.001
120	-22.897	2.026	20.046	1.988	20.071	0.620	-0.038	-20.600	-9.567	2037.226	-0.002
240	-22.879	2.025	19.683	2.000	19.699	0.621	-0.025	-24.972	-14.773	*****	-0.001
360	-22.893	2.026	19.326	1.981	19.356	0.620	-0.045	-4.316	-8.110	*****	-0.002
480	-22.901	2.026	18.985	1.979	19.017	0.620	-0.048	-49.477	-7.551	827.166	-0.003
720	-22.820	2.021	18.311	1.967	18.348	0.622	-0.055	-15.917	-6.605	*****	-0.003
840	-22.836	2.025	17.981	1.955	18.028	0.622	-0.070	-11.341	-5.150	1899.075	-0.004
1020	-22.811	2.021	17.508	1.950	17.555	0.622	-0.071	27.330	-5.087	*****	-0.004
1224	-22.860	2.022	16.962	1.934	17.021	0.621	-0.088	-14.525	-4.122	1013.068	-0.005
1584	-22.771	2.026	16.067	1.940	16.124	0.623	-0.086	11.813	-4.238	-375.134	-0.005
1704	-22.844	2.026	15.776	1.914	15.850	0.621	-0.112	-8.925	-3.229	916.024	-0.007

TIME (secs)	STRAIN (%)	CELL (ksc)	V.STS (ksc)	PORE P (ksc)	V.E.STS (ksc)	VOID RATIO,e	DEL U (ksc)	DEL K (*10 cm/	TOT. K (*10 cm/s)	D (ksc)	Ub/Ov
1944	-22.783	2.026	15.213	1.910	15.290	0.623	-0.116	11.023	-3.124	-803.369	-0.008
2184	-22.859	2.031	14.660	2.004	14.677	0.621	-0.026	-50.993	-13.714	*****	-0.002
2424	-22.855	2.026	14.142	1.894	14.230	0.621	-0.132	-4.738	-2.753	528.532	-0.009
2664	-22.760	2.027	13.634	1.888	13.727	0.623	-0.139	-4.214	-2.610	638.351	-0.010
2904	-22.687	2.029	13.156	1.869	13.263	0.625	-0.160	5.813	-2.274	*****	-0.012
3144	-22.727	2.026	12.672	1.878	12.770	0.624	-0.148	-5.635	-2.464	594.343	-0.012
3504	-22.614	2.026	11.997	1.870	12.102	0.626	-0.156	2.125	-2.331	*****	-0.013
3864	-22.645	2.026	11.350	1.877	11.449	0.626	-0.149	6.730	-2.448	*****	-0.013
4224	-22.701	2.026	10.746	1.889	10.837	0.624	-0.137	-8.862	-2.663	267.693	-0.013
4464	-22.566	2.021	10.374	1.866	10.477	0.627	-0.155	7.830	-2.354	-275.311	-0.015
4585	-22.638	2.026	10.197	1.900	10.280	0.626	-0.125	-7.828	-2.906	846.212	-0.012
5485	-22.477	2.026	8.828	1.886	8.922	0.629	-0.141	2.228	-2.601	1204.759	-0.016
6385	-22.384	2.025	7.726	1.922	7.794	0.631	-0.102	5.303	-3.594	8394.309	-0.013
6685	-22.380	2.026	7.380	1.878	7.478	0.631	-0.147	0.142	-2.489	698.898	-0.020
7585	-22.245	2.026	6.433	1.873	6.535	0.634	-0.153	5.806	-2.409	923.031	-0.024
8485	-22.154	2.033	5.601	1.883	5.701	0.636	-0.150	1.087	-2.465	842.624	-0.027
9385	-22.074	2.032	4.873	1.813	5.019	0.638	-0.219	2.854	-1.686	408.146	-0.045
10285	-21.911	2.027	4.233	1.845	4.354	0.641	-0.181	3.618	-2.046	688.132	-0.043
11185	-21.830	2.026	3.669	1.835	3.796	0.643	-0.190	0.988	-1.953	256.258	-0.052
12085	-21.637	2.026	3.175	1.835	3.302	0.647	-0.191	2.722	-1.957	*****	-0.060
12985	-21.646	2.026	2.737	1.811	2.880	0.647	-0.215	0.072	-1.739	172.309	-0.079
13885	-21.434	2.026	2.370	1.810	2.514	0.651	-0.216	-0.155	-1.742	193.452	-0.091
14785	-21.265	2.026	2.041	1.805	2.188	0.655	-0.220	-0.019	-1.712	149.651	-0.108
15685	-21.090	2.023	1.771	1.791	1.926	0.658	-0.233	2.801	-1.627	214.855	-0.132
16585	-20.966	2.026	1.521	1.817	1.660	0.661	-0.209	0.439	-1.823	84.155	-0.137
17485	-20.702	2.023	1.315	1.840	1.438	0.666	-0.184	0.840	-2.086	84.351	-0.140
18385	-20.504	2.026	1.136	1.823	1.271	0.671	-0.203	5.014	-1.896	96.850	-0.179
19285	-20.332	2.025	1.000	1.869	1.104	0.674	-0.156	2.447	-2.476	93.696	-0.156
20185	-20.199	2.019	0.875	1.862	0.980	0.677	-0.157	-0.037	-2.473	54.048	-0.179
21085	-20.014	2.026	0.751	1.833	0.880	0.681	-0.193	3.799	-2.018	82.570	-0.257
22285	-19.891	2.025	0.709	1.923	0.778	0.683	-0.102	-2.999	-3.814	41.634	-0.144
23185	-19.814	2.030	0.695	1.955	0.746	0.685	-0.076	-2.390	-5.175	23.125	-0.109
24085	-19.660	2.025	0.677	1.975	0.710	0.688	-0.050	7.338	-7.892	1002.462	-0.074
25285	-19.657	2.025	0.658	1.989	0.682	0.688	-0.036	1.554	-10.903	35.803	-0.055
26785	-19.548	2.025	0.616	1.984	0.643	0.691	-0.041	9.080	-9.640	68.633	-0.066
27985	-19.525	2.018	0.625	2.014	0.627	0.691	-0.004	89.519	-92.880	18.058	-0.007
30385	-19.402	2.024	0.602	2.019	0.605	0.694	-0.005	139.313	-77.452	98.358	-0.008
32786	-19.285	2.025	0.443	1.954	0.490	0.696	-0.071	4.817	-5.593	34.877	-0.160
35186	-18.914	2.024	0.255	1.865	0.361	0.704	-0.160	0.626	-2.509	19.174	-0.626
36425	-18.594	2.023	0.190	1.859	0.300	0.711	-0.164	36.417	-2.453	1.611	-0.866

 CONSOLIDATION AT CONSTANT RATE OF STRAIN
 MIT GEOTECHNICAL LAB

File Name: CRS03.PRN

 1. Test Name: CRS 03
 2. Date: 2/12/89
 3. Initial Height of Sample (cm): 2.339
 4. Initial Water Content of Sample (%): 41.02
 5. Area of Sample (sq cm): 31.64
 6. DCDT
 Zero: 0.21181
 CF: -1.8526 cm/V/V
 7. Cell Pressure
 Zero: -0.00004
 CF: 705.735 ksc/V/V
 8. Vertical Load Cell
 Zero: 0.00006
 CF: 27013.98 kg/V/V
 9. Pore Pressure
 Zero: -0.0010
 CF: 965.359 ksc/V/V

TIME (secs)	STRAIN (%)	CELL (ksc)	V.STS (ksc)	PORE P (ksc)	V.E.STS (ksc)	VOID RATIO,e	DEL U (ksc)	DEL K (*10 cm/(*10 cm/s)	TOT. K	D (ksc)	Ub/Ov
39480	0.000	2.055	0.148	2.119	0.105	1.145	0.064	12.121	9.614	69.451	0.435
40080	-0.039	2.055	0.169	2.111	0.132	1.142	0.056	11.705	11.057	30.555	0.330
40680	-0.145	2.056	0.198	2.106	0.164	1.139	0.050	9.424	12.307	23.031	0.253
41280	-0.276	2.055	0.223	2.097	0.195	1.136	0.042	13.697	14.512	12.759	0.190
41880	-0.403	2.059	0.254	2.124	0.211	1.134	0.064	8.636	9.496	45.672	0.254
42480	-0.502	2.055	0.290	2.106	0.256	1.132	0.051	8.571	11.965	40.758	0.176
43080	-0.606	2.062	0.326	2.104	0.298	1.129	0.042	10.865	14.560	12.972	0.128
43680	-0.766	2.055	0.364	2.121	0.319	1.126	0.066	10.556	9.154	38.120	0.183
44280	-0.890	2.055	0.404	2.112	0.366	1.123	0.057	9.478	10.704	16.742	0.140
44880	-1.016	2.055	0.439	2.132	0.387	1.121	0.077	7.133	7.818	63.389	0.176
45480	-1.132	2.054	0.489	2.096	0.461	1.118	0.042	12.000	14.410	14.012	0.086
47280	-1.503	2.055	0.616	2.211	0.513	1.110	0.155	3.325	3.850	73.664	0.252
47880	-1.620	2.055	0.640	2.117	0.599	1.108	0.061	8.198	9.737	76.760	0.096
48480	-1.643	2.054	0.650	2.104	0.617	1.107	0.050	2.028	12.004	30.731	0.076
49080	-1.684	2.055	0.653	2.089	0.629	1.106	0.035	5.052	17.240	-0.050	0.053
49680	-1.736	2.048	0.659	2.093	0.629	1.105	0.045	4.951	13.271	61.466	0.068
50880	-1.776	2.062	0.668	2.083	0.654	1.104	0.021	2.708	27.913	-58.294	0.032
51480	-1.784	2.056	0.670	2.086	0.650	1.104	0.030	1.107	19.644	28.924	0.045
52080	-1.799	2.055	0.672	2.082	0.654	1.104	0.027	2.381	22.024	-12.398	0.040
52680	-1.838	2.055	0.676	2.094	0.649	1.103	0.040	4.208	14.981	85.745	0.059
53280	-1.859	2.054	0.683	2.079	0.667	1.103	0.025	3.634	24.181	17.765	0.036
53880	-1.909	2.055	0.690	2.075	0.676	1.101	0.021	10.415	28.921	6.392	0.030
54480	-1.890	2.054	0.692	2.081	0.675	1.102	0.026	-3.017	22.475	34.124	0.038
55680	-1.951	2.055	0.708	2.074	0.695	1.101	0.019	3.208	30.720	26.225	0.027
56280	-2.010	2.057	0.752	2.118	0.711	1.099	0.061	4.160	9.669	100.844	0.081
56880	-2.052	2.055	0.779	2.093	0.753	1.098	0.038	4.654	15.511	24.535	0.049
57480	-2.099	2.056	0.787	2.090	0.765	1.097	0.034	5.962	17.570	34.210	0.043
58680	-2.205	2.056	0.841	2.116	0.801	1.095	0.060	2.747	9.899	50.723	0.071
59280	-2.297	2.057	0.877	2.100	0.847	1.093	0.044	8.792	13.396	42.092	0.050
59880	-2.406	2.056	0.924	2.102	0.893	1.091	0.045	10.219	12.963	26.859	0.049
60480	-2.515	2.057	0.960	2.113	0.923	1.089	0.056	8.197	10.466	26.804	0.058
61080	-2.653	2.061	0.994	2.113	0.960	1.086	0.052	11.115	11.236	26.969	0.052
61680	-2.805	2.056	1.036	2.109	1.001	1.082	0.052	12.211	11.110	17.722	0.051
62280	-2.944	2.057	1.072	2.127	1.025	1.079	0.070	8.336	8.336	34.846	0.065
62880	-3.060	2.057	1.104	2.114	1.066	1.077	0.057	8.438	10.132	29.582	0.052
63480	-3.172	2.051	1.137	2.109	1.099	1.074	0.058	8.082	10.010	16.995	0.051

TIME (secs)	STRAIN (%)	CELL (ksc)	V.STS (ksc)	PORE P (ksc)	V.E.STS (ksc)	VOID RATIO,e	DEL U (ksc)	DEL K (*10 cm/(*10 cm/s)	TOT. K (*10 cm/s)	D (ksc)	Ub/Ov
64080	-3.339	2.059	1.164	2.113	1.127	1.071	0.054	12.683	10.583	42.477	0.047
64680	-3.476	2.068	1.211	2.106	1.185	1.068	0.038	14.945	15.193	11.777	0.031
66480	-3.845	2.057	1.271	2.121	1.229	1.060	0.063	7.788	9.008	20.260	0.050
68280	-4.246	2.059	1.349	2.117	1.310	1.051	0.059	7.958	9.669	17.478	0.043
69480	-4.482	2.059	1.397	2.128	1.351	1.046	0.069	7.195	8.159	19.278	0.049
70680	-4.775	2.059	1.456	2.131	1.408	1.040	0.072	7.153	7.745	18.825	0.050
71880	-5.094	2.059	1.510	2.122	1.468	1.033	0.063	10.243	8.790	16.803	0.042
73080	-5.388	2.060	1.568	2.135	1.517	1.027	0.076	8.315	7.302	18.310	0.048
74280	-5.642	2.061	1.614	2.136	1.564	1.022	0.075	7.281	7.320	27.389	0.047
75480	-5.959	2.066	1.685	2.117	1.651	1.015	0.051	11.052	10.736	20.301	0.030
77280	-6.392	2.062	1.781	2.125	1.738	1.005	0.064	10.193	8.482	22.381	0.036
78480	-6.652	2.062	1.851	2.143	1.797	1.000	0.081	5.750	6.619	19.940	0.044
79680	-6.954	2.062	1.908	2.139	1.857	0.993	0.077	8.601	6.947	29.291	0.040
83280	-7.797	2.071	2.139	2.123	2.104	0.975	0.052	9.572	10.005	18.742	0.025
84480	-8.129	2.063	2.215	2.137	2.166	0.968	0.074	6.829	7.043	30.992	0.033
85680	-8.404	2.065	2.298	2.135	2.251	0.962	0.070	6.958	7.381	18.279	0.031
86280	-8.556	2.054	2.342	2.148	2.279	0.959	0.094	5.989	5.482	33.143	0.040
87480	-8.839	2.065	2.435	2.158	2.373	0.953	0.093	6.163	5.527	36.409	0.038
88680	-9.140	2.064	2.526	2.130	2.483	0.947	0.066	8.327	7.743	33.122	0.026
90480	-9.577	2.066	2.681	2.146	2.627	0.937	0.080	7.428	6.292	38.478	0.030
91680	-9.834	2.066	2.785	2.154	2.726	0.932	0.088	5.291	5.684	32.776	0.032
92880	-10.162	2.065	2.891	2.152	2.834	0.925	0.086	6.968	5.773	39.441	0.030
94080	-10.409	2.066	3.024	2.204	2.931	0.919	0.139	3.801	3.572	47.687	0.046
95280	-10.705	2.066	3.126	2.146	3.072	0.913	0.081	5.772	6.094	39.659	0.026
96480	-10.988	2.066	3.243	2.154	3.184	0.907	0.088	6.150	5.576	37.459	0.027
97080	-11.134	2.067	3.298	2.155	3.239	0.904	0.088	5.798	5.512	56.873	0.027
98280	-11.387	2.066	3.428	2.134	3.383	0.898	0.068	7.056	7.160	40.329	0.020
99480	-11.693	2.067	3.568	2.159	3.507	0.892	0.092	6.511	5.231	52.016	0.026
100680	-11.972	2.066	3.711	2.155	3.652	0.886	0.089	4.552	5.383	52.347	0.024
101880	-12.223	2.068	3.854	2.175	3.783	0.881	0.107	3.263	4.446	55.932	0.028
103080	-12.505	2.067	4.005	2.163	3.941	0.874	0.096	3.925	4.921	76.677	0.024
104280	-12.754	2.067	4.158	2.108	4.131	0.869	0.040	11.958	11.692	48.891	0.010
106080	-13.183	2.067	4.408	2.167	4.341	0.860	0.101	5.437	4.626	62.063	0.023
107280	-13.471	2.068	4.582	2.160	4.520	0.854	0.092	6.276	5.022	74.480	0.020
108480	-13.699	2.068	4.749	2.156	4.690	0.849	0.089	5.449	5.187	47.835	0.019
109680	-14.004	2.068	4.934	2.214	4.836	0.842	0.147	2.893	3.112	93.041	0.030
110880	-14.269	2.070	5.150	2.171	5.083	0.837	0.101	5.680	4.501	86.245	0.020
112080	-14.496	2.068	5.346	2.170	5.278	0.832	0.102	4.651	4.415	80.146	0.019
113280	-14.750	2.067	5.551	2.172	5.482	0.826	0.104	2.581	4.308	86.837	0.019
114480	-15.009	2.069	5.786	2.189	5.706	0.821	0.120	1.868	3.705	92.579	0.021
115680	-15.277	2.068	6.017	2.162	5.954	0.815	0.094	4.763	4.690	79.820	0.016
116880	-15.584	2.068	6.272	2.176	6.200	0.809	0.108	4.236	4.072	131.707	0.017
118080	-15.843	2.069	6.524	2.044	6.541	0.803	-0.026	-19.368	-16.926	74.882	-0.004
119280	-16.059	2.069	6.786	2.194	6.702	0.798	0.125	2.297	3.476	94.551	0.018
120480	-16.371	2.069	7.077	2.189	6.997	0.792	0.120	3.551	3.593	114.893	0.017
121680	-16.619	2.069	7.367	2.197	7.282	0.786	0.128	3.387	3.364	113.891	0.017
122880	-16.903	2.068	7.669	2.162	7.606	0.780	0.094	5.344	4.520	116.636	0.012
124080	-17.158	2.068	7.994	2.203	7.903	0.775	0.135	3.095	3.131	147.165	0.017
125280	-17.370	2.069	8.317	2.222	8.215	0.770	0.152	2.565	2.764	138.112	0.018
126480	-17.634	2.069	8.671	2.205	8.580	0.765	0.136	2.045	3.072	130.314	0.016
127680	-17.913	2.068	9.040	2.213	8.943	0.759	0.145	2.980	2.861	155.093	0.016
128880	-18.161	2.068	9.424	2.212	9.328	0.753	0.144	2.372	2.864	134.637	0.015
130080	-18.461	2.067	9.819	2.197	9.732	0.747	0.130	4.062	3.162	172.162	0.013
131280	-18.690	2.066	10.227	2.217	10.126	0.742	0.151	2.219	2.696	147.875	0.015
132480	-18.976	2.067	10.669	2.247	10.549	0.736	0.181	2.059	2.244	217.177	0.017
133680	-19.195	2.066	11.122	2.213	11.024	0.731	0.147	2.097	2.742	167.751	0.013

TIME (secs)	STRAIN (%)	CELL (ksc)	V.STS (ksc)	PORE P (ksc)	V.E.STS (ksc)	VOID RATIO,e	DEL U (ksc)	DEL K (*10 cm/(*10 cm/s)	TOT. K (*10 cm/s)	D (ksc)	Ub/Ov
134880	-19.468	2.065	11.590	2.225	11.483	0.725	0.160	2.294	2.504	235.468	0.014
136080	-19.680	2.065	12.093	2.232	11.981	0.721	0.167	1.453	2.386	185.653	0.014
137280	-19.954	2.064	12.604	2.236	12.490	0.715	0.172	1.787	2.305	198.156	0.014
138480	-20.215	2.064	13.124	2.240	13.007	0.709	0.176	2.084	2.229	285.722	0.013
139680	-20.487	2.064	13.672	1.897	13.784	0.703	-0.167	-2.492	-2.332	135.997	-0.012
140880	-20.740	2.063	14.263	2.264	14.129	0.698	0.201	1.782	1.925	248.785	0.014
142080	-20.984	2.063	14.857	2.245	14.736	0.693	0.182	1.400	2.123	227.262	0.012
143280	-21.248	2.061	15.458	2.245	15.335	0.687	0.184	1.611	2.080	286.544	0.012
144480	-21.476	2.063	16.107	2.241	15.988	0.682	0.178	1.769	2.140	322.792	0.011
145680	-21.680	2.063	16.773	2.254	16.646	0.678	0.191	1.581	1.984	264.704	0.011
146880	-21.938	2.062	17.460	2.257	17.329	0.672	0.196	1.224	1.920	261.123	0.011
148080	-22.203	2.062	18.164	2.276	18.022	0.667	0.214	1.655	1.748	276.148	0.012
149280	-22.449	2.062	18.907	2.369	18.702	0.661	0.307	1.237	1.208	326.127	0.016
150480	-22.700	2.062	19.673	2.290	19.521	0.656	0.228	1.386	1.617	237.739	0.012
151201	-22.852	2.062	19.978	2.206	19.882	0.653	0.144	1.595	2.554	36.105	0.007
151617	-22.683	2.063	19.762	1.975	19.821	0.656	-0.088	11.145	-4.189	138.033	-0.004
152217	-22.726	2.063	19.933	2.142	19.880	0.656	0.080	1.609	4.610	1165.943	0.004
152517	-22.744	2.063	20.173	2.196	20.084	0.655	0.133	0.697	2.770	149.034	0.007
152684	-22.759	2.063	20.176	2.167	20.107	0.655	0.104	1.372	3.536	754.831	0.005
153284	-22.795	2.063	20.485	2.223	20.378	0.654	0.160	0.594	2.295	-73.866	0.008
62101	-23.191	2.045	20.112	2.083	20.086	0.646	0.039	0.047	9.455	-10.477	0.002
0.2	-23.412	2.029	20.097	2.080	20.063	0.641	0.051	*****	7.073	781.250	0.003
180	-23.409	2.029	20.072	2.073	20.043	0.641	0.044	0.944	8.282	7770.152	0.002
360	-23.403	2.029	19.591	2.042	19.582	0.641	0.013	-26.790	27.441	7288.535	0.001
720	-23.389	2.029	18.549	2.024	18.552	0.641	-0.005	39.494	-67.454	2148.637	-0.000
900	-23.367	2.029	18.047	1.993	18.072	0.642	-0.036	5.192	-9.949	*****	-0.002
1620	-23.360	2.029	16.156	2.001	16.174	0.642	-0.028	-2.059	-13.082	*****	-0.002
2220	-23.354	2.028	14.748	1.996	14.770	0.642	-0.033	7.863	-11.060	924.026	-0.002
2280	-23.341	2.029	14.620	1.996	14.642	0.642	-0.033	10.918	-10.951	4958.555	-0.002
2340	-23.338	2.029	14.487	1.992	14.511	0.642	-0.037	1.853	-9.809	9725.373	-0.003
2400	-23.337	2.029	14.357	1.994	14.381	0.642	-0.035	0.997	-10.307	*****	-0.002
2520	-23.335	2.029	14.093	1.995	14.115	0.642	-0.034	-5.316	-10.815	1609.949	-0.002
2580	-23.328	2.029	13.965	1.993	13.989	0.643	-0.036	5.622	-9.967	1027.698	-0.003
2670	-23.310	2.030	13.780	1.983	13.811	0.643	-0.046	40.033	-7.843	9764.139	-0.003
2970	-23.304	2.029	13.164	1.987	13.193	0.643	-0.042	0.778	-8.551	1817.898	-0.003
3270	-23.272	2.029	12.577	1.981	12.610	0.644	-0.048	3.460	-7.497	3549.650	-0.004
3570	-23.256	2.029	12.020	1.982	12.051	0.644	-0.047	1.756	-7.761	2712.327	-0.004
3870	-23.237	2.029	11.484	1.974	11.521	0.645	-0.055	1.853	-6.591	7635.320	-0.005
4170	-23.230	2.028	10.959	1.973	10.996	0.645	-0.055	0.654	-6.606	1190.925	-0.005
4470	-23.189	2.028	10.468	1.971	10.506	0.646	-0.058	3.719	-6.288	1476.425	-0.006
4735	-23.160	2.029	10.054	1.972	10.092	0.646	-0.056	2.962	-6.476	1552.006	-0.006
5335	-23.105	2.028	9.190	1.971	9.227	0.647	-0.057	2.582	-6.446	2083.300	-0.006
5935	-23.066	2.028	8.375	1.957	8.422	0.648	-0.070	1.440	-5.181	1403.904	-0.008
6535	-23.014	2.028	7.638	1.958	7.685	0.649	-0.070	1.960	-5.189	770.396	-0.009
7135	-22.928	2.029	6.972	1.953	7.023	0.651	-0.075	3.006	-4.857	1235.175	-0.011
7735	-22.877	2.028	6.339	1.948	6.393	0.652	-0.081	1.665	-4.539	805.334	-0.013
8335	-22.807	2.028	5.770	1.933	5.833	0.654	-0.096	1.923	-3.847	1565.738	-0.017
8935	-22.774	2.028	5.243	1.912	5.321	0.654	-0.116	0.743	-3.160	611.239	-0.022
9535	-22.698	2.028	4.770	1.899	4.856	0.656	-0.129	1.566	-2.860	476.567	-0.027
10135	-22.609	2.028	4.347	1.902	4.430	0.658	-0.125	1.893	-2.946	636.414	-0.029
10735	-22.548	2.028	3.947	1.886	4.042	0.659	-0.142	1.146	-2.609	359.692	-0.036
11335	-22.452	2.027	3.588	1.865	3.696	0.661	-0.163	1.578	-2.282	300.985	-0.045
11935	-22.339	2.028	3.255	1.875	3.356	0.664	-0.153	1.975	-2.435	430.974	-0.047
12535	-22.269	2.028	2.954	1.878	3.054	0.665	-0.150	1.256	-2.488	182.624	-0.051
13135	-22.139	2.028	2.685	1.830	2.817	0.668	-0.198	1.764	-1.891	390.846	-0.074
13735	-22.066	2.028	2.431	1.876	2.532	0.670	-0.152	1.291	-2.462	177.058	-0.063

TIME (secs)	STRAIN (%)	CELL (ksc)	V.STS (ksc)	PORE P (ksc)	V.E.STS (ksc)	VOID RATIO,e	DEL U (ksc)	DEL K (*10 cm/(*10 cm/s)	TOT. K (*10 cm/s)	D (ksc)	Ub/Ov
14335	-21.935	2.028	2.201	1.881	2.299	0.672	-0.147	2.417	-2.554	140.187	-0.067
14935	-21.795	2.028	2.002	1.875	2.104	0.675	-0.153	2.475	-2.465	183.996	-0.076
15535	-21.692	2.028	1.812	1.873	1.914	0.678	-0.154	1.816	-2.454	121.700	-0.085
16135	-21.556	2.028	1.648	1.876	1.749	0.681	-0.152	2.444	-2.498	167.599	-0.092
16735	-21.466	2.027	1.494	1.872	1.597	0.683	-0.156	1.590	-2.446	104.835	-0.104
17335	-21.333	2.027	1.357	1.877	1.458	0.685	-0.150	2.441	-2.544	118.149	-0.111
17935	-21.226	2.027	1.226	1.869	1.332	0.688	-0.158	1.846	-2.416	131.093	-0.129
18535	-21.139	2.028	1.117	1.877	1.218	0.690	-0.151	1.598	-2.542	73.460	-0.135
19135	-20.995	2.028	1.016	1.884	1.112	0.693	-0.144	2.770	-2.673	94.926	-0.142
19735	-20.911	2.028	0.953	1.909	1.032	0.694	-0.118	1.965	-3.261	65.119	-0.124
20335	-20.848	2.028	0.888	1.873	0.991	0.696	-0.155	1.137	-2.499	89.155	-0.174
20935	-20.718	2.028	0.789	1.898	0.875	0.699	-0.130	2.801	-2.991	60.524	-0.164
21535	-20.619	2.028	0.746	1.924	0.815	0.701	-0.104	2.646	-3.732	39.329	-0.140
22135	-20.517	2.028	0.735	1.967	0.775	0.703	-0.060	4.749	-6.451	33.849	-0.082
22735	-20.453	2.028	0.723	1.983	0.753	0.704	-0.045	4.003	-8.656	128.862	-0.062
23335	-20.424	2.028	0.684	1.980	0.716	0.705	-0.048	1.671	-8.078	16.438	-0.071
23935	-20.332	2.028	0.680	1.996	0.701	0.707	-0.032	8.009	-12.127	145.358	-0.048
24535	-20.315	2.028	0.663	2.006	0.677	0.707	-0.021	2.202	-18.411	80.377	-0.032
25135	-20.291	2.028	0.644	2.008	0.657	0.708	-0.020	3.466	-19.670	38.958	-0.031
25735	-20.251	2.028	0.642	2.027	0.642	0.709	-0.000	302.681	-1055.795	4.998	-0.001
26335	-20.208	2.028	0.647	2.039	0.640	0.709	0.012	-10.468	34.028	13.937	0.018
26935	-20.136	2.028	0.639	2.042	0.630	0.711	0.014	-14.597	28.112	268.566	0.022
27535	-20.124	2.027	0.629	2.074	0.597	0.711	0.047	-0.725	8.376	-42.181	0.075
28135	-20.081	2.027	0.625	2.042	0.615	0.712	0.015	-8.156	26.388	31.559	0.024
28735	-20.053	2.027	0.620	2.048	0.606	0.713	0.021	-3.868	18.907	6.326	0.034
29335	-20.023	2.028	0.626	2.060	0.605	0.713	0.032	-2.618	12.420	22.891	0.051
29935	-20.008	2.028	0.622	2.059	0.601	0.714	0.031	-1.409	12.610	-226.628	0.050
30535	-20.009	2.027	0.620	2.060	0.598	0.714	0.032	0.106	12.177	15.358	0.052
31135	-19.979	2.027	0.617	2.062	0.594	0.714	0.035	-2.410	11.148	-23.846	0.057
31735	-20.000	2.027	0.611	2.061	0.589	0.714	0.034	1.730	11.650	19.867	0.055
32335	-19.983	2.027	0.605	2.057	0.585	0.714	0.030	-1.623	13.379	140.074	0.049
32935	-19.959	2.027	0.549	2.023	0.552	0.715	-0.004	15.351	-90.161	2.767	-0.008

 CONSOLIDATION AT CONSTANT RATE OF STRAIN
 MIT GEOTECHNICAL LAB

File Name: CRS08.PRN

-
- 1. Test Name: CRS 08
 - 2. Date: 5/30/89
 - 3. Initial Height of Sample (cm): 2.08
 - 4. Initial Water Content of Sample (%): 39.59
 - 5. Area of Sample (sq cm): 31.64
 - 6. DCDT
 - Zero: 0.291
 - CF: -1.8526 cm/V/V
 - 7. Cell Pressure
 - Zero: -0.00009
 - CF: 705.735 ksc/V/V
 - 8. Vertical Load Cell
 - Zero: 0.00009
 - CF: 27013.98 kg/V/V
 - 9. Pore Pressure
 - Zero: -0.0010
 - CF: 965.359 ksc/V/V

TIME (secs)	STRAIN (%)	CELL (ksc)	V.STS (ksc)	PORE P (ksc)	V.E.STS (ksc)	VOID RATIO,e	DEL U (ksc)	DEL K (*10 cm/(*10 cm/s)	TOT. K (ksc)	D (ksc)	Ub/Ov
840	-0.012	1.988	0.225	2.150	0.117	1.102	0.162	23.331	27.010	25.944	0.719
960	-0.224	1.990	0.323	2.217	0.172	1.097	0.227	16.689	19.141	40.129	0.702
1080	-0.411	1.990	0.438	2.275	0.247	1.093	0.286	11.737	15.164	50.394	0.653
1200	-0.576	1.990	0.537	2.299	0.330	1.090	0.309	9.507	13.958	44.908	0.576
1320	-0.793	1.990	0.637	2.304	0.428	1.085	0.314	12.220	13.671	41.551	0.493
1440	-1.022	1.991	0.736	2.311	0.523	1.081	0.320	12.621	13.355	50.940	0.435
1560	-1.218	1.990	0.836	2.310	0.623	1.076	0.320	10.763	13.315	64.008	0.383
1680	-1.385	1.990	0.941	2.307	0.730	1.073	0.317	9.260	13.389	50.331	0.337
1800	-1.567	1.985	1.036	2.307	0.821	1.069	0.323	9.818	13.112	37.190	0.311
1920	-1.807	1.985	1.129	2.312	0.911	1.064	0.328	12.777	12.859	40.044	0.290
2040	-2.019	1.985	1.213	2.312	0.995	1.060	0.327	11.203	12.824	40.472	0.269
2160	-2.215	1.985	1.296	2.316	1.075	1.056	0.332	10.187	12.589	33.280	0.256
2280	-2.420	1.990	1.368	2.327	1.143	1.051	0.337	10.436	12.341	24.718	0.246
2400	-2.686	1.991	1.438	2.334	1.209	1.046	0.343	13.245	12.048	21.346	0.239
2520	-2.949	1.990	1.505	2.350	1.265	1.040	0.360	12.399	11.435	30.067	0.239
2577	-3.043	1.991	1.531	2.348	1.293	1.038	0.357	9.419	11.510	20.212	0.233
2757	-3.425	1.990	1.623	2.368	1.370	1.030	0.379	11.295	10.763	20.933	0.233
2937	-3.788	1.990	1.712	2.389	1.446	1.022	0.399	10.135	10.133	18.815	0.233
3117	-4.188	1.989	1.799	2.405	1.522	1.014	0.416	10.589	9.634	16.344	0.231
3297	-4.561	1.989	1.886	2.443	1.583	1.006	0.455	8.983	8.753	16.534	0.241
3477	-4.938	1.989	1.964	2.468	1.645	0.998	0.479	8.541	8.239	16.547	0.244
3657	-5.326	1.988	2.047	2.494	1.709	0.990	0.506	8.258	7.732	17.939	0.247
3837	-5.720	1.986	2.140	2.526	1.780	0.982	0.540	7.805	7.190	18.750	0.252
4017	-6.108	1.982	2.231	2.551	1.853	0.974	0.568	7.235	6.776	20.064	0.255
4197	-6.514	1.984	2.326	2.572	1.934	0.965	0.589	7.245	6.486	16.055	0.253
4377	-6.904	1.984	2.414	2.610	1.997	0.957	0.627	6.480	6.042	19.529	0.259
4557	-7.294	1.983	2.501	2.624	2.073	0.949	0.642	6.275	5.851	18.077	0.257
4737	-7.727	1.983	2.591	2.643	2.151	0.940	0.660	6.713	5.635	21.151	0.255
4917	-8.120	1.983	2.691	2.667	2.234	0.931	0.685	5.815	5.384	22.140	0.255
5097	-8.510	1.983	2.791	2.688	2.320	0.923	0.705	5.566	5.186	26.203	0.253
5277	-8.887	1.983	2.896	2.698	2.419	0.915	0.715	5.272	5.072	26.352	0.247
5457	-9.280	1.980	3.008	2.707	2.523	0.907	0.727	5.344	4.944	30.788	0.242
5637	-9.642	1.980	3.133	2.728	2.634	0.899	0.748	4.746	4.769	29.173	0.239
5817	-10.038	1.980	3.255	2.737	2.750	0.891	0.757	5.082	4.668	30.880	0.233
5997	-10.390	1.980	3.375	2.754	2.858	0.884	0.774	4.386	4.531	31.110	0.229
6177	-10.782	1.980	3.510	2.775	2.980	0.875	0.795	4.718	4.374	32.308	0.226

TIME (secs)	STRAIN (%)	CELL (ksc)	V.STS (ksc)	PORE P (ksc)	V.E.STS (ksc)	VOID RATIO,e	DEL U (ksc)	DEL K (*10 cm/(*10 cm/s)	TOT. K (*10 cm/s)	D (ksc)	Ub/Ov
6357	-11.165	1.980	3.645	2.791	3.104	0.867	0.811	4.479	4.249	37.486	0.223
6537	-11.533	1.980	3.793	2.806	3.242	0.860	0.826	4.199	4.141	40.386	0.218
6717	-11.886	1.980	3.951	2.829	3.385	0.852	0.849	3.879	3.994	37.184	0.215
6897	-12.248	1.980	4.101	2.852	3.520	0.845	0.872	3.844	3.859	38.015	0.213
7077	-12.641	1.979	4.233	2.825	3.669	0.836	0.846	4.254	3.940	51.246	0.200
7257	-12.979	1.979	4.452	2.894	3.842	0.829	0.915	3.366	3.615	41.194	0.205
7437	-13.361	1.979	4.617	2.905	3.999	0.821	0.926	3.718	3.541	46.651	0.201
7617	-13.743	1.979	4.812	2.931	4.178	0.813	0.952	3.591	3.414	52.520	0.198
7797	-14.102	1.975	5.015	2.949	4.366	0.806	0.974	3.262	3.309	58.018	0.194
7977	-14.455	1.978	5.225	2.959	4.571	0.798	0.981	3.170	3.258	61.433	0.188
8157	-14.816	1.976	5.455	2.969	4.793	0.791	0.993	3.170	3.193	63.212	0.182
8337	-15.180	1.978	5.692	2.982	5.023	0.783	1.005	3.127	3.128	64.897	0.176
8517	-15.541	1.976	5.950	3.015	5.257	0.775	1.039	2.985	3.000	68.274	0.175
8697	-15.904	1.976	6.227	3.060	5.505	0.768	1.083	2.847	2.851	69.785	0.174
8877	-16.262	1.976	6.491	3.080	5.755	0.760	1.104	2.733	2.775	74.780	0.170
9057	-16.623	1.976	6.780	3.109	6.025	0.753	1.133	2.663	2.680	82.014	0.167
9237	-16.977	1.977	7.088	3.137	6.315	0.745	1.160	2.525	2.595	80.466	0.164
9417	-17.337	1.977	7.392	3.158	6.604	0.738	1.181	2.502	2.527	81.721	0.160
9597	-17.695	1.977	7.695	3.174	6.897	0.730	1.197	2.437	2.472	90.931	0.156
9777	-18.045	1.977	8.045	3.221	7.215	0.723	1.245	2.268	2.357	92.400	0.155
9957	-18.391	1.977	8.388	3.255	7.536	0.715	1.279	2.171	2.275	100.751	0.152
10137	-18.721	1.977	8.732	3.273	7.868	0.709	1.296	2.019	2.226	102.356	0.148
10317	-19.068	1.977	9.105	3.301	8.222	0.701	1.324	2.060	2.160	115.357	0.145
10497	-19.392	1.977	9.495	3.325	8.596	0.694	1.349	1.877	2.105	117.149	0.142
10677	-19.726	1.977	9.903	3.349	8.987	0.687	1.373	1.883	2.050	124.749	0.139
10857	-20.053	1.977	10.335	3.385	9.396	0.681	1.408	1.786	1.983	128.632	0.136
11037	-20.373	1.977	10.770	3.420	9.807	0.674	1.444	1.687	1.918	151.316	0.134
11217	-20.663	1.977	11.227	3.448	10.246	0.668	1.471	1.492	1.869	151.990	0.131
11397	-20.963	1.977	11.710	3.489	10.702	0.661	1.512	1.488	1.804	167.031	0.129
11577	-21.249	1.978	12.205	3.517	11.180	0.655	1.539	1.386	1.761	159.638	0.126
11757	-21.562	1.977	12.727	3.547	11.680	0.649	1.570	1.477	1.712	156.878	0.123
11937	-21.888	1.978	13.268	3.591	12.192	0.642	1.613	1.482	1.652	169.361	0.122
12117	-22.198	1.978	13.817	3.630	12.715	0.635	1.652	1.361	1.600	181.489	0.120
12297	-22.495	1.977	14.382	3.666	13.256	0.629	1.690	1.271	1.553	200.174	0.117
12477	-22.783	1.977	14.985	3.708	13.831	0.623	1.731	1.190	1.505	202.520	0.116
12657	-23.075	1.977	15.589	3.726	14.423	0.617	1.750	1.187	1.477	238.320	0.112
12837	-23.334	1.978	16.231	3.762	15.042	0.612	1.784	1.028	1.439	246.483	0.110
13017	-23.596	1.978	16.908	3.811	15.686	0.606	1.833	1.001	1.391	226.714	0.108
13197	-23.890	1.978	17.603	3.851	16.354	0.600	1.873	1.094	1.351	239.225	0.106
13377	-24.183	1.978	18.330	3.892	17.054	0.594	1.914	1.056	1.312	253.413	0.104
13557	-24.470	1.978	19.095	3.950	17.780	0.588	1.972	0.996	1.263	264.995	0.103
13737	-24.759	1.978	19.899	4.005	18.548	0.582	2.027	0.972	1.220	327.059	0.102
13802.	-24.848	1.978	20.202	4.024	18.839	0.580	2.045	0.808	1.206	-122.146	0.101
0	-24.956	1.977	19.475	3.130	18.707	0.577	1.153	*****	2.134	92.591	0.059
120	-25.023	1.979	19.337	2.832	18.769	0.576	0.853	0.795	2.879	173.714	0.044
240	-25.358	1.983	20.346	3.478	19.350	0.569	1.494	2.248	1.628	156.398	0.073
360	-25.460	1.983	20.260	3.108	19.510	0.567	1.125	0.912	2.158	134.063	0.056
300	-25.656	1.983	20.212	2.642	19.772	0.563	0.659	155.123	3.663	93.568	0.033
600	-25.753	1.983	20.160	2.429	19.863	0.561	0.446	0.868	5.403	-73.882	0.022
688	-25.777	1.983	20.076	2.329	19.845	0.560	0.346	0.946	6.960	89.008	0.017
1588	-25.928	1.983	20.090	2.149	19.980	0.557	0.166	1.199	14.462	-8.902	0.008
2488	-26.017	1.983	20.031	2.072	19.972	0.555	0.089	1.309	26.879	238.164	0.004
3388	-26.076	1.983	20.167	2.063	20.114	0.554	0.080	0.983	29.870	-235.448	0.004
4288	-26.121	1.983	20.039	2.028	20.009	0.553	0.045	1.310	53.526	-50.997	0.002
5188	-26.156	1.983	20.016	2.020	19.992	0.552	0.036	1.271	65.745	155.850	0.002
6088	-26.189	1.983	20.061	2.011	20.043	0.552	0.028	1.531	84.764	627.936	0.001

TIME (secs)	STRAIN (%)	CELL (ksc)	V.STS (ksc)	PORE P (ksc)	V.E.STS (ksc)	VOID RATIO,e	DEL U (ksc)	DEL K (*10 cm/(*10 cm/s)	TOT. K	D (ksc)	Ub/Ov
6988	-26.214	1.983	20.226	2.016	20.204	0.551	0.033	1.016	72.005	-965.140	0.002
7888	-26.234	1.983	20.030	2.001	20.018	0.551	0.018	1.397	132.095	1774.450	0.001
8788	-26.253	1.983	20.384	2.024	20.357	0.550	0.040	0.617	58.749	-903.761	0.002
9688	-26.275	1.983	20.172	2.001	20.160	0.550	0.017	1.635	136.254	-855.346	0.001
10588	-26.289	1.984	20.047	1.997	20.038	0.549	0.014	1.347	171.125	2020.326	0.001
11488	-26.303	1.984	20.336	2.004	20.323	0.549	0.020	0.919	118.268	-948.400	0.001
12388	-26.318	1.984	20.191	1.995	20.184	0.549	0.011	1.686	208.502	*****	0.001
13288	-26.328	1.982	20.085	1.991	20.079	0.549	0.009	1.450	265.391	7006.093	0.000
14188	-26.333	1.982	20.498	2.024	20.470	0.549	0.042	0.173	56.427	-935.463	0.002
15088	-26.350	1.982	20.320	1.996	20.311	0.548	0.014	1.602	170.631	*****	0.001
15988	-26.360	1.984	20.210	1.991	20.205	0.548	0.007	1.755	317.386	-805.005	0.000
16888	-26.370	1.984	20.129	1.989	20.125	0.548	0.006	2.349	427.701	*****	0.000
17788	-26.376	1.982	20.062	1.987	20.059	0.548	0.005	1.601	486.678	*****	0.000
18688	-26.380	1.982	20.006	1.988	20.002	0.548	0.005	0.986	453.635	*****	0.000
19588	-26.383	1.984	19.953	1.986	19.952	0.547	0.002	1.594	1087.859	6230.138	0.000
20488	-26.393	1.982	20.600	2.008	20.582	0.547	0.026	0.511	91.887	-837.964	0.001
21388	-26.409	1.982	20.459	1.993	20.452	0.547	0.011	1.866	217.068	*****	0.001
22288	-26.416	1.982	20.368	1.990	20.363	0.547	0.008	1.256	293.148	-953.762	0.000
23188	-26.424	1.982	20.296	1.987	20.293	0.547	0.005	2.020	502.311	*****	0.000
24088	-26.429	1.982	20.238	1.987	20.235	0.547	0.005	1.439	484.070	5049.265	0.000
24988	-26.437	1.982	20.656	1.996	20.647	0.546	0.013	0.794	176.738	*****	0.001
25888	-26.447	1.982	20.550	1.991	20.544	0.546	0.009	1.393	263.965	-898.452	0.000
26788	-26.455	1.982	20.472	1.988	20.468	0.546	0.005	2.024	437.887	*****	0.000
27688	-26.461	1.982	20.407	1.987	20.404	0.546	0.005	1.505	483.652	*****	0.000
28588	-26.465	1.984	20.354	1.986	20.353	0.546	0.002	2.544	1012.016	*****	0.000
29488	-26.470	1.982	20.307	1.988	20.304	0.546	0.005	1.188	452.526	-987.282	0.000
30388	-26.474	1.984	20.267	1.987	20.264	0.546	0.003	1.536	695.548	-786.577	0.000
31288	-26.479	1.984	20.231	1.986	20.229	0.545	0.002	2.696	1094.743	*****	0.000
32188	-26.481	1.984	20.197	1.985	20.196	0.545	0.002	1.724	1469.537	-687.124	0.000
33088	-26.486	1.984	20.164	1.984	20.164	0.545	0.000	16.428	6404.409	*****	0.000
33988	-26.490	1.984	20.687	1.993	20.681	0.545	0.009	0.631	250.360	*****	0.000
34888	-26.497	1.984	20.668	1.989	20.605	0.545	0.006	1.575	424.750	*****	0.000
35788	-26.503	1.983	20.547	1.987	20.544	0.545	0.004	1.907	592.398	*****	0.000
36688	-26.508	1.983	20.494	1.986	20.492	0.545	0.003	2.239	807.478	*****	0.000
37588	-26.510	1.983	20.447	1.986	20.445	0.545	0.002	1.173	986.555	-666.504	0.000
38488	-26.516	1.984	20.407	1.987	20.404	0.545	0.003	2.325	687.014	-330.964	0.000
38622	-26.518	1.984	20.399	1.985	20.398	0.545	0.001	11.534	1585.458	*****	0.000
40422	-26.523	1.983	20.326	1.985	20.324	0.545	0.002	1.541	1046.171	5317.535	0.000
42222	-26.529	1.983	20.633	1.987	20.630	0.544	0.004	0.830	524.390	*****	0.000
44022	-26.539	1.983	20.533	1.986	20.531	0.544	0.003	2.121	801.109	*****	0.000
45822	-26.545	1.983	20.465	1.986	20.463	0.544	0.003	1.274	755.608	*****	0.000
47622	-26.549	1.983	20.415	1.983	20.415	0.544	0.000	8.921	7647.269	-654.306	0.000
49422	-26.556	1.981	20.370	1.985	20.368	0.544	0.004	1.235	623.028	-835.593	0.000
51222	-26.561	1.981	20.330	1.984	20.328	0.544	0.003	1.176	905.714	-555.544	0.000
53022	-26.571	1.981	20.272	1.980	20.273	0.544	-0.001	-9.499	-3450.295	844.565	-0.000
54822	-26.569	1.981	20.257	1.981	20.257	0.544	0.000	-2.416	4765.408	-692.647	0.000
56622	-26.571	1.981	20.242	1.980	20.243	0.544	-0.001	-2.501	-4457.645	-812.857	-0.000
58422	-26.574	1.978	20.222	1.981	20.220	0.543	0.003	0.614	795.345	*****	0.000
60222	-26.575	1.975	20.172	1.978	20.170	0.543	0.003	0.281	777.566	*****	0.000
62022	-26.578	1.976	20.138	1.977	20.137	0.543	0.002	0.925	1388.107	-556.481	0.000
63822	-26.580	1.975	20.126	1.977	20.125	0.543	0.002	0.645	1087.284	-675.000	0.000
65622	-26.581	1.975	20.115	1.976	20.114	0.543	0.001	1.159	2702.252	*****	0.000
67422	-26.585	1.979	20.064	1.979	20.064	0.543	0.000	19.236	19729.130	1210.340	0.000
69222	-26.570	1.976	19.889	1.980	19.886	0.544	0.004	-2.306	570.164	*****	0.000
71022	-26.577	1.975	19.792	1.978	19.790	0.543	0.003	1.562	867.702	115.007	0.000
72822	-26.570	1.976	19.786	1.982	19.782	0.544	0.006	-0.776	419.190	7025.000	0.000

TIME (secs)	STRAIN (%)	CELL (ksc)	V.STS (ksc)	PORE P (ksc)	V.E.STS (ksc)	VOID RATIO,e	DEL U (ksc)	DEL K (*10 cm/(*10 cm/s)	TOT. K (*10 cm/s)	D (ksc)	Ub/Ov
74622	-26.571	1.978	19.828	1.983	19.824	0.544	0.005	0.071	433.562	*****	0.000
76422	-26.570	1.980	19.839	1.983	19.837	0.544	0.003	-0.182	863.465	5118.519	0.000
78222	-26.570	1.979	19.854	1.984	19.851	0.544	0.005	0.035	461.802	*****	0.000
80022	-26.569	1.980	19.868	1.982	19.866	0.544	0.002	-0.326	968.598	2107.317	0.000
81822	-26.569	1.979	19.878	1.984	19.875	0.544	0.005	0.053	471.039	-406.061	0.000
83622	-26.569	1.980	19.879	1.985	19.876	0.544	0.005	-0.042	459.849	-746.154	0.000
83766.	-26.569	1.977	19.881	1.986	19.875	0.544	0.009	0.118	268.053	45.003	0.000
0	-26.457	1.986	19.822	1.983	19.824	0.546	-0.003	*****	-760.206	*****	-0.000
120	-26.462	1.986	17.999	1.592	18.262	0.546	-0.395	-0.124	-5.983	*****	-0.022
240	-26.472	1.984	15.494	1.370	15.903	0.546	-0.614	-0.163	-3.848	7552.751	-0.040
360	-26.446	1.986	13.403	1.222	13.913	0.546	-0.764	0.336	-3.093	3226.662	-0.057
480	-26.392	1.988	11.546	1.065	12.161	0.547	-0.922	0.575	-2.566	4072.205	-0.080
600	-26.353	1.985	9.896	0.948	10.587	0.548	-1.037	0.364	-2.285	2012.851	-0.105
720	-26.285	1.986	8.478	0.861	9.228	0.550	-1.125	0.588	-2.110	2123.302	-0.133
840	-26.230	1.984	7.247	0.785	8.046	0.551	-1.198	0.456	-1.984	1019.816	-0.165
960	-26.129	1.984	6.184	0.727	7.021	0.553	-1.257	0.786	-1.897	992.697	-0.203
1080	-26.039	1.986	5.247	0.667	6.127	0.555	-1.319	0.674	-1.811	567.331	-0.251
1200	-25.903	1.985	4.433	0.607	5.352	0.558	-1.378	0.981	-1.740	517.464	-0.311
1320	-25.771	1.984	3.717	0.554	4.670	0.560	-1.430	0.915	-1.683	368.220	-0.385
1440	-25.611	1.986	3.095	0.506	4.081	0.564	-1.480	1.078	-1.633	245.564	-0.478
1560	-25.401	1.988	2.557	0.474	3.566	0.568	-1.513	1.393	-1.606	256.117	-0.592
1680	-25.231	1.985	2.141	0.501	3.130	0.572	-1.484	1.154	-1.645	176.960	-0.693
1800	-25.001	1.985	1.697	0.444	2.724	0.577	-1.541	1.511	-1.595	130.987	-0.908
1920	-24.743	1.988	1.359	0.448	2.386	0.582	-1.540	1.712	-1.607	233.668	-1.133
2040	-24.617	1.986	1.077	0.465	2.091	0.585	-1.521	0.849	-1.632	181.886	-1.412
2160	-24.482	1.986	0.845	0.487	1.845	0.587	-1.500	0.928	-1.661	123.695	-1.774
2280	-24.310	1.984	0.658	0.522	1.633	0.591	-1.462	1.213	-1.712	99.680	-2.220
2400	-24.128	1.986	0.502	0.563	1.451	0.595	-1.424	1.329	-1.766	76.474	-2.836
2520	-23.920	1.986	0.369	0.602	1.293	0.599	-1.385	1.563	-1.826	72.114	-3.750
2640	-23.731	1.986	0.265	0.649	1.156	0.603	-1.337	1.482	-1.900	62.088	-5.048
2760	-23.537	1.986	0.161	0.674	1.036	0.607	-1.312	1.558	-1.946	52.385	-8.156
2880	-23.332	1.986	0.082	0.716	0.928	0.612	-1.270	1.713	-2.022	36.498	*****
3000	-23.092	1.986	0.026	0.764	0.841	0.617	-1.222	2.091	-2.114	3.641	*****

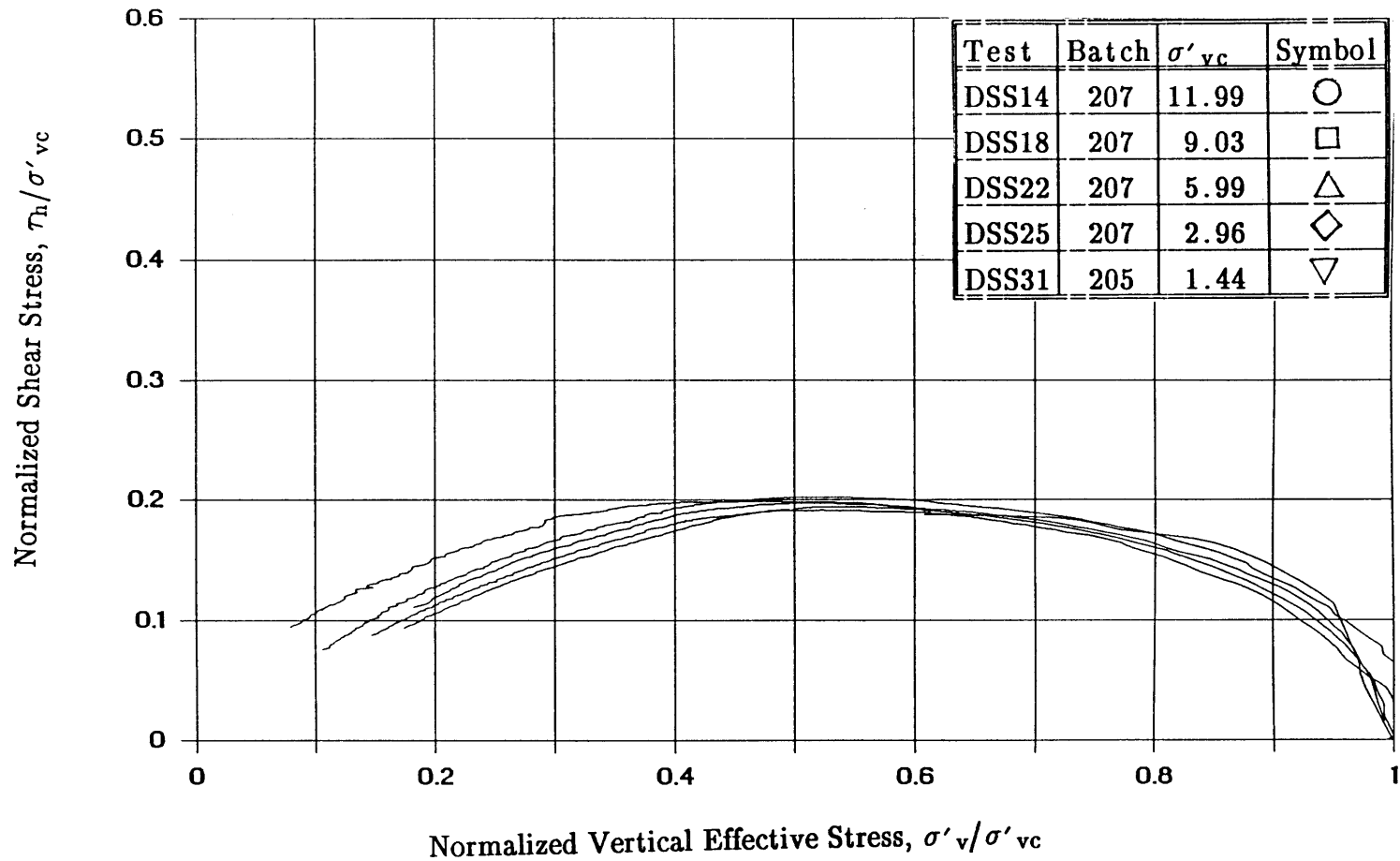


Figure 6.1: Normalized Stress Paths from CK_0 UDSS Tests on Normally Consolidated Boston Blue Clay.